

ÉCOLE DOCTORALE DES SCIENCES CHIMIQUES

UMR 7509

THÈSE

présentée par

Thibault GENDRON

soutenue le : **23 novembre 2012**

pour obtenir le grade de

Docteur de l'université de Strasbourg

Discipline / Spécialité : Chimie

Synthesis and evaluation of the antiparasitic activity of diarylideneacetones and their related thiopyranone and S-oxide prodrugs

THÈSE dirigée par :

Mme DAVIOUD-CHARVET Elisabeth

Docteur, Université de Strasbourg

RAPPORTEURS :

M. FIGADÈRE Bruno

Docteur, Université Paris XI

Mme MAHUTEAU-BETZER Florence

Docteur, Institut Curie

MEMBRES DU JURY :

M. COURTEMANCHE Gilles

Docteur, Sanofi-Aventis

M. LOISEAU Philippe

Professeur, Université Paris XI

M. MIESCH Michel

Docteur, Université de Strasbourg

*À mes parents,
À mes sœurs,
À mes proches.*

Pour leurs encouragements
et leur indéfectible soutien.

Men are not prisoners of fate, but only prisoners of their own minds

Franklin Delano Roosevelt

Remerciements

Avant tout, je souhaiterais remercier les membres du jury pour avoir accepté de lire et d'évaluer ce travail de thèse : Dr. Florence Mahuteau-Betzer, Dr. Bruno Figadère, Dr. Gilles Courtemanche, Pr. Philippe Loiseau et Dr. Michel Miesch.

Un très grand merci au Dr. Elisabeth Davioud-Charvet, ma directrice de thèse, qui m'a accueilli, conseillé et guidé durant ces trois années de thèse. C'est avec sincérité que je te témoigne ma gratitude pour la confiance et la liberté que tu m'as accordées pour mes recherches. Merci également pour les nombreuses discussions enrichissantes que nous avons pu avoir : ton enthousiasme et ta passion pour la chimie médicinale sont indubitablement communicatifs !

J'adresse un remerciement tout particulier au Dr. Don Antoine Lanfranchi pour son accompagnement tout au long de cette thèse. Que de choses à dire ! Merci de m'avoir fait partager tes connaissances et ta passion pour la chimie organique, tes nombreuses et précieuses astuces expérimentales, ta rigueur dans l'exécution des protocoles... Ton encadrement et ta participation ont été décisifs pour la réussite de ce projet. Mais notre collaboration ne se résume pas à des casse-tête stéréochimiques : travailler avec toi c'est aussi et surtout des discussions passionnées sur tous les sujets, scientifiques ou non, de franches rigolades, des expressions bizarres, bref en un mot comme en cent, la chaleur Corse !

J'exprime toute ma gratitude au Pr. Philippe Loiseau, au Pr. Louis Maes et à tous les membres de leurs équipes pour avoir testé rapidement tous les produits décrits dans cette thèse. Sans les biologistes, la chimie médicinale n'est que peu de choses, merci à eux. De même, je tiens à remercier le Pr. Thomas Müller ainsi que tous mes collègues de l'Université de Düsseldorf pour leur accueil durant notre collaboration.

Je souhaiterais également remercier tous les membres du laboratoire de Chimie Bioorganique et Médicinale. Elena, Katharina, Xavier, Didier et Mourad, merci à tous pour votre bonne humeur qui rend le travail au R5N1 si agréable. Merci aussi aux anciens, Laure et Alexandra, qui m'ont aidé à mon arrivée à Strasbourg et pour qui je garde une amitié toute particulière, et Karène, redoutable d'énergie et de détermination. Enfin il ne serait pas juste d'oublier les étudiants de Master : Hripsimée, Roxanne, Benoît, et Benjamin. Je tiens tout particulièrement à remercier Hripsimée qui, malgré mon exigence et des délais serrés, est parvenue avec brio à synthétiser nombre des produits décrits dans cette thèse.

Je remercie également les membres permanents de l'UMR 7509 et notamment le Dr. Frédéric Leroux et le Dr. Gilles Hanquet pour leur précieux avis et conseils en chimie organique. Je n'oublie pas non plus mes collègues : Florence, Marie, Anaïs, Margareta, Matthieu, Mickael, Nicolas, Thomas et tous les autres. Un grand merci en particulier à Pierre-Antoine et Camille qui ont tous deux été à mes côtés pendant ces trois ans et avec qui j'ai partagé de nombreux moments d'amitié et de bonne humeur, si précieux lorsque l'on s'aventure dans le désert hostile d'un doctorat.

Merci à Michel Schmitt pour sa disponibilité et son enseignement de la pratique des appareillages RMN : du vénérable 200 MHz au moderne 300 MHz, juges arbitraires de la paix de mes nuits/week-end. Merci aussi à tous les membres des Services Communs d'Analyses de l'Université de Strasbourg.

Merci à mes amis de l'Ecole de Chimie de Rennes, pour leur présence, leur soutien et pour m'avoir permis de m'évader du laboratoire quand cela été nécessaire. Merci en particulier à Chloé pour son intarissable joie de vivre, à Lucie pour m'avoir fait l'honneur d'être son Témoin, à Élise pour les nombreuses et précieuses heures passées à discuter ensembles, à Katya la plus attachante des chimistes théoriciennes, à Stéphanie pour son entrain et sa vivacité, à Gaëlle, à Régine, à mon Binôme Rémi, à mes co-Binômes Aurore et Geoffrey, à Jo et à Cédric.

Enfin, je remercie de tout cœur mes parents et mes sœurs, qui ont su me faire confiance et m'ont toujours soutenu dans mes choix. C'est grâce à vous que j'ai pu en arriver là aujourd'hui ! Un grand merci à ma maman qui a eu le courage et l'abnégation de relire l'intégralité de cette thèse, chassant inlassablement tous les "at", "of", et autres "s" récalcitrants. Place aux jeunes : merci à ma nièce, Othilie, et à mes neveux, Pierre-Hugo et Louis, pour leur vivacité, pour leur bonne humeur enfantine mais néanmoins communicative, et pour avoir parfaitement su comment occuper mes vacances sans penser à la chimie et au laboratoire.

Abbreviations

ADMET	absorption, distribution, metabolism, excretion, and toxicity
ANOVA	analysis of variance
ATP	adenosine-5'-triphosphate
BBD	Box-Behnken design
CHP	cumyl hydroperoxide
CIR	coupling isomerization reaction
conc.	concentrated
δ	chemical shift
d	doublet
DAA	diarylideneacetone
2,6-DA-4-THTP	2,6-diaryl-4 <i>H</i> -tetrahydrothiopyran-4-one
DBA	dibenzylideneacetone
DBU	1,8-diazabicyclo[5.4.0]undec-7-ene
DCE	1,2-dichloroethane
DCM	dichloromethane
dec.	decomposition
DMF	dimethylformamide
DNA	deoxyribonucleic acid
DoE	design of experiment
ECG	electrocardiogram
EDG	electron donating group
EMG	enone masking group
equiv.	equivalent
ESI	electron spray ionization
Et ₃ N	triethylamine
EtOAc	ethyl acetate
EtOH	ethanol
EWG	electron withdrawing group
γ GCS	glutamylcysteine synthetase
GR	glutathione reductase
GSH	glutathione
GSSG	glutathione disulfide
h	hour(s)
HAT	human African trypanosomiasis
<i>h</i> MRC-5	human diploid embryonic lung fibroblast MRC-5 cells
HO1	heme oxygenase 1
HPLC	high pressure liquid chromatography
HTS	high-throughput screening
IC ₅₀	50 % inhibitory concentration
<i>J</i>	coupling constant
LAH	lithium aluminium hydride
LHS	left hand side
μ L	microliter

M	molarity
m	multiplet
m.p.	melting point
<i>m</i> CPBA	<i>meta</i> -chloroperbenzoic acid
Me	methyl
MeOH	methanol
MHz	megahertz
min	minute(s)
MMOA	molecular mechanism of action
mmol	millimole
MS	mass spectroscopy
MTBE	methyl <i>tert</i> -butyl ether
NADP ⁺	nicotinamide adenine dinucleotide phosphate (oxidized)
NADPH	nicotinamide adenine dinucleotide phosphate (reduced)
<i>n</i> BuLi	<i>n</i> -butyllithium
NFκB	nuclear factor κB
NMR	nuclear magnetic resonance
Nrf2	nuclear factor (erythroid-derived 2)-like 2
PCC	pyridinium chlorochromate
pH	potential hydrogen
Ph	phenyl
ppm	parts per million
PRT	3-phosphoribosyltransferase
ref.	reference
R _f	retention factor
RHS	right hand side
ROS	reactive oxygen species
RT	room temperature
s	singlet, second
SAR	structure activity relationship
sat.	saturated
S _N Ar	nucleophilic aromatic substitution
t	triplet
T(SH) ₂	trypanothione
TBHP	<i>tert</i> -butylhydroperoxide
TFA	trifluoroacetic acid
THF	tetrahydrofuran
TLC	thin layer chromatography
TPP	target Product Profile
TR	trypanothione reductase
TS ₂	trypanothione disulfide
UV	ultraviolet
Vis.	visible
WHO	world health organisation

Résumé en français

Les maladies parasitaires représentent un réel problème de santé public dans de nombreux pays et notamment ceux en voie de développement. L'ensemble de ces maladies cause plus de deux millions de morts par an et constitue un frein important pour le développement économique des pays touchés.^{1,2} Si le paludisme est sans doute la parasitose la plus médiatisée, à raison, puisqu'il entraîne à lui seul la mort d'un million de personnes par an, d'autres maladies parasitaires sont responsables d'une morbidité et d'une mortalité considérables. Tout aussi fatales, les leishmanioses, les trypanosomiasés, ou encore la schistosomiase, font malheureusement l'objet de recherches moins importantes, et ce en dépit d'une réponse thérapeutique peu satisfaisante.³ En effet, peu de médicaments sont disponibles sur le marché et la plupart, relativement anciens, s'accompagnent d'une longue liste d'effets indésirables potentiellement mortels. Il y a donc un besoin urgent en termes de recherche et de développement de nouveaux principes actifs pour le traitement de ces diverses parasitoses.

S'inscrivant parfaitement dans cette thématique, le travail de recherche ici présenté en vue de l'obtention d'un doctorat en chimie organique de l'Université de Strasbourg, est plus particulièrement dédié à la lutte contre les trypanosomiasés et les leishmaniosés. Effectué au sein du laboratoire de Chimie Bioorganique et Médicinale sous la direction du Dr. Elisabeth Davioud-Charvet et co-encadré par le Dr. Don Antoine Lanfranchi, ce doctorat a été mené à l'interface de plusieurs domaines, alliant des travaux de chimie de synthèse et de méthodologie, à des études de relations structure-activité tout en utilisant des outils de physicochimie et de biochimie pour étudier les propriétés et les effets des molécules synthétisées. Ce document résume ces trois années de recherche.

Les bis-(accepteurs de Michael), de nouveaux agents antiparasitaires

Criblage primaire et cibles potentielles

Lors d'un criblage à haut débit d'inhibiteurs de disulfure réductases NADPH-dépendantes visant à découvrir de nouveaux agents antipaludiques ou trypanocides, une structure base de Mannich insaturée s'est avérée particulièrement intéressante

(Figure 1).⁴⁻⁶ Nicole Wenzel, doctorante m'ayant précédé sur le sujet, a effectué au cours de sa thèse (2005-2009) une étude approfondie sur cette série, défrichant les relations structure-activité (RSA) à la recherche d'autres motifs bis-(accepteurs de Michael) actifs, tout en élucidant partiellement le mécanisme d'action.⁷ Sur ce dernier point, il est apparu que ces molécules

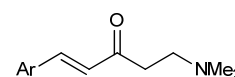


Figure 1 | Base de Mannich insaturée

interagissaient avec les thiols assurant l'équilibre redox du parasite. Dans la plupart des cellules eucaryotes c'est le système glutathion/glutathion réductase qui est chargé de maintenir l'homéostasie réductrice dans la cellule pour lutter contre le stress oxydant. Chez les parasites de l'ordre des kinétoplastidés (regroupant les trypanosomes et les leishmanies), ce système est remplacé par un système unique basé sur un dithiol appelé trypanothion ($T(SH)_2$), et une flavoenzyme, la trypanothion réductase (TR). Le trypanothion est une bis(glutathionyl)spermidine, dithiol cytosolique spécifique et majoritaire chez ces parasites flagellés. La glutathion réductase humaine et la trypanothion réductase parasitaire sont des flavoenzymes NADPH-dépendantes qui partagent environ 41% d'identité dans leur structure primaire (Schéma 1).

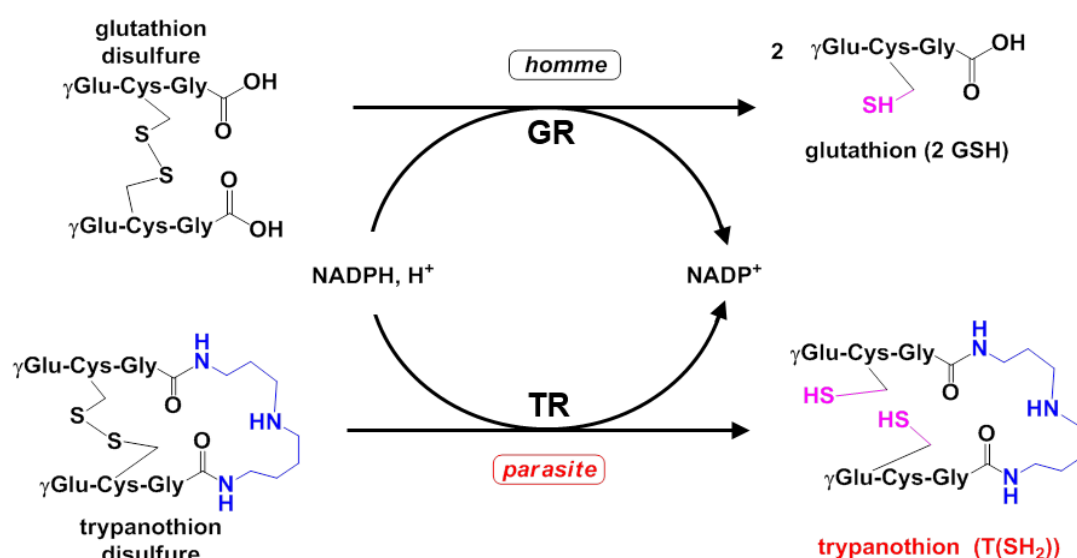


Schéma 1 | Systèmes enzymatiques responsables du maintien de l'équilibre redox chez l'homme et le parasite.

L'élucidation du mécanisme d'action des bases de Mannich insaturées a montré que ces molécules réagissent directement avec le trypanothion pour former un polymère mixte. La formation de ce polymère a pu être confirmée par ESI-MS et HPLC. D'autre part, la base de Mannich peut se dégrader pour former une divinylcétone qui, par alkylation de la cystéine 52 du site actif, inhibe de manière irréversible la trypanothion réductase.^{4,5} Ces deux mécanismes conduisent à la mort du parasite, probablement par une déplétion importante en thiols.

En dépit de très bonnes activités antiparasitaires, les propriétés pharmacocinétiques des bases de Mannich insaturées sont décevantes. Leur instabilité en solution notamment, s'est avérée totalement incompatible avec une administration en tant que médicament. Dès lors, il devenait nécessaire de trouver une structure proche, susceptible de présenter le même mode d'action sans avoir les désavantages des bases de Mannich insaturées.

La présence de deux sites électrophiles étant essentielle au mécanisme d'action, les recherches se sont portées vers la synthèse de molécules plus stables en solution, possédant deux centres électrophiles. Finalement, des diarylidèneacétones symétriques (DAA) diversement substituées (Figure 2) ont été

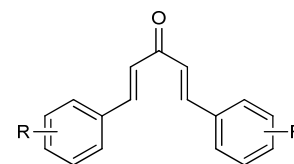


Figure 2 | Diarylidèneacétone

sélectionnées comme pharmacophore d'intérêt. Ainsi, une première bibliothèque d'une quinzaine de DAA a-t-elle été synthétisée par le Dr. Nicole Wenzel. Les résultats des tests biologiques étaient très satisfaisants du point de vue de l'activité antiparasitaire mais, comme on pouvait s'y attendre, ces molécules sont aussi toxiques vis-à-vis des cellules humaines.⁷ Afin de déterminer s'il était possible de dissocier l'activité antiparasitaire de la toxicité, le premier objectif du travail de thèse ici présenté fut de compléter la bibliothèque de DAA avec de nouvelles substitutions. En effet, la sélectivité de ces molécules vis-à-vis des parasites pourrait être améliorée par la reconnaissance spécifique de certaines substitutions par des transporteurs parasites. De même, du fait de la différence de réactivité existant entre le trypanothion et le glutathion, un ajustement fin de la réactivité des centres électrophiles pourrait permettre une meilleure sélectivité. Dans un second temps, nous avons donc cherché à modifier la répartition électronique des DAA synthétisées, modulant ainsi les propriétés d'électrophilie des centres réactifs.

Synthèse et évaluation de diarylidèneacétones à visée antiparasitaire

Synthèse de diarylidèneacétones *via* une réaction de Claisen-Schmidt

Les diarylidèneacétones sont usuellement synthétisées selon un protocole de condensation de Claisen-Schmidt en milieu acide ou basique concentré. Selon les substitutions aryliques, ces conditions doivent être adaptées. A partir des travaux précédemment publiés,^{7,8} nous sommes parvenus à mettre au point un protocole général, compatible avec une très large variété de substitutions (Schéma 2).

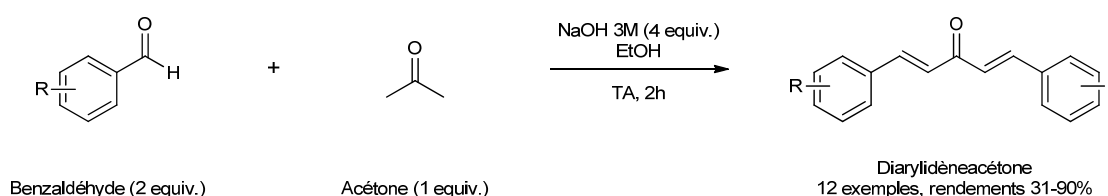


Schéma 2 | Synthèse de diarylidèneacétone symétriques *via* une réaction de Claisen-Schmidt.

Ces mêmes conditions ont pu être adaptées à la synthèse de molécule dissymétriques, à condition de procéder alors en deux étapes (Schéma 3).

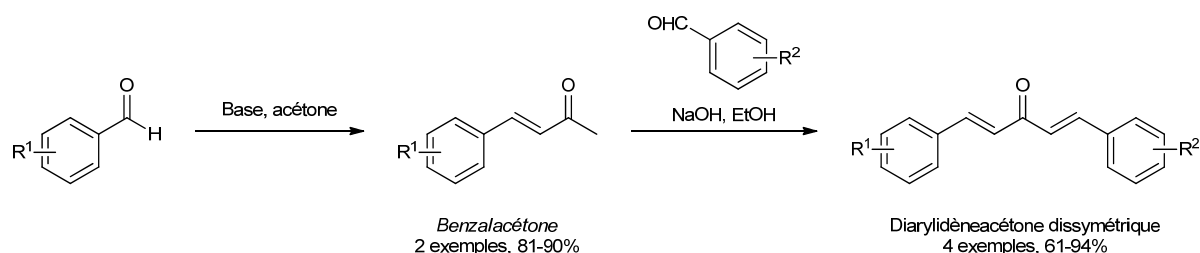


Schéma 3 | Synthèse de diarylidèneacétone dissymétriques via une réaction de Claisen-Schmidt.

Une première condensation de l'acétone (utilisée comme solvant de réaction), sur un benzaldéhyde conduit à la formation d'une benzalacétone intermédiaire. Celle-ci réagit ensuite avec un second benzaldéhyde en milieu basique pour donner la diarylidèneacétone dissymétrique attendue.

Quoique particulièrement simples à mettre en œuvre, ces protocoles souffrent de plusieurs limitations. Ils nécessitent des conditions drastiques (base concentrée ou chlorure d'hydrogène) qui ne sont pas forcément compatibles avec les substitutions nécessaires à l'étude de RSA. En particulier, ces protocoles ne permettent pas l'utilisation d'aldéhydes hétérocycliques azotés.^{9,10} Ces divers problèmes nous ont conduits à envisager une nouvelle voie d'accès aux DAA dissymétriques.

Synthèse de diarylidèneacétone via une réaction pallado-catalysée

Au cours du travail de thèse de N. Wenzel, une collaboration avec le Pr. Thomas Müller, (université de Düsseldorf), avait permis d'essayer la méthodologie intitulée *Coupling-Isomerization Reaction* (CIR) pour la préparation et l'évaluation de divinylcétone. Initialement dédiée à la synthèse de chalcones, cette procédure repose sur un couplage de Sonogashira entre un halogénoaryle et un alcool propargylique, suivie d'une isomérisation *in situ* en conditions basiques (Schéma 4).^{11,12} Les essais ont abouti à l'abandon des divinylcétone ($\text{R} = \text{CH}=\text{CH}_2$), trop réactives, et à celui des alcools propargyliques intermédiaires, trop toxiques.

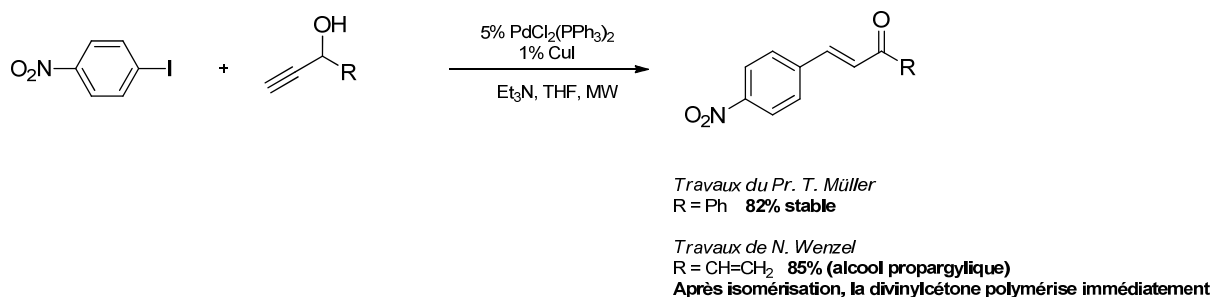


Schéma 4 | Synthèse de chalcones et de divinylcétone via le protocole de Coupling-Isomerization Reaction.

Considérant la similarité structurale existant entre les chalcones et les diarylidèneacétone, nous avons décidé d'adapter la procédure CIR à la synthèse de DAA

dissymétriques. Ce projet a fait l'objet d'un stage de recherche de quatre mois à l'Université de Düsseldorf.

Les premières tentatives de couplage ont permis d'obtenir la DAA **3a** avec un rendement moyen de 40 % (Schéma 5).

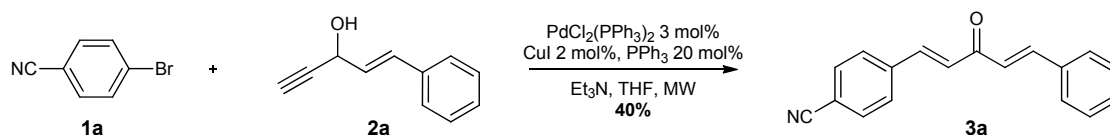


Schéma 5 | Premiers essais de synthèse.

Encouragés par ces résultats, nous avons décidé d'optimiser les conditions opératoires. Deux types de facteurs ont été étudiés :

- Les facteurs discrets : type de solvant, de base et de catalyseur,
- et les facteurs continus : température, concentration et durée de réaction.

Cette optimisation s'est faite en utilisant la méthodologie des plans d'expériences et notamment un plan de type Box-Behnken.¹³

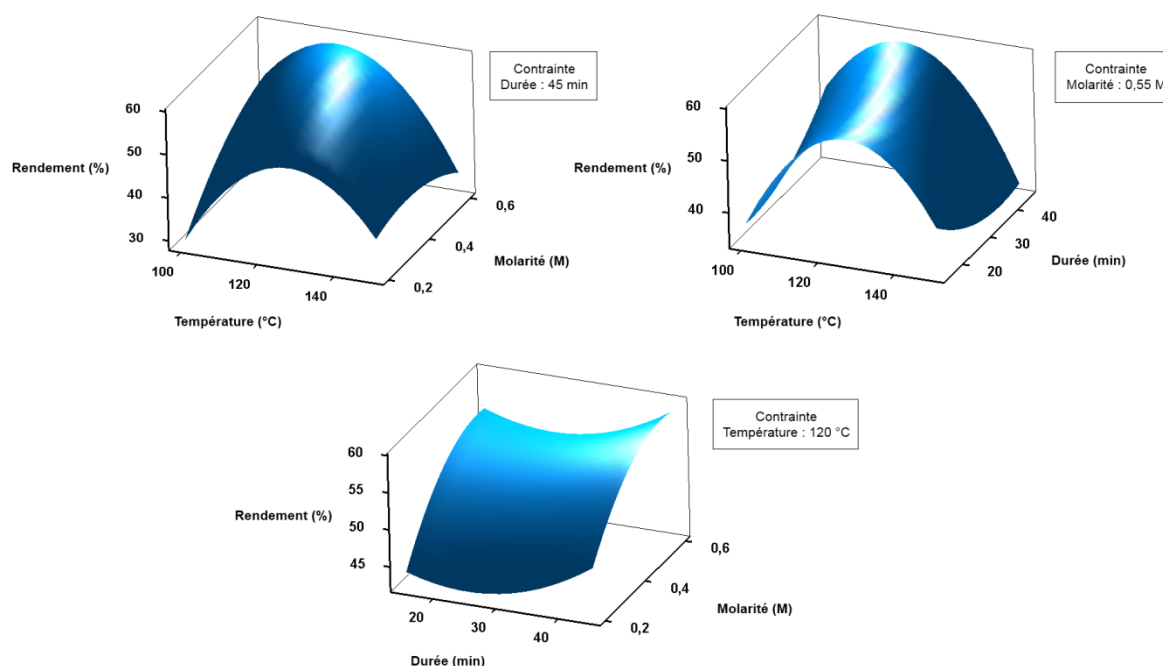


Figure 3 | Surfaces de réponse obtenues après analyse statistique des résultats du plan de Box-Behnken.

Le tracé des surfaces de réponse (Figure 3) correspondant à la représentation tridimensionnelle du système, ainsi qu'une régression multivariée, ont permis de déterminer les conditions opératoires optimales, résumées sur le Schéma 6.

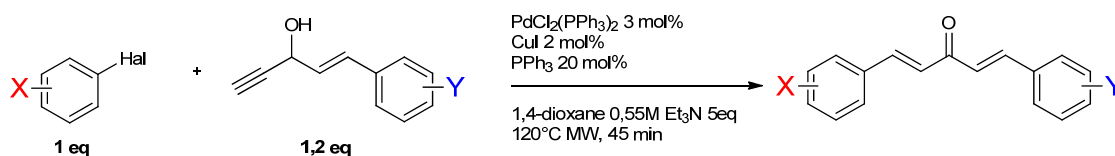


Schéma 6 | Conditions optimisées pour la synthèse de diarylidèneacétone dissymétriques par Coupling-Isomerization Reaction.

Afin de vérifier la polyvalence de cette réaction, nous l'avons testée sur divers substrats, et notamment ceux qui posaient problème lors des condensations de Claisen-Schmidt. La Figure 4 présente ces diverses structures. Les halogénoaryles fluorés (**3b** et **3i**) donnent de bons rendements, tout comme les hétéroaromatiques, qu'ils soient de type pyridine, pyrimidine ou encore thiazole (**3f-h** et **3j-l**). En revanche, les halogénoaryles riches en électrons ou neutres ne réagissent pas dans ces conditions (**3c-e**).

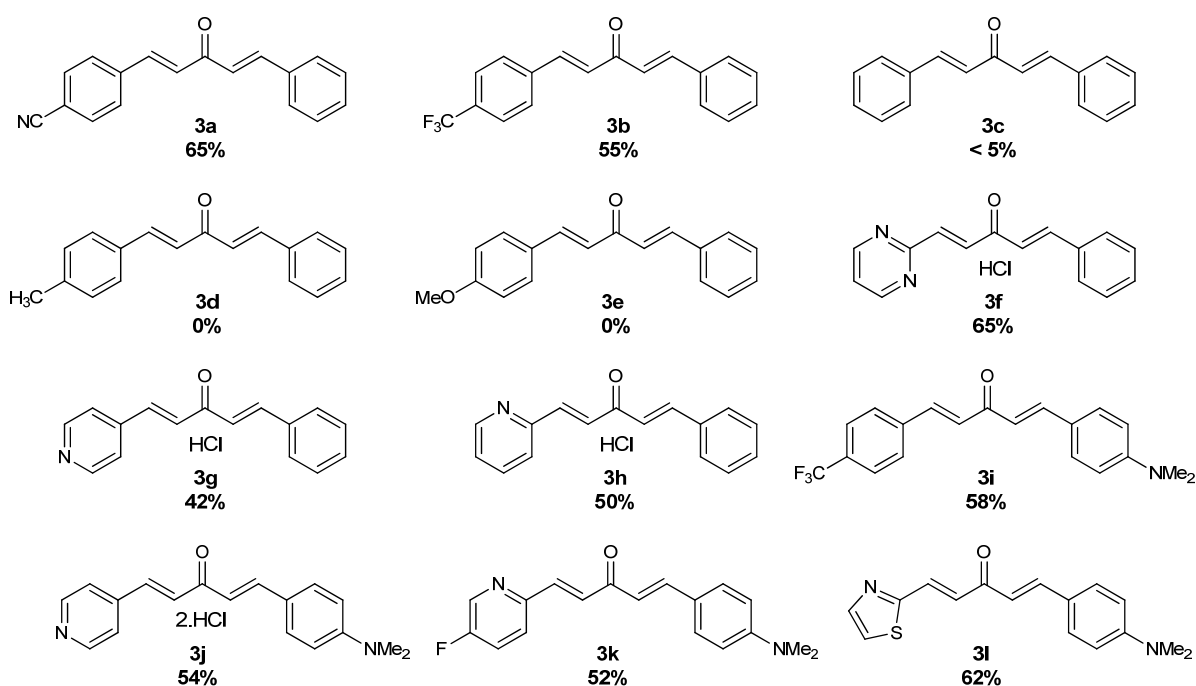


Figure 4 | Généralisation des conditions optimisées.

Confirmant les résultats obtenus pour la synthèse des chalcones, nous avons pu montrer que la densité électronique de l'alcool propargylique insaturé n'influence pas le rendement ; il est ainsi possible d'utiliser des alcools portant des groupes donneurs d'électrons (**3i-l**). Enfin, nous avons démontré qu'il était possible d'utiliser cette réaction à plus grande échelle. Ainsi avons-nous pu synthétiser le produit **3a**, avec un rendement constant de 68 %, sur une échelle de trois grammes, limite imposée par la taille des réacteurs disponibles pour notre micro-onde de laboratoire.

Evaluation des (hétéro)diarylidèneacétones synthétisées

L'ensemble des molécules synthétisées –symétriques et dissymétriques– a été testé *in vitro* sur les parasites en cultures : *Trypanosoma brucei* (responsable de la maladie du sommeil), *Trypanosoma cruzi* (responsable de la maladie de Chagas), *Leishmania infantum* et *Leishmania donovani* (responsables des leishmanioses). La cytotoxicité est aussi évaluée sur des cellules humaines de lignée hMRC-5 et des macrophages de souris. Ces tests sont réalisés dans le cadre de collaborations avec l'équipe du Pr. Philippe Loiseau de la Faculté de pharmacie de Chatenay-Malabry (Université Paris Sud, BioCIS, UMR8076 CNRS) ainsi qu'avec le groupe du Pr. Louis Maes de l'Université d'Anvers.

De manière générale, ces molécules se sont avérées très actives sur les parasites, présentant des valeurs d'IC₅₀ inférieures à 1 µM pour les substitutions de type hétérocycles azotés (**3f-h**) et entre 0,25 µM et 15 µM pour les substitutions fluorées et nitriles (**3a-b** et **3i**). Malheureusement, cette activité s'accompagne d'une importante cytotoxicité sur cellules humaines. Ainsi les substitutions de type hétérocycles azotés (**3f-h**) ont-elles des IC₅₀(hMRC-5) de l'ordre de 1 µM qui leur confère une sélectivité pour ainsi dire nulle. Les diarylidèneacétones symétriques substituées par des groupements phenyl, *p*-trifluorométhylphenyl, *p*-benzonitrile ou encore *p*-aniline substitué présentent des indices de sélectivité légèrement supérieurs (de 50 à 130) mais qui s'accompagne pour certaines d'une toxicité importante sur les macrophages de souris.

Après une analyse fine des résultats, il paraît clair qu'il est difficile de dissocier l'activité antiparasitaire de la cytotoxicité sur cellules humaines pour cette série diarylidèneacétone. Qu'elles soient symétriques, ou dissymétriques, avec une répartition homogène ou délocalisée des électrons, la plupart des diarylidèneacétones testées sont insuffisamment sélectives, tuant aussi bien les parasites que les cellules de l'hôte. Forts de cette expérience, nous avons poursuivi nos recherches par la conception de molécules prodrogues et de leurs potentiels métabolites *S*-oxydes.

Stratégie prodrogue et synthèse diastéréosélective de 2,6-diaryl-4H-tetrahydro-thiopyran-4-ones

Principes de la stratégie prodrogue

Comme nous venons de le voir, le principal problème de la série diarylidèneacétone est sa toxicité intrinsèque sur les cellules de l'hôte. Si l'on se reporte aux modes d'actions démontrés pour les bases de Mannich, et en faisant l'hypothèse que les DAA agissent de manière similaire, il apparaît que les centres électrophiles jouent un rôle crucial. Or, s'ils peuvent réagir avec le trypanothion parasitaire, ces centres électrophiles réagissent aussi avec le glutathion humain, provoquant une cytotoxicité sur cellule humaine importante. La formation de bis(adduits) de glutathion a été prouvée par HPLC et spectrométrie de masse.⁷

Dès lors, il est envisageable de masquer temporairement ces centres électrophiles pour les rendre moins réactifs et, une fois la molécule internalisée dans le parasite, de régénérer la diarylidèneacétone et restaurer l'activité antiparasitaire (Schéma 7).

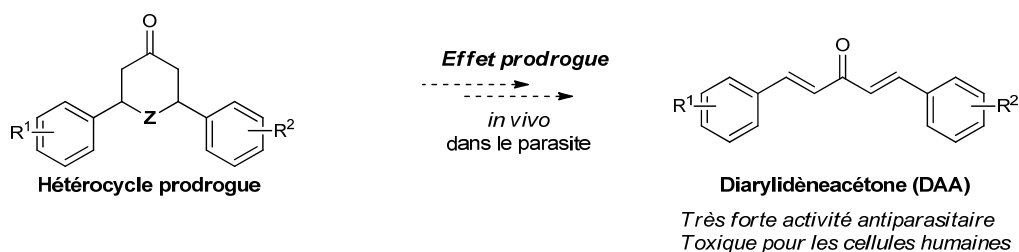


Schéma 7 | Principe illustré de la stratégie prodrogue

La conception d'une prodrogue efficace est déterminée par le choix de la méthode de protection temporaire des centres électrophiles. La molécule doit être assez inerte pour ne pas réagir avec les systèmes biologiques de l'hôte, mais doit pouvoir régénérer une espèce réactive dans les conditions métaboliques spécifiques du parasite (acides, oxydantes etc.).

Les sulfures, sulfones et sulfoxydes sont connus en chimie pour être susceptibles de subir une β -élimination amenant à la formation d'une double liaison.¹⁴ Trois mécanismes sont possibles : péricyclique,¹⁵ ionique,¹⁶ ou radicalaire.¹⁷ Un hétérocycle de type 2,6-diaryl-4H-tetrahydrothiopyran-4-one (2,6-DA-4-THTP) est donc une cible intéressante pour notre stratégie prodrogue (Figure 5).

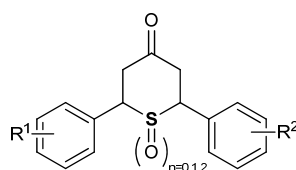


Figure 5 | Structure du noyau 2,6-diaryl-4H-tetrahydrothiopyran-4-one

Les réactions de β -élimination étant d'autant plus faciles que le soufre est oxydé, nous avons choisi de synthétiser et tester les sulfoxides et sulfones en plus des sulfures.

Etude du motif 2,6-diaryl-4H-tetrahydrothiopyran-4-one

Quoique relativement simple en apparence, le noyau 2,6-DA-4-THTP possède deux carbones asymétriques qui rendent sa synthèse et son étude spectroscopique particulièrement intéressantes. Ainsi, si l'on considère une même substitution sur les aromatiques de part et d'autre du cycle, on dénombre deux diastéréoisomères, le *cis* (mésó) et le (\pm)-*trans* (potentiellement optiquement actif) ; ces deux isomères étant par ailleurs soumis aux équilibres conformationnels (Schéma 8). Si l'on considère l'arrangement des substituant aryliques, il apparaît que l'isomère *cis* est le plus stable thermodynamiquement (deux aryles en positions équatoriales). L'isomère (\pm)-*trans* quant à lui serait donc l'isomère cinétique, ce que des travaux antérieurs tendent à confirmer.¹⁸

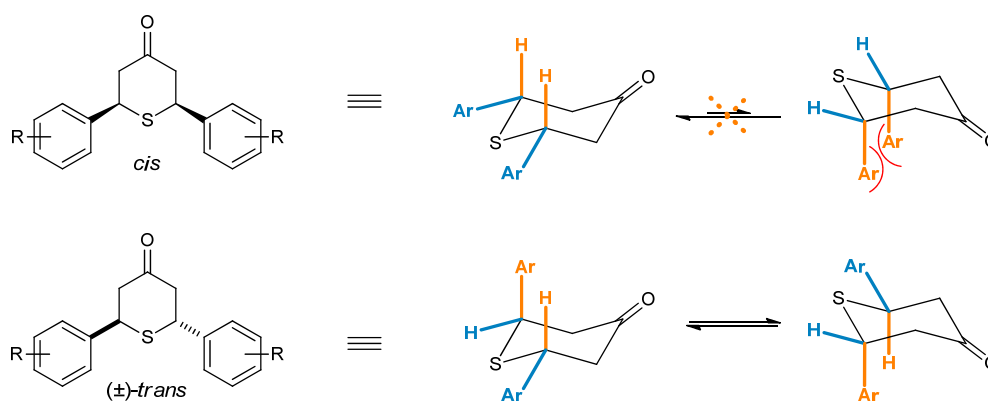


Schéma 8 | Stéréochimies et conformations du noyau 2,6-diaryl-4H-tetrahydrothiopyran-4-one

Une étude de relation structure-activité rigoureuse nécessite une connaissance parfaite et un contrôle total de la stéréochimie des molécules testées. Malheureusement, il existe peu d'exemples dans la littérature décrivant précisément la synthèse de 2,6-diaryl-4H-tetrahydrothiopyran-4-ones. Au plus une dizaine d'articles, la plupart assez anciens, proposent un protocole de synthèse utilisant l'hydrogène sulfuré, gaz hautement toxique.¹⁹⁻²¹ Par ailleurs, la plupart de ces exemples discutent peu, voire ignorent complètement, l'aspect stéréochimique de la synthèse.

Considérant le peu de données disponibles et la dangerosité des procédures proposées, nous avons décidé de travailler à l'élaboration de nouveaux protocoles diastéréosélectifs et plus sûrs.

Conception d'une nouvelle voie de synthèse diastéréosélective des 2,6-diaryl-4H-tetrahydrothiopyran-4-ones

Nous nous sommes intéressés dans un premier temps à la détermination des critères essentiels à la sécurité, à la chimiosélectivité, et à la diastéréosélectivité de la réaction.

L'utilisation du sulfure d'hydrogène étant un problème majeur, tant en terme de sécurité que de contrôle de la stœchiométrie de la réaction, nous avons en premier lieu remplacé l'hydrogène sulfuré par sa base conjuguée, l'hydrogénosulfure de sodium ($\text{NaHS}\cdot x\text{H}_2\text{O}$). Ceci fait, nous avons étudié l'effet de la température, du solvant et d'éventuelles bases utilisées comme additifs de réaction. *In fine*, nous sommes parvenus à établir deux procédures préliminaires distinctes permettant la synthèse sélective de l'isomère *cis* ou du (\pm)-*trans* (Schéma 9).

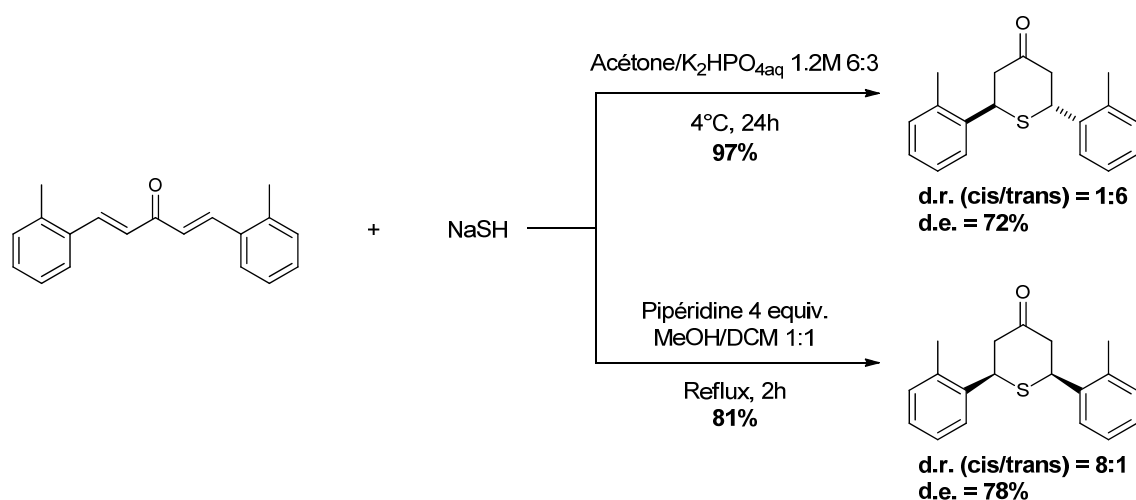


Schéma 9 | Résultats préliminaires pour la synthèse diastéréosélective des 2,6-diaryl-4H-tetrahydrothiopyranones

Ces premiers résultats nous ont, en outre, permis d'établir des critères spectroscopiques fiables pour la détermination de la configuration de chaque isomère. En effet, les données spectroscopiques n'étant pas précises et/ou fiables dans la littérature, nous avons dû acquérir une certaine expertise dans la détermination de la stéréochimie de ce type de cycle. D'abord pressenties par des expériences de RMN, utilisant notamment les constantes de système ABX ou encore le γ -syn effect,²² les différentes stéréochimies ont été confirmées par diffraction des rayons X (Figure 6).

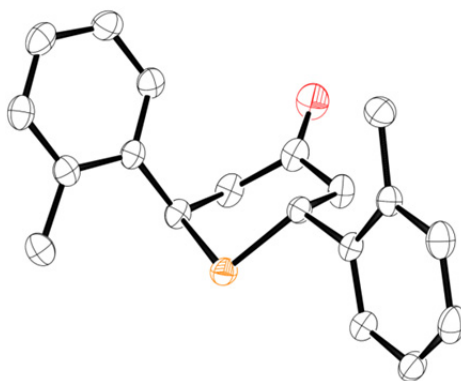


Figure 6 | Structure aux rayons X de la (±)-*trans* 2,6-di-*o*-tolyl-4H-tetrahydrothiopyran-4-one.

A partir de ces résultats préliminaires, nous avons entrepris l'optimisation des deux synthèses diastéréosélectives.

Optimisation des synthèses diastéréosélectives des 2,6-diaryl-4H-tetrahydrothiopyran-4-ones

Synthèse diastéréosélective de l'isomère (±)-*trans*

Peu de modifications se sont avérées nécessaires pour l'optimisation du rendement et de l'excès diastéréoisomérique. Parmi les différents solvants testés, le tétrahydrofurane s'est clairement démarqué, permettant une augmentation significative de l'excès diastéréoisomérique, passant de 72 % à 92 %. Contrairement à ce qui était mentionné dans la littérature, nous n'avons pas pu démontrer d'effet significatif de la quantité de base utilisée. *In fine*, nous sommes parvenus à déterminer des conditions opératoires optimales (Schéma 10).

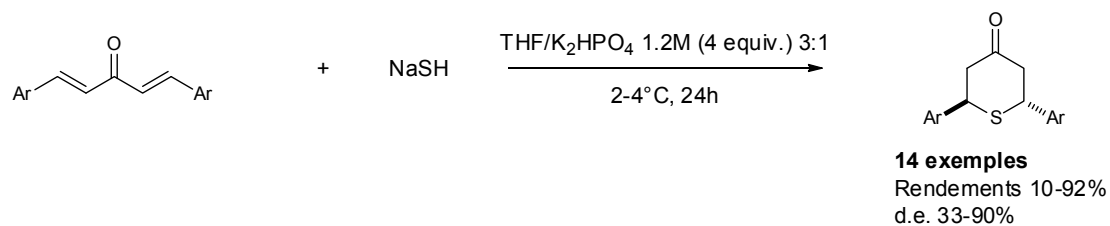


Schéma 10 | Conditions opératoires optimisées pour la synthèse diastéréosélectives de l'isomère (±)-*trans*

Ces conditions ont été utilisées pour la synthèse d'une quinzaine de molécules portant des substitutions très diverses, et ce avec de très bons rendements et des excès diastéréoisomériques satisfaisants.

Synthèse diastéréosélective de l'isomère *cis* en conditions purement organiques

A partir des premiers essais de synthèse, effectués en milieu purement organique, nous avons étudié l'influence du solvant et de la base. Dans ce protocole, le NaSH a peu de chance d'être protoné sous la forme d' H_2S ; dès lors l'utilisation d'une base n'apparaissait plus indispensable. De fait, nous avons pu prouver que, en milieu purement méthanolique et sans base, de meilleurs résultats étaient obtenus (Schéma 11).

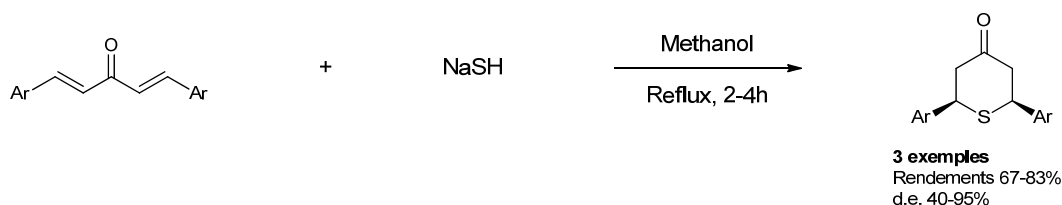


Schéma 11 | Synthèse diastéréosélective de l'isomère *cis* en milieu purement organique.

Malheureusement ces conditions se sont révélées difficiles à généraliser, notamment avec des substituants aryliques sensibles à la substitution nucléophile. Nous nous sommes donc consacrés à l'élaboration d'une nouvelle stratégie plus douce et chimiosélective.

Synthèse diastéréosélective de l'isomère *cis* par catalyse de transfert de phases

Partant de l'hypothèse que le problème majeur du protocole précédent était la présence massive d'anions hydrosulfure très réactif dans le milieu, nous avons cherché à apporter le réactif soufré par petites quantités. Considérant la nature antinomie des deux réactifs impliqués –un réactif inorganique, le NaSH, et un réactif organique, la DAA– il nous est apparu qu'un protocole basé sur une catalyse de transfert de phase pourrait avantageusement solutionner les problèmes rencontrés.

Nous avons donc conçu et optimisé une nouvelle méthodologie de synthèse utilisant l'Aliquat® 336 comme catalyseur de transfert de phase. Les meilleurs résultats ont été obtenus dans un mélange diphasique de méthyl *tert*-butyl ether et d'une solution aqueuse de phosphate de potassium diphasique 1,2 M, chauffé à 55 °C pendant une journée complète (Schéma 12).

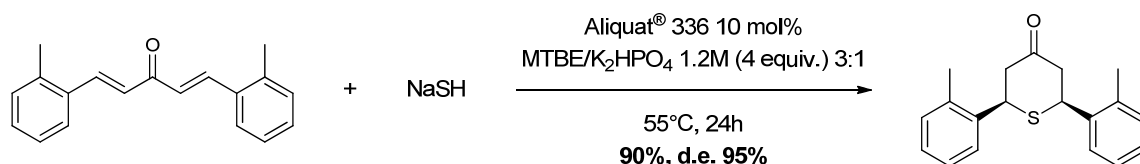


Schéma 12 | Synthèse diastéréosélective de l'isomère *cis* par catalyse de transfert de phase.

Une étude cinétique approfondie de ce nouveau protocole a démontré qu'en réalité l'isomère *cis* n'est pas obtenu directement dans la synthèse ; l'isomère (\pm)-*trans* (cinétique) est d'abord synthétisé et s'isomérise ensuite lentement en isomère *cis* (thermodynamique) (Figure

7). Le temps de réaction est donc une donnée importante pour l'optimisation de l'excès diastéréoisomérique.

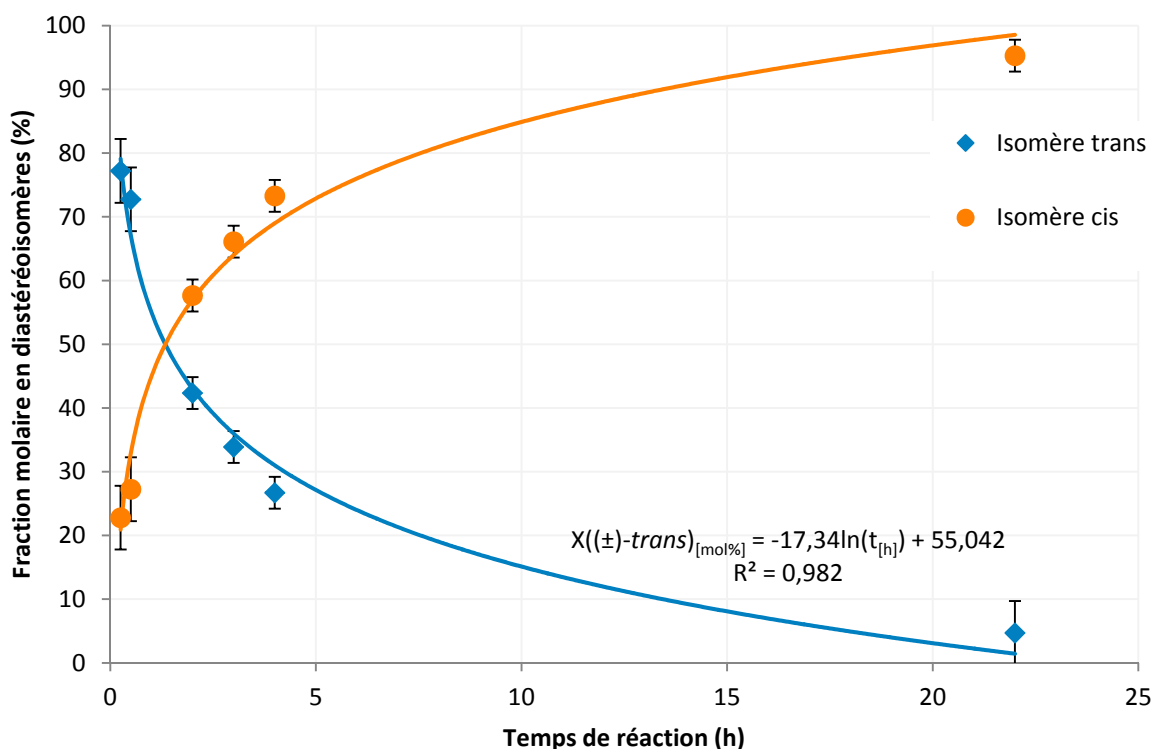


Figure 7 | Suivi cinétique de la fraction molaire en diastereoisomers (\pm)-*trans* et *cis*

Ces résultats, et notamment l'étude cinétique, ayant été obtenus dans les tous derniers temps de ce doctorat, nous n'avons pu être en mesure d'effectuer la généralisation de ce nouveau protocole sur une durée de réaction de 24 heures. En revanche, nous avons pu obtenir des résultats encourageants après 9 heures de réaction sur six substitutions différentes qui n'avaient pu être synthétisées avec le protocole précédent (rendements de 75 à 93 % et d.e. de 40 à 70 %). La répétition de ces mêmes réactions sur 24 heures ou plus permettra sans aucun doute d'améliorer les excès diastéréoisomériques.

Synthèses des S-oxydes associés

Les sulfures étant synthétisés, nous nous sommes ensuite intéressés à l'obtention des sulfoxydes et sulfones associés. En dépit de nombreuses tentatives, les protocoles "classiques" d'oxydation du sulfure (peroxydes, peracides, procédure de Kagan, Kagan modifié etc...)²³⁻²⁵ n'ont pas donné de résultats probants. Ce n'est qu'avec l'utilisation de l'oxaziridine de Davis que les sulfoxydes attendus ont pu être obtenus avec d'excellents rendements (Schéma 13).²⁶

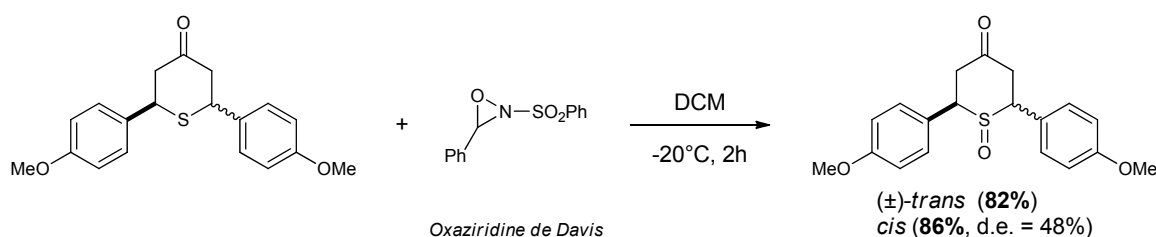


Schéma 13 | Synthèse des sulfoxyde avec l'oxaziridine de Davis.

De manière surprenante, il nous a été difficile d'obtenir les sulfones directement par suroxydation du sulfure. En revanche, nous avons pu les synthétiser avec des rendements quasi-quantitatifs par oxydation lente du sulfoxyde avec l'acide *m*-chloroperbenzoïque (Schéma 14).

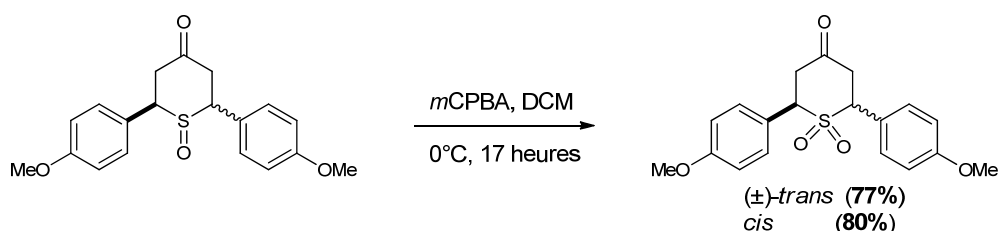


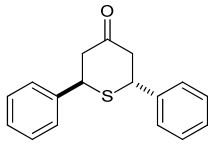
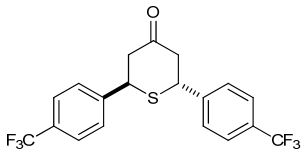
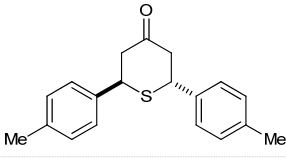
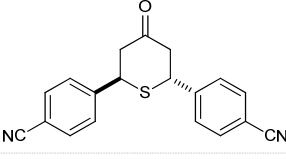
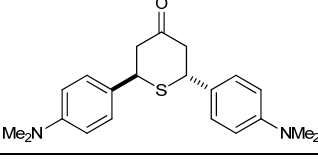
Schéma 14 | Synthèse des sulfones par oxydation lente du sulfoxyde.

Deux séries chimiques complètes (sulfoxydes et sulfones) portant les substitutions *p*-méthoxy et *o*-pyridine, ont ainsi été synthétisées. Ces molécules, ainsi que les autres sulfures précédemment synthétisés, ont été envoyées en test *in vitro*.

Activités antiparasitaires des 2,6-diaryl-4H-tetrahydrothiopyran-4-ones et oxydes associés

Les 2,6-diaryl-4H-tetrahydrothiopyran-4-ones synthétisées ont été soumises aux mêmes tests biologiques, effectués dans les mêmes conditions et par les mêmes équipes que ceux que nous avons précédemment étudiés. D'une manière générale, les sulfures se sont révélés être bien moins toxiques que les diarylidèneacétones parentes. En revanche, cette réduction de la toxicité s'accompagne, pour la plupart des molécules testées, d'une réduction de l'activité antiparasitaire. Les cinq substitutions les plus actives dans cette série sont présentées en table I.

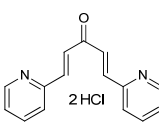
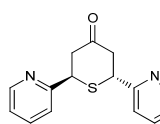
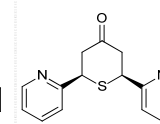
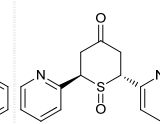
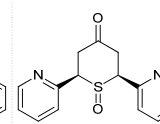
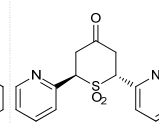
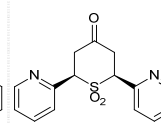
Table I | Activités antiparasitaires et toxicité des cinq 2,6-diaryl-4H-tetrahydrothiopyran-4-ones les plus actives.

Entrée	Structure	<i>In vitro</i> – IC ₅₀ (μM)				Tox.
		<i>hMRC-5</i>	<i>T. cruzi</i>	<i>T. brucei</i>	<i>L. infantum</i>	
1		27.57	4.57	≤ 0.25	8.11	T2
2		10.20	2.49	0.50	32.46	T1
3		24.25	3.70	0.77	≥ 64	
4		≥ 64	42.47	1.23	≥ 64	
5		4.96	2.5	1.47	43.07	

De manière très intéressante, nous pouvons retrouver dans cette série 2,6-DA-4-THTP les substitutions qui avaient déjà été déterminées comme étant les plus actives dans la série des diarylidèneacétones. Comme nous l'espérons, il semblerait donc qu'une corrélation puisse s'établir entre les activités des deux séries.

Si l'on s'intéresse aux effets de la stéréochimie et de l'oxydation du soufre, les résultats obtenus sont intéressants à plus d'un titre ; nous nous focaliserons ici sur ceux de la série *o*-pyridine (table II).

Table II : Résultats des tests *in vitro* pour les 4H-thiopyran-4-ones et oxydes associés de la série *o*-pyridine

IC ₅₀ (μM)							
<i>hMRC-5</i>	1,91	> 64	> 64	8,00	8,06	7,86	7,47
<i>T. brucei</i>	0,03	26,1	29,1	0,13	0,13	0,51	0,13

Du point de vue de la stéréochimie, la synthèse diastéréosélective des 2,6-diaryl-4H-tetrahydrothiopyran-4-ones ne semble pas cruciale pour l'activité biologique. À degré

d'oxydation constant, les isomères *cis* et (\pm)-*trans* ont des activités biologiques comparables. Comme nous pouvions nous y attendre, le degré d'oxydation du soufre a, lui, une influence considérable. L'oxydation du soufre en sulfoxyde ou sulfone permet de retrouver l'activité initiale tout en conservant une $IC_{50}(hMRC-5)$ plus élevée que celle de la DAA parente (Table II).

Quoiqu'encore relativement modestes, ces résultats sont extrêmement encourageants dans le sens où la cyclisation en 2,6-DA-4-THTP permet de diminuer de façon significative la toxicité des molécules, tandis que l'oxydation du soufre permet de retrouver une certaine activité antiparasitaire.

Conclusion

Du point de vue de la synthèse, nous retiendrons la mise au point de nouvelles méthodologies, spécifiques aux structures et substitutions désirées. Ainsi, le nouveau protocole de synthèse des diarylidèneacétones dissymétriques par voie palladocatalysée permet-il l'accès à des structures jusqu'à présent inconnues. Structures qui, outre l'aspect médicinal, peuvent être intéressantes pour d'autres applications, comme par exemple en catalyse ou en synthèse d'hétérocycles par réaction de Nazarov. De même, le travail effectué sur la synthèse des 2,6-diaryl-4*H*-tetrahydrothiopyran-4-ones et des oxydes associés, a permis de mettre au point des protocoles fiables, sûrs et diastéréosélectifs. L'expérience acquise sur les propriétés spectroscopiques de ces hétérocycles n'est pas non plus à négliger tant les données sont peu nombreuses dans la littérature.

Si l'on considère les activités antiparasitaires des molécules synthétisées, deux constats s'imposent. Les diarylidèneacétones, qu'elles soient symétriques ou dissymétriques présentent d'excellentes activités ; nous avons cependant prouvé que cette activité semble être indissociablement liée à une très forte toxicité sur les cellules humaines. Cependant, ce travail nous a permis d'identifier les substitutions les plus actives. Deuxième constat, la série des 2,6-diaryl-4*H*-tetrahydrothiopyran-4-ones est particulièrement prometteuse ; permettant une réduction remarquable de la toxicité tout en conservant une activité puissante contre les parasites kinétoplastidés, cette famille de molécules répond à nos critères de développement.

Considérant le nombre encore réduit de molécules testées dans cette nouvelle série, il est, pour l'instant, encore difficile de conclure sur son réel potentiel en termes de candidat-médicaments. Cependant, l'utilisation des nouveaux protocoles de synthèse mis au point au cours de ce doctorat devrait permettre rapidement la constitution d'une bibliothèque étendue de molécules, ouvrant ainsi la voie à des études de relation structure-activité, de pharmacocinétique et de métabolisme plus poussées.

Références bibliographiques du résumé

- (1) Guddat, L. Editorial [Hot Topic: Drug Targets for the Treatment of Protozoan Parasitic Diseases (Guest Editor: Luke Guddat)]. *Current Topics in Medicinal Chemistry* **2011**, *11*, 2010–2011.
- (2) Singer, P. A.; Berndtson, K.; Tracy, C. S.; Cohen, E. R. M.; Masum, H.; Lavery, J. V.; Daar, A. S. A tough transition. *Nature* **2007**, *449*, 160–163.
- (3) Cavalli, A.; Bolognesi, M. L. Neglected Tropical Diseases: Multi-Target-Directed Ligands in the Search for Novel Lead Candidates against Trypanosoma and Leishmania. *Journal of Medicinal Chemistry* **2009**, *52*, 7339–7359.
- (4) Davioud-Charvet, E.; McLeish, M. J.; Veine, D. M.; Giegel, D.; Arscott, L. D.; Andricopulo, A. D.; Becker, K.; Müller, S.; Schirmer, R. H.; Williams, C. H.; Kenyon, G. L. Mechanism-Based Inactivation of Thioredoxin Reductase from Plasmodium falciparum by Mannich Bases. Implication for Cytotoxicity. *Biochemistry* **2003**, *42*, 13319–13330.
- (5) Lee, B.; Bauer, H.; Melchers, J.; Ruppert, T.; Rattray, L.; Yardley, V.; Davioud-Charvet, E.; Krauth-Siegel, R. L. Irreversible Inactivation of Trypanothione Reductase by Unsaturated Mannich Bases: A Divinyl Ketone as Key Intermediate. *Journal of Medicinal Chemistry* **2005**, *48*, 7400–7410.
- (6) Wenzel, I. N.; Wong, P. E.; Maes, L.; Müller, T. J. J.; Krauth-Siegel, R. L.; Barrett, M. P.; Davioud-Charvet, E. Unsaturated Mannich Bases Active Against Multidrug-Resistant Trypanosoma brucei Strains. *ChemMedChem* **2009**, *4*, 339–351.
- (7) Wenzel, I. N. Synthesis and Mechanism of Antiparasitic Mannich Base Derivatives Affecting the Redox Equilibrium of Trypanosomes and Malaria Parasites, Ruprecht-Karls-Universität Heidelberg: Heidelberg, 2009.
- (8) Conard, C. R.; Dolliver, M. A. Dibenzalacetone. *Organic Syntheses* **1932**, *12*, 22.
- (9) Marvel, C. S.; Stille, J. K. Preparation of the Pyridalacetones and the Inductive Effect of Nitrogen on the Dehydration of the Intermediate Aldols. *Journal of Organic Chemistry* **1957**, *22*, 1451–1457.
- (10) Sehna, P.; Taghzouti, H.; Fairlamb, I. J. S.; Jutand, A.; Lee, A. F.; Whitwood, A. C. Heteroaromatic Analogues of Dibenzylideneacetone (dba) and Pd₂(het-dba)₃ Complexes: Effect of a Thienyl Moiety on the Reactivity of Pd(η²-th[n]-dba)(PPh₃)₂/Pd(PPh₃)₂ (n=1 or 2) and Pd(η²-th₂-dba)(dppe)/Pd(dppe) in Oxidative Addition Reactions with Iodobenzene. *Organometallics* **2009**, *28*, 824–829.
- (11) Braun, R. U.; Ansoorge, M.; Müller, T. J. J. Coupling–Isomerization Synthesis of Chalcones. *Chemistry - A European Journal* **2006**, *12*, 9081–9094.
- (12) Schramm (née Dediu), O. G.; Müller, T. J. J. Microwave-Accelerated Coupling-Isomerization Reaction (MACIR) – A General Coupling-Isomerization Synthesis of 1,3-Diarylprop-2-en-1-ones. *Advanced Synthesis & Catalysis* **2006**, *348*, 2565–2570.
- (13) Box, G. E. P.; Behnken, D. W. Some New Three Level Designs for the Study of Quantitative Variables. *Technometrics* **1960**, *2*, 455–475.
- (14) Trost, B. M. α-Sulfonylated carbonyl compounds in organic synthesis. *Chemical Reviews* **1978**, *78*, 363–382.
- (15) Cubbage, J. W.; Guo, Y.; McCulla, R. D.; Jenks, W. S. Thermolysis of Alkyl Sulfoxides and Derivatives: A Comparison of Experiment and Theory. *The Journal of Organic Chemistry* **2001**, *66*, 8722–8736.
- (16) Bordwell, F. G.; Happer, D. A. R.; Cooper, G. D. Concerning driving forces for β-elimination reactions. *Tetrahedron Letters* **1972**, *13*, 2759–2762.
- (17) Cubbage, J. W.; Vos, B. W.; Jenks, W. S. Ei Elimination: An Unprecedented Facet of Sulfone Chemistry. *Journal of the American Chemical Society* **2000**, *122*, 4968–4971.
- (18) Baxter, C. A. R.; Whiting, D. A. Stereochemistry and structure in the tetrahydro-1-thio-4-pyrone and tetrahydro-4-pyrone series. *Journal of the Chemical Society C: Organic* **1968**, 1174.
- (19) Rule, N. G.; Detty, M. R.; Kaeding, J. E.; Sinicropi, J. A. Syntheses of 4H-Thiopyran-4-one 1,1-Dioxides as Precursors to Sulfone-Containing Analogs of Tetracyanoquinodimethane. *The Journal of Organic Chemistry* **1995**, *60*, 1665–1673.
- (20) Chaykovsky, M.; Lin, M.; Rosowsky, A.; Modest, E. J. 2,4-Diaminothieno[2,3-d]pyrimidines as antifolates and antimalarials. 2. Synthesis of 2,4-diaminopyrido[4',3':4,5]thieno[2,3-d]pyrimidines and 2,4-diamino-8H-thiopyrano[4',3':4,5]thieno[2,3-d]pyrimidines. *Journal of Medicinal Chemistry* **1973**, *16*, 188–191.
- (21) Parthiban, P.; Aridoss, G.; Rathika, P.; Ramkumar, V.; Kabilan, S. Synthesis, spectral, crystal and antimicrobial studies of biologically potent oxime ethers of nitrogen, oxygen and sulfur heterocycles. *Bioorganic & Medicinal Chemistry Letters* **2009**, *19*, 2981–2985.
- (22) Kalinowski, H.-O.; Berger, S.; Braun, S. *Carbon-13 NMR spectroscopy*; Wiley: Chichester; New York, 1988.
- (23) Wojaczynska, E.; Wojaczynski, J. Enantioselective Synthesis of Sulfoxides: 2000–2009. *Chemical Reviews* **2010**, *110*, 4303–4356.
- (24) Brunel, J. M.; Kagan, H. B. Catalytic Asymmetric Oxidation of Sulfides With High Enantioselectivities. *Synlett* **1996**, 1996, 404–406.
- (25) Song, Z. J. Asymmetric Catalysis Special Feature Part II: An efficient asymmetric synthesis of an estrogen receptor modulator by sulfoxide-directed borane reduction. *Proceedings of the National Academy of Sciences* **2004**, *101*, 5776–5781.
- (26) Davis, F. A.; Lal, S. G.; Durst, H. D. Chemistry of oxaziridines. 10. Selective catalytic oxidation of sulfides to sulfoxides using N-sulfonyloxaziridines. *The Journal of Organic Chemistry* **1988**, *53*, 5004–5007.

Communications et publications

Communications orales

1. *Découverte et optimisation d'une nouvelle voie palladocatalysée pour la synthèse de diarylidèneacétones substituées.* T. Gendron, T. Müller, E. Davioud-Charvet
Journée des Doctorants en Chimie 2010, Strasbourg, 10 novembre **2010**
2. *Discovery and optimization of a new palladium-catalyzed methodology for the synthesis of substituted dibenzylideneacetones.* T. Gendron, T. Müller, E. Davioud-Charvet
New Trends in Infectious Disease Research, Ellwangen, Allemagne, 22-24 novembre **2010**
3. *Synthèse diastéréosélective de tetrahydrothiopyran-4-ones comme prodrogues de dibenzylidènes acétones à activité antiparasitaire.* T. Gendron, D. A. Lanfranchi, Elisabeth Davioud-Charvet
SCF Grand Est 7, Reims, 29-30 mars **2012**

Communications par affiche

1. *Synthesis of starting-blocks for medicinal chemistry of antiparasitics.* D. A. Lanfranchi, L. Johann, A. Novodomská, T. Gendron, G. Hanquet, F. Leroux, E. Davioud-Charvet
New Trends in Infectious Disease Research, Heidelberg, Allemagne, 19-21 novembre **2009**
2. *Development of a new synthesis of dibenzylideneacetones and evaluation of their antiparasitic activities.* T. Gendron, E. Davioud-Charvet, T. Müller.
XVIII^e Journée Jeunes Chercheurs de la SCT, Paris, 4 février **2011**
3. *Medicinal Chemistry of antiparasitic compounds. Redox-active naphthoquinone derivatives and bis(Michael acceptors) and prodrugs.* E. Cesar, E. Davioud-Charvet, T. Gendron, L. Johann, D. A. Lanfranchi.
AERES, Strasbourg, novembre **2011**
4. *Design and synthesis of prodrugs of bis-Michael acceptors as antitrypanosomal drug-candidates*
T. Gendron, D. A. Lanfranchi, E. Davioud-Charvet
Rencontres Internationales de Chimie Thérapeutique, Poitiers, 4-6 Juillet **2012**

Brevet

1. *Compounds useful against Kinetoplastideae parasites.* T. Gendron, I. N. Wenzel, T. J. J. Müller, G. Hanquet, D. A. Lanfranchi, F. Leroux, E. Davioud-Charvet.
PCT Int. Appl. (**2011**), WO 2011033115-A2

Livres

1. *Redox-active agents in reactions involving the trypanothione/trypanothione reductase-based system to combat kinetoplastid parasites.* T. Gendron, D. A. Lanfranchi, E. Davioud-Charvet
in Drug Discovery for Trypanosomatid Diseases, Vol. 4, **2012**, from the series Drug Discovery in Infectious Diseases, (Ed.: P. M. Selzer), Wiley-VCH Verlag GmbH & Co. KGaA, Weinheim (in press)

Publications internationales avec comité de lecture

1. *Dissymmetric (hetero)dibenzylideneacetones: a versatile access by a Pd-catalyzed Coupling-Isomerisation Reaction.* T. Gendron, E. Davioud-Charvet, T. Müller
Soumis à *Synthesis*.
2. *Diastereoselective preparation of 2,6-diaryl-4H-tetrahydrothiopyran-4-ones and their S-oxides.*
En preparation
3. *Antitrypanosomal and antileishmanial activities of DAA, 4H-thiopyran-4-ones and their S-oxides – Interactions with trypanothione versus glutathione.*
En preparation

Chapter I. Trypanosomatid diseases: physiopathology and drug discovery

Human African trypanosomiasis	7
PARASITE'S LIFE-CYCLE	7
EPIDEMIOLOGY.....	8
CLINICAL PRESENTATION	10
<i>Phase I: haemolymphatic stage</i>	10
<i>Phase II: meningoencephalitic stage</i>	10
TREATMENTS.....	11
<i>Vector control</i>	11
<i>Drug used in Phase I</i>	11
<i>Drug used in Phase II</i>	13
Chagas disease	16
PARASITE'S LIFE-CYCLE	16
EPIDEMIOLOGY.....	18
CLINICAL PRESENTATION	19
<i>Acute phase</i>	19
<i>Long-term asymptomatic phase</i>	19
<i>Chronic phase</i>	19
TREATMENTS.....	20
<i>Vector control</i>	20
<i>Therapeutic response</i>	20
Leishmaniasis	23
PARASITE'S LIFE-CYCLE	23
EPIDEMIOLOGY.....	24
CLINICAL PRESENTATION	25
TREATMENTS.....	26
Drug discovery in trypanosomatid diseases	29
TARGET PRODUCT PROFILE OF ANTIPARASITIC	29
THE DRUG DISCOVERY PIPELINE.....	31
DIFFERENT STRATEGIES TO ASSESS THE POTENCY OF COMPOUNDS	33
DRUGGABLE TARGETS OR BIOLOGICAL PATHWAYS IN TRYPANOSOMATIDS.....	35
<i>Glycolytic pathway</i>	36
<i>Sterol pathway</i>	37
<i>Purine metabolism and salvage pathway</i>	38
<i>Polyamine pathway</i>	39
<i>Trypanothione pathway</i>	40

The trypanothione pathway and the redox equilibrium inside parasites	41
REDOX HOMEOSTASIS IN HUMANS AND PARASITES.....	41
TARGETING THE TRYPANOTHIONE PATHWAY	44
<i>Direct thiol depletion</i>	44
<i>Trypanothione reductase inhibition</i>	45
<i>Subversive substrate approach</i>	46
BACKGROUND OF THE PROJECT: FROM THE HIT-DISCOVERY OF MANNICH BASES WITH ANTITRYPANOSOMAL ACTIVITY TO THE DIARYLIDENEACETONE SERIES.....	48
<i>Mannich bases as potent antitrypanosomal agents</i>	48
<i>The divinylketone, a key intermediate</i>	49
<i>The diarylideneacetone scaffold, a new series to explore</i>	50

Chapter II. Synthesis and evaluation of diarylideneacetones derivatives as antiparasitic agents

Synthesis of diarylideneacetone derivatives via the Claisen-Schmidt pathway	57
REPORTED USES AND SYNTHESIS OF DIARYLIDENEACETONES – A LITERATURE REVIEW	57
<i>Reported uses of diarylideneacetone derivatives</i>	57
<i>History of the synthesis of diarylideneacetones</i>	58
SYNTHESIS OF SYMMETRIC DIARYLIDENEACETONES	59
SYNTHESIS OF DISSYMMETRIC DIARYLIDENEACETONES	61
SYNTHESIS OF HETEROCYCLIC DIARYLIDENEACETONES.....	63
<i>Synthesis of 2-furan derivatives</i>	63
<i>Synthesis of pyridine derivatives</i>	64
LIMITATIONS OF THE CLAISEN-SCHMIDT PATHWAY	66
The coupling isomerization reaction	67
THE COUPLING ISOMERIZATION REACTION.....	67
<i>The coupling isomerization reaction at a glance</i>	67
<i>Would the coupling isomerization reaction fit to the synthesis of diarylideneacetones?</i>	69
RETROSYNTHETIC ANALYSIS.....	69
SYNTHESIS OF CINNAMALDEHYDE DERIVATIVES	70
<i>The oxidative approach</i>	71
<i>The reductive approach</i>	71
<i>The Wittig approach</i>	72
<i>The Grignard approach</i>	73
<i>Comparison of the different approaches</i>	74
SYNTHESIS OF UNSATURATED PROPARGYL ALCOHOLS	75
FIRST ATTEMPTS.....	77

Optimization of the synthesis of dissymmetric (hetero)diarylideneacetones via Pd-catalyzed coupling isomerization reaction	78
SET-UP AND VALIDATION OF THE QUANTIFICATION METHOD.....	78
<i>Choice of the method</i>	78
<i>Calibration and validation</i>	80
<i>Summary</i>	82
OPTIMIZATION OF DISCRETE FACTORS.....	82
<i>Base screening</i>	83
<i>Solvent screening</i>	84
<i>Catalyst screening</i>	84
OPTIMIZATION OF CONTINUOUS FACTORS.....	84
<i>Box-Behnken design of experiment</i>	85
<i>Statistical analysis of the results</i>	86
<i>Optimized reaction conditions</i>	88
SCOPE OF THE REACTION.....	89
<i>In vitro</i> activities against trypanosomatid parasites	92
PROTOCOLS.....	92
<i>Parasitic assays</i>	92
<i>Toxicity</i>	93
<i>Representation of the results</i>	93
ANTIPARASITIC ACTIVITIES OF SYMMETRIC DIARYLIDENEACETONES.....	95
<i>Polyphenol pattern – Curcumin-like substitutions</i>	95
<i>Monosubstituted aromatics</i>	97
<i>Sterically hindered diarylideneacetones</i>	99
<i>Heteroaromatics</i>	100
ANTIPARASITIC ACTIVITIES OF DISSYMMETRIC DIARYLIDENEACETONES.....	101
<i>Heteroaromatics</i>	101
<i>Monosubstituted aromatics</i>	102
<i>Antileishmanial activities</i>	104
DISCUSSION.....	105
<i>Dissociation of the toxicity from the activity</i>	105
<i>Effect of the electronic distribution</i>	106
<i>Effect of lipophilicity</i>	108
Conclusion	110

Chapter III. Synthesis and evaluation of 2,6-diaryl-4H-tetrahydrothiopyran-4-ones and their relative S-oxides as prodrugs

Introduction to the prodrug strategy	115
BASEMENTS OF THE STRATEGY	115
<i>Prodrugs of ketones</i>	116
<i>Prodrugs of alkenes</i>	118
<i>Choice of the masking strategy</i>	119
HETEROCYCLIC PRODRUGS OF DIARYLIDENEACETONES.....	120
<i>2,6-diarylpiperidine-4-ones as candidates for the prodrug strategy</i>	121
<i>2,6-diaryl-4H-tetrahydrothiopyran-4-ones as candidates for the prodrug strategy</i>	124
The 2,6-diaryl-4H-tetrahydrothiopyran-4-one core at a glance	128
OVERVIEW OF THE 2,6-DIARYL-4H-TETRAHYDROTHIOPYRAN-4-ONES – CONFORMATION AND CONFIGURATION OF THE RING.....	128
REPORTED USES AND SYNTHESIS OF 2,6-DIARYL-4H-TETRAHYDROTHIOPYRAN-4-ONES – A LITERATURE REVIEW	129
<i>Reported uses of 2,6-diphenyl-4H-tetrahydrothiopyran-4-one derivatives</i>	129
<i>Synthesis of 2,6-diaryl-4H-tetrahydrothiopyran-4-ones</i>	130
<i>Limitations</i>	132
DESIGN OF A NEW METHODOLOGY FOR THE DIASTEREOSELECTIVE SYNTHESIS OF 2,6-DIARYL-4H-TETRAHYDROTHIOPYRAN-4-ONES	133
<i>Source of sulfur</i>	133
<i>Control of the reaction temperature</i>	133
<i>Influence of the solvent</i>	134
<i>Control of the basicity of the medium</i>	134
<i>Summary and first results</i>	135
Optimization of the diastereoselective synthesis of 2,6-diaryl-4H-tetrahydrothiopyran-4-ones	136
SET-UP AND VALIDATION OF THE QUANTIFICATION METHOD.....	136
<i>Spectroscopic characterization of diastereoisomers</i>	136
<i>Choice of the method</i>	140
<i>Calibration and validation</i>	141
<i>Summary</i>	141
OPTIMIZATION OF THE SELECTIVE SYNTHESIS OF (±)-TRANS DIASTEREOISOMERS.....	143
<i>Effects of the solvent</i>	143
<i>Effect of the base stoichiometry</i>	145
<i>Scope of the reaction</i>	145
<i>Concluding remarks on the diastereoselective synthesis of (±)-trans-2,6-diaryl-4H-tetrahydrothiopyran-4-ones</i>	148

OPTIMIZATION OF THE SELECTIVE SYNTHESIS OF CIS DIASTEREISOMERS	148
<i>Synthesis in purely organic medium</i>	148
<i>Phase-transfer catalyzed synthesis</i>	152
<i>Concluding remarks on the diastereoselective synthesis of cis-2,6-diaryl-4H-tetrahydrothiopyran-4-ones</i>	160
Synthesis of the putative S-oxide metabolites	161
SYNTHESIS OF SULFOXIDE DERIVATIVES	161
<i>Literature review</i>	161
<i>Screening of new oxidation protocols for the synthesis of the desired sulfoxides</i>	162
<i>Use of Davis's oxaziridine for the synthesis of sulfoxide derivatives</i>	164
<i>Characterization of cis sulfoxide derivatives – stereochemical and spectroscopic aspects</i>	167
<i>Concluding remarks on the synthesis of sulfoxide derivatives</i>	168
SYNTHESIS OF SULFONE DERIVATIVES	169
<i>Literature review</i>	169
<i>Screening of new oxidation protocols for the synthesis of the desired sulfone</i>	169
<i>Synthesis of sulfone derivatives by smooth oxidation of sulfoxides</i>	171
Antiparasitic activities of 2,6-diaryl-4H-tetrahydrothiopyran-4-ones and their relative S-oxides	172
FOREWORD	172
<i>Protocols</i>	172
<i>Representation of the results</i>	172
ANTIPARASITIC ACTIVITIES OF 2,6-DIARYL-4H-TETRAHYDROTHIOPYRAN-4-ONES.....	173
<i>Polyphenol pattern – Curcumine-like substitutions</i>	173
<i>Monosubstituted aromatics</i>	174
<i>Sterically hindered 2,6-diaryl-4H-tetrahydrothiopyran-4-ones</i>	177
<i>Heteroaromatics</i>	177
ANTIPARASITIC ACTIVITIES OF PUTATIVE S-OXIDE METABOLITES	178
<i>Sulfoxide derivatives</i>	178
<i>Sulfone derivatives</i>	180
<i>Antileishmanial activities</i>	181
DISCUSSION	182
<i>Dissociation of the toxicity from the activity</i>	183
<i>Effects of the stereochemical configuration</i>	184
<i>Effects of sulfur oxidation</i>	186
Conclusion	187

General introduction

Parasitic diseases represent a major public health concern in numerous countries, and especially in developing ones. The global burden imputable to these diseases is estimated to exceed two millions deaths annually, hampering dramatically both economic and social development in endemic areas.^{1,2} Whereas the scientific community is paying close attention to malaria, dedicating huge investments and researches to this disease, other parasitosis are underinvestigated and less known by the general public. Diseases like Human African Trypanosomiasis (HAT), Chagas disease, leishmaniasis or schistosomiasis are endemic in more than half of the surface of the earth and kill at least half a million people every year.³ Despite this threatening status, these diseases have received little consideration for decades, resulting in their classification as Neglected Tropical Diseases (NTDs). As listed by the World Health Organization (WHO), NTDs are a subset of infectious diseases that are responsible for dramatic morbidity and mortality (Table I.1). The collective term "neglected tropical diseases" does, however, imply two important shared features.⁴ On one hand, these diseases are predominately endemic in tropical areas. Though a hot climate is required for the development and the spread of these parasitosis, the burden is all the more dramatic as these diseases disproportionately affect poor populations, with limited access to safe water, sanitation, appropriate housing and health care facilities. NTDs generate a vicious circle as massive contamination of the population leads to a dramatic decrease in the work force and in both the family and national income, which, in turn, limits the access to adequate drugs and medical care. On the other hand, these diseases have been neglected for decades by funders, researchers, pharmaceutical companies and policy-makers. Figures speak from themselves: out of more than 1 200 new drugs introduced on the market between 1975 and 1999, only 13 were dedicated to the treatment of NTDs.⁵ This is also visible in terms of funding: tuberculosis and tropical diseases represent less than 0.1% of the investments in pharmaceutical research although these diseases contribute to about 5% of the global disease burden.⁶ This lack of commitment is easily explained by the low, or even null, return on investments on the development of treatments for this kind of diseases.⁷ The cost for the development of the eight urgently needed new drugs for NTDs was recently evaluated to US\$ 1 billion, which is more than the annual research budget of most drug companies.⁸ Moreover, this huge amount cannot be balanced by any return on investment since treatments are usually donated for free to WHO or nongovernmental organization (NGOs) as poor population cannot afford the drugs. As a result, big pharmaceutical companies have widely neglected this area of research during most of the twentieth century.

Table I.1 | Neglected tropical diseases – toll and clinical manifestations.

Disease	Causative agent	Prevalence (millions)	Areas of highest prevalence	Estimated DALYs lost (millions)	Clinical manifestations
Ascariasis	<i>A. lumbricoides</i> (Helminthes)	807 – 1 221	Saharan Africa Latin America	1.8	Gastrointestinal disorders, impaired growth, reduced school performance
Dracunculiasis	<i>D. medinensis</i> (Helminthes)	0.002	Asia, Africa	Unknown	Painful skin ulcer from which a worm protrudes
Hookworm infection	<i>A. duodenale</i> <i>N. americanus</i> (Helminthes)	576 – 740	Asia, Africa	0.06	Gastrointestinal disorders, anemia, impaired growth, reduced school performance
Lymphatic filariasis	<i>W. bancrofti</i> <i>B. malayi</i> <i>B. timori</i> (Helminthes)	120	Asia, Africa	5.8	Hydrocele, lymphedema, and elephantiasis
Onchocerciasis	<i>O. volvulus</i> (Helminthes)	37	Saharan Africa	0.5	Skin impairments, blindness
Schistosomiasis	<i>Schistosoma</i> spp. (Helminthes)	200	Africa	1.7	Hematuria, bladder and renal impairments periportal fibrosis, portal hypertension, ascites and varices
Trichuriasis	<i>Trichuris trichiuria</i> (Helminthes)	604 – 795	Asia, Africa and Latin America	1.0	Colitis, chronic dysentery, rectal prolapsed, impaired growth, reduced school performance
Chagas disease	<i>T. cruzi</i> (Protozoa)	8 – 9	Latin America	0.7	Cardiomyopathy, cardiac dysrhythmia, mega-oesophagus, mega-colon
Human African Trypanosomiasis	<i>T. brucei</i> ssp. (Protozoa)	0.3	Sub-Saharan Africa	1.5	Fever, headache, lymphadenopathy, neurological disorders, coma, death
Leishmaniasis	<i>Leishmania</i> spp. (Protozoa)	12	Southern-Asia, Sub-Saharan Africa, Latin America, Mediterranean area	2.1	skin ulcer, oropharyngeal destruction, fevers, night sweats, weight loss, anaemia, immunosuppression
Buruli ulcer	<i>M. ulcerans</i> (Bacterium)	Unknown	Sub-Saharan Africa, Asia	Unknown	Skin ulcer with an undermined edge
Leprosy	<i>M. leprae</i> (Bacterium)	0.4	Asia, Africa, Latin America	0.2	Skin changes, anaesthesia
Trachoma	<i>C. trachomatis</i> (Bacterium)	84	Asia, Africa	2.3	Conjunctivitis, trachomatous scarring, trichiasis, corneal opacity, blindness

Among the thirteen NTDs, human African trypanosomiasis, Chagas diseases and leishmaniasis are usually quoted as the "Most Neglected Tropical Diseases". Indeed, these diseases have the highest morbidity and mortality rate among the NTDs, while their therapeutic management is still inadequate.^{7,9} These three NTDs are parasitic diseases resulting from the infection of human being by trypanosomatid parasites. Trypanosomatids are unicellular flagellated eukaryotes that belong to the class of kinetoplastid protozoa (Figure I.1). They are quite old organisms as they belong to one of the earliest diverging branch of the eukaryotic evolutionary tree (during the mid-Cretaceous, approximately 100 million years before now).^{10–12} In spite of their taxonomic similarities, the different species of trypanosomatids widely differ in their foci, life cycles and in the symptoms that they induce

after infection. However, the common feature of these parasitic infections is that treatment modalities mostly rely on drugs dating back over 50 years and suffering from limited efficacy, high toxicity, and above all increasing resistance.^{6,7}

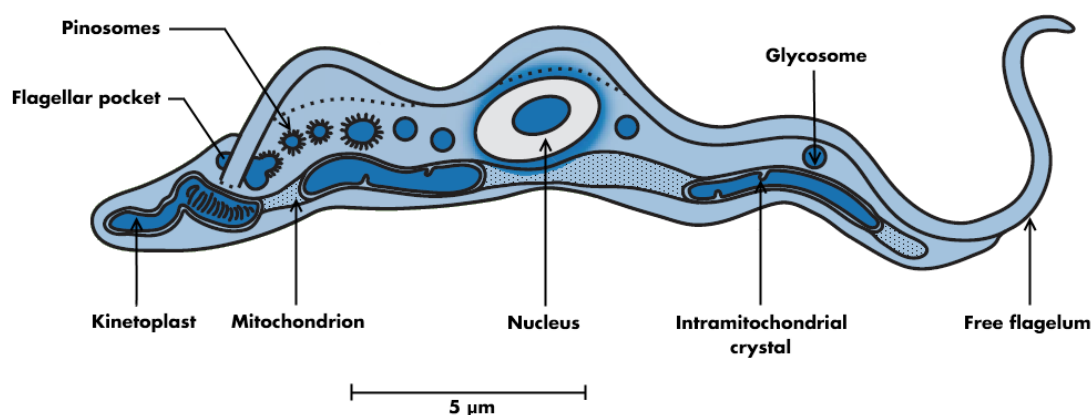


Figure 1.1 | Schematic representation of a trypanosomatid parasite

Following large epidemic episodes that occurred in southern-Africa in the 90's and the emergence of resistance to the old drugs, WHO and NGOs sounded the alarm bell, emphasizing the urgent need for new adequate responses to these diseases, both on a medical and a socioeconomic point of view. Considering the wide diversity of NTDs, their large spread throughout the world, and the cost incurred by development of new drugs, it became obvious that such global threats require a global response. The entire process of research and development (R&D) has to be reviewed and this led to the emergence of new public-private partnerships (PPPs).¹³ On one hand, the public sector has long taken an interest in stimulating the development of new therapy, and thus has gained a deep knowledge in the rationale of diseases and in numerous drug targets. However, public sector usually does not have any drug development infrastructure. On the other hand, the pharmaceutical industry has developed expertise in medicinal chemistry and other technologies for the conversion of basic scientific discoveries into new therapies and has efficient drug development infrastructures. Introduced in early 2000's, the concept of PPPs aims at stimulating R&D interest in neglected tropical diseases through the combination of knowledge and experience of the public sector with drug development infrastructures of the pharmaceutical industry.

Consolidated by the injection of new funds from philanthropic foundations, this approach is able to compensate for market failure by reducing the costs and risks involved for both public- and private-sector partners. This new way of drug development requires an efficient organization, management powers and, above all, the set-up of clear and precise agreements between the different partners, especially in term of industrial property. One of the first achievements of these partnerships was the full sequencing of parasite genomes by

the academic sector, leading to target identification and hit selection by pharmaceutical companies. Little by little, this pharmacological reengagement with neglected tropical diseases is starting to yield encouraging results, and about twenty compounds are currently under development for several applications.⁶

As part of this pharmacological commitment, present PhD thesis will be focused on the search for new antiparasitic drugs, targeting the three most neglected tropical diseases, namely human African trypanosomiasis, Chagas diseases and leishmaniasis. Based on results that have been previously obtained in the laboratory,¹⁴ this work aimed at exploring the chemistry and the antiparasitic activities of bis-(Michael acceptors) and their associated prodrugs. Before studying the chemistry and the structure-activity relationship of these products, the three diseases will be briefly introduced (Chapter 1). In this same part, a short overview of the parasitic drug targets and a state-of-the-art of the on-going research projects will be given. The chemistry and the antiparasitic activities of diarylideneacetones (Chapter 2) and their associated 2,6-diaryl-4*H*-tetrahydrothiopyran-4-one prodrugs and putative metabolites will next be discussed (Chapter 3).

Chapter I

Trypanosomatid diseases: physiopathology and drug discovery

Human African trypanosomiasis

Human African Trypanosomiasis (HAT), more commonly known as sleeping sickness, is a disease caused by kinetoplastid parasites *Trypanosoma brucei* ssp. This neglected tropical disease is a serious public health concern in Africa, where approximately 60 million persons are at risk.⁷

Parasite's life-cycle

HAT is a vector-borne infection transmitted to mammals mainly by blood-sucking flies of the genus *Glossina*, commonly named "Tsetse" flies. At least thirty species or subspecies of tsetse flies have been listed, with different habitats and variable infectivity levels.¹⁵ Among the five subspecies of *T. brucei* that *Glossina* can transmit, only two are responsible for the human form of the disease: *T. brucei gambiense* and *T. brucei rhodesiense*. Trypanosomes are unicellular organisms of 15-30 μm length. It is important to notice that, unlike *Trypanosoma cruzi* (*vide infra*), *Trypanosoma brucei* ssp. are exclusively extracellular parasites; they are constantly moving in the host's fluids using their highly efficient flagellum. During their development inside the fly and next in the host, *T. brucei* ssp. will adopt different forms: metacyclic, bloodstream and procyclic trypomastigotes, and epimastigote. The complete life cycle of *T. brucei* ssp. is depicted in Figure I.2.

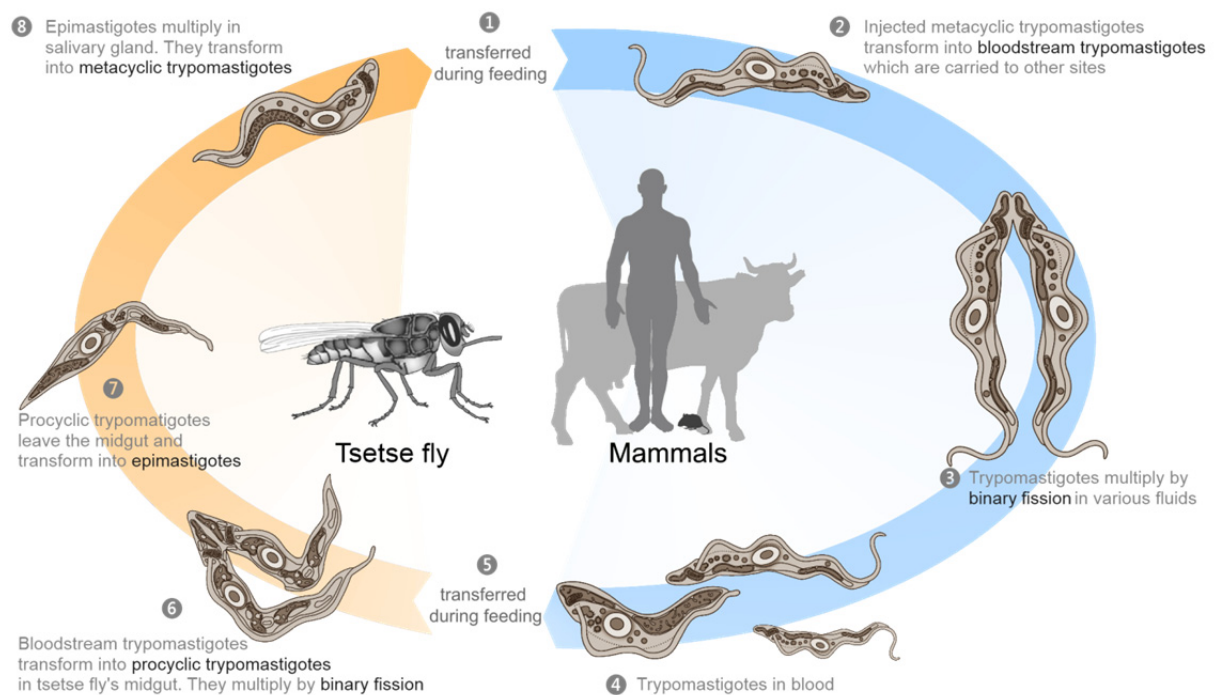


Figure I.2 | *Trypanosoma brucei* parasite life cycle

During a blood meal on the mammalian host, the fly injects metacyclic trypomastigotes into skin tissue. The parasites get into both the lymphatic system and the bloodstream, ①. Inside the host, they transform themselves into bloodstream trypomastigotes, ②, are carried to other sites throughout the body, reach other blood fluids (e.g. lymph, spinal fluid), and continue their replication by binary fission, ③. The tsetse fly becomes infected with bloodstream trypomastigotes when taking a blood meal on an infected mammalian host (④, ⑤). In the fly's midgut, the parasites transform themselves into procyclic trypomastigotes, multiply by binary fission, ⑥, leave the midgut, and transform themselves into epimastigotes, ⑦. The epimastigotes reach the fly's salivary glands and keep multiplying by binary fission, ⑧.

Maturation of trypanosomes in the fly is a long and complex process which takes from three to five weeks, while the life expectancy of tsetse life is about three months. As a result, this maturation is rarely reached, and only about 0.1 % of flies are really able to transmit the disease.¹⁵ However, the vector-borne transmission is all the more facilitated as other mammals are playing the role of reservoir. The reservoir of *T. brucei gambiense* was proved to be mainly human beings, while *T. brucei rhodesiense* uses animals, and especially cattle, as reservoir.¹⁶ Transmission of HAT is exclusively vector-mediated. To our knowledge, no inter-human transmissions, as well as contaminations through food, were reported.

Epidemiology

Human African Trypanosomiasis is endemic in 36 countries, mainly in Sub-Saharan Africa (Figure I.3).^{15,17} The two pathogens responsible for the disease have clearly separated endemic areas. Thus, *T. b. gambiense* is found in central and western-Africa, while its counterpart *T. b. rhodesiense* is circumscribed to the southeastern part of the continent. Although few cases were reported in cities, the disease is currently still limited to rural areas.¹⁵ However, climate changes, travels and population movements are constantly increasing the risk of a spread of HAT.¹⁷ WHO estimates that 60 million people are at risk, with a global prevalence over 300 000 people, and about 50 000 new cases each year.^{7,18} However, evaluating of both the prevalence and the annual incidence is all the more difficult as most of endemic countries are underdeveloped, with almost no access to medical care or follow-up. Therefore, most of the figures available are considered as underestimated by WHO. The mortality imputable to HAT is estimated to 48 000 deaths per year.⁷

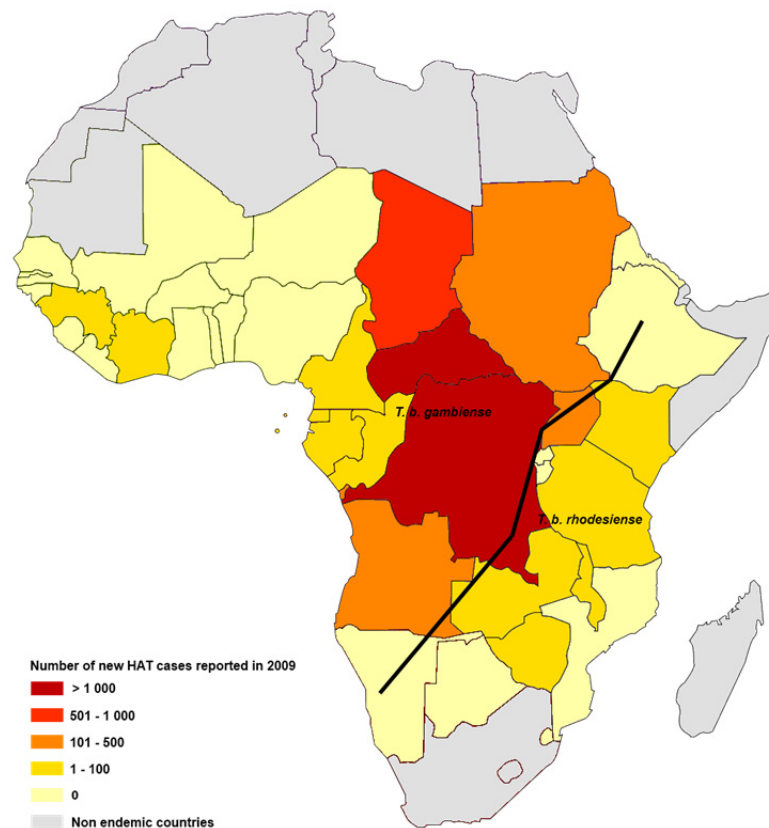


Figure I.3 | Endemic areas of human African trypanosomiasis. Number of cases reported in 2009, adapted from ref.¹⁵

Human African Trypanosomiasis mostly arises through epidemic episodes. This first reported major outbreak of HAT occurred between 1896 and 1906. During this period more than 800 000 deaths were attributed to the disease. In the next decades, efforts in vector control and in medication from European colonial governments resulted in an outstanding decrease in the prevalence of HAT and in 1960's the disease was almost eradicated. Unfortunately, after the advent of independence, surveillance and control activities were neglected in many endemic countries. Reinforced by civil conflicts and their resulting numerous population movements, the disease spread again, causing many death in Democratic Republic of Congo, Angola, Central African Republic, southern-Sudan and Uganda during the 1990's. Further to political and socio-economic stabilizations, governmental reengagements –supported by WHO and Non-Governmental Organizations (NGO)– led to a progressive decrease in the number of reported cases; between 1997 and 2006 this number was reduced by 69%.¹⁵ This history of HAT outbreaks perfectly illustrates the close link existing between the spread of the disease and the socio-economic background in the endemic areas. It also demonstrates that eradication of the disease should be possible but will require a strong political will, combined with large-scale control vector, efficient diagnosis and treatments of the disease.¹⁹

Clinical presentation

Human African Trypanosomiasis evolves in two stages, first haemolympathic stage followed by the second meningoencephalitic stage, characterized by invasion of the Central Nervous System (CNS). Both *T. b. gambiense* and *T. b. rhodesiense* are following this clinical pattern. However, they differ in their rate of evolution if left untreated. *T. b. gambiense* induces a slow chronic HAT that evolves progressively, leading to the death within about three years.²⁰ On the contrary; the infection caused by *T. b. rhodesiense* is usually acute and death occurs within weeks or months.²¹

Phase I: haemolympathic stage

Following the inoculation from the tsetse fly, a reaction at the site of the bite (Trypanosoma chancre) might appear. However this is not HAT-specific as *T. b. gambiense* usually does not induce this reaction, while only 19% of patients infected by *T. b. rhodesiense* show this symptom.¹⁵ Subsequent invasion of blood and lymph induces several symptoms the most commons of which are an intermittent fever, headache, pruritus, lymphadenopathy, and, to a lesser extent, hepatosplenomegaly.¹⁵ In the case of *T. b. gambiense* infection, these symptoms are usually limited to a general malaise feeling common place in rural Africa. This results in a difficult diagnosis of the early stage of *T. b. gambiense* HAT. On the other hand, the phase I symptoms of *T. b. rhodesiense* are acute and highly disabling which, in endemic areas, usually leads to early presentation by patients at clinic.²² Whatever the subspecies, if phase I is left untreated, the disease will necessarily evolve to the meningoencephalitic stage.

Phase II: meningoencephalitic stage

With the time and the increasing parasitemia, bloodstream trypanosomes manage to reach the CNS by passing through the Blood-Brain Barrier (BBB). This time-dependent penetration of the brain remains unclear. Among the several mechanisms that have been suggested, a penetration through intracellular junctions of the BBB mediated by inflammatory response of the host is the most agreed.^{23,24} Once inside the CNS, trypanosomes have dramatic deleterious neurological and psychiatric effects. First manifestations of the phase II are sleep disorders that gave the disease its name. Unlike the popular belief about HAT, patients do not sleep more than healthy subjects, but rather, experience a deregulation of their circadian rhythm that results in fragmentation and disruption of the sleeping pattern with daytime somnolence.^{15,22} Neurological symptoms include tremor, fasciculation, general motor weakness, paralysis of a limb, hemiparesis, akinesia, dyskinesia.¹⁵ Most of these symptoms are similar to those that occur in Parkinson disease. However, in the case of HAT psychiatric symptoms also occurs; they involve irritability, psychotic reaction, aggressive behavior or apathy.¹⁵ Combination of these

two patterns in endemic area is HAT-specific and requires urgent medical care and drug treatment. In the absence of any therapy, phase II of the disease is fatal in 100 % of the cases.

Treatments

Vector control

The control campaigns that were carried out in the 60's and since the late 90's demonstrated the great efficiency of such measures. This control implies both the eradication of the tsetse fly and massive antiparasitic treatment of reservoirs. Regarding the first point, insecticides or tsetse fly traps have dramatically decreased the number of flies, leading in almost complete eradication of the species in some areas. However the use of insect repellents is not satisfactory as few flies are sensitive to these products.¹⁵ Concerning the control of reservoirs, as we previously mentioned, the two parasites have different reservoirs. In the case of *T. b. gambiense*, human beings constitute the reservoir for the disease; control and cure of this reservoir is possible if adapted medical care, large-scale diagnosis and treatment campaign are carried out. On the other hand, controlling cattle and animal reservoir of *T. b. rhodesiense* appears far more difficult. In addition to the numerous individuals that should be treated, most of cattle and other mammals are asymptomatic-carriers. It is therefore difficult to treat only infected animals, the only way would be to treat the entire reservoir which is highly improbable in Africa for both financial and logistic reasons.¹⁵

Drug used in Phase I

The main goal of drugs that are used in HAT phase I is to eradicate the parasite from all the body fluids before it reaches the CNS. This requires chemical drug treatment as, in most of the cases, the immune response of the host is unable to kill the parasite. Indeed, *T. b. gambiense* and *T. b. rhodesiense* show a very variable composition in glycoprotein at their surface.²² Although the Trypanosome Lytic Factor (TLF) of human serum is able to destroy animal forms of the disease (*T. b. brucei*, *T. evansi*, and *T. congolense*), it is useless with regards to the high antigenic variation of *T. b. gambiense* and *T. b. rhodesiense*.²⁵ For similar reasons, the development of an efficient vaccine for HAT is very unlikely, leaving the chemotherapy as the only effective mean to eradicate the parasite from the host.

Two drugs are used in early stage disease, pentamidine and suramin (Figure I.4).

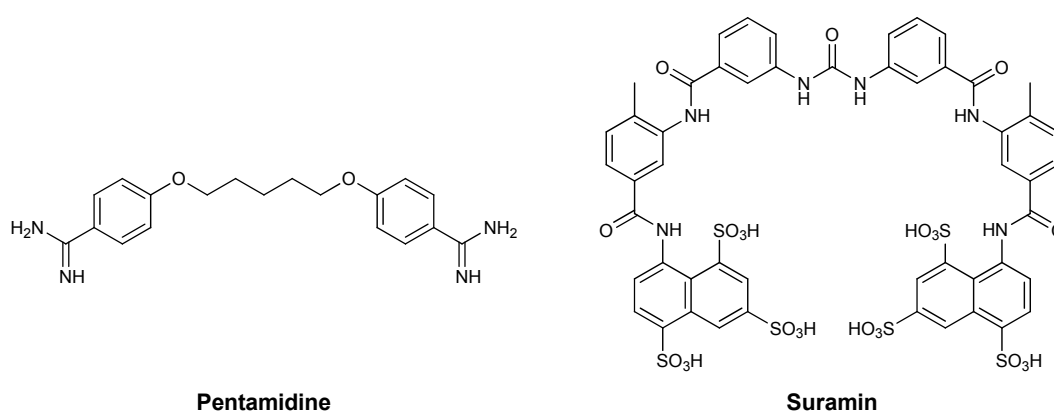


Figure I.4 | Drugs used in the early stage of human African Trypanosomiasis.

Pentamidine is the drug of choice for the treatment of phase I *T. b. gambiense* infections. It has to be administered through intramuscular injection at 4 mg/kg daily or on alternate days for seven to ten days.²² Although usually well tolerated, pentamidine induces several side effects such as hypoglycemia (5-40 % of the patients), nephrotoxicity, leucopenia, liver enzyme abnormalities, pain at the site of injection, swelling, abdominal pain, or gastro-intestinal disorders.^{15,22} Pentamidine is concentrated in trypanosomes to high level (low millimolar range) probably by P2-transporters active uptake.²⁶ Once in the parasite, the drug seems to target the mitochondrion but its mode of action remains unclear. As a di-cation, pentamidine interacts electrostatically with macromolecules and especially DNA, leading to devastating damages to the genomes of the parasite.²²

The second drug, suramin, is dedicated to treatments of phase I *T. b. rhodesiense* infections. It is also active against *T. b. gambiense*, but suramin induces severe allergic reactions when patients are co-infected with *Onchocerca* spp. which is often the case in endemic areas of *T. b. gambiense*. Recommended dose regimens for suramin are complex; the drug is injected intravenously at 20 mg/kg once a week, during five weeks, with a maximum dose per injection of 1 g. In addition, the handling of suramin is problematic as it is unstable to air and therefore must be used immediately after solubilization.¹⁵ Neuropathy, nephrotoxicity, bone-marrow toxicity, rash, fatigue, anemia, hyperglycemia, hypoglycemia, coagulopathies, neutropenia, renal insufficiency and liver enzyme abnormalities often occur during the treatment. Suramin can also trigger severe anaphylactic reaction.^{15,22} In spite of several attempts, the mechanism of action of suramin is still unknown. It is believed that the drug enters the parasite by pinocytosis. As a highly negatively charged molecule, suramin might interact with numerous biological macromolecules and, among them, glycolytic enzymes are supposed to be the target of suramin.²²

Drug used in Phase II

This second stage of the disease is characterized by a massive parasitic infection of the CNS and of the cerebrospinal fluid (CSF). Any drug aiming at reaching the parasites must first cross the BBB or the blood-CSF barrier.²² Due to their high polarity, drugs used in phase I cannot achieve brain penetration and are therefore unable to cure phase II infections.

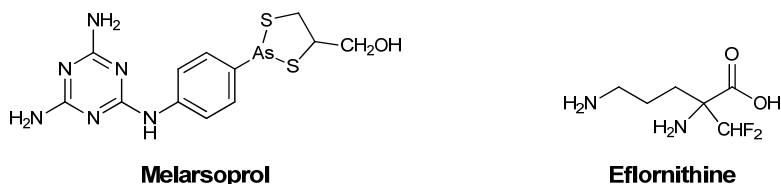
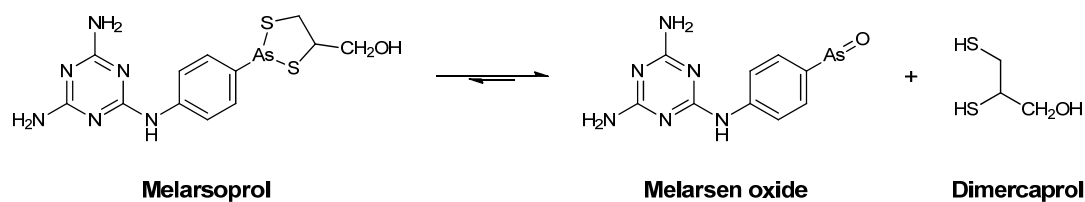


Figure I.5 | Drug used in the second stage of human African Trypanosomiasis.

The first drug introduced on the market for the treatment of phase II HAT, was melarsoprol in 1949 (Figure I.5). This melaminophenyl-based organic arsenical compound is active both on *T. b. rhodesiense* and *T. b. gambiense*. A recent standardized shortened protocol of treatment consists in 2.2 mg/kg given intravenous once a day for ten days. Although melarsoprol can achieve complete relief of phase II HAT, this drug suffers from frequent severe side effects. Among them, reactive encephalopathy triggered by arsenical poisoning of the CNS occurs in 5-10% of patients of which more than the half dies!^{15,22} Due to this risk of neurological complication, patients treated with melarsoprol must be carefully monitored in hospital settings. Besides this severe adverse reaction, pruritus, maculopapular eruptions, bullous eruptions, peripheral motor or sensorial neuropathies, or thrombophlebitis are also frequent.¹⁵ Melarsoprol acts as a prodrug and is rapidly metabolized in highly toxic melarsen oxide which is responsible for the antiparasitic activity (Scheme I.1).²⁷



Scheme I.1 | Metabolic activation of melarsoprol.

Melarsoprol and its metabolite principally enter *T. brucei* spp. parasites by P2 aminopurine transporters which is recognizing the melamine moiety of melarsoprol.²⁸ However, it has been demonstrated that the dithiol ligand is also playing an important role in the adsorption and the distribution of the drug, both in the host and in parasites.^{29,30} Once inside the parasite, the mechanism of action of the drug is not entirely known. The organic arsenic is believed to form stable interactions with thiols, and especially with trypanothione, which might trigger an oxidative stress, leading to the death of the parasite.³¹ Perturbation of the glycolytic pathway also seems to play an important role in the lysis of the parasite.²² Efficiency of melarsoprol is

limited by its high toxicity, but also by the recent emergence of resistance. Thus in several foci, treatment failure have reached 30 %, probably due to mutations in the aminopurine pathway that limits the uptake of the drug by lower efficiency of P2 transporters. Melarsoprol is truly affordable which makes it the first intent choice in several endemic areas, in spite of its numerous drawbacks.¹⁵

Initially developed for cancer therapy, eflornithine (Figure I.5) was approved in 1991 for the treatment of both phases of *T. b. gambiense* HAT, but not for *T. b. rhodesiense* on which the drug displays limited activity.²² Eflornithine, otherwise named D,L- α -difluoromethylornithine (DFMO), is the only recently developed drug for the treatment of HAT which achieved a true improvement in the toxicity profile of antitypanosomal drugs. Indeed, this molecule has shown a clearly reduced mortality compared to melarsoprol which would normally makes it as first line treatment. Unfortunately, eflornithine suffers from a poor pharmacokinetic profile with a short half-life (about 3 h) and more than 80% of the drug excreted unchanged in the urine after 24 h. As a result, the required dose of eflornithine is as high as 100 mg/kg, injected intravenously four times a day for two weeks.^{15,22} Main side effects are bone-marrow toxicity, cytopenia (20-50%), gastrointestinal syndromes (10-39%), convulsion (7%).¹⁵ Eflornithine uptake in the parasite occurs through amino-acid transporters. Subsequent irreversible inhibition of ornithine decarboxylase enzyme (ODC, EC 4.1.1. 17) deprives trypanosomes of net polyamine synthesis. It is of interest to notice that eflornithine has similar affinity for mammals' ODC and parasites' ODC. However, ODC is replenished much more slowly in the case of *T. b. gambiense* ($t_{1/2} \approx 19$ h) than in *T. b. rhodesiense* ($t_{1/2} \approx 4$ h) and mammals ($t_{1/2} \approx 10$ -30 min).³² As a result, inhibited ODC is quickly replaced in *T. b. rhodesiense* and mammals whereas *T. b. gambiense* is dramatically affected by the alteration of its crucial enzyme. This explains the selectivity of the drug.³² In spite of a better toxicity profile and a clear knowledge of the drug target, eflornithine remained less used than melarsoprol, mainly due to its very expensive cost (more than 500 US\$ for one treatment, Table I.2).¹⁷ Efforts have been made from Sanofi-Aventis to reduce the cost, and from WHO to developed all-in-one kits, in order to promote the use of this treatment instead of melarsoprol. Since 2009, this results in a great diminution in the number of patients treated with melarsoprol, from 88% to 38% in favor of eflornithine.¹⁷

Table I.2 | Treatments used in human African Trypanosomiasis

INN (DoA) ^a	Brand name	Stage	Mode of Action ²²	Dosing ^{15,33}	Side effects	Cost of a full treatment ^a
<i>Trypanosoma brucei gambiense</i>						
Pentamidine (1939)	Pentacarnat [®] (Sanofi-Aventis)	First	Unclear. Might interact electrostatically with macro-molecules and especially DNA, damaging the genomes of the parasite.	4 mg/kg IM on alternate days for seven to ten days	Hypoglycemia, nephrotoxicity, leucopenia, liver enzyme abnormalities, pain at the site of injection, swelling, abdominal pain, gastro-intestinal disorders.	170 US\$ ^b
Eflornithine ^c (1991)	Ornidyl [®] (Sanofi-Aventis)	Second	Irreversible inhibition of Ornithine decarboxylase enzyme deprives trypanosomes of net polyamine synthesis.	100 mg/kg IV four times a day for two weeks	Bone-narrow toxicity, cytopenia, gastrointestinal syndromes, convulsion.	692 US\$ ³⁴
<i>Trypanosoma brucei rhodesiense</i>						
Suramin (1920)	Germanine [®] (Bayer)	First	Unclear. Might interact with low-density lipoprotein carriers, leading to depletion in sterols and phospholipids. ³⁵	20 mg/kg IV once a week, during five weeks	Sever anaphylactic reactions, neuropathy, nephrotoxicity, bone-narrow toxicity, rash, fatigue, anemia, hyperglycemia, hypoglycemia, coagulopathies, neutropenia, renal insufficiency, liver enzyme abnormalities	33 US\$ ³⁶
Melarsoprol (1949)	Arsobal [®] (Speca)	Second	Assumed to involve both trypanothione depletion that leads to oxidative stress, and perturbation of the glycolytic pathway.	2.2 mg/kg IV once a day for ten days	Reactive encephalopathy, pruritus, maculopapular eruptions, bullous eruptions, peripheral motor or sensorial neuropathies, thrombophlebitis	40 US\$ ³⁶

^a For a patient weighing 35 kg, based on an exchange rate of 1 € = 1.25 US\$^b Courtesy of Dr. R. Passemard, Hôpitaux Universitaires de Strasbourg (personal communication).^c Might be substituted by melarsoprol when eflornithine is not available or not considered as first-line treatment according to national guideline, although not recommended by WHO considering toxicity and resistance issues of melarsoprol.

Abbreviations: INN = International Nonproprietary Names, DoA = Date of Approval (or of first described curative use), IM = Intramuscular, IV = Intravenous, po = per os

Chagas disease

Chagas disease is a chronic, systemic, parasitic infection caused by the kinetoplastid *Trypanosoma cruzi*. Recognized by WHO as one of the Neglected Tropical Diseases, it affects about eight million people in Latin America.

Parasite's life-cycle

Chagas disease is transmitted to mammals mainly by blood-sucking bugs of the subfamily *Triatominae*. Although more than 130 species of triatomines bugs have been identified, less than a dozen are competent vectors for *T. cruzi*. Among them, *Triatoma infestans*, *Rhodnius prolixus*, and *Triatoma dimidiata* are the three most important vectors.³⁷ During its development inside the bugs and next in the host, *T. cruzi* will adopt different forms: trypomastigote, amastigote and epimastigote. Trypomastigote and amastigote are only found in the host, the latter being the intracellular replicative form while trypomastigote form is only found in bloodstream and cannot replicate. Epimastigote is the replicative form of the parasite which is adapted to life-conditions inside triatomines. The complete life cycle of *T. cruzi* is depicted in Figure I.6.

An infected triatomine vector takes a blood meal and releases trypomastigotes in its feces near the site of the bite wound, ①. Trypomastigotes enter the host through the bite site, skin abrasions caused by the victim scratching the bite, or through intact mucosal membranes, such as the conjunctiva, ②. Once metacyclic trypomastigotes pass through the skin, they briefly migrate in the bloodstream and then colonize muscle and neuron tissues, where they differentiate into intracellular amastigotes, ③. The amastigotes multiply by binary fission differentiating into trypomastigotes, and then they are released into the circulation as bloodstream trypomastigotes. When triatomine insect feeds on blood from an infected animal or human, they ingest trypomastigotes, ④. These trypomastigotes turn into epimastigotes in the vector's midgut, ⑤, which are more able to survive in the internal of the bug where the parasite proliferates and transforms to metacyclic trypomastigotes that will be released in the feces of the insect, ①. This will, in turn, infect a new host. Unlike malaria, HAT or leishmaniasis, *T. cruzi* is not directly inoculated through a bite. This is a significant difference which greatly reduces the risk of transmission *via* a contact with an infected triatomine to about 1 %.³⁸

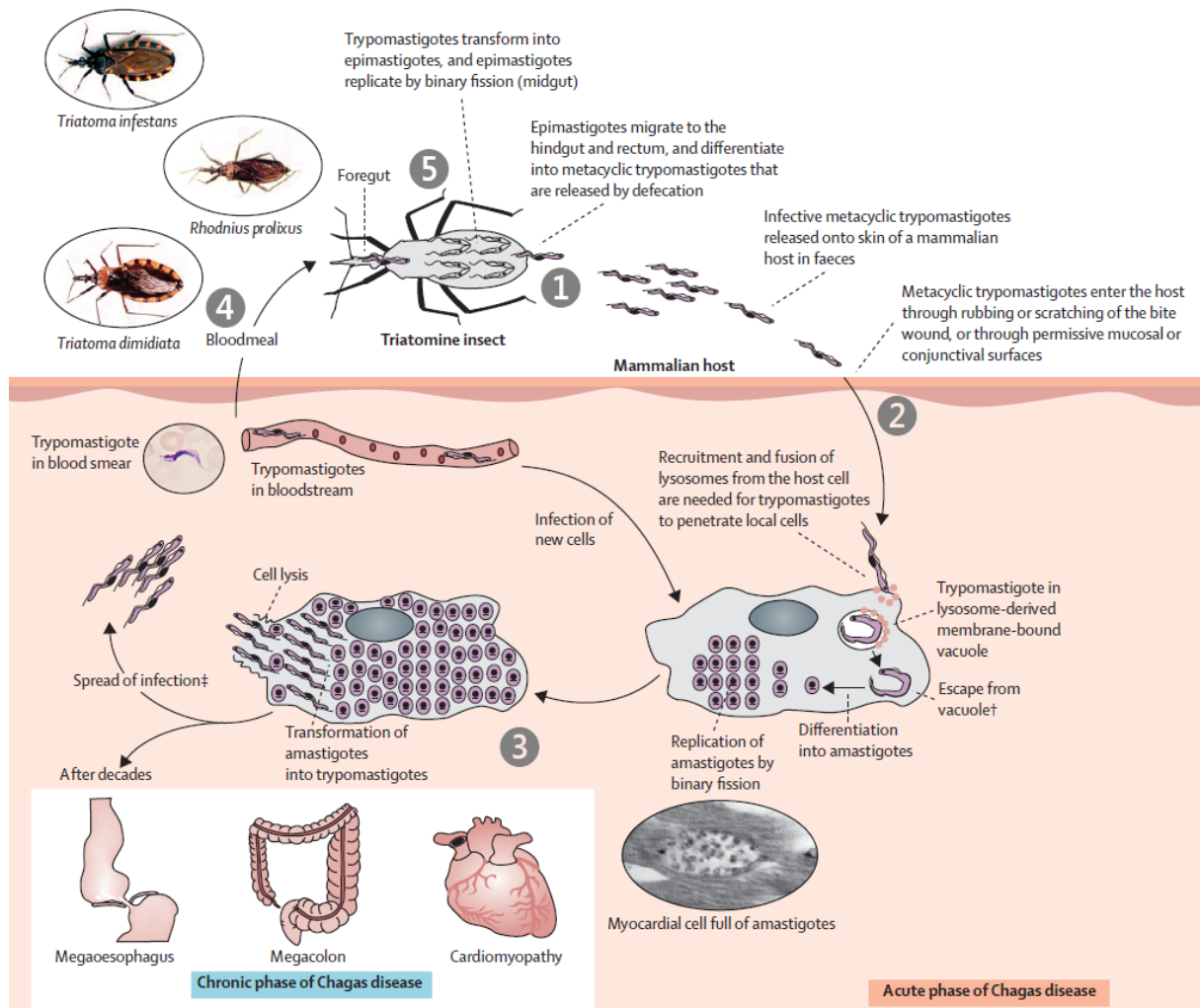


Figure I.6 | *Trypanosoma cruzi* parasite's life cycle. Adapted from ref. ³⁷

Although the vector-borne transmission is the major source of infection, other mechanisms of transmission exist. Patients can contract the disease following a blood transfusion from an infected blood donor. The risk of contamination is rather low, between 10 % and 20 %, depending on the parasite concentration, the blood component transfused, and the immunity of the receiver.^{39,40} Nevertheless, this route of entry is the second most common mechanism of transmission, especially in non-endemic countries that welcome numerous immigrants from Latin-America (e.g. the United States or Spain...⁴¹). In a similar manner, *T. cruzi* infections were reported after solid organ or bone marrow transplantations in endemic areas as well as in non-endemic regions.³⁷ Congenital transmission is also possible and estimated to an average of 1-5 % of pregnancies at risk, depending on the region.³⁷ Finally, oral transmissions of Chagas disease are relatively rare. However, when they occur, such contaminations are responsible for regional outbreaks of acute infection. Thus, ingestion of contaminated food such as sugar cane juice, palm berry juice or raw meat is generally associated with massive parasitic infestation, resulting in severe acute clinical presentation and high mortality.⁴²

Epidemiology

Chagas disease was originally confined to poor, rural areas of South and Central America. However, climate changes, travels and population movements contribute to the spread of the disease in all South America and Caribbean region (Figure I.7). WHO estimated that 25 million people are at risk, with a global prevalence over 8 million people. However, evaluation of Chagas disease prevalence is all the more difficult as it is a chronic disease which remains asymptomatic for years (*vide infra*). Therefore, most of the available figures are considered as underestimated by WHO. The mortality related to Chagas disease is estimated to 21 000 deaths per year.⁴³

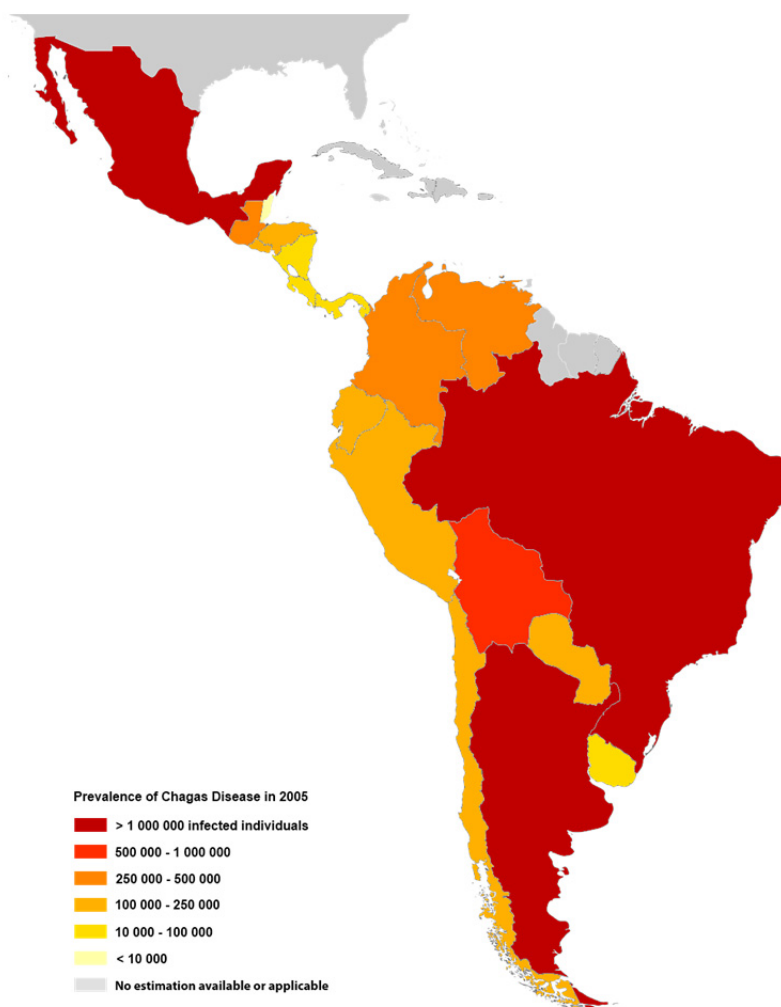


Figure I.7 | Endemic areas of Chagas disease in Central- and Southern-America.

The recent influx of immigrants from endemic regions to countries of the North hemisphere contributed to the spread of the disease in non-endemic areas. Thus, Chagas disease is becoming an important health issue in the United States, Canada and many countries of Europe and western Pacific. With more than 300 000 individuals, the USA has the highest number of infected immigrants, mainly coming from Mexico, followed by Spain (about 50 000 individuals).⁴⁴

Clinical presentation

Chagas disease evolves in three successive phases. Following contamination and an incubation period, the acute phase is characterized by a high parasitic charge, both in bloodstream and tissue, and non-specific symptoms. During the subsequent long-term undetermined phase, patients are seropositive but asymptomatic. Finally, the chronic phase of the disease usually occurs ten to thirty years after the infection and is characterized by severe life-threatening symptoms that lead to premature deaths.⁴⁵

Acute phase

The incubation period in human being usually takes two to ten weeks after exposure to infected triatomines bugs or up to few months in case of transfusion or transplantation of contaminated material. Further to this period starts the acute phase of the Chagas disease. Symptoms are mild and usually limited to local inflammation at the site of infection, and non-specific manifestations (fever, anorexia, lymphadenopathy, mild hepatosplenomegaly and myocarditis).⁴⁵ During the acute phase, macrophages and then muscle cells are the primary target for the parasite. The extremely high parasitic charge in bloodstream results in a strong immune response which, as time goes by, achieves a substantial reduction in parasitemia to subpatent concentrations. This marks the end of the acute phase. Mortality during this phase is lower than 10 %.³⁷

Long-term asymptomatic phase

In spite of the immune response of the host, parasites are not completely eliminated and infection of specific tissues, such as muscles or enteric ganglia will continue for years without any specific symptoms. Little by little, intracellular parasitic colonization severely damaged the structural integrity of organs. These injuries may be caused either by cell lysis, due to parasitic invasion itself, or by the host's acute immuno-inflammatory response, or both. As soon as symptoms associated to these damages declare, the chronic phase of the disease starts. About 30-40 % of infected patients will develop clinically apparent chronic phase, whereas 60-70 % will stay in the long-term asymptomatic phase for the rest of their life.³⁷

Chronic phase

Chronic phase of Chagas disease mainly involve cardiac, digestive or cardiodigestive symptoms. In chronic Chagas heart disease, a low-intensity, slowly evolving myocarditis leads to disorder in contractile function. The progressive destruction of the cardiac muscle and the resulting fibrosis dramatically increase the risk of heart failure and ventricular arrhythmias.³⁷ Sudden cardiac arrest is the main cause of death in this pathology (65 %), followed by refractory heart failure (25-30 %) and thromboembolism (10-15 %).⁴⁶ On the other hand,

chronic Chagas gastrointestinal disease predominantly affects the oesophagus or colon with the development of corresponding mega-oesophagus or mega-colon pathologies. They both refer to a wide dilation of the tract (oesophagus or colon), associated with trouble in smooth muscle contractions and partial to complete disappearance of alimentary bolus's motility. The mega-oesophagus leads to dysphagia combined with epigastric pain, regurgitation, pytalism, and malnutrition in severe cases. An increased prevalence of cancer of oesophagus was observed in patients with mega-oesophagus. Mega-colon produces prolonged constipation, abdominal distension, and occasionally large bowel obstruction.³⁷ Gastrointestinal manifestations are less life-threatening than cardiac impairments, though very disabling in daily life.

Treatments

Vector control

Efforts in controlling Chagas disease have been undertaken in various regions of America since the early 1990's. Chemical control with insecticides used to be questioned because of the risk of environmental pollution and human toxicity. However, synthetic pyrethroids that are now used, exhibit low direct and indirect toxicity, while their insecticide properties allow a huge reduction in triatomine invasion.⁴³ In the meantime, improvements in housing and health conditions limit the contact of infected triatomines with human being and stop the spread of the disease. Finally, laboratory bioassays performed on blood samples and solid organs efficiently decreased the number of contamination due to medical procedures.³⁹⁻⁴¹ These initiatives have successfully led to an overall 50% reduction in the number of infected individuals between 1980 and 2005.^{37,45}

Therapeutic response

The therapeutic response for Chagas disease involves both antitrypanosomal drugs and treatments to cure the symptoms of the chronic phase of the disease. Protocols for treatments of the later are now well established and rely on safe and efficient drugs or surgery. Therefore, we will only focus on the antiparasitic aspect of the therapeutic response.

Currently the antiparasitic response is exclusively based on two approved drugs: nifurtimox (Nfx) and benznidazole (Bz) (Figure I.8).

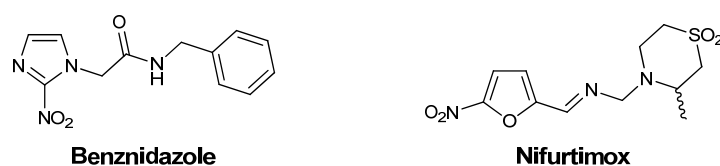


Figure I.8 | Approved drugs for the treatment of Chagas disease.

Benznidazole has the best safety and efficacy profile, and therefore is used for first line treatment. Typical dosage for adults is 5 mg/kg per day orally for 60 days.³⁷ Dermatitis (20-25% of patients), digestive intolerance (5% of patients), polyneuritis, depression of bone-marrow and toxic hepatitis, are the most severe side effects. Other side effects such as anorexia, headache, exhaustion, myalgia or insomnia are more common but normally do not force the patient to stop the medication.^{7,45} The mode of action of Bz is still unclear. However, it is usually accepted that covalent bonding of nitro-reduced derivatives of Bz to parasitic macromolecules –such as DNA– might be involved.⁴⁷

Although it was the first marketed drug for the treatment of Chagas disease, nifurtimox is now recommended as a second line treatment, mainly due to its severe side effects. Typical dosage for adults is 8-10 mg/kg per day orally in three divided doses for 90 days. Side effects usually include anorexia, weight loss, psychic alteration, excitability or sleepiness, nausea, vomit, intestinal colic, diarrhea, skin rashes, peripheral neuritis, bone-marrow depression, and loss of memory.⁴⁵ Due to the high risk of teratogenicity and genotoxicity, pregnant women should not be treated with nifurtimox. As for Bz, the mode of action of Nfx is still discussed. However, Nfx is believed to act as redox cyler, perturbing the redox equilibrium of the parasite. This point will be discussed in details in the last section of this chapter.

Despite a potent activity in acute phase of the disease, with a recovery rate higher than 80 %, these two drugs have very limited effect in the chronic phase.⁴⁵ In addition, the several side effects of these drugs, combined to the long term treatment, are responsible for premature stop of the treatment in numerous patients, increasing dramatically the risk of parasite selection and appearance of resistance.³⁷

Table I.3 | Treatments used in Chagas disease.

INN (DoA) ⁶	Brand name	Mode of Action ⁶⁷	Dosing ³⁷	Side effects	Cost of a full treatment ^a
Benznidazole (1974)	Rochagan [®] (Hoffman-La Roche)	Unknown. Covalent bonding of nitro-reduced derivatives of Bz to parasitic macromolecules might be involved.	5 mg/kg po daily for 60 days	Anorexia, headache, fatigue, myalgia or insomnia, dermatitis, digestive intolerance, polyneuritis, depression of bone-marrow, toxic hepatitis.	3 US\$ ^b
Nifurtimox (1970)	Lampit [®] (Bayer)	Perturbation of the redox equilibrium by redox cycling and thiols depletion. Resulting oxidative stress kills the parasite.	8-10 mg/kg po per day in 3 divided doses for 90 days	Anorexia, weight loss, psychic alteration, excitability or sleepiness, nausea, vomit, intestinal colic, diarrhea, skin rashes, peripheral neuritis, bone-marrow depression, loss of memory, teratogenicity.	94 US\$

^a For a patient weighing 35 kg, based on exchange rate of 1 € = 1.25 US\$. ^b Courtesy of Dr. R. Passemard, Hôpitaux Universitaires de Strasbourg (personal communication). Abbreviations: INN = International Nonproprietary Names, DoA = Date of Approval (or of first described curative use), IM = Intramuscular, IV = Intravenous, po = per os

Leishmaniasis

Leishmaniasis is a group of parasitic diseases caused by at least twenty different species of the kinetoplastid parasites named *Leishmania*. This great variety in the species implies a wide spectrum of clinical manifestations which are usually divided into three major pathologies: Cutaneous Leishmaniasis (CL), Visceral Leishmaniasis (VL) and, to a lesser extent, Mucocutaneous Leishmaniasis (MCL).⁴⁸

Parasite's life-cycle

Leishmania parasites enter the mammalian host following the bite of specific sandflies belonging to the *Phlebotomus* species (Figure I.9, step ①). Promastigotes –infective forms of the parasites– are phagocytized by macrophages and other types of mononuclear phagocytic cells, ②. Once inside the cells, promastigotes transform themselves into the tissue form of the parasite, named amastigote. Under this specific form, parasites are able to multiply by simple cellular division, ③. This multiplication proceeds until the damaged host cell explodes, liberating parasites which can then infect other cells of various tissues (including macrophages), mostly depending on which *Leishmania* species is involved, ④. In turn, the mammalian host is now able to transmit infected cells to sandflies during blood meals, ⑤. In sandflies, amastigotes transform themselves into promastigotes, develop in the midgut (⑥,⑦), and migrate to the pharyngeal tract (proboscis), ⑧. At this stage, sandflies infect a new mammalian host during the next blood meal.

More than thirty species of *Phlebotomus* can transmit leishmaniasis. Each of these species has its own living area, its own lifestyle, and usually transmits one specific species of *Leishmania*.⁴⁹ The vector-borne transmission is all the more facilitated as other mammals are playing the role of reservoir; in particular, dogs are the main reservoir for *Leishmania* parasites, although leishmaniasis are often asymptomatic in these animals. As example, in southern-France, prevalence of *L. infantum* in dogs was evaluated to 80%, of which 68% were asymptomatic.⁴⁹ Besides the transmission by vectors, inter-human contamination might occur. Parasites can go through the placenta and infect unborn child, while transplantations and transfusion were reported to be at risk in endemic areas, and, though to a lesser extent, also in non-endemic areas.⁵⁰⁻⁵² However, in developed countries, transmission through syringes of drug addicts remains the main source of inter-human contamination.⁵³

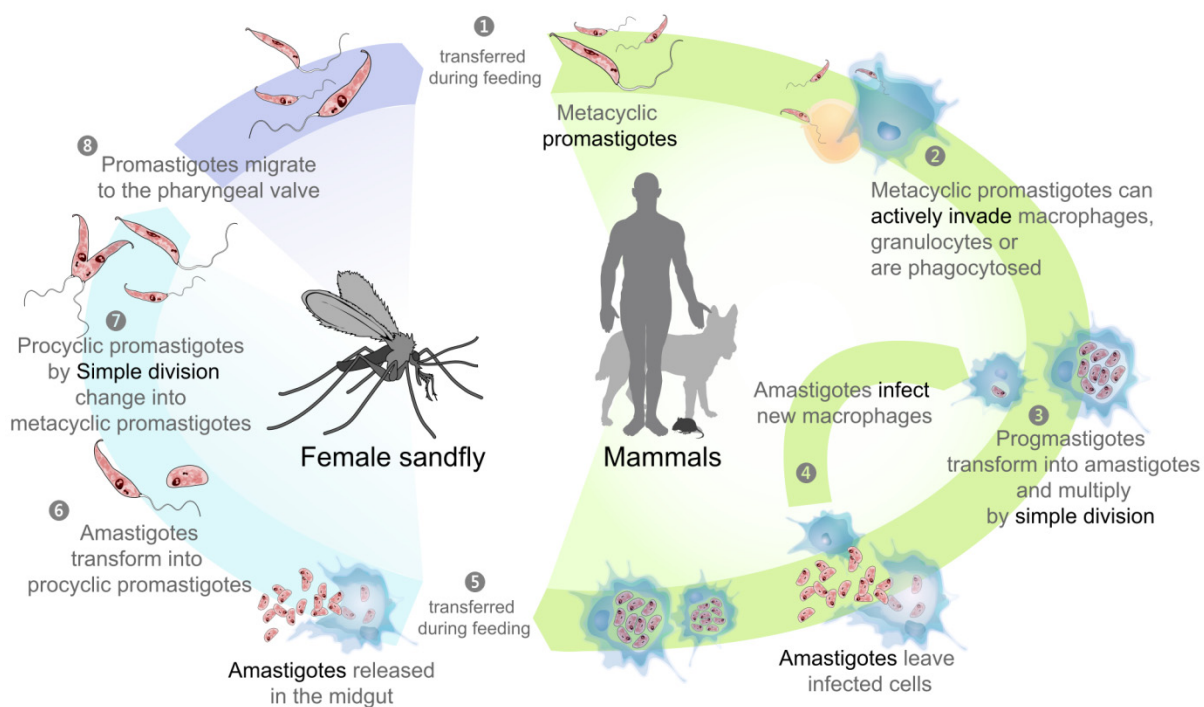


Figure I.9 | *Leishmania* parasite's life cycle.

Epidemiology

The multiplicity of vectors also explains the large spread of leishmaniasis, which are endemic in about 90 countries, representing a population at risk of 350 million people (Figure I.10).⁷ It is important to notice that leishmaniasis are not restricted to developing countries. Climate changes, travels and population movements contribute to the spread of the disease to the Mediterranean coasts of developed countries (e.g. France, Italy, Spain, Greece ...).⁴⁹ WHO estimates that currently 12 million people are infected, with an incidence of 500 000 cases of visceral Leishmaniasis and 1.5-2.0 million cases of the cutaneous form each year.⁵⁴

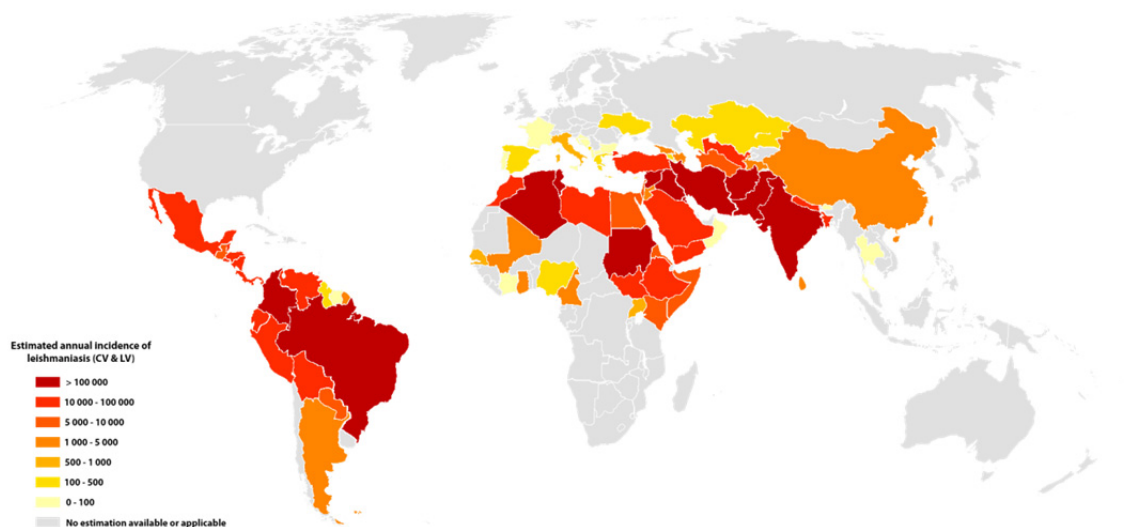


Figure I.10 | Endemic areas of leishmaniasis. Data from ref.⁵⁵

Leishmaniasis can also arise through epidemic episodes as it was the case in southern-Sudan in the 80's when one third of the population was decimated by VL.⁵⁶ This epidemic was a dreadful example of how socio-economic factors and wars can influence the course of the diseases. Indeed, numerous studies have reported that population movements, malnutrition and poor health conditions occurring during wars dramatically contributed to both the spread and the development of the disease. It is also important to notice that co-infection with Human Immunodeficiency Virus (HIV) is a major aggravating factor as it increases the risk of developing the disease by a factor of 100 (*vide infra*).⁵⁷ This may explain the spread of leishmaniasis in countries where HIV is also widespread and not under control.

Clinical presentation

About twenty species of *Leishmania* (e.g. *L. major*, *L. tropica*, *L. aethiopica*, *L. guyanensis*, *L. infantum*, *L. mexicana*) cause CL and some are also known to induce the visceral form of the disease. The species causing VL in Africa, Asia and Europe are *L. donovani* and *L. infantum*. In America *L. chagasi* is predominant for VL infection. Thus, depending on the infective species and on the global health condition of the patient, the clinical presentation ranges from long-term asymptomatic carriage to severe alterations of vital functions. It is somehow interesting to notice that, for immunocompetent patients having a healthy lifestyle, leishmaniasis is normally asymptomatic. Thus, in southern-France, *L. infantum* asymptomatic carriage was evaluated by Polymerase Chain Reaction (PCR) to 58% of the population.⁵⁸ However, as soon as the immune system of the host is weakened, leishmaniasis turns to an acute phase, which usually includes erratic fever, splenomegaly and cytopenias.⁴⁹ These non-specific symptoms make it more complex to diagnose the diseases which can only be confirmed by western blot (WB) or, even better, by PCR. As it has already been mentioned, the expression of the disease is mainly triggered by immuno-compromising conditions, including malnutrition, viral infection (e.g. hepatitis, HIV...), or immuno-suppressive treatments. In the case of HIV co-infection, the disease is evolving far more quickly and intensively. Indeed, both *Leishmania* parasites and HIV virus target immune cells, leading to a deleterious synergistic effect on the immune response.⁵⁷ In addition, it has been demonstrated that some drugs used for the treatment of leishmaniasis might stimulate the replication process of the virus. *In fine*, more than 30% of the patients who have been diagnosed with leishmaniasis were co-infected with HIV.⁵⁸ And this figure can raise above 50% in highly HIV-spread endemic areas. If left untreated, acute visceral leishmaniasis is lethal due to the infection of several vital organs, especially liver. Cutaneous and mucocutaneous leishmaniasis are normally less dramatic as patient may survive the diseases, but huge scars, disfigurements or limbs injuries are very disabling in daily life.

Treatments

Unlike some other parasitic diseases such as malaria, the control of the spread of the disease is complex and almost inefficient. Indeed, each of the thirty species of *Phlebotomus* live in a different manner, either in the field or in the houses and the canine reservoir is so important and so contaminated that it is almost impossible to eradicate this source of propagation. Thus the only way to reduce the impact of the disease is to cure infected mammals by medical treatments.⁴⁹

Unfortunately, as for trypanosomiasis, treatments are mostly based on drugs that date back over fifty years and that suffer from poor efficacy, high toxicity, and, above all, increasing resistance. Historically, first-line treatments are pentavalent antimonials meglumine antimoniate and sodium stibogluconate (Figure I.11).⁵⁹ Recovery rates of these cheap drugs were initially higher than 95%, but they now suffer from resistance which finally forced countries like India to give up their use as they are now no longer effective. This was reinforced by the toxicity profile of antimonial drugs which ranges from reversible intolerance to severe life-threatening intoxication.

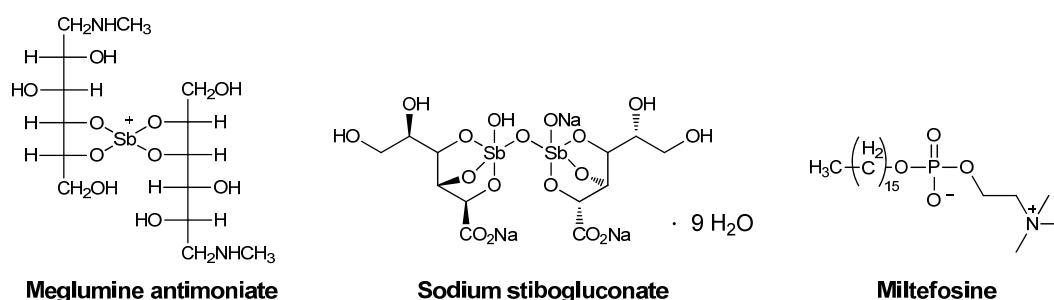


Figure I.11 | Drugs used to cure leishmaniasis.

Ten years ago, a new alternative oral treatment for VL emerged with the use of miltefosine (Figure I.11), which was originally developed for antiproliferative purpose.^{7,49} Although this drug allows recovery rate above 90% in *L. donovani* infections, its efficiency towards *L. infantum* is rather low. Furthermore, miltefosine exhibits severe gastrointestinal side effects, its teratogenicity makes it contraindicated in women of childbearing age, and resistance to this drug has already been reported. Research for new anti-leishmanial compounds has shown that amphotericin B (Figure I.12) exhibits interesting activity, with recovery rate higher than 95% and no reported resistance.^{7,49} The nephrotoxicity of the drug is efficiently overcome by the use of a liposomal formulation. The major drawback of this treatment is its high cost (above 250 U.S.\$ for an average course) which drastically restricts its use in poor leishmaniasis-endemic areas.

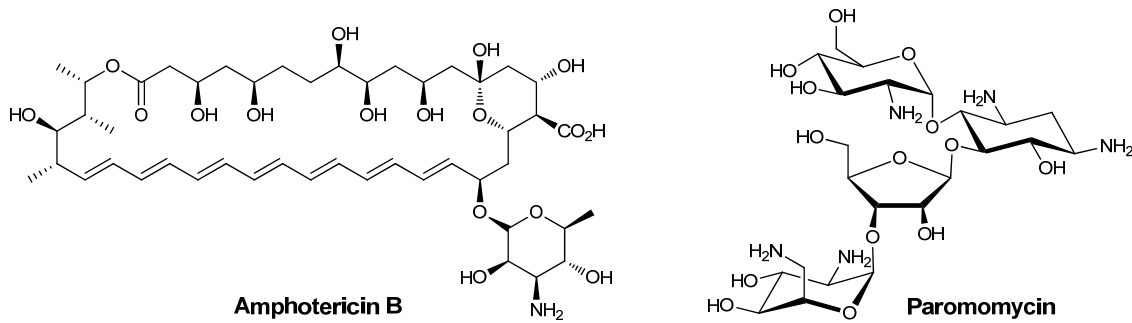


Figure I.12 | Drugs recently approved for their use in antibiotherapy against *Leishmania* parasites.

In 2006, paromomycin (an aminoglycoside antibiotic, Figure I.12) was registered in India for the treatment of leishmaniasis. Clinical trials have shown its excellent efficacy and safety with no nephrotoxicity.⁷ Considering its low-cost (15 U.S.\$ per treatment), and if these results are confirmed on a larger scale, paromomycin might be an acceptable alternative to amphotericin B. Nevertheless, as for all antibiotics, a wide use of paromomycin would certainly lead to arise new cross-resistances in other pathogens, including bacteria.

Table I.4 | Treatments used in leishmaniasis.

INN (DoA)	Brand name	Usage	Mode of Action	Dosing ⁵⁵	Side effects	Cost of a full treatment ^a
Meglumine antimoniate (1950) ⁶	Glucantime® (Sanofi-Aventis)	CL & VL	Unclear. Parasite-mediated reduction in toxic Sb(III) species, inhibition of parasite's macromolecular biosynthesis, and activation of host immune system have been proposed. ⁵⁹	20 mg/kg IM per day 20 days of treatment for CL 30 days of treatments for VL	Pancreatitis, dyspnea, rash, dizziness, headache, face oedema, abdominal pains; increased liver enzyme activity.	39.5 US\$ (CL) 59.3 US\$ (VL)
Sodium stibogluconate (1945) ⁶⁰	Pentostam® (GSK)	CL & VL	Assumed similar to Glucantime	20 mg/kg slow IV per day 20 days of treatment for CL 30 days of treatments for VL	Phlebotoxicity, thrombosis, pancreatitis, loss of appetite, metallic taste in mouth, nausea, vomiting, diarrhea, headache, tiredness, joint pains, muscle aches, dizziness, anaphylaxis.	37.2 US\$ (CL) 55.8 US\$ (VL)
Miltefosine (2002) ⁶	Impavido® (Zentaris)	VL	Induction of a process of programmed cell death (apoptosis-like death). ^{61,62}	100 mg po daily for 28 days	Nausea, vomiting, abdominal pains, teratogenicity.	65-150 US\$
Liposomal amphotericin B (1997) ⁶³	AmBisome® (Gilead)	VL	Destruction of membranes of <i>Leishmania</i> parasites by binding of Amphotericin B to ergosterol has been proposed. ⁶³	20 mg/kg IV for 2-4 days	Nausea, vomiting, rash, dyspnea, dizziness, headache, fever, chill, tachycardia, hypokalemia.	252 US\$
Paromomycine (2006)	Humatin® (Monarch)	VL	Inhibition of protein synthesis by targeting several of the proteins involved in the translational machinery, in particular the ribosomal ones. ^{64,65}	15 mg/kg po daily for 21 days	Nausea, vomiting, abdominal pains.	15 US\$

^a For a patient weighing 35 kg, according to ref. ⁵⁵

Abbreviations: INN = International Nonproprietary Names, DoA = Date of Approval (or of first described curative use), IM = Intramuscular, IV = Intravenous, po = per os

Drug discovery in trypanosomatid diseases

Target Product Profile of antiparasitic

As any other process of discovery, developing a new drug requires a well-defined preliminary study. Results of such a study will be used to define the Target Product Profile (TPP) of the desired drug.⁶⁶ A simple definition of the TPP would be "a collection of clinical specifications of the intended drug". Thus, the TPP is listing the entire essential criteria needed for the desired drug to be clinically successful. The TPP aims at being a strategic planning and decision-making tool dedicated to research.⁶⁷ Though the TPP is defining essential criteria for the progression from one phase of the development to another, its most useful role is to remove from the pipeline any series of product that does not meet these criteria, and this as early as possible in the process. Therefore, the sooner the TPP is defined, the better it is, as it may significantly reduce the risk of wasting time and money on series that will never end-up in a clinical successful drug.

In practice, the TPP has to contain information about the therapeutic area, the spectrum of activity, the targeted population, the desired drug regimen, the acceptable level of toxicity and safety profile, and the stability. Marketing information –such as the final cost of the treatment or the expected return on investment– are often included in the TPP,⁶⁷ however this is not the initial aim of the TPP. TPP is dedicated to medicinal chemists, biologists and clinicians; it is not supposed to be a business tool.⁶⁶ Antiparasitic drug development is a specific field which requires a slightly different TPP compared to the ones defined for drugs dedicated to "traditional" diseases of the developing world. As an example, we summarized basic TPP for trypanosomatid diseases in Table I.5.^{67,68} For a practical insight, we correlated some essential criteria to their chemical implications. In addition, as the cost of the drug is a major "chokepoint" in antiparasitic drug discovery, it was included in the TPP, despite the previously mentioned remarks.

Table I.5 | Target product profile of antitrypanosomatid drugs. Adapted from ref. ^{6,67,68}

Essential specifications	Chemical implications
General desired features for a drug against trypanosomatid diseases	
Active against all species and all strains of the considered parasite	
Short course of treatment (≤ 14 days)	
Oral formulation preferably	Compound soluble in polar medium, or adequate formulation of it
Injectable with reduced treatment time acceptable	Compound soluble at blood pH, or adequate formulation of it
Stable under tropical conditions (shelf life > 2 years)	Avoid sensitive function, use stable substitution pattern Start early studies on chemical and thermal stability
Safer than available treatments	Compounds free of heavy metals.
Safe for children and pregnant women	Limit the use of molecular structures identified as potentially toxic and teratogenic. Plan an early assessment of cytotoxicity.
Low potential of developing parasite resistance	Adapt the molecular structure according to the metabolism pathway to obtain an adequate half-life. Avoid structures that are deemed to have already raised resistances (e.g. melamine core of melarsoprol).
Cheaper than current treatments	Short synthesis based on affordable and commercially available starting material.
Human African Trypanosomiasis	
Active against melarsoprol refractory strains	Avoid amino-purine transporters for uptake in parasite
Efficacy against early and late-stage desirable	Adjust polarity of compounds to allow them to cross the brain blood barrier
Injectable for late-stage acceptable	
Chagas disease	
Active against blood and tissue form of the disease	
Active in chronic forms of the disease	
Leishmaniasis	
Active both in visceral and cutaneous leishmaniasis	
Topical application for CL desired	Adjust polarity of compounds to allow them to cross the skin or create adequate formulation of them

Besides the optimization of the activity, the TPP for antiparasitic drugs highlights the three main challenges for medicinal chemists: the optimal balance between solubility, stability, and safety. In the context of endemic developing countries with few clinical facilities, an oral formulation is always preferable. This normally implies a polar molecule liable to solubilize in aqueous medium at physiological pH. However, this has to be counterbalanced by the possible need to target the central nervous system, as it is the case for late-stage of human African trypanosomiasis. Solubility is also important for *in vitro* assays that may be biased if the tested compound is not much soluble. The second parameter that needs to be taken into consideration is the stability of the drug. Once again, populations at risk mainly live in tropical regions; hot and humid climate associated to a limited access to adequate storage conditions put a strong strain on chemical entities. Sensitive substitutions, and especially thermal sensitive ones (> 30 °C), have therefore to be banned from the substitution pattern of leads and candidates. Finally, the safety issue is probably the most important point in antiparasitic drug development. We already mentioned that most of the drugs currently in use induce

severe side effects. It is therefore crucial that new drugs developed for these therapeutic applications show a better safety profile. However, this goal is all the more difficult to achieve as several parasitic biological pathways, including detoxification ones, are very similar to their mammalian equivalents. Thus, it is very challenging to develop a drug that would selectively kill parasites and not human cells. This will be one of the major goals of the drug discovery process. Although these three requirements might be satisfied through the usual medicinal chemistry drug discovery process, the contribution of formulation and galenic must not be underestimated. Indeed, specific encapsulated systems might advantageously deliver toxic drugs to targeted parasites with a limited toxicity toward human cells; liposomal formulation of amphotericin B is a successful example of such an approach.⁶⁹

The drug discovery pipeline

Three approaches can be used for the development of new treatments: combination of existing drugs, new indication for existing drugs, and *de novo* drug discovery.^{68,70} The two first approaches are obviously quicker and less expensive as they rely on products which have already been thoroughly studied and approved. In spite of interesting results –as for nifurtimox-eflornithine combination therapy, the raise of resistances and the scarce library of antiparasitic drugs drastically limit these strategies. We will therefore focus our attention on the last approach, the *de novo* drug discovery.

De novo drug discovery is a long and costly process which requires the synergy of numerous domains of science, from chemistry through biology, genetics, informatics and clinical studies. It focuses on the identification of new potent chemical entities and on the synthesis and evaluation of analogues. However, "*de novo*" does not mean that researchers are starting from scratch. They usually have a precise starting point; this may be a well-described validated biological target, a synthetic molecule or class of molecules that exhibit interesting potency, or a natural product which has beneficial effects toward the disease. At the same time, the development of a biological assay to determine the activity of compounds is also required *via* one of the following two different approaches: phenotypic assays or target-based assays. As the choice between these two methodologies is often questioned, discussion on this specific point will be given later (*vide infra*). Whatever the selected method, the assay must be reliable, reproducible, easy to perform with the highest throughput as possible, and at an acceptable cost. Once these preliminary parameters are set, the drug discovery process can be launched. This iterative process is typically carried out in several discrete stages (Figure I.13).⁶

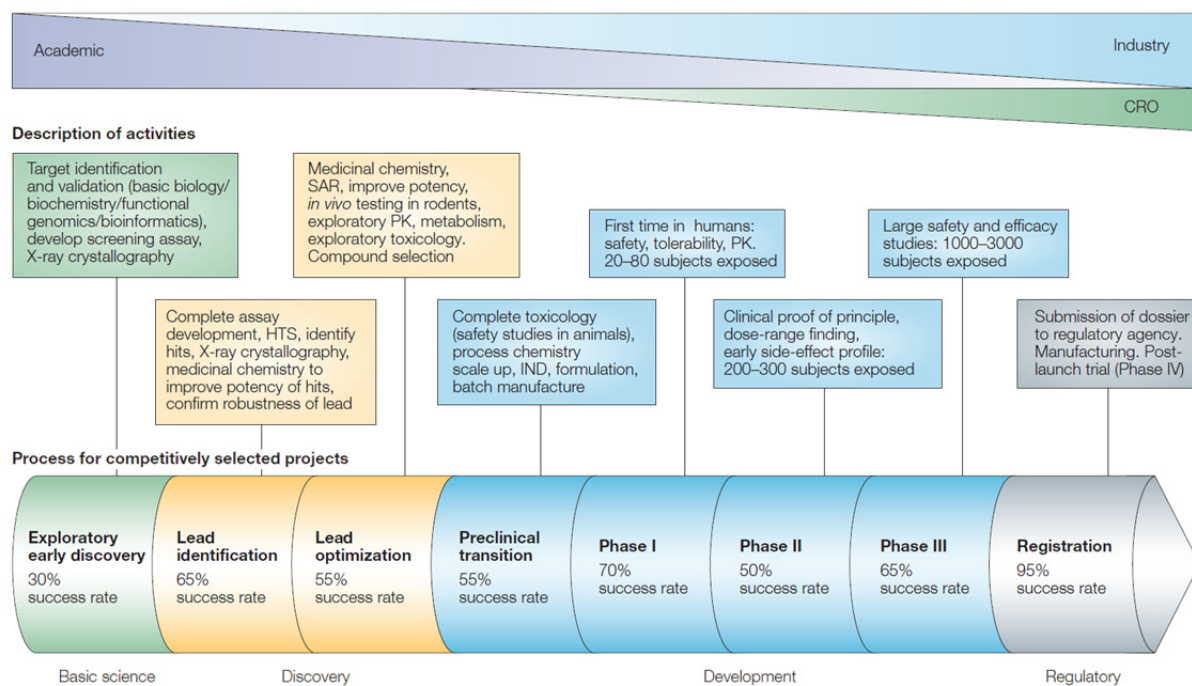


Figure 1.13 | The drug discovery pipeline. According to ref. ¹³.

HTS, high-throughput screening; IND, Investigational New Drug application; PK, pharmacokinetics; SAR, structure–activity relationships.

From the identified hits, a broad library of analogues is synthesized by medicinal chemists. Potency of these molecules is next assessed and, depending on the results, a structure or a substitution pattern is selected to define lead compounds. During the subsequent lead optimization stage, medicinal chemists carry out modifications of the structure and analyze the effects on the activity; this step is commonly known as the Structure Activity Relationship (SAR) study. For each new compound, the potency, as well as several other parameters related to Absorption, Distribution, Metabolism, Excretion, and Toxicity (ADMET) are evaluated to be optimized. Out of thousand molecules synthesized, only about six candidates will enter the next clinical development phases.⁸ The research work of the organic medicinal chemist usually stops at that point, leaving further studies to experts in development, formulation and scale-up for the chemistry part, and to biologists and clinicians for the medical part.

Statistically, it takes at least 12 years to put a new anti-infective drug on the market, half of this time being dedicated to clinical development and approval phase.^{67,71} Each drug successfully approved for clinical use has required an investment of about 800 million US\$.⁶⁷ Considering this huge cost, starting any new project is at risk, especially with respect to the high attrition rate in drug development. Indeed, only 1 out of 5 projects survive through preclinical development and less than 1 out of 10 enters clinical development and finally leads to approval.⁶⁷ This high and costly attrition rate is mainly due to compounds that fall down in the late stages of the clinical trial. Reasons for such failures are numerous: a target not being a chokepoint in the network of metabolic pathways, a lack of efficacy in human, ADMET issues

etc. Although this risk is inherent to drug discovery, several authors agree on the fact that an adequate choice of the method to assess potency, and an extensive knowledge of the parasitic biological pathways that are "druggable" (i.e. that can be targeted by a drug), should limit in a great extent the risk of failure.^{6,67,68}

Different strategies to assess the potency of compounds

As previously mentioned, choosing the proper method to assess the activity of molecules is crucial. Two methods are available: phenotypic assays or target-based assays. The goal of this rapid review is not to determine whether one method is better than the other, but to summarize briefly specificities, advantages and drawback of these complementary approaches.

Phenotypic assays are the historical way to determine the potency of compounds. It consists in incubating the whole cells with the product of interest and in subsequently observing the biological response of the system. The main advantage of this methodology is that the assay is performed on a whole complex system; the drug needs to find access to its own target by crossing the membranes and surviving to the cell's detoxification system.⁷² Considering the strong similarity between this *in vitro* assay and the *in vivo* complexity, results obtained through the phenotypic approach usually translate in biological and clinical response. Another advantage of the phenotypic approach is that it does not require a precise knowledge of the target and of the Molecular Mechanism Of Action (MMOA), multiple targets are evaluated concomitantly inside the whole cell.^{72,73} However this may also be considered as a drawback. Indeed, the phenotypic approach is similar to a "black-box", putting together a compound and an extremely complex system with a limited knowledge of their possible interactions.⁷² This lack of knowledge on the relation between the structure of the molecule and its biological effects makes the optimization work very difficult for medicinal chemists. In most of the cases, further improvements in the potency and in the pharmacological properties of compounds usually require the target and the MMOA to be elucidated, which can be a very long and challenging research.⁷³

On the other hand, the **target-based approach** relies on a precise knowledge of a biological target, which is essential for the activity. This methodology arose in the 1990's with the expansion of genetics. Sequencing of genomes allows a better understanding of the biological function of numerous targets such as enzymes, receptors, or ion channels. Subsequent expression of genes encoding these targets allows the purification of the proteins and thus their use in isolated assays. Screening technologies are well established in this

domain and can be performed in high-throughput.⁷² In addition, X-ray crystallography and resolution of three-dimensional structures provide important structural information about ligand-interacting cavities and mechanism of catalytic processes. This is the rationale of a structure-based drug design where homology model or 3D dockings methods are used to improve the fit of a molecule inside a target. Using these modern tools, medicinal chemists can easily identify whether a part of the molecules is essential for the activity or not, and thus can improve both the potency and the ADMET profile of the compound. However, this approach also suffers from several limitations.^{6,72} The most awkward is that target-based activity often does not translate into biological response once *in vivo*. There can be several explanations to this drawback. Being conducted on the isolated target, such an assay does not evaluate the ability of compounds to go across biological membranes and to survive to detoxification systems. In addition, the entire approach is based on the selection of one unique target. However, the validity of this target must be questioned before starting the project. Indeed, biological structures, such as enzymes or receptors, are part of a network with cross-talk and homeostatic control mechanisms; evolution has tailored this complex system to ensure the robustness of pathways critical to life. Therefore, feedbacks loops, metabolic by-pass or genetic knockdown of the target might significantly limit the clinical activity of drugs that have been selected through the target-based approach. Kinetic considerations are also disregarded in this approach. For example, a drug that irreversibly inhibits an enzyme which is immediately regenerated by the cell is completely useless. As an example, we already mentioned the case of DFMO which is inactive toward *T. b. rhodesiense* due to such kinetic effects (*vide supra*). It is therefore essential to take into account lifetime and regenerating time of the target, as well as the kinetic profile of the drug candidate, which is not the case in target-based assay. Furthermore, target-based approach sometimes leads to an excessive focus on the optimization of the affinity at a given target with little regard to the other essential parameters of a drug (e.g. ADMET profile). *In fine*, out of the 75 first-in-class small drugs with a new MMOA that have been approved between 1999 and 2008, only 17 (23%) were discovered through target-based assays (Figure I.14).⁷³ To date, eflornithine is the only antiparasitic drug that has been successfully translated into a clinically used drug following a target-based approach of ornithine decarboxylase.

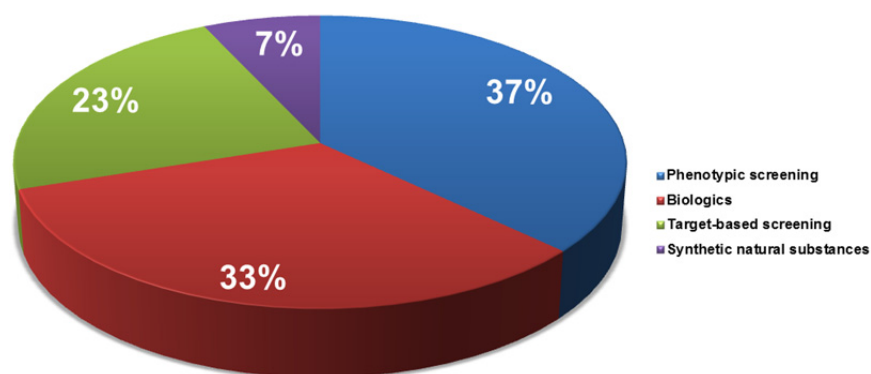


Figure 1.14 | The distribution of new drugs discovered between 1999 and 2008, according to the discovery strategy.

To summarize, we can say that there is no ideal approach. Choosing one approach or the other will depend on the disease, on the availability of whole-cell or target-based assays, and on the affordability of them. An optimal way to proceed would be to conciliate the best of the two methods, while keeping in mind that, to be efficient, a drug needs to act on an essential pathway, with a broad specificity among various druggable targets.⁷²

Druggable targets or biological pathways in trypanosomatids

The genomes of the three major trypanosomatids parasites were completely sequenced and published in 2005.^{74–76} It demonstrated that each genome contains about 10 000 protein-coding genes, of which 6 200 are common to all three genomes.⁷⁷ This later point highlights the high similarities existing between *T. brucei*, *T. cruzi* and *Leishmania spp.*, and thus the opportunity of developing a drug which might target similar and essential pathways in all the trypanosomatid parasites. At least, this reinforced the absolute necessity to always test compounds over the three species of trypanosomatids. This major breakthrough was crucial for the discovery and the elucidation of some of the most promising pathways in the search for potential anti-trypanosomatid drug. In the following section, we will describe some of these biochemical pathways and targets. However, this brief description is definitely not exhaustive; here will only be considered the most promising pathways, and especially the most distinct as compared to the mammalian host.

Glycolytic pathway

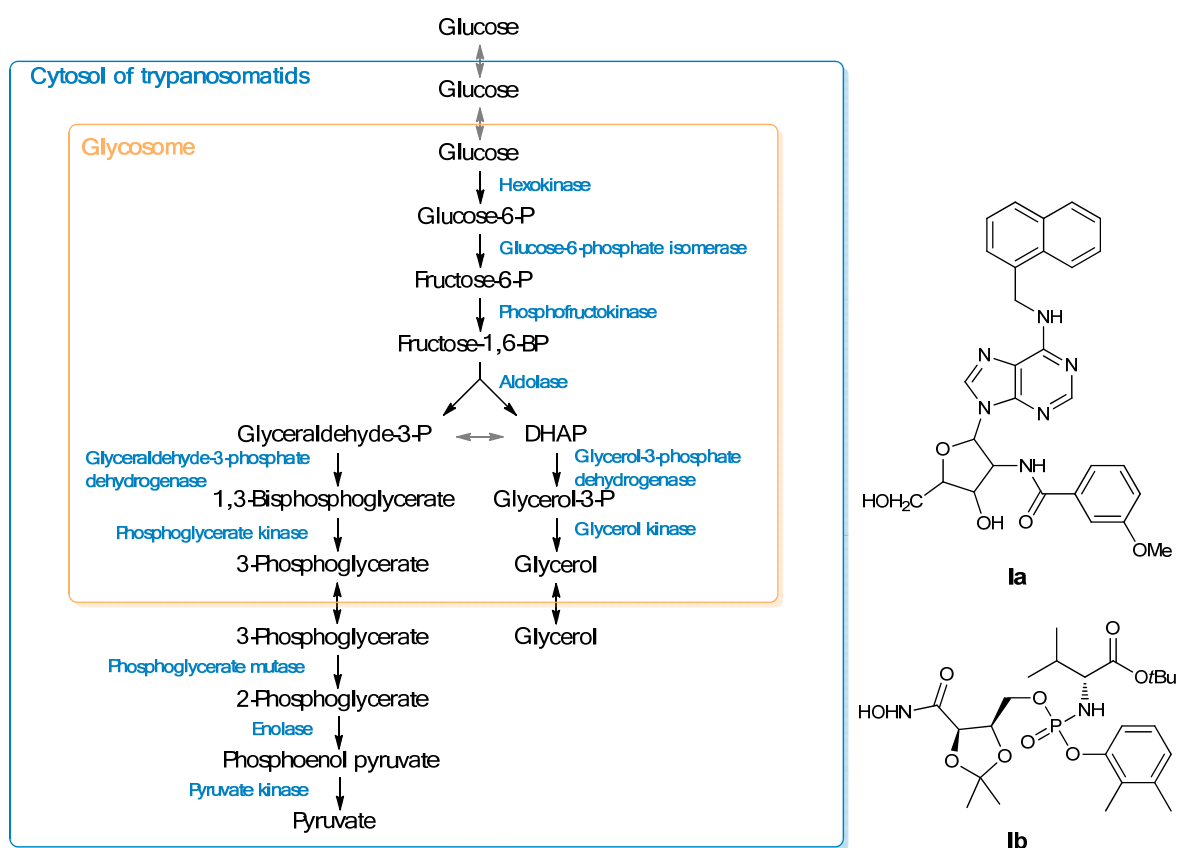


Figure I.15 | Description of the glycolytic pathway in trypanosomatids (left) and two examples of drugs in development that are targeting this pathway (right).

Trypanosomatids lack a functional Krebs cycle. Therefore, the energy metabolism of parasites, and especially the synthesis of adenosine-5'-triphosphate (ATP), only relies on the glycolysis of carbohydrates uptaken from the host (Figure I.15). Seven glycolytic enzymes are responsible for this activity and their coding-sequence was found to be very different from their mammalian's counterparts.⁵⁴ In addition, parasitic enzymes are compartmentalized in the glycosome, a peroxisome-like organelle, which is a unique feature of trypanosomatids.⁷⁸ Considering these two specificities, the glycolytic pathway is regarded as a very interesting target for the design of new anti-trypanosomatid drug. One of the first most promising agents was product **1a** (Figure I.15), an analogue of adenosine targeting the glyceraldehyde-3-phosphate dehydrogenase. This product was evaluated toward *L. mexicana* and showed a very promising activity, inhibiting growth of parasites with an IC_{50} value of 0.28 μM .⁷⁹ More recently, a series of phosphoramidates targeting the 6-phosphogluconate dehydrogenase enzyme was synthesized and evaluated toward *T. brucei brucei*. Several compounds have proved to be very potent, and the most active one was product **1b** (Figure I.15) with a trypanocidal activity of 8 nM.⁸⁰

Sterol pathway

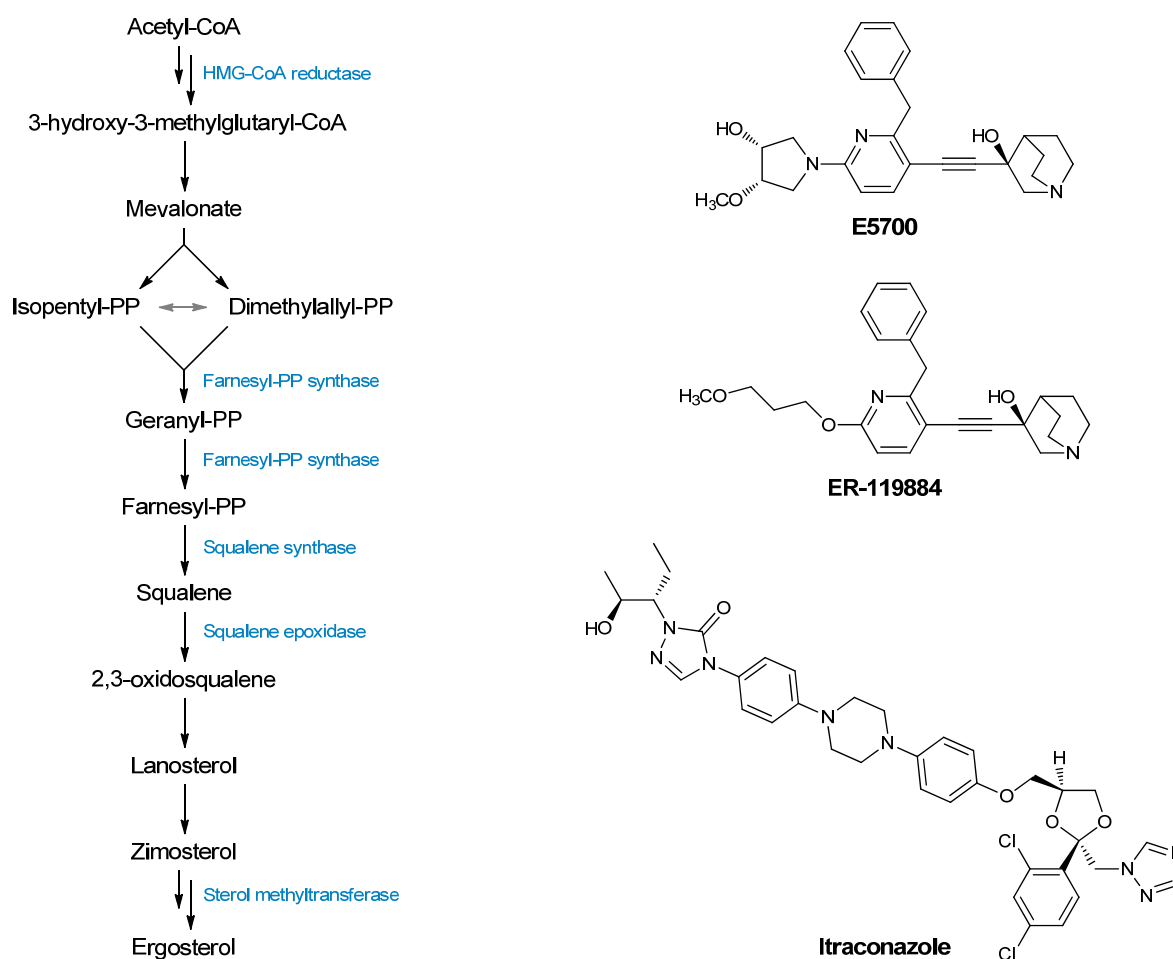


Figure I.16 | Description of the sterol pathway in trypanosomatids (left) and three examples of drugs in development that are targeting this pathway (right).

Unlike mammalian cells for which cholesterol is a major component of membrane sterol, trypanosomatids synthesize ergosterol and other 24-methyl sterols for cell viability and proliferation. Biological pathway to the synthesis of ergosterol involves numerous enzymes (Figure I.16). Inhibition of some of these enzymes has been proved to be effective against these parasites and the pathway is therefore considered as an important drug target.⁵⁴ In that matter, itraconazole (Figure I.16) was one of the most promising compounds against *T. cruzi* infection.⁴⁷ Although it was very potent both *in vitro* and *in vivo* in rodent, clinical trials were less successful. Over the 135 patients suffering from chronic Chagas disease treated with itraconazole, parasitological cure and normalization of the electrocardiogram (ECG) was observed in only 36.5% and new ECG abnormalities appeared in the 48.2% of the patients after treatments.⁸¹ In spite of these disappointing results, azoles are still considered as a promising series, and newer, and probably more effective, trypanocidal triazoles are currently under study.^{82,83} More recently, novel arylquinuclidine derivatives developed as cholesterol-lowering agents, were shown to be potent *in vitro* growth inhibitors of both proliferative stages of

Leishmania amazonensis.⁸⁴ Thus, compounds **ER-119884** and **E5700** (Figure I.16) displayed IC₅₀ values of 10 and 30 nM respectively against *L. amazonensis* promastigotes. It was demonstrated that these two compounds were very potent noncompetitive inhibitors of native *L. amazonensis* squalene synthase, leading to depletion of the parasite's main endogenous sterols. Further investigations on this promising series, especially *in vivo* and toxicity assessments, are currently under development.

Purine metabolism and salvage pathway

Being involved in the synthesis of the ATP, of the DNA bases nucleoside triphosphates and of several other important endogenous molecules, purines are indispensable to all life. Unlike their mammalian and insect hosts, trypanosomatids lack the metabolic machinery to biosynthesize purine nucleotides *de novo* and must therefore rely on preformed purines available in the hosts. These are captured through the so called "purine salvage system" and next converted into various substrates essential to parasites by several enzymes.⁵⁴ This pathway is known since decades and three main options have been described to target it. One of the first ways would be to block the uptake of purines at the membrane of the parasite. Several transporters have been identified but their amount and diversity make the design of efficient and selective inhibitors very challenging.⁵⁴ Nevertheless, this pathway remains a promising target as parasitic transporters are very different from mammalian's ones. On another way, once internalized in the parasites, dephosphorylated purines are transformed into nucleoside monophosphate. 3-phosphoribosyltransferase (PRT) is the enzyme that catalyzes this specific reaction and might therefore be targeted. Allopurinol (Figure I.17) was developed against Chagas disease on this base. Considering the potency of this compound both *in vivo* and *in vitro*, it was progressed to the clinical phase. However, variable results were obtained and, in the best case, only 44% of the patients were cured from *T. cruzi* infection.^{45,81} These disappointing results might be explained by the fact that PRT was subsequently demonstrated not to be essential for parasites' survival. Targeting the uptake and metabolism of purines seems thus rather problematic.

The third possibility is slightly different from the first two ones. Here the aim is not to deprive parasites of purines, but just to use the pathway to internalize drugs that will subsequently act on another target. This strategy was widely applied as it is the rationale of the uptake of melarsoprol and pentamidine.²⁶ Pentamidine analog pafuramidine (Figure I.17) was similarly developed and progressed to clinical trials. However, due to toxicity issues, the development of this molecule was stopped in phase III. Novel arylimidamides were recently synthesized and evaluated for their use in the treatment of visceral leishmaniasis.⁸⁵ In particular, **DB745** and **DB766** (Figure I.17) were exceptionally active (IC₅₀ < 0.12 μM) against

intracellular *L. donovani*, *L. amazonensis*, and *L. major* and did not exhibit mutagenicity in an Ames screen. Most notably, **DB766** (100 mg/kg per day for 5 days) reduced liver parasitemia in mice and hamsters by 71% and 89%, respectively.

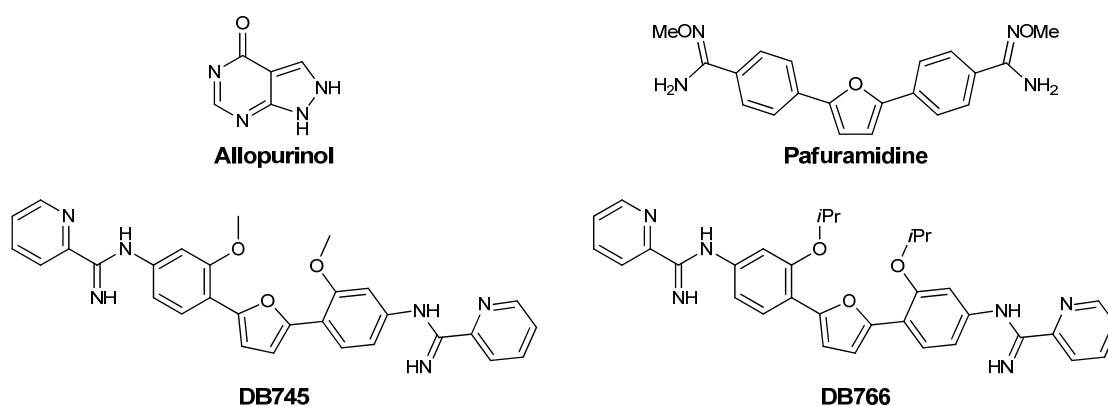


Figure I.17 | Drugs that are targeting the purine pathway to fight trypanosomatids.

The opportunity of developing new drugs that are targeting purine transporters to be internalized might be questioned with respect to pentamidine or melarsoprol resistance. Indeed, it is now well known that melarsoprol-resistance is mainly due to genetic mutations of purine transporters, and can therefore affect the potency of any new drug that is using P2 transporters for its uptake in parasite.²⁸ However, several sub-types of P2-transporters are involved in the uptake of amidine- or melamine-based drug, resulting in several by-pass for the internalization of these drugs. In addition, it has been demonstrated that parasites which develop numerous genetic mutations at different purine transporters are highly weakened, therefore becoming sensitive to the immune response of the host.⁸⁶ As a result, drugs that are targeting purine transporters are still of high interest.

Polyamine pathway

Polyamines are ubiquitous small cationic molecules required for growth and proliferation in eukaryotic cells and in most bacteria. They play an important role in several biological processes, including gene expression, chromatin structure and stabilization, ion channel regulation, and, in general, they are substrates for the synthesis of numerous more complex endogenous molecules.⁸⁷ One of this polyamine –the spermidine– is crucial for trypanosomatids. Indeed, this molecule is required for the synthesis of trypanothione, an essential dithiol responsible for maintaining the redox homeostasis in the parasite (*vide infra*).^{45,87} Depletion in spermidine might lead to the death of the parasite through oxidative stress. Furthermore, parasites lack the regulatory control mechanism of polyamine biosynthesis that is found in mammals, and enzymes implied in this biosynthesis differ significantly between the parasite and the human host.⁴⁵ With regards to these specific features, the polyamine pathway can therefore be considered as a promising target. The most

important example in this area is eflornithine which targets the ornithine decarboxylase enzyme (*vide supra*). Besides this successful molecule, few compounds were developed to specifically target the polyamine pathway of parasites. However, a huge amount of data has already been collected on the inhibition of the polyamine pathway for cancer therapy.⁸⁸ There is no doubt that the compound collection will play an important part in further drug-combination screening of antiparasitic drugs that target the polyamine pathway and another synergetic chokepoint.

Trypanothione pathway

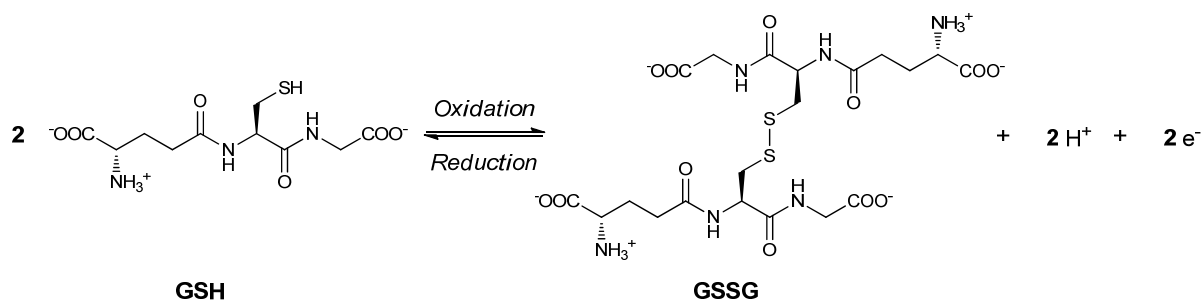
The mammalian redox defense system is based on oxidized glutathione and glutathione reductase (GR). This system is replaced in trypanosomes by an analogous, but different, system based on trypanothione and trypanothione reductase (TR). This enzyme is unique to trypanosomatids and is responsible for maintaining trypanothione in its reduced dithiol form. Therefore, it plays a crucial role in the thiol redox metabolism and is essential for parasites to resist to oxidative attacks of host's immune system.⁸⁹ Due to these findings and the structural differences between the parasite enzyme and host glutathione reductase, the whole system based on trypanothione/TR has been identified as a promising target for anti-trypanosomatid drug development. Numerous products targeting this system have been proposed, including marketed melarsoprol and nifurtimox. Considering the expertise of the laboratory in redox active compounds and the previous studies performed on this topic, the trypanothione pathway was the target of choice for the present thesis. Therefore, this system will be described in details in the next part of this chapter.

The trypanothione pathway and the redox equilibrium inside parasites

Oxygen is vital for aerobic living organisms that are using it in many biological reactions, from cells respiration and metabolism, to immune response. However, these reactions are usually associated with the formation of reactive oxygen species (ROS) such as hydrogen peroxide, superoxide anion or hydroxyl radical. Accumulation of such ROS can be life-threatening as they might damage several biological structures through oxidation. There is therefore a need for a strict control of the redox potential inside the cells. Although the general mechanism of action of the redox control is similar in mammals and in trypanosomatids, the two systems differ in the nature of the enzyme and of the low-molecular thiol that are involved.

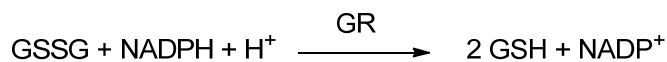
Redox homeostasis in humans and parasites

In humans, the couple glutathione/glutathione reductase is responsible for redox homeostasis within cells.^{90,91} First, glutathione (GSH) is a low-molecular tripeptide composed of the amino acids, glycine, cysteine and γ -glutamic acid. Glutathione in its reduced form represents the most abundant intracellular non-protein thiol and is in equilibrium with its oxidized form glutathione disulfide (GSSG) (Scheme I.2).



Scheme I.2 | Redox half-reaction of glutathione.

The thiol group of glutathione is the reactive entity which confers its redox properties to the tripeptide. Indeed, oxidizing agents are reduced by two molecules of GSH, resulting in the formation of one molecule of glutathione disulfide and two protons (Scheme I.2). The chemical reduction allows the destruction of ROS and other deleterious molecules. However, glutathione is consumed in this step and without a regenerating system it would be difficult for cells to sustain high glutathione fluxes. Concomitantly to the *de novo* synthesis of glutathione, the role of the glutathione reductase enzyme is to maintain glutathione pulses. Glutathione reductase (GR, E.C. 1.8.1.7, formerly EC 1.6.4.2) is a homodimeric flavoenzyme belonging to the family of oxidoreductases. The main function of GR is to catalyze the reduction of glutathione disulfide to its thiol form glutathione at the expense of NADPH (Scheme I.3).



Scheme I.3 | Reduction of glutathione disulfide to glutathione by the enzyme glutathione reductase.

The mechanism of this reaction involves several steps (Figure I.18). At first, the electrons are transferred from NADPH, *via* the FAD isoalloxazine ring, to a cysteine disulfide residue, ①. This forms a charge transfer complex between the isoalloxazine ring and the thiolate anion of Cys 63, ②. In the second step, the cysteine thiolate Cys 58 reacts with the disulfide bridge of GSSG forming a transient covalent mixed disulfide intermediate, ③. His 467' acts as a proton donor/acceptor in the reaction. Finally, the oxidized enzyme is regenerated, while glutathione is released by an attack of the neighbor thiolate Cys 63 on the mixed glutathione-enzyme disulfide bridge, ④.⁹²

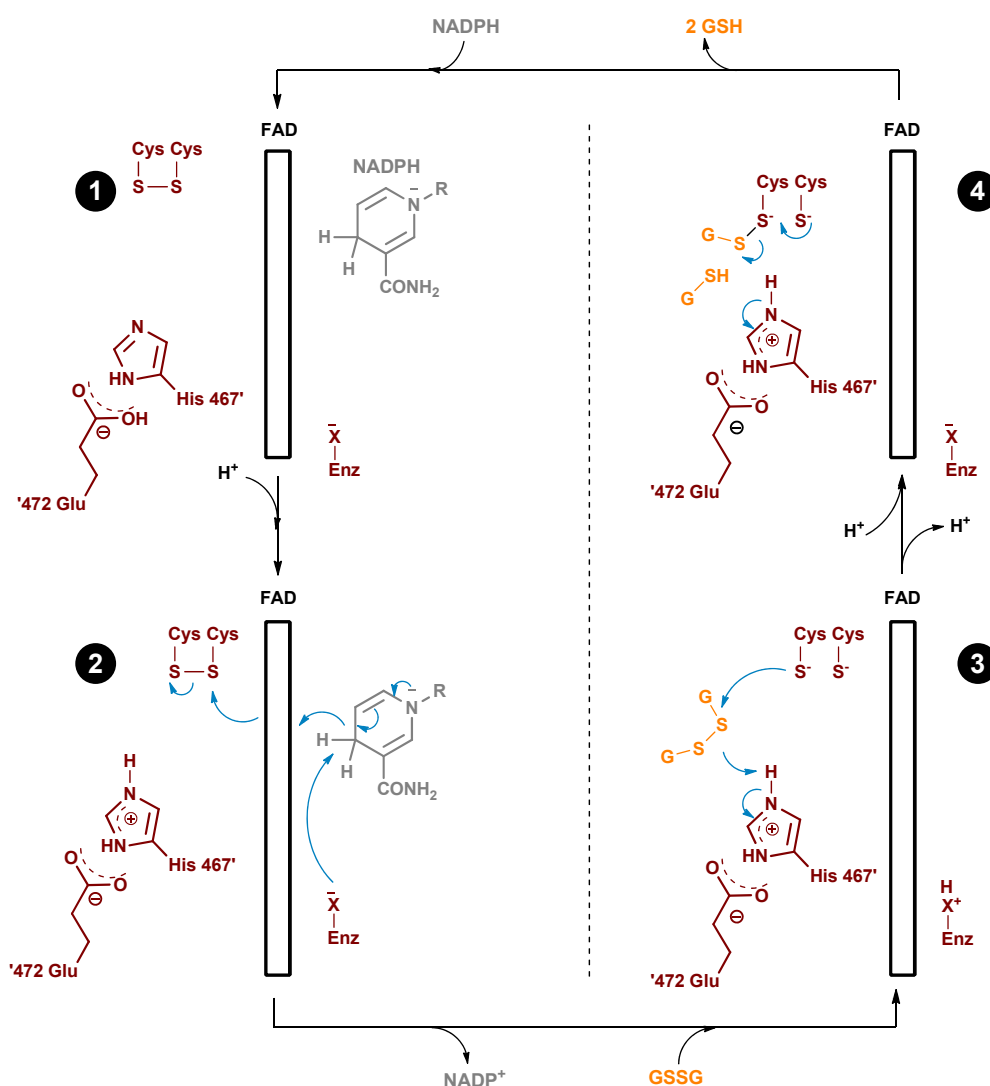
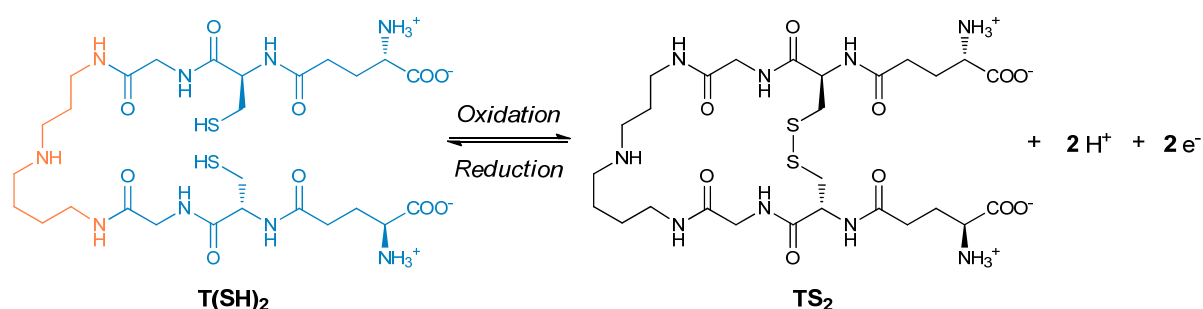


Figure I.18 | Enzymatic mechanism of the glutathione disulfide reduction by glutathione reductase

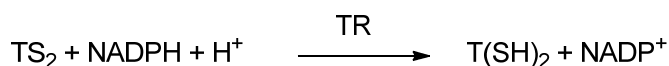
Through this enzymatic reduction, the glutathione is regenerated to its ground reduced state, ready to reduce in turn a new oxidized entity, allowing to maintain the redox potential within the cell.

By contrast, trypanosomatids solely rely on the trypanothione/trypanothione reductase system instead of the GSH/GR system of mammals. This unusual system is exclusively found in all kinetoplastid parasites and *Euglena algae* cells.^{93–95} In trypanosomatids trypanothione is replacing glutathione as major thiol in parasitic cells. It is a low-molecular weight dithiol composed of two glutathionyl units (Scheme I.4, in blue) linked by a spermidine (in orange) through amide bonds at the glycine residues.⁹⁶



Scheme I.4 | Redox half-reaction of trypanothione.

Like glutathione, trypanothione (T(SH)₂) is oxidized by oxidizing agents to trypanothione disulfide (TS₂) through the creation of an intramolecular disulfide bridge between the two glutathionyl units. In trypanosomatids, the equivalent of GR is trypanothione reductase (TR, EC 1.8.1.12). This homodimeric flavin adenine dinucleotide (FAD)-containing enzyme also belongs to the family of NADPH-dependent oxidoreductases. And like GR, TR is responsible for maintaining trypanothione in its reduced dithiol form (Scheme I.5).



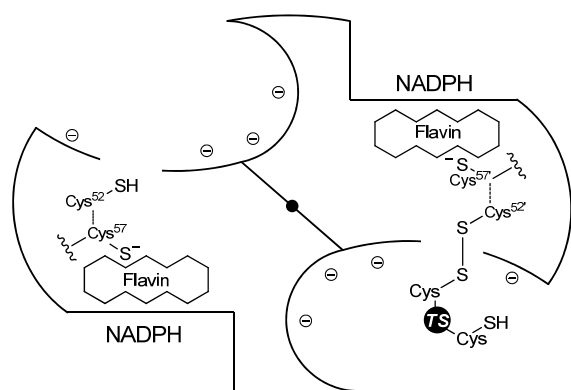
Scheme I.5 | Reduction of trypanothione disulfide to trypanothione by the enzyme trypanothione reductase.

The TR enzyme has been subjected to less mechanistic studies, however, it is suggested that its mechanism should be similar, if not identical, to that of GR.

Although these two systems seem very similar, it is important to point out several differences that can be useful for the design of drug targeting the trypanothione pathway. Regarding the two enzymes structure, GR and TR share about 41% identity.⁹⁷ However, TR/GR substrate recognition is ruled by a difference in the charge of the active site which makes these enzymes mutually exclusive towards their disulfide substrates (Figure I.19).⁹⁸ Indeed, the active site of TR is negatively charged due to Glu 18, while an Arg residue at the cognate position 37 in GR gives a positively charged one.⁹⁹ Additionally, the active site of TR can accommodate

larger ligands and is more hydrophobic due to Met 113 and Trp 21. This specific hydrophobic pocket of TR can interact with substrates through cation- π and π - π interactions.^{89,100}

a) Trypanothione reductase



b) Glutathione reductase

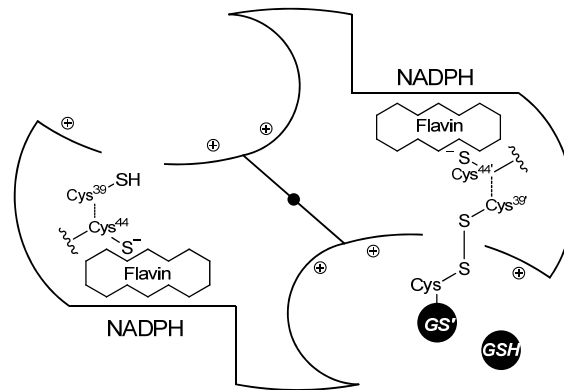


Figure 1.19 | Comparison of the active sites of trypanothione reductase (a) and glutathione reductase (b).

In addition, on a reactivity point of view, it is interesting to notice that trypanothione is rather more reactive than glutathione.¹⁰¹ Indeed, although glutathione is a better nucleophile than trypanothione, the latter is more reactive because it is more ionized in a large pH range. This specificity might be advantageously used to obtain selective drugs that target the trypanothione pathway. With regard to the uniqueness of the trypanothione pathway and to the specific differences between the two enzymes and thiols, the redox-regulating system of trypanosomatids is considered as a very promising target for future therapy.

Targeting the trypanothione pathway

Two components of this pathway are unique to trypanosomatids; therefore, it might be considered either to inhibit the activity of trypanothione reductase, or to deplete the *de novo* biosynthesis of trypanothione. A third approach would be a combination of the first two with the use of subversive substrates. In the following, we will describe in detail these three possibilities to target the trypanothione pathway.

Direct thiol depletion

The ability of the trypanothione system to maintain the redox homeostasis within the parasite partly relies on the reactivity of thiols of trypanothione. Any molecule able to form thiol-adducts will therefore have a dramatic impact on trypanosomatids survival. Indeed, a rapid and massive thiol depletion prevents the parasite from detoxifying the ROS resulting both from its own metabolism and from the host immune system. This oxidative stress leads to the death of parasites. Such a mechanism of action was postulated for numerous anti-trypanosomatid drugs, including melarsoprol,²² benznidazole,⁴⁷ meglazole,¹⁰² and, to a lesser extent, nifurtimox.¹⁰³ The main disadvantage of such an approach is that thiols are widely present in endogenous molecules including mammals' ones. Forming thiol adducts with

human proteins or with glutathione greatly increases the risk of toxicity toward the host. To achieve this strategy successfully, compounds have to react as most selectively as possible with trypanothione, and, above all, they must be quickly internalized with a great selectivity inside the parasite. Melarsoprol is an example of this strategy as it is composed of a melamine motif allowing a rapid drug uptake and an arsenic atom, prone to react with thiols.

Trypanothione reductase inhibition

As we mentioned in the previous part, one of the prerequisites for an enzyme to be employed as a drug target molecule is that it should be essential to the parasite. Different genetic (RNA interference, knock-out),^{104,105} chemical (inhibitors), and metabolomics (analysis of the trypanothione and polyamine pathways) approaches have unequivocally shown that TR is essential. Thus, bloodstream African trypanosomes with less than 10% of wild-type TR activity were unable to multiply but remained alive.¹⁰⁵ In the same experiment, these knocked-out parasites *tr* were highly sensitive towards hydrogen peroxide and were unable to induce parasitemia in mice. These results proved that the *de novo* synthesis of trypanothione and residual levels of TR are sufficient to maintain resting thiol levels, but insufficient to cope with oxidative stress situations. TR is therefore a validated drug target for anti-trypanosomatid drug discovery. Considering their ability to alkylate thiols, trivalent arsenical drugs were suggested as irreversible inhibitors of trypanothione reductase. Thus, it has been demonstrated that melarsen oxide, the active metabolite of melarsoprol (*vide supra*), is a potent inhibitor of TR *in vitro*, through alkylation of cysteine residues in the active site of the enzyme.¹⁰⁶ However, this enzyme inhibition is far from being selective, and melarsoprol tends to react with any nucleophile, including trypanothione and mammalian's thiols which definitely confers its toxicity to the drug. Facing this selectivity issue, many promising lead compounds that inhibit TR have been identified through a target-based approach.¹⁰⁷ Thus, polyamines derivatives,¹⁰⁸ tricyclics,¹⁰⁹ and aminodiphenyl sulfides,^{110–113} turned out to be very potent in *in vitro* enzymatic assays (Figure I.20). Unfortunately, up to now, none of these compounds selected for TR inhibition has been successfully transposed clinically.

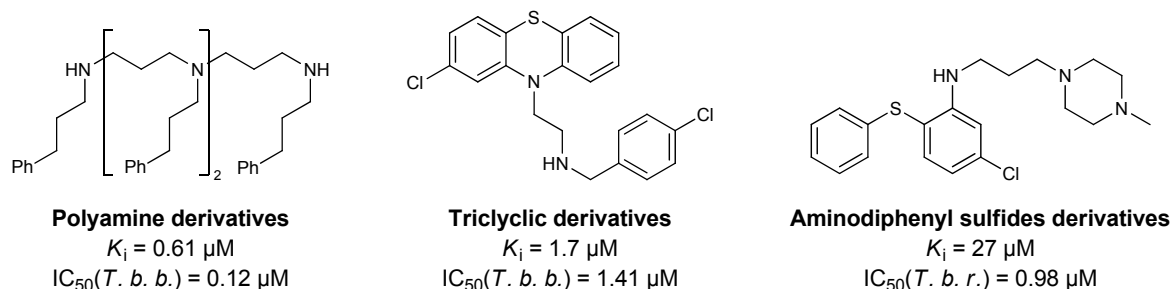
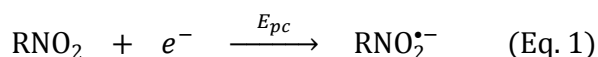


Figure I.20 | Examples of compounds in development that are targeting the trypanothione pathway.

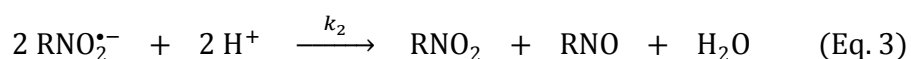
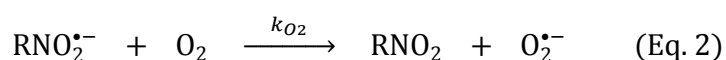
Subversive substrate approach

The term subversive substrate (or turncoat inhibitor) is defined from a pharmacological perspective; it indicates that this compound switches the physiological function of the enzyme to the opposite.^{114,115} In order to give a better understanding of this concept, we will take the molecular mechanism of action of nifurtimox as an example.

It is now well admitted that nifurtimox is a good substrate of TR. The one electron reduction of the nitro group of nifurtimox leads to the formation of a radical anion (Eq. 1).¹⁰²



Subsequent quenching of this nitro-anion radical can follow two different pathways. The radical anion can react with molecular oxygen, resulting in the regeneration of nifurtimox and in the formation of superoxide anion (Eq. 2),¹¹⁶ or it can dismutate into the relative nitroso compound, nifurtimox, and water (Eq. 3).¹⁰²



Electrochemical studies have demonstrated that the reaction kinetic with molecular oxygen is very fast, the first pathway (Eq. 2) thus prevailing over the second one.¹¹⁶ As nifurtimox is regenerated, it is again available to be reduced by TR, causing a continuous activity of the enzyme to the detriment of the natural substrate, the trypanothione. This permanent cycle is usually called *redox cycle* or *futile cycle* because of the continuous waste of NADPH (Figure I.21). The redox-active substrate is called *redox-cycler* or *subversive substrate* or *turncoat inhibitor*.

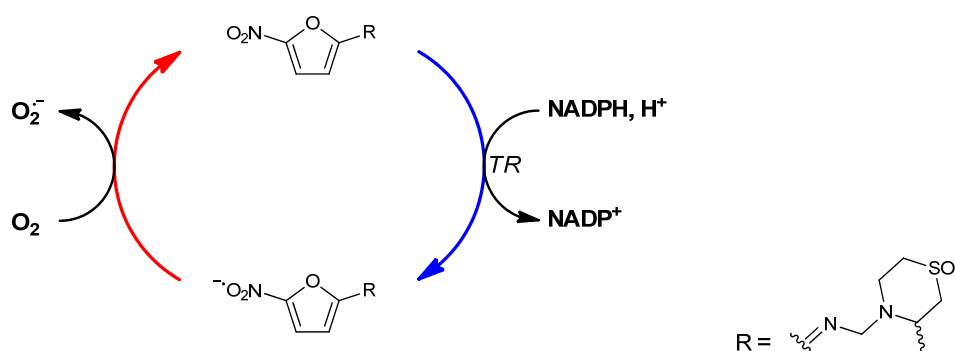


Figure I.21 | Redox cycle of nifurtimox in aerobic conditions.

However, this is only one part of the MMOA of nifurtimox. According to (Eq. 2), the decay of the radical anion leads to the formation of superoxide. As the parasite is particularly sensitive to ROS, the production of superoxide might contribute to the antiparasitic effect of the drug.

Finally, recent metabolic studies performed with nifurtimox have evidenced a nitroreductase-mediated formation of new cytotoxic nitrile metabolites (Michael acceptors) liable to react with several cellular components, including thiols.¹¹⁷

To summarize, nifurtimox, and subversive substrates in general, have three main deleterious effects on parasite metabolism:¹¹⁴

- they inhibit the reduction of disulfides causing trypanothione depletion,
- they generate reactive oxygen species and free radicals, and
- they cause futile consumption of NADPH.

Nifurtimox was the first drug with this MMOA to be approved for the treatment of Chagas disease. Although very active on the acute phase of the disease, nifurtimox is of no use at the chronic stage. In addition, the drug still induces some severe side effects. However, as this subversive substrate approach has proven its efficacy, extensive studies –mainly focused on nitroaromatics– were done. Among these data, we present here the few examples of compounds that were promising leads *in vivo* in animal models.

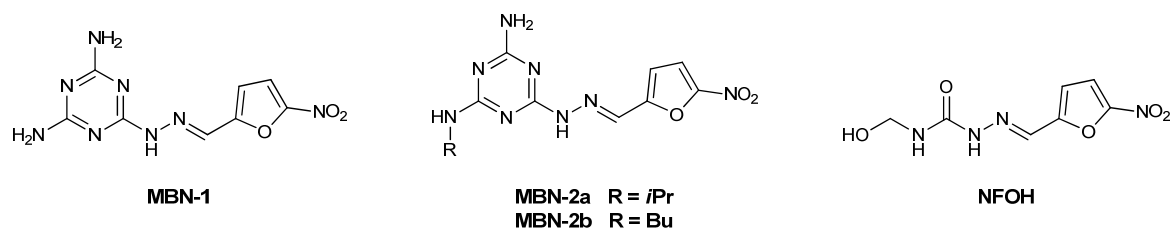


Figure I.22 | New subversive substrates currently in development.

In order to gain in selectivity *versus* the host cells, the vectorization through the aminopurine transporters was investigated with the evaluation of melamine-based nitrofurans (**MBN**, Figure I.22).^{118,119} In *T. brucei brucei*-infected murine model, **MBN-1** cured all mice at a dose of 20 mg/kg for four days, even with P2-deficient trypanosome mutants. With compounds **MBN-2a** and **MBN-2b** (Figure I.22), *T. brucei rhodesiense*-infected mice were treated at a dose of 50 mg/kg intraperitoneally for four days. Once again, all mice were cured with an appreciable survival time (> 30 days). In spite of a toxicity increase toward L6 cells, no overt sign of toxicity was found in mice.¹¹⁹ Recently, product **NFOH-121** was suggested as anti-trypanosomatid candidate (Figure I.22). This is a prodrug of nitrofurazone, one of the first active nitrofurans which was withdrawn from the market due to its toxicity. The activity of **NFOH-121** was evaluated *in vivo* in a murine model of Chagas disease.¹²⁰ The group treated with the **NFOH-121** displayed the lowest mortality rate (16%), followed by benznidazole (33%), placebo (66%)

and finally nitrofurazone (75%). Therefore, this molecule emerges as a promising candidate for antitrypanosomatid treatments.

To summarize, all the results obtained through these three approaches demonstrate that the trypanothione pathway is one of the most promising targets in the field of anti-trypanosomatid drug discovery. Considering these numerous advantages and the previous studies that have been done (*vide infra*), the trypanothione pathway was therefore chosen as target of the medicinal chemistry project of the present PhD thesis.

Background of the project: from the hit-discovery of Mannich bases with antitrypanosomal activity to the diarylideneacetone series

Mannich bases as potent antitrypanosomal agents

In 2002, a large screening of the Pfizer library (350 000 compounds) highlighted some unsaturated Mannich base as potent inhibitors of *Plasmodium falciparum* thioredoxin reductase (Figure I.23).^{121,122} Further studies demonstrated that these molecules also irreversibly inhibit *T. cruzi* trypanothione reductase.^{123,124} Considering the potential interest of such a new class of antitrypanosomatid agents, the mechanism of inhibition was thoroughly studied (Figure I.24).¹²⁵

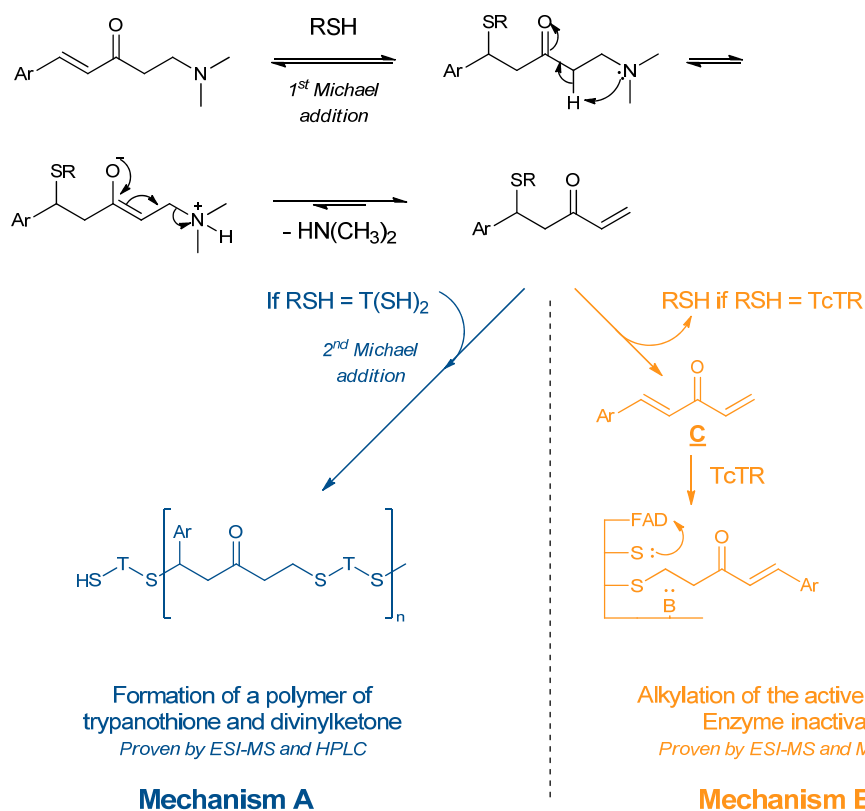
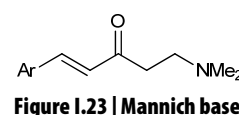


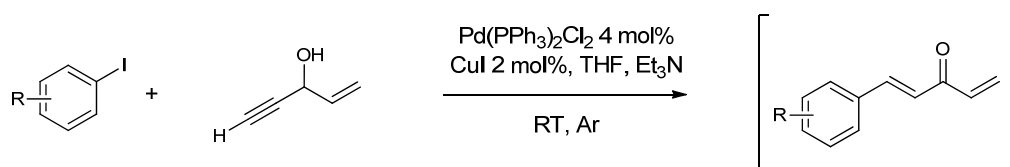
Figure I.24 | Mechanism of action of Mannich bases.

At first, a thiol attacks the double bond of the Mannich base to generate the first reversible adduct (Figure I.24, upper line). Subsequent base-catalyzed elimination of the *N,N*-dialkylamino moiety leads to the formation of a new highly reactive Michael-acceptor. This intermediate can next evolve following two different pathways. In mechanism A (left blue side, Figure I.24), addition of a new thiol, such as trypanothione, allows the formation of an oligomer. Both sides of this oligomer are terminated by a thiol function which can, in turn, react with another highly reactive intermediate, resulting in polymer elongation. On the other hand, in mechanism B (right orange side, Figure I.24), a divinylketone is formed following dethiolation reaction. This intermediate is able to covalently bond the Cys 52 of *T. cruzi* TR active site, leading to an irreversible inhibition of the enzyme. These two mechanisms are responsible for the death of the parasite, probably by thiol depletion.

Once the mechanism of action was elucidated, a broad library of compounds was synthesized and evaluated *in vitro* for anti-trypanosomatid activity by Dr. Nicole Wenzel during her PhD thesis.^{14,125} Unfortunately, in spite of a very good potency, the pharmacokinetic properties of unsaturated Mannich bases were disappointing. Above all, their instability in solution was problematic and not compatible with their use as drug candidates. As a result, there was a need for a new lead structure that would show the same mode of action but without these drawbacks.

The divinylketone, a key intermediate

As demonstrated in the reactivity mechanism, two electrophilic centers are required for the drugs to inhibit the trypanothione pathway (Figure I.24). The divinylketone **C** being identified as an important intermediate for enzyme inactivation, a first approach was to synthesize and evaluate such compounds. Thanks to the nascent collaboration with Prof. Thomas Müller from the University of Heidelberg, Dr. Wenzel used a Coupling Isomerization Reaction (CIR) under palladium catalysis to obtain these molecules (Scheme I.6).^{14,125}



Scheme I.6 | Synthesis of divinylketones through a coupling isomerization reaction.

Unfortunately, the resulting divinylketones were highly reactive and prone to polymerization in solution. Of course, such reactivity was considered incompatible with their use as potential drugs. A new scaffold was therefore required to achieve the design of new drugs with a similar mechanism of action than the one which had previously been described.

The diarylideneacetone scaffold, a new series to explore

Identifying a new molecular core having two electrophilic centers and being stable in solution was therefore the objective. These criteria are met by a well-known structure, the diarylideneacetone core (DAA), namely 1,5-diaryl penta-1,4-dien-3-one (Figure I.25).

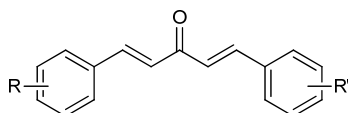


Figure I.25 | General structure of diarylideneacetones.

This scaffold was found to be all the more relevant as it is fairly closed to the natural product "curcumin" (Figure I.26)

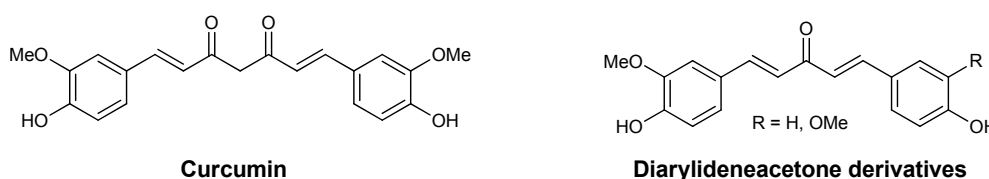


Figure I.26 | Structures of curcumin and diarylideneacetone derivatives that have been identified in *curcuma* extracts.

Curcumin is the major component of extracts of *Curcuma longa* which is the base of turmeric spice. Besides its gustative and food coloring (E100) usage, this spice is known since antiquity for its therapeutic properties.¹²⁶ *Curcuma* extracts have been used in decoction or cataplasm for anti-inflammatory and antioxidant effects.¹²⁷ These ancient prescriptions have been confirmed by modern biological and genomic studies. Thus, it has been proved that curcumin inhibits the transcription factor NFκB (nuclear factor κB) which is involved in the expression regulation of various genes responsible for the synthesis of pro-inflammatory molecules. The down regulation of this pathway by curcumin drastically decreases the inflammatory response.¹²⁶

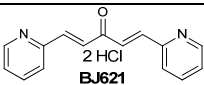
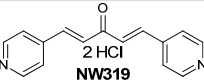
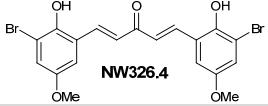
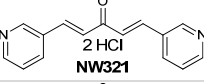
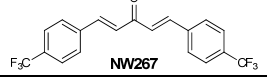
On the other hand, the antioxidant properties of curcumin are due to both the chemical structure of the molecule and its ability to interact with biological targets. Structurally speaking, the enol form of the β-diketone moiety, as well as phenol groups reacts as powerful radical scavengers. Curcumin also acts as a substrate of Nrf2 (nuclear factor (erythroid-derived 2)-like 2) pathway, inducing a biological cascade that triggers the overexpression of enzymes playing a crucial role in redox homeostasis.¹²⁶

Last but not least, the most outstanding application of curcumin is undoubtedly its anticancer activities. Thus, curcumin is currently in clinical trials (phase I and II) for the prevention and the treatment of the most life-threatening cancers (e.g. colorectal cancers, resistant pancreatic cancers).^{128,129}

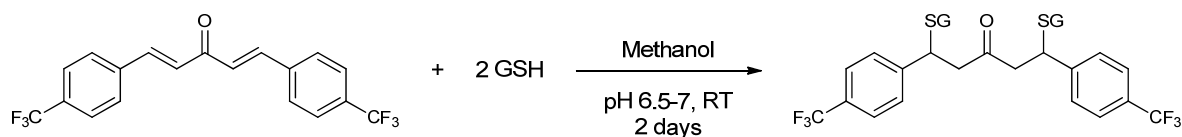
Like curcumin, diarylideneacetone derivatives have many reported medicinal applications. It is noteworthy to mention that some diarylideneacetone derivatives have also been identified in extracts of *Curcuma longa* (Figure I.26).¹²⁷ Like curcumin, these derivatives displayed interesting anti-inflammatory and antioxidant activities.^{130,131} However, the most promising results were obtained in cancer therapy. Indeed, DAA derivatives exhibit growth-suppressive activity against a variety of cancer cells and demonstrate definite chemopreventive properties.^{132–136} Although the mode of action of DAA is still unclear, it has been suggested that a down-regulation of the NFκB pathway might play an important role.^{137,138} More recently, the use of diarylideneacetone derivatives as radiolabelled probes for β-amyloid plaques imaging has been considered.¹³⁹

In spite of these numerous applications, only few studies were reporting the use of curcuminoids or DAA derivatives for antiparasitic purposes.^{140,141} Considering the promising results that she has previously obtained with Mannich bases, Dr. Nicole Wenzel focused her attention on the synthesis and the evaluation of diarylideneacetones as antiparasitic agents. Thus, a library of about twenty symmetric DAA, with various substitution patterns on the aromatic rings was built up during her PhD thesis.¹⁴ Unlike Mannich bases or divinylketones, these products were stable both in solid state and in solution and were therefore screened in parasitic assays. This has allowed the determination of the most active substitution pattern. In terms of potency, the results were excellent, with IC₅₀ values in the nanomolar range for the pyridine substituted derivatives (Table I.6). However, unsurprisingly, the antitrypanosomal activity of these molecules was associated with high toxicity (in the micromolar range) toward human cells (represented by the *hMRC-5* IC₅₀ in Table I.6).

Table I.6 | Antiparasitic activities of top-five substituted DAA synthesized by Dr. Wenzel.¹⁴

	<i>In vitro</i> assays – IC ₅₀ (μM)			
	<i>hMRC-5</i>	<i>T. cruzi</i>	<i>T. b. brucei</i>	<i>L. infantum</i>
 2 HCl BJ621	1.91	0.29	0.03	0.38
 2 HCl NW319	1.13	≤ 0.32	≤ 0.32	1.04
 NW326.4	0.96	≤ 0.32	≤ 0.32	1.04
 2 HCl NW321	1.09	0.91	≤ 0.32	1.04
 NW267	26.18	1.60	0.25	≥ 64

The observed cytotoxicity is likely to be due to high reactivity of the electrophilic centers of DAA with human glutathione. Indeed, Dr Wenzel demonstrated the formation of double-adducts of glutathione on DAA's electrophilic centers (Scheme I.7).



Scheme I.7 | Formation of double-adducts of glutathione on DAA's electrophilic centers.

In a similar manner, trypanothione reacts with these structures to form oligomers which were evidenced by Dr. Wenzel in ESI-MS analyses. It has been hypothesized that these polymeric entities resulted from a tail-to-tail addition of trypanothione on the electrophilic centers of a DAA molecule. Unlike glutathione, trypanothione has two reactive centers (the two thiols) as well as the DAA (the two alkenes). Copolymerization of these two monomers was confirmed (Figure I.27, step A). It has been previously demonstrated that sulfide polymers are prone to be oxidized and to undergo polymer fragmentation through β -*syn*-elimination (Figure I.27, step B and C).¹⁴² Here such elimination would regenerate an α,β -unsaturated ketone which could, in turn, reacts again with trypanothione, resulting in polymer elongation (Figure I.27, step D). In our topic, the repetition of these steps might be considered as a redox cycle since a reactive species is sequentially oxidized and reduced, resulting in the futile consumption of trypanothione and NADPH. This redox cycle might finally kill the parasite due to both an oxidative stress and the generation of damaging species such as sulfinic or sulfonic acids (Figure I.27).

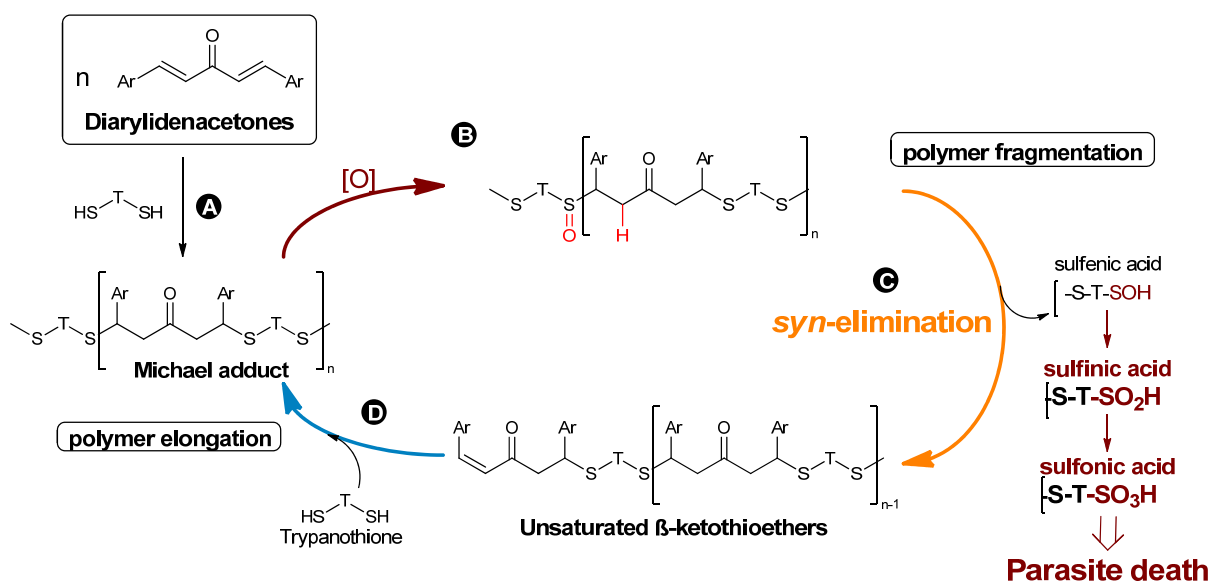


Figure I.27 | Proposed mechanism for trypanothione depletion through polymer formation.

Unlike double-adducts of glutathione-DAA that should be rapidly extruded from cells by ATP-dependent pumps, the extrusion of such high molecular weight trypanothione-based polymers is expected to be more difficult and slower than oxidation kinetic. Although elusive starting from DAA, such a mechanism has already been described with Mannich bases in polymer chemistry.¹⁴² Therefore it was considered as a plausible rationale for the description of trypanothione-DAA polymeric entities and consequently, for the antiparasitic activity of DAA.

Considering the mechanism hypothesis, the DAA series was continued with the aim of carrying structural modifications that would reduce the reactivity toward glutathione and, as a result, the toxicity. We already mentioned the fact that trypanothione is more reactive than glutathione, therefore it might be expected that a fine tuning of the electrophilicity of the reactive centers will achieve a better selectivity. Consequently, we decided to study the relationship between antiparasitic activity and the electron distribution. To achieve this goal, we intended to:

- synthesize new symmetric diarylideneacetones with electron-donating or electron-withdrawing groups,
- synthesize new dissymmetric diarylideneacetones with push-pull, pull-pull or push-push electronic repartition,
- synthesize new heterocyclic substituted diarylideneacetones, both symmetric and dissymmetric.

These were the first objective of the present PhD thesis and will now be detailed.

Chapter II

Synthesis and evaluation of diarylideneacetones derivatives as antiparasitic agents

Synthesis of diarylideneacetone derivatives via the Claisen-Schmidt pathway

Reported uses and synthesis of diarylideneacetones – a literature review

Reported uses of diarylideneacetone derivatives

As we previously mentioned, the diarylideneacetone core (DAA), namely 1,5-diaryl penta-1,4-dien-3-one (Figure II.1), is a widely represented structure, both in synthetic and natural compounds. Before studying the synthesis of such compounds, we would like to give a brief overview of all the current and potential usages of DAA.

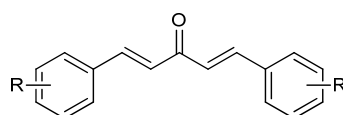
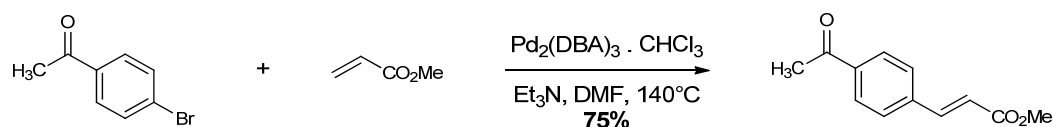


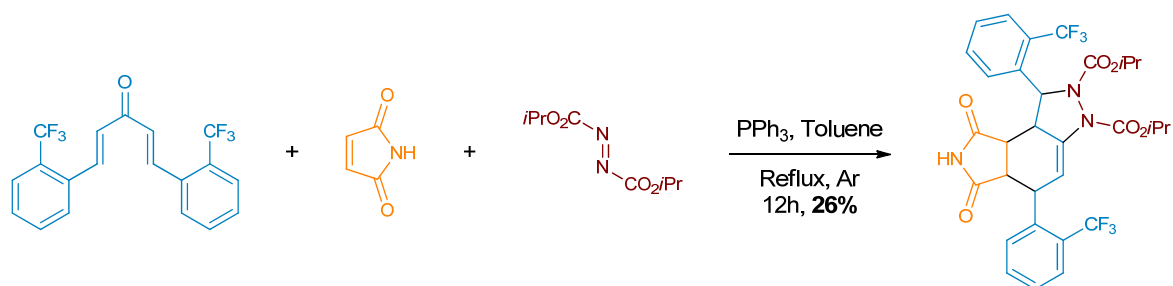
Figure II.1 | General structure of diarylideneacetones.

Besides its uses in medicinal chemistry that have already been detailed (*vide supra*), this scaffold was found very useful in the field of advanced organic chemistry. The dibenzylideneacetone (Figure II.1, R = H) is especially very important in organometallic catalysis. Its use as palladium's ligand for the Suzuki-Miyaura coupling,¹⁴³ or for the Heck reaction,¹⁴⁴ is well documented (Scheme II.1). Dibenzylideneacetone (DBA) has numerous advantages over traditional phosphine ligands. Indeed, due to a better stability against moisture and air, bis(dibenzylideneacetone)palladium(0) is easier to handle. Affordability is also an argument as this complex is commercially available at a lower cost. Furthermore, it is easier to synthesize substituted DBA ligands than to prepare phosphine derivatives; therefore, it is possible to study the effects of electronic distribution on the catalytic efficiency.¹⁴³



Scheme II.1 | Use of dibenzylideneacetone as ligand in palladium-catalyzed coupling reactions.

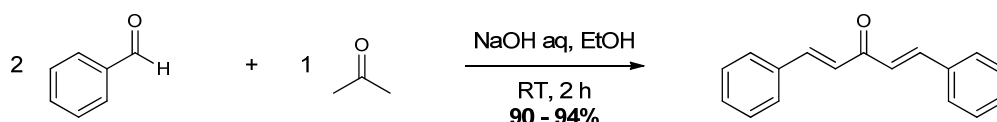
Diarylideneacetones can also be used as starting material for the synthesis of several heterocycles. Highly substituted cyclopentenones are obtained from divinylketones through a Nazarov type cyclization.^{145,146} Their use in multicomponent reactions has also been demonstrated, leading to the synthesis of highly functionalized vinyl pyrazoline or indazole derivatives (Scheme II.2).¹⁴⁷



Scheme II.2 | Preparation of indazole derivatives through a multicomponent reaction using diarylideneacetone as starting material.

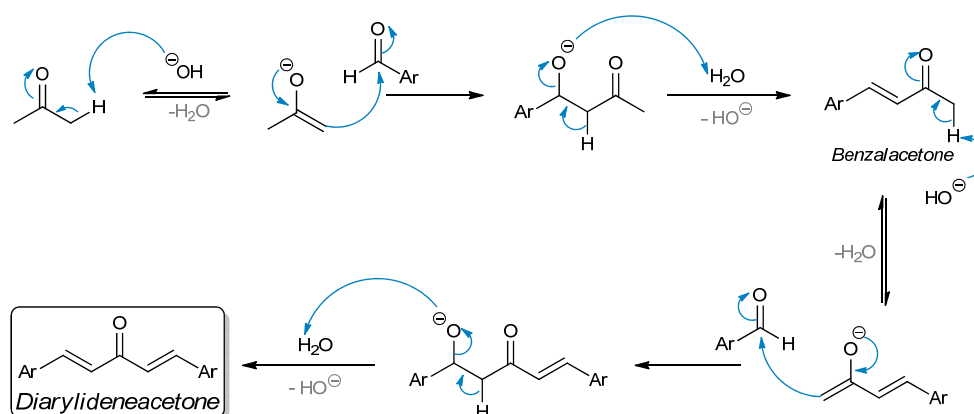
History of the synthesis of diarylideneacetones

To the best of our knowledge, the synthesis of the dibenzylideneacetone was published for the first time in 1932 by Charles R. Conard and Morris A. Dolliver.¹⁴⁸ The desired product was straightforwardly obtained from a classic Claisen-Schmidt reaction (Scheme II.3).



Scheme II.3 | Synthesis of dibenzylideneacetone as described by Conard and Dolliver.

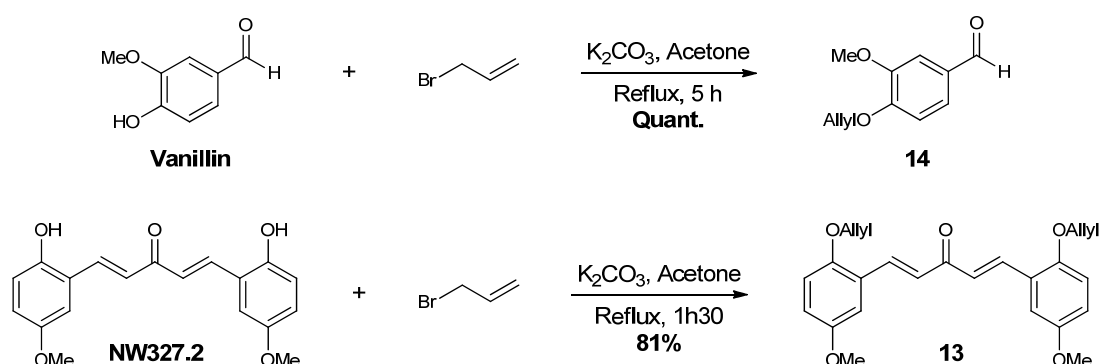
In this procedure, acetone is deprotonated by sodium hydroxide to give the reactive enolate which subsequently reacts in an aldol condensation step to give the intermediate benzalacetone. The acidic proton of benzalacetone is next subjected to acid/base equilibrium leading to a new reactive enolate which, in turn, can react with the second equivalent of aldehyde in an aldol condensation step to give the desired product (Scheme II.4).



Scheme II.4 | Mechanism of the formation of diarylideneacetones via the Claisen-Schmidt pathway.

Synthesis of symmetric diarylideneacetones

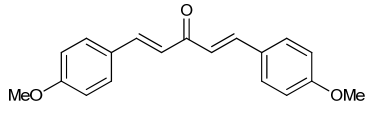
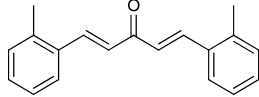
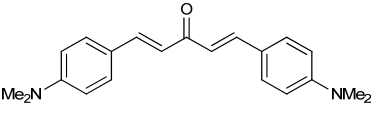
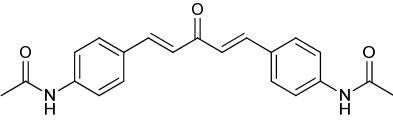
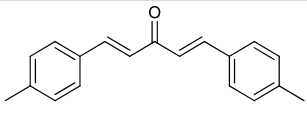
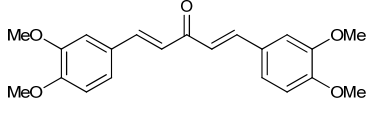
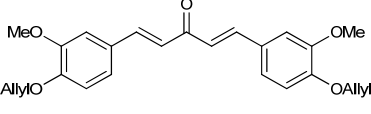
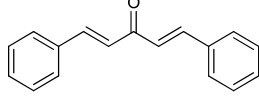
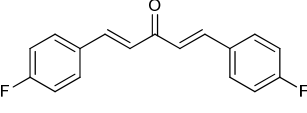
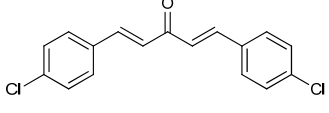
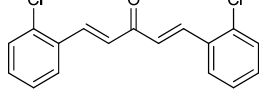
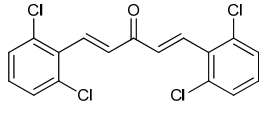
In our hands, the reaction conditions described by Conard and Dolliver proved to be fairly general. We successfully applied this methodology to the synthesis of several DAA in moderate to excellent yields (Table II.1). All these synthesis were performed on a large scale, between 10 g and 15 g. Most of the products were obtained from commercially available benzaldehydes. The only exception is product **7** which was synthesized from the *O*-allylated vanillin. This starting material was quantitatively prepared by reacting vanillin with allyl bromide in acetone (Scheme II.5, upper line). Likewise, the *ortho* allylated diarylideneacetone **13** was prepared from a phenolic DAA that have been previously synthesized by Dr. Nicole Wenzel (Scheme II.5, lower line).¹⁴



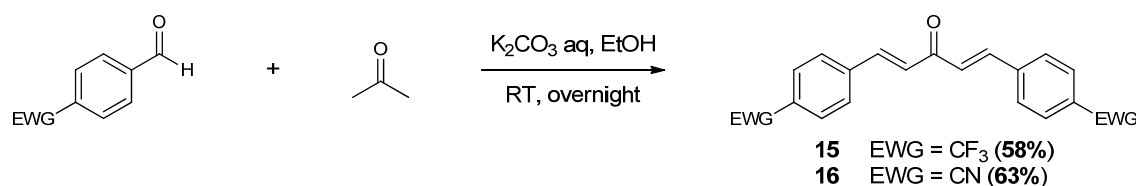
Scheme II.5 | Alkylation reactions of vanillin and diarylideneacetone NW327.2.

On a practical point of view, we found out that two parameters did influence the yield of the Claisen-Schmidt procedure. The first one, the most obvious, is the amount of acetone that must be strictly controlled. Indeed, an excess of acetone will lead to a non-negligible amount of intermediate benzalacetone while a default will leave some unreacted benzaldehyde starting material. The second one is the rate of addition of the benzaldehyde in the reaction mixture that appeared to be crucial. As an example, when the 2-methylbenzaldehyde is added with a rate of 10 mmol.min⁻¹, product **2** is obtained in 69 % yield; if the rate of addition is decreased to 2.5 mmol.min⁻¹, the yield of the reaction is increased up to 82 %. The reaction temperature as well as the concentration of the medium has little effect on the conversion. However, it is important to maintain a sufficient concentration to initiate the precipitation of the desired DAA, allowing a simple and quick recovery of the product.

Table II.1 | Yields of the synthesis of symmetric diarylideneacetones *via* the Claisen-Schmidt pathway.

Entry	Compound	Diarylideneacetone	Yield (%)
1	1		85
2	2		82
3	3		57
4	4		80
5	5		63
6	6		88
7	7		31
8	8		85
9	9		69
10	10		80
11	11		38
12	12		90

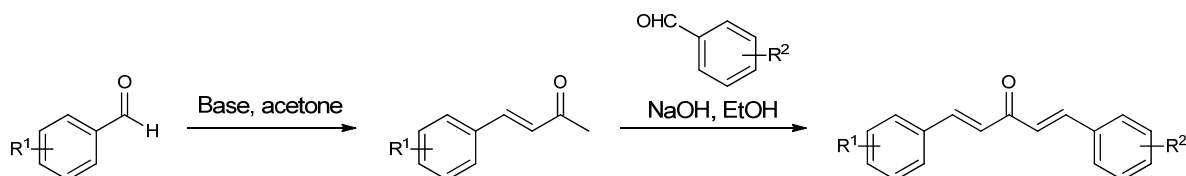
Substitution patterns of the aromatic part of the molecule were chosen to range from electron donating (Table II.1, entries 1 to 7) to electron withdrawing groups (Table II.1, entries 9 to 12). No general correlation can be established between the electron density and the yield of the reaction. However, when highly electron-deficient benzaldehydes were used, the yield of the reaction dropped significantly, with a concomitant raise in the amount of by-products. The synthesis of DAA bearing such substitution requires less drastic conditions, and we found that diluted potassium carbonate in aqueous ethanol overnight allows the smooth formation of the desired product (Scheme II.6).



Scheme II.6 | Specific conditions for the synthesis of diarylideneacetones bearing electron-deficient substituents.

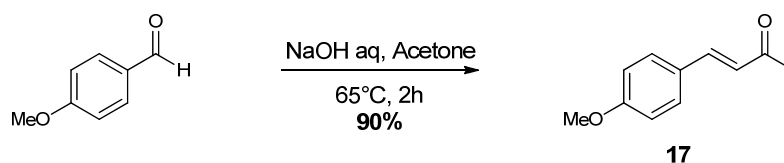
Synthesis of dissymmetric diarylideneacetones

The Claisen-Schmidt pathway described by Conard and Dolliver can also be adapted to the synthesis of dissymmetric diarylideneacetones, that is to say DAA bearing different aromatic substitution patterns on the left hand side (LHS) and on the right hand side (RHS) of the structure. To achieve this goal, the reaction is performed in two separate steps; the first one is the synthesis of a benzalacetone derivative which is subsequently allowed to react with a second benzaldehyde to give the desired dissymmetric DAA (Scheme II.7).



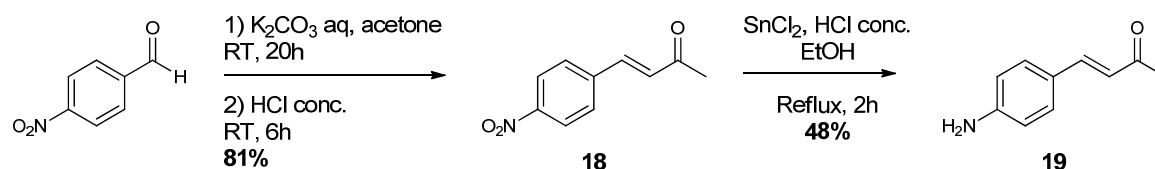
Scheme II.7 | The two-steps Claisen-Schmidt protocol for the preparation of dissymmetric diarylideneacetones.

The benzalacetone (where $\text{R}^1 = \text{H}$) is commercially available at a low cost. Other substitution patterns need to be synthesized from the corresponding benzaldehyde. Following this pathway, *p*-methoxybenzalacetone **17** was obtained in 90 % yield (Scheme II.8).



Scheme II.8 | Synthesis of *p*-methoxybenzalacetone 17.

The synthesis of *p*-aminobenzalacetone **19** was less straightforward. Indeed, due to its ambident nature, the *p*-aminobenzaldehyde cannot be used as a starting material. Therefore, *p*-nitrobenzalacetone **18** has to be synthesized first and next reduced to the amino derivative (Scheme II.9).¹³⁹ The overall yield of the reaction is rather low (39%), the limiting step being the reduction with tin chloride. However, this reaction was only performed once, on a large scale; the yield is therefore likely to be optimized with further experiments or with other reductive conditions like the use of zinc, sodium borohydride or sodium sulfide.^{125,149}



Scheme II.9 | Synthesis of *p*-aminobenzalacetone **19.**

Once the benzalacetone in hands, the last condensation step with benzaldehyde was performed in aqueous ethanolic solution of sodium hydroxide, at room temperature, until total consumption of starting materials. The dissymmetric DAA were obtained in good to excellent yields (Table II.2).

Table II.2 | Yields of the synthesis of dissymmetric diarylideneacetones *via* the Claisen-Schmidt pathway.

Entry	Compound	Dissymmetric DAA	Yield (%)
1	20		94
2	21		80
3	22		61
4	23		82

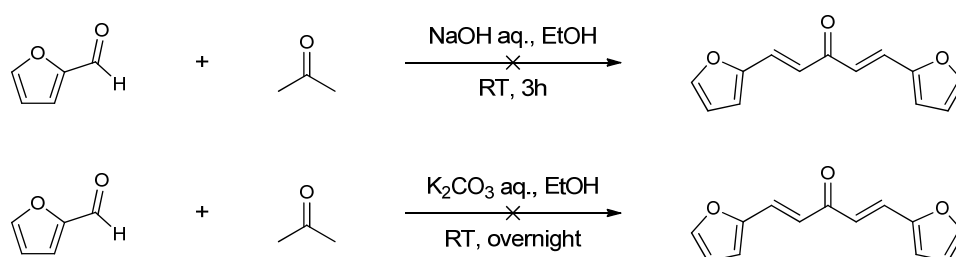
Synthesis of heterocyclic diarylideneacetones

As mentioned in Chapter 1, the most active compounds discovered by Dr. Nicole Wenzel were bearing a pyridyl moiety as aromatic substitution.¹⁴ Furthermore, the introduction of a heteroatom in the aromatic part of DAA is expected to improve the solubility of the compounds which is a recurrent issue in this series. Finally, it also adds a new degree of freedom in the structure-activity relationship as the position of the heteroatom can be changed; this usually results in significant variations in the potency as well as in the ADMET properties of the molecule. We were therefore interested in developing the chemistry of heterocyclic diarylideneacetones.

Synthesis of 2-furan derivatives

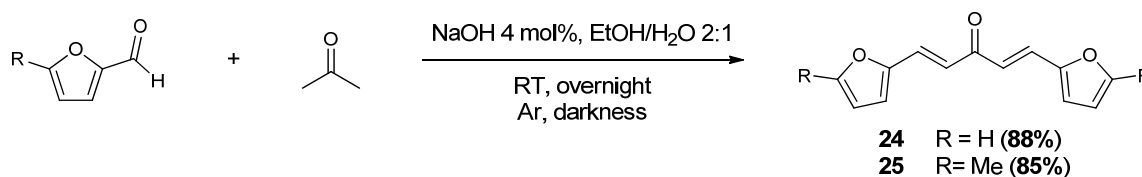
Furans play an important role in the field of antiparasitic drug development. Furan-based moieties are potent antitrypanosomal agents as it is the case in the nitrofurans drugs. Therefore, we aimed at evaluating the activity of heterocyclic diarylideneacetones bearing a 2-furan moiety as aromatic substitution.

The synthesis of 2-furan derivatives according to the usual Claisen-Schmidt conditions was unsuccessful; the reaction mixture quickly turned to a black solid residue, even in the darkness under an atmosphere of argon (Scheme II.10, first reaction). Considering the high reactivity of furfuraldehyde and its propensity to polymerize, we applied the less drastic conditions that were used for the synthesis of electron deficient DAA (*vide supra*). Unfortunately, this also did not lead to the desired product (Scheme II.10, second reaction).



Scheme II.10 | First attempts in the synthesis of 2-furan-substituted diarylideneacetones.

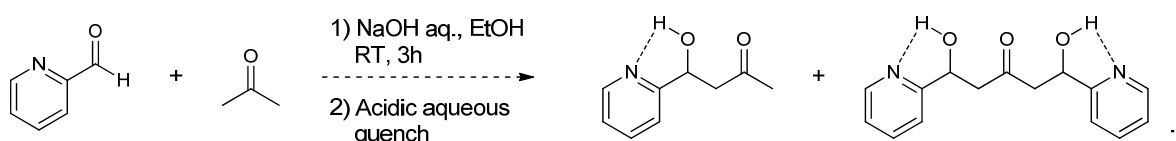
This synthetic issue was overcome by the use of a catalytic amount of sodium hydroxide instead of an excess.¹⁵⁰ Under these modified conditions, the desired 2-furan DAA derivatives were obtained in good yields (Scheme II.11).



Scheme II.11 | Base-catalyzed synthesis of 2-furan-substituted diarylideneacetones.

Synthesis of pyridine derivatives

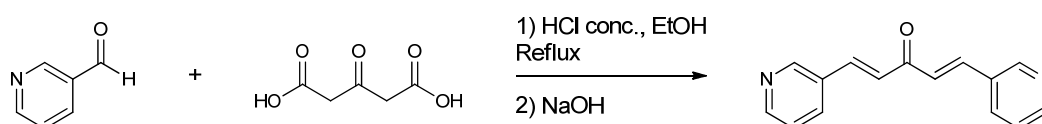
Pyridyl substituted diarylideneacetones were found to be the most potent molecules – in this series– toward trypanosomatids.¹⁴ In order to extend the structure-activity relationships on this particular core, we wanted to prepare new pyridyl substituted DAA. However, this substitution is very difficult to obtain through the usual aldol approach. It has been demonstrated in the literature that, although the enol is effectively added on the pyridinecarboxaldehyde, subsequent elimination of water to yield the desired unsaturated product does not efficiently occur, neither in acidic nor in basic catalysis (Scheme II.12).¹⁵¹ This might be due to a combination of the inductive effect of the nitrogen and of hydrogen bonds, which both tend to deactivate the dehydration of the intermediate aldol.



Scheme II.12 | Possible explanation of the failure in the synthesis of 2-pyridyl-substituted diarylideneacetones through the usual Claisen-Schmidt protocol.

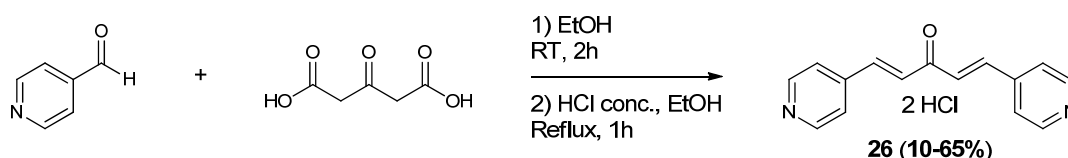
Considering the complexity and the number of by-products, none of our attempts to characterize the reaction mixture was successful.

Three alternatives are described in the literature for the synthesis of this scaffold. The first one is the reaction of nicotinaldehyde with 1,3-acetonedicarboxylic acid under strong acid and high temperature conditions (Scheme II.13).^{14,130}



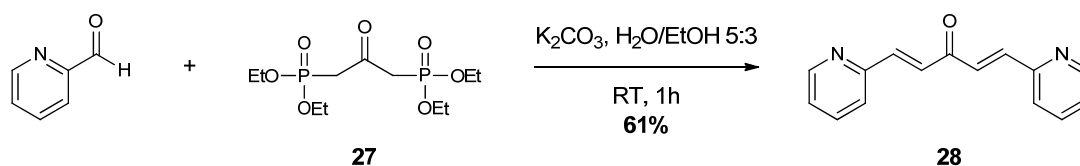
Scheme II.13 | Alternative synthesis using 1,3-acetonedicarboxylic acid as starting material.

Here, we adapted and scaled-up these conditions to the synthesis of the 4-pyridyl substituted DAA (Scheme II.14). However, yields were moderate and non-reproducible, ranging from 65 % to 10 %, depending on the batch and on the scale.



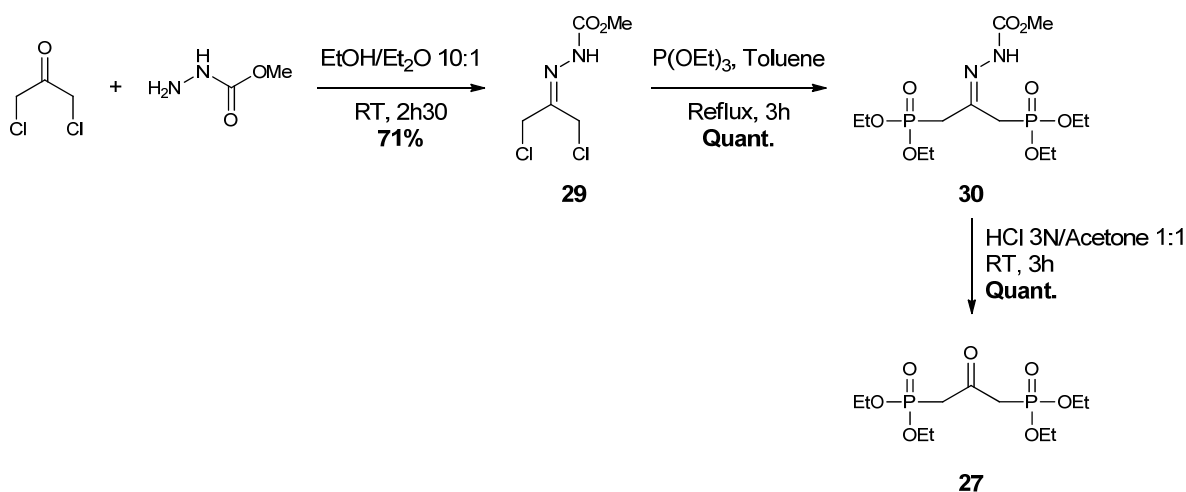
Scheme II.14 | Synthesis of 4-pyridyl-substituted derivatives.

The second pathway relies on an Horner–Wadsworth–Emmons reaction of two equivalents of pyridinecarboxaldehyde with one equivalent of bis(phosphonate) **27** in the presence of K_2CO_3 (Scheme II.15).¹⁵²



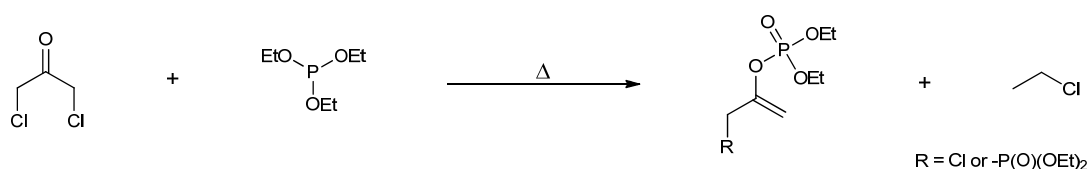
Scheme II.15 | Synthesis of pyridyl derivatives via an Horner–Wadsworth–Emmons reaction.

This approach is efficient, allowing the synthesis of the desired product in very mild conditions and on multigram scale. Bis(phosphonate) **27** starting material is obtained in three steps (Scheme II.16).¹⁵³



Scheme II.16 | Synthesis of bis(phosphonate) **27**.

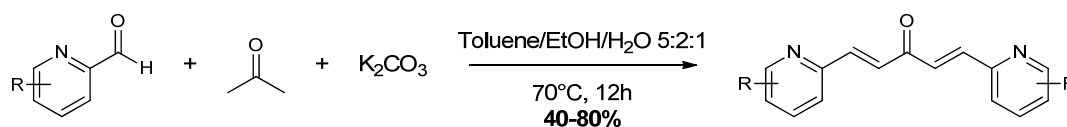
The 1,3-dichloroacetone is firstly protected with a methoxycarbonylhydrazono group in 71 % yield. Subsequent Arbuzov reaction between hydrazone **29** and triethyl phosphite provides quantitatively hydrazone-protected phosphonate **30**. This material is finally deprotected in acidic conditions to give desired phosphonate **27**. It is noteworthy to mention that the initial step is required to avoid the risk of synthesizing an enol phosphate through a Perkow reaction in the second step of the synthesis (Scheme II.17).¹⁵⁴



Scheme II.17 | Perkow reaction that is expected to occur if the 1,3-dichloroacetone is used unprotected in the Arbuzov reaction.

In spite of its efficiency, this Horner–Wadsworth–Emmons approach suffers from two major drawbacks: the three-steps synthesis of bis(phosphonate) **27** is relatively long, and this Wittig reagent does not allow the preparation of dissymmetric heterocyclic diarylideneacetones.

Finally, very recently, Cao *et al.* published a new synthesis of pyridinyl analogues of dibenzylideneacetone based on an improved Claisen-Schmidt protocol.¹⁵⁵ Starting from the usual Claisen-Schmidt conditions, the authors explored solvent and base effects. The best results were obtained with two equivalents of potassium carbonate in a mix of three solvents (toluene/ethanol/water 5:2:1), stirred at 70 °C for twelve hours (Scheme II.18).



Scheme II.18 | Optimized reaction conditions for the synthesis of 2-pyridyl derivatives via a Claisen-Schmidt reaction.

As this publication dates from 2012, we were not able to use it in our project. However, at a first glance, this procedure might not be suitable to our specific needs as it suffers from several limitations. Thus, the control of the reaction conditions is crucial and rather troublesome; little deviation in the temperature or in the solvent ratio makes the yield to fall critically.¹⁵⁵ Furthermore, the scale of the reaction was limited to 1 mmol, whereas the scale-up of such precise conditions is expected to be tricky. Finally, all the examples are substituted by a 2-pyridyl moiety and no experiments were carried out with the nitrogen in positions 3- or 4-.

Limitations of the Claisen-Schmidt pathway

In fine, more than twenty final compounds were obtained through the Claisen-Schmidt pathway in moderate to good yields. This protocol allows the synthesis of both symmetric and dissymmetric diarylideneacetones with various substitution patterns. However, several limitations remain:

- the drastic reaction conditions are not compatible with sensitive substitution patterns,
- highly electron-deficient benzaldehydes, especially fluorinated ones, do not efficiently yield the desired DAA,
- (hetero)diarylideneacetones are not easily obtained through this pathway in both symmetric and dissymmetric series.

In order to circumvent these drawbacks, we aimed at developing a novel approach allowing the one-pot synthesis of dissymmetric (hetero)diarylideneacetones under mild conditions.

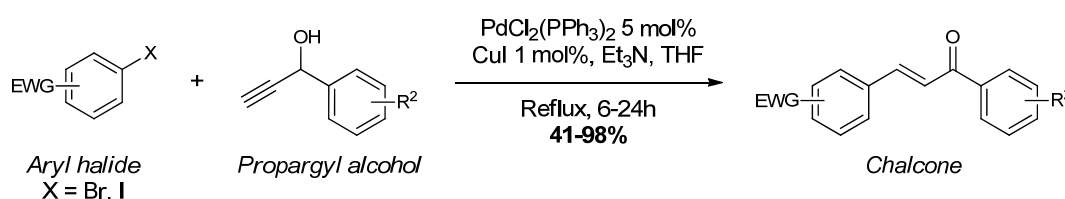
The coupling isomerization reaction

With regard to the limitations of the Claisen-Schmidt protocol for the synthesis of diarylideneacetones, a new versatile pathway was investigated. Essential specifications of the new procedure should include a wide chemical compatibility, especially with sensitive substitution patterns, a good chemoselectivity, a good reactivity with heteroaromatic starting material, ideally a similar reactivity with both electron-rich and electron-deficient substitutions, and the capacity of easily scaling-up the process. Considering these different criteria, we decided to investigate a new convenient catalytic pathway based on the research conducted by Prof. Dr. Thomas J. J. Müller and his team at the University of Düsseldorf.

The coupling isomerization reaction

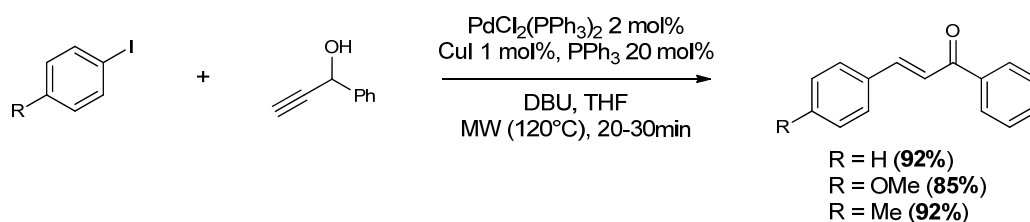
The coupling isomerization reaction at a glance

A few years ago, a new catalytic procedure for the synthesis of chalcones has been published by the research group of Prof. Dr. Thomas J. J. Müller.^{156,157} In this procedure, an aryl halide reacts with a propargyl alcohol to give the desired chalcone under palladium catalysis and in basic medium (Scheme II.19).



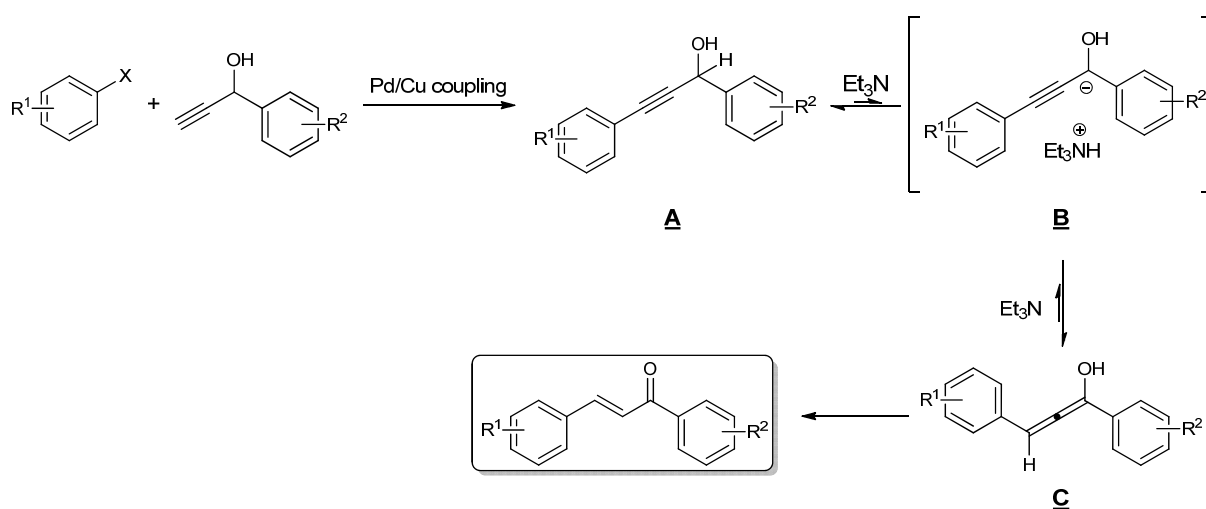
Scheme II.19 | Synthesis of chalcones via a coupling isomerization reaction under thermal heating.

Under thermal heating, the reaction takes between six hours and one day to complete, depending on the starting materials. Furthermore, the aryl halide starting material have to be functionalized by an electron-withdrawing group in *para* position, otherwise the desired product is not obtained. These limitations to the procedure were next abolished by the use of microwave irradiation instead of the traditional thermal heating, and the switch of the base from triethylamine to 1,8-diazabicyclo[5.4.0]undec-7-ene (DBU). Under these improved conditions, chalcones were obtained in half an hour in excellent yields, whatever the electronic properties of the aromatic substituents (Scheme II.20).¹⁵⁸



Scheme II.20 | Improved synthesis of chalcones via a coupling isomerization reaction under microwave irradiation.

On a mechanistic point of view, this reaction proceeds through a coupling followed by an *in situ* isomerization, under basic conditions (Scheme II.21).¹⁵⁶ At first, the Sonogashira coupling occurs between the aryl halide and the propargyl alcohol resulting in the formation of intermediate **A**. Subsequent base-catalyzed deprotonation of this intermediate gives the propargyl anion **B** as a short-lived intermediate, which is protonated back either to the propargyl alcohol **A** or the allenol **C**. The latter then isomerizes to the desired chalcone. On a kinetic point of view, the deprotonation of **A** to give **B** was proven to be the rate-determining step. This sequence of elementary steps gave its name to the procedure: Coupling Isomerization Reaction (CIR).



Scheme II.21 | Mechanistic rationale of the coupling isomerization reaction, proved by deuterium incorporation studies.

Further studies have highlighted a strong dependence on the basicity of the applied amine; this correlates with the fact that the deprotonation step is rate determining. Bases with a pK_a comparable to triethylamine or pyrrolidine were found effective for electron-deficient aryl halides, whereas stronger bases, like DBU, are required for the isomerization of electron rich aryl halides.^{156,158} Screening of solvents showed that the reaction proceeded preferably in solvents such as ethanol, methanol, tetrahydrofuran (THF), acetonitrile or dimethylformamide (DMF).¹⁵⁶ However, under dielectric heating, THF turned out to be the most efficient solvent.¹⁵⁸

Would the coupling isomerization reaction fit to the synthesis of diarylideneacetones?

Chalcones are obviously structurally related to diarylideneacetones; these two structures are vinylogous (Figure II.2).

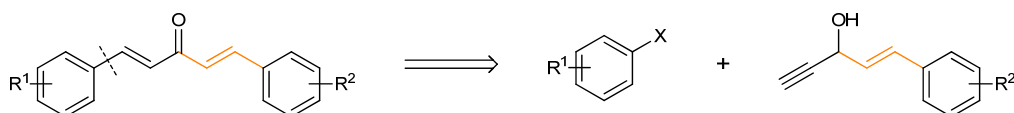


Figure II.2 | Structural similarities between chalcones and diarylideneacetones.

Therefore, it is questionable whether the synthesis of chalcone through the coupling isomerization reaction can be adapted to the synthesis of diarylideneacetones or not. Indeed, the preparation of DAA through this pathway might be a solution for numerous issues that have been raised by the Claisen-Schmidt protocol. The CIR displays very good reactivity with electron-deficient substitution pattern as well as with hetero aryl substituents. Furthermore, the palladium catalysis provides a very good chemoselectivity and is usually compatible with a large panel of chemical functions. These arguments were an incentive to adapt the coupling isomerization pathway to the synthesis of diarylideneacetones. With the aim to investigate this new reaction, a collaboration was established with the research group of Prof. Dr. Thomas Müller, giving me the opportunity to develop this project for four months at the University of Düsseldorf, *via* the Deutscher Akademischer Austausch Dienst (DAAD) program. This collaborative work was initiated in 2009 when our research unit in Strasbourg was not yet equipped with a chemistry-dedicated microwave.

Retrosynthetic analysis

Formally, the retrosynthetic analysis of DAA's synthesis through a coupling isomerization reaction is not so different that the one used for the synthesis of chalcones (Scheme II.22). However, for the synthesis of DAA, the propargyl alcohol starting material is unsaturated; it is the vinylogous counterpart of the propargyl alcohol used in the synthesis of chalcones.

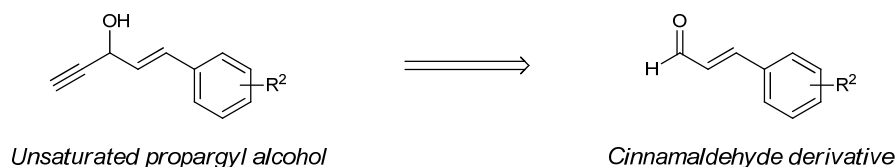


Scheme II.22 | Retrosynthetic analysis of the preparation of diarylideneacetone derivatives through a coupling isomerization reaction.

Two starting materials are required: an aryl halide and an unsaturated propargyl alcohol. Due to their use in numerous coupling reactions, aryl halides are widely commercially available, even with complex substitution pattern. Furthermore, a small library of highly substituted aryl iodides had been previously built in the laboratory. Therefore, we will focus

our discussion on the preparation of the unsaturated propargyl alcohol instead of the synthesis of the aryl halides.

Such unsaturated propargyl alcohols are obviously not commercially available and therefore have to be prepared in the lab. Few procedures are available in the literature, all of them using a cinnamaldehyde as a precursor (Scheme II.23).



Scheme II.23 | Cinnamaldehydes are obvious precursors of unsaturated propargyl alcohols.

This approach is similar to the experiments that have been performed on the synthesis of chalcones where the propargyl alcohol was obtained from a benzaldehyde (Scheme II.24).^{156,159}



Scheme II.24 | Preparation of propargyl alcohols starting material in the synthesis of chalcones.

Considering the results that have been obtained through this approach, we adopted a similar pathway, starting from a cinnamaldehyde derivative for the synthesis of the unsaturated propargyl alcohol. However, very few cinnamaldehyde derivatives are commercially available; we will now discuss the synthesis of such entities.

Synthesis of cinnamaldehyde derivatives

Although they are unsaturated aromatics aldehydes, the synthesis of cinnamaldehydes is not really different from the synthesis of alkyl or aryl aldehydes. Four main strategies are described in the literature (Figure II.3): the reductive pathways (from a carboxylic acid or an ester), the oxidative pathway (from an alcohol), the Wittig pathway, and the Grignard pathway (both from a benzaldehyde). Here we will briefly discuss these different strategies and correlate these approaches with the availability and affordability of starting material. These last data are based on a survey done from the top-five chemical suppliers' website (January 2010). Forty compounds were selected, of which 10 cinnamaldehydes (25%), 3 cinnamic alcohols (7.5%), 22 cinnamic acids (55%), 5 cinnamate methyl esters (12.5%) and 9 cinnamate ethyl esters (22.5%).

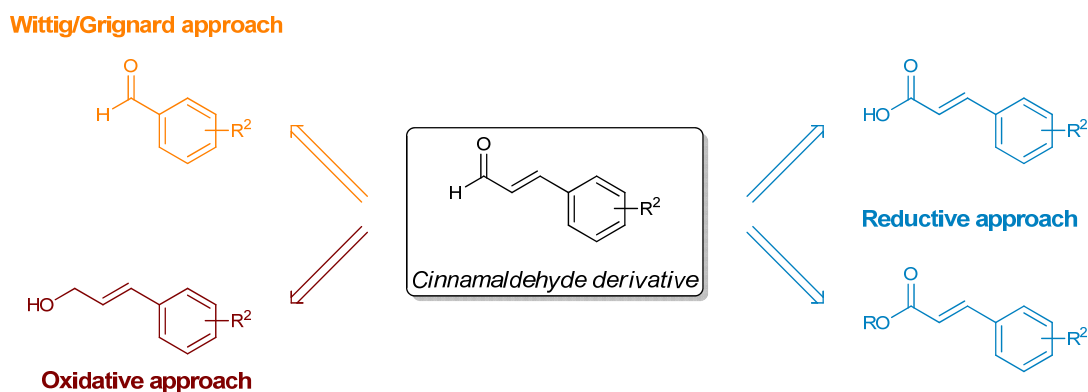
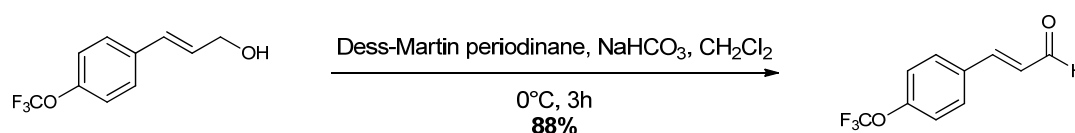


Figure II.3 | Different approaches for the preparation of cinnamaldehyde derivatives.

The oxidative approach

The one-step synthesis of cinnamaldehyde derivatives from the oxidation of alcohols can be achieved both with the Dess Martin's reagent in dichloromethane at 0°C (Scheme II.25),^{160,161} or with the usual pyridinium chlorochromate (PCC) in dichloromethane at room temperature.^{162,163}

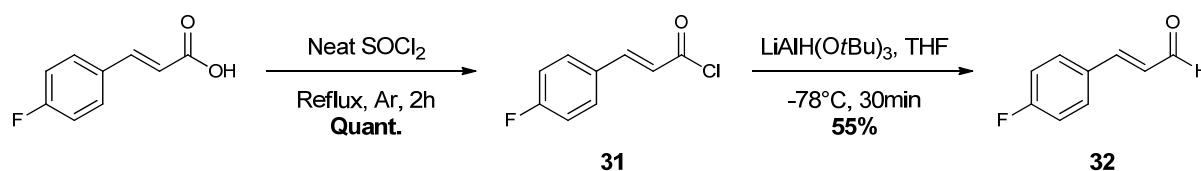


Scheme II.25 | Published procedure for the synthesis of *p*-trifluoromethoxy cinnamaldehyde through the oxidation of the corresponding alcohol.

These reactions occurred with moderate to good yields (66 % up to 90 %). Over-oxidation is an inherent risk in this pathway, though it has not been reported in the literature. However, this route is mainly limited by the few unsaturated alcohols starting material that are commercially available and by their very expensive prices; thus only three compounds were available (7.5 %) at an average cost between 50 €/g and 1 500 €/g. Therefore, we did not investigate this approach.

The reductive approach

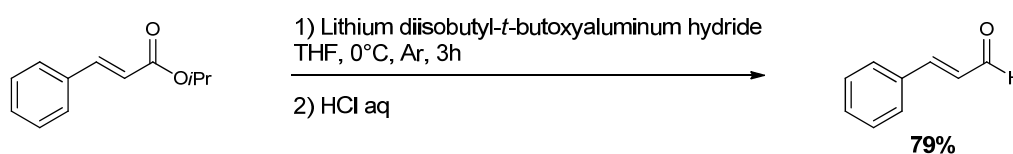
Along the reductive pathway, two starting materials might be used. Starting from the carboxylic acid implies its conversion to acid chloride followed by the reduction of this intermediate by palladium-catalyzed hydrogenation (Rosenmund reduction),¹⁶⁴ or by metal hydrides, such as lithium tri-*tert*-butoxyaluminumhydride.¹⁶⁵ The latter strategy was investigated with the synthesis of 4-fluorocinnamaldehyde **32**. Commercially available 4-fluorocinnamic acid was converted to corresponding acyl chloride **31** which was subsequently reduced by commercial lithium tri-*tert*-butoxyaluminumhydride (Scheme II.26).



Scheme II.26 | Hydride reduction of 4-fluorocinnamoyl chloride for the synthesis of 4-fluorocinnamaldehyde 32.

Although the desired product was obtained in 55 % yield, this procedure is limited by the amount of by-product likely to be generated by the highly reactive metal hydride. This is balanced by the wide availability and affordability of cinnamic acid; more than half of the commercially available starting materials is cinnamic acid at a cost ranging from 1.5 €/g to 100 €/g.

On the other hand, cinnamaldehyde derivatives might also be prepared from the reduction of methyl, ethyl or isopropyl esters. Direct reduction to aldehydes is carried out by the use of DIBAL-H or lithium diisobutyl-*t*-butoxyaluminum hydride in THF at 0°C (Scheme II.27).¹⁶⁶



Scheme II.27 | Published procedure for the synthesis of cinnamaldehyde through an ester reduction.

Another possibility is to reduce the ester in alcohol with the use of a strong hydride such as Lithium Aluminum Hydride (LAH) and next re-oxidized the product in aldehyde with Dess Martin's reagent or PCC (*vide supra*). Once again, the main limitation of the use of cinnamate esters is the availability of starting materials; only 14 esters are commercially available at an average cost between 5.8 €/g and 45 €/g. Therefore, we did not investigate this pathway.

The Wittig approach

The Wittig pathway is the most obvious route when it comes to synthesize products with complex substitution on the aryl part. Indeed, there are numerous benzaldehydes, including highly substituted ones, that are commercially available and usually at an affordable cost. Along this pathway, two Wittig reagents can be used.

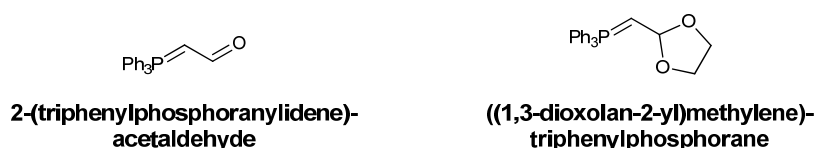
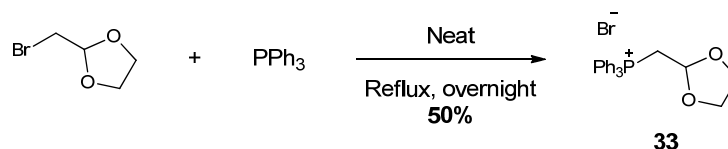


Figure II.4 | Ylide that can be used for the synthesis of cinnamaldehyde derivatives.

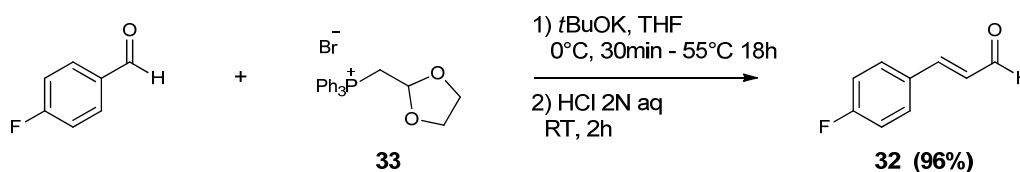
The first one, derived from the unprotected acetaldehyde, is the 2-(triphenylphosphoranylidene)acetaldehyde (Figure II.4).^{162,167,168} However, this reagent might induce multiple homologations as it bears itself a reactive function, which is able to react in turn with

the ylide. In order to avoid this issue, the dioxolane-protected ylide is preferably used (Figure II.4).¹⁶⁹⁻¹⁷¹ (1,3-Dioxolan-2-ylmethyl)triphenylphosphonium bromide **33**, is commercially available but it can easily be prepared from the 2-bromomethyl-1,3-dioxolane (Scheme II.28).¹⁷¹



Scheme II.28 | Synthesis of (1,3-Dioxolan-2-ylmethyl)triphenylphosphonium bromide 33.

Considering the mild reaction condition and the wide availability and affordability of starting materials, we decided to investigate this pathway for the synthesis of 4-fluorocinnamaldehyde **32**. Protected phosphonium salt **33** was obtained in 50 % yield (Scheme II.28). Subsequent Wittig reaction yields the protected cinnamaldehyde which was directly deprotected in 2 M aqueous chlorohydric acid to give desired 4-fluorocinnamaldehyde **32** in 96 % yield (Scheme II.29).

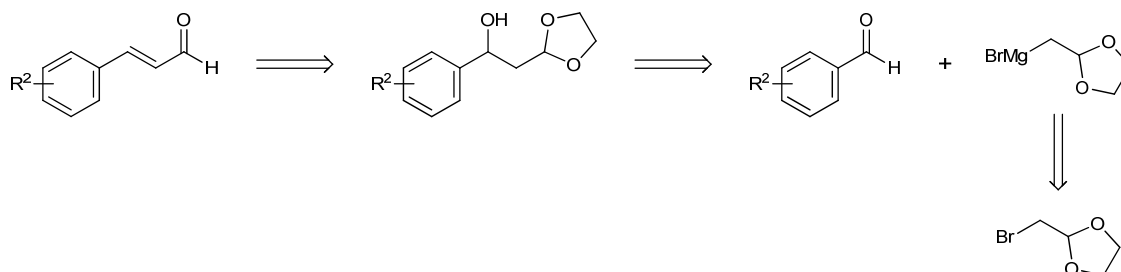


Scheme II.29 | Synthesis of 4-fluorocinnamaldehyde 32 through the Wittig pathway.

The only limitation of this procedure is the huge mass of phosphonium salt required for the reaction to occur (above 1 g per millimole of final compound).

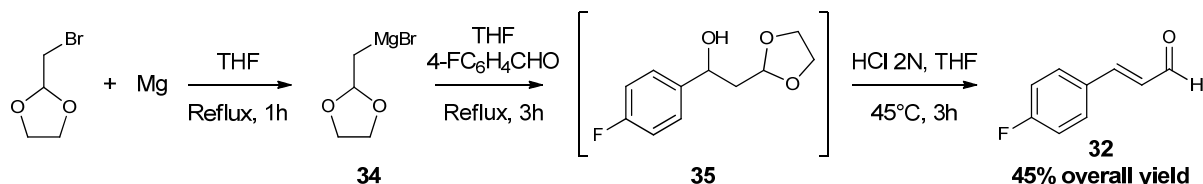
The Grignard approach

To the best of our knowledge, no synthesis of cinnamaldehyde derivatives was carried out through a Grignard strategy. Therefore, we investigated this possibility and finally suggested the use of 2-bromomethyl-1,3-dioxolane as precursor for the homologation of benzaldehyde derivatives (Scheme II.30).



Scheme II.30 | Retrosynthetic analysis of the preparation of cinnamaldehyde derivatives via a Grignard strategy.

We applied this strategy to the synthesis of our test compound **32** (Scheme II.31). In the first step of the procedure 2-bromomethyl-1,3-dioxolane reacted with magnesium to give the Grignard intermediate **34**. Subsequent 1,2-addition on the 4-fluorobenzaldehyde gave intermediate β -hydroxydioxolane **35** which, after hydrolysis and dehydration resulted in the formation of the desired product in 45 % overall yield.



Scheme II.31 | Grignard synthesis of 4-fluorocinnamaldehyde 32.

This promising result is expected to be significantly improved further to optimization process. Furthermore, a great advantage of this procedure is that all reactions are performed in one-pot. Starting materials are commercially available at an affordable cost, and Grignard reactions are known to be easily scaled-up.

Comparison of the different approaches

To conclude on the synthesis of cinnamaldehyde derivatives, we aimed at comparing the most promising synthetic pathways that we investigated. Therefore, all the features of each of the three tested pathways are summarized in Table II.3.

Table II.3 | Comparison of the three tested pathways for the synthesis of 4-fluorocinnamaldehyde.

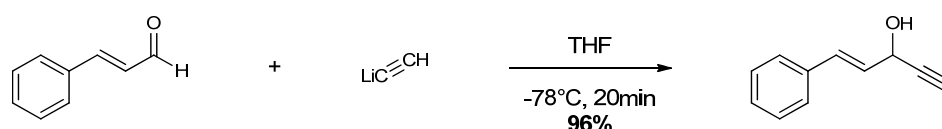
Pathway	Commercial (Sigma Aldrich)	Reductive	Wittig	Grignard
Starting material availability	-	Moderate	Excellent	Excellent
Steps	-	2	3	3 (one pot)
Purification	-	Chromatography	Trituration	Distillation
Preparation Time (h)	-	6	20	10
Chemoselectivity	-	Moderate	Good	Moderate
Cost (€/g)	241	21	27	7

According to this table, the Grignard pathway is the most interesting in terms of cost and purification process, and even more if we consider that the procedure has not been yet optimized. However, the main argument to choose one specific procedure rather than another is the chemical compatibility of the substrate's substituents with the reagent being used. In that matter, the Wittig pathway displays the best compromise as ylides are usually compatible with a large panel of chemical functions.

Synthesis of unsaturated propargyl alcohols

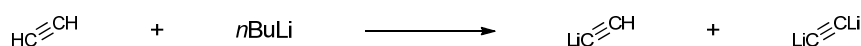
Once the cinnamaldehyde derivatives have been obtained, they have to be converted into unsaturated propargyl alcohols. Several protocols are described in the literature for the preparation of such an alkyne. Most of them start from acetylene (or an acetylenic derivative) which is converted to a nucleophilic species and then allowed to react with the electrophilic carbon of the aldehyde.

The obvious way to generate a nucleophilic species from acetylene is a lithiation with *n*-butyllithium or methyl lithium.^{172,173} Subsequent addition to the aldehyde in anhydrous THF at -78°C, usually yields to the desired product in 70 % to 96 % yield (Scheme II.32).¹⁷⁴



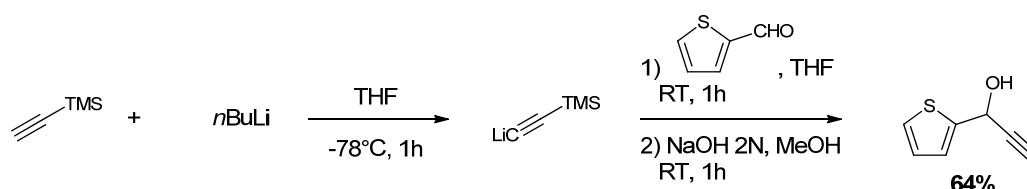
Scheme II.32 | Propargylation of cinnamaldehyde derivatives using lithium acetylide.

However, this simple strategy suffers from two major drawbacks. Acetylene is a highly flammable gas, difficult to handle, which significantly limits the control of the stoichiometry. In addition, the use of *n*-butyllithium in the presence of the two acidic protons of acetylene involves a risk of generating the dilithium acetylide (Scheme II.33). The only possibility to circumvent this issue is to strictly control the temperature, the reaction time, as well as the stoichiometry.¹⁷⁴



Scheme II.33 | Risk of acetylene dilithiation.

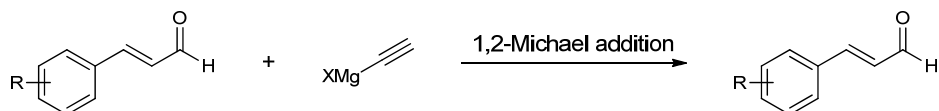
More recently, the use of protected acetylenic derivatives was suggested to overcome the dilithiation issue. In this strategy, one of the protons of acetylene is replaced by a protecting group –usually a trimethylsilyl– which can be removed at the end of the synthesis (Scheme II.34).¹⁵⁶



Scheme II.34 | Propargylation reaction using trimethylsilylacetylene.

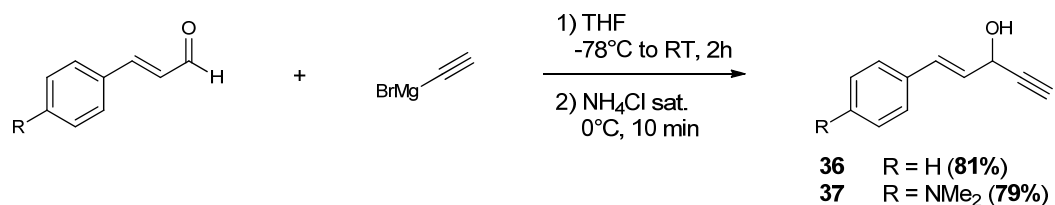
In spite of the additional desilylation step, overall yields are moderate to good through this approach. This methodology has the advantage of using a liquid acetyating reagent instead of a gas, which results in an easier and safer handling. However, the cost of trimethylsilylacetylene tends to limit the use of this approach on a large scale.

Last but not least, a Grignard strategy can also be considered for the synthesis of unsaturated propargyl alcohols. Indeed, an organomagnesium acetylenic derivative might be used to react on the aldehyde of cinnamaldehyde derivatives in a 1,2-Michael addition (Scheme II.35).



Scheme II.35 | Grignard approach for the propargylation of cinnamaldehyde derivatives.

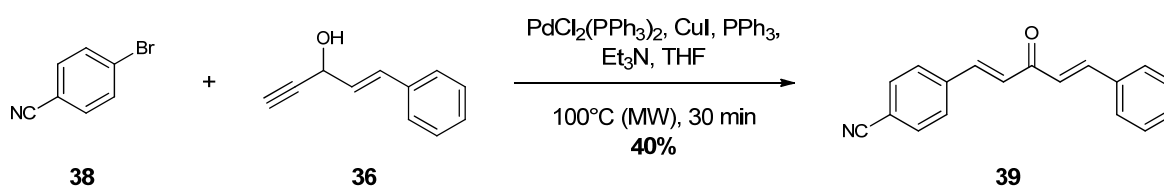
Although such a Grignard reagent may be prepared in the laboratory, ethynylmagnesium bromide was recently put on the market by Sigma-Aldrich at a very affordable cost. This reagent does not involve any risk of side reaction due to dilithium acetylide, it is liable to be used in large scale, and being commercially available in 0.5 M THF solution, it is easy to handle. Considering these numerous advantages, this strategy was chosen for the synthesis of precursors. For preliminary studies on the synthesis of DAA through a CIR, we decided to limit our experiments to two unsaturated propargyl alcohols, 1-phenylpent-1-en-4-yn-3-ol **36** and 1-(4-(dimethylamino)phenyl)pent-1-en-4-yn-3-ol **37**, which were obtained in 81 % and 79 % yield, respectively (Scheme II.36).



Scheme II.36 | Synthesis of unsaturated propargyl alcohols 36 and 37.

First attempts

With all the starting materials in hands, preliminary experiments were performed. Reaction conditions (temperature, duration, concentration, solvent, base, catalytic system) as well as starting materials were selected further to previous studies on the synthesis of chalcones.^{156,158} Thus, experiments were performed using 1-phenylpent-1-en-4-yn-3-ol **36** and 4-bromobenzonitrile **38** as starting materials. The catalytic system was composed of $\text{Pd}(\text{PPh}_3)_2\text{Cl}_2$ and copper iodide as a co-catalyst. The reaction was carried out in THF at 120 °C (dielectric heating) for half an hour with triethylamine as the base of choice (Scheme II.37).



Scheme II.37 | First attempts in the synthesis of dissymmetric diarylideneacetone 39 through a coupling isomerization reaction

Under these conditions, desired product **39** was obtained in 40% yield. This encouraging result was an incentive to try to optimize the reaction conditions in order to achieve better yields, while being compatible with a large panel of substitutions.

Optimization of the synthesis of dissymmetric (hetero)diarylideneacetones via Pd-catalyzed coupling isomerization reaction

Optimization of a synthetic reaction is often a time-consuming and costly process. Keeping in mind that our collaboration within the laboratory of Prof. Dr. Müller was time-limited, we had to streamline this task as much as possible. Our goal was to develop a reliable methodology to quickly determine which parameters of the reaction are crucial for the yield.

Parameters involved in the CIR can be divided into two categories: discrete factors (solvent, base, catalytic system), and continuous factors (temperature, duration and concentration). These two sets of parameters were studied independently; effects of discrete factors were analyzed through an usual iterative process, while the effects of continuous factors were evaluated according to the Design of Experiment (DoE) methodology.¹⁷⁵

Nevertheless, with regard to the short reaction duration of the CIR under microwave irradiation, extraction and purification are the most time-consuming steps in the process. This issue can be advantageously overcome through the use of a quantitative analysis of the crude reaction mixture. This is the reason why we initiated our optimization process with setting-up a reliable analytical method for quantification of product **39**.

Set-up and validation of the quantification method

Choice of the method

When it comes to defining a new quantification method for an unknown product, several parameters have to be considered. One of the first is the analytical instrument that will be used. This choice is mainly guided by the required degree of accuracy, the duration of an analysis, and the samples properties. In our case, we had to analyze a complex system in a solution containing at least three different chemical entities: the two reactants (**38** and **36**) and the desired product **39**. A chromatographic separation was therefore selected. The selection of the detection method was mainly determined by the physical properties of compounds. Both starting materials and product absorb in the range 250-300 nm (Figure II.5). In addition, **39** is a highly yellow-colored product, resulting in a high absorption coefficient at $\lambda_{\max} = 325$ nm ($\epsilon_{325\text{nm}} = 2.05 \cdot 10^4 \text{ L} \cdot \text{mol}^{-1} \cdot \text{cm}^{-1}$).

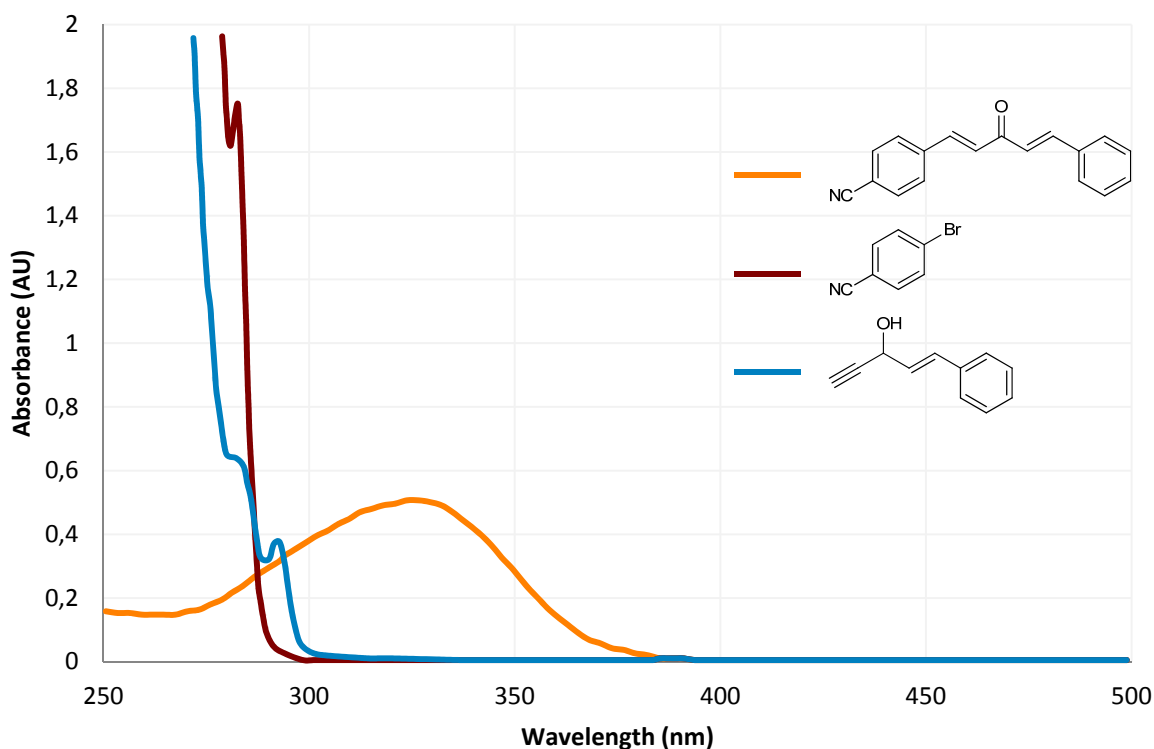


Figure II.5 | UV-Vis spectra of products 36, 38, and 39.

Therefore, a UV-Vis detector was found to be adequate for both detection and quantification of the compounds. The availability of an apparatus meeting these criteria was fortunately ensured as a Hewlett-Packard High Pressure Liquid Chromatography (HPLC) was available within the laboratory in free access. Besides its ability to separate compounds, an HPLC analysis constitutes a reliable, accurate and, above all, fast method, which perfectly meets all the requirements for an optimization process.

Far from being a straightforward procedure, separation and quantification of an intricate system also need to be developed and optimized. Especially, selecting the proper column and adequate elution program is crucial. Here, a silica-column of chromatography was selected (Nucleosil®) and the best separation was observed with dichloromethane containing 1 vol% of isopropanol at $0.6 \text{ mL}\cdot\text{min}^{-1}$. Under these conditions, resolution reached 2.74 between compounds **38** and **39**, and 8.04 between compounds **39** and **36** (Figure II.6). Such a fine separation resulted in an accurate peak picking and integration which are essential conditions for the calibration of the method.

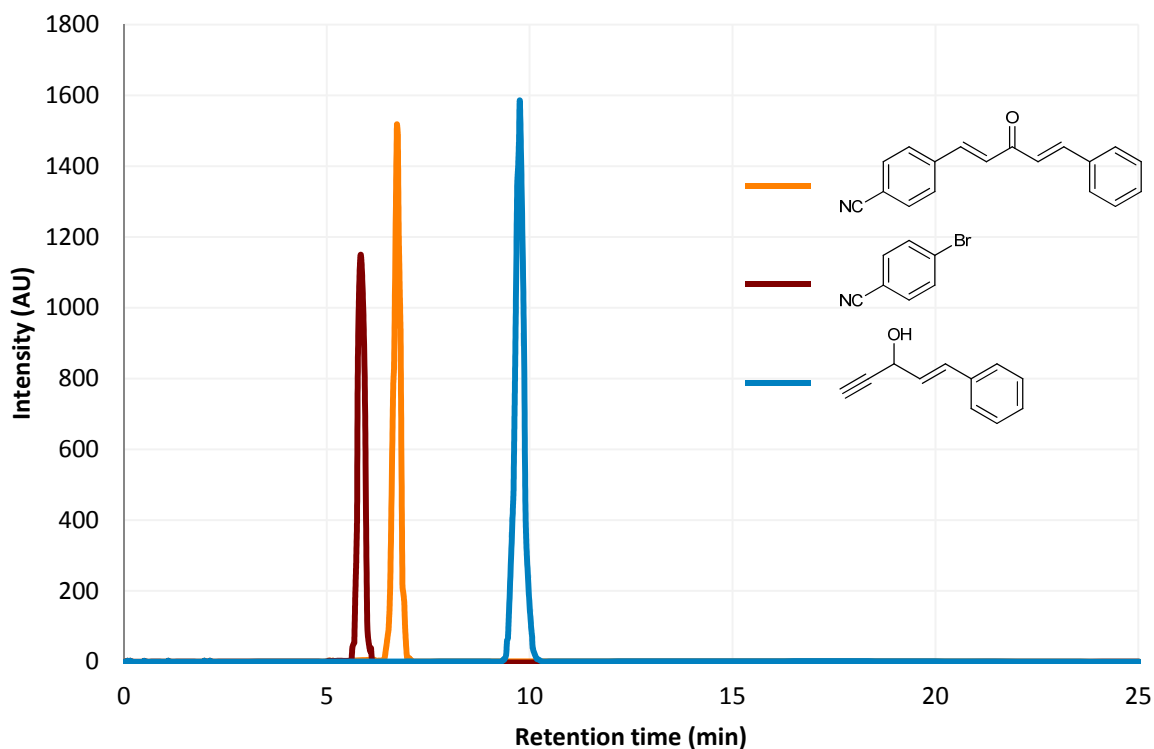


Figure II.6 | Chromatograms of products 36, 38, and 39.

Calibration and validation

In order to obtain reliable measurements, the analytical method was calibrated and validated as well. A range of solutions of product **39** at different concentrations was therefore prepared. Concentrations were chosen according to the expected molarity of the reaction, the saturation level of the detector and the observed linear range of the detector for this specific product. *In fine*, seven samples were prepared with concentrations ranging from $1.50 \pm 0.03 \text{ mg.mL}^{-1}$ to $0.050 \pm 0.002 \text{ mg.mL}^{-1}$. It is necessary to mention that product **39** can be detected both at 254 nm and 325 nm, the latter wavelength allowing more sensitive and accurate measurements. Using the diode array detector of the HPLC apparatus, two chromatograms were recorded at 254 nm and 325 nm for each analysis. Consequently, two calibration curves were plotted (Figure II.7 and II.8). The accuracy and the repeatability of the calibration were assessed through triplicate analysis of three samples of known concentration. For each sample, the value we deduced from the calibration curves was found to be in excellent agreement with the expected concentration within the experimental errors. As a result, the calibration of the method was considered as validated.

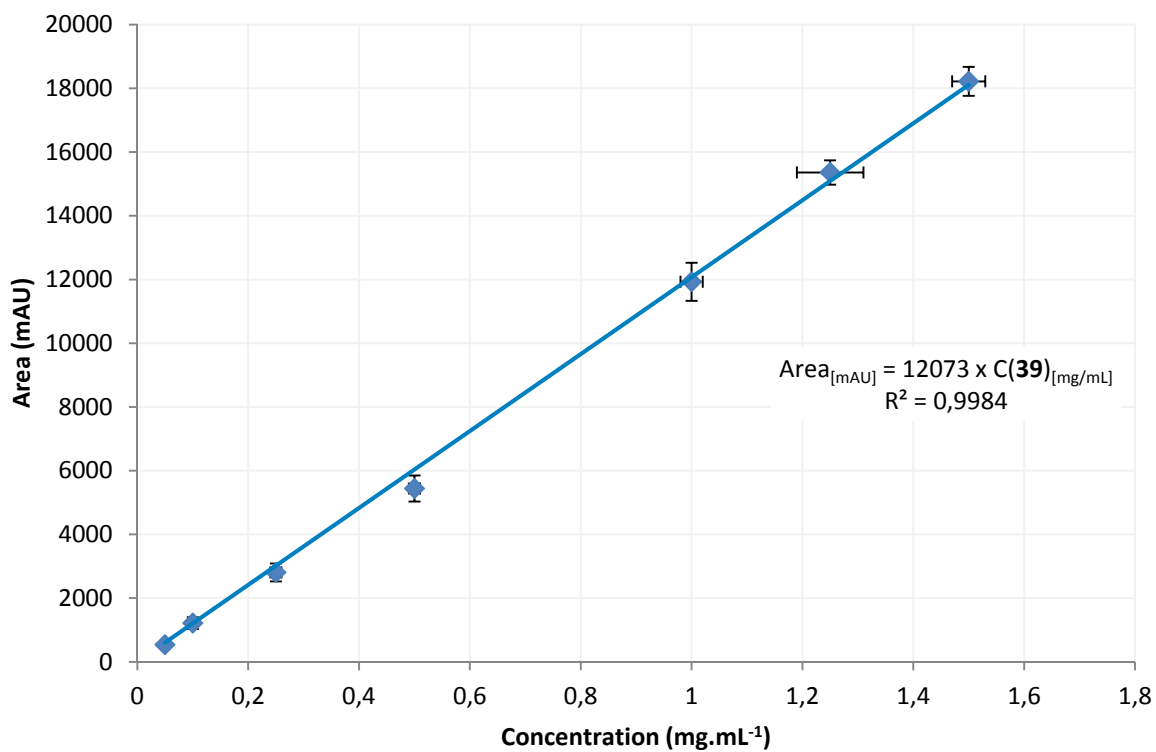


Figure II.7 | Calibration curve of product 39 at 254 nm.

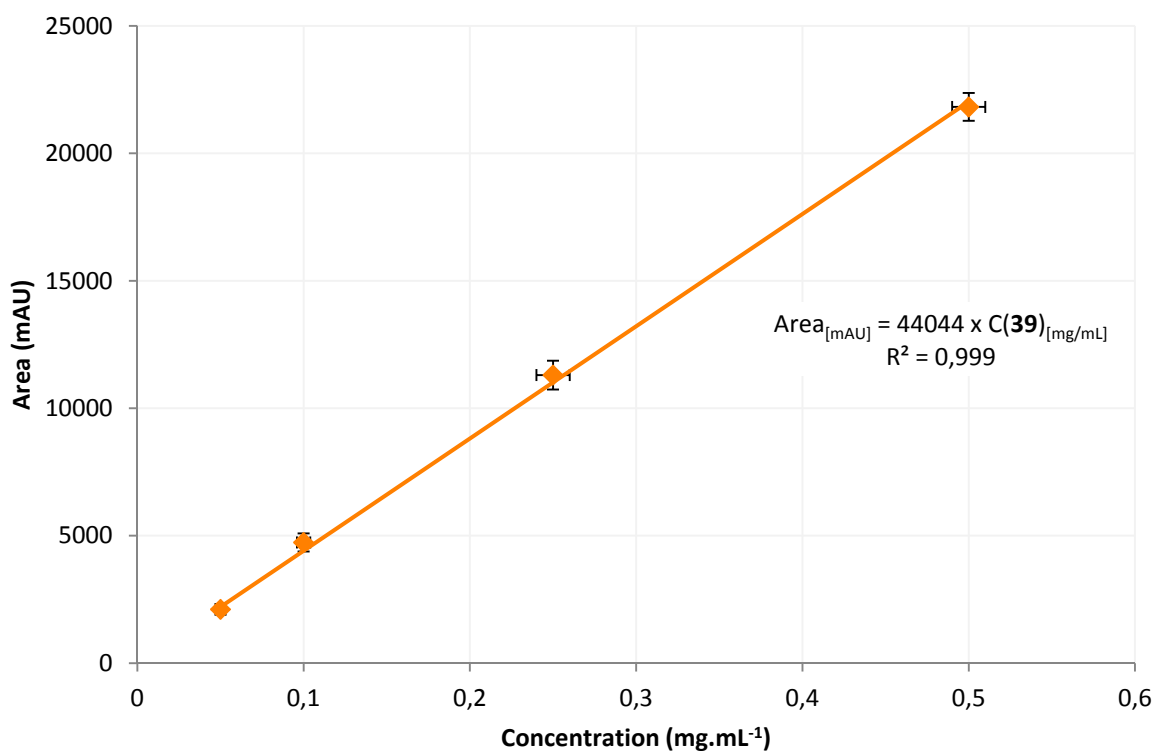


Figure II.8 | Calibration curve of product 39 at 325 nm.

Summary

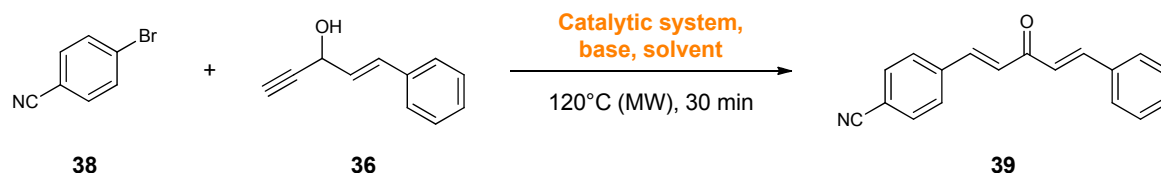
The main parameters of the quantitative HPLC analysis of product **39** are summarized in Table II.4.

Table II.4 | Quantitative HPLC determination of product 39.

	Calibration at 254 nm	Calibration at 325 nm
Limit of detection	2 $\mu\text{g}\cdot\text{mL}^{-1}$	0.5 $\mu\text{g}\cdot\text{mL}^{-1}$
Limit of quantification	50 $\mu\text{g}\cdot\text{mL}^{-1}$	50 $\mu\text{g}\cdot\text{mL}^{-1}$
Saturation	2.00 $\text{mg}\cdot\text{mL}^{-1}$	0.7 $\text{mg}\cdot\text{mL}^{-1}$
Linear calibration range	0.05 – 1.50 $\text{mg}\cdot\text{mL}^{-1}$	0.05 – 0.5 $\text{mg}\cdot\text{mL}^{-1}$
Correlation (R^2)	0.9984	0.9990

With respect to accuracy and sensitivity, calibration established at $\lambda = 325$ nm was selected for the quantification of product **39**. Chromatograms recorded at $\lambda = 254$ nm were used to confirm the value and to qualitatively evaluate the amount of the remaining starting materials. Considering the limited time dedicated to this optimization step, subsequent analyses of reaction mixtures were only duplicated; however, this might be considered sufficient for an optimization of the reaction conditions.

Optimization of discrete factors



Scheme II.38 | Discrete factors influencing the coupling isomerization reaction.

The coupling isomerization reaction is controlled by several parameters. Among them, three discrete factors can influence the yield: the catalytic system, the base and the solvent (Scheme II.38). In order to make the optimization process easier, these factors were considered independently from each other. Therefore, for each experiment only one factor was varied; combinations of variation were not examined. In such a simplified study, the order of examination may have a drastic effect on the conclusion to be drawn. Here, the importance of different factors was evaluated and classified further to the result of previous studies.^{156,158} As a result, the influence of the base was firstly studied, followed by the effects of the solvent, and finally two different catalytic systems were evaluated (Table II.5).

Table II.5 | Optimization of the discrete factors.^a

Entry	Base	Solvent	Catalyst	HPLC yield (%)
1	Cs ₂ CO ₃	THF	PdCl ₂ (PPh ₃) ₂	5
2	DBU	THF	PdCl ₂ (PPh ₃) ₂	0
3	Pyrrolidine	THF	PdCl ₂ (PPh ₃) ₂	0
4	Piperidine	THF	PdCl ₂ (PPh ₃) ₂	0
5	DIPEA	THF	PdCl ₂ (PPh ₃) ₂	21
6	Triethylamine	THF	PdCl ₂ (PPh ₃) ₂	40
7	Triethylamine	DMF	PdCl ₂ (PPh ₃) ₂	58
8	Triethylamine	Neat Et ₃ N	PdCl ₂ (PPh ₃) ₂	52
9	Triethylamine	1,4-dioxane	PdCl ₂ (PPh ₃) ₂	62
10	Triethylamine	1,4-dioxane	Pd(PPh ₃) ₄	60

^aReactions performed at 0.3 M, with 5 equivalents of base, heated at 120 °C under microwave irradiation for 30 min.

Base screening

Since the isomerization step of the CIR is a base-catalyzed process, the choice of the base is expected to be essential. Six bases have been selected according to their pK_a and their nucleophilic properties: cesium carbonate (Cs₂CO₃), triethylamine (Et₃N), piperidine, pyrrolidine, diisopropylethylamine (DIPEA), and 1,8-diazabicyclo[5.4.0]undec-7-ene (DBU) (Table II.5). Inorganic base like cesium carbonate resulted in a limited amount of desired product (Table II.5, entry 1). Switching to organic bases, with the use of DBU, no product was detected (Table II.5, entry 2). Although 4-bromobenzonitrile **38** was still present in the mixture, neither the desired product nor 1-phenylpent-1-en-4-yn-3-ol **36** was detected. DBU as a base might be too strong, inducing decomposition of the unsaturated propargyl alcohol. In the case of pyrrolidine, both starting materials were entirely consumed to form a new product, not the desired one, that we were not able to identify (Table II.5, entry 3). With piperidine no reaction occurred, and starting materials were still present (Table II.5, entry 4). The use of nucleophilic secondary amines seems therefore problematic. On the other hand, non-nucleophilic tertiary amines DIPEA and triethylamine worked well (Table II.5, entries 5 and 6). In the case of DIPEA, the coupling reaction occurred but the isomerization seemed to be slower, resulting in lower yield. The higher steric hindrance of DIPEA is likely to explain the lower reactivity compared to triethylamine. Consequently, triethylamine was selected as the base for this reaction.

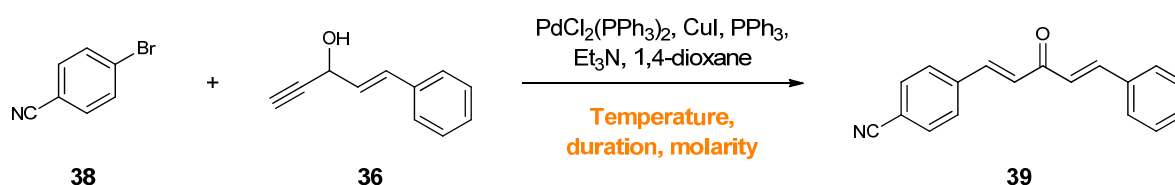
Solvent screening

Although the choice of solvent under conventional heating is very important, it becomes even more crucial under microwave irradiation. Indeed, besides polarity and (a)protic properties, the ability of the solvent to absorb microwave energy and to convert it into heat has to be carefully considered.¹⁷⁶ Taking into account these specificities, four different solvents were tested: tetrahydrofuran, 1,4-dioxane, dimethylformamide, and neat triethylamine. All solvents gave satisfactory yields but THF was clearly less efficient than the others. 1,4-Dioxane, DMF and neat triethylamine showed comparable results (Table II.5, entries 7-9). However, as 1,4-dioxane gave the highest yield and is much easier to remove during the work-up, it was selected as the preferred solvent for this reaction.

Catalyst screening

The first step in the CIR is a Sonogashira coupling which is usually performed using a palladium phosphane ligand complex as a catalyst in the presence of a catalytic amount of a copper(I) salt, most often copper iodide. Regarding the palladium precatalyst, Pd(PPh₃)₄ or Pd(PPh₃)₂Cl₂ are the most commonly used in this type of reaction.¹⁷⁷ We evaluated both of them and yields were 60 % and 62 %, respectively (Table II.5, entries 6 and 9). In all cases, 20 mol% of triphenylphosphine were added to the reaction mixture to stabilize the palladium catalyst.¹⁵⁸ Being easier to synthesize, store and handle, bis(triphenylphosphine)palladium(II) dichloride was preferred as catalyst.

Optimization of continuous factors



Scheme II.39 | Continuous factors influencing the coupling isomerization reaction.

In the case of the coupling isomerization reaction, a minimum of three continuous factors may affect the yield: temperature, duration, and molarity of the reaction (Scheme II.39). Optimization of such continuous factors is always a complex process. Indeed, combinations are infinite and the probability to find the optimal conditions by chance is rather low. The use of the Design of Experiments (DoE) methodology is a valuable alternative to overcome these difficulties.

Box-Behnken design of experiment

Design of experiment, also called experimental design, is a structured and organized way to evaluate the effects of factors on a response variable.¹⁷⁵ This methodology relies on predetermined matrix of experiment, called "design", which specifies for each factor, the level at which the individual runs in the experiment are to be conducted. Matrix calculation and statistical analysis subsequently result in the determination of a predictive model. This model is then used to determine the optimal value of each factor.

As opposed to the conventional experimental method consisting in changing one factor at a time, DoE is able to highlight effects that are caused by several factors acting in combination, or, on the contrary, parameters which, statistically, are not significantly influencing the response. This procedure is also much easier to implement and carry-out, and provides accurate data faster and cheaper than the former approach.

Considering the great advantage of the DoE methodology, we decided to use a Box-Behnken design (BBD).¹⁷⁸ This design uses a centered quadratic model to calculate the three dimensional representation (response surfaces) of multivariate systems, allowing the optimization of the process.¹⁷⁹ When it comes to use this design, it is, at first, necessary to define factors, variation ranges and observed response. Here, the effects on the yield of three factors upon three levels were studied. Levels were chosen according to preliminary results and previous studies (Table II.6).^{156,158}

Table II.6 | Variation ranges of the studied continuous factors.

Factor	Low level (-1)	Center (0)	High level (+1)
Temperature (°C)	100	125	150
Duration (min)	15	30	45
Molarity (mol.L ⁻¹)	0.2	0.4	0.6

Three factors required fifteen experiments for the development of a Box-Behnken design. Conditions of each run are chosen based on the specific matrix of experiments of the BBD (Table II.7). Experiments were conducted under these conditions and an HPLC quantitative analysis (*vide supra*) of each crude was performed twice to determine the average yield of each reaction (Table II.7). In order to make use of these raw results, data were submitted to a computer-aided statistical analysis using the Minitab 16 software.

Table II.7 | Optimization of the continuous factors

Entry	Temperature (°C)	Duration (min)	Concentration (M)	HPLC yield (%)
1	100	15	0.4	35
2	100	30	0.2	17
3	100	30	0.6	39
4	100	45	0.4	44
5	125	15	0.2	47
6	125	15	0.6	54
7	125	30	0.4	53
8	125	30	0.4	53
9	125	30	0.4	53
10	125	45	0.2	52
11	125	45	0.6	58
12	150	15	0.4	44
13	150	30	0.2	38
14	150	30	0.6	37
15	150	45	0.4	35

*Reaction performed in 1,4-dioxane, with 5 equivalents of triethylamine, and PdCl₂(PPh₃)₂ as a catalyst.

Statistical analysis of the results

Processing the raw data was performed in three steps: multivariate quadratic regression, analysis of the variance, and response optimization. In a Box-Behnken design, the system is supposed to follow a quadratic law. In the case of our reaction, this model therefore consists of ten terms: three second-degree terms, three terms of interaction, three linear terms, and the constant.

$$\begin{aligned}
 \text{Yield} = & \alpha \times \text{Temperature}^2 + \beta \times \text{Duration}^2 + \gamma \times \text{Molarity}^2 \\
 & + \delta(\text{Temperature} \times \text{Duration}) + \varepsilon(\text{Temperature} \times \text{Molarity}) + \epsilon(\text{Duration} \times \text{Molarity}) \\
 & + \theta \times \text{Temperature} + \vartheta \times \text{Duration} + \mu \times \text{Molarity} + K
 \end{aligned}$$

The multivariate quadratic regression of the raw results is used to adjust each coefficient in order to properly fit the model to the observed experimental response variations. Once the regression is achieved, it is possible to plot graphical representations of the equation (response surfaces). These three-dimensional plots help to depict primary trends and to get a better understanding of the system (Figure II.9).

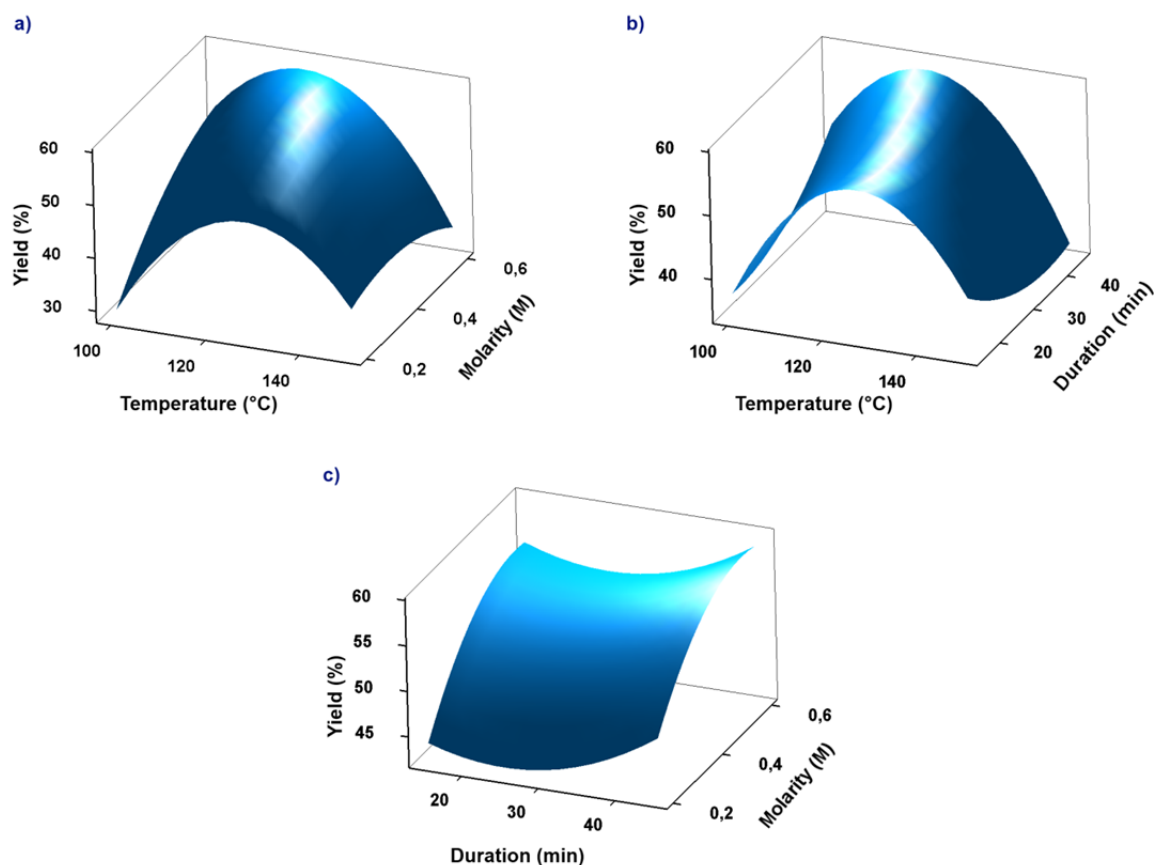


Figure II.9 | Plots of response surfaces. Hold values: a) duration = 45 min, b) molarity = 0.55 M c) Temperature = 120 °C

At first glance, temperature shows a drastic influence on the yield. A maximum is clearly reached around 120 °C, although higher or lower temperatures decreased the yield significantly (Figure II.9, plots a and b). The molarity also plays an important part, as it is often the case in microwave reactions. The higher seems to be the better but a plateau is reached between 0.5 and 0.6 mol.L⁻¹ (Figure II.9, plots a and c). Finally, the effect of irradiation hold time is less obvious as no tendency could be clearly detected (Figure II.9, plots b and c). Nonlinear specific effects of microwave irradiation might explain this observation.¹⁷⁶ This experimental observation would tend to demonstrate that the hold time term may not be statistically significant for the model. This hypothesis can be easily verified by the analysis of the variance.

The analysis of the variance (ANOVA) is used to determine if a factor is statistically significant for the model used to describe the response. ANOVA relies on the statistical Fisher test which is used to determine if, at a fixed significance level, a hypothesis is statistically verified. Regarding the data obtained during the DoE of the optimization of the CIR, the analysis of the variance demonstrated that, at a significance level of $\alpha = 95 \%$, the duration term and all combinations of it are not statistically significant for the model. Likewise, the quadratic term of molarity is also not statistically significant (Box 1).

Box 1 | Analysis of Variance for Yield

Source	DF	Seq SS	Adj SS	Adj MS	F	P
Regression	9	1549.68	1549.68	172.19	13.61	0.005
Linear	3	199.75	1313.97	437.99	34.62	0.001
Temperature	1	45.13	1240.83	1240.83	98.09	0.000
Duration	1	10.12	10.57	10.57	0.84	0.403
Molarity	1	144.50	192.70	192.70	15.23	0.011
Square	3	1136.43	1136.43	378.81	29.95	0.001
Temperature*Temperature	1	1045.20	1035.92	1035.92	81.89	0.000
Duration*Duration	1	46.00	39.00	39.00	3.08	0.139
Molarity*Molarity	1	45.23	45.23	45.23	3.58	0.117
Interaction	3	213.50	213.50	71.17	5.63	0.047
Temperature*Duration	1	81.00	81.00	81.00	6.40	0.053
Temperature*Molarity	1	132.25	132.25	132.25	10.45	0.023
Duration*Molarity	1	0.25	0.25	0.25	0.02	0.894
Residual Error	5	63.25	63.25	12.65		
Lack-of-Fit	3	63.25	63.25	21.08		
Pure Error	2	0.00	0.00	0.00		
Total	14	1612.93				

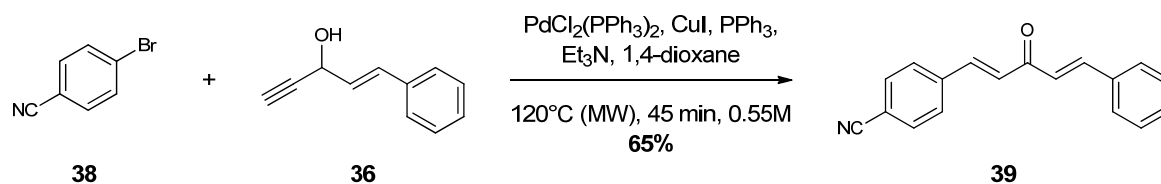
Note: with $\alpha = 95\%$, a factor is significant if $P < 0.05$

These results confirmed the experimental observations about the effect of the irradiation hold time. They also demonstrated that the reaction is following non-linear law as the quadratic term of temperature, as well as the combination term of temperature with molarity, are statistically significant. Taking these new information into account, the quadratic model may be simplified as follows:

$$\text{Yield} = \alpha \times \text{Temperature}^2 + \varepsilon(\text{Temperature} \times \text{Molarity}) + \theta \times \text{Temperature} + \mu \times \text{Molarity} + K$$

Optimized reaction conditions

This new equation can be used to determine the optimized reaction conditions and the corresponding theoretical yield.^{178,180} Here, the maximal yield was predicted to reach 59 % after 45 min of microwave irradiation at a temperature of 120 °C and at a concentration of 0.55 mol.L⁻¹. To meet this expectation, we performed an experiment with starting materials **38** and **36** under the calculated optimal reaction conditions. The final yield after isolation and purification was 65 %, confirming the computed prediction (Scheme II.40).

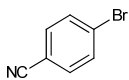
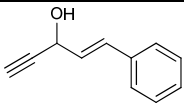
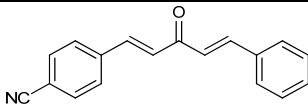
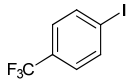
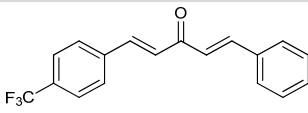
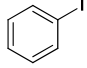
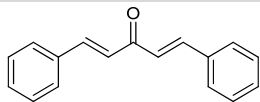
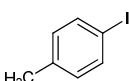
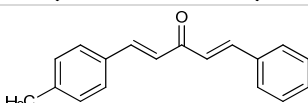
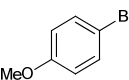
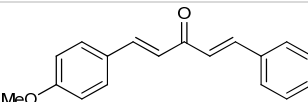
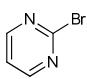
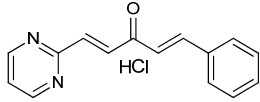
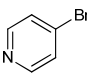
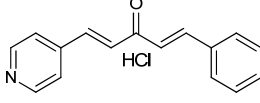
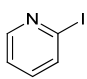
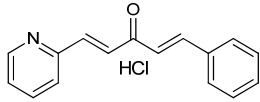


Scheme II.40 | Synthesis of **39** under the predicted optimal reaction conditions.

Scope of the reaction

The methodology under the optimized reaction conditions was then extended to the synthesis of several dissymmetric (hetero)diarylideneacetones (Table II.8). All the (hetero)aryl halides were commercially available, and previously synthesized compounds **36** and **37** were used as propargyl alcohol starting materials (*vide supra*).

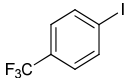
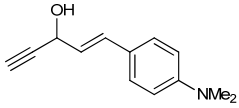
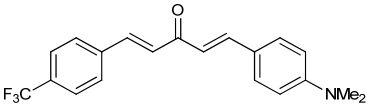
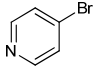
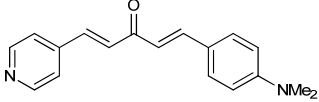
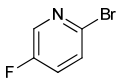
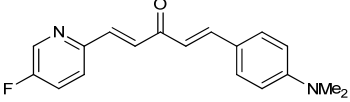
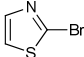
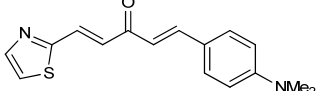
Table II.8 | Scope of the reaction.^a

Entry	(hetero)aryl halide	Propargyl alcohol	Diarylideneacetone	Yield (%) ^b
1		 36	 39	65 68 ^c
2		36	 40	55
3		36		traces
4		36		nd
5		36		nd
6		36	 41	65
7		36	 42	42
8		36	 43	50

^aReaction performed on a 1 mmol scale using the optimized conditions.

^bIsolated yields. ^cScale-up; reaction performed on a 10 mmol scale

Table II.8 | Scope of the reaction.^a (continued)

Entry	(hetero)aryl halide	Propargyl alcohol	Diarylideneacetone	Yield (%) ^b
9				58
10		37		54
11		37		52
12		37		62

^aReaction performed on a 1 mmol scale using the optimized conditions.^bIsolated yields. ^cScale-up; reaction performed on a 10 mmol scale

With respect to the aryl halide, the reaction appeared to be fairly general for electron deficient aryl halides (Table II.8, entries 1, 2, and 9). Unfortunately, electron-rich aryl halides could not successfully be transformed into the title compounds (Table II.8, entries 3-5). This limitation was already observed on the synthesis of chalcones and was overcome by the use of DBU as a base; however, this solution is not applicable to the synthesis of DAA as we demonstrated that the propargyl alcohol does not tolerate a strong base like DBU (*vide supra*). On the other hand, heteroaryl halides, such as pyridyl, pyrimidinyl, and thiazolyl halides were transformed in good yields, to the desired substituted (hetero)diarylideneacetones (Table II.8, entries 6-8 and 10-12). Furthermore, the reaction also displayed a good chemoselectivity toward fluorinated substitutions as the fluorinated pyridyl DAA **46** was obtained in 52 % yield (Table II.8, entry 11).

With regard to the right hand side (RHS) of the molecule, only two substitutions were tested. Indeed, in previous works done on the synthesis of chalcones through CIR, the reaction showed a wide tolerability toward the substitution pattern of the propargyl alcohol. Therefore it was decided to focus our attention on the reactivity of the aryl halide, limiting our investigations of the RHS to only two substrates, namely compounds **36** and **37**. As expected, these two starting materials were successfully coupled to the aryl halide and underwent the isomerization step to give the desired product. The donating effect of the nitrogen of **37** is not likely to influence the reaction. Indeed, phenyl and *p*-dimethyl aniline substitutions displayed

comparable results with satisfactory yields (Table II.8, entries 2-9 and 7-10). This might be advantageously used to obtain dissymmetric DAA with electron-donating group.

Finally, we investigated the possibility to extend this procedure to the preparation of larger batch of product. Indeed, at the end of year 2010, our research unit in Strasbourg purchased a chemistry-dedicated microwave allowing the use of bigger vials (up to 20 mL). Thus, the synthesis of **39** was conducted on a 10 mmol scale –instead of 1 mmol during the optimization process. Optimized reaction conditions were applied exactly as they were initially defined, resulting in the desired product in 68 % yield. The possibility to scale-up the reaction was therefore demonstrated and larger batch should probably be obtained. Until now, regarding the scale of the reaction, the only remaining limitation is the volume of the microwave cavity.

The whole library of dissymmetric (hetero)diarylideneacetones, as well as compounds obtained according to the Claisen-Schmidt procedure, were submitted for biological evaluation in antiparasitic assays. We will now focus our attention on the result of these assays with the aim to give a better understanding on the structure-activity relationship of this series.

In vitro activities against trypanosomatid parasites

Protocols

Parasitic assays

Assessing the activity of compounds is probably the most crucial step in the medicinal chemistry pipeline. Indeed, these results are guiding the whole drug discovery process, leading to discontinue some series in favor of others. An acute attention has therefore to be granted to the protocols of biological assessments to guarantee meaningful data. During the thesis, all compounds were sent for biological evaluation to two laboratories: the Laboratory of Antiparasitic Chemotherapy, led by Prof. Philippe Loiseau at the University of Paris XI (BioCIS, UMR8076 CNRS), and the Laboratory of Microbiology, Parasitology and Hygiene, led by Prof. Louis Maes at the University of Antwerp.

At the University of Antwerp, compounds were evaluated through High-Throughput Screening (HTS) using fluorimetric assays (*T. brucei brucei* and *T. cruzi*) or microscopic counting (*L. infantum*). Within Prof. Loiseau's team, compounds were tested individually and manually using fluorimetric assays (*T. brucei brucei* and *L. donovani*) or microscopic counting (*L. donovani*). Detailed protocols for growth cultures and cell viability assessments are described in the experimental part. The different parasite strains and reference drugs that have been used are summarized in Table II.9.

Table II.9 | Parasites strains and associated reference drugs used in assays.

Parasite strain	Reference drug (IC ₅₀ (μM))
<i>T. brucei brucei</i> Squib 427	Suramin (0.12±0.07 μM)
<i>T. cruzi</i> Tulahuen CL2 β-galactosidase	Nifurtimox (0.845±0.2 μM)
<i>L. infantum</i> MHOM/MA(BE)/67 – Amastigotes	Miltefosine (5.2±0.8 μM)
<i>L. donovani</i> MHOM/ET/67/HU3 – Amastigotes	Miltefosine (19.1±0.1 μM)
<i>L. donovani</i> MHOM/ET/67/HU3 – Promastigotes	Miltefosine (12.8±0.6 μM)
<i>L. donovani</i> R40 Miltefosine-resistant – Promastigotes	Miltefosine (67.8±5.9 μM)

Testing compounds in two different laboratories using different procedures was an interesting opportunity to cross-compare the results and obtain reliable data. In spite of slight differences, it is important to emphasize that both Prof. Loiseau and Prof. Maes used a phenotypic-like screening approach as compounds were evaluated on whole parasites/cells.

Toxicity

As it was previously highlighted, developing less toxic drugs is the main challenge in antiparasitic treatments. Therefore, the assessment of compounds' toxicity was essential in this project. These biological assays were only performed at the University of Antwerp. Cytotoxicity of compounds is evaluated toward human diploid embryonic lung fibroblast *hMRC-5_{SV2}* cells; this cell strain derived from fetal lung tissues was firstly described in 1970.¹⁸¹ It is noteworthy to mention that reference cytotoxic drugs are usually not included in the test because of health hazards for laboratory personnel. Additionally, toxicity toward mouse macrophages is qualitatively observed in *Leishmania* spp. assays. Three concentrations are tested toward these cells (64, 16 and 4 μM) and the range of toxicity is indicated as follows, from the less toxic compound to the most toxic one: T1 (toxic at 64 μM), T2 (toxic at 64 and 16 μM) and T3 (toxic at 64, 16 and 4 μM).

Representation of the results

Further to the biological experiments, results are provided as 50 % inhibitory concentration (IC_{50}) expressed in micromolar. In the following sections these will be shown in table for each parasite and each compound. For easier reading and analysis, compounds will be sorted depending on their activity against *Trypanosoma brucei* rather than on their occurrence.

Aiming at thoroughly analyzing these data, we will plot them on graphs in order to study the correlation between biological activity and several parameters (toxicity, electronic distribution, polarity etc.). These graphs will be expressed in term of $p\text{IC}_{50}$, that is to say $-\text{Log}(\text{IC}_{50})$, where the IC_{50} is expressed in $\text{mol}\cdot\text{L}^{-1}$. As a result, **the higher the $p\text{IC}_{50}$ is, the more active is the compound**. As an example, the graph of the correlation between activity and toxicity is given below (Figure II.10).

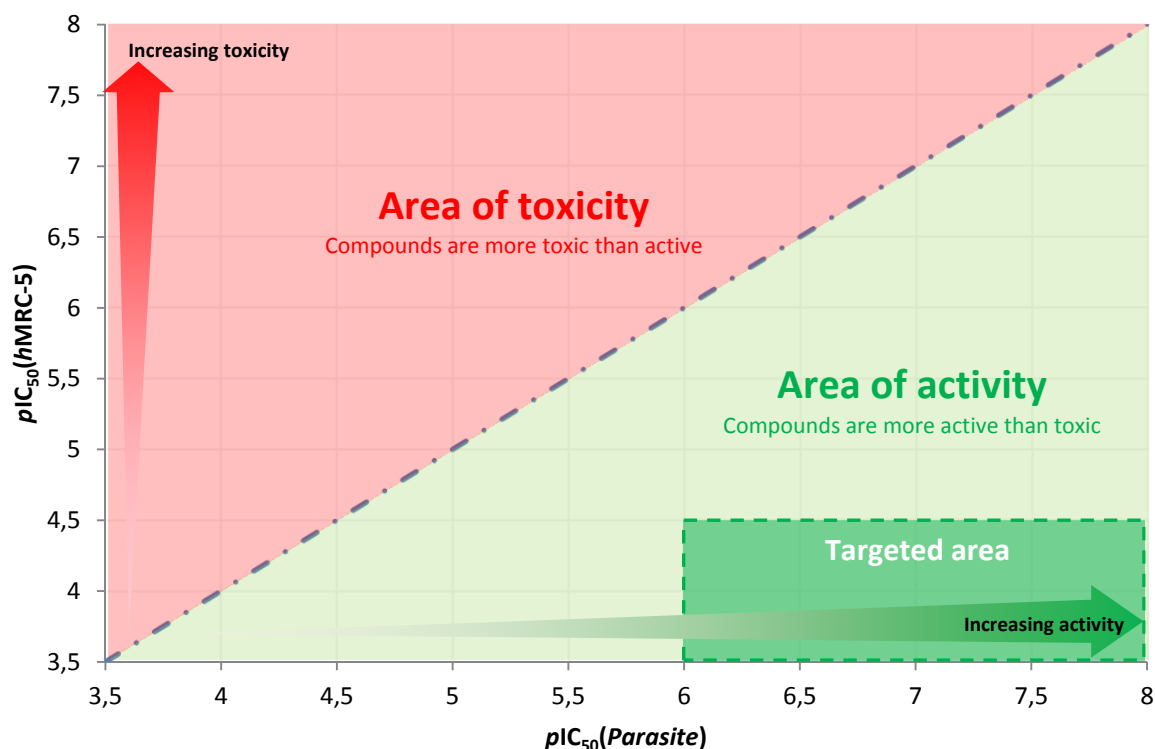


Figure II.10 | Important areas in the plot of antiparasitic activity versus toxicity.

Such a graphical representation allows a rapid identification of compounds meeting the criteria of the drug development process. Indeed, the plot can be divided into three areas:

- Above the first bisector are compounds that are more toxic towards human cells than parasites; these compounds are obviously removed from the pipeline.
- Below the first bisector are compounds that have a higher activity toward parasites than towards human cells. Depending on their selectivity index, these compounds might be interesting and will be subjected for further investigations.
- Finally, compounds located in the targeted area are of high interest as they display low micromolar antiparasitic activity while maintaining a low toxicity towards human cells. Bounds of this area are defined as follows: $IC_{50}(Parasite) < 1 \mu M$ (i.e. $pIC_{50}(Parasite) > 6$) and $CC_{50}(hMRC-5) > 32 \mu M$ (i.e. $pCC_{50}(hMRC-5) < 4.5$).

In addition, the selective plotting of a defined sub-family of molecules (e.g. electron deficient, electron rich, symmetric, dissymmetric etc.) can be used to depict primary trends on the structure-activity relationships. This will be discussed in the last section of this chapter.

Antiparasitic activities of symmetric diarylideneacetones

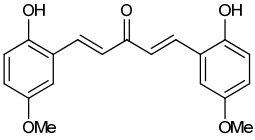
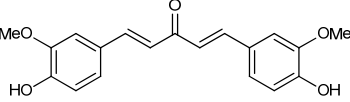
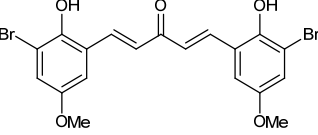
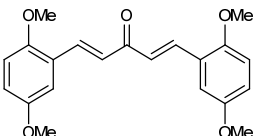
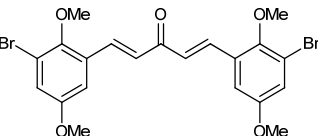
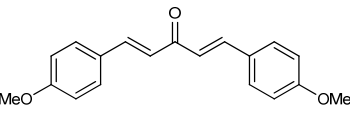
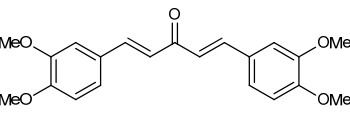
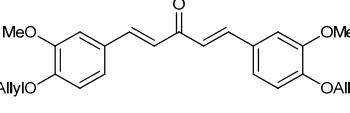
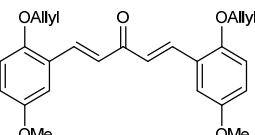
In fine, as part of this thesis, thirteen symmetric diarylideneacetones were synthesized and evaluated for their antiparasitic activity against trypanosomatid parasites. For the sake of an extended discussion on the structure-activity relationship, the most active compounds previously synthesized by Dr. Nicole Wenzel have also been included.¹⁴ These last compounds are identified with a code-name beginning by "NW" or "BJ". In order to make the process of data mining easier, compounds have been clustered depending on their general structure (heteroaromatics, polyphenols etc.) and will be presented further to this classification.

Polyphenol pattern – Curcumin-like substitutions

As previously mentioned, curcumin is well known for its numerous therapeutic properties. In the field of antiparasitic treatments, Dr. Wenzel initiated the exploration of the polyphenol substitution pattern in the DAA series, while a similar investigation on curcuminoid analogs was concomitantly performed and published by Changtam and coworkers.^{14,140} This latter work demonstrated that the *m*-methoxy, *p*-phenol substitution pattern of curcumin was the minimal pattern for antiparasitic activity. The most potent compounds in this series were the ones with a protected alcohol in *para* position ideally with 3,3-dimethylallyl group but methyl, ethyl, allyl groups also displayed a very promising activity in the low micromolar range against *T. b. brucei*.

Based on these promising results, a library of diarylideneacetone bearing this kind of substitution pattern was synthesized and evaluated for antiparasitic activity (Table II.10).

Table II.10 | *In vitro* antiparasitic activities of polyphenolic diarylideneacetones.

Entry	Compound	<i>In vitro</i> assays – IC ₅₀ (μM)				
		<i>hMRC-5</i>	<i>T. cruzi</i>	<i>T. brucei</i>	<i>L. infantum</i>	Tox.
1	 NW327.2	1.88	1.03	≤ 0.32	≥ 32	
2	 NW300	1.06	1.00	≤ 0.32	≥ 32	
3	 NW326.4	0.96	≤ 0.32	≤ 0.32	1.04	T1
4	 NW331	1.02	1.08	0.79	10.36	T1
5	 NW324.1	0.85	0.92	0.94	10.36	T1
6	 NW247	≥ 64	10.7	1.24	≥ 64	
7	 6	6.9	2.09	2.06	30.05	T1
8	 7	≥ 64	36.93	6.78	≥ 64	
9	 13	≥ 16	24.25	26.58	≥ 64	

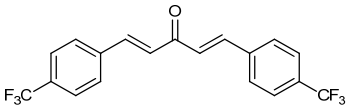
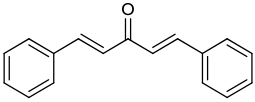
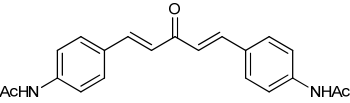
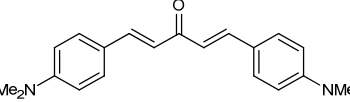
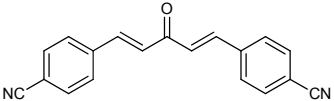
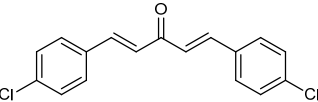
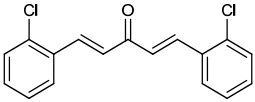
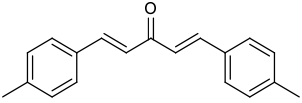
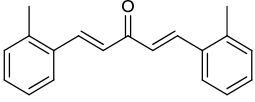
As expected, the curcumin substitution pattern showed a very good activity (Table II.10, entry 2) with IC_{50} values around 1 μ M for *T. cruzi* and *T. brucei*. The isomer **NW327.2** displayed similar results. Unfortunately, this potent activity goes with a very high toxicity, also in the micromolar range. In order to see whether it would be possible to improve this profile several derivatives have been synthesized. Brominated compounds **NW326.4** and **NW326.4** (Table II.10, entries 3 and 5) were also very active but showed an increased toxicity with CC_{50} below the micromolar. Alkylated derivatives were also synthesized and evaluated. However, in spite of the previous results in the curcuminoid series,¹⁴⁰ in the diarylideneacetone series the hydroxyl alkylation clearly resulted in lowered activity. Indeed, when comparing the activity of free phenols **NW327.2**, **NW300**, **NW326.4** to their respective methylated derivatives **NW331**, **6**, **NW324.1**, it appeared that the activity was reduced more than twice in average; and this with no significant reduction in the toxicity. Allylated derivatives **7** and **13** were almost completely inactive, both toward parasites and human MRC-5 cells (Table II.10, entries 8 and 9). The only compound showing an interesting profile was molecule **NW247** which is quite different from the usual curcumin pattern. Generally speaking, none of these compounds were active against *L. infantum* except highly cytotoxic brominated derivative **NW326.4**.

Monosubstituted aromatics

The use of monosubstituted aromatics is quite common during the initial drug discovery process. Indeed, this kind of substitution is obtained from simple starting materials which are widely commercially available at a low cost. In addition, the large amount of functional groups with different electronic properties, combined to the multitude of available isomers, allows a quasi-infinite number of combinations. As a result, the use of such building blocks usually provides valuable and reliable information that can be subsequently used for the design of more elaborated lead compounds.

Eight of these monosubstituted diarylideneacetones were synthesized and evaluated for antiparasitic activity (Table II.11). Once again, one compound synthesized by Dr. Wenzel has been added to the list.

Table II.11 | *In vitro* antiparasitic activities of monosubstituted diarylideneacetones.

Entry	Compound	<i>In vitro</i> assays – IC ₅₀ (μM)				
		<i>hMRC-5</i>	<i>T. cruzi</i>	<i>T. brucei</i>	<i>L. infantum</i>	Tox.
1	 NW267	26.18	1.60	0.25	≥ 64	
2	 8	52.86	16.00	0.38	20.32	T1
3	 4	33.99	10.21	0.51	8.11	T2
4	 3	62.28	36.93	0.81	≥ 64	
5	 16	57.41	11.89	1.47	5.08	T2
6	 10	42.44	35.6	2.14	≥ 60	
7	 11	29.37	12.02	7.81	6.82	T2
8	 5	32.46	41.90	9.27	≥ 64	
9	 2	≥ 64	51.71	≥ 64	8.11	T2

Here we can see that the potency significantly depends on the substituent. Compared to the dibenzylideneacetone **8**, the *p*-trifluoromethyl derivative **NW267** showed a better activity, although its toxicity was twice more important (Table II.11, entries 1 and 2). Substituted anilines had an interesting profile with activity on *T. brucei* below 1 μM at an acceptable level of toxicity (Table II.11, entries 3 and 4). Compound **4** is especially interesting as it showed potency towards *L. infantum* ($\text{IC}_{50} = 8.11 \mu\text{M}$). Similarly, *p*-nitrile disubstituted product **16** was also very potent against *L. infantum* ($\text{IC}_{50} = 5.08 \mu\text{M}$), comparable to the potency of the marketed drug miltefosine. This same compound was also active against *T. cruzi* and *T. brucei* with limited toxicity toward human cells (Table II.11, entry 5). However, toxicity toward mouse macrophages was reported during the biological assays. This might partially explain the good potency against *L. infantum* as these parasites were maintained in mouse macrophages during the test. Finally, chloro- and methyl-substituted derivatives **10**, **11**, **5**, and **2** had a limited activity towards parasites (Table II.11, entries 6 to 9). However, these compounds perfectly illustrate the dramatic effect of a change in the position of a substituent. Indeed, here we can see that, switching from a *para*-methyl-substituted DAA to an *ortho*-methyl, the activity toward *T. brucei* was almost completely suppressed (Table II.11, entry 8 and 9). Chlorine-substituted DAA basically behaved similarly, although to a lesser extent (Table II.11, entries 6 and 7).

In fine, this exploration of monosubstituted DAA highlights four substitution patterns showing a reasonable potency as well as a selectivity index (based on *T. brucei*) about 50 or higher. These substituents are: trifluoromethyl, *N,N*-dimethylamine, nitrile and *N*-acetyl.

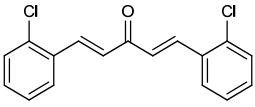
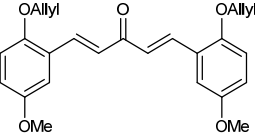
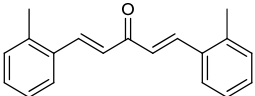
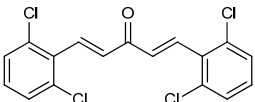
Sterically hindered diarylideneacetones

Among many other parameters, steric hindrance can be used to finely tune the potency of molecules. Supposing that steric hindrance close to the electrophilic reactive centers of DAA might reduce the toxicity by rate-limiting the reaction with glutathione, few compounds with bulky *ortho*-substituents were prepared and evaluated (Table II.12).

The effect of such a steric hindrance is very clear. All the compounds lost almost completely their toxicity but also their activity toward parasites, being the less active molecules in the series. This is particularly obvious when comparing the dichlorinated compound **12** to its mono-chlorinated relative compound **11** (Table II.12, entries 1 and 4).

Although it is impossible to generalize a rule based on four examples only, it might be considered that a large steric hindrance in *ortho* position is likely to decrease significantly the antiparasitic activity, at least in this series.

Table II.12 | *In vitro* antiparasitic activities of sterically hindered diarylideneacetones.

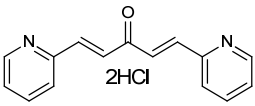
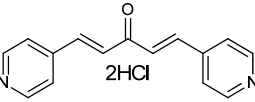
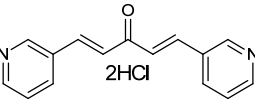
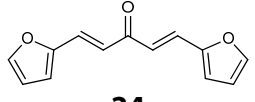
Entry	Compound	<i>In vitro</i> assays – IC ₅₀ (μM)				
		<i>hMRC-5</i>	<i>T. cruzi</i>	<i>T. brucei</i>	<i>L. infantum</i>	Tox.
1	 11	29.37	12.02	7.81	6.82	T2
2	 13	≥ 16	24.25	26.58	≥ 64	
3	 2	≥ 64	51.71	≥ 64	8.11	T2
4	 12	≥ 64	39.52	≥ 64	32.46	T1

Heteroaromatics

Heteroaromatics are more and more subjected to investigation in medicinal chemistry. Indeed, as compared to substituted-phenyls they offer new degrees of freedom to investigate the structure-activity relationships. The position of the heteroatom in the ring can therefore significantly affect the potency as well as the properties of the molecules –especially its solubility– and mesomeric as well as inductive effects of the heteroatom are of considerable importance.

Aiming at investigating this chemical space, Dr. Wenzel synthesized three pyridine-based DAA which were evaluated in antiparasitic assays; as part of this thesis, one furan derivative was synthesized and evaluated (Table II.13). Pyridine-based compounds **BJ621**, **NW319** and **NW321** showed very high potency toward *T. cruzi*, *T. brucei* and *L. infantum* (Table II.13, entries 1 to 3). Unfortunately, this high-nanomolar activity was counterbalanced by an unacceptable cytotoxicity toward human cells in the low-micromolar range. Interestingly, the position of the nitrogen atom in the ring had no significant effect, neither on the antiparasitic activity nor on the cytotoxicity. Finally, compound **24** showed very limited potency. Unless newly synthesized furan-derivatives give good results, this series will probably be discontinued.

Table II.13 | *In vitro* antiparasitic activities of heteroaromatic diarylideneacetones.

Entry	Compound	<i>In vitro</i> assays – IC ₅₀ (μM)				
		<i>h</i> MRC-5	<i>T. cruzi</i>	<i>T. brucei</i>	<i>L. infantum</i>	Tox.
1	 BJ621	1.91	0.29	0.03	0.38	T3
2	 NW319	1.13	≤ 0.32	≤ 0.32	1.04	T3
3	 NW321	1.09	0.91	≤ 0.32	1.04	T1
4	 24	≥ 64	39.83	7.58	32.46	T1

To summarize, pyridine-based DAA are very potent molecules but their cytotoxicity is a major concern which significantly limit their use as lead compound. However, new derivatives based on this core, especially dissymmetric DAA, were considered in order to determine if the toxicity is intrinsically linked with the pyridyl moiety.

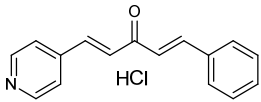
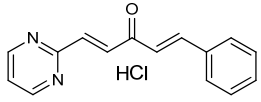
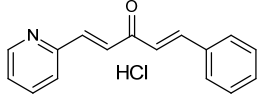
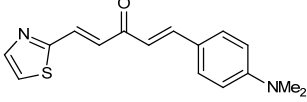
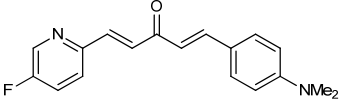
Antiparasitic activities of dissymmetric diarylideneacetones

The synthesis and the evaluation of dissymmetric diarylideneacetones were one of the main objectives of the present thesis. These molecules were designed to study the effect of dissymmetric electronic distribution (Push-Pull effects) on the activity. *In fine*, eleven molecules were sent for biological evaluation.

Heteroaromatics

As we just mentioned, symmetric heteroaromatic diarylideneacetones showed unacceptable toxicity. A library of dissymmetric molecules bearing this heteroaromatic substitution as left hand side was synthesized and evaluated for antiparasitic activity (Table II.14). As expected, DAA based on pyridyl or pyrimidyl moieties showed very good potency, with IC₅₀ below the micromolar range (Table II.14, entries 1 to 3). However, toxicity was still present at an unacceptable level.

Table II.14 | *In vitro* antiparasitic activities of dissymmetric (hetero)diarylideneacetones.

Entry	Compound	<i>In vitro</i> assays – IC ₅₀ (μM)				Tox.
		<i>hMRC-5</i>	<i>T. cruzi</i>	<i>T. brucei</i>	<i>L. infantum</i>	
1	 42	1.99	≤ 0.25	≤ 0.25	0.5	T3
2	 41	1.56	≤ 0.25	≤ 0.25	0.4	T3
3	 43	1.53	0.55	≤ 0.25	1.27	T3
4	 47	33.44	11.02	0.4	38.05	
5	 46	≥ 64	≥ 64	13.3	32.46	T1

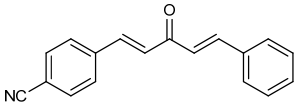
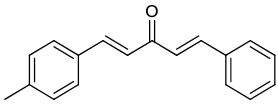
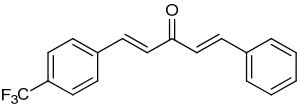
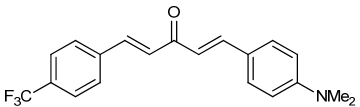
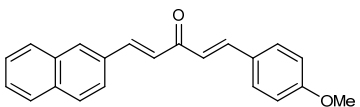
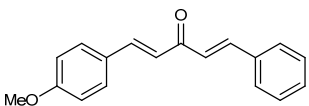
Interestingly, compound **47** bearing a thiazolyl residue as left hand side and a *p*-aniline as right hand side, displayed IC₅₀ value in *T. brucei* assays in the high nanomolar range while the toxicity was limited (Table II.14, entry 4). This might be a good starting point for a future investigation of a new series based on this heterocycle. Finally, the adjunction of a fluorine atom in *para* position with concomitant use of *p*-aniline as right hand side drastically diminished both the activity and the toxicity (Table II.14, entry 5).

Although the number of evaluated compounds is rather low, it might be considered that desymmetrization of pyridine-based DAA may not be sufficient to completely suppress the toxicity of this series while maintaining the activity. At first glance, the toxicity seems to be intrinsically linked to the pyridyl core.

Monosubstituted aromatics

With respect to the interesting activities that monosubstitution pattern demonstrated in symmetric series, we considered the evaluation of such monosubstituted aromatic substituents in dissymmetric series (Table II.15).

Table II.15 | *In vitro* antiparasitic activities of dissymmetric monosubstituted diarylideneacetones.

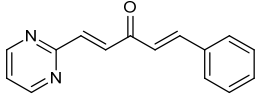
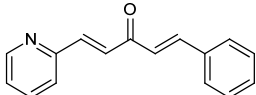
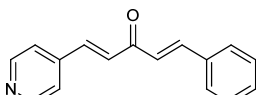
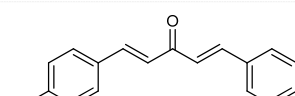
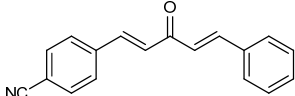
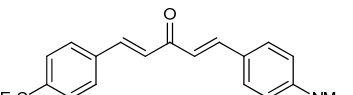
Entry	Compound	<i>In vitro</i> assays – IC ₅₀ (μM)				
		<i>hMRC-5</i>	<i>T. cruzi</i>	<i>T. brucei</i>	<i>L. infantum</i>	Tox.
1	 39	38.73	3.34	≤ 0.25	6.96	T1
2	 20	47.03	2.65	0.5	32.46	T1
3	 40	≥ 64	33.84	2.16	≥ 64	
4	 44	≥ 64	31.71	9.22	8	T1
5	 22	32	9.62	24.59	≥ 64	
6	 21	>64	53.47	>64	>64	T1

Although these molecules have an interesting profile in term of activity and toxicity, the desymmetrization did not achieve further improvements compared to the symmetric molecules that have been previously described. Furthermore, it is noteworthy that dissymmetric compound **21** is completely inactive although its symmetric counterpart **NW247** was selected as the best compound in the polyphenol series.

Antileishmanial activities

A selection of dissymmetric molecules was evaluated by Prof. Loiseau toward promastigotes of two strains of *L. donovani*, a wild type strain (WT) and a miltefosine-resistant strain (R40) (Table II.16).

Table II.16 | *In vitro* antileishmanial activities of dissymmetric diarylideneacetones.

Entry	Compound	<i>In vitro</i> assays – IC ₅₀ (μM)			Tox.
		hMRC-5	<i>L. donovani</i> WT	<i>L. donovani</i> R40	
1	 41	1.56	0.21	0.13	T3
2	 43	1.53	0.6	0.35	T3
3	 42	1.99	1.1	0.9	T3
4	 40	≥ 64	3.6	2.2	
5	 39	38.73	4.4	2.4	T1
6	 44	≥ 64	14	14.3	T1

Reference: Miltefosine, IC₅₀(WT) = 5.1±0.3 μM, IC₅₀(R40) = 67.8±5.9 μM

Once again, the most active compounds were highly cytotoxic pyridine-based DAA **41**, **43** and **42** (Table II.16, entries 1 to 3). Interestingly, trifluoromethylated product **40** displayed a very potent activity toward both strains without any toxicity neither toward human MRC-5 cells nor toward mouse macrophages (Table II.16, entry 4). The use of a *p*-*N,N*-dimethylaniline as a substitute for phenyl as right hand side significantly decreased the activity (Table II.16, entry 6 compared to entry 4).

Beside the potency values, these data are of crucial interest as they demonstrate that the mechanism of action of diarylideneacetones is significantly different from the one of miltefosine, as the miltefosine-resistant strain was still sensitive to our compounds.

Discussion

Correlating the structure of molecules with their *in vitro* activity on targets is always a complex and risky process. Many factors have to be considered and, with a few rare exceptions, it is not common to find a simple quantitative law. In addition, reliable information can only be obtained from the analysis of hundreds of compounds.

Considering the limited library of compounds that has already been tested, the aim of this section is not to establish a precise correlation between molecular descriptors and the antiparasitic activity of DAA. Here, we will only give some general trends resulting from the comparison of the activity *versus* several criteria such as toxicity, electronic distribution and polarity. Compounds synthesized by Dr. Wenzel will be included in each of the following graphs to provide more accurate data. In addition, with respect to the moderate activities of DAA toward *Leishmania* spp., the activity toward *Trypanosoma* parasites will be the only one to be considered in the discussion.

Dissociation of the toxicity from the activity

Since its exploration by Dr. Wenzel and the following experiments performed during her PhD thesis, the diarylideneacetone series suffers from a recurrent issue with the toxicity of compounds. Although several structures were very promising, only very few of them might be safer enough to be considered as good starting point for lead evaluation. Therefore, the main question to answer is: would it be possible to dissociate the toxicity from the activity?

Answering this question needs a thorough analysis of the data obtained from the biological evaluation. In order to facilitate this work, the graphical representation of $pCC_{50}(hMRC-5)$ as a function of $pIC_{50}(\text{parasites})$ was plotted (Figure II.11). At first glance, we can see that most of the compounds are located below the first bisector. Therefore they are more active against parasites than toward human cells. However, many compounds are located near the first bisector, which might mean that the antiparasitic activity is correlated to the toxicity toward human cells. Finally, we can see that only few compounds are located in the targeted area. Furthermore, these compounds are very close to the acceptable limit of toxicity, with a moderate activity against *T. brucei* and almost no potency toward *T. cruzi* or *Leishmania* spp.

In spite of these disappointing results, it might be useful to study these data in detail to determine if some general trends could be drawn. This is the reason why we decided to investigate the impacts of electronic distribution and polarity on the antiparasitic activity.

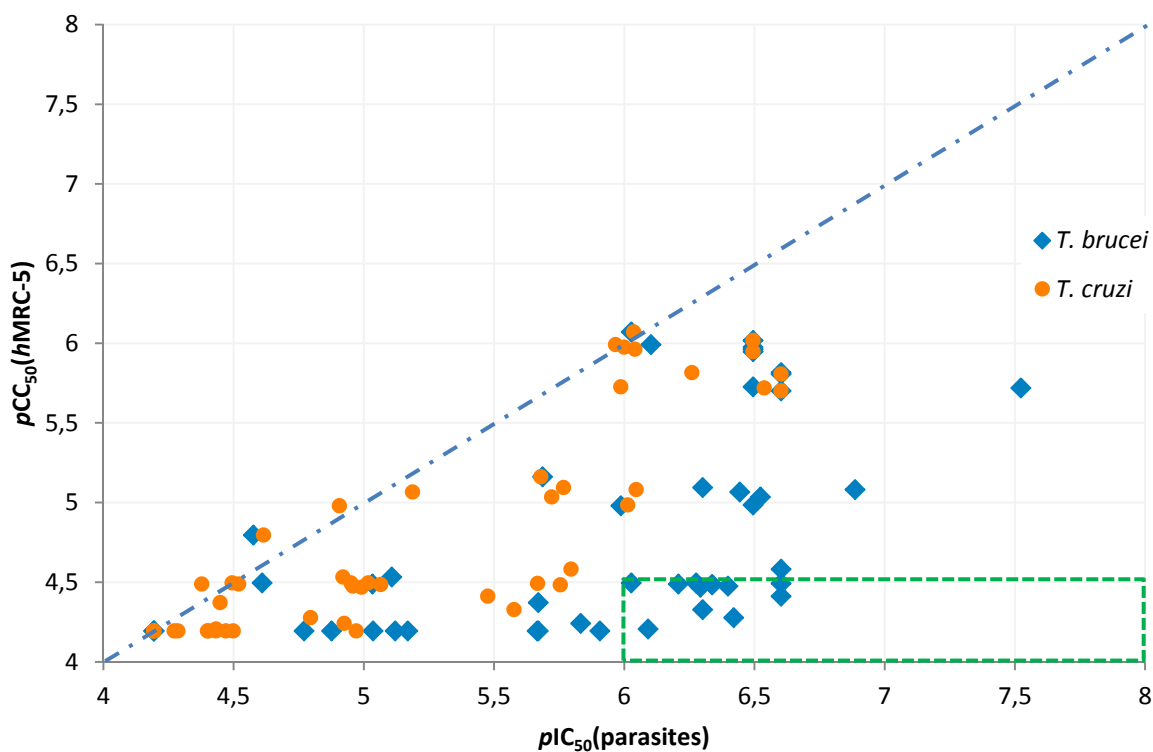


Figure II.11 | Antiparasitic activities versus toxicity plot of the whole diarylideneacetone series.

Effect of the electronic distribution

As we already mentioned several times, the activity of DAA is supposed to result from the Michael-addition of thiols on their electrophilic reactive centers. As the reactivity of such electrophilic carbons is significantly affected by the distribution of the electronic density, it might be interesting to see if the antiparasitic activity can be correlated with the electronic properties of substituents. In the following graph, symmetric compounds have been categorized depending on the electron-withdrawing (EWG), electron-neutral (ENG) and electron-donating (EDG) properties of the substituents (Figure II.12). A similar graph was plotted for the electronic distribution on dissymmetric DAA (Figure II.13). To achieve this goal, three categories were considered:

- push-neutral: when an EDG substituent is on one side of the molecule and a phenyl on the other side,
- pull-neutral: when an EWD substituent is on one side and a phenyl on the other,
- and finally, push-pull: when an EDG is donating its electrons to an EWG through the conjugation of the molecule

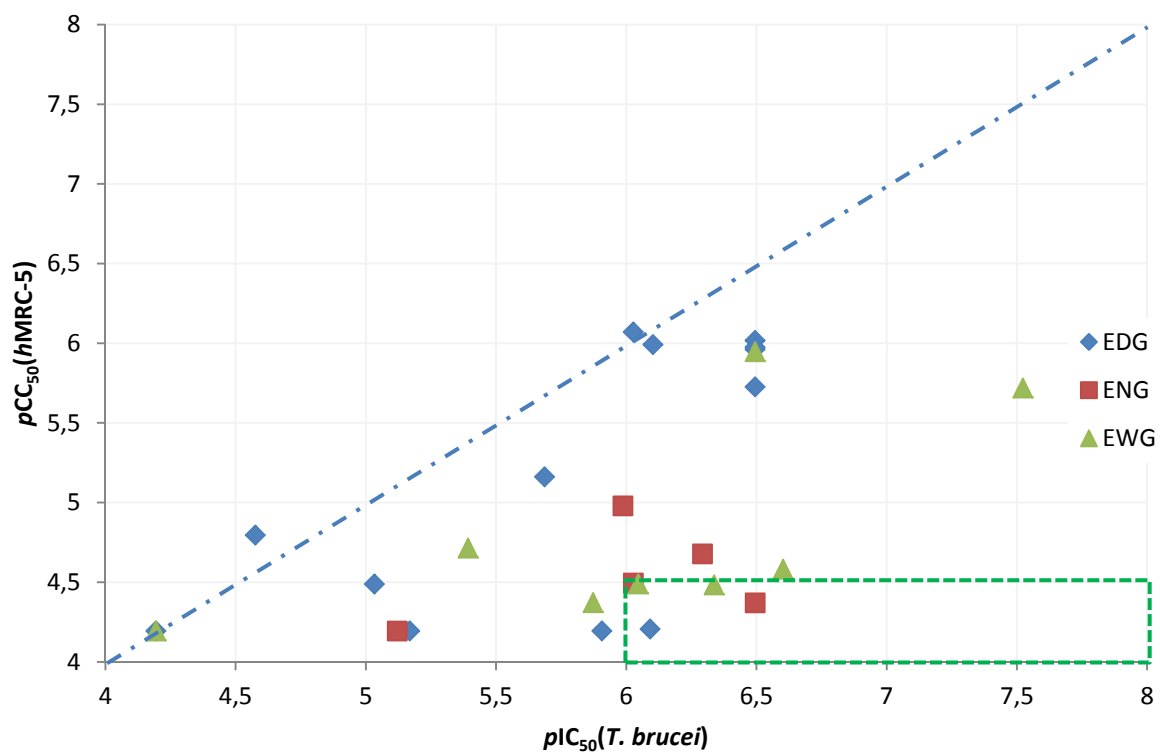


Figure II.12 | Effect of the electronic distribution in the symmetric diarylideneacetone sub-series.

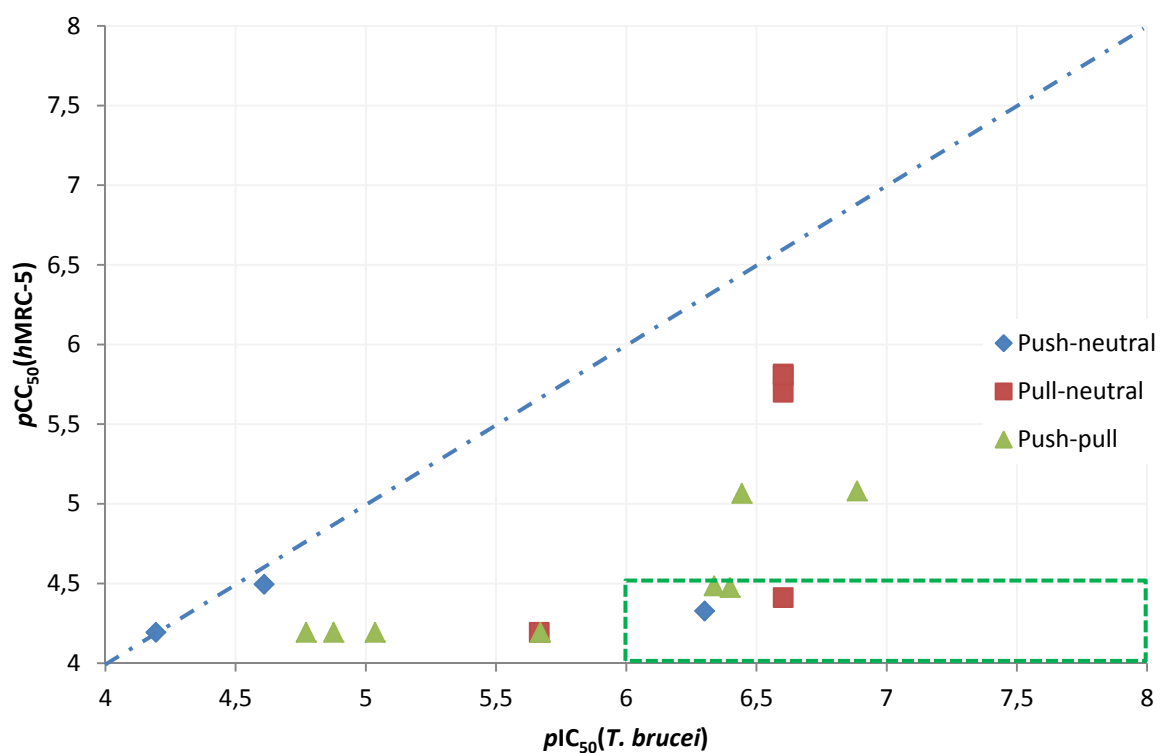


Figure II.13 | Effect of the electronic distribution in the dissymmetric diarylideneacetone sub-series.

Unfortunately, no clear tendency can be outlined from these two graphs. Although compounds bearing electron donating groups seem to have a higher toxicity, some of them are also located in the targeted area (Figure II.12). On the other hand, electron withdrawing groups might contribute to the activity but some of them are also highly toxic (pyridine-based DAA). This lack of relationship between the electronic distribution and the activity can also be noticed for dissymmetric compounds (Figure II.13)

In fine, the effect of electronic distribution is far from being obvious. No clear correlation could be established between the inductive or mesomer properties of substituent and the antiparasitic activity. However, this does not imply that the electronic distribution is not linked to the activity; we can just conclude that the electronic repartition is likely to influence the activity but among several other parameters which makes this correlation complex to demonstrate.

Effect of lipophilicity

Lipophilicity of molecules is an important parameter for drug development. Although it can be neglected in the preliminary steps of a target-based approach, it has to be carefully considered in phenotypic assays. Indeed, compounds have to go across several barriers, either by simple diffusion through membranes –for which the lipophilicity is known to be crucial– or by active transport by specific transporters. In order to assess the possible link between the lipophilicity and the activity of our compounds, the lipophilicity index (logP) of each molecule was calculated using the ALOGPS 2.1 program.^{182,183} It is important to emphasize that these values are only predicted values. However, as they are obtained using the same algorithm, it can be assumed that, in case there is a bias compared to experimental values, then this bias should affect each value, especially on a chemically homogenous series. To feature these data, the graph of the anti-trypanosomal activity as a function of the lipophilicity index was plotted (Figure II.14).

This graph tends to demonstrate a link between the lipophilicity index and the antiparasitic activity as an overall trend is clearly visible. Thus, it can be observed that, with a variation of about four decades in logP, the activity increased in an average of two decades toward *T. brucei*. And the effect is even more visible toward *T. cruzi*. It is noteworthy that this rationale confirmed the experimental observations; indeed, it was shown that the most active compounds were molecules bearing an alkylated amine substituent, a pyridyl/pyrimidyl moiety, or a polyphenol pattern, which are all polar residues.

Nevertheless, the validity of this rationale may be questioned. Indeed, provided the predictive character of these values, it can be argued that this correlation may result from

solubility issues. Although the solubility is expected to be checked during the biological assay, it is possible that molecules with a high lipophilicity index are not completely soluble in the aqueous medium. At a same concentration, this would certainly result in lower observed activities compared to those of more polar molecules.

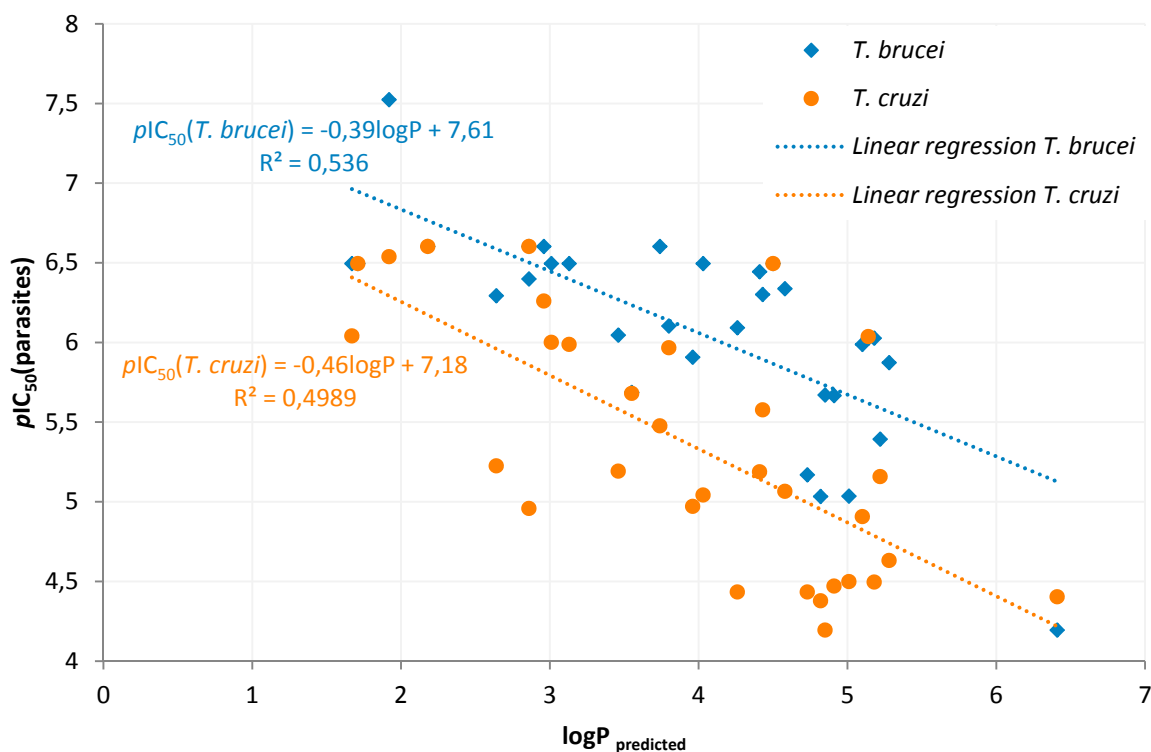


Figure II.14 | Effect of the lipophilicity on the antiparasitic activity.

On the contrary, this trend might express a real need for the drug to be active. Until now, the uptake route of DAA is unknown. Passive transport across the membranes usually required lipophilic molecules. But these highly lipophilic molecules might also remain stuck in the fatty-acids bilayers or in vesicles, resulting in lowered activity. On the other hand, if an active transport is hypothesized, this is achieved through specific transporters which might have higher affinity with less lipophilic compounds. In addition, the intracellular medium in the parasite is mainly aqueous, and polar compounds are therefore more likely to stay in solution, without being expelled from the parasite.

It is obvious that trends based on predicted values cannot be considered as gold-rule for a structure-activity relationship. However this predicted behavior is confirmed by several experimental examples in that series. Therefore, this discussion on the correlation between lipophilicity and activity might be an interesting starting point for further developments which should invalidate or confirm the existence of such a correlation. To achieve this goal, a nascent collaboration is being initiated with Dr. De Koning (University of Glasgow) who identified a *T. b. brucei* transporter specific to curcuminoid analogues (unpublished results).

Conclusion

Following the identification of novel substituted diarylideneacetones as anti-trypanosomatid agents during previous research work in our laboratory, an extended library of molecules was synthesized. Symmetric diarylideneacetones were obtained according to the usual Claisen-Schmidt pathway. Homogenization of the reaction conditions with regards to the nature of the substituents allowed the synthesis of the desired compounds in good to excellent yields. In addition, these protocols appeared to be convenient on a multigram scale (up to 15 g). However, as previously reported in the literature, our experiments confirmed the problematic access to diarylideneacetones bearing heteroaromatic rings as substituents. Furthermore, the synthesis of dissymmetric molecules having this kind of heteroaromatic core was scarcely described. We therefore intended the setup of a new synthetic pathway for the synthesis of dissymmetric (hetero)diarylideneacetones.

We based our new strategy on the work published by Prof. Dr. Thomas Müller's group on the synthesis of chalcones. The authors have described the preparation of this structure through a palladium-catalyzed coupling isomerization reaction under microwave irradiation. Considering structural similarities between chalcones and diarylideneacetones, we aimed at adapting this approach to the synthesis of dissymmetric (hetero)diarylideneacetones. Further to encouraging preliminary results, we implemented an optimization process of the reaction conditions, using the design of experiment methodology. A library of novel dissymmetric (hetero)diarylideneacetones was synthesized through the optimized reaction conditions in moderate to good yields. This new procedure allowed the preparation of diarylideneacetones bearing substituted heteroaromatic rings as substituents which cannot be obtained with the usual synthetic pathways. Furthermore, this approach has proven to be fast and was easily scaled-up on a gram scale.

Both libraries of symmetric and dissymmetric (hetero)diarylideneacetones were evaluated for antiparasitic activities in phenotypic assays with *Trypanosoma cruzi*, *Trypanosoma brucei brucei*, *Leishmania donovani* and *Leishmania infantum*. Several substitution patterns were highlighted for their potency toward parasites. Among them, curcumin-like substitution pattern, *p*-nitrile-, *p*-trifluoromethyl-, and *N*-substituted *p*-aniline were the most promising structures in terms of activity and toxicity. Pyridine and pyrimidine-based diarylideneacetones showed an outstanding nanomolar activity. However an unacceptable cytotoxicity towards human cells seems to be intrinsically linked to these nitrogen-containing heterocycles. Generally speaking, the toxicity remains the major issue of the

diarylideneacetones series. Furthermore, investigations on the structure-activity relationship have demonstrated that the toxicity is correlated to the activity for most of the compounds in this series. However, we were unable to correlate neither the activity nor the toxicity to the electron distribution on the molecules, both in symmetric or dissymmetric series. A correlation was underlined between the activity and the lipophilicity of the molecules. However, as this finding was based on predicted values of the lipophilic index, these data have to be considered with pragmatism and circumspection. Further investigation are therefore needed to definitely determine if less lipophilic molecule are really more potent than more lipophilic compounds or if it is only an artifact of solubility limitation.

When analyzed altogether, these results clearly established the fact that diarylideneacetones cannot be considered as lead compounds. However, the underlying mechanism of action between an electrophilic species and the trypanothione system is definitely a promising approach. We therefore shifted our strategy to the design of prodrugs of diarylideneacetones and their putative metabolites.

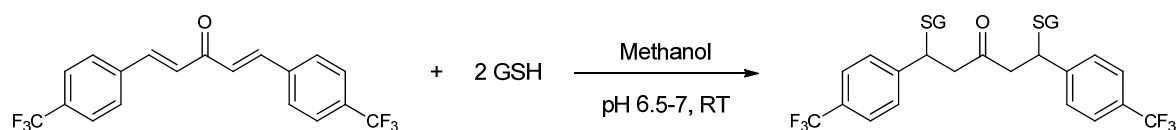
Chapter III

Synthesis and evaluation of 2,6-diaryl-*4H*-tetrahydrothiopyran-4-ones and their relative *S*-oxides as prodrugs

Introduction to the prodrug strategy

Basements of the strategy

In the previous chapter, we reviewed the chemistry and the biological activities of diarylideneacetones. Although most of the molecules in this series are potent toward trypanosomatids, we demonstrated that the toxicity toward human cells is really difficult to dissociate from the antiparasitic activity. This intrinsic toxicity is believed to result from the high reactivity of the two electrophilic centers of the structure toward dithiols. Indeed, Dr. Nicole Wenzel has previously demonstrated that glutathione quickly reacts with DAA to form double-adducts of $\text{DAA}(\text{GS})_2$ (Scheme III.1).¹⁴



Scheme III.1 | Formation of double-adducts of glutathione on DAA's electrophilic centers in biomimetic conditions.

In vivo, DAA are expected to be rapidly quenched by the detoxification system of the host, even before reaching any parasite. The compound's high reactivity would therefore be responsible for its very short half-life, which is non-compatible with its use as a drug. Nevertheless, the *in vitro* observed antiparasitic activity is also likely to result from these same electrophilic centers through perturbation of the trypanothione pathway. Facing this paradox, we then decided to discontinue the research on the direct use of diarylideneacetones as lead compounds.

To address this issue, we considered the development of a new series of compounds which would act as prodrugs of diarylideneacetones. To achieve this goal, we designed a system in which electrophilic centers of the enone are temporary masked, thus reducing significantly side-reactions with the host system. In addition, if the chemical entity used to mask the enone is tailored to be cleaved in specific conditions only found in the parasite, the active diarylideneacetone will be regenerated specifically in the parasite, resulting in an enhanced selectivity. This rationale is the basis for the prodrug strategy illustrated in Figure III.1.

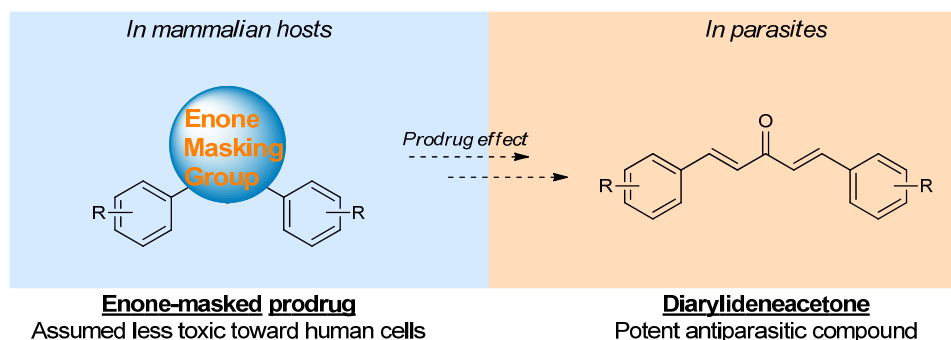


Figure III.1 | Representation of the targeted prodrug effect.

The choice of the Enone Masking Group (EMG) is of utmost importance as the whole strategy relies on the ability of this group to be specifically released in the parasite, regenerating at the same time the active DAA. Furthermore, the introduction of the EMG creates a new degree of freedom in the drug design. This group offers several benefits and may be used to modify and improve ADMET profile as well as the selectivity of the molecule. Several EMG can be considered for this specific application, and we will now give a short overview of the different masking-strategies that can be implemented on the diarylideneacetone series. The aim of this non-exhaustive list is to give some specific examples of marketed prodrugs from which either a ketone, or an unsaturated system, is temporary masked to improve the ADMET profile.

Prodrugs of ketones

A significant decrease in the reactivity of an enone group can be achieved through chemical modifications of the carbonyl function. Indeed, without the ketone group, the electron-delocalization on the molecule is no longer possible and the electrophilicity is therefore clearly reduced. Among the several chemical modifications that can be considered, the reduction of the ketone is probably the most drastic. However, the subsequent unsaturated secondary alcohol is very stable and its re-oxidation in biological conditions might be awkward. Therefore, with the aim of developing a temporary EMG, it appears more favorable to investigate the protection or derivatization of the ketone group. Acetal, imine and oxime derivatizations are probably the easiest way to temporary modify a keto-group. Only few examples of such prodrug are currently marketed. Among them we can quote the norgestimate which is used in hormonal contraceptives. Indeed, it has been demonstrated that norgestimate itself is not responsible for the progestational activity. This oxime acts as a prodrug and it is one of its metabolite, the levonorgestrel, which is the active entity (Figure III.2).^{184,185} Potent levonorgestrel is obtained through a metabolic cascade involving a deacetylation and an oxidation (Figure III.2). The acetyl ester saponification is likely to occur either by simple hydrolysis in biological medium or through enzymatic digestion. On the other

hand, it has been suggested that the oxidation of the oxime to regenerate the ketone might occur mainly in liver microsomes, probably mediated by cytochromes P450.^{186,187}

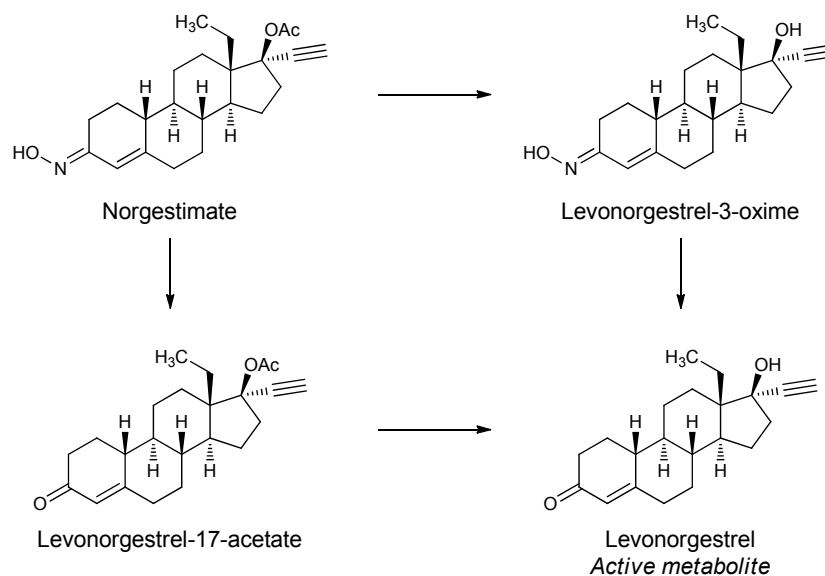


Figure III.2 | Metabolic fate of prodrug norgestimate.

The introduction of the oxime group has also been considered to improve ADMET profile. Thus, the solubility of the antileishmanial drug buparvaquone was significantly enhanced by the chemical transformation of one quinone group to a phosphorylated oxime. The resulting prodrug was highly soluble in aqueous medium, therefore allowing its administration *per os*. The lipophilic buparvaquone is regenerated through a quick alkaline phosphatase hydrolysis followed by an oxidation, most likely mediated by cytochromes P450 (Figure III.3).^{186–188}

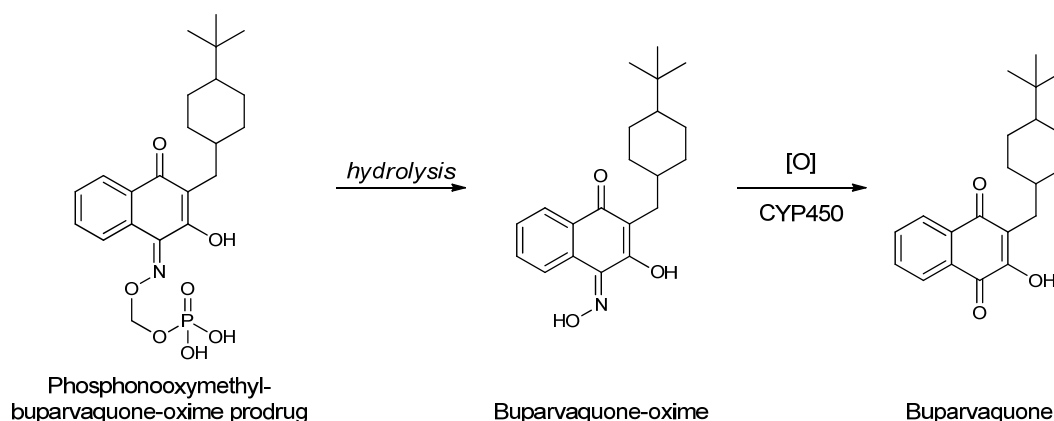
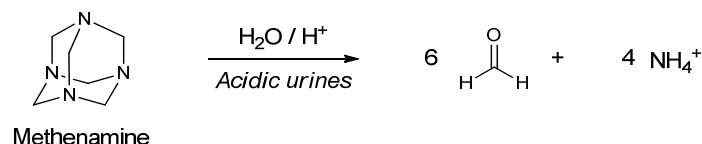


Figure III.3 | Metabolic fate of prodrug buparvaquone.

Being highly sensitive to hydrolysis, imines and acetals are rarely found in drug structures. However, some examples have been reported in the literature. Most of them take advantage of this lack of stability to release the active drug in a specific area of the human body. This is the case of methenamine, an *N*-acetal prodrug of formaldehyde used to cure

infections of the urinary tract.¹⁸⁹ In spite of its powerful antiseptic activity, formaldehyde is toxic for most of the biological systems. Therefore, the use of this product as an antiseptic agent requires a method to selectively deliver it to the urinary tract. Methenamine is encapsulated in tablets that do not dissolve in the acidic environment of the stomach but do dissolve once they reach the basic environment of the intestine. After its absorption through the intestinal lumen, methenamine reaches the acidic medium of the urinary tract where it is hydrolyzed, releasing the antiseptic formaldehyde (Scheme III.2).



Scheme III.2 | Regeneration of formaldehyde from methenamine in the acidic medium of the urinary tract.

To the best of our knowledge, this very specific example is one of the rare cases of a prodrug in which a carbonyl is protected to avoid toxicity issues.

Prodrugs of alkenes

Another approach to limit the toxicity of DAA would be to mask the unsaturated carbon-carbon bonds. This is usually achieved through substitution of double bonds by groups which can be subsequently eliminated in specific conditions. For example, halogens, alcohols, sulfur-derivatives, or carboxylic acids can regenerate a double bond further to dehalogenation, dehydration, desulfurization and oxidative decarboxylation, respectively. This concept is the basis of the mechanism of action of oxamniquine which is used to kill *Schistosoma mansoni* worms responsible for schistosomiasis.¹⁸⁹ The active metabolite is obtained further to activation of parent oxamniquine by a sulfotransferase enzyme expressed by the worm. Once converted in sulfate ester, the free alcohol of oxamniquine is easily eliminated, resulting in the formation of a highly reactive quinone methide imine. The electrophilic center of the terminal alkene immediately alkylates the DNA of *Schistosoma*, preventing DNA replication and leading to the death of the worm (Figure III.4).

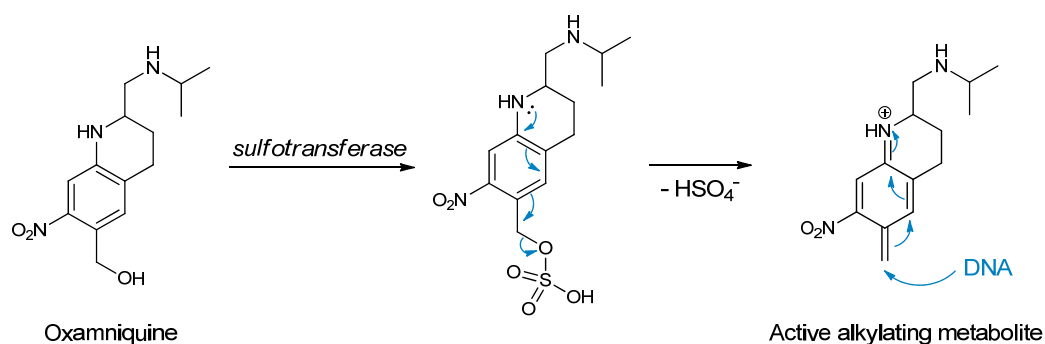


Figure III.4 | Metabolic activation of the alkene reactive center of prodrug oxamniquine.

It is important to notice that this type of deactivated prodrug is usually very stable over a wide range of biological conditions. Indeed, regenerating the active metabolite often requires an activation, either chemically- or enzymatically-mediated, prior to the elimination step. In addition, by removing the unsaturation, the electronic delocalization is normally completely blocked, thus decreasing the reactivity of active centers.

Considering the structure of diarylideneacetones, the deactivation of the unsaturated conjugated systems would require two masking groups (Figure III.5).

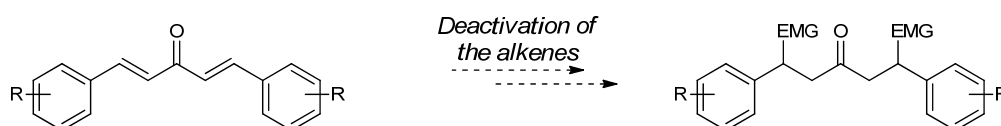


Figure III.5 | Diarylideneacetones have two unsaturated bonds to deactivate.

However, with regard to the specific arrangement of the double α,β -unsaturated ketone, a six-membered ring would be very favored further to the addition of a first masking group (Figure III.6).

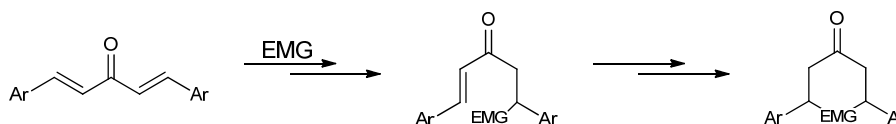


Figure III.6 | Diarylideneacetone deactivation through cyclization.

The resulting heterocycle is expected to efficiently stabilize the masked form of the active DAA. This prolonged half-life of the inactive prodrug should allow a large distribution of the product within the host before it starts reacting with any endogenous nucleophile (cysteines, glutathione etc.). Finally, the three dimensional arrangement of the cyclized prodrug is very different from the one of the parent diarylideneacetones. It is well known that such spatial changes can significantly modify biological activities.¹⁸⁹

Choice of the masking strategy

The choice of the enone masking strategy was mainly ruled by the need to develop a stable prodrug. With regard to their very limited stability in biological medium, imines and acetals were considered as too labile EMG and therefore not matching our criteria. Although oximes are more stable toward acidic and basic aqueous conditions, their high reactivity with cytochromes P450 was a source of concern. Indeed, this might imply that the active DAA would be regenerated in considerable amount in the liver, causing significant hepatotoxicity. *In fine*, the transient derivatization of the keto-group does not appear as a promising strategy for the development of prodrugs of DAA.

On the other hand, the deactivation of the alkenes through the formation of a cyclized prodrug is expected to significantly stabilize the structure. Depending on the nucleophilic EMG used to cyclize, further derivatization may be done on this group, creating a new degree of freedom to optimize the pharmacokinetic and pharmacodynamic profiles. Furthermore, as we previously mentioned, the spatial arrangement around the heterocycle can also significantly modify the biological activity. Last but not least, the chemistry of these six-membered heterocyclic ketones is not extensively developed in the literature; exploring the synthesis of such small heterocycles is always a very interesting challenge that often results in the discovery of new methodologies. Considering these arguments altogether, the deactivation of DAA through the formation of heterocyclic derivatives was selected for the development of our prodrug strategy.

Heterocyclic prodrugs of diarylideneacetones

Further to the choice of the masking strategy, we defined the essential structural specifications of the heterocyclic prodrugs that we intended to develop. These features are summarized on Figure III.7.

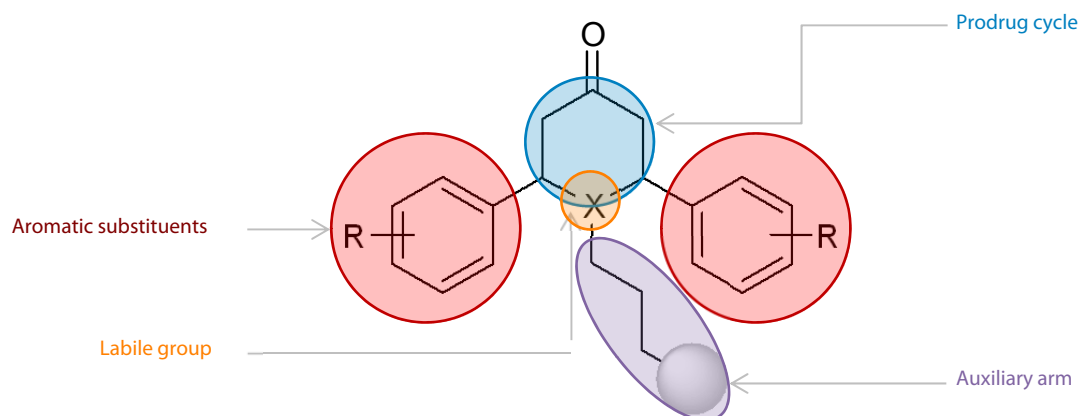


Figure III.7 | Design of the targeted diarylideneacetone prodrug structure.

Four specific items can be distinguished:

- The **prodrug cycle**, which stabilizes the prodrug through the creation of a favored six-membered ring that temporarily deactivates the electrophilic centers of the enone.
- The **labile group**, at the heart of the heterocycle, which is supposed to be easily eliminated, regenerating at the same time the two double bonds of the parent DAA. Ideally, this group has to be chosen for being eliminated only in parasites.
- The **two aromatic substituents**, which allow a fine tuning of the electrophilicity –and consequently of the antiparasitic activity– of the parent DAA. Substitution pattern of these aromatic substituents will be chosen according to previous SAR results obtained

on the DAA series. Can also be used for the inclusion of structural patterns specifically recognized by the parasite.

- The **auxiliary arm**, optional, this additive chain is to be used for the optimization of the ADMET profile or, ideally, for the inclusion of structural patterns specifically recognized by the parasite.

The next step in the design consisted in selecting the labile group to be used to form the heterocycle. Possibilities are rather limited as only oxygen-, nitrogen-, sulfur- or phosphorus-containing groups might be used. Phosphorus heterocycles are very exotic species, not so much described in the literature and very rarely used in drug design. Pyranones and their relative oxygen-containing heterocycles are known to be stable and do not easily undergo elimination to regenerate double bonds. Finally, only nitrogen- and sulfur-containing heterocycles might match the criteria of our prodrug strategy.

2,6-diarylpiperidine-4-ones as candidates for the prodrug strategy

Nitrogen containing heterocycles are commonly used in drug design. Interactions with biological (macro)molecules and metabolic fate of such compounds are well known and can be of great benefit for the prodrug strategy. Thus, the *N*-methyl-2,6-diarylpiperidine-4-one core was investigated by Dr. Nicole Wenzel during her doctoral work. The choice of this specific core was supported by the fact that numerous prodrugs are including methylated nitrogen which, in the human body, is prone to be demethylated by several enzymes. As an example, this is the case of marketed diazepam and hexobarbitone. These two CNS-targeting drugs are believed to act as prodrugs, releasing their respective active metabolites after *N*-demethylation (Figure III.8).¹⁸⁹

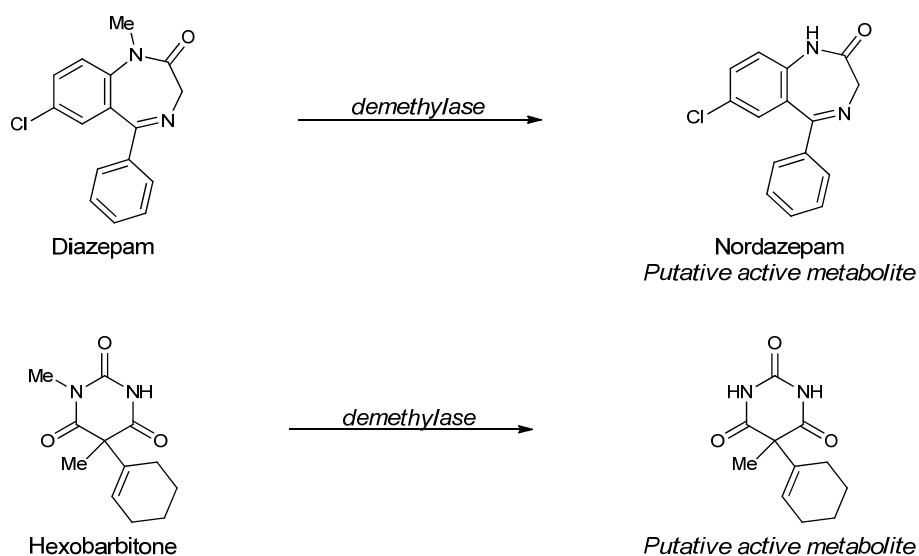


Figure III.8 | Example of prodrug activation through *N*-demethylation.

In the case of *N*-methyl-2,6-diaryl-4H-tetrahydrothiopyran-4-one, two different metabolic pathways are expected to take place (Figure III.9).

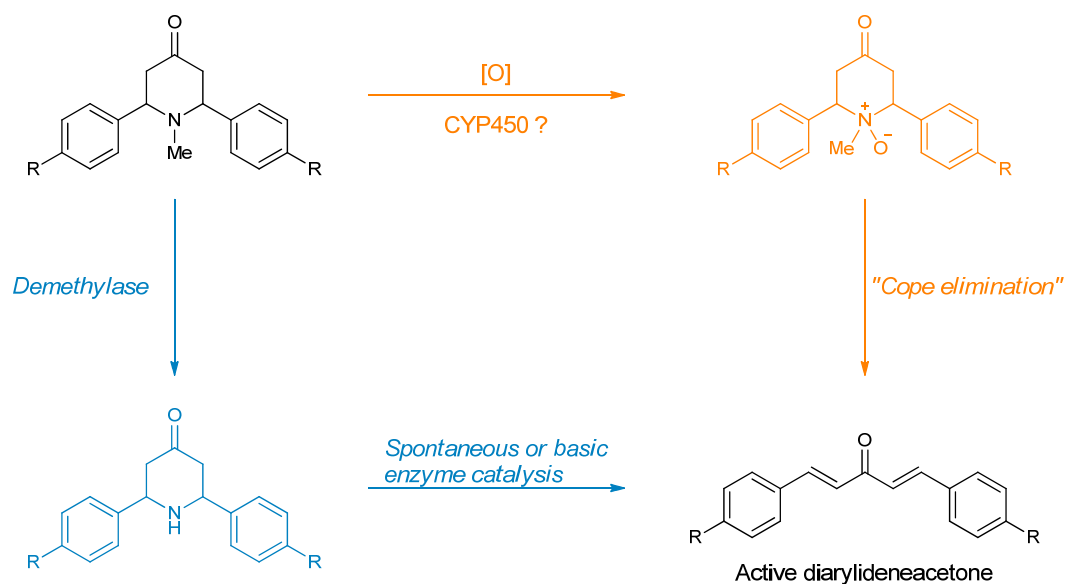
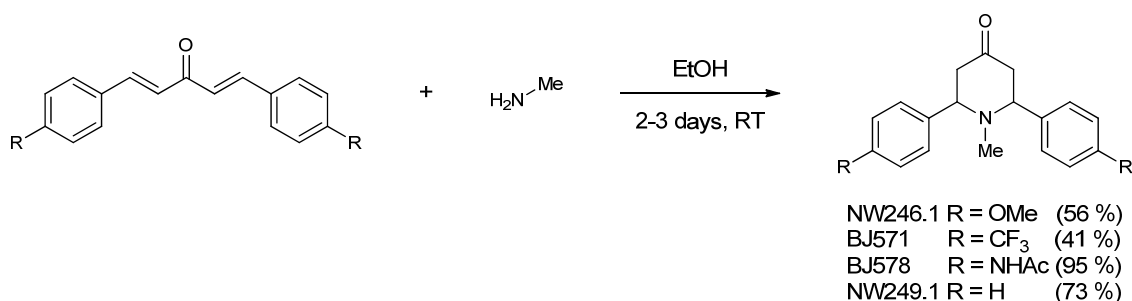


Figure III.9 | Putative metabolic cascade resulting in the regeneration of a diarylideneacetone starting from a *N*-methyl-2,6-diaryl-4H-tetrahydrothiopyran-4-one

Following the first pathway (Figure III.9, in blue), prodrug might firstly be enzymatically demethylated (*vide supra*) giving the free amine intermediate which subsequently reacts to release the active DAA and ammoniac, either by spontaneous degradation or under basic enzyme catalysis. On the other hand (Figure III.9, in orange), prodrug would be oxidized first giving an *N*-oxide intermediate. This product might next undergo a pseudo Cope elimination in biological conditions resulting in the formation of the active DAA and of the *N*-methylhydroxylamine.

N-methyl-2,6-diaryl-4H-tetrahydrothiopyran-4-ones were synthesized by nucleophilic addition of methylamine on the parent DAA (Scheme III.3).



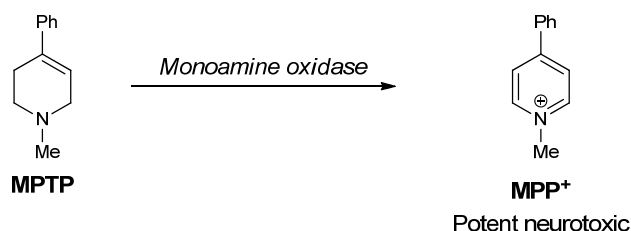
Scheme III.3 | Synthesis of *N*-methyl-2,6-diaryl-4H-tetrahydrothiopyran-4-one and yields previously obtained by Dr. Wenzel.

Resulting diastereoisomeric mixtures were evaluated for their antiparasitic activity and displayed very good potency with IC_{50} values in the low micromolar range (Table III.1).

Table III.1 | *In vitro* antiparasitic activities of *N*-methyl-2,6-diarylpiperidine-4-ones.

Entry	Compound	<i>In vitro</i> assays – IC_{50} (μ M)				Tox.
		<i>h</i> MRC-5	<i>T. cruzi</i>	<i>T. brucei</i>	<i>L. infantum</i>	
1	NW249.1	≥ 64	4.50	≤ 0.25	≥ 64	
2	BJ578	8.52	2.13	0.50	8.11	
3	BJ571	32.22	8.26	0.79	32.00	
4	NW246.1	≥ 64	23.97	8.46	≥ 64	

Unfortunately, *in vivo* studies in rodents were disappointing. Although completely cured, most of the animals died from the treatment, developing significant symptoms of neurological disorders (shivers, dizziness, drowsiness etc.). One possible explanation of this toxicity toward the CNS might be the formation of *N*-methylpyridinium derivatives that are known to be very potent neurotoxic compounds.¹⁹⁰ This was demonstrated with 1-methyl-4-phenyl-1,2,3,6-tetrahydropyridine (MPTP) which is converted by monoamine oxidase in neurotoxic 1-methyl-4-phenylpyridinium (MPP⁺) (Scheme III.4).¹⁹⁰

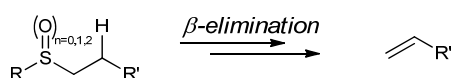


Scheme III.4 | Example of monoamine oxidase-mediated reaction resulting in the formation of neurotoxic 1-methyl-4-phenylpyridinium.

Such toxic analog metabolites might be obtained in a similar manner with the 2,6-diarylpiperidine-4-one compounds. Considering the high neurologic toxicity of tested compounds, the *N*-methyl-2,6-diarylpiperidine-4-one series was temporary discontinued.

2,6-diaryl-4H-tetrahydrothiopyran-4-ones as candidates for the prodrug strategy

The last element that may be used for the prodrug strategy is sulfur. Sulfur containing heterocycles are also common in organic chemistry as well as in drug development, although to a lesser extent than nitrogen-containing heterocycles. Sulfur is especially interesting due to its several degrees of oxidation and its many and varied metabolic fates once in human body. These different pathways have been subjected to numerous researches and are now perfectly known.^{191–195} In the field of organic chemistry, the synthesis and the reactivity of sulfur-containing compounds have also been extensively studied and described in the literature.^{196,197} In particular, it is well known that sulfide, sulfoxide and sulfone can undergo β -elimination, thus resulting in the formation of a double bond (Scheme III.5).

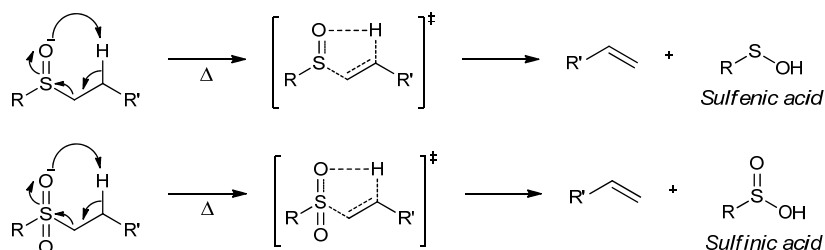


Scheme III.5 | Regeneration of double bonds through β -elimination of sulfurated groups.

This elimination of a sulfurated leaving group can occur according three different mechanisms: pericyclic, ionic or radical.

Pericyclic pathway

Under thermal conditions, a pericyclic β -*syn*-elimination is liable to occur spontaneously. Sulfoxides will lead to the formation of a sulfenic acid whereas sulfones give a sulfinic acid (Scheme III.6).^{198,199}

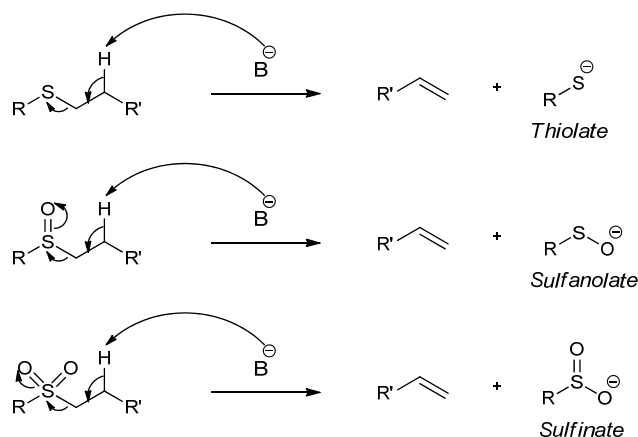


Scheme III.6 | Pericyclic reactions of sulfurated species resulting in the regeneration of a double bond.

The activation temperature of this reaction is really substrate-dependent and *syn*-elimination of some sulfoxides has been observed from 0 °C.²⁰⁰

Ionic pathway

In this case, a base is needed to deprotonate the proton which is in *beta* position to the sulfur atom. Subsequent elimination of the leaving group results in the formation of the double bond and of different anionic sulfur-derivatives, depending on the oxidation state of the sulfur (Scheme III.7).^{201,202}

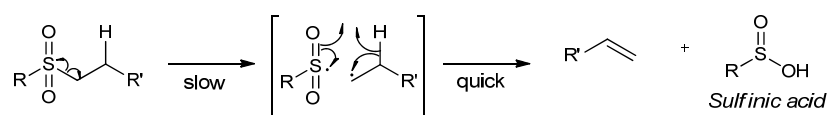


Scheme III.7 | Base-mediated β -elimination of sulfurated groups resulting in the regeneration of a double bond.

It has been demonstrated that, in this mechanism, the deprotonation step is the rate-limiting step.²⁰³ With R and R' fixed, the pK_a of the proton in beta position to the sulfur atom is generally lower for sulfoxides and sulfones than for sulfides. As a consequence, this ionic mechanism is expected to be facilitated with oxidized forms of sulfur.

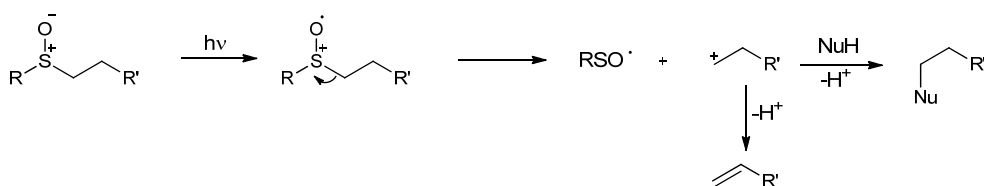
Radical pathway

The last possible pathway for the β -elimination of a sulfur-containing group is to create radicals on the structure. As often in radical reactions, numerous mechanisms can be considered. Here we will only discuss two of them. It is now well known that a carbon-sulfur bond is longer and less strong than C-C, C-O or C-N bonds. Therefore, the homolytic break of the carbon-sulfur bond can lead to the formation of two radicals. Subsequent rearrangement results in the formation of the alkene and of different sulfur-derivatives, depending on the oxidation state of the sulfur (Scheme III.8).¹⁹⁸



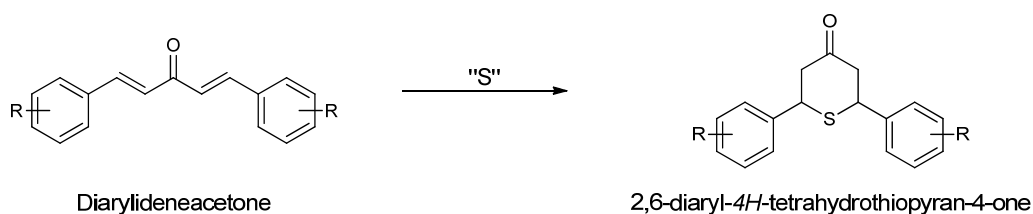
Scheme III.8 | Homolytic break of a C-S bond resulting in the regeneration of a double bond.

Another possibility is to create a radical on the oxygen of a sulfoxide. This can be achieved through photochemical irradiation or chemical activation. Subsequent heterolytic rupture of the carbon-sulfur bond results in the formation of a carbocation which can then undergo β -elimination or nucleophilic quenching (Scheme III.9).²⁰⁴



Scheme III.9 | Photochemical irradiation of sulfoxides resulting in the regeneration of a double bond.

These experimental data are supporting the hypothesis that sulfur-containing compounds are prone to regenerate double bonds further to β -elimination and are therefore interesting candidates for the prodrug strategy. Starting from diarylideneacetones, the addition of sulfur will result in the formation of 2,6-diaryl-4H-tetrahydrothiopyran-4-ones (2,6-DA-4-THTP) (Scheme III.10).



Scheme III.10 | 2,6-diaryl-4H-tetrahydrothiopyran-4-ones selected as prodrug for diarylideneacetones.

Further to the different elimination mechanisms that we previously described (*vide supra*), 2,6-DA-4-THTP are expected to be metabolized *in vivo* to the active DAA. Targeting the pericyclic elimination pathway would imply designing drugs which spontaneously react at the human body temperature. This is obviously not desirable as such compounds would be highly reactive and not stable in standard conditions, and even less under the tropical climate of the endemic areas. On the other hand, ionic and radical pathways can reasonably be considered as potential metabolic fate for 2,6-DA-4-THTP. Indeed, the host immune response is responsible for a highly oxidative stress near parasites implying considerable amount of ROS and free radicals. Although less obvious and more elusive, a basic catalysis is also always possible in any enzymatic pocket or specific biological compartments. We previously mentioned that the elimination step is all the more facilitated as the sulfur atom is oxidized. Therefore, it might be possible that the regeneration of the active DAA requires the preparation of oxidized forms of the prodrug, either chemically through the synthesis of S-oxides, or enzymatically directly from the sulfide. These different metabolic pathways are summarized in Figure III.10.

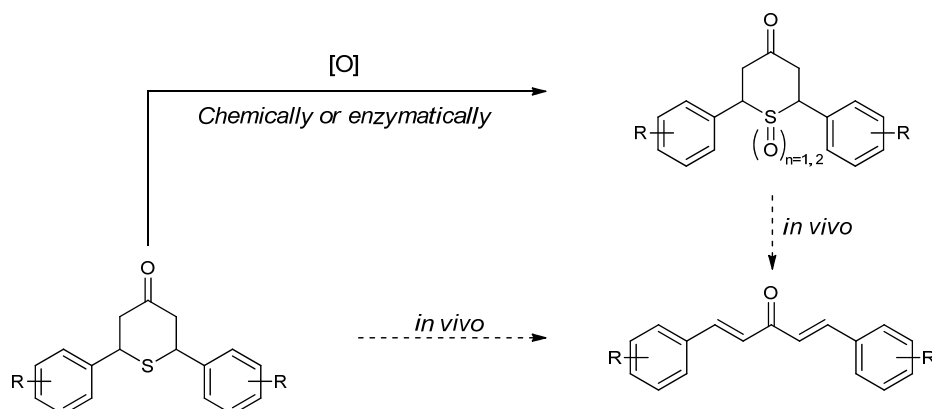


Figure III.10 | Expected metabolic cascade resulting in the regeneration of a diarylideneacetone starting from a 2,6-diaryl-4H-tetrahydrothiopyran-4-one.

Considering all these promising leads, we focused our research on the 2,6-diaryl-4H-tetrahydrothiopyran-4-one core and more specifically on:

- the set-up of new reaction conditions, their test and the characterization of the obtained products,
- the optimization of the new diastereoselective synthesis of both diastereoisomers of 2,6-diaryl-4H-tetrahydrothiopyran-4-ones, in safe and mild conditions,
- the synthesis of the relative S-oxides and their characterization,
- and the evaluation of the antiparasitic activities of this new class of products.

These different points will be discussed in the following sections.

The 2,6-diaryl-4H-tetrahydrothiopyran-4-one core at a glance

Heterocyclic chemistry is one of the most appealing and important field of research in organic chemistry. Whereas the chemistry of nitrogen or oxygen heterocycles was thoroughly researched, the sulfur-containing heterocyclic chemistry was subjected to less investigation. In the following sections we will detail the previously reported uses and syntheses of 2,6-diaryl-4H-tetrahydrothiopyran-4-ones, highlighting the numerous drawbacks of these aged procedures. Aiming at overcoming these issues, we will suggest a new methodology for the diastereoselective synthesis of 2,6-DA-4-THTP.

Overview of the 2,6-diaryl-4H-tetrahydrothiopyran-4-ones – Conformation and configuration of the ring

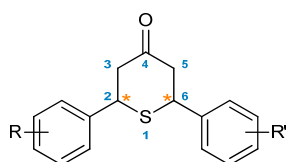


Figure III.11 | 2,6-diaryl-4H-tetrahydrothiopyran-4-one ring.

In spite of its apparent simplicity, the 2,6-diaryl-4H-tetrahydrothiopyran-4-one ring has two asymmetric carbons on a saturated six-membered ring subjected to conformational equilibrium (Figure III.11). As a consequence, conformational and configurational aspects have to be carefully considered. As part of this thesis, we limited our

exploration of the series to symmetric molecules, that is to say where $R = R'$ (Figure III.11). Therefore, all stereochemical and conformational properties described hereafter refer to symmetrical molecules.

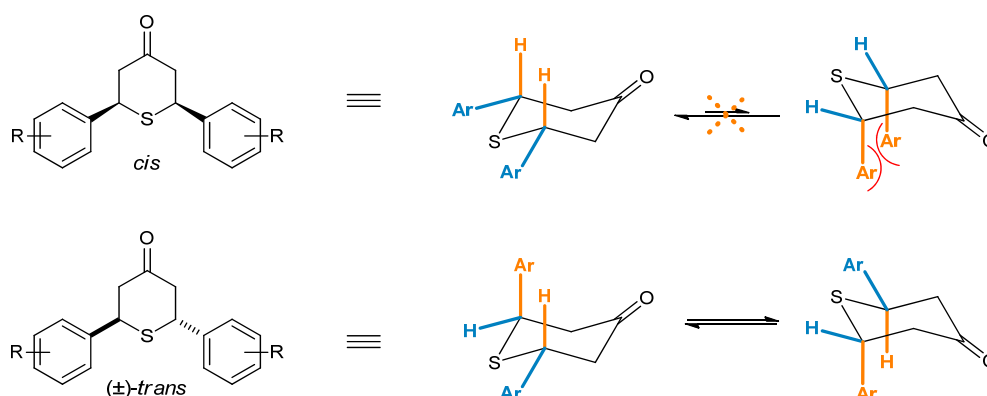


Figure III.12 | Configurational and conformational aspects of the 2,6-diaryl-4H-tetrahydrothiopyran-4-one ring.

On a stereochemical point of view, symmetric 2,6-diaryl-4H-tetrahydrothiopyran-4-ones might be obtained as two diastereoisomers: the *cis* –when both aryls are on the same side of the symmetry plan of the molecule– and the *trans* –when the two aryls are on both side of the symmetry plan. Figure III.12 shows the four main chair conformations that can be expected from a six membered ring sulfur heterocycle such as 2,6-DA-4-THTP. Indeed, it has been

previously demonstrated that this core is predominantly arranged in chair, both in liquid and solid state.^{205–208}

On Figure III.12 we can see that, for the *cis* isomer, aryls might be both in equatorial position or both in axial position. The latter being highly thermodynamically disfavored due to diaxial interactions, this axial conformer is assumed to be negligible. Thus, the *cis* isomer presents one unique conformer, the equatorial one, which, on a stereochemistry point of view, is a *meso* stereoisomer. Substituents of the *trans* diastereoisomer have an equal probability to be placed on an axial or an equatorial position (Figure III.12). Indeed, due to the symmetry plan of the molecule, the resulting two conformers have exactly the same energy, and thus the conformational equilibrium is assumed to be rapid and perfectly balanced; this hypothesis has been corroborated by spectroscopic analysis.²⁰⁶ Unlike the *cis*, two different enantiomers might be obtained from the synthesis of the *trans*; without any evidence of optical activity, *trans* product is assumed to be a racemic mixture, and will be next referred to (\pm)-*trans* isomer.

According to these configuration and conformational analysis, the *cis* isomer is expected to be the product of lower energy and thus thermodynamically favored. Consequently, the (\pm)-*trans* isomer is supposed to be thermodynamically less favored.

Reported uses and synthesis of 2,6-diaryl-4H-tetrahydrothiopyran-4-ones – A literature review

Reported uses of 2,6-diphenyl-4H-tetrahydrothiopyran-4-one derivatives

Although this six membered heterocyclic compound has not been yet isolated from natural sources, it has a wide range of properties, and thus might be considered as a promising series for numerous applications.²⁰⁹ This core and its derivatives were firstly studied for their electronic and redox properties.

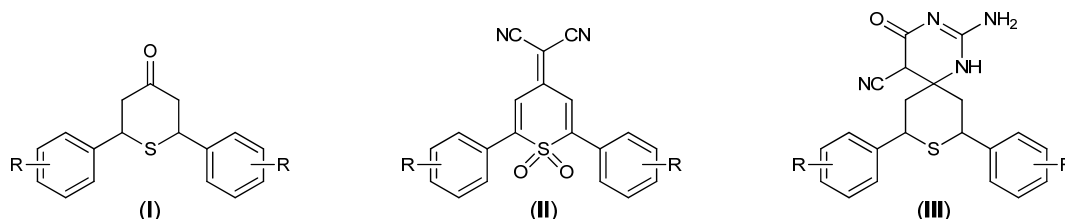


Figure III.13 | Examples of 2,6-diaryl-4H-tetrahydrothiopyran-4-one derivatives reported in the literature.

The *cis* 2,6-diphenyl-4H-tetrahydrothiopyran-4-one (Figure III.13, compound I where R = H) was demonstrated to behave as an inhibitor of copper corrosion in sulfuric medium.²¹⁰ This product is also the starting material for the synthesis of 2,6-diaryl-4-thianones and dicyanomethylene

derivatives (Figure III.13, compound II) which show interesting electron transport properties. Such products were successfully used as laser dyes, organic conductors or as electrophotographic elements in xerography processes.^{150,211,212} In total synthesis, 2,6-diaryl-4H-tetrahydrothiopyran-4-ones were used in the synthesis of fused heterocyclic systems. Indeed, it can be easily converted into bicyclic systems where the first cycle is a six membered sulfur heterocycle, and the second can be a pyrazole, an isoxazole, or a pyridine.²¹³ Novel spirocycles (Figure III.13, compound III) were also reported to be synthesized starting from 2,6-diphenyl-4H-tetrahydrothiopyran-4-one.²¹⁴

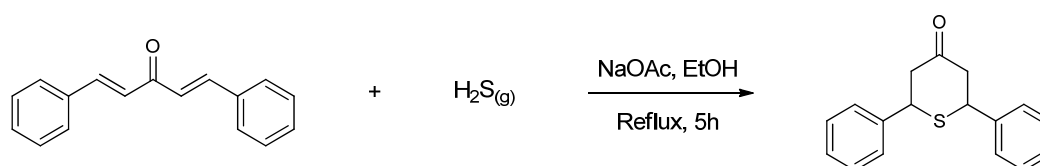
Minimum inhibitory concentration (µg/mL)	(IV)	(V)
<i>Staphylococcus aureus</i>	100	12.5
<i>Pseudomonas aeruginosa</i>	50	25
<i>Escherichia coli</i>	100	50

Figure III.14 | Antibacterial activities of 2,6-diaryl-4H-tetrahydrothiopyran-4-one oximes.

Besides these synthetic uses, 4H-tetrahydrothiopyran-4-ones were also considered as promising compounds for the treatment of several diseases. They were firstly evaluated for their use as antimicrobial and antimalarial agents.²¹⁵ Despite their moderate activities against malarial parasites, 2,6-diaryl-4H-tetrahydrothiopyran-4-ones and their oxime or azine derivatives showed potent antibacterial and antifungal activities (Figure III.14).²¹⁶⁻²¹⁸

Synthesis of 2,6-diaryl-4H-tetrahydrothiopyran-4-ones

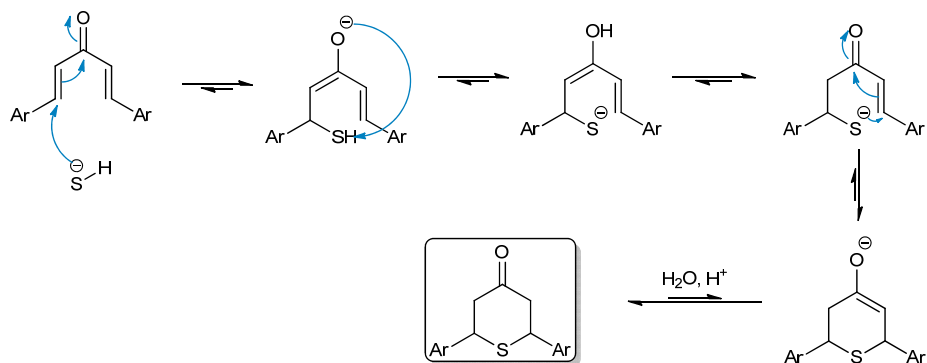
The synthesis of 2,6-diphenyl-4H-tetrahydrothiopyran-4-one was firstly described by Arndt *et al.* in 1925.²¹⁹ In this procedure, the dibenzylideneacetone was subjected to a double Michael addition of gaseous hydrogen sulfide under basic ethanolic conditions (Scheme III.11).



Scheme III.11 | Synthesis of 2,6-diaryl-4H-tetrahydrothiopyran-4-one as described by Arndt and coworkers.

This reaction is expected to occur through a sequence of 1,4-Michael additions of sulfide anion on the enone (Scheme III.12). At first, deprotonated hydrogen sulfide (either under the form of sodium hydrosulfide or sulfide anion) is attacking a first electrophilic center of the enone. Subsequent keto-enol tautomerism resulted in the activation of sulfide which, in turn, reacts

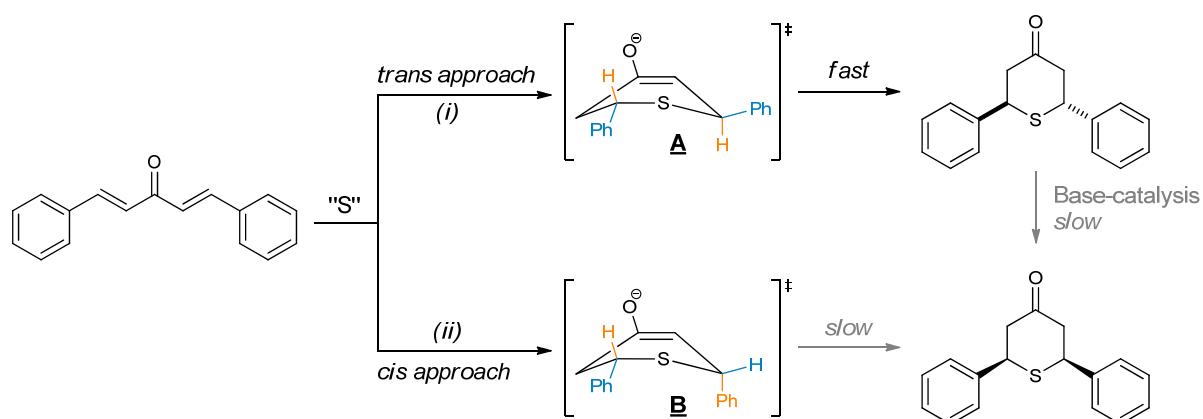
through a 1,4-Michael addition on the second double bond. Acidic aqueous quench of the resulting keto-enol tautomer gives the desired 2,6-DA-4-THTP.



Scheme III.12 | Mechanism of 2,6-diaryl-4H-tetrahydrothiopyran-4-ones cyclization.

The yield of the reaction is not reported, but Arndt *et al.* were aware of the diastereoisomeric mixture issue as they mentioned the isolation of two types of crystals which melt at different temperature (87 °C and 113 °C). The authors noticed that the amount of sodium acetate introduced in the reaction seemed to influence the final ratio between both isomers.

Baxter and Whiting were the first to clearly establish the configuration of both isomers.²²⁰ In this study, they demonstrated through deuterated experiments that the (\pm)-*trans* isomer is kinetically favored. To explain this kinetic effect, they postulated that the intermediate cyclized enol could adopt a quasi-boat conformation (Scheme III.13). Thus, *trans* enol **A** would have both phenyl groups in equatorial, whereas *cis* enol **B** would have one phenyl in axial and one in equatorial. It is then likely that the *trans* enol is the most stable, and, consequently, step (i) in the Scheme is faster than step (ii). As the subsequent ketonization is fast, the (\pm)-*trans* isomer is more quickly formed in the reaction.



Scheme III.13 | Kinetic and thermodynamic hypotheses suggested by Baxter and Whiting to explain the diastereoselectivity of the 2,6-diaryl-4H-tetrahydrothiopyran-4-one synthesis.

Furthermore, they unambiguously proved that a slow thermodynamic shift results in the interconversion of the (\pm)-*trans* isomer to the thermodynamically more stable *cis* isomer under base-catalysis (Scheme III.13).

Unfortunately, these very important results were never used to design a new diastereoselective synthetic pathway. Timorous attempts to evaluate the effect of gas injection rate or base amounts are reported but they were contradictory from one study to another.^{205,218,220} In the next decades, the procedure was used again in several experiments with only few changes and almost no optimization.^{205,215,218,220,221}

Limitations

As a result from this lack of rationale studies, numerous drawbacks were linked to the synthesis of 2,6-diphenyl-4H-tetrahydrothiopyran-4-one when we initiated this work:

- The sulfur source is gaseous hydrogen sulfide which is known for its very high toxicity, its unpleasant smelling and its difficult handling and stoichiometric control.
- Reaction was performed in refluxing ethanol with a large excess of base, thus being not compatible with sensitive substitution patterns.
- Stereochemistry of the reaction is absolutely not controlled in this procedure, giving non reproducible results and almost exclusively the *cis* isomer.
- As a direct consequence, the (\pm)-*trans* isomer was never thoroughly studied and characterized.

All these limitations were incompatible with our prodrug strategy. Indeed, it was expected that several substitutions will not withstand the reaction conditions. In addition, stereochemistry is known to significantly influence biological activities;¹⁸⁹ thus, it would have been much less valuable to send diastereoisomeric mixture for biological assays and we therefore wanted to test both diastereoisomers separately. Consequently, we decided to develop a new methodology for the diastereoselective synthesis of 2,6-diaryl-4H-tetrahydrothiopyran-4-ones.

Design of a new methodology for the diastereoselective synthesis of 2,6-diaryl-4H-tetrahydrothiopyran-4-ones

With the aim of designing a new efficient, safe, and easy procedure for the synthesis of 2,6-DA-4-THTP, we focused our attention on the essential sources of concern that we identified in the published procedure. The solutions that we implemented are listed below.

Source of sulfur

Both the toxicity and the difficult control of gaseous hydrogen sulfide were a major concern in the published procedure. Facing this issue, we decided to use solid sodium hydrosulfide (NaSH) as the source of nucleophilic sulfur. This choice was supported by several previous works which were reporting the use of this reagent for Michael addition and sulfur-cyclisation.^{150,222,223} Commercial sodium hydrosulfide is available as hydrated pellets. These were finely powdered, dried under high vacuum and back titrated with the iodine/sodium thiosulfate system to accurately determine the amount of active sulfur. Depending on the batch, the amount of pure anhydrous sodium hydrosulfide was found to be in the range of 75 to 80 wt% which roughly corresponds to a monohydrated salt. Stored under argon in a desiccator, sodium hydrosulfide kept its water content constant over at least six months.

Control of the reaction temperature

The most obvious parameter which has been identified for orientating the diastereoisomeric of the reaction is the effect of the temperature. We previously mentioned that the (\pm)-*trans* isomer is kinetically favored due to its lower-energy transition state. On another hand, the *cis* isomer is expected to result from both direct formation of the product and slow base-catalyzed isomerization of the (\pm)-*trans* isomer. Consequently, a low temperature should contribute to the formation of (\pm)-*trans* isomer, while higher reaction temperatures are clearly supposed to slowly increase the amount of *cis* isomer.²⁰⁵ Nevertheless, this parameter was not much studied in the previous experiments, most of the reactions being performed at reflux of the ethanol. We therefore decided to carry out reactions at two different temperatures: around 0 °C for the selective synthesis of the (\pm)-*trans* isomer and at the reflux of the solvent for the selective synthesis of the *cis* isomer.

Influence of the solvent

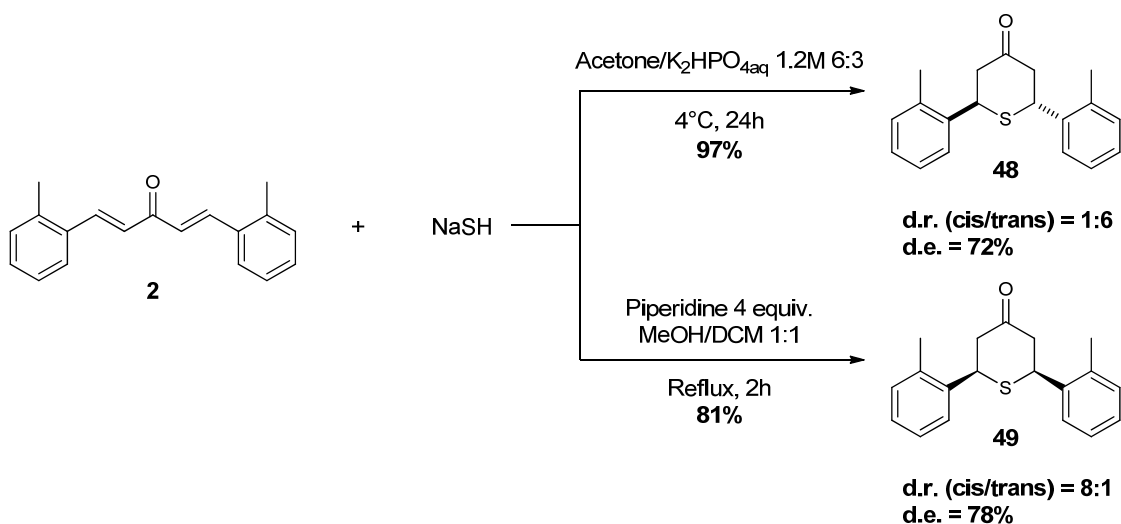
Solvent effects are known to influence significantly the stereochemistry of Michael addition.²²⁴ Chelating and solvating effects modulate the nucleophilicity of the sulfur and thus orientate the stereochemistry, partly by rate-determining effects. Once again, this aspect has been clearly neglected in the previous researches, as most of them were describing the use of alcohols such as ethanol or methanol. Preliminary investigations on the effects of solvent led us to choose a diphasic mixture of water and acetone for the synthesis of the (\pm)-*trans* isomer, while a purely organic medium mixing methanol (for solubilization of NaSH) and dichloromethane (for solubilization of DAA) was found to be promising for the selective synthesis of the *cis* isomer.

Control of the basicity of the medium

When gaseous hydrogen sulfide was used, a base had to be added in the reaction generating the active nucleophilic sulfur. This base was claimed to significantly influence the diastereoselectivity. However, contradictory results were obtained; high base concentration was reported to help the major formation of the (\pm)-*trans*,²⁰⁵ whereas other studies determined that this same (\pm)-*trans* isomer is preferentially obtained with lower base concentration.²²⁰ As the sulfur source that we intended to use is the basic form of hydrogen sulfide ($pK_a(\text{H}_2\text{S}/\text{HS}^-) = 7.0$, $pK_a(\text{HS}^-/\text{S}^{2-}) = 11.9$) the role of the base is expected to be less crucial. Nevertheless, we investigated the necessity and the effects of such a base in our search for diastereoselectivity. For the synthesis of the (\pm)-*trans* isomer we chose the system described by Rule *et al.* (dibasic hydrogen phosphate in water).¹⁵⁰ Being conducted in purely organic medium, the synthesis of the *cis* isomer was firstly investigated with piperidine as the base of choice.

Summary and first results

Reaction conditions selected for the first attempts in the diastereoselective synthesis of 2,6-DA-4-THTP are summarized on Scheme III.14. 1,5-Di-*o*-tolylpenta-1,4-dien-3-one **2** was chosen as starting material since the resulting two diastereoisomers are clearly separated, both on HPLC chromatogram and NMR spectra, allowing an accurate quantification of the diastereoisomeric ratio and of the yield (*vide infra*).



Scheme III.14 | Preliminary reaction conditions for the diastereoselective synthesis of 2,6-diaryl-4H-tetrahydrothiopyran-4-ones.

At a low temperature, (\pm)-*trans* 2,6-di-*o*-tolyl-4H-tetrahydrothiopyran-4-one **48** was obtained in 97 % yield with a diastereoisomeric excess (d.e.) of 72 %. On the other hand, under reflux, *cis* 2,6-di-*o*-tolyl-4H-tetrahydrothiopyran-4-one **49** was obtained in 81 % yield with a d.e. of 78 %. From these encouraging results, we then tried to optimize the reaction conditions.

Optimization of the diastereoselective synthesis of 2,6-diaryl-4H-tetrahydrothiopyran-4-ones

Based on the first promising results that we obtained in the search for a new diastereoselective synthesis of 2,6-diaryl-4H-tetrahydrothiopyran-4-ones, we intended an optimization of both the yield and the diastereoisomeric excess of the reaction. The main goal of this work was to achieve a procedure which would be compatible with a large panel of substitutions, including nucleophile-sensitive ones. As we proceeded for the optimization of the synthesis of dissymmetric DAA, we chose to develop an analytical method for fast quantitative determination of the yield and the d.e.

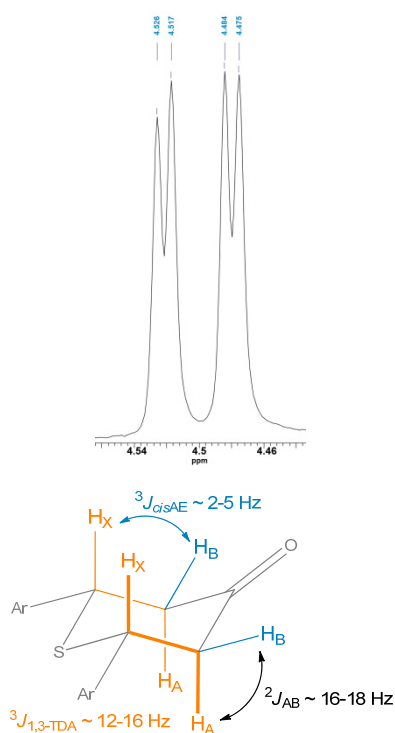
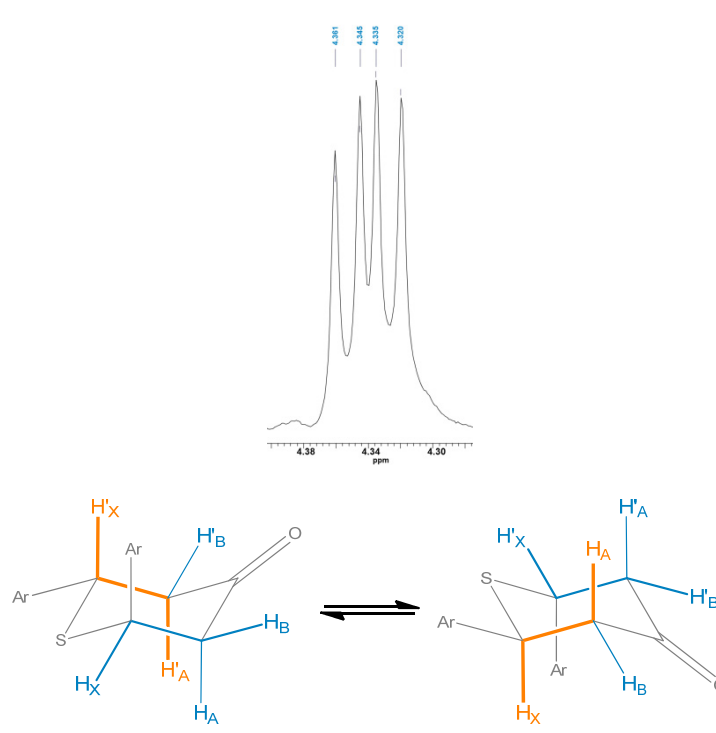
Set-up and validation of the quantification method

One prerequisite for developing the method was obviously to definitely determine which isolated isomer is the *cis* and which is the (\pm)-*trans*. A special care was taken in characterizing these isomers in order to provide very reliable data that are currently missing in the literature.

Spectroscopic characterization of diastereoisomers

The exact determination of the stereochemistry of 2,6-DA-4-THTP was an important part of the present work. With the aim of clearly establishing a reliable method to detect and quantify the two diastereoisomers, ^1H NMR, ^{13}C NMR (1D and 2D) were recorded and analyzed. Areas of interest in these spectra are the $-\text{CH}$ and $-\text{CH}_2$ domains relative to chiral centers of the heterocycle and their surroundings.

Proton NMR spectra are displaying a typical ABX system, where X is the methine proton (Figure III.15, H_X) and A and B the two diastereotopic protons of the methylene group (Figure III.15, H_A and H_B). The spectra for those two diastereoisomers differ in their specific coupling constants. On one hand, in the *cis* isomer, the two ABX systems are equivalent. As a result, the signal of H_X shows a well-defined doublet-of-doublet with a high 1,3-*trans*-diaxial coupling constant ($^3J_{1,3\text{-TDA}} \approx 12\text{-}16$ Hz) resulting from the coupling of axial protons H_X with axial protons H_A . The second coupling constant of the doublet is lower ($^3J_{\text{cisAE}} \approx 2\text{-}5$ Hz) and results from the *cis*-axial-equatorial coupling of protons H_X with equatorial protons H_B (Figure III.15, case A).

A) *cis* isomerB) *trans* isomer**Figure III.15 | NMR spectra of the X part of the ABX system in both diastereoisomers.**

On the other hand, the (\pm)-*trans* isomer has two different ABX systems, one with the aryl substituent in equatorial position, and the other in axial position. This should result in two different patterns. However, due to the rapid conformational equilibrium, these two ABX systems are averaged, resulting in broader signals. Thus proton H_X usually appears as a broad doublet-of-doublet which, depending on the analyzed product, can sometimes even appear as a triplet, due to signals averaging and overlapping. The coupling constants that have been observed for this proton are typically in the range of 6-8 Hz for the averaged coupling and 2-5 Hz for the *cis*-axial-equatorial coupling.

With regard to the AB part of spectra, it is more difficult to draw precise trends as there is a great variability depending on the substitution pattern of the tetrahydrothiopyran-4-one ring. For the *cis* isomers, it is usually possible to attribute protons H_A and H_B as the two patterns are well resolved ($\Delta\nu/J \approx 5$). Signal for H_A is the combination of a geminal coupling constant with proton H_B ($^2J_{AB} \approx 13-16$ Hz) and a typical 1,3-*trans*-diaxial coupling constant with proton H_X ($^3J_{1,3-TDA} \approx 12-16$ Hz). Regarding proton H_B , the signal is the combination of the same geminal coupling constant with proton H_A ($^2J_{AB} \approx 13-16$ Hz) and a smaller *cis*-axial-equatorial coupling with proton H_X ($^3J_{cisAE} \approx 2-5$ Hz). This results in a broad triplet (or doublet-of-doublet) for proton H_A and a fine doublet-of-doublet for proton H_B (Figure III.16, case A).

The AB part for the (\pm)-*trans* isomer is obviously more complex as signals are averaged. In this case, it is more difficult to distinguish protons H_A and H_B as a typical fused ABX pattern is observed (*i.e.* lower values of the ratio $\Delta\nu/J$) (Figure III.16, case B).

A) *cis* isomer – $\Delta\nu/J \approx 5$

B) *trans* isomer – $\Delta\nu/J \approx 3$

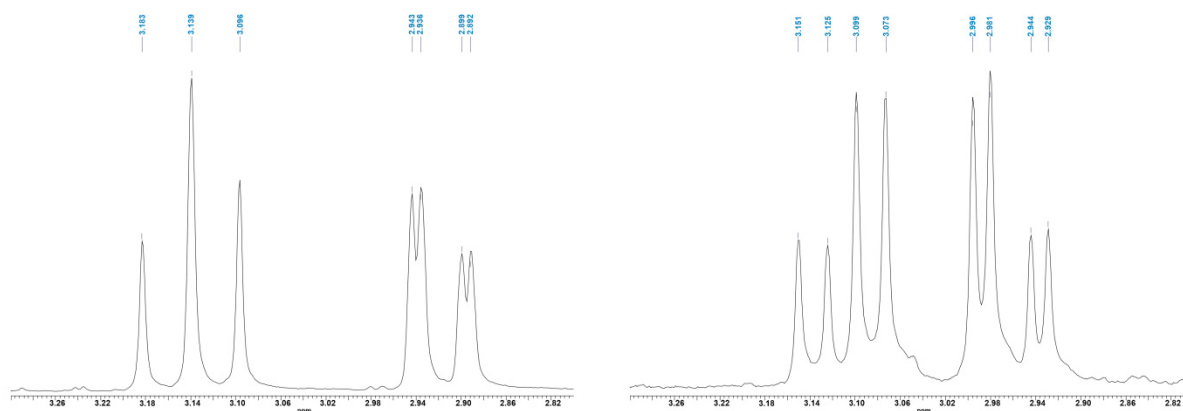


Figure III.16 | NMR spectra of the AB part of the ABX system in both diastereoisomers.

These results on ¹H NMR were reinforced by ¹³C NMR data. For *cis* isomer **49**, the chemical shift of the methines was 44.6 ppm, whereas in (\pm)-*trans* analogue **48** this same carbon has a chemical shift of 39.8 ppm ($\Delta\delta = -4.8$ ppm relative to the *cis*). This shielding of the methine of (\pm)-*trans* isomers is consistent with a γ -*syn* effect between the axial aryl substituent and the methine carbon (Figure III.17).^{225,226}

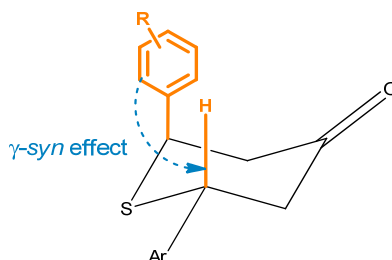


Figure III.17 | γ -*syn* effect on the (\pm)-*trans* 2,6-diaryl-4H-tetrahydrothiopyran-4-one core.

To confirm all these data and definitely establish them as evidences for the stereochemical determination, an X-ray diffraction of (\pm)-*trans* 2,6-di-*o*-tolyl-4H-tetrahydrothiopyran-4-one was recorded (Figure III.18). At first glance, we can see that the *trans* arrangement of the two aryls is confirmed, as well as the chair conformation. Interestingly, the crystal packing of such compounds is mainly ruled by Π - Π interactions through the two aryl moieties, leading to the formation of tetramer subunits. Both *face-to-face* and *edge-to-face* associations of the aromatic rings were observed and are responsible for this specific arrangement.²⁰⁸ Finally, this X-ray analysis confirmed the presence of the two enantiomers of the *trans* in the unit cell.

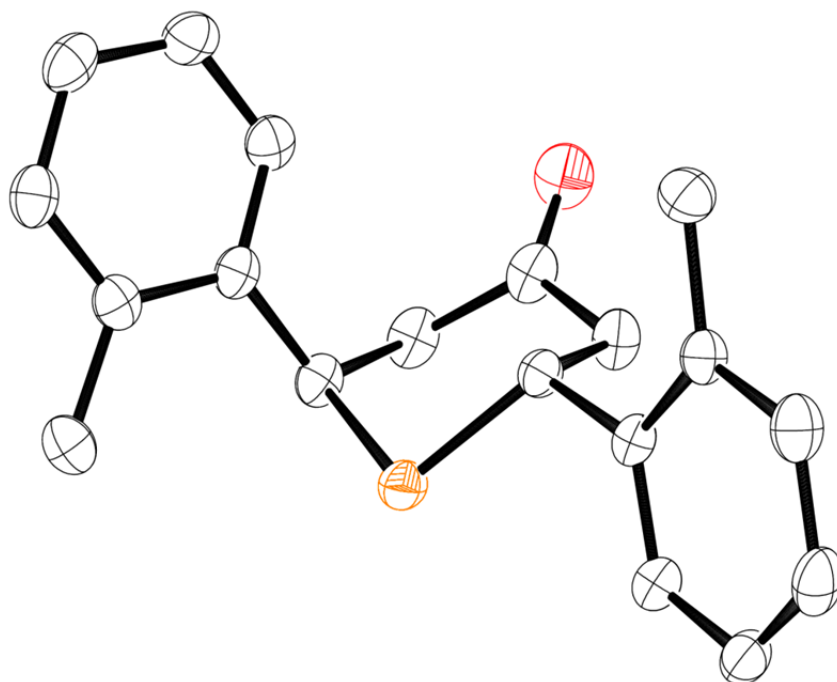


Figure III.18 | X-ray structure of (\pm)-*trans* 2,6-di-*o*-tolyl-4H-tetrahydrothiopyran-4-one.

To summarize, we clearly and surely established a relation between specific spectroscopic data and the configuration of the diastereoisomers. Thus, the following NMR observations were demonstrated and have therefore been used for the assignment of each 2,6-DA-4-THTP synthesized as part of this thesis:

- on ^1H NMR, *cis* isomers display a well separated doublet-of-doublet for the methine proton with a high 1,3-*trans*-diaxial coupling constant between 12 Hz and 16 Hz and a smaller *cis*-axial-equatorial coupling constant between 2 Hz and 5 Hz, whereas the same proton in (\pm)-*trans* isomer appears as a broader signal with smaller coupling constants,
- on ^{13}C NMR, a shielding of about -5 ppm (relative to the *cis*) of the methine carbon is characteristic of the (\pm)-*trans* isomer,
- finally, although less reliable, the general aspect of the AB part of the ^1H NMR spectra can be used to confirm the deduced configuration as the *cis* isomer usually shows a well resolved AB part with $\Delta\nu/J$ generally higher than 5.

Once the two isomers were unambiguously identified, we were able to develop a quantitative method to determine yields and d.e. during the optimization process.

Choice of the method

For the same reasons as described in the section relative to the synthesis of dissymmetric DAA, we analyzed crude mixtures by HPLC. Being performed on an older apparatus available within our laboratory in Strasbourg, the detection had to be restricted to only one wavelength. Considering the spectroscopic properties of starting material **2** and products **48** and **49**, a standard UV detection at 254 nm was selected. Column, solvent and elution program were adequately chosen in order to maximize the separation ratio between the three expected compounds on chromatograms. *In fine*, the best separation was achieved with a Nucleodur® C18 column, eluted using a gradient of water and acetonitrile at 0.800 mL.min⁻¹.

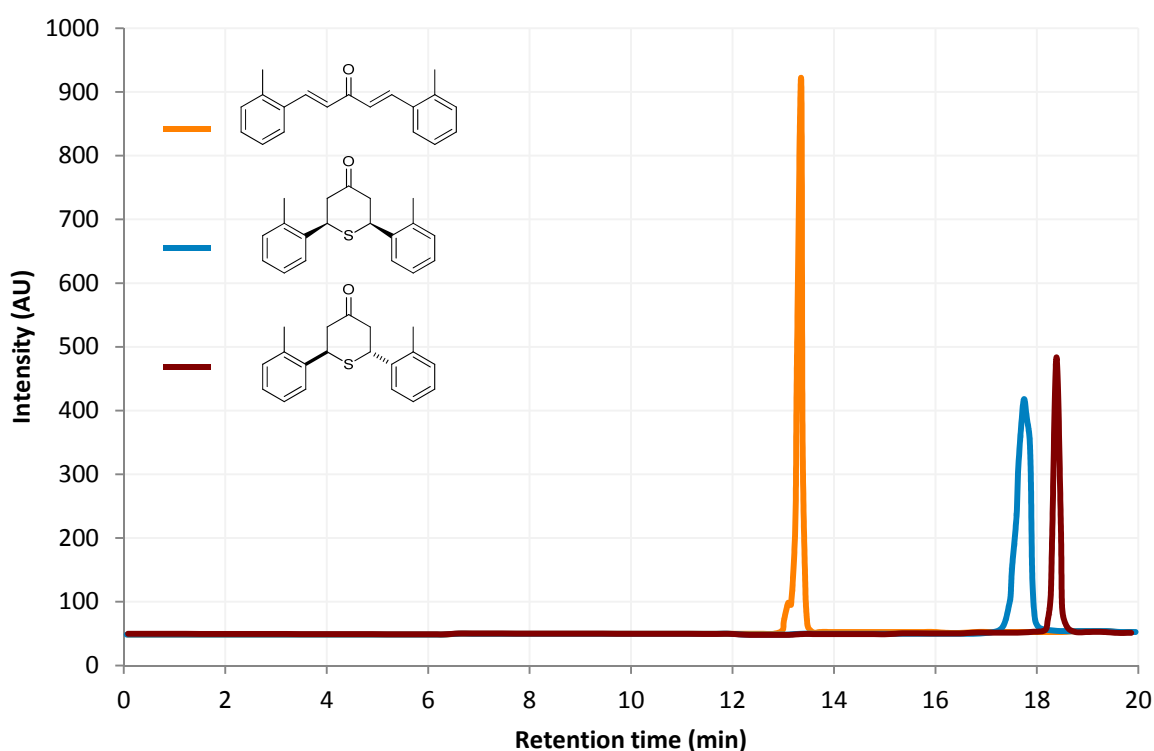


Figure III.19 | Chromatograms of products 2, 48, and 49.

Under these conditions, resolution reached 1.3 between the two diastereoisomers **48** and **49** (Figure III.19). Although this resolution might appear rather low, it is sufficient for the separation and to achieve accurate peak picking and integration of the two diastereoisomers.

Calibration and validation

The process of calibration and validation was similar to previous works. Two series of solutions of diastereoisomers **48** and **49** ranging from $1.05 \pm 0.01 \text{ mg.mL}^{-1}$ to $0.21 \pm 0.005 \text{ mg.mL}^{-1}$ were prepared. These were analyzed under the previously mentioned HPLC elution conditions and the corresponding two calibration curves were plotted (Figure III.20 and III.21). The accuracy and the repeatability of these calibrations were assessed through triplicate analysis of three samples of known concentration. For each sample, the value deduced from the calibration curves was found to perfectly match with the expected concentration within the experimental errors. As a result, the calibration of the method was considered as validated.

Summary

Main parameters of the quantitative HPLC analysis of diastereoisomers **48** and **49** are summarized in Table III.2.

Table III.2 | Quantitative HPLC determination of diastereoisomers 48 and 49.

Limit of detection	$7 \mu\text{g.mL}^{-1}$
Limit of quantification	$200 \mu\text{g.mL}^{-1}$
Saturation	1.7 mg.mL^{-1}
Linear calibration range	$0.20 - 1.10 \text{ mg.mL}^{-1}$
Correlation (R^2)	0.999

As for the optimization of the synthesis of dissymmetric DAA, analyses of reaction mixtures were only duplicated.

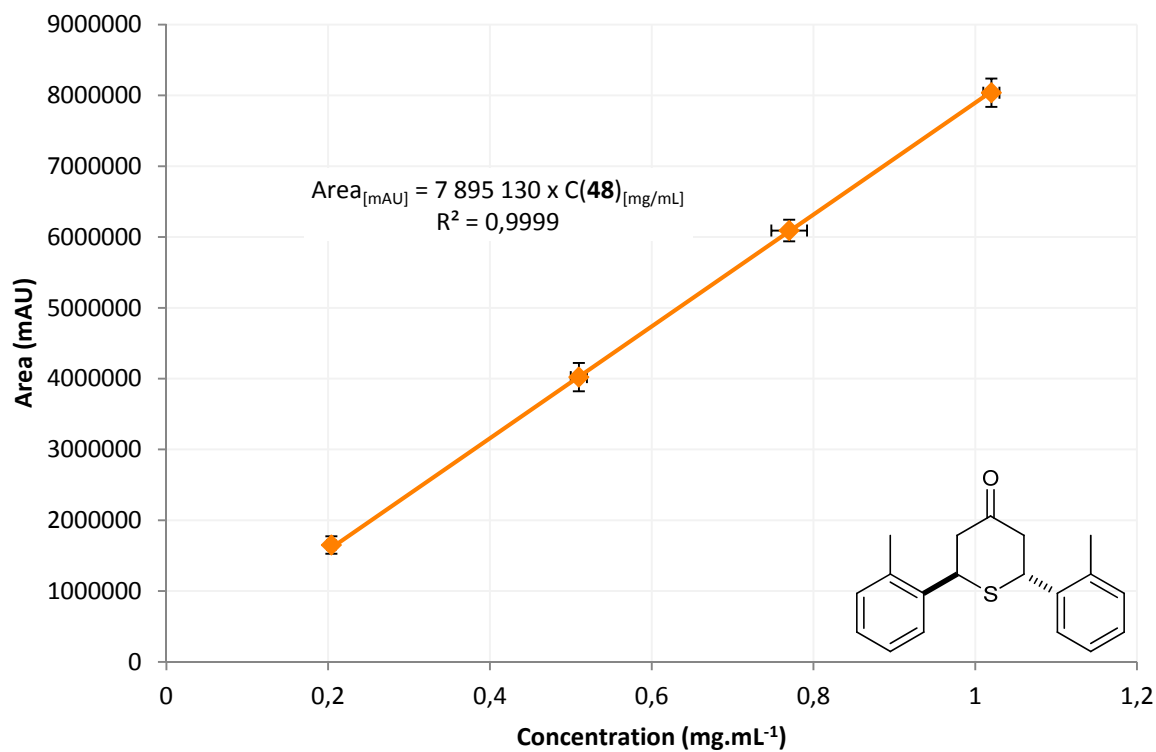


Figure III.20 | Calibration curve of product 48.

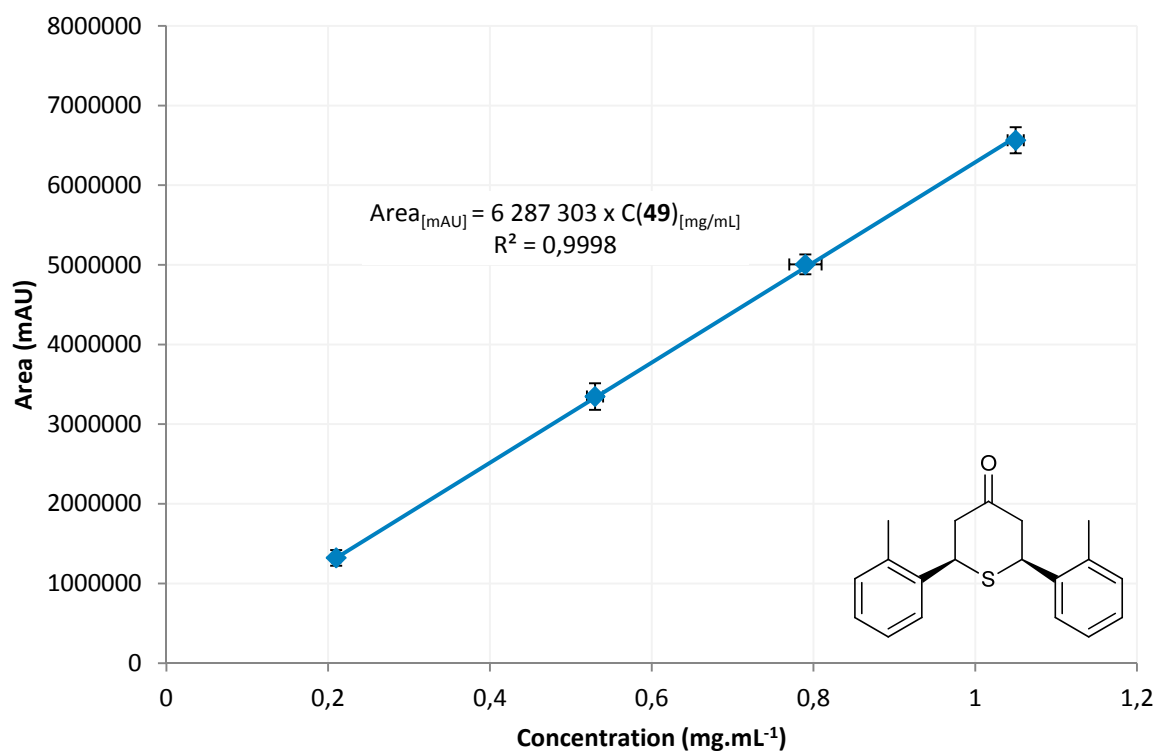


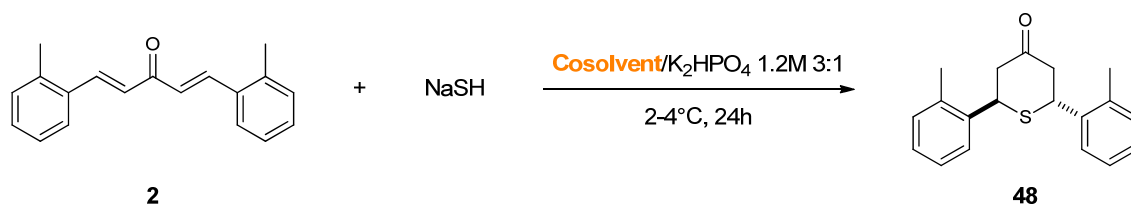
Figure III.21 | Calibration curve of product 49.

Optimization of the selective synthesis of (\pm)-*trans* diastereoisomers

Further to the essential parameters that we identified at the beginning of this chapter, we studied more specifically the effects of solvent and base. As (\pm)-*trans* diastereoisomers are kinetic products, they are expected to be preferably formed at lower temperatures. We therefore performed all the reactions described below between 2 °C and 4 °C in a temperature-controlled container, allowing the continuous stirring of reactions even on longer reaction times.

Effects of the solvent

Solvents are known to have significant effects on the stereoselectivity of Michael addition.²²⁴ The rationale behind these solvent effects is usually difficult to find out as many parameters, such as chelating, polarity or protic properties, can influence the orientation of the reaction. In the case of the synthesis of (\pm)-*trans* isomers, first results were successful in an aqueous basic medium containing an organic cosolvent solubilizing the DAA starting material. Keeping the aqueous phase fixed, we firstly considered the effect of the organic cosolvent (Scheme III.15).



Scheme III.15 | Effects of the cosolvent on the selective synthesis of (\pm)-*trans* diastereoisomers.

The choice of this cosolvent was mainly guided by its aqueous miscibility, its ionic dissociation power and its ability to solubilize the diarylideneacetone starting material. Taking into account these specificities, five different solvents were tested: methanol, dimethylsulfoxide (DMSO), acetonitrile, acetone and tetrahydrofuran (THF). The results are summarized in Table III.3.

Table III.3 | Effects of cosolvent.

Entry	Cosolvent	Base (equiv.)	d.r. (cis/trans) ^a	d.e. (%) ^a	HPLC yield (%)
1	Methanol	K ₂ HPO ₄ (4 equiv.)	n.d.	n.d.	0
2	DMSO	K ₂ HPO ₄ (4 equiv.)	7:10	18	91
3	Acetonitrile	K ₂ HPO ₄ (4 equiv.)	1:4	60	98
4	Acetone	K ₂ HPO ₄ (4 equiv.)	1:6	72	97
5	THF	K ₂ HPO ₄ (4 equiv.)	1:33	94	92

^aDetermined by HPLC.

All solvents gave satisfactory yields except methanol. Indeed, the diarylideneacetone starting material was not solubilized in this solvent at 4 °C and, as a result, reaction did not occur (Table III.3, entry 1). Regarding the diastereoselectivity of the reaction, DMSO is clearly less efficient, giving a poor diastereoisomeric excess (Table III.3, entry 2). Acetonitrile and acetone allowed the d.e. to reach 60 % and 72 %, respectively (Table III.3, entry 3 and 4). The best result was obtained with the use of THF (Table III.3, entry 6). With this less polar solvent, desired (\pm)-*trans*-2,6-di-*o*-tolyl-4H-tetrahydrothiopyran-4-one **48** was obtained in 92 % yield with a d.e. of 94 %, reaching the limit of quantification of our HPLC and NMR methods.

It is noteworthy to notice that the resulting diastereoisomeric excess seems to be correlated with the dielectric constant of the solvent (Figure III.22). The lower the dielectric constant, the better is the diastereoisomeric excess.

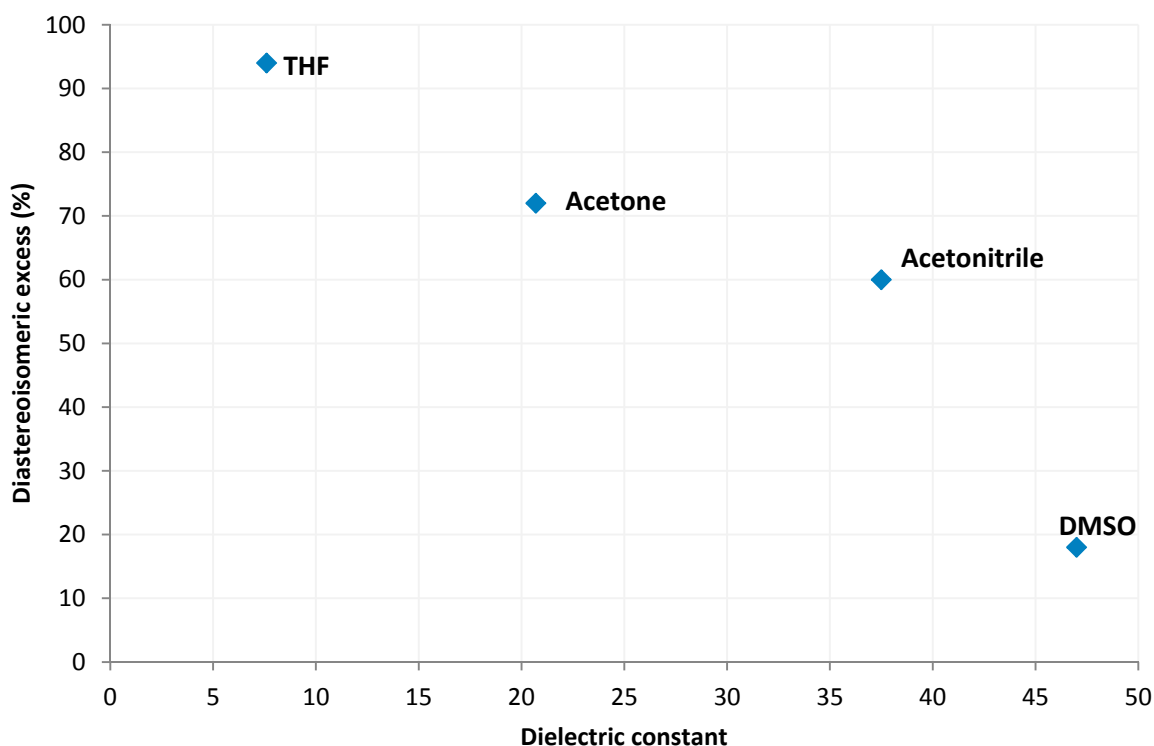
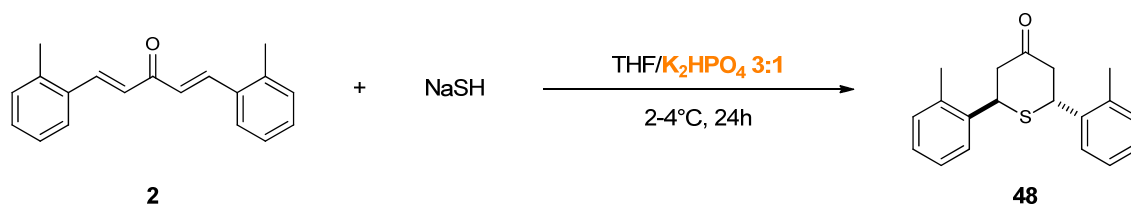


Figure III.22 | Correlation of the cosolvent dielectric constant with the observed diastereoisomeric excess.

However, the solvent has to be polar enough, and miscible to water, to allow the active hydrosulfide anion to reach the organic phase and react with the DAA. Considering the good properties of THF and the excellent d.e. obtained through the use of this solvent, THF was selected as a solvent for the diastereoselective synthesis of (\pm)-*trans*-2,6-DA-4-THTP.

Effect of the base stoichiometry



Scheme III.16 | Effects of the base stoichiometry on the selective synthesis of (±)-*trans* diastereoisomers.

As we previously mentioned, effects of base stoichiometry on the d.e. were debated in the literature. In order to determine the real impact of the amount of base, we subsequently carried out two further experiments, respectively with two equivalents and six equivalents of base (Table III.4).

Table III.4 | Effects of base stoichiometry.

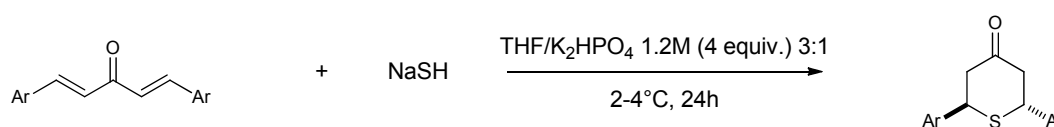
Entry	Solvent	Base (equiv.)	d.r. (cis/trans) ^a	d.e. (%) ^a	HPLC yield (%)
1	THF	K ₂ HPO ₄ (2 equiv.)	1:40	95	90
2	THF	K ₂ HPO ₄ (4 equiv.)	1:33	94	92
3	THF	K ₂ HPO ₄ (6 equiv.)	1:33	94	91

^aDetermined by HPLC.

With regard to these results, we can certainly conclude that the amount of base has no crucial effects, neither on the yield, nor on the diastereoselectivity, at least under these reaction conditions. However, in order to prevent any protonation of the hydrosulfide anion which would result in gaseous hydrogen sulfide, we decided to keep four equivalents of potassium phosphate dibasic in the medium.

Scope of the reaction

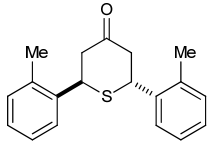
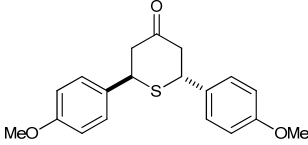
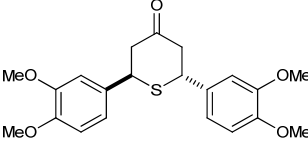
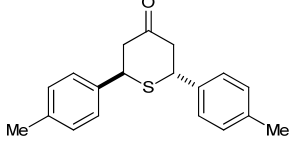
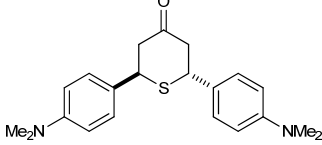
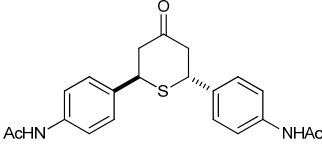
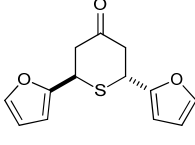
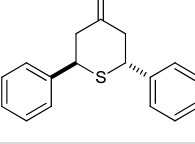
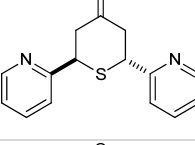
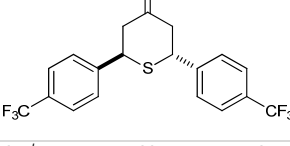
The optimization process has led to the determination of reaction conditions that maximize both the yield and the diastereoisomeric excess of the selective synthesis of (±)-*trans* isomers. Under these conditions, one equivalent of DAA is reacting with three equivalents of sodium hydrosulfide, in a 3:1 mixture of THF and aqueous potassium phosphate dibasic 1.2 M, at 4 °C for one day (Scheme III.17).



Scheme III.17 | Optimized reaction conditions for the selective synthesis of the (±)-*trans* isomer.

The methodology under these optimized conditions was then extended to the synthesis of several (±)-*trans*-2,6-diaryl-4H-tetrahydrothiopyran-4-ones (Table III.5). All these reactions were performed on a multigram scale (≈ 5 g), starting from the previously synthesized DAA.

Table III.5 | Yields of the diastereoselective synthesis of the (±)-*trans* diastereoisomer.^a

Entry	Compound	Structure	d.r. (cis/trans) ^b	d.e. (%) ^b	Yield (%) ^c
1	48		1:32	94	92
2	50		1:40	95	76
3	51		1:9	80	63
4	52		1:15	88	70
5	53		1:19	90	10 ^d
6	54		1:19	90	74
7	55		1:14	87	69
8	56		1:14	87	67
9	57		1:3.5	55	64 ^{d,e}
10	58		1:2	33	80

^aReaction performed on a 15 mmol scale. ^bDetermined by NMR. ^cIsolated yield. ^dPerformed in acetone. ^e*cis* isomer **63** was isolated.

Table III.5 | Yields of the diastereoselective synthesis of the (±)-*trans* diastereoisomer.^a (continued)

Entry	Compound	Structure	d.r. (cis/trans) ^b	d.e. (%) ^b	Yield (%) ^c
11	59		n.d.	> 95	50
12	60		1:11	83	77
13	61		1:7	75	63
14	62		n.d.	> 95	67

^aReaction performed on a 15 mmol scale. ^bDetermined by NMR. ^cIsolated yield.

Substitutions on the aromatic part were chosen to range from electron-donating groups (Table III.5, entries 1-6) to electron-withdrawing group (Table III.5, entries 9-14). No general correlation can be established between the electron density and the yield or the diastereoisomeric excess. Generally speaking, yields and d.e. were good to excellent. The lower yield of product **53** is explained by the really poor solubility of the DAA starting material in the reaction medium, even when the cosolvent was switched to acetone; 80 % of the DAA was recovered at the end of the reaction. A fine buffering of the pH might allow concomitant presence of deprotonated sulfide and protonated aniline thus allowing a better solubilization of the starting material while maintaining the reactivity of sulfur; however, such an approach is challenging and time-consuming, and was therefore not intended.

It is noteworthy to mention that the values indicated in Table III.5 were obtained after purification over column of chromatography without separation of the two isomers; better d.e. are therefore likely to be achieved further to subsequent recrystallization steps.

Concluding remarks on the diastereoselective synthesis of (\pm)-*trans*-2,6-diaryl-4H-tetrahydrothiopyran-4-ones

To summarize this part of our work, we developed a new method for the diastereoselective synthesis of (\pm)-*trans*-2,6-diaryl-4H-tetrahydrothiopyran-4-ones. The use of a water-miscible organic solvent at low temperature allows the diastereoisomeric excesses to reach excellent values, mostly above 90 %. These mild reaction conditions proved to be compatible with a large panel of substitution patterns, from electron-rich to electron-deficient aromatic rings, including nucleophile-sensitive ones (such as aryl halides, *N*-acetamide substituted phenyl etc.). Finally, this new protocol is easier and safer than the old procedure, even on large scales.

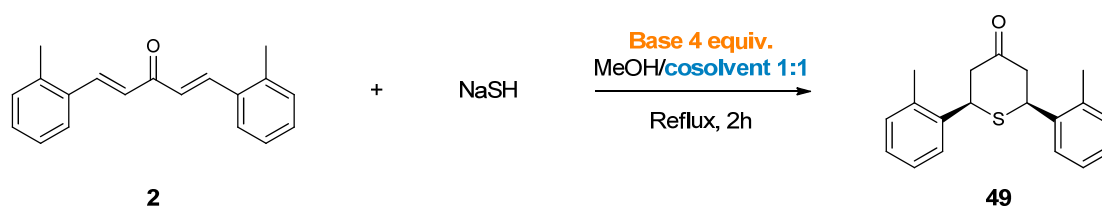
These thirteen (\pm)-*trans*-2,6-diaryl-4H-tetrahydrothiopyran-4-ones were submitted for biological evaluation of their antiparasitic activities (*vide infra*).

Optimization of the selective synthesis of *cis* diastereoisomers

As we previously mentioned, *cis* diastereoisomers are thermodynamically more stable than their (\pm)-*trans* counterparts. As a consequence, they are expected to be preferentially formed at high temperature. Based on our preliminary experimental results, our first stage consisted in investigating the selective synthesis of *cis* isomers at the reflux of a purely organic medium. Although the optimization of this protocol allowed the efficient synthesis of toluyl- and anisyl-substituted *cis*-2,6-diaryl-4H-tetrahydrothiopyran-4-ones, we next demonstrated that it was not compatible with nucleophile-sensitive substitution patterns. In a second stage, we successfully designed and optimized a novel methodology for the diastereoselective synthesis of *cis*-2,6-DA-4-THTP under the very mild conditions of a phase-transfer catalysis. These two protocols will be detailed below.

Synthesis in purely organic medium

Preliminary studies that have been performed resulted in excellent yields and satisfactory diastereoisomeric excess. In these first attempts, the piperidine was used as a base and dichloromethane as a cosolvent (Scheme III.18).



Scheme III.18 | Synthesis of *cis* isomers in purely organic medium.

As for the optimization of the preparation of (\pm)-*trans* isomers, we investigated the effect of the base and the solvent system.

Effects of the base

Unlike the selective synthesis of the (\pm)-*trans* isomer, the reaction was here performed in a purely organic medium. Consequently, the protonation of sodium hydrosulfide is not likely to occur. Thus, the use of a base might be theoretically avoided, a slight excess of NaSH being sufficient to catalyze the keto-enolic equilibrium occurring in the synthesis. The effects as well as the need for such a base were therefore investigated (Table III.6).

Table III.6 | Effects of the base.

Entry	Base (equiv.)	d.r. (cis/trans) ^a	d.e. (%) ^a	HPLC yield (%)
1	Piperidine (4 equiv.)	6:1	71	86
2	Triethylamine (4 equiv.)	4.7:1	65	86
3	DIPEA (4 equiv.)	5:1	67	81
4	Piperidine (1 equiv.)	12:1	84	75
5	Piperidine (0.1 equiv.)	15:1	87	84
6	-	16:1	88	85

^aDetermined by HPLC.

Organic amines used in excess resulted in good yields but d.e. were moderate, being comprised between 65 % and 71 % (Table III.6, entries 1 to 3). Decreasing the concentration of piperidine resulted in a significant raise in the diastereoselectivity (Table III.6, entries 4 and 5). However, similar results were obtained by simply removing the base (Table III.6, entry 6). This clearly confirmed the hypothesis that in purely organic condition, no additional base is required neither for the diastereoselectivity of the reaction nor for the yield. As a consequence, further experimentations were performed without any other base than sodium hydrosulfide itself.

Effects of the solvent system

The solvent system was composed of methanol and an organic cosolvent. In methanol, we evaluated the solubility of NaSH to 90 g.L⁻¹ whereas this value drops to 30 g.L⁻¹ in ethanol. Furthermore, this inorganic salt was found almost insoluble in most of the other solvents (acetone, higher alcohols, acetonitrile etc.). Methanol is therefore required. As a strong influence of the solvent was observed in the selective synthesis of the (\pm)-*trans* isomer, similar effects were expected for the synthesis of the *cis* diastereoisomer. In order to study potential effects of the cosolvent, we screened several of them (Table III.7).

Table III.7 | Effects of the cosolvent.

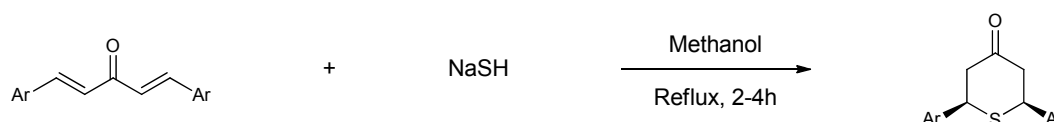
Entry	Cosolvent	d.r. (cis/trans) ^a	d.e. (%) ^a	HPLC yield (%)
1	<i>tert</i> -butanol	2.4:1	41	52
2	1,4-dioxane	6:1	71	37
3	methyl <i>tert</i> -butyl ether	17:1	89	54
4	dichloromethane	16:1	88	85
5	methanol	14:1	87	83

^aDetermined by HPLC.

Regarding both the yield and the d.e., *tert*-butanol and 1,4-dioxane are clearly less efficient than the other cosolvents (Table III.7, entries 1 and 2). The use of methyl *tert*-butyl ether (MTBE) resulted in excellent d.e. but the yield dropped to 54 % (Table III.7, entry 3). Finally, dichloromethane and methanol (*i.e.* without cosolvent) were both efficient, providing high yields and excellent d.e. (Table III.7, entries 4 and 5). As it is always easier to set-up reactions without cosolvent, and considering the fact that pure methanol can be heated at a higher temperature than a mixture of methanol and dichloromethane, we finally chose to use methanol as the unique solvent for the reaction.

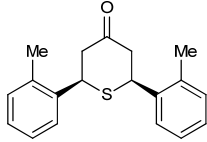
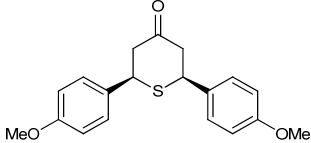
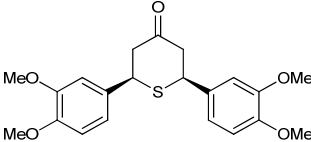
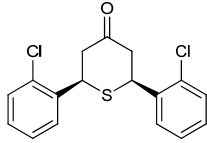
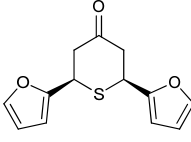
Generalization

Optimization process has allowed to determine the reaction conditions that maximize both the yield and the diastereoisomeric excess of the selective synthesis of *cis* isomers in a purely organic medium. Under these conditions, one equivalent of DAA is reacting with two equivalents of sodium hydrosulfide, in refluxing methanol until consumption of starting material (Scheme III.19).

**Scheme III.19 | Optimized reaction conditions for the selective synthesis of the *cis* isomer in purely organic medium.**

We then tried to extend this procedure to the synthesis of several *cis*-2,6-diaryl-4H-tetrahydrothiopyran-4-ones (Table III.8).

Table III.8 | Yields of the diastereoselective synthesis of the *cis* diastereoisomer in purely organic medium.^a

Entry	Compound	Structure	d.r. (cis/trans)	d.e. (%)	Yield (%)
1	49		n.d.	> 95	83
2	64		32:1	94	73
3	65		2.3:1	40	67
4	66		-	-	0
5	67		-	-	0

^aReaction performed on a 15 mmol scale. ^bDetermined by NMR. ^cIsolated yield.

Anisyl- and toluyl-substituted *cis*-2,6-DA-4-THTP were obtained in good yields with excellent diastereoisomeric excesses (Table III.8, entries 1 and 2). Synthesis of product **65** was less efficient as the d.e. dropped to 40 % while the yield remained satisfying (Table III.8, entry 3). Unfortunately, all other attempts for the synthesis of *cis*-2,6-DA-4-THTP bearing a more sensitive substitution pattern failed. As an example, synthesis of chloro- and 2-furyl-substituted 2,6-DA-4-THTP according this procedure resulted in a black sticky-chewing-gum-like material (Table III.8, entries 4 and 5); further analysis of these crudes demonstrated the presence of poly-sulfurated entities.

These failures might be explained by the lack of chemoselectivity of this procedure. In refluxing methanol, the hydrosulfide anion is less solvated than in water, resulting in a slightly higher reactivity. Moreover, sodium hydrosulfide is introduced in excess. As a result, a large amount of highly reactive nucleophilic sulfide is able to react with any reactive center, including the double bonds of DAA, but also any centers prone to undergo a nucleophilic substitution. In particular, it has been demonstrated in the literature that sulfide anion is able to undergo nucleophilic aromatic substitution (S_NAr) on chlorinated aromatics.^{222,223} In the case

of the synthesis of product **66**, such a lack of chemoselectivity might result in a multitude of by-products, including polymerized ones.

Considering the lack of chemoselectivity of this procedure, and its resulting limited scope, we decided to investigate a new procedure, which would allow the diastereoselective synthesis of *cis*-2,6-DA-4-THTP bearing all type of substitution patterns, including nucleophile-sensitive ones.

Phase-transfer catalyzed synthesis

In the previously established protocol, we identified two main issues: hydrosulfide anion is too reactive in the medium and is in a too large amount. Considering the opposite nature of reagents, one being an organic product whereas the other is an inorganic salt, a phase-transfer catalysis appeared an interesting approach. Indeed, in this strategy, the inorganic sodium hydrosulfide will be deactivated in a non-dissociating aqueous phase and brought by a phase-transfer catalyst to react with the DAA substrate in the organic phase (Figure III.23).

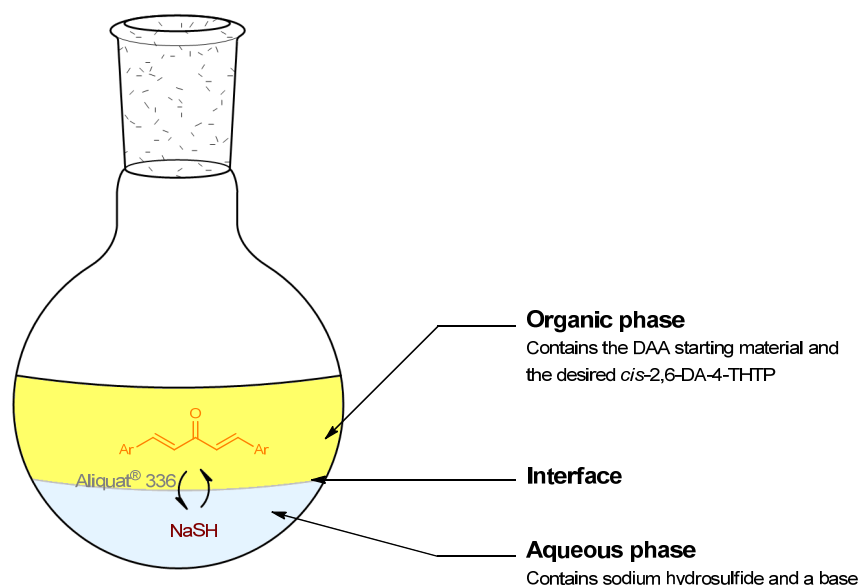


Figure III.23 | Phase-transfer catalysis for the diastereoselective synthesis of *cis* diastereoisomers.

The controlled released of hydrosulfide anion in the organic phase is expected to overcome the drawbacks of the previous strategy.

To the best of our knowledge, such an approach has never been implemented for the synthesis of 2,6-diaryl-4H-tetrahydrothiopyran-4-ones. As a result, we started from scratch and we had to carefully investigate the effects of several parameters, including:

- the phase-transfer catalyst,
- the solvent used in the organic phase,
- and the base.

With regard to the work of Baxter and Whiting that we previously reported (*vide supra*),²²⁰ we suspected an important kinetic effect for the formation of the *cis* diastereoisomer. As a consequence, we also studied the kinetic of the reaction under the optimized conditions.

Choice of the phase-transfer catalyst

We decided to use a phase-transfer catalyst named "Aliquat® 336" (Figure III.24). This quaternary ammonium salt had already been used in the laboratory for mild methylation of salicaldehydes (Scheme III.20).²²⁷ In this procedure Aliquat® 336 allowed a controlled release of hydroxide anion in the organic phase, and thus the deprotonation of phenols that subsequently reacted with dimethyl sulfate.

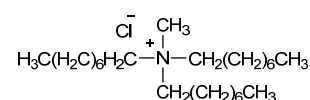
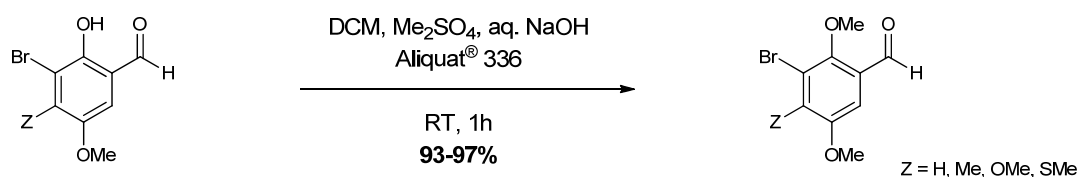


Figure III.24 | Aliquat® 336

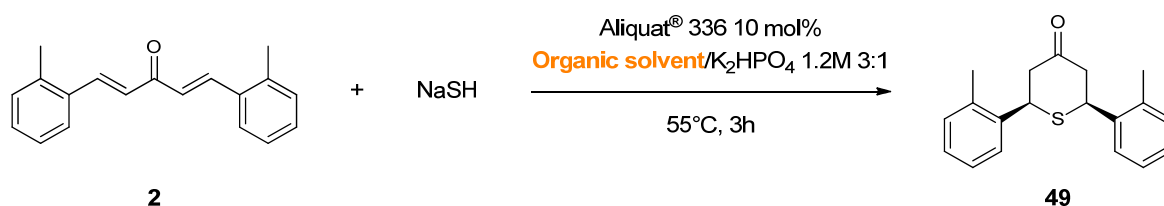


Scheme III.20 | Methylation of salicaldehydes under phase-transfer catalysis mediated by Aliquat® 336

In homogenous medium, this synthesis was previously reported as troublesome.²²⁸ The use of Aliquat® 336 in a diphasic mixture resulted in the quantitative formation of the desired methylated product.

Considering the similarities between NaOH and NaSH, the good results that have been previously obtained, and the very affordable price of Aliquat® 336, this phase-transfer catalyst was selected for the development of our new strategy.

Effects of the organic solvent



Scheme III.21 | Effects of the organic solvent.

In a phase-transfer catalyzed reaction, the choice of the organic solvent is of significant importance. Indeed, this solvent must have a very limited miscibility with water whereas, in the meantime, it has to allow the transfer of reactants from the aqueous phase. Furthermore, in this specific synthesis, the organic solvent must be heated at least at 50 °C in order to favor the thermodynamic diastereoisomer. To meet these criteria, and considering the previous results that have been obtained in this series, we chose to test chloroform, 1,2-dichloroethane (DCE), methyl *tert*-butyl ether, and toluene (Table III.9). For these reactions, the aqueous phase was similar to the one used in the synthesis of (\pm)-*trans* isomers, being composed of four equivalents of potassium phosphate dibasic. Finally, reactions were stopped after a short time (three hours) in order to highlight potential kinetic effects.

Table III.9 | Effects of the organic solvent.

Entry	Solvent	d.r. (cis/trans) ^a	d.e. (%) ^a	HPLC yield (%)
1	1,2-dichloroethane	1:7	-75	61
2	chloroform	1:3.5	-55	91
3	toluene	1.5:1	18	81
4	methyl <i>tert</i> -butyl ether	2.3:1	40	88

^aDetermined by HPLC.

At first, regarding the yield of reactions, except for 1,2-dichloroethane (Table III.9, entry 1), all solvents resulted in satisfying values being comprised between 81 % and 91 % (Table III.9, entries 2 to 4). Furthermore, after three hours, no remaining DAA starting material was observed on the chromatogram. On a stereochemical point of view, it is important to highlight that both DCE and chloroform resulted in an excess of the undesired (\pm)-*trans* isomer after three hours of reaction (Table III.9, entry 1 and 2). Toluene gave a very modest excess in favor of the *cis* isomer whereas MTBE was the most promising solvent with a d.e. value of 40 %.

These observations tend to confirm the hypothesis suggested by Baxter and Whiting who argued that the sulfide-addition step is very fast, the subsequent thermodynamic equilibrium between *cis* and (\pm)-*trans* isomers being the rate-limiting step. As MTBE seemed to be the most promising solvent, it was selected for this new synthetic pathway

Effects of the base



Scheme III.22 | Effects of the base.

Unlike the first procedure that we proposed for the selective synthesis of *cis* isomers, the phase-transfer catalyzed synthesis required the dissolution of sodium hydrosulfide in an aqueous medium. Considering the pK_a value of the couple $\text{H}_2\text{S}/\text{NaSH}$, at least half of the material is liable to be protonated in gaseous hydrogen sulfide. Consequently, a base is required in the process to prevent this protonation (Scheme III.22). However, the choice of this base is restricted by several criteria:

- It must not be soluble in the organic phase.
- A non-nucleophilic base is required in order to prevent any phase-catalyst-mediated nucleophilic substitution on the DAA starting material.
- The pK_a of the base has to be comprised between 8 and 10.

Only very few bases are meeting these criteria, the choice being limited to phosphate and carbonate bases. Therefore, we evaluated three bases, potassium carbonate, cesium carbonate, and potassium phosphate dibasic (Table III.10).

Table III.10 | Effects of the base.

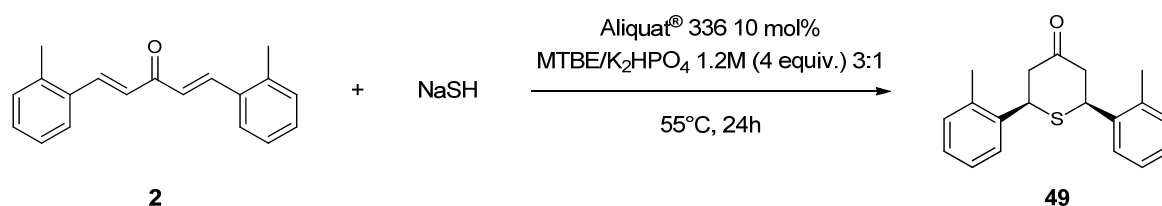
Entry	Base	d.r. (cis/trans) ^a	d.e. (%) ^a	HPLC yield (%)
1	Cs_2CO_3	1.9:1	30	73
2	K_2CO_3	1.8:1	28	76
3	K_2HPO_4	2.3:1	40	88

^aDetermined by HPLC.

Carbonate bases resulted in very similar results both in terms of yields and diastereoisomeric excesses (Table III.10, entries 1 and 2). However, contrary to the reaction performed with phosphate base, some DAA starting material was still observed on the chromatograms; the rate of sulfide addition seems therefore to be lowered with carbonates. Furthermore, d.e. obtained with these bases are about one third lower than the d.e. observed with K_2HPO_4 (Table III.10, entries 1 and 2 compared to entry 3).

As it gave better results, and matched our concern to keep consistency between the different procedures that we developed, potassium phosphate dibasic was selected for this reaction.

Kinetic studies



Scheme III.23 : Reaction conditions used for the kinetic studies.

Further to the optimization experiments, we decided to study the kinetic of the reaction under the optimized conditions (Scheme III.23). As a matter of comparison, we also performed the reaction without the phase-transfer catalyst. The evolution of both systems was followed during one day, with measurements at 15 min, 30 min, 2 h, 3 h, 4 h and 22 h. The amount of diastereoisomers was determined through HPLC analysis and the decrease of DAA starting material was estimated by UV-Vis spectrometry measurement at $\lambda_{\max} = 322 \text{ nm}$ ($\epsilon_{322\text{nm}} = 2.28 \cdot 10^4 \text{ L} \cdot \text{mol}^{-1} \cdot \text{cm}^{-1}$) (Figure III.25 and III.26).

At first, these experiments confirmed the crucial importance of the phase-transfer catalyst. Indeed results shown on Figure III.25 and III.26 (dark red curves) clearly demonstrate that absolutely no reaction occurred if the catalyst was not added in the mixture.

With the catalyst, considering the consumption of the DAA (Figure III.25), we can see that the starting material has almost completely disappeared after one hour of reaction. Concomitantly, the desired 2,6-DA-4-THTP is quickly formed, at first under the form of the (\pm)-*trans* diastereoisomer (Figure III.26, blue curve). This (\pm)-*trans*-2,6-DA-4-THTP is then slowly and quantitatively transformed into its *cis*-2,6-DA-4-THTP counterpart (Figure III.26, orange curve).

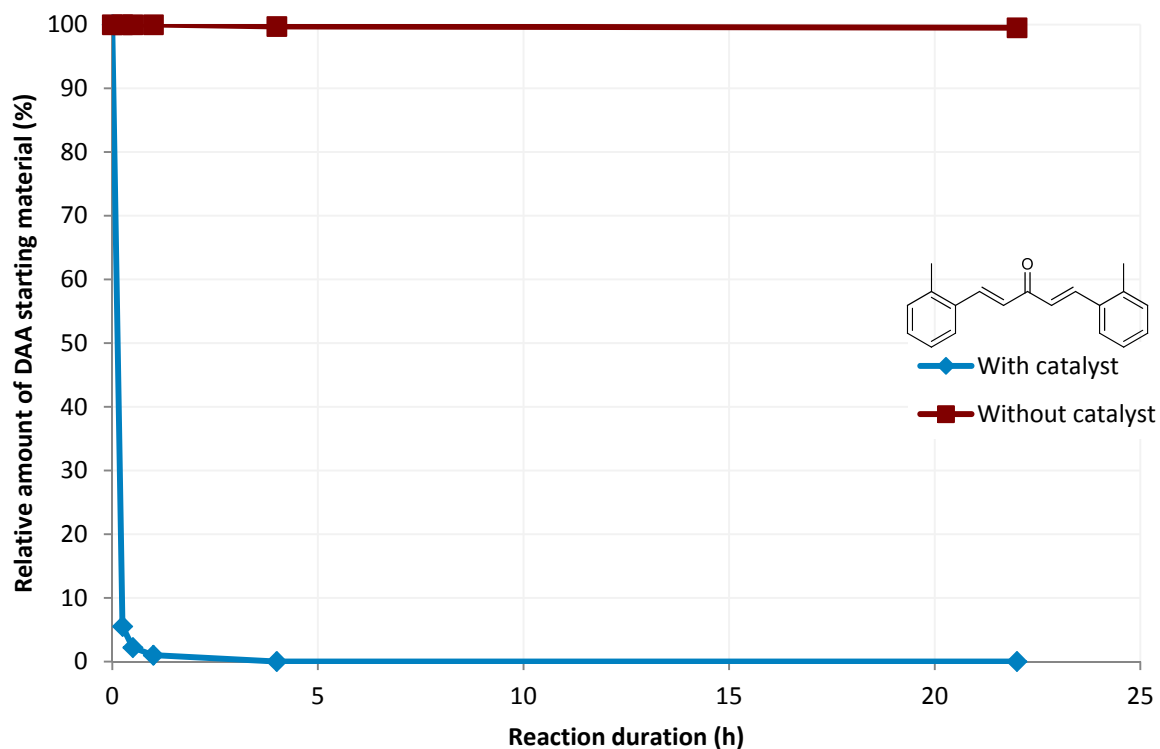
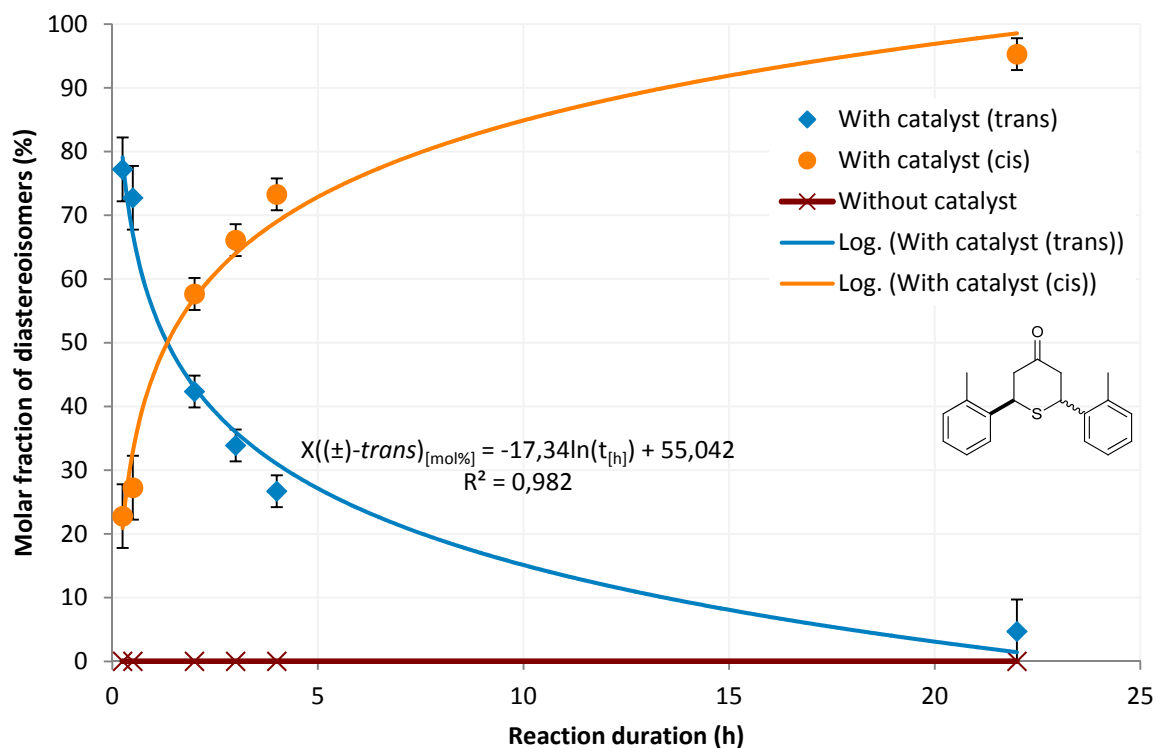
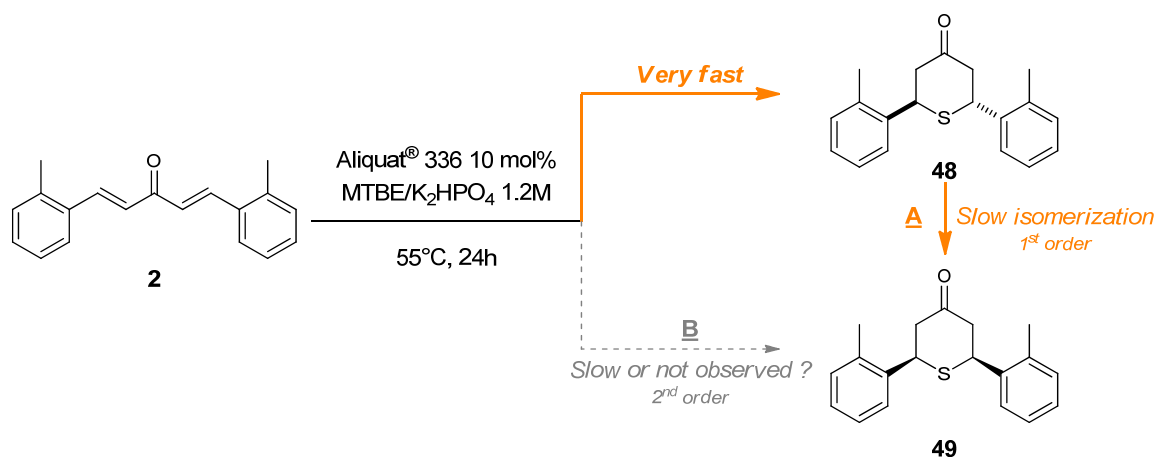


Figure III.25 | Kinetic follow-up of the diarylideneacetone starting material.

Figure III.26 | Kinetic follow-up of the *cis* isomer synthesis.

Though obtained under different reaction conditions, these results clearly confirmed and completed the preliminary observations that have been previously published by Baxter and Whiting.²²⁰ *In fine*, our kinetic studies have unambiguously demonstrated that, under these conditions, the sulfide addition step is very fast, resulting in the quick formation of the kinetic (\pm)-*trans* diastereoisomer. This isomer then undergoes a rate-limiting isomerization to form the thermodynamically more stable *cis* diastereoisomer (Scheme III.24).

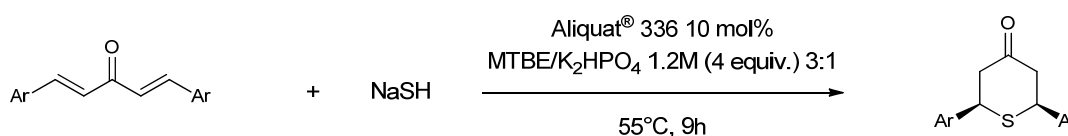


Scheme III.24 | Summary of the kinetic study results.

On a kinetic point of view, the direct formation of the *cis* isomer should follow a second order kinetic law (as the sulfur is not in large excess). Experimentally, the purely logarithmic form of the kinetic curve tends to prove that the formation of the *cis* isomer is a first order, which matches with a formation through an isomerization step (path **A**). As a result we can hypothesize that the direct synthesis of the *cis* isomer (path **B**) is not possible or at least very minor. However, with this unique experiment it is impossible to surely conclude on this point.

Scope of the reaction

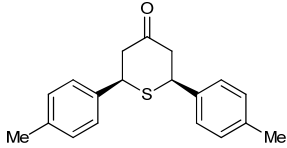
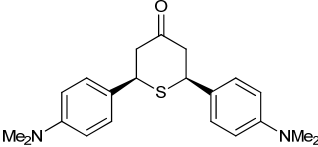
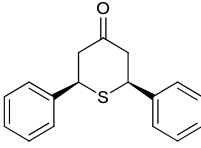
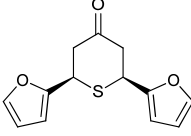
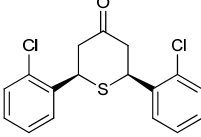
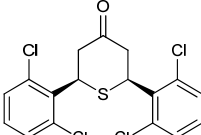
The optimization process has led to the determination of reaction conditions that maximize both the yield and the diastereoisomeric excess of the selective synthesis of *cis* isomers in phase-transfer catalysis. Under these conditions, one equivalent of DAA is reacting with two equivalents of sodium hydrosulfide, in a mixture of methyl *tert*-butyl ether and aqueous potassium phosphate dibasic 1.2 M (3:1), at 55 °C, and with 10 mol% of Aliquat® 336 (Scheme III.25).



Scheme III.25 | Reaction conditions used for the generalization of the diastereoselective synthesis of *cis* isomers.

The methodology under these optimized conditions was extended to the synthesis of several *cis*-2,6-diaryl-4H-tetrahydrothiopyran-4-ones (Table III.11).

Table III.11 | Yields of the diastereoselective synthesis of the *cis* diastereoisomer in phase-transfer catalysis.^a

Entry	Compound	Structure	d.r. (<i>cis/trans</i>) ^b	d.e. (%) ^b	yield (%) ^c
1	68		5.7:1	70	90
2	69		2.3:1	40	82
3	70		4:1	54	88
4	67		3:1	50	75
5	66		2.3:1	40	85
6	71		4.2:1	62	93

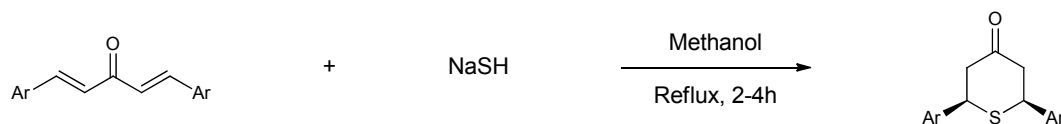
^aReaction performed on a 2 mmol scale. ^bDetermined by NMR. ^cIsolated yield.

At first glance, it is remarkable that this new procedure resulted in the formation of desired products in good to excellent yields, for electron-rich starting materials (Table III.11, entries 1 and 2), as well as for electron-deficient (Table III.11, entry 5) or bulky substrates (Table III.11, entry 6). Products that were not successfully synthesized through the previous procedure were here obtained uneventfully (Table III.11, entry 4 and 5).

Diastereoisomeric excesses were moderate for almost all the reactions, being comprised between 40 % and 70 %. These disappointing results are certainly explained by the relatively short reaction duration; here, the syntheses were stopped after only nine hours whereas the kinetic study has demonstrated that at least one day of reaction is required to achieve good diastereoisomeric excess. Unfortunately, as these experiments were performed in the very last days of the present thesis, we were not able to reproduce these syntheses on a longer reaction time. However, it is almost certain that a prolonged heating of the reaction will significantly improve the d.e. while keeping excellent overall yields.

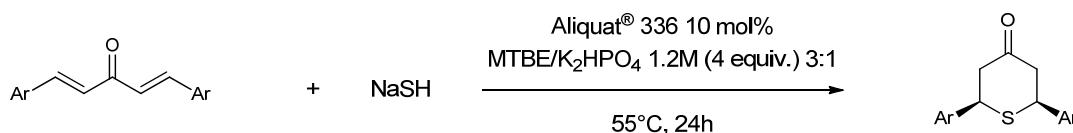
Concluding remarks on the diastereoselective synthesis of *cis*-2,6-diaryl-4H-tetrahydrothiopyran-4-ones

To summarize this part of our work, we developed two different methods for the diastereoselective synthesis of *cis*-2,6-diaryl-4H-tetrahydrothiopyran-4-ones.



Scheme III.26 | Optimized synthesis of *cis* diastereoisomers in organic medium.

The first one, in purely organic medium, proved to be very efficient for robust substitution patterns, resulting in the desired *cis*-2,6-DA-4-THTP in excellent yields and good diastereoisomeric excesses. However, transposition of these conditions on more sensitive substitution patterns failed.



Scheme III.27 | Optimized synthesis of *cis* diastereoisomers under phase-transfer catalysis.

In order to overcome this limitation, we developed a novel approach based on phase-transfer catalysis. These mild reaction conditions were turned out to be compatible with a large panel of substitution patterns, from electron-rich to electron-deficient aromatic rings, including nucleophile-sensitive ones (such as aryl halides, 2-furyl etc.). In addition, kinetic studies have clearly demonstrated that, under these conditions, the addition of the sulfide anion on the double-bonds of the DAA is very fast compared to the rate-limiting isomerization step that slowly transforms the kinetic (\pm)-*trans* diastereoisomer into its thermodynamic *cis* counterpart.

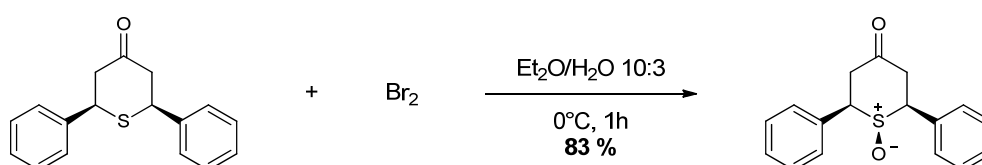
Synthesis of the putative S-oxide metabolites

The reactivity of sulfur containing heterocycle suggests that the β -elimination step is all the more facilitated as the sulfur atom is oxidized. We mentioned in this chapter introduction that this oxidation can be achieved *in vivo* through several ways (e.g. by cytochromes P450, by the ROS generated by the immune response of the host, or in the parasite), resulting in the activated prodrug. In order to determine whether this activation really participates to the antiparasitic activity, we synthesized the oxidized forms –sulfoxides and sulfones– of 2,6-diaryl-4H-tetrahydrothiopyran-4-ones.

Synthesis of sulfoxide derivatives

Literature review

To the best of our knowledge, the synthesis of sulfoxide derivatives of 2,6-DA-4-THTP has been documented in only three articles and was limited to the oxidation of the *cis* isomer.^{229–231} In each case, wet bromine was used to oxidize the sulfur, with variable yield up to 83 % (Scheme III.28).

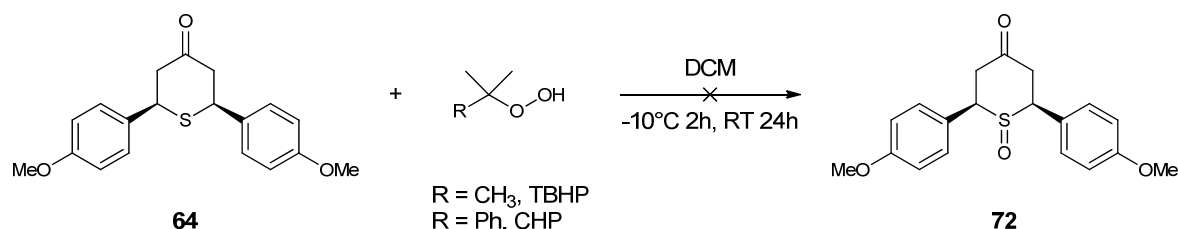


Scheme III.28 | Published procedure for the synthesis of sulfoxide derivatives.

We were able to reproduce this result with the unsubstituted 2,6-diphenyl-4H-tetrahydrothiopyran-4-one which was obtained in a slightly lower yield. However, when this procedure was used on more complex substrates, much lower yields were observed, especially with substituents such as anisyl, *N,N*-dimethylaniline, or furyl. Analysis of the crude showed that the starting material was entirely converted to a small quantity of the desired product and a large amount of by-products. This might be explained by the lack of chemoselectivity of bromine which easily reacts with electron-rich aromatic rings, resulting in the bromination of these aryls. Furthermore, the amount of bromine injected is not well controlled in this procedure; authors recommended adding bromine "*dropwise to the stirred mixture until the brown color of the Br, no longer faded*" without more precisions. In our experiments, we calculated that a four-fold excess of bromine was required to reach this point. Finally, we encountered solubility issues as most of the 2,6-diaryl-4H-tetrahydrothiopyran-4-ones starting materials had limited solubility in the reaction mixture. Facing these difficulties, we investigated a new procedure for the synthesis of these sulfoxides.

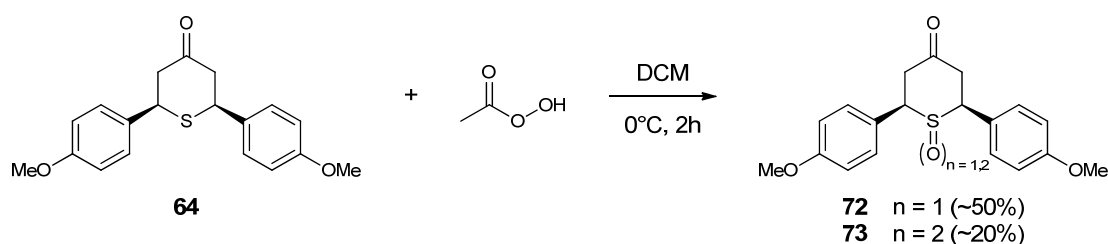
Screening of new oxidation protocols for the synthesis of the desired sulfoxides

In the large panel of oxidizing agents that are described to oxidize sulfide to sulfoxide,¹⁴⁹ we decided to investigate the use of peracids and hydroperoxides. The latter proved to be inefficient as the desired product was obtained neither with *tert*-butylhydroperoxide nor with cumyl hydroperoxide (Scheme III.29).



Scheme III.29 | Attempts of sulfoxide synthesis with hydroperoxides.

On the other hand, the use of peracetic acid yielded to the desired sulfoxide in about 50 % yield with concomitant formation of the sulfone, in spite of a precise control in the stoichiometry of the peracid (Scheme III.30).



Scheme III.30 | Attempts of sulfoxide synthesis with peracetic acid.

This over-oxidation was all the more problematic as the two products are very difficult to separate from each other, either by column of chromatography or by recrystallization. We also evaluated the use of *meta*-chloroperbenzoic acid (*m*CPBA) in similar conditions; with this peracid only traces of sulfoxide and sulfone were both detected.

Facing these difficulties, and with the aim of developing a new mild and, if possible, stereocontrolled synthesis of our sulfoxide derivatives, we looked in the literature for chemoselective, mild or catalyzed methodology.²³² We started our research with the well-known conditions described by Brunel and Kagan.²³³ This protocol –based on the work of Sharpless– was originally developed to achieve the enantiomeric synthesis of chiral sulfoxides. The stereoselectivity is believed to result from the specific configuration of the titanium complex which is formed during the reaction (Figure III.27).²³⁴ The primary source of chirality is the optically pure diethyl tartrate (either the D- or the L-enantiomer). Being chelated on the titanium species, this chiral ligand leaves one unique way for the transient chelation of the hydroperoxide and for the approach of the sulfide.

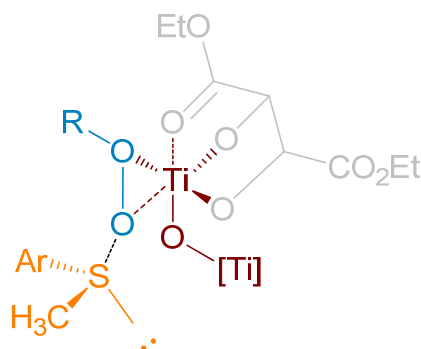
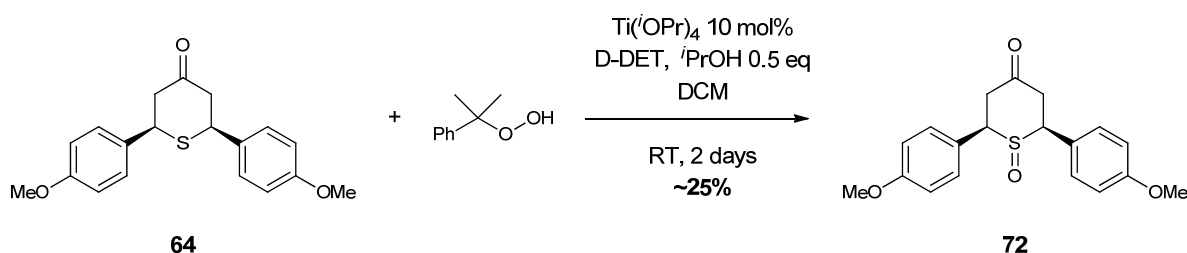


Figure III.27 | Putative structure of the chiral chelate that is expected to provide the chirality on the sulfoxide.

This simplified view is controversial as several authors argued that it does not explain the stoichiometry of the reaction which requires two equivalents of diethyl tartrate and an half equivalent of isopropanol.²³⁵ Therefore, until now, the exact structure of the active titanium species is not known and it is assumed that several complexes are interfering in the reaction mixture. Apart from these theoretical considerations, this procedure usually leads to the formation of the desired sulfoxide in moderate to good yield with excellent enantiomeric excesses.²³² We therefore applied these conditions to product **64**, using cumyl hydroperoxide as oxidizing agent (Scheme III.31).

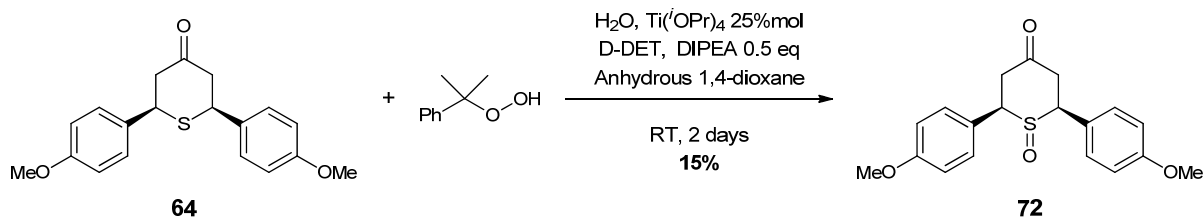


Scheme III.31 | Kagan's protocol for the synthesis of sulfoxide derivatives.

Under these conditions, only about 25 % of the desired sulfoxide was identified and most of the starting material was still present in the crude, even after two days of reaction. However, it is noteworthy to notice that these results tend to demonstrate that the titanium catalytic system might also have an influence on the energy of activation of the oxidation reaction. Indeed, oxidation with cumyl hydroperoxide under the condition described by Kagan gives the sulfoxide in 25 % yield, while no product was observed without the catalytic system (*vide supra*).

With the aim of improving this result, modified conditions of Kagan's protocol were subsequently used (Scheme III.32). Indeed, it has been demonstrated that, in some cases, the addition of *N,N*-diisopropylethylamine can significantly improve the yield.^{236,237} Unfortunately these modifications were to the detriment of the desired product, as the sulfoxide was

detected in a lower yield (15 %). Starting material was still present in the crude as well as traces of the parent diarylideneacetone, probably regenerated due to the presence of the base.



Scheme III.32 | Modified Kagan's conditions for the synthesis of sulfoxide derivatives.

Considering these disappointing results obtained under usual oxidative conditions, we focused our attention on the search for efficient and chemoselective oxidative agents which would be compatible with our substrate, and, more specifically, which could be used in neutral or slightly acidic conditions at a low temperature. Oxaziridines were found to efficiently meet these different criteria.

Use of Davis's oxaziridine for the synthesis of sulfoxide derivatives

Although oxaziridines were well-known for their ability to transfer nitrogen,²³⁸ Davis and coworkers have demonstrated the exceptional ability of 2-sulfonyloxaziridines to transfer an oxygen atom to various nucleophiles.²³⁹ Thus, 2-sulfonyloxaziridines have been used in the oxidation of sulfides to sulfoxides,²⁴⁰ disulfides to thiosulfonates,²⁴⁰ selenides to selenoxides,²⁴¹ thiols to sulfenic acids,^{242–244} organometallic reagents to alcohols and phenols,²⁴⁵ ketone and ester enolates to α -hydroxy carbonyl compounds,²⁴⁶ in the epoxidation of alkenes,^{247,248} and in the conversion of chiral amide enolates to optically active α -hydroxy carboxylic acids (Figure III.28).^{249,250}

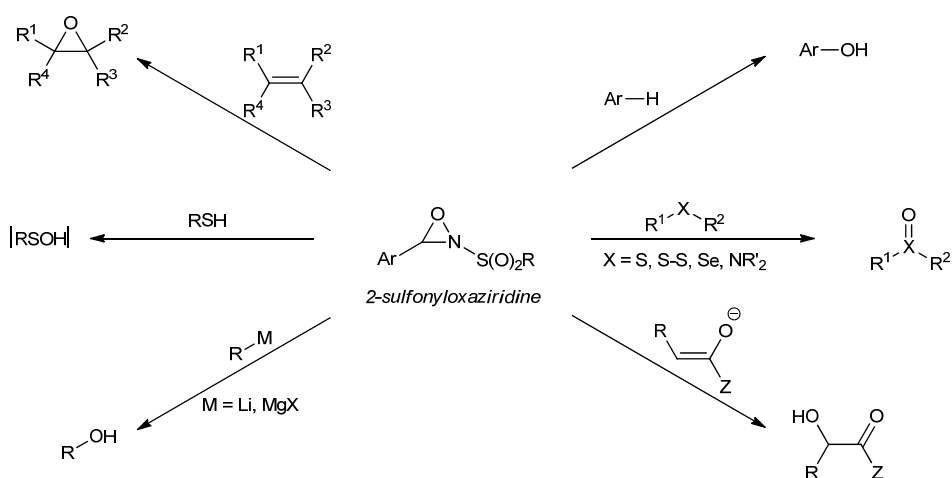
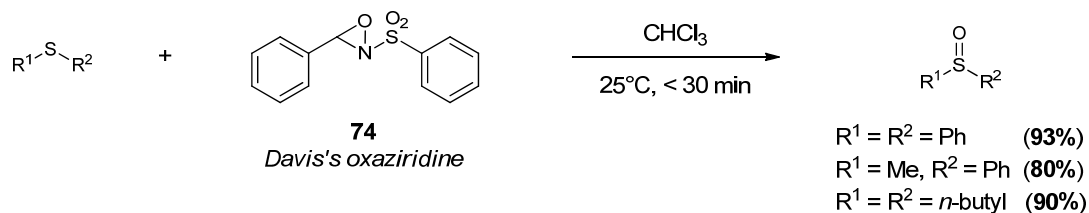


Figure III.28 | Scope of application of 2-sulfonyloxaziridines.

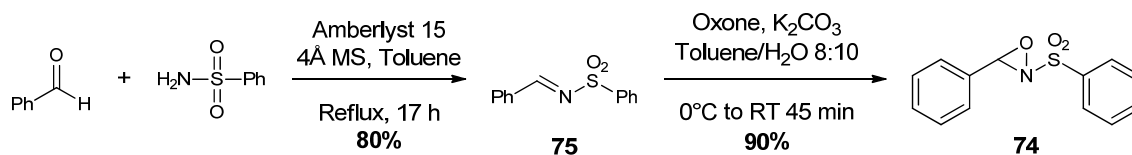
For the specific oxidation of sulfide to sulfoxide, the so called Davis's oxaziridine was demonstrated to be very efficient and particularly chemoselective (Scheme III.33).²⁴⁰



Scheme III.33 | Published sulfoxide synthesis with Davis's oxaziridine as oxidizing agent.

Considering these promising results, we decided to investigate the oxidation of 2,6-DA-4-THTP with Davis's oxaziridine.

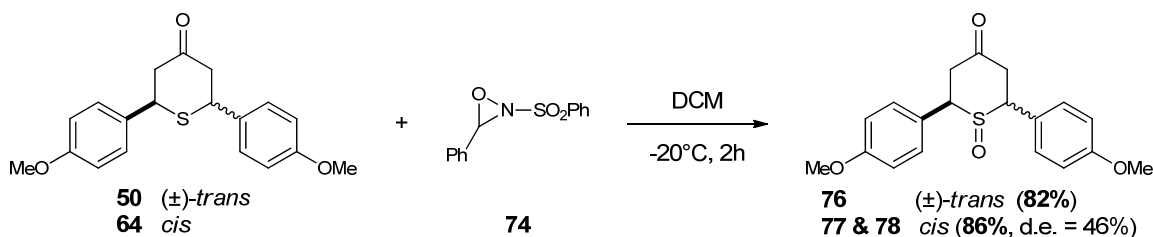
Davis's oxaziridine **74** was quickly and simply synthesized in two steps (Scheme III.34).²⁵¹ The first step in the synthesis consists in the condensation of benzenesulfonamide on benzaldehyde catalyzed by Amberlyst® 15 in refluxing toluene. In addition to 4Å powdered molecular sieves, a Dean-Stark apparatus was used in order to prevent water accumulation in the reaction mixture. Desired imine **75** was obtained in 80 % yield after recrystallization in ethyl acetate and pentane. Subsequent epoxidation of the imine double bond with Oxone® in basic aqueous toluene resulted in the formation of oxaziridine **74** in 90 % yield after recrystallization in toluene.



Scheme III.34 | Synthesis of Davis's oxaziridine.

Hazard statement: although Davis's oxaziridine is considered to be stable under normal conditions of handling and storage, this reagent is a powerful oxidizing agent which can react unexpectedly. Thus, exothermic decomposition of a 500 g quantity after two weeks of storage at room temperature was reported by Dr. G. C. Crockett of Aldrich Chemical Company, Inc.²⁵² The generated force was powerful enough to shatter the container and char the oxaziridine. This may explain why Davis's oxaziridine is no longer commercially available within Sigma-Aldrich or any other important chemical supplier. This was an incentive to apply enhanced security measures, working on single-gram scale, behind the closed protective screen of a fume hood at any time. Special care must be taken during the evaporation of the final crude and the recrystallization step which were performed behind a blast shield and at a reasonable heating-temperature. Pure oxaziridine was stored under an inert atmosphere of argon at -20 °C.

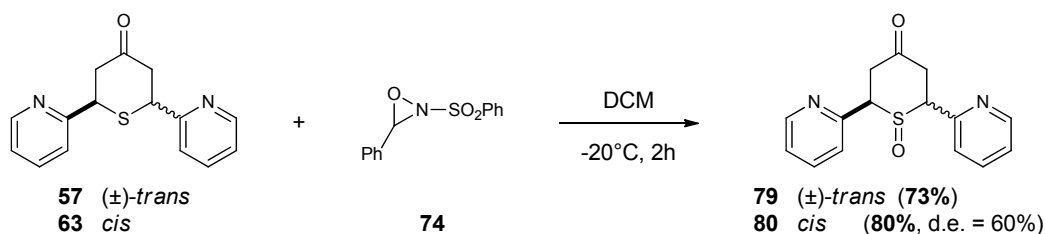
The oxaziridine being synthesized, we investigated the oxidation of 2,6-diaryl-4H-tetrahydrothiopyran-4-ones with this new reagent. With regard to the conditions described by Davis and coworkers,²⁴⁰ anhydrous dichloromethane was substituted to chloroform, molarity was slightly decreased and synthesis were firstly performed at -20 °C to prevent any side reactions. First attempts done with substrate **64** were very successful as the desired sulfoxide was obtained in 86 % yield. Unsurprisingly, similar results were obtained with (±)-*trans* isomer **50** (Scheme III.35).



Scheme III.35 | Synthesis of desired sulfoxides (*p*-anisyl series).

It is important to highlight that the reactions carried out on the *cis* isomer resulted in the formation of the two expected diastereoisomers. These two products were separated by column of chromatography yielding **77** (63 %) and **78** (23 %). This stereochemical aspect of the reaction will be discussed in the following section (*vide infra*). Regarding the effects of the reaction temperature, further test-reactions were carried out successively at -78°C, -20°C and 0°C without significant changes in yield, purity or reaction time.

The procedure was next extended to the synthesis of 2-pyridyl-substituted 2,6-DA-4-THTP (Scheme III.36). Similarly, excellent yields were obtained on this series. It is noteworthy to mention that reactions were performed with no specific protection of the nitrogen on the pyridyl ring. No oxidation was observed on this specific site, thus demonstrating the chemoselectivity of the methodology.



Scheme III.36 | Synthesis of desired sulfoxides (*o*-pyridyl series).

The two diastereoisomers of the *cis* product were also formed during the reaction. Unfortunately, in spite of numerous attempts, we were not able to separate these two products, neither by recrystallization nor by column of chromatography.

Characterization of *cis* sulfoxide derivatives – stereochemical and spectroscopic aspects

On a stereochemistry point of view, the oxidation of the *cis* sulfide should give two different diastereoisomers, depending on the position of the oxygen. In one case it is in equatorial position (hereafter quoted as *anti-cis* sulfoxide isomer), whereas in the other case it is in axial position (hereafter quoted as *syn-cis* sulfoxide isomer) (Figure III.29).

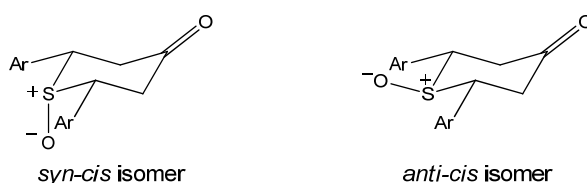


Figure III.29 | Two diastereoisomers are expected from the synthesis of *cis* sulfoxides.

The most stable configuration of the sulfoxide for this kind of heterocycles has been discussed in several studies.^{229,253,254} According to these works, the axial position seems more stable than the equatorial one; the *syn-cis* is therefore expected to be the major isomer, if not the unique one.

One unique old publication briefly described NMR data for sulfoxide derivatives of 2,6-DA-4-THTP.²²⁹ In this article, Klein and Stollar used the significant deshielding of axial proton in beta position to the sulfoxide as proof of the axial positioning of the oxygen atom. This argument was supported by one previous study done on similar sulfoxide-containing heterocycles.²⁵³ Basing our investigations on these weak NMR data, we considered the variation of chemical shifts for relevant protons of sulfoxide isomers compared to same protons in sulfide (Table III.12).

Table III.12 | NMR chemical shifts of relevant protons for configuration determination of sulfoxide isomers.

	64	77		78	
Proton	δ (ppm)	δ (ppm)	$\Delta\delta$ (ppm)	δ (ppm)	$\Delta\delta$ (ppm)
$H_{X(ax)}$	4.28	4.07	-0.21	4.12	-0.16
$H_{A(ax)}$	3.01	3.73	+0.72	3.24	+0.23
$H_{B(eq)}$	2.93	2.67	-0.26	3.01	+0.08

Regarding the axial proton in α position to the sulfoxide ($H_{X(ax)}$), variations of the chemical shift are similar in both oxidized isomers **77** and **78** with a shielding of about 0.20 ppm. On the other hand, protons in β position to the sulfoxide, and especially axial ones, are significantly

influenced by the presence of the oxygen. Product **77** is the most affected as the deshielding of $H_{A(ax)}$ reaches 0.72 ppm. In the meantime equatorial proton $H_{B(eq)}$ is shielded by about 0.26 ppm. Isomer **78** is significantly less affected as almost no variation is observed for the equatorial proton, whereas the axial is shifted to lower field from 0.23 ppm.

According to these observations, and further to the aforementioned studies, it might be concluded that isomer **77** -which is the major one- has its oxygen in axial position, thus being the *syn-cis* isomer. However, this conclusion is in contradiction with the literature published by Davis and coworkers who concluded on an equatorial positioning of the oxygen when sulfoxides are obtained further to oxidation with Davis's oxaziridine.²⁴⁰

Without any reliable references it was very challenging to attribute configurations of each isolated isomers and we will therefore not conclude on this point. An X-rays crystallographic analysis would have been very valuable in this enterprise; unfortunately, in spite of several attempts, we never managed to obtain crystals from the cotton-like pure products.

Concluding remarks on the synthesis of sulfoxide derivatives

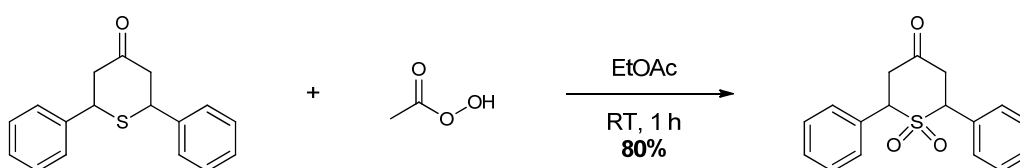
To summarize this part of our work, we developed a new method for the efficient oxidation of 2,6-DA-4-THTP to their relative sulfoxide. The use of oxaziridine as oxidative agent that we suggest offers several advantages. The high chemoselectivity and tolerance of this reagent allows the selective oxidation of the sulfur, without side reactions. A wide range of temperature –from -78 °C to 0 °C– is suitable for this reaction, thus being compatible with thermo-sensitive molecules. Finally, Davis's oxaziridine is easy to prepare and handle, stable over months, and, above all, less toxic and hazardous than bromine, which is a great advantage compared to earlier procedures.

The five synthesized sulfoxides were submitted for biological evaluation (*vide infra*) and would be used as references for the analytical determination of metabolites of 2,6-diaryl-4H-tetrahydrothiopyran-4-ones.

Synthesis of sulfone derivatives

Literature review

We previously described the uses of 2,6-diaryl-4H-tetrahydrothiopyran-4-one derivatives for electronic applications (*vide supra*). Most of the compounds used in this field were sulfone derivatives. As a result, the oxidation of 2,6-DA-4-THTP to their sulfone derivatives is more described in the literature than the synthesis of sulfoxide species.^{150,211} The reported protocol consists in the mixing of the 2,6-diaryl-4H-tetrahydrothiopyran-4-one with an excess of peracetic acid (3 equivalents) in ethyl acetate or dichloromethane, and at high molarity (1.5 M) (Scheme III.37).

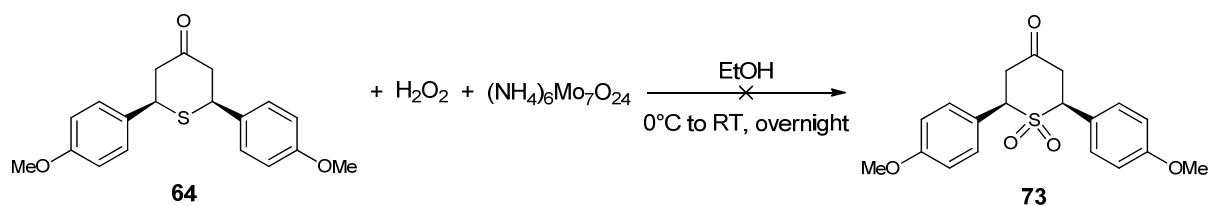


Scheme III.37 | Published protocol for the synthesis of sulfone derivatives.

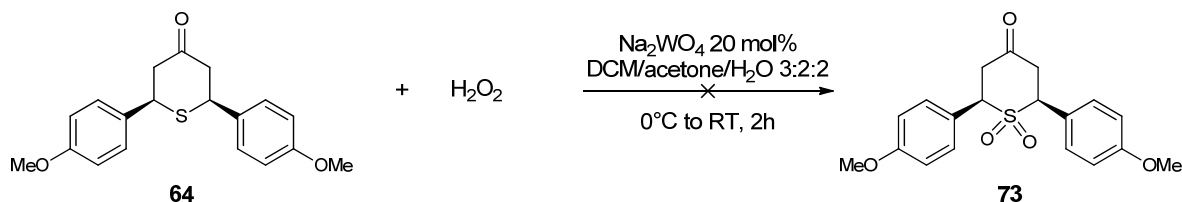
In our hands, this procedure was successful only with the unsubstituted 2,6-diphenyl-4H-tetrahydrothiopyran-4-one but we never managed to apply it on more complex substitution patterns. Each of our attempts resulted in an entire consumption of the starting material to produce a large amount of unidentified by-products. This might be explained by the relatively high concentration of the medium and, above all, by the high oxidizing and acidic strength of peracetic acid. Therefore, with the constant aim of developing less drastic procedures, we looked for milder or catalytic protocol for the synthesis of sulfone derivatives of 2,6-DA-4-THTP.

Screening of new oxidation protocols for the synthesis of the desired sulfone

Numerous protocols are described in the literature for the direct oxidation of sulfide to sulfone. The use of simple inorganic reagents such as potassium permanganate or potassium hydrogen persulfate is well documented.¹⁴⁹ However, an excess of these strong oxidizing agent is commonly used, increasing the high risk of side reactions as we observed with peracetic acid. Therefore, we discarded all these procedures. Likewise, protocols which were performed in basic conditions were not considered in order to avoid the risk of *in situ* β -elimination. We firstly focused our attention on new green catalytic processes of oxidation. Thus, we investigated the use of ammonium molybdate and sodium tungstate as a catalyst for hydrogen peroxide-mediated oxidation (Scheme III.38 and III.39).^{255,256}



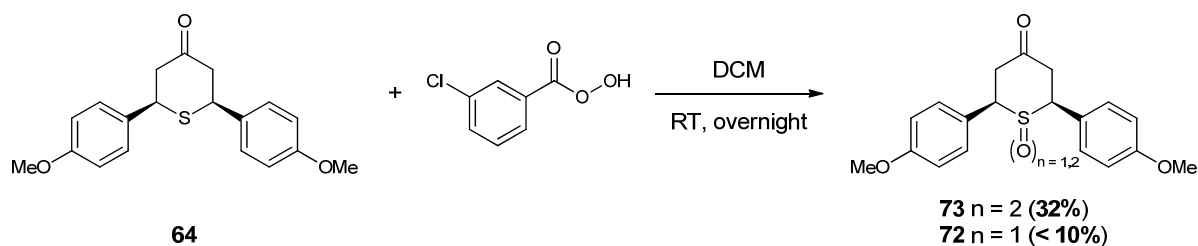
Scheme III.38 | Ammonium molybdate catalysis for the hydrogen peroxide-mediated synthesis of sulfones.



Scheme III.39 | Sodium tungstate catalysis for the hydrogen peroxide-mediated synthesis of sulfones.

Unfortunately, none of these two procedures resulted in the desired sulfone. In both cases the oxidation did not occur, even with a very large excess of hydrogen peroxide (up to twenty equivalents). Starting material was almost completely recovered.

In the discussion about the synthesis of sulfoxide derivatives, we mentioned that the use of one equivalent of *m*CPBA resulted in the formation of both sulfoxide and sulfone species at trace level. We therefore tried to oxidize sulfide to sulfone with a large excess of *m*CPBA, overnight at room temperature (Scheme III.40).

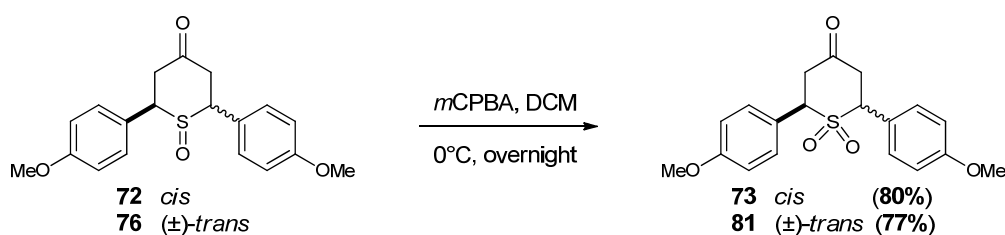
Scheme III.40 | Synthesis of sulfone derivatives with *m*-chloroperbenzoic acid oxidation.

Unfortunately, in spite of the excess of oxidant and of the long reaction time, only 32% of the desired sulfone was recovered, in mixture with traces of the intermediate sulfoxide.

With regard to the difficult direct oxidation of sulfide to sulfone, we turned out our strategy to the use of previously synthesized sulfoxides as starting material for the synthesis of sulfones.

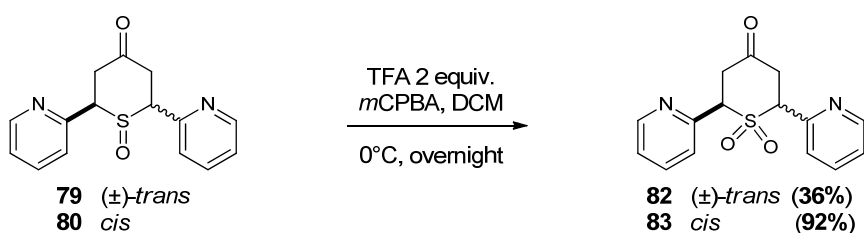
Synthesis of sulfone derivatives by smooth oxidation of sulfoxides

As the over-oxidation of sulfide to sulfone was troublesome, we hypothesized that starting from the sulfoxide species would make the process of oxidation easier. On the 2,6-diaryl-4H-tetrahydrothiopyran-4-one series this approach was successful as the sulfone derivatives were finally obtained in excellent yields by smooth and slow oxidation of parent sulfoxides with *m*CPBA in dichloromethane at low temperature (Scheme III.41). As the chirality on the sulfur atom disappeared with the formation of the sulfone, the diastereoisomeric mixture of *cis* isomers was used as starting material.



Scheme III.41 | Successful synthesis of sulfone derivatives by slow oxidation of their relative sulfoxides (*p*-anisyl series).

Likewise, the procedure was applied to the synthesis of 2-pyridyl-substituted 2,6-DA-4-THTP (Scheme III.42). Results were satisfactory, the disappointing yield of the (±)-*trans* isomer being explained by its poor solubility in all organic solvents which made the purification step tricky. However, it is important to notice that, unlike Davis's oxaziridine, *m*CPBA is absolutely not chemoselective. Without protection of the aromatic nitrogen, very complex mixtures of by-products were obtained with only limited amounts of desired products. This issue was simply overcome by the addition of two equivalent of trifluoroacetic acid prior to the *m*CPBA. The resulted protonated amine was thus protected from undesirable oxidation.



Scheme III.42 | Successful synthesis of sulfone derivatives by slow oxidation of their relative sulfoxides (*o*-pyridyl series).

The four synthesized sulfones were submitted for biological evaluation (*vide infra*) and would be used as references for the analytical determination of metabolites of 2,6-diaryl-4H-tetrahydrothiopyran-4-ones.

Antiparasitic activities of 2,6-diaryl-4H-tetrahydrothiopyran-4-ones and their relative S-oxides

Foreword

Protocols

Prodrugs and their putative metabolites were assessed *in vitro* in the same conditions as the antiparasitic assays that were performed with diarylideneacetones. Thus, compounds were submitted to cellular growth assays on whole parasites at the Laboratory of Antiparasitic Chemotherapy, led by Prof. Philippe Loiseau at the University of Paris XI (BioCIS, UMR8076 CNRS), and the Laboratory of Microbiology, Parasitology and Hygiene, headed by Prof. Louis Maes at the University of Antwerp. Testing protocols and parasite strains remained identical (see experimental part for details).

Representation of the results

Further to the biological experiments, results are provided as 50 % inhibitory concentration (IC_{50}) expressed in micromolar. In the following sections these will be shown in table for each parasite and each compound. For an easier reading and analysis, compounds will be sorted depending on their activity against *Trypanosoma brucei* rather than on their occurrence.

The discussion will be based on similar plots than those used for describing the SAR of DAA. The targeted area remains the same for the evaluation of prodrugs and putative metabolites: $IC_{50}(Parasite) < 1 \mu M$ (i.e. $pIC_{50}(Parasite) > 6$) and $CC_{50}(hMRC-5) > 32 \mu M$ (i.e. $pCC_{50}(hMRC-5) < 4.5$).

Considering the lower number of 2,6-DA-4-THTP synthesized and tested, it would be more difficult to draw primary trends regarding the electronic repartition or the lipophilicity as it was the case in the SAR of diarylideneacetones. Nevertheless, the effect of the stereochemistry as well as of the sulfur oxidation state will be discussed in the last section of this chapter.

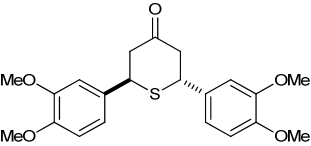
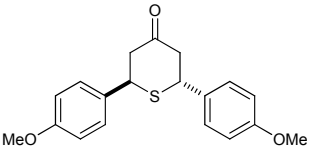
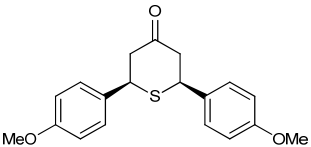
Antiparasitic activities of 2,6-diaryl-4H-tetrahydrothiopyran-4-ones

In fine, as part of this thesis, seventeen 2,6-diaryl-4H-tetrahydrothiopyran-4-ones were synthesized and evaluated for their antiparasitic activity against trypanosomatids. For the sake of the comparison, in each table, **bracketed small gray values refer to the IC₅₀/CC₅₀ values of the parent diarylideneacetone** as quoted in Chapter 2. As for the analysis of DAA's bioassays, compounds have been clustered according to their general structure (heteroaromatics, polyphenols etc.) and will be presented further to this classification.

Polyphenol pattern – Curcumine-like substitutions

Further to the exploration of this substitution pattern in the DAA series, we picked-up the two most promising structures in term of selectivity index, *i.e.* the anisyl- and *O*-methylated vanillin-substituted DAA. This resulted in the evaluation of compounds **51**, **50** and **64** (Table III.13).

Table III.13 | *In vitro* antiparasitic activities of polyphenol-substituted sulfides.

Entry	Compound	<i>In vitro</i> assays – IC ₅₀ (μM)				Tox.
		<i>hMRC-5</i>	<i>T. cruzi</i>	<i>T. brucei</i>	<i>L. infantum</i>	
1	 <p style="text-align: center;">51</p>	9.26 (6.90)	7.27 (2.09)	8.11 (2.06)	32.46 (30.05)	T1
2	 <p style="text-align: center;">50</p>	≥ 64 (≥ 64)	≥ 64 (10.70)	≥ 64 (1.24)	≥ 64 (≥ 64)	
3	 <p style="text-align: center;">64</p>	≥ 64 (≥ 64)	≥ 64 (10.70)	≥ 64 (1.24)	≥ 64 (≥ 64)	

Although the toxicity of product **51** was slightly decreased compared to the parent DAA, antiparasitic activities were almost four times lowered, resulting in a worst selectivity index (1.1 for the prodrug compared to 3.3 for the parent DAA). Cyclization of anisyl-substituted DAA in 2,6-DA-4-THTP was also to the detriment of the potency. Indeed, the formation of the prodrug cycle resulted in a complete loss of the activity for both compounds **50** and **64**.

Monosubstituted aromatics

Ten 2,6-DA-4-THTP were evaluated as part of this category (Table III.14). Substitutions were chosen according to the results obtained in the DAA series. Generally speaking, most of tested compounds show lowered toxicity toward human cells. Regarding the antiparasitic activities, it is noteworthy to mention that the most active substitution patterns highlighted in the diarylideneacetones series are also the most potent in the 2,6-DA-4-THTP series. Thus, the two most active compounds were still the phenyl and *p*-trifluoromethyl derivatives (Table III.14, entries 1-2). Phenyl substituted 2,6-DA-4-THTP **56** was a little bit more active in this series than *p*-trifluoromethyl derivative **51**. Toxicity of these two compounds was worrying although not alarming, being expressed at minimum twenty-fold the therapeutic $IC_{50}(T. brucei)$ value. In addition, **56** was the only 2,6-DA-4-THTP to have an activity toward *L. infantum* ($IC_{50} = 8.11 \mu M$). However, toxicity on mouse macrophages was reported during the biological assays. This might partially explains the good potency on *L. infantum* as these parasites were maintained in mouse macrophages during the test.

Three other compounds, namely compounds **52**, **59** and **53**, showed interesting antiparasitic activities with $IC_{50}(T. brucei)$ values in the micromolar range (Table III.14, entries 3-5). Compound **59** was not toxic toward both human cells and mouse macrophages while **59** displayed a limited toxicity against hMRC-5 cells. Surprisingly compound **53** was not selective, being toxic for parasites as well as human cells although its parent DAA was not toxic at all.

The five remaining sulfide were not active and not toxic (Table III.14, entries 6-10). Chlorinated DAA were especially affected by the heterocycle formation. Indeed, although they had an interesting profile in the DAA series, here we can see that they were almost completely inactive (Table III.14, entries 6-8).

In fine, this exploration of monosubstituted 2,6-diaryl-4H-tetrahydrothiopyran-4-ones highlighted four substitution patterns displaying a reasonable potency as well as a satisfying selectivity index (based on *T. brucei*). Although *N*-substituted anilines did not display interesting profiles in this series, *p*-trifluoromethylphenyl, *p*-benzotrile, phenyl and *p*-toluyl are definitely confirmed as very promising substitution patterns.

Table III.14 | *In vitro* antiparasitic activities of monosubstituted sulfides.

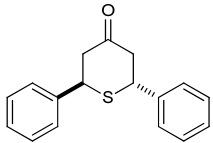
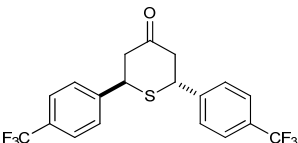
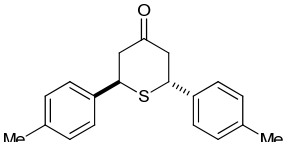
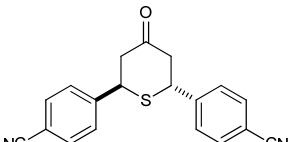
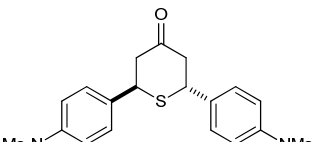
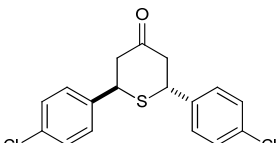
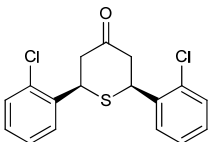
Entry	Compound	<i>In vitro</i> assays – IC ₅₀ (μM)				Tox.
		<i>hMRC-5</i>	<i>T. cruzi</i>	<i>T. brucei</i>	<i>L. infantum</i>	
1	 56	27.57 (52.86)	4.57 (16.00)	≤ 0.25 (0.38)	8.11 (20.32)	T2
2	 58	10.20 (26.18)	2.49 (1.60)	0.50 (0.25)	32.46 (0.64)	T1
3	 52	24.25 (32.46)	3.70 (41.90)	0.77 (9.27)	≥ 64 (≥ 64)	
4	 59	≥ 64 (57.41)	42.47 (11.89)	1.23 (1.23)	≥ 64 (5.08)	
5	 53	4.96 (62.28)	2.5 (36.93)	1.47 (0.81)	43.07 (≥ 64)	
6	 60	≥ 64 (42.44)	≥ 64 (35.6)	27.43 (2.14)	33.19 (≥ 60)	
7	 66	≥ 64 (29.37)	35.00 (12.02)	37.60 (7.81)	≥ 64 (6.82)	

Table III.14 | *In vitro* antiparasitic activities of monosubstituted sulfides. (Continued)

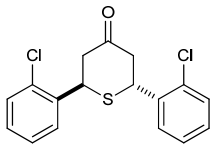
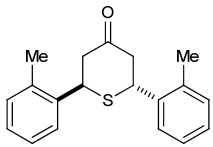
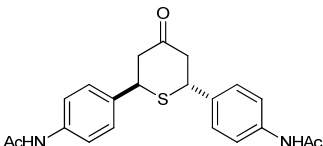
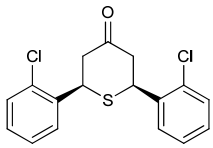
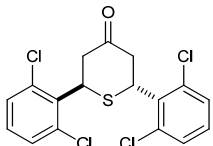
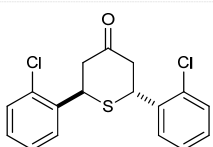
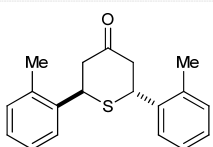
Entry	Compound	<i>In vitro</i> assays – IC ₅₀ (μM)				Tox.
		<i>hMRC-5</i>	<i>T. cruzi</i>	<i>T. brucei</i>	<i>L. infantum</i>	
8	 <p>61</p>	≥ 64 (29.37)	≥ 64 (12.02)	≥ 64 (7.81)	32.00 (6.82)	
9	 <p>48</p>	≥ 64 (≥ 64)	≥ 64 (51.71)	≥ 64 (≥ 64)	43.07 (8.11)	
10	 <p>54</p>	≥ 64 (33.99)	≥ 64 (10.21)	≥ 64 (0.51)	≥ 64 (8.11)	

Table III.15 | *In vitro* antiparasitic activities of sterically hindered sulfides.

Entry	Compound	<i>In vitro</i> assays – IC ₅₀ (μM)				Tox.
		<i>hMRC-5</i>	<i>T. cruzi</i>	<i>T. brucei</i>	<i>L. infantum</i>	
1	 <p>66</p>	≥ 64 (29.37)	35.00 (12.02)	37.60 (7.81)	≥ 64 (6.82)	
2	 <p>62</p>	≥ 64 (≥ 64)	≥ 64 (39.52)	≥ 64 (≥ 64)	2.03 (32.46)	T3
3	 <p>61</p>	≥ 64 (29.37)	≥ 64 (12.02)	≥ 64 (7.81)	32.00 (6.82)	
4	 <p>48</p>	≥ 64 (≥ 64)	≥ 64 (51.71)	≥ 64 (≥ 64)	43.07 (8.11)	

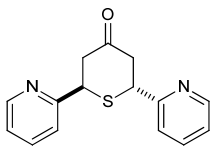
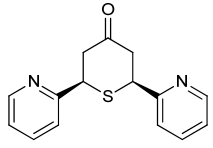
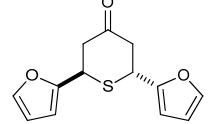
Sterically hindered 2,6-diaryl-4H-tetrahydrothiopyran-4-ones

In the diarylideneacetones series, we demonstrated that a high steric hindrance close to the reactive electrophilic centers significantly lowered both the activity and the toxicity. We expected that 2,6-diaryl-4H-tetrahydrothiopyran-4-ones would show a similar tendency and biological tests confirmed this assumption (Table III.15). None of the compounds tested in this category showed potency or toxicity. However, it is noteworthy to mention that, although it showed no activity toward *Trypanosoma*, bulky compound **62** was highly potent toward *L. infantum*, being twice more active than the marketed drug miltefosine (Table III.15, entry 2). However, once again, this product was found to be toxic on mouse macrophages, which might explain this potent activity toward *Leishmania*.

Heteroaromatics

Being the most active compounds in the diarylideneacetone series but suffering from an unacceptable toxicity, pyridyl-substituted 2,6-diaryl-4H-tetrahydrothiopyran-4-ones were carefully considered (Table III.16). At first glance, we can notice that sulfide **57** and **63** were not anymore toxic toward human cells. Unfortunately, the concomitant loss of potency toward trypanosomatid parasites limits the interest of these cyclized compounds (Table III.16, entries 1 and 2). 2-furyl derivatives showed only limited activities in the DAA series and this was also the case in the prodrugs series (Table III.16, entry 3).

Table III.16 | *In vitro* antiparasitic activities of heteroaromatic derivatives.

Entry	Compound	<i>In vitro</i> assays – IC ₅₀ (μM)				
		<i>hMRC-5</i>	<i>T. cruzi</i>	<i>T. brucei</i>	<i>L. infantum</i>	Tox.
1	 57	≥ 64 (1.91)	≥ 64 (0.29)	26.10 (0.03)	≥ 64 (0.38)	
2	 63	≥ 64 (1.91)	≥ 64 (0.29)	29.06 (0.03)	≥ 64 (0.38)	
3	 55	≥ 64 (≥ 64)	≥ 64 (39.83)	≥ 64 (7.58)	≥ 64 (32.46)	

Antiparasitic activities of putative S-oxide metabolites

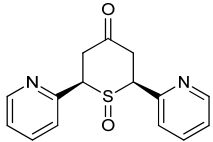
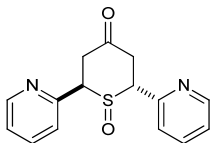
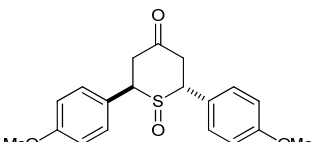
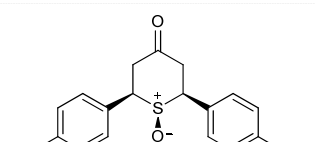
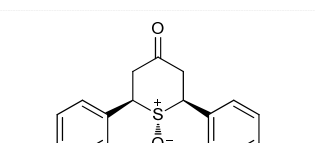
As they are prone to easily undergo β -elimination, sulfoxide and sulfone derivatives of 2,6-DA-4-THTP are expected to allow a rapid regeneration of the active DAA and, as a consequence, of the antiparasitic activity. This might compensate for the lack of activity that we observed in most of parent sulfides. In order to check the validity of this hypothesis, five sulfoxides and four sulfones were submitted to biological evaluation. Regarding the time-limitation of a thesis, we had to restrict our preliminary studies to two different substitution patterns; based on the results obtained in the DAA series, we chose the anisyl- and 2-pyridyl-substituents as representative examples for the evaluation of putative S-oxide metabolites. For the sake of the comparison, in each table, **bracketed small blue values refer to the IC₅₀/CC₅₀ values of the parent sulfide** as quoted in the previous section.

Sulfoxide derivatives

At first glance, we can notice that the antitrypanosomal activity was significantly restored compared to parent sulfide (Table III.17). Although anisyl- and 2-pyridyl-substituted sulfide were all displaying IC₅₀(trypanosomatids) values higher than 26 μ M, their relative sulfoxides have IC₅₀ values in the low micromolar range. Unfortunately, a concomitant raise of the toxicity toward human cells was observed. Thus, pyridyl-substituted sulfoxides showed toxicity around 10 μ M (Table III.17, entries 1 and 2). However, this toxicity is far more limited compared to the original DAA and the selectivity index is about 60. Interestingly, products **79** and **80** were the firsts metabolites that show a good potency toward both *Trypanosoma* and *Leishmania* parasites while having an acceptable selectivity index. Similarly, sulfoxides bearing the anisyl substituent were significantly more active than their relative sulfides (Table III.17, entries 3 to 5). However, the toxicity of the oxidized form was slightly higher than the parent DAA, resulting in a little decrease of the selectivity index.

On a stereochemical point of view, it is interesting to notice that the two separated *cis*-sulfoxides **78** and **77** behaved differently. Indeed, although **77** was completely inactive against both *T. cruzi* and *L. infantum*, its diastereoisomer counterpart **78** showed moderate potency against these two parasites. Furthermore, the toxicity of sulfoxide **78** was higher than the one of **77**. These results tend to prove that the sulfoxide stereochemistry might affect the biological activities. However, as the exact configuration of both sulfoxides is unknown, and considering the fact that we had only one example illustrating such an effect, it is difficult to conclude on this observation.

Table III.17 | *In vitro* antiparasitic activities of sulfoxide derivatives.

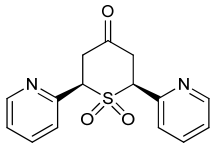
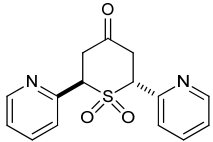
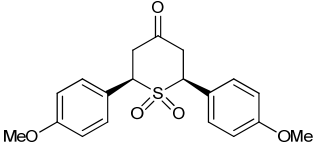
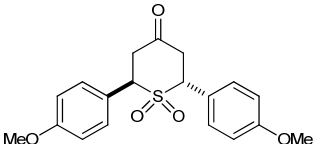
Entry	Compound	<i>In vitro</i> assays – IC ₅₀ (μM)				Tox.
		<i>hMRC-5</i>	<i>T. cruzi</i>	<i>T. brucei</i>	<i>L. infantum</i>	
1	 <p>80^a</p>	8.06 (≥ 64) (1.91)	0.54 (≥ 64) (0.29)	0.13 (29.6) (0.03)	2.03 (≥ 64) (0.38)	T3
2	 <p>79</p>	8.00 (≥ 64) (1.91)	0.80 (≥ 64) (0.29)	0.13 (26.10) (0.03)	2.03 (≥ 64) (0.38)	T3
3	 <p>76</p>	32.22 (≥ 64) (≥ 64)	8.86 (≥ 64) (10.7)	3.14 (≥ 64) (1.24)	≥ 64 (≥ 64) (≥ 64)	
4	 <p>78</p>	32.00 (≥ 64) (≥ 64)	8.51 (≥ 64) (10.7)	2.39 (≥ 64) (1.24)	27.27 (≥ 64) (≥ 64)	T1
5	 <p>77</p>	≥ 64 (≥ 64) (≥ 64)	≥ 64 (≥ 64) (10.7)	2.35 (≥ 64) (1.24)	≥ 64 (≥ 64) (≥ 64)	

^a Diastereoisomeric mixture.

Sulfone derivatives

Results obtained in the series of sulfone derivatives were very similar to the ones that had been observed with sulfoxide derivatives (Table III.18). 2-Pyridyl-substituted sulfones **83** and **82** had IC_{50} values in the high nanomolar range toward *Trypanosoma* whereas they showed excellent potency against *L. infantum* (Table III.18, entries 1 and 2). As in the sulfoxide series, toxicity was about five times lower compared to the parent DAA. Anisyl-substituted sulfones were less potent than their sulfoxide counterparts, product **81** being even almost inactive (Table III.18, entries 3 and 4). However, we were surprised by the high insolubility of anisyl-substituted sulfones, which, contrary to their sulfoxide equivalents, were insoluble in almost all types of solvent, even at very low concentration. As we previously mentioned, the solubility of compounds can significantly influence the results of biological assays. Consequently, the insolubility of compounds **73** and **81** might be one explanation for the higher IC_{50} values that were measured.

Table III.18 | *In vitro* antiparasitic activities of sulfone derivatives.

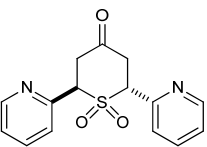
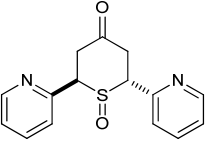
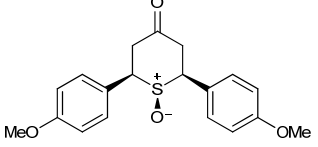
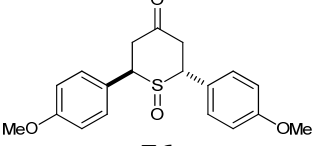
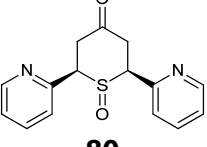
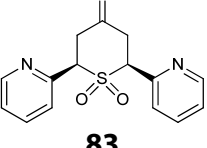
Entry	Compound	<i>In vitro</i> assays – IC_{50} (μ M)				Tox.
		<i>hMRC-5</i>	<i>T. cruzi</i>	<i>T. brucei</i>	<i>L. infantum</i>	
1	 83	7.47 (≥ 64) (1.91)	0.41 (≥ 64) (0.29)	0.13 (29.6) (0.03)	2.03 (≥ 64) (0.38)	T3
2	 82	7.89 (≥ 64) (1.91)	0.42 (≥ 64) (0.29)	0.51 (26.10) (0.03)	2.03 (≥ 64) (0.38)	T3
3	 73^a	≥ 64 (≥ 64) (≥ 64)	34.38 (≥ 64) (10.7)	2.14 (≥ 64) (1.24)	20.32 (≥ 64) (≥ 64)	T1
4	 81^a	≥ 64 (≥ 64) (≥ 64)	≥ 64 (≥ 64) (10.7)	43.29 (≥ 64) (1.24)	≥ 64 (≥ 64) (≥ 64)	

^a Solubility issues.

Antileishmanial activities

All the S-oxides and their relative sulfide were evaluated by Prof. Loiseau toward two stages of *L. donovani* LV9, the promastigote stage and the intra-macrophage amastigote stage. Six S-oxides showed interesting activities and are populated in Table III.19. The three remaining S-oxides were completely inactive ($IC_{50} \geq 100 \mu\text{M}$) and were therefore omitted.

Table III.19 | *In vitro* antileishmanial activities.

Entry	Compound	<i>In vitro</i> assays – <i>L. donovani</i> – IC_{50} (μM)			
		<i>hMRC-5</i>	<i>Promastigotes</i>	<i>Amastigotes</i>	Tox.
1	 82	7.89 (≥ 64) (1.91)	1.2 \pm 0.2 (≥ 100) (0.14)	5.0 \pm 1.5	T3
2	 79	8.00 (≥ 64) (1.91)	2.7 \pm 0.1 (≥ 100) (0.14)	20.5 \pm 2.1	T3
3	 78	32.00 (≥ 64) (≥ 64)	31.5 \pm 9.4 (≥ 100) (74.30)	35.0 \pm 6.5	T1
4	 76	32.22 (≥ 64) (≥ 64)	≥ 100 (≥ 100) (74.30)	50.2 \pm 1.2	
5	 80	8.06 (≥ 64) (1.91)	2.5 \pm 0.1 (≥ 100) (0.14)	50.1 \pm 5.2	T3
6	 83	7.47 (≥ 64) (1.91)	1.6 \pm 0.1 (≥ 100) (0.14)	50.2 \pm 5.0	T3

Besides product **82**, the most active compounds were the sulfoxides derivatives (Table III.19, entries 2-5). Once again, 2-pyridyl-substituted products were more potent than anisyl derivatives (Table III.19, entries 3 and 4). With regard to their relative sulfides, all the tested S-oxides have a higher activity, the oxidation of the sulfur allowing the potency to be restored at a similar level as the parent DAA.

Generally speaking, S-oxides are more active toward promastigotes (except product **76**). However, they are also active against intra-macrophage amastigotes which tends to demonstrate that these products are able to penetrate the macrophage to kill parasites. Considering that most of the S-oxides turned out to be toxic against mouse macrophages, another explanation would be that these compounds are damaging the whole macrophage and consequently *Leishmania* which are parasitizing these cells. Determining whether these compounds are active by direct interaction with the parasite or by destruction of the host cells will need further investigation, and particularly the test of new S-oxides based on the most active and less toxic substitution patterns recently highlighted in the sulfide series.

Discussion

We previously demonstrated that the DAA series was not a promising series for lead development, mainly due to the dramatic toxicity that is likely to be intrinsic to the structure of these molecules. The prodrug strategy was intended to cope with these issues. Here we will discuss the biological results and see whether this strategy fulfilled its promises or not.

As the library of prodrugs was even smaller than the library of DAA, establishing a precise correlation between molecular descriptors and the antiparasitic activity is not possible. Consequently, in the following sections, we will only give some general trends resulting from the comparison of the activity with several criteria including the toxicity, the stereochemical configuration and the degree of oxidation of the sulfur atom. In addition, with respect to the few prodrugs that are potent toward *Leishmania* spp., the activity toward *Trypanosoma* parasites will be the only one to be considered in the discussion (preliminary discussion on the antileishmanial activities has been previously given, *vide supra*).

Dissociation of the toxicity from the activity

As we previously mentioned, the toxicity was the major concern in the DAA series. The most potent DAA were also the most toxic ones and we have observed that dissociating the toxicity from the activity would be a very difficult task on this series. As their reactive electrophilic centers are deactivated, 2,6-diaryl-4H-tetrahydrothiopyran-4-ones and their relative S-oxide are expected to be less toxic. To check this hypothesis, the graph of $pCC_{50}(hMRC-5)$ as a function of $pIC_{50}(\text{parasites})$ was plotted (Figure III.30).

At first glance, we can notice that most of the compounds are located below the first bisector. Therefore, their activity against parasites is more important than their toxicity toward human cells. Furthermore, considering the potency toward *T. brucei* (Figure III.30, blue diamonds), we can see that most of the compounds are far from the first bisector, which means that a good selectivity is achieved. Regarding the activity toward *T. cruzi* (Figure III.30, orange circles), mixed results were obtained as few compounds show a very good potency without toxicity. Unfortunately, we can see that no compound is located in the targeted area. Despite this later point, the prodrug strategy might be considered promising as the overall toxicity is lowered in this series. In order to get a better comprehension of this series, we will now study in detail the effects of the stereochemical configuration and of the oxidation of the sulfur atom.

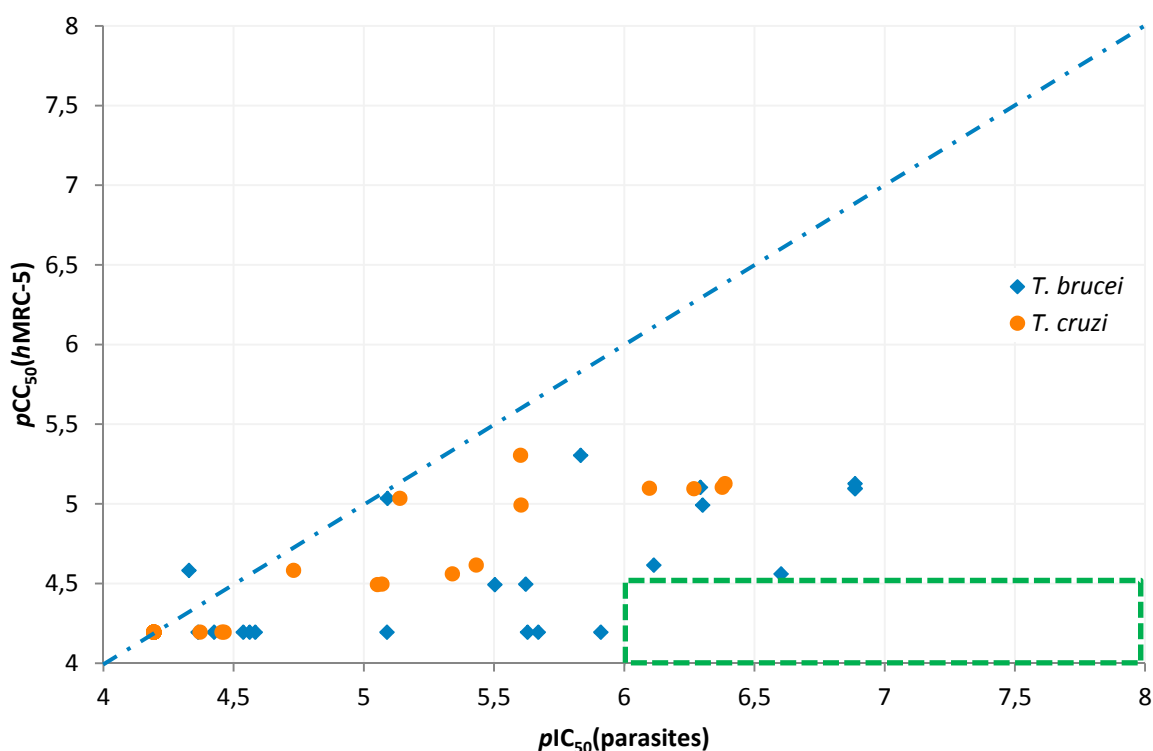


Figure III.30 | Antiparasitic activities versus toxicity plot of the whole 2,6-diaryl-4H-tetrahydrothiopyran-4-one series, including the S-oxides.

Effects of the stereochemical configuration

In the chemistry-related section, we described our efforts to develop novel diastereoselective synthesis of 2,6-diaryl-4H-tetrahydrothiopyran-4-ones. This effort was motivated by the fact that stereochemistry is known to significantly influence the biological activities and therefore it would have been impossible to deconvolve the results obtained from diastereoisomeric mixtures.¹⁸⁹ However, further to the biological results it would be interesting to find out if the configuration of the prodrug heterocycle really affects the antiparasitic activity.

To answer this question, we will analyze the results on a complete homogenous series (sulfides and S-oxides). As the anisyl substitution did not show interesting activities, we chose the 2-pyridyl series for this work (Table III.20). Considering each pair of diastereoisomers, variations were very limited and did not exceed 10 % of the activity, which can be considered in the error range of such *in vitro* measurements. Consequently, we can conclude that there is no difference in the IC₅₀ values between diastereoisomers, neither for the sulfides nor for the S-oxides.

Several hypotheses can be suggested to explain the experimental results. The most obvious one is that the activity does not depend on recognition mechanism, or at least on stereochemical sensitive ones. Another possibility would be that the *cis* and the (\pm)-*trans* isomers might have a similar reactivity in biological medium, resulting in similar activities. Finally, we can hypothesize that, in biological medium, the (\pm)-*trans* isomer might be quickly isomerized into the thermodynamically more stable *cis* isomer, which will obviously result in the same activity for the two diastereoisomers. This later hypothesis is supported by the fact that we observed the isomerization of the (\pm)-*trans* into the *cis* diastereoisomer in organic conditions (*vide supra*) but also in biomimetic conditions (100 μ M of product in an aqueous PBS buffer at pH 7.4 for 24 h at 37 °C). Determining which of these three hypotheses is the most plausible will require new experiments and mechanistic studies to determine if an active transport is occurring during the uptake on compounds and to explore the pharmacokinetic of these series both in mammals (*e.g.* metabolic studies over liver microsomes) and in parasites. Even if it is questionable to conclude on one unique series, we decided to focus our attention on the (\pm)-*trans* isomers for primary assays that we just described; in the future, the *cis* isomer will probably be synthesized and tested in a second time and only with the most promising substitution patterns.

Table III.20 | Comparison of the *in vitro* antiparasitic activities depending on the configuration of the heterocycle.

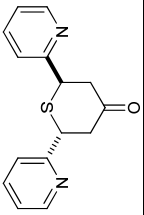
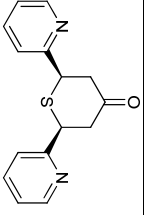
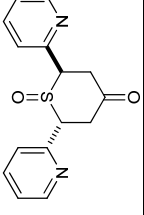
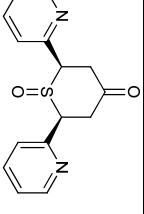
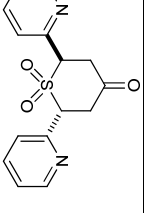
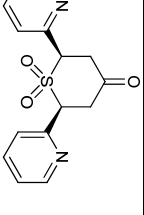
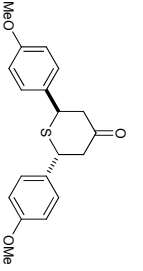
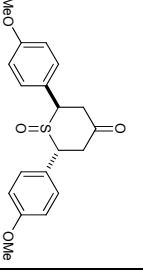
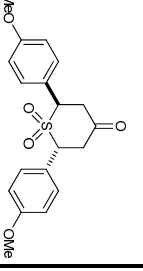
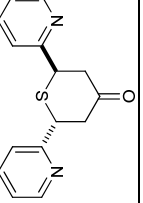
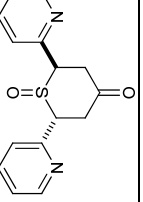
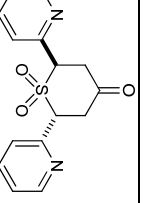
IC ₅₀ (μM)						
57	63	79	80	82	83	
hMRC-5	≥ 64	≥ 64	8.00	8.06	7.89	7.47
<i>T. cruzi</i>	≥ 64	≥ 64	0.80	0.54	0.42	0.41
<i>T. brucei</i>	26.10	29.06	0.13	0.13	0.51	0.13

Table III.21 | Comparison of the *in vitro* antiparasitic activities depending on the sulfur oxidation degree.

IC ₅₀ (μM)						
50	76	81	57	79	82	
hMRC-5	≥ 64	32.22 ^a	≥ 64 ^a	≥ 64	8.00	7.89
<i>T. cruzi</i>	≥ 64	8.86 ^a	≥ 64 ^a	≥ 64	0.80	0.42
<i>T. brucei</i>	≥ 64	3.14 ^a	43.29 ^a	26.10	0.13	0.51

^a Solubility issues

Effects of sulfur oxidation

Due to their reactivity that can result in the regeneration of double bonds through β -elimination, S-oxides were highlighted in the prodrug strategy as putative metabolites. To assess the real impact of the degree of sulfur oxidation, these products were also screened in biological assays. We have already mentioned that the reactivity of sulfur in β -elimination is higher when the sulfur is oxidized. Therefore, we would expect a similar behavior for the antiparasitic activity.

To analyze the real impact on the antiparasitic activity of the sulfur oxidation, we will compare the antiparasitic activities of sulfide, sulfoxide and sulfone in two homogenous chemical series, namely the anisyl and 2-pyridyl series (Table III.21). Unlike the stereochemical configuration, we can note that the degree of sulfur oxidation significantly affects the antiparasitic activity. Indeed, on both series the oxidation of sulfide to sulfoxide clearly restored the antiparasitic activity that was abolished by the heterocyclic-sulfide formation. In the same way, the over-oxidation of sulfide **57** to sulfone **82** resulted in an enhanced activity toward both *T. cruzi* and *T. brucei*. We already mentioned the fact that this was not the case with sulfone **81** which was completely inactive, probably due to solubility issues. Regarding the toxicity, all the S-oxides are more toxic than their parent sulfides. However, this increased toxicity is not such an issue as it is less important than the gain in activity. In addition, it is now well defined that the 2-pyridyl series showed unacceptable toxicity issues. Hence, the same oxidative strategy on more selective substitution patterns (e.g. *p*-benzotrile, *p*-toluyl or *p*-trifluoromethylphenyl) should result in very good activity with even more limited toxicity.

To summarize, it is obvious that the oxidation of the sulfur atom significantly improved the activity toward parasites. The observed residual toxicity issues are expected to be solved by the use of more selective substitution patterns that we recently highlighted. According to these preliminary results, sulfoxide derivatives are all the more promising as they are much more soluble than their relative sulfides, parent DAA or even their sulfone counterparts. However, these observations on the effect of the oxidation have to be confirmed with several new substitution patterns to be generalized.

Conclusion

In spite of their potent antiparasitic activities, diarylideneacetones suffered from a recurrent toxicity issue which seems to be intrinsically linked to the structure of this series. As the highly reactive enone system was supposed to be responsible from this host toxicity, we intended to synthesize diarylideneacetone prodrugs. To achieve this goal, we designed a new structure where the enone system is temporary masked in a heterocyclic structure. Being able to regenerate double bonds of diarylideneacetones through β -elimination, the 2,6-diaryl-4H-tetrahydrothiopyran-4-one scaffold was selected for this prodrug strategy. We also hypothesized that relative S-oxides derivatives might also be putative active metabolites. We therefore intended the synthesis of these different structures. As two asymmetric carbons are present in the structure, a particular care was paid to the diastereoselectivity of the synthesis.

Unfortunately, only few procedures were reported in the literature and most of them suffer from a limited scope and a moderate diastereoselectivity. Furthermore, the use of toxic gaseous hydrogen sulfide was a major source of concern. Considering these numerous drawbacks, we designed and optimized new synthetic pathways for the diastereoselective synthesis of 2,6-diaryl-4H-tetrahydrothiopyran-4-ones. The establishment of reliable criteria for the unambiguous spectroscopic determination of the diastereoisomeric configuration was an important stage prior to the synthetic work. Further to the identification of key parameters liable to influence both the yield and the diastereoisomeric ratio, we followed an optimization process similar to the one used for the synthesis of dissymmetric diarylideneacetones. This approach resulted in the identification of three sets of conditions for the selective synthesis of the (\pm)-*trans* and the *cis* isomers. These optimized reactions conditions were applied to a wide panel of substitution patterns, with moderate to good diastereoisomeric excesses and good to excellent yields.

As for the synthesis of sulfide, the synthesis of the S-oxide derivatives was not extensively described in the literature. The few available procedures were using highly reactive oxidizing agents such as bromine or peracids. With the constant aim of developing mild reaction conditions that would be compatible with all the substitutions patterns required by the medicinal chemistry project, we developed new synthetic protocols. Sulfoxide derivatives were obtained through the use of Davis's oxaziridine which proved to be highly chemoselective. With regard to the diastereoselectivity of the *cis*-isomer oxidation, a moderate diastereoisomeric excess was achieved with the use of the oxaziridine. The exact configuration of the major isomer is still to be determined. Sulfone derivatives were synthesized by slow and mild oxidation of the sulfoxide with *m*-chloroperbenzoic acid.

In fine, the synthetic work performed on this new series allowed the selective synthesis of each diastereoisomer on demand, as summarized on Figure III.31. Further to the optimization work, each step was controlled and performed under mild conditions which are compatible with a wide panel of substitution patterns.

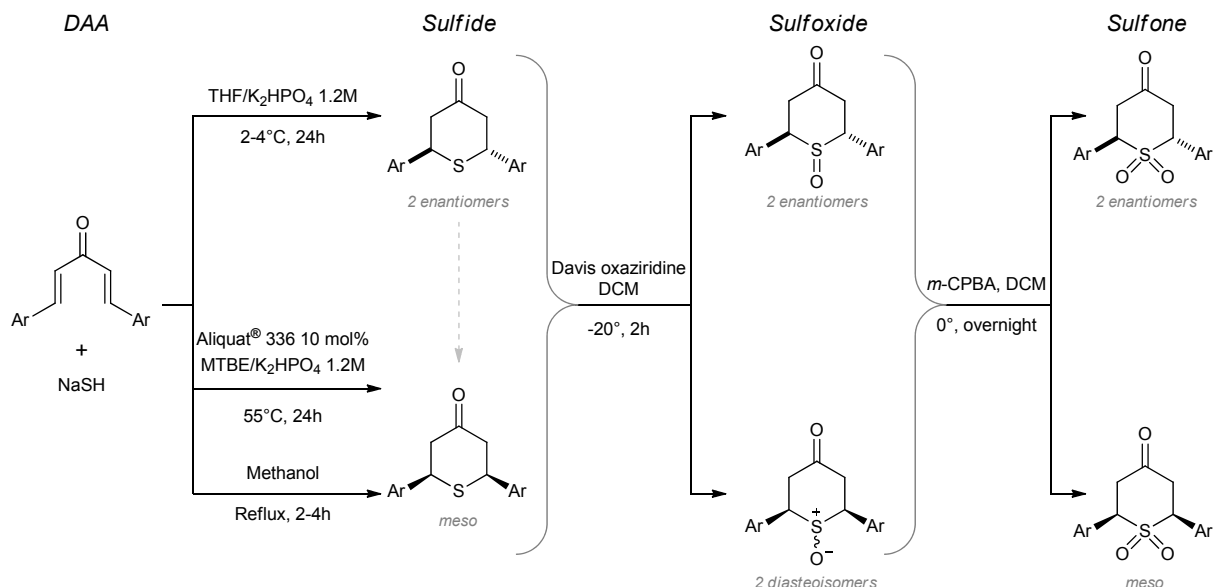


Figure III.31 | Synthetic platform of 2,6-diaryl-4H-tetrahydrothiopyran-4-one and their relative S-oxides

Both libraries of sulfides and S-oxides were evaluated for antiparasitic activities in biological assays against *Trypanosoma cruzi*, *Trypanosoma brucei brucei*, *Leishmania donovani* and *Leishmania infantum*. Generally speaking, most of the sulfides were not toxic toward human cells but only showed moderate or no activity against trypanosomatid parasites. Nevertheless, several substitution patterns were confirmed as promising scaffold: *p*-phenyl-, *p*-benzotrile-, *p*-trifluoromethylphenyl-, or *p*-toluyl- substituted 2,6-diaryl-4H-tetrahydrothiopyran-4-ones have interesting profiles. Interestingly, we noticed that the heterocycle configuration seemed to affect neither the antiparasitic activity nor the toxicity. Finally, as expected, we demonstrated that S-oxide putative metabolites showed an enhanced potency toward parasites while the toxicity toward human cell was limited.

To conclude, we can consider that the first objective of the prodrug strategy was achieved as the heterocycle formation resulted in an almost complete loss of the toxicity toward human cells. However, this decrease in the toxicity is counterbalanced by a concomitant reduction in the potency. Preliminary results obtained with the S-oxides series tend to prove that an oxidation of the sulfur atom is liable to allow a partial recovery of the activity. Nevertheless, these results have to be confirmed by further phenotypic assays and *in vivo* studies, especially with S-oxides substituted with the most active patterns.

General conclusion

"We have never had such a sophisticated arsenal of technologies for treating diseases, yet the gap in health outcomes keep getting wider. This is unacceptable". With these few words, Margaret Chan –former director-general of WHO– dramatically summarized the paradox of Neglected Tropical Diseases. In spite of significant advances in the understanding of parasitic diseases, the drug discovery pipeline in this domain remained almost dried for many years. The recent emergence of new partnerships was a promising sign of a slow but efficient pharmacological reengagement. As part of these efforts, the present PhD thesis aimed at discovering a new class of chemical agents showing potency against parasites responsible for human African trypanosomiasis, Chagas disease or leishmaniasis. To achieve this goal, we focused our attention on two different series, the diarylideneacetone core and the 2,6-diaryl-4H-tetrahydrothiopyran-4-one scaffold.

Further to the work initiated by Dr. Nicole Wenzel during her PhD thesis, we extended the diarylideneacetone series. Particular attention was paid to the standardization of protocols for the synthesis of symmetric entities. This work successfully allowed the scale-up and the generalization of the reactions conditions to a wide panel of substitution patterns. With the aim of investigating the effects of the electronic distribution, we also developed the synthesis of dissymmetric (hetero)diarylideneacetones. As the usual Claisen-Schmidt pathway proved to be troublesome in several cases, we designed and optimized a palladium-catalyzed coupling isomerization synthesis during a four-month collaboration at the University of Düsseldorf. This new methodology allowed the preparation of several dissymmetric heteroaromatic derivatives which were submitted for biological evaluation with the whole library of symmetric compounds. In spite of some promising substitution patterns, the assays demonstrated a recurrent toxicity issue in this series.

To address this issue, we considered the development of a new series of compounds which would act as prodrugs of diarylideneacetones. Being able to regenerate the enone system of diarylideneacetones through β -elimination, the 2,6-diaryl-4*H*-tetrahydrothiopyran-4-one scaffold was selected for this strategy. The dramatic lack of reliable, safe and selective published protocols led us to design and optimize novel diastereoselective methodologies which would be compatible with the large panel of substitution patterns. Once these conditions were successfully established, a full control of the whole series was achieved, each diastereoisomer being able to be synthesized on demand. A dozen of variously substituted sulfides, as well as two full series of *S*-oxide derivatives were submitted for biological assays. The preliminary results obtained with this small library were encouraging as a significant decrease of toxicity was achieved while the putative *S*-oxides metabolites proved to be potent antiparasitic agents.

In fine, this PhD work was an opportunity to develop and optimize new methodologies for the synthesis of specific structures required by our medicinal chemistry project. These efforts resulted in novel, robust, and general procedures which allowed the constitution of small libraries of compounds. Antiparasitic screenings of these libraries demonstrated three main points (i) dissociation of the toxicity from the activity is challenging in the diarylideneacetone series, (ii) cyclization in sulfide lowers both the toxicity and the activity (iii) oxidation of these sulfides in their putative *S*-oxide active metabolites enhances the potency with the toxicity kept limited. These results demonstrated the validity of the prodrug strategy rationale.

In the future, the reliable procedures that have been established during this PhD work will be applied to synthesize new derivatives, and thus to achieve a thorough structure-activity relationship. This should help to gain a better understanding of the mechanisms of action of this series which remain unidentified. Thus, the uptake route, the metabolic fate, the real active species, or the precise parasitic target will have to be investigated. Finding answers to each of these questions will be a long-term run which would finally conclude on the viability of the 2,6-diaryl-4*H*-tetrahydrothiopyran-4-one scaffold as lead structure.

Experimental section

Generality

Commercially available starting materials were purchased from Sigma-Aldrich, ABCR GmbH & Co. KG, Alfa Aesar, and Apollo Scientific and were used without further purification. Solvents were obtained from Sigma-Aldrich and Carlos Erba; unless noticed reagent grade was used for reactions and column of chromatography and analytical grade was used for recrystallizations. When specified, anhydrous solvents were required; dichloromethane (DCM) was distilled over CaH₂ under argon. Tetrahydrofuran (THF) was distilled over sodium/benzophenone under argon or dried by passage through an activated alumina column under argon. 1,4-Dioxane and dimethylformamide (DMF) were purchased anhydrous over molecular sieves from Sigma-Aldrich. Triethylamine (Et₃N), diisopropylethyl amine (DIPEA), pyrrolidine, piperidine were distilled over KOH under argon and stored over KOH.

All reactions were performed in standard glassware. Microwave reactions were carried out on two different apparatus (Biotage Initiator™ and CEM) with comparable results (cross compared); supplier standard microwave vials were used. Thin Layer Chromatography (TLC) were used to monitor reactions (*vide infra*).

Crude mixtures were purified either by recrystallization or by flash column of chromatography. The latter were performed using silica gel 60 (230-400 mesh, 0.040-0.063 mm) purchased from E. Merck. Automatic flash chromatographies were carried out in a Biotage Puriflash apparatus with UV-Vis detection at 254 nm (unless otherwise specified).

Monitoring and primary characterization of products were achieved by Thin Layer Chromatography on aluminum sheets coated with silica gel 60 F254 purchased from E. Merck. Eluted TLC's were revealed under UV (325 nm and 254 nm) and with chemicals (*vide infra*).

High Pressure Liquid Chromatography (HPLC) experiments were performed on a Hewlett Packard HPLC with dual UV-Vis detection (254 nm and 325 nm) or on a Hitachi HPLC (detection at 254 nm). A standard Nucleosil silica column was used on the first apparatus while a Nucleodur® C18 was used on the Hitachi apparatus.

Nuclear Magnetic Resonance (NMR) spectra were recorded on a Bruker AC 300, Bruker AC 400 or Avance DRX500 with solvent peaks as reference. Carbon multiplicities were assigned by Distortionless Enhancement by Polarization Transfer (DEPT) experiments. ¹H and ¹³C signals were assigned by correlation spectroscopy (COSY), Heteronuclear Single Quantum Correlation (HSQC), and Heteronuclear Multiple-Bond Correlation spectroscopy (HMBC). In the following NMR assignments, coupling constants (*J*) will be expressed in Hertz (Hz), multiplicity are described with (s) as singlet, (d) as doublet, (t) as triplet and (q) as quadruplet, "b-" prefix means that the considered signal is broad. In addition, the following acronyms will be used: ³*J*_{trans}: ³*J* coupling constant between the two alkenyl protons of the enone; ³*J*_{1,3-TDA}: 1,3-*trans*-diaxial coupling constant between the axial H_X proton and the axial H_A proton of an ABX system; ³*J*_{cisAE}: *cis*-axial-equatorial coupling constant between the H_X proton (either in axial or in equatorial position) and the equatorial H_B proton of an ABX system; ArH: aromatic proton; H_{vin}: vinylic proton of an enone; C_q: quaternary carbon; CH₂: secondary carbon; Me: methyl group. When a carbon is attributed without any doubt to a tertiary aromatic carbon, this carbon is abbreviated to "Ar". Otherwise tertiary

carbon (aromatic or not) are abbreviated to "CH". Numbering on structures are not following the official IUPAC rules; these indications are only provided to make the reading of spectra easier.

Infrared (IR) spectra (cm^{-1}) were recorded neat on a Perkin-Elmer Spectrum One Spectrophotometer. UV-Vis spectra were recorded on a Varian Cary 50 spectrophotometer.

ESI-HRMS mass spectra were carried out on a Bruker MicroTOF spectrometer. LC-MS were performed on a ThermoFisher apparatus with ESI ionization. Elemental analysis were obtained from "Service commun d'analyses" from the University of Strasbourg. Melting points were measured on a Stuart Melting Point 10 apparatus and are given uncorrected; when measured after recrystallization, the solvent is mentioned between brackets.

In the following sections, solvents will be abbreviated as follows: DCM: dichloromethane; CyHex: Cyclohexane; EtOAc: Ethyl acetate; Tol.: toluene; Et₂O: diethyl ether; MTBE: methyl *tert*-butyl ether; THF: tetrahydrofurane.

A mixture of methanolic ammonia in dichloromethane was used for the elution and purification of highly polar compounds. This was prepared as follows: commercial solution of 7 M ammonia in methanol (14 mL) was dissolved in methanol (86 mL) and dichloromethane (900 mL). This resulted in a 10 % (1 M NH₃ in methanol) in dichloromethane solution which was next used for TLC and flash chromatography elution. This will be abbreviated as (1 M NH₃ in MeOH) in DCM.

TLC dips:

Mostaïne

Ammonium molybdate (5 g)
Ceric sulfate (0.05 g)
Sulfuric acid 10 vol% (100 mL)
Store in the dark

Phosphomolybdic acid (PMA)

Phosphomolybdic acid (12 g)
Ethanol (250 mL)

p-Anisaldehyde

p-Anisaldehyde (0.5 mL)
Conc. sulfuric acid (5 mL)
Methanol (85 mL)
Acetic acid (100 mL)
Store at 4 °C

2,4-Dinitrophenyl hydrazine (*2,4*-DNPH)

2,4-Dinitrophenyl hydrazine (12 g)
Conc. sulfuric acid (60 mL)
Water (80 mL)
Ethanol (200 mL)

Potassium permanganate (KMnO₄)

Potassium permanganate (1 g)
Potassium carbonate (7 g)
Sodium hydroxide 1M (2 mL)
Water (100 mL)

Dragendorff's reagent

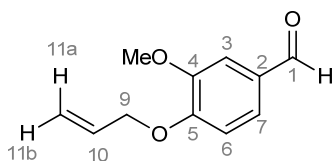
Basic bismuth nitrate (0.17 g)
Acetic acid (2 mL)
Water (8 mL)

Potassium iodide (4 g)
Acetic acid (10 mL)
Water (20 mL)

Both solutions are mixed and diluted to 100 mL of water. Store in the dark.

Synthesis of symmetric diarylideneacetones

Synthesis of precursor 4-(allyloxy)-3-methoxybenzaldehyde (**14**)



Colorless oil
 Chemical Formula: C₁₁H₁₂O₃
 Molecular Weight: 192.21 g.mol⁻¹
 Yield: ≥ 95%

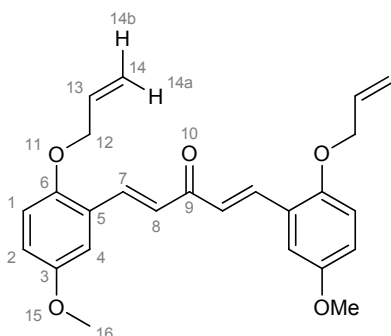
Vanillin (1 g, 6.57 mmol, 1.0 equiv.) and potassium carbonate (1.82 g, 13.14 mmol, 2.0 equiv.) were suspended in acetone (20 mL). To this well stirred suspension was added allyl bromide (685 μ L, 7.89 mmol, 1.2 equiv.) and the mixture was subsequently refluxed for five hours. The resulting crude mixture was filtered and washed with acetone (3 x 10 mL). The filtrate was evaporated under reduced pressure, and purified by flash chromatography (SiO₂, EtOAc/CyHex) to yield desired product **14** as a colorless oil (1.27 g, 6.57 mmol, quantitative).

¹H NMR (300 MHz, CDCl₃) δ (ppm): 9.85 (s, 1H, CHO), 7.43 (d, ³J = 8.7 Hz, 1H, H6 or H7), 7.41 (s, 1H, H3), 6.97 (d, ³J = 8.7 Hz, 1H, H7 or H6), 6.08 (ddt, ³J = 17.5 Hz, 10.5 Hz, 5.4 Hz, 1H, H10), 5.44 (dd, ³J_{trans} = 17.2 Hz, ²J = 1.5 Hz, 1H, H11a), 5.34 (dd, ³J_{cis} = 10.5 Hz, ²J = 1.5 Hz, 1H, H11b), 4.71 (dt, ³J = 5.4 Hz, ⁴J = 1.4 Hz, 2H, H9), 3.94 (s, 3H, OMe)

¹³C NMR (75.5 MHz, CDCl₃) δ (ppm): 190.9 (CHO), 153.5 (C5), 149.9 (C4), 132.2 (C10), 130.2 (C2), 126.6 (Ar), 118.8 (C11), 111.9 (Ar), 109.3 (Ar), 69.8 (C9), 56.0(OMe)

LC/MS (ESI): [M+H]⁺ m/z 193.4

TLC (SiO₂): 30% ethyl acetate in cyclohexane R_F = 0.4 Dark blue with Mostaïne

(1E,4E)-1,5-bis(2-(allyloxy)-5-methoxyphenyl)penta-1,4-dien-3-one (13)

Yellow powder

Chemical Formula: C₂₅H₂₆O₅Molecular Weight: 406.47 g.mol⁻¹

Yield: 81 %

Diarylideneacetone NW327.2 (653 mg, 2 mmol, 1.0 equiv.) and potassium carbonate (1.38 g, 10 mmol, 5.0 equiv.) were suspended in acetone (7 mL). To this well stirred suspension was added allyl bromide (435 μ L, 5 mmol, 2.5 equiv.) and the mixture was subsequently refluxed for one hour and half. The reaction was next allowed to cool at room temperature and the crude was filtered over a pad of Celite and washed with acetone (3 x 10 mL). The filtrate was evaporated under reduced pressure, and purified by flash chromatography (SiO₂, EtOAc/CyHex) to yield desired product **13** as a yellow powder (655 mg, 1.6 mmol, 81 %).

¹H NMR (300 MHz, CDCl₃) δ (ppm): 8.06 (d, ³J_{trans} = 16.1 Hz, 2H, H7), 7.89 (m, 4H, H1-H2), 7.17 (d, ³J_{trans} = 16.1 Hz, 2H, H8), 7.15 (s, 2H, H4), 6.09 (ddt, ³J_{H13-H14a} = 17.3 Hz, ³J_{H13-H14b} = 10.5 Hz, ³J_{H13-H12} = 5.2 Hz, 2H, H13), 5.43 (dq, ³J_{H13-H14a} = 17.3 Hz, J = 1.6 Hz, 2H, H14a), 5.30 (dq, ³J_{H13-H14b} = 10.5 Hz, J = 1.6 Hz, 2H, H14b), 4.59 (dt, J = 5.3 Hz, 1.6 Hz, 4H, H12), 3.81 (s, 6H, OMe)

¹³C NMR (75.5 MHz, CDCl₃) δ (ppm): 189.9 (CHO), 153.7 (C6 or C3), 152.1 (C6 or C3), 138.1 (CH), 133.2 (CH), 126.4 (CH), 125.0 (C5), 117.7 (C14), 117.3 (CH), 114.3 (CH), 113.1 (CH), 70.1 (C12), 55.8 (C16)

LC/MS (ESI): [M+H]⁺ m/z 407.4

Elemental analysis: Calcd. C 73.87 H 6.45

Found C 73.98 H 6.43

m.p. = 83°C

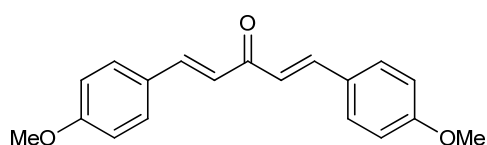
TLC (SiO₂): 40 % ethyl acetate in cyclohexane

R_F = 0.52

Yellow with Mostaine

General procedure A for the synthesis of symmetric diarylideneacetones

Ethanol, aqueous sodium hydroxide (3M, 4.0 equiv.) and acetone (1.0 equiv.) were introduced in a round-bottomed flask (molarity = 0.4 mol.L⁻¹). To this was added dropwise (≈ 2.5 mmol.min⁻¹) the aldehyde starting material (2.0 equiv.). The reaction mixture was stirred at room temperature until total consumption of the starting material (TLC). The resulting precipitate was filtered off on a Büchner apparatus, thoroughly washed with a 3:1 cold mixture of ethanol in water, and dried under high vacuum. The desired product was then recrystallized in boiling ethanol or in a mixture of solvent.

(1E,4E)-1,5-bis(4-methoxyphenyl)penta-1,4-dien-3-one (1)

Yellow needles

Chemical Formula: C₁₉H₁₈O₃Molecular Weight: 294.34 g.mol⁻¹

Yield: 85 %

Commercially available *p*-anisaldehyde (11.44 g, 84 mmol) was used as the starting material and treated according to general procedure A. Recrystallization in ethanol gave desired product **1** as yellow crystals (10.6 g, 36 mmol, 85 %).

¹H NMR (300 MHz, CDCl₃) δ (ppm): 7.70 (d, ³J_{trans} = 15.9 Hz, 2H, H_{vin}), 7.57 (d, ³J = 8.7 Hz, 4H, ArH), 6.95 (d, ³J_{trans} = 15.9 Hz, 2H, H_{vin}), 6.93 (d, ³J = 8.7 Hz, 4H, ArH), 3.86 (s, 6H, OMe)

¹³C NMR (75.5 MHz, CDCl₃) δ (ppm): 188.4 (C=O), 160.9 (C_q), 142.4 (CH), 129.9 (Ar), 127.6 (C_q), 123.5 (CH), 114.4 (Ar), 55.3 (OMe)

Elemental analysis: Calcd. C 77.53 H 6.16

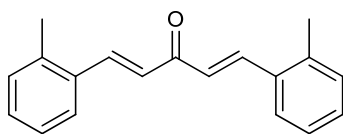
Found C 77.45 H 6.16

m.p. = 127 °C (EtOH)

TLC (SiO₂): 10 % ethyl acetate in toluene

R_F = 0.3

Yellow with Mostaine

(1E,4E)-1,5-di-*o*-tolylpenta-1,4-dien-3-one (2)

Yellow crystals

Chemical Formula: C₁₉H₁₈OMolecular Weight: 262.35 g.mol⁻¹

Yield: 82 %

Commercially available *o*-tolualdehyde (11.65 g, 97 mmol) was used as the starting material and treated according to general procedure A. Recrystallization in ethanol gave desired product **2** as yellow crystals (10.4 g, 40 mmol, 82 %).

¹H NMR (300 MHz, CDCl₃) δ (ppm): 7.8 (d, ³J_{trans} = 15.8 Hz, 2H, H_{vin}), 7.41 (d, ³J = 7.7 Hz, 2H, ArH), 6.9-7.1 (m, 6H), 6.7 (d, ³J_{trans} = 15.8 Hz, 2H, H_{vin}), 2.24 (s, 6H, Me)

¹³C NMR (75.5 MHz, CDCl₃) δ (ppm): 188.8 (C=O), 140.9 (CH), 138.2 (C_q), 133.8 (C_q), 130.9 (CH), 130.2 (Ar), 126.7 (Ar), 126.4 (Ar), 126.3 (Ar), 19.8 (Me)

HRMS (ESI+): [M+Na]⁺ Calcd. m/z 285.125

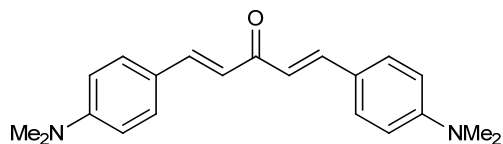
Found m/z 285.122

m.p. = 101 °C (EtOH)

TLC (SiO₂): 10 % ethyl acetate in toluene

R_F = 0.64

Orange with Mostaïne

(1E,4E)-1,5-bis(4-(dimethylamino)phenyl)penta-1,4-dien-3-one (3)

Red powder

Chemical Formula: C₂₁H₂₄N₂OMolecular Weight: 320.43 g.mol⁻¹

Yield: 57 %

Commercially available 4-(dimethylamino)benzaldehyde (6.61 g, 43 mmol) was used as the starting material and treated according to general procedure A. Recrystallization in ethanol and water gave desired product **3** as a red powder (3.92 g, 12.2 mmol, 57 %).

¹H NMR (300 MHz, CDCl₃) δ (ppm): 7.71 (d, ³J_{trans} = 15.7 Hz, 2H, H_{vin}), 7.53 (d, ³J = 8.8 Hz, 4H, ArH), 6.91 (d, ³J_{trans} = 15.7 Hz, 2H, H_{vin}), 6.70 (d, ³J = 8.8 Hz, 4H, ArH), 3.04 (s, 12H, Me)

¹³C NMR (75.5 MHz, CDCl₃) δ (ppm): 188.9 (C=O), 151.7 (C_q), 142.9 (CH), 129.9 (Ar), 122.8 (C_q), 121.2 (CH), 111.7 (Ar), 40.2 (Me)

HRMS (ESI+): [M+Na]⁺ Calcd. m/z 343.179

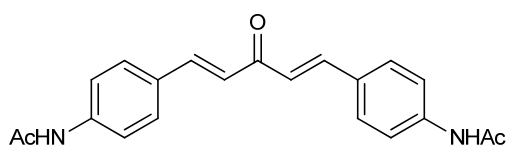
Found m/z 343.177

m.p. = 190°C (EtOH/H₂O)

TLC (SiO₂): 30 % ethyl acetate in cyclohexane

R_F = 0.2

Orange with Dragendorff

***N,N'*-(((1*E*,4*E*)-3-oxopenta-1,4-diene-1,5-diyl)bis(4,1-phenylene))diacetamide (4)**

Yellow powder

Chemical Formula: C₂₁H₂₀N₂O₃Molecular Weight: 348.40 g.mol⁻¹

Yield: 80 %

Commercially available 4-acetamidobenzaldehyde (17.71 g, 109 mmol) was used as the starting material and treated according to general procedure A. Trituration in diethyl ether gave desired product **4** as a yellow powder (15.21 g, 44 mmol, 80 %).

¹H NMR (300 MHz, DMSO-*d*₆) δ (ppm): 10.25 (bs, 2H, NH), 7.70 (m, 10H), 7.21 (d, ³J_{trans} = 16 Hz, 2H, H_{vin}), 2.07 (s, 6H, Me)

¹³C NMR (75.5 MHz, DMSO-*d*₆) δ (ppm): 118.1 (C=O), 168.6 (C_q), 142.1 (C_q), 141.4 (CH), 129.4 (Ar), 124.1 (CH), 118.9 (Ar), 24.1 (Me)

HRMS (ESI+): [M+Na]⁺ Calcd. m/z 371.137

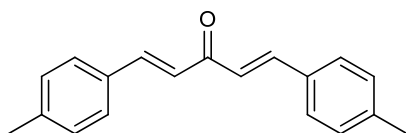
Found m/z 371.132

m.p. = 254 °C

TLC (SiO₂): ethyl acetate

R_F = 0.40

Brown with Mostaïne

(1*E*,4*E*)-1,5-di-*p*-tolylpenta-1,4-dien-3-one (5)

Yellow crystals

Chemical Formula: C₁₉H₁₈OMolecular Weight: 262.35 g.mol⁻¹

Yield: 63 %

Commercially available *p*-tolualdehyde (11.65 g, 97 mmol) was used as the starting material and treated according to general procedure A. Recrystallization in a mixture of ethyl acetate and cyclohexane gave desired product **5** as yellow crystals (8.04 g, 44 mmol, 63 %).

¹H NMR (300 MHz, CDCl₃) δ (ppm): 7.73 (d, ³J_{trans} = 15.9 Hz, 2H, H_{vin}), 7.43 (d, ³J = 8.1 Hz, 4H, ArH), 7.23 (d, ³J = 8.1 Hz, 4H, ArH), 7.05 (d, ³J_{trans} = 15.9 Hz, 2H, H_{vin}), 2.40 (s, 6H, Me)

¹³C NMR (75.5 MHz, CDCl₃) δ (ppm): 189.11 (C=O), 143.1 (CH), 141.0 (C_q), 132.1 (C_q), 129.7 (CH), 128.4 (CH), 124.6 (Ar), 21.5 (Me)

HRMS (ESI+): [M+Na]⁺ Calcd. m/z 285.125

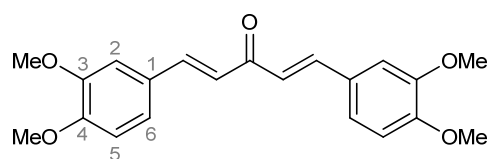
Found m/z 285.125

m.p. = 180 °C (EtOAc/CyHex)

TLC (SiO₂): 10 % ethyl acetate in toluene

R_F = 0.58

Yellow with Mostaïne

(1E,4E)-1,5-bis(3,4-dimethoxyphenyl)penta-1,4-dien-3-one (6)

Yellow-orange powder
 Chemical Formula: C₂₁H₂₂O₅
 Molecular Weight: 354.40 g.mol⁻¹
 Yield: 88 %

Commercially available 3,4-dimethoxybenzaldehyde (10.0 g, 60 mmol) was used as the starting material and treated according to general procedure A. Recrystallization in ethanol gave desired product **6** as a yellow-orange powder (9.40 g, 26.5 mmol, 88 %).

¹H NMR (300 MHz, CDCl₃) δ (ppm): 7.71 (d, ³J_{trans} = 15.8 Hz, 2H, H_{vin}), 7.22 (dd, ³J = 8.3 Hz, ⁴J = 1.9 Hz, 2H, H₆), 7.16 (d, ⁴J = 1.9 Hz, 2H, H₂), 6.97 (d, ³J_{trans} = 15.8 Hz, 2H, H_{vin}), 6.91 (d, ³J = 8.3 Hz, 2H, H₅), 3.96-3.95 (2s, 12H, OMe)

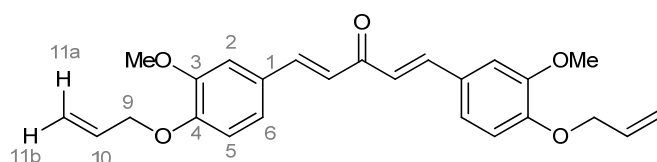
¹³C NMR (75.5 MHz, CDCl₃) δ (ppm): 188.7 (C=O), 151.3 (C1 or C2), 149.3 (C1 or C2), 143.1 (CH), 127.9 (C5), 123.6 (CH), 123.1 (CH), 111.1 (CH), 109.9 (CH), 56.0 (OMe), 55.9 (OMe)

LC/MS (ESI): [M+H]⁺ m/z 355.3

Elemental analysis: Calcd. C 69.90 H 5.56
 Found C 69.95 H 5.53

m.p. = 78°C (EtOH)

TLC (SiO₂): 50 % ethyl acetate in cyclohexane R_F = 0.34 Purple with Mostaïne

(1E,4E)-1,5-bis(4-(allyloxy)-3-methoxyphenyl)penta-1,4-dien-3-one (7)

Yellow sticky-solid
 Chemical Formula: C₂₅H₂₆O₅
 Molecular Weight: 406.47 g.mol⁻¹
 Yield: 31 %

Previously prepared allylated vanillin **14** (0.76 g, 4 mmol) was used as the starting material and treated according to general procedure A. Flash column of chromatography (SiO₂, Et₂O/CyHex) gave desired product **7** as a yellow sticky-solid (240 mg, 0.6 mmol, 31 %).

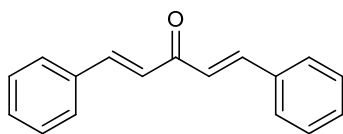
¹H NMR (300 MHz, CDCl₃) δ (ppm): 7.68 (d, ³J_{trans} = 15.9 Hz, 2H, H_{vin}), 7.15 (m, 4H, H₂-H₆), 6.95 (d, ³J_{trans} = 15.9 Hz, 2H, H_{vin}), 6.89 (d, ³J = 8.1 Hz, 2H, H₅), 6.08 (ddt, ³J_{trans} = 17.3 Hz, ³J_{cis} = 10.5 Hz, ³J = 5.4 Hz, 2H, H₁₀), 5.42 (dd, ³J_{trans} = 17.3 Hz, ⁴J = 1.3 Hz, 2H, H_{11a}), 5.42 (dd, ³J_{cis} = 10.5 Hz, ⁴J = 1.3 Hz, 2H, H_{11b}), 4.66 (d, ³J = 5.6 Hz, 4H, H₉), 3.94 (s, 6H, OMe)

¹³C NMR (75.5 MHz, CDCl₃) δ (ppm): 188.7 (C=O), 150.3 (C₄), 149.6 (C₃), 143.0 (CH), 132.7 (C₁₀), 128.1 (C₁), 123.7 (CH), 122.9 (CH), 118.4 (C₁₁), 112.9 (Ar), 110.4 (Ar), 69.8 (C₉), 56.0 (OMe)

LC/MS (ESI): [M+H]⁺ m/z 407.3

Elemental analysis: Calcd. C 73.87 H 6.45
 Found C 73.58 H 6.45

TLC (SiO₂): 70 % diethylether in cyclohexane R_F = 0.25 Brown with PMA

(1E,4E)-1,5-diphenylpenta-1,4-dien-3-one (8)

Yellow crystals

Chemical Formula: C₁₇H₁₄OMolecular Weight: 234.29 g.mol⁻¹

Yield: 85 %

Commercially available benzaldehyde (13.2 g, 125 mmol) was used as the starting material and treated according to general procedure A. Recrystallization in ethanol gave desired product **8** as yellow crystals (12.4 g, 53 mmol, 85 %).

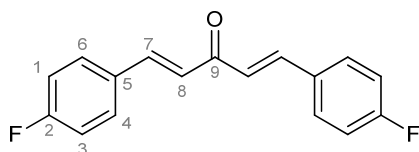
¹H NMR (300 MHz, CDCl₃) δ (ppm): 7.79 (d, ³J_{trans} = 15.9 Hz, 2H, H_{vin}), 7.67-7.65 (m, 4H, ArH), 7.46-7.44 (m, 6H, ArH), 7.12 (d, ³J_{trans} = 15.9 Hz, 2H, H_{vin})

¹³C NMR (75.5 MHz, CDCl₃) δ (ppm): 189.3 (C=O), 143.7 (CH), 135.2 (C_q), 130.9 (CH), 129.4 (CH), 128.8 (CH), 125.8 (CH)

Elemental analysis: Calcd. C 87.15 H 6.02

Found C 87.21 H 6.03

m.p. = 105 °C (EtOH)

(1E,4E)-1,5-bis(4-fluorophenyl)penta-1,4-dien-3-one (9)

Fine yellow powder

Chemical Formula: C₁₇H₁₂F₂OMolecular Weight: 270.27 g.mol⁻¹

Yield: 69 %

Commercially available 4-fluorobenzaldehyde (6.21 g, 50 mmol) was used as the starting material and treated according to general procedure A. Recrystallization in ethanol gave desired product **9** as a fine yellow powder (4.64 g, 17.1 mmol, 69 %).

¹H NMR (300 MHz, CDCl₃) δ (ppm): 7.72 (d, ³J_{trans} = 15.9 Hz, 2H, H7), 7.62 (m, 4H, H4-H6), 7.13 (m, 4H, H1-H3), 7.01 (d, ³J_{trans} = 15.9 Hz, 2H, H8)

¹³C NMR (75.5 MHz, CDCl₃) δ (ppm): 188.4 (C=O), 164.1 (d, ¹J_{C-F} = 253 Hz, C2), 142.1 (C8), 131.0 (d, ⁴J_{C-F} = 3.5 Hz, C5), 130.3 (d, ³J_{C-F} = 8.7 Hz, C4), 125.1 (d, ⁵J_{C-F} = 2.4 Hz, C7), 116.2 (d, ²J_{C-F} = 22.1 Hz, C1)

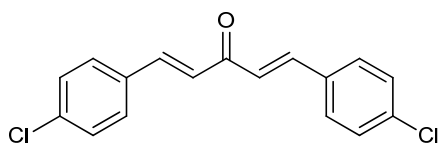
LC/MS (ESI): [M+H]⁺ m/z 271.3

m.p. = 153°C (EtOH)

TLC (SiO₂): 20 % ethyl acetate in cyclohexane

R_F = 0.47

Yellow with Mostaine

(1E,4E)-1,5-bis(4-chlorophenyl)penta-1,4-dien-3-one (10)

Yellow crystals

Chemical Formula: C₁₇H₁₂Cl₂OMolecular Weight: 303.18 g.mol⁻¹

Yield: 80 %

Commercially available 4-chlorobenzaldehyde (14.06 g, 100 mmol) was used as the starting material and treated according to general procedure A. Recrystallization in a mixture of ethyl acetate and *n*-hexane gave desired product **10** as yellow crystals (12.17 g, 40.1 mmol, 80 %).

¹H NMR (300 MHz, CDCl₃) δ (ppm): 7.70 (d, ³J_{trans} = 15.9 Hz, 2H, H_{vin}), 7.56 (d, ³J = 8.5 Hz, 4H, ArH), 7.41 (d, ³J = 8.5 Hz, 4H, ArH), 7.05 (d, ³J_{trans} = 15.9 Hz, 2H, H_{vin})

¹³C NMR (75.5 MHz, CDCl₃) δ (ppm): 188.3 (C=O), 142.1 (CH), 136.5 (C_q), 133.2 (C_q), 129.5 (Ar), 129.3 (Ar), 125.7 (CH)

HRMS (ESI+): [M+Na]⁺ Calcd. m/z 325.016

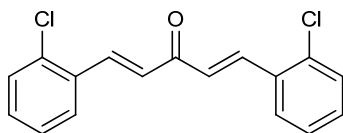
Found m/z 325.013

m.p. = 183 °C (EtOAc/*n*-hexane)

TLC (SiO₂): 20 % ethyl acetate in cyclohexane

R_F = 0.40

Yellow with Mostaïne

(1E,4E)-1,5-bis(2-chlorophenyl)penta-1,4-dien-3-one (11)

Yellow powder

Chemical Formula: C₁₇H₁₂Cl₂OMolecular Weight: 303.18 g.mol⁻¹

Yield: 38 %

Commercially available 2-chlorobenzaldehyde (14.06 g, 100 mmol) was used as the starting material and treated according to general procedure A. Recrystallization in a mixture of ethyl acetate and *n*-hexane gave desired product **11** as a yellow powder (5.77 g, 19 mmol, 38 %).

¹H NMR (300 MHz, CDCl₃) δ (ppm): 8.15 (d, ³J_{trans} = 16 Hz, 2H, H_{vin}), 7.74 (m, 2H, ArH), 7.48-7.32 (m, 6H, ArH), 7.09 (d, ³J_{trans} = 16 Hz, 2H, H_{vin})

¹³C NMR (75.5 MHz, CDCl₃) δ (ppm): 188.83 (C=O), 139.40 (CH), 135.43 (C_q), 133.06 (C_q), 131.23 (CH), 130.27 (Ar), 127.52 (Ar), 127.57 (Ar), 127.15 (Ar)

HRMS (ESI+): [M+Na]⁺ Calcd. m/z 325.016

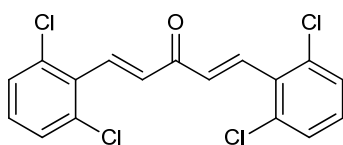
Found m/z 325.013

m.p. = 108 °C (EtOAc/*n*-hexane)

TLC (SiO₂): 20 % ethyl acetate in cyclohexane

R_F = 0.46

Blue with Mostaïne

(1E,4E)-1,5-bis(2,6-dichlorophenyl)penta-1,4-dien-3-one (12)

Fine yellowish powder

Chemical Formula: C₁₇H₁₀Cl₄OMolecular Weight: 372.07 g.mol⁻¹

Yield: 90 %

Commercially available 2,6-dichlorobenzaldehyde (10.45 g, 60 mmol) was used as the starting material and treated according to general procedure A. Recrystallization in a mixture of ethyle acetate and *n*-hexane gave desired product **12** as a fine yellowish powder (9.90 g, 26 mmol, 90 %).

¹H NMR (300 MHz, CDCl₃) δ (ppm): 7.84 (d, ³J_{trans} = 16.5 Hz, 2H, H_{vin}), 7.40 (d, ³J = 7.9 Hz, 4H, ArH in *ortho* to ArCl), 7.24 (d, ³J_{trans} = 16.5 Hz, 2H, H_{vin}), 7.23 (t, ³J = 7.9 Hz, 2H, ArH in *meta* to ArCl)

¹³C NMR (75.5 MHz, CDCl₃) δ (ppm): 188.8 (C=O), 137.3 (CH), 135.2 (C_q), 133.1 (Ar), 132.3 (C_q), 130.0 (CH), 128.9 (Ar)

HRMS (ESI+): [M+Na]⁺ Calcd. m/z 394.935

Found m/z 394.931

m.p. = 160 °C (EtOAc/*n*-hexane)

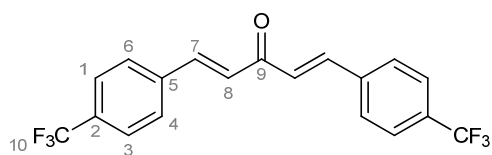
TLC (SiO₂): 20 % ethyl acetate in cyclohexane

R_F = 0.45

Blue with Mostaïne

General procedure B for the synthesis of symmetric diarylideneacetones

Potassium carbonate (2.5 equiv.) and acetone (1.0 equiv.) were introduced in a round-bottomed flask and dissolved in a 1:1 mixture of ethanol and water (molarity = 0.3 mol.L⁻¹). To this was added dropwise the aldehyde starting material (2.0 equiv.). The reaction mixture was stirred at room temperature until total consumption of the starting material (TLC). The resulting precipitate was filtered off on a Büchner apparatus, thoroughly washed with a 3:1 cold mixture of ethanol in water, and dried under high vacuum. The desired product was then recrystallized in boiling ethanol or in a mixture of solvent.

(1E,4E)-1,5-bis(4-(trifluoromethyl)phenyl)penta-1,4-dien-3-one (15)

Yellow powder

Chemical Formula: C₁₉H₁₂F₆OMolecular Weight: 370.29 g.mol⁻¹

Yield: 58 %

Commercially available 4-trifluoromethylbenzaldehyde (10.45 g, 60 mmol) was used as the starting material and treated according to general procedure B. Recrystallization in a mixture of ethyl acetate and cyclohexane gave desired product **15** as a yellow powder (6.39 g, 17.2 mmol, 58 %).

¹H NMR (300 MHz, CDCl₃) δ (ppm): 7.78 (d, ³J_{trans} = 15.9 Hz, 2H, H_{vin}), 7.72 (m, 8H, ArH), 7.16 (d, ³J_{trans} = 15.9 Hz, 2H, H_{vin})

¹³C NMR (75.5 MHz, CDCl₃) δ (ppm): 188.1 (C=O), 141.9 (C7), 138.0 (C5), 132.1 (q, ²J_{C-F} = 33.1 Hz, C2), 128.5 (C4-C6), 127.2 (C8), 126.0 (q, ³J_{C-F} = 3.9 Hz, C1-C3), 123.8 (q, ¹J_{C-F} = 273.4 Hz, C19)

Elemental analysis: Calcd. C 61.63 H 3.27

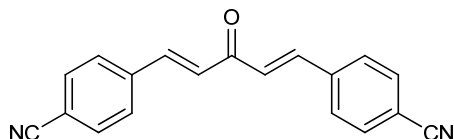
Found C 61.45 H 3.30

m.p. = 149 °C (EtOAc/CyHex)

TLC (SiO₂): 20 % ethyl acetate in cyclohexane

R_F = 0.45

Yellow with Mostaïne

4,4'-((1E,4E)-3-oxopenta-1,4-diene-1,5-diyl)dibenzonitrile (16)

Yellow powder

Chemical Formula: C₁₉H₁₂N₂OMolecular Weight: 284.31 g.mol⁻¹

Yield: 63 %

Commercially available 4-formylbenzonitrile (13.2 g, 100.0 mmol) was used as the starting material and treated according to general procedure B. Trituration in ethanol gave desired product **16** as a yellow powder (9.0 g, 31.6 mmol, 63 %).

¹H NMR (300 MHz, DMSO-*d*₆) δ (ppm): 7.96 (m, 8H, ArH), 7.86 (d, ³J_{trans} = 16.2 Hz, 2H, H_{vin}), 7.50 (d, ³J_{trans} = 16.2 Hz, 2H, H_{vin})

¹³C NMR (75.5 MHz, DMSO-*d*₆) δ (ppm): 188.45 (C=O), 141.20 (CH), 139.18 (C_q), 132.79 (Ar), 129.12 (Ar), 128.34 (CH), 118.56 (C_q), 112.31 (CN)

Elemental analysis: Calcd. C 80.27 H 4.25

Found C 80.15 H 4.30

m.p. = 137 °C

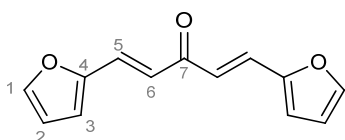
TLC (SiO₂): 10 % ethyl acetate in toluene

R_F = 0.26

Blue with Mostaïne

General procedure C for the synthesis of symmetric (hetero)diarylideneacetones

Aldehyde starting material (2.0 equiv.) and acetone (1.0 equiv.) were introduced in a round-bottomed flask and diluted in a 7:4 mixture of ethanol and water (molarity = 0.65 mol.L⁻¹). To this was added sodium hydroxide 3M (500 μ L, 0.04 equiv.). The reaction mixture was stirred at room temperature until total consumption of the starting material (TLC). The desired product was then purified as noticed.

(1E,4E)-1,5-di(furan-2-yl)penta-1,4-dien-3-one (24)

Orange solid at -20 °C

Chemical Formula: C₁₃H₁₀O₃

Molecular Weight: 214.22 g.mol⁻¹

Yield: 88 %

Commercially available furfural (9.93 g, 103 mmol) was used as the starting material and treated according to general procedure C. Crude mixture was extracted with chloroform (3 x 50 mL). The combined organic layers were washed with brine (2 x 30 mL), dried over MgSO₄ and evaporated to dryness. The residue was purified by flash chromatography (SiO₂, EtOAc/CyHex) to yield desired product **24** as an orange oil which solidified at -20 °C (9.79 g, 45.7 mmol, 88 %).

¹H NMR (300 MHz, CDCl₃) δ (ppm): 7.52 (d, ³J = 3.5 Hz, 2H, H1), 7.50 (d, ³J_{trans} = 15.7 Hz, 2H, H5), 6.92 (d, ³J_{trans} = 15.7 Hz, 2H, H6), 6.70 (d, ³J = 3.5 Hz, 2H, H3), 6.51 (dd, ³J = 3.5 Hz, 2H, H2)

¹³C NMR (75.5 MHz, CDCl₃) δ (ppm): 188.0 (C=O), 151.5 (C4), 144.8 (C5), 129.2 (C1), 123.2 (C6), 115.8 (C3), 112.6 (C2)

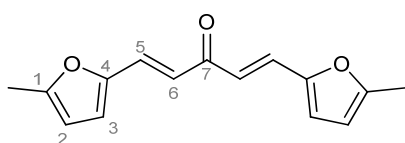
HRMS (ESI+): [M+Na]⁺ Calcd. m/z 237.052

Found m/z 237.049

TLC (SiO₂): 30 % ethyl acetate in cyclohexane

R_F = 0.37

Black with Mostaïne

(1E,4E)-1,5-bis(5-methylfuran-2-yl)penta-1,4-dien-3-one (25)

Orange solid

Chemical Formula: C₁₅H₁₄O₃

Molecular Weight: 242.27 g.mol⁻¹

Yield: 85 %

Commercially available 5-methyl-2-furaldehyde (2.75 g, 20.6 mmol) was used as the starting material and treated according to general procedure C. Crude mixture was extracted with chloroform (3 x 20 mL). The combined organic layers were washed with brine (2 x 15 mL), dried over MgSO₄ and evaporated to dryness. The residue was purified by flash chromatography (SiO₂, EtOAc/CyHex) to yield desired product **25** as an orange solid (2.11 g, 8.7 mmol, 85 %).

¹H NMR (300 MHz, CDCl₃) δ (ppm): 7.43 (d, ³J_{trans} = 15.5 Hz, 2H, H5), 6.85 (d, ³J_{trans} = 15.5 Hz, 2H, H6), 6.60 (d, ³J = 3.3 Hz, 2H, H2), 6.12 (bd, ³J = 3.3 Hz, 2H, H3), 2.38 (s, 6H, Me)

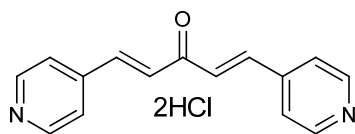
¹³C NMR (75.5 MHz, CDCl₃) δ (ppm): 188.1 (C=O), 155.7 (C_q), 150.3 (C_q), 129.0 (C5), 121.8 (C6), 117.6 (C2), 109.2 (C3), 13.9 (Me)

LC/MS (ESI): [M+H]⁺ m/z 243.3

TLC (SiO₂): 30 % ethyl acetate in cyclohexane

R_F = 0.56

Black with Mostaïne

(1E,4E)-1,5-di(pyridin-4-yl)penta-1,4-dien-3-one dihydrochloride salt (26)

Yellow cotton-like powder

Chemical Formula: C₁₅H₁₄Cl₂N₂OMolecular Weight: 309,19 g.mol⁻¹

Yield: 65 %

1,3-Acetonedicarboxylic acid (6.43 g, 44 mmol, 1.0 equiv.) was dissolved in ethanol (60 mL) in a round-bottomed flask. The solution was stirred at room temperature for fifteen minutes and 4-pyridinecarboxaldehyde (8.4 mL, 88 mmol, 2.0 equiv.) was added dropwise. The reaction was stirred at room temperature for two hours. Concentrated hydrochloric acid (30 mL) was subsequently added and the yellowish solution was heated at 80 °C for one hour. After being cooled at room temperature, the crude was filtered and the solid was thoroughly washed with acetone. This material was next recrystallized in boiling water; acetone was then added to initiate precipitation and to yield desired product **26** as a yellow cotton-like powder (8.85 g, 28.6 mmol, 65 %).

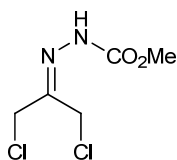
¹H NMR (300 MHz, D₂O) δ (ppm): 8.77 (d, ³J = 6.8 Hz, 4H, ArH in *ortho* to the nitrogen), 8.25 (d, ³J = 6.8 Hz, 4H, ArH in *meta* to the nitrogen), 7.85 (d, ³J_{trans} = 16.2 Hz, 2H, H_{vin}), 7.62 (d, ³J_{trans} = 16.2 Hz, 2H, H_{vin})

¹³C NMR (75 MHz, D₂O) δ (ppm): 191.5 (C=O), 153.1 (C_q), 142.6 (CH), 139.8 (CH), 134.8 (CH), 126.8 (CH)

Elemental analysis: Calcd. C 56.63 H 4.85

Found C 56.60 H 4.78

m.p. = 244 °C (H₂O/Acetone)

Methyl 2-(1,3-dichloropropan-2-ylidene)hydrazinecarboxylate (29)

White powder

Chemical Formula: C₅H₈Cl₂N₂O₂Molecular Weight: 199.04 g.mol⁻¹

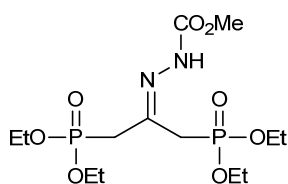
Yield: 71 %

1,3-Dichloroacetone (5.00 g, 39.4 mmol, 1.00 equiv.) was dissolved in ethanol (45 mL) and diethyl ether (4 mL). To this was added methyl hydrazinecarboxylate (3.72 g, 41.3 mmol, 1.05 equiv.) and the reaction was stirred at room temperature for three hours. Crude reaction mixture was filtered and washed with cold ethanol (2 x 10 mL). The resulting white powder was dried *in vacuo* to give desired product **29** as a white powder (5.55 g, 27.9 mmol, 71 %).

¹H NMR (200 MHz, CDCl₃) δ (ppm): 8.82 (bs, 1H, NH), 4.32 (s, 2H, CH₂), 4.24 (s, 2H, CH₂), 3.88 (s, 3H, Me)

¹³C NMR (75.5 MHz, CDCl₃) δ (ppm): 154.2 (C=O), 143.9 (C=N), 53.6 (OMe), 45.8 (CH₂), 33.3 (CH₂)

m.p. = 136 °C (Litt. 138 °C)

Methyl 2-(1,3-bis(diethoxyphosphoryl)propan-2-ylidene)hydrazinecarboxylate (30)

Light yellow oil

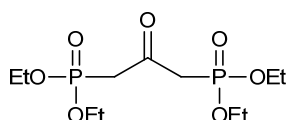
Chemical Formula: C₁₃H₂₈N₂O₈P₂Molecular Weight: 402.32 g.mol⁻¹

Yield: ≥ 95 %

Triethylphosphite (8.18 g, 49.2 mmol, 2.1 equiv.) was diluted in toluene (25 mL) in a three-necked round-bottomed flask. The solution was refluxed and protected dichloroacetone **29** (4.66 g, 23.4 mmol, 1.0 equiv.) was added dropwise over 10 min. After three hours under reflux, the reaction was allowed to cool at room temperature. Solvent was removed under reduced pressure and the residue was diluted in water (70 mL). The product was extracted with chloroform (3 x 40 mL), the combined organic layers were dried over MgSO₄ and evaporated under reduced pressure to give desired product **30** as a light yellow oil (9.4 g, 23.3 mmol, quantitative) which was used in the next step without further purification.

¹H NMR (200 MHz, CDCl₃) δ (ppm): 9.48 (bs, 1H, NH), 4.15 (m, 8H, P-OCH₂-), 3.8 (s, 3H, OMe), 3.16 (d, ²J_{H-P} = 24 Hz, 2H, -H₂C-P), 3.01 (d, ²J_{H-P} = 24 Hz, 2H, -H₂C-P), 1.34 (t, ³J = 7.1 Hz, 6H, P-OCH₂CH₃), 1.33 (t, ³J = 7.1 Hz, 6H, P-OCH₂CH₃)

¹³C NMR (75.5 MHz, CDCl₃) δ (ppm): 140.75 (dd, ²J_{C-P} = 10.5 Hz, ²J_{C-P} = 8.4 Hz, C=N), 63.1 (d, ²J_{C-P} = 6.8 Hz, P'-OC'H₂-), 62.6 (d, ²J_{C-P} = 6.8 Hz, P-OCH₂-), 52.7 (OMe), 36.1 (d, ¹J_{C-P} = 137 Hz, -H₂C-P), 30.1 (d, ¹J_{C-P} = 137 Hz, -H₂C-P), 16.4 (P'-OCH₂CH₃), 16.3 (P-OCH₂CH₃)

Tetraethyl (2-oxopropane-1,3-diyl)bis(phosphonate) (27)

Light yellow oil

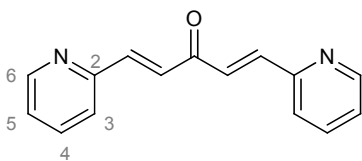
Chemical Formula: C₁₁H₂₄O₇P₂Molecular Weight: 330.25 g.mol⁻¹

Yield: ≥ 95 %

Protected phosphonate **30** (9.4 g, 23.3 mmol, 1.0 equiv.) was diluted in acetone (15 mL) in a round-bottomed flask. The mixture was cooled to 0° C and 3 M hydrochloric acid (15 mL, 42 mmol, 1.8 equiv.) was added dropwise. Once the addition was finished, the reaction was warmed to room temperature and stirred for three hours. Water (50 mL) was added and acetone was removed under reduced pressure. Product was extracted with chloroform (3 x 40 mL). The combined organic layers were dried over MgSO₄ and evaporated under reduced pressure to give desired product **27** as a light yellow oil (7.68 g, 23.2 mmol, quantitative) which was used in the next step without further purification.

¹H NMR (200 MHz, CDCl₃) δ (ppm): 4.16 (dq, ³J_{H-P} = 8.1 Hz, ³J = 7.1 Hz, 8H, P-OCH₂-), 3.35 (d, ²J_{H-P} = 23 Hz, 2H, -H₂C-P), 1.34 (td, ³J = 7.1 Hz, ³J_{H-P} = 1.6 Hz, 22H, P-OCH₂CH₃)

¹³C NMR (75.5 MHz, CDCl₃) δ (ppm): 193.8 (t, ²J_{C-P} = 6.2 Hz, C=O), 62.7 (t, ²J_{C-P} = 3.3 Hz, P-OCH₂-), 43.3 (d, ¹J_{C-P} = 126 Hz, -H₂C-P), 16.3 (m, P-OCH₂CH₃)

(1E,4E)-1,5-di(pyridin-2-yl)penta-1,4-dien-3-one (28)

Yellow crystals

Chemical Formula: C₁₅H₁₂N₂OMolecular Weight: 236.27 g.mol⁻¹

Yield: 61 %

Bis(phosphonate) **27** (7.5 g, 19.3 mmol, 1.0 equiv.) and 2-pyridinecarboxaldehyde (4.13 g, 38.6 mmol, 2.0 equiv.) were introduced in a round-bottomed flask. To this was added potassium carbonate (36 g, 260 mmol, 13.5 equiv.) in ethanol (20 mL) and water (35 mL). The biphasic mixture was vigorously stirred for two hours at room temperature. Crude mixture was transferred in a separating funnel, diluted with brine (50 mL) and the product was extracted with ethyl acetate (4 x 80 mL). The combined organic layers were dried over MgSO₄, and evaporated to dryness. The residue was purified by flash chromatography (SiO₂, EtOAc) to give desired product **28** as a yellow crystals (2.80 g, 11.9 mmol, 61 %).

Note: the product tends to crystallize in the column. A better way to purify it would be to do an acid/base extraction followed by a recrystallization.

¹H NMR (300 MHz, CDCl₃) δ (ppm): 8.7 (dd, ³J = 4.8 Hz, ⁴J = 1.5 Hz, 2H, H₆), 7.77 (d, ³J_{trans} = 15.8 Hz, 2H, H_{vin}), 7.76 (td, ³J = 7.7 Hz, ⁴J = 1.5 Hz, 2H, H₄), 7.63 (d, ³J_{trans} = 15.8 Hz, 2H, H_{vin}), 7.51 (bd, ³J = 7.7 Hz, 2H, H₃), 7.31 (ddd, ³J = 7.7 Hz, 4.8 Hz, ⁴J = 1.2 Hz, 2H, H₅)

¹³C NMR (75.5 MHz, CDCl₃) δ (ppm): 189.5 (C=O), 153.2 (C_q), 150.2 (CH), 142.1 (CH), 136.8 (CH), 128.8 (CH), 124.9 (CH), 124.4 (CH)

LC/MS (ESI): [M+H]⁺ m/z 235.3

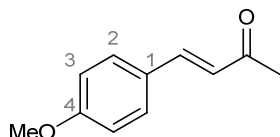
TLC (SiO₂): 70 % ethyl acetate in cyclohexane

R_F = 0.25

Orange with Dragendorff

Synthesis of dissymmetric diarylideneacetones *via* the Claisen-Schmidt pathway

(*E*)-4-(4-methoxyphenyl)but-3-en-2-one (**17**)



Light yellow crystals

Chemical Formula: C₁₁H₁₂O₂

Molecular Weight: 176.08 g.mol⁻¹

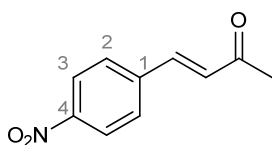
Yield: 90 %

p-Anisaldehyde (4.1 g, 30 mmol, 1.00 equiv.) and acetone (6.6 mL, 90 mmol, 3.00 equiv.) were diluted in water (17 mL) in a round-bottomed flask. The resulting solution was heated at 65 °C under stirring. 1 M Sodium hydroxide (4 mL, 3.9 mmol, 0.13 equiv.) in water (10 mL) was subsequently introduced dropwise over twenty minutes and the reaction was carried on for two hours at 65 °C under vigorous stirring. After the mixture was allowed to cool at room temperature, it was quenched by 1 M hydrochloric acid (20 mL) and the product was extracted with DCM (2 x 20 mL). The combined organic layers were washed with saturated ammonium chloride solution (2 x 5 mL), dried over MgSO₄ and evaporated to dryness under reduced pressure. The resulting yellow solid was recrystallized in ethyl acetate and pentane to give desired product **17** as light yellow crystals (4.5 g, 27 mmol, 90 %).

¹H NMR (300 MHz, CDCl₃) δ (ppm): 7.49 (d, ³J_{trans} = 16.2 Hz, 1H, H_{vin}), 7.48 (d, ²J = 8.7 Hz, 2H, H₂), 6.91 (d, ²J = 8.7 Hz, 2H, H₃), 6.60 (d, ³J_{trans} = 16.2 Hz, 1H, H_{vin}), 3.84 (s, 3H, OMe), 2.35 (s, 3H, Me)

¹³C NMR (75.5 MHz, CDCl₃) δ (ppm): 198.4 (C=O), 161.6 (C₄), 143.2 (CH), 130.0 (C₂), 127.1 (C₁), 125.0 (CH), 114.5 (C₃), 55.4 (OMe), 27.4 (Me)

LC/MS (ESI): [M+H]⁺ m/z 177.2

(E)-4-(4-nitrophenyl)but-3-en-2-one (18)

Light yellow powder

Chemical Formula: C₁₀H₉NO₃Molecular Weight: 191.18 g.mol⁻¹

Yield: 81 %

4-Nitrobenzaldehyde (6.04 g, 40 mmol, 1.0 equiv.) and potassium carbonate (1.38 g, 10 mmol, 0.25 equiv.) were solubilized in acetone (150 mL) and water (10 mL) in a round-bottomed flask. The orange solution was stirred at room temperature for twenty hours. Concentrated hydrochloric acid (20 mL) was subsequently carefully added while the mixture was maintained at room temperature with external cooling. The reaction was next carried on at room temperature under stirring for six hours. Crude mixture was poured in a mixture of crushed ice and water (200 mL) and the resulting precipitate was filtered, washed with a 1:3 cold mixture of ethanol and water until complete neutralization of the filtrate. The solid was dried under high vacuum to give desired product **18** as a light yellow powder (6.2 g, 32.4 mmol, 81 %) which was used in the next steps without further purification.

¹H NMR (300 MHz, CDCl₃) δ (ppm): 8.28 (d, ³J = 8.8 Hz, 2H, H₃), 7.71 (d, ³J = 8.8 Hz, 2H, H₂), 7.55 (d, ³J_{trans} = 16.3 Hz, 1H, H_{vin}), 6.84 (d, ³J_{trans} = 16.3 Hz, 1H, H_{vin}), 2.44 (s, 3H, Me)

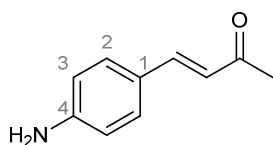
¹³C NMR (75.5 MHz, CDCl₃) δ (ppm): 197.5 (C=O), 148.6 (C_q), 140.7 (C_q), 140.1 (CH), 130.4 (CH), 128.8 (Ar), 124.2 (Ar), 28.1 (Me)

LC/MS (ESI): [M+H]⁺ m/z 192.2

TLC (SiO₂): 50% ethyl acetate in cyclohexane

R_F = 0.43

Pink with *p*-Anisaldehyde

(E)-4-(4-aminophenyl)but-3-en-2-one (19)

dark orange powder

Chemical Formula: C₁₀H₁₁NOMolecular Weight: 161.20 g.mol⁻¹

Yield: 48 %

Benzalacetone **18** (1.92 g, 10 mmol, 1.0 equiv.) and tin chloride (3.8 g, 20 mmol, 2.0 equiv.) were dissolved in ethanol (80 mL) and concentrated hydrochloric acid (5 mL, 60 mmol, 6.0 equiv.) in a round-bottomed flask. The reaction was refluxed under vigorous stirring for two hours. After cooling, the resulting dark brown solution was basified with 3 M sodium hydroxide (until pH 11-12) and the product was extracted with ethyl acetate (3 x 75 mL). The combined organic layers were dried over MgSO₄ and evaporated under reduced pressure to give viscous orange oil. This residue was purified by flash chromatography (SiO₂, DCM/(1 M NH₃ in MeOH) in DCM) to afford desired product **19** as a dark orange powder (777 mg, 4,8 mmol, 48 %) which was used in the next steps without further purification.

¹H NMR (300 MHz, CDCl₃) δ (ppm): 7.45 (d, ³J_{trans} = 16.2 Hz, 1H, H_{vin}), 7.39 (d, ³J = 8.4 Hz, 2H, H₂), 6.68 (d, ³J = 8.4 Hz, 2H, H₃), 6.56 (d, ³J_{trans} = 16.2 Hz, 1H, H_{vin}), 4.02 (s, 2H, NH₂), 2.37 (s, 3H, Me)

¹³C NMR (75.5 MHz, CDCl₃) δ (ppm): 198.6 (C=O), 149.0 (C_q), 144.0 (CH), 130.2 (Ar), 124.5 (C_q), 123.3 (CH), 114.9 (Ar), 27.3 (Me)

LC/MS (ESI): [M+H]⁺ m/z 162.3

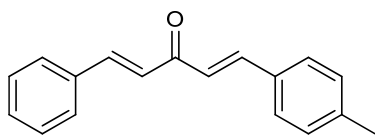
TLC (SiO₂): 70% ethyl acetate in cyclohexane

R_F = 0.40

Pink with Ninhydrin

General procedure D for the synthesis of dissymmetric diarylideneacetones via the Claisen-Schmidt protocol

Benzalacetone starting material (1.0 equiv.) was solubilized in ethanol and aqueous sodium hydroxide (3M, 3.0 equiv.) in a round-bottomed flask (molarity = 0.5 mol.L⁻¹). To this was quickly added the aldehyde starting material (1.0 equiv.). The reaction mixture was stirred at room temperature until total consumption of the starting material (TLC). The resulting precipitate was filtered off on a Büchner apparatus, thoroughly washed with a 3:1 cold mixture of ethanol in water, and dried under high vacuum. The desired product was then recrystallized in boiling ethanol or in a mixture of solvent.

(1E,4E)-1-phenyl-5-(p-tolyl)penta-1,4-dien-3-one (20)

Yellow crystals

Chemical Formula: C₁₈H₁₆OMolecular Weight: 248.32 g.mol⁻¹

Yield: 94 %

Commercially available *p*-tolualdehyde (807 μ L, 6.84 mmol) and commercially available benzalacetone (1 g, 6.84 mmol) were used as the starting material and treated according to general procedure D. Recrystallization in ethyl acetate and pentane gave desired product **20** as yellow crystals (1.60 g, 6.4 mmol, 94 %).

¹H NMR (300 MHz, CDCl₃) δ (ppm): 7.75 (two doublets, ³J_{trans} \approx 16 Hz, 2H, H_{vin}), 7.64 (m, 2H, Ph), 7.54 (d, ³J = 8.1 Hz, 2H, ArH), 7.43 (m, 3H, Ph), 7.24 (d, ³J = 8.1 Hz, 2H, ArH in *ortho* to ArMe), 7.11 (d, ³J_{trans} = 15.9 Hz, 1H, H_{vin}), 7.06 (d, ³J_{trans} = 15.9 Hz, 1H, H_{vin}), 2.41 (s, 3H, Me)

¹³C NMR (75.5 MHz, CDCl₃) δ (ppm): 189.0 (C=O), 143.4 (CH), 143.1 (CH), 141.1 (C_q), 134.9 (C_q), 132.1 (C_q), 130.4 (Ph), 129.7 (Ar), 129.0 (Ar), 128.4 (Ph), 128.3 (Ph), 125.5 (CH), 124.6 (CH), 21.3 (Me)

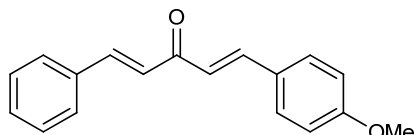
HRMS (ESI+): [M+Na]⁺ Calcd. m/z 271.109

Found m/z 271.109

TLC (SiO₂): 30% ethyl acetate in cyclohexane

R_F = 0.57

Yellow with Mostaïne

(1E,4E)-1-(4-methoxyphenyl)-5-phenylpenta-1,4-dien-3-one (21)

Yellow powder

Chemical Formula: C₁₈H₁₆O₂Molecular Weight: 264.32 g.mol⁻¹

Yield: 95 %

Commercially available *p*-anisaldehyde (832 μ L, 6.84 mmol) and commercially available benzalacetone (1 g, 6.84 mmol) were used as the starting material and treated according to general procedure D. Recrystallization in ethyl acetate and pentane gave desired product **21** as yellow crystals (1.72 g, 6.5 mmol, 95 %).

¹H NMR (300 MHz, CDCl₃) δ (ppm): 7.75 (d, ³J_{trans} = 16 Hz, 1H, H_{vin}), 7.74 (d, ³J_{trans} = 16 Hz, 1H, H_{vin}), 7.63 (m, 2H, Ph), 7.60 (d, ³J = 8.9 Hz, 2H, ArH), 7.42 (m, 3H, Ph), 7.10 (d, ³J_{trans} = 16 Hz, 1H, H_{vin}), 6.99 (d, ³J_{trans} = 16 Hz, 1H, H_{vin}), 6.96 (d, ³J = 8.9 Hz, 2H, ArH in *ortho* to ArOMe), 3.87 (s, 3H, OMe)

¹³C NMR (75.5 MHz, CDCl₃) δ (ppm): 188.9 (C=O), 161.7 (C_q), 143.2 (CH), 142.3 (CH), 135.0 (C_q), 130.4 (CH), 130.2 (CH), 128.9 (CH), 128.3 (CH), 127.5 (C_q), 125.6 (CH), 123.3 (CH), 114.5 (CH), 55.4 (OMe)

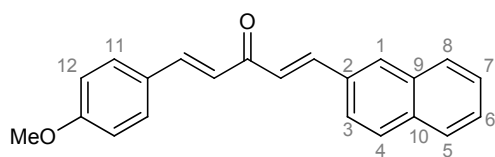
HRMS (ESI+): [M+Na]⁺ Calcd. m/z 287.104

Found m/z 287.104

TLC (SiO₂): 30% ethyl acetate in cyclohexane

R_F = 0.45

Orange with Mostaïne

(1E,4E)-1-(4-methoxyphenyl)-5-(naphthalen-2-yl)penta-1,4-dien-3-one (22)

Creamy-white powder

Chemical Formula: C₂₂H₁₈O₂Molecular Weight: 314.38 g.mol⁻¹

Yield: 61 %

Commercially available 2-naphthaldehyde (100 mg, 0.64 mmol) and previously prepared anisylacetone **17** (113 mg, 0.64 mmol) were used as the starting material and treated according to general procedure D. Recrystallization in ethyl acetate and *n*-hexane gave desired product **22** as a creamy-white yellow powder (122 mg, 0.39 mmol, 61 %).

¹H NMR (300 MHz, CDCl₃) δ (ppm): 8.04 (s, 1H, H1), 7.92 (d, ³J_{trans} = 16 Hz, 1H, H_{vin}), 7.89 (m, 4H, H3-H4-H8-H5), 7.55 (m, 2H, H7-H6), 7.77 (d, ³J_{trans} = 16 Hz, 1H, H_{vin}), 7.62 (d, ³J = 8.7 Hz, 2H, H11), 7.21 (d, ³J_{trans} = 16 Hz, 1H, H_{vin}), 7.03 (d, ³J_{trans} = 16 Hz, 1H, H_{vin}), 6.97 (d, ³J = 8.7 Hz, 2H, H12), 3.89 (s, 3H, OMe)

¹³C NMR (75.5 MHz, CDCl₃) δ (ppm): 188.8 (C=O), 161.7 (C_q), 143.2 (CH), 142.9 (CH), 134.3 (C_q), 133.4 (C_q), 132.5 (C_q), 130.4 (CH), 130.2 (C11), 128.7 (CH), 128.6 (CH), 127.8 (CH), 127.6 (C_q), 127.3 (CH), 126.7 (CH), 125.8 (CH), 123.7 (CH), 123.5 (CH), 114.5 (C12), 55.4 (OMe)

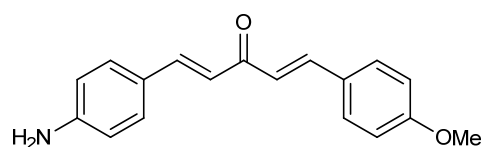
HRMS (ESI+): [M+Na]⁺ Calcd. m/z 337.120

Found m/z 337.118

TLC (SiO₂): DCM

R_F = 0.69

Pink with Mostaine

(1E,4E)-1-(4-aminophenyl)-5-(4-methoxyphenyl)penta-1,4-dien-3-one (23)

Orange powder

Chemical Formula: C₁₈H₁₇NO₂Molecular Weight: 279.33 g.mol⁻¹

Yield: 82 %

Commercially available *p*-anisaldehyde (573 μL, 4.7 mmol) and previously synthesized *p*-anilinacetone **19** (760 mg, 4.7 mmol) were used as the starting material and treated according to general procedure D. Recrystallization in ethyl acetate gave desired product **23** as an orange powder (1.07 g, 3.8 mmol, 82 %).

¹H NMR (300 MHz, CDCl₃) δ (ppm): 7.70 (d, ³J_{trans} = 16.0 Hz, 1H, H_{vin}), 7.69 (d, ³J_{trans} = 16.0 Hz, 1H, H_{vin}), 7.58 (d, ³J = 8.5 Hz, 2H, ArH), 7.46 (d, ³J = 8.5 Hz, 2H, ArH), 6.97 (d, ³J_{trans} = 16.0 Hz, 1H, H_{vin}), 6.95 (d, ³J = 8.5 Hz, 2H, ArH), 6.91 (d, ³J_{trans} = 16.0 Hz, 1H, H_{vin}), 6.69 (d, ³J = 8.5 Hz, 2H, ArH), 4.01 (bs, 2H, NH₂), 3.87 (s, 3H, OMe)

¹³C DEPT135 NMR (75.5 MHz, CDCl₃) δ (ppm): 188.9 (C=O), 161.4 (C_q), 148.9 (C_q), 143.4 (CH), 142.2 (CH), 130.3 (Ar), 130.0 (Ar), 127.8 (C_q), 125.2 (C_q), 123.7 (CH), 121.8 (CH), 114.9 (Ar), 114.4 (Ar), 55.4 (OMe)

LC/MS (ESI): [M+H]⁺ m/z 280.3

TLC (SiO₂): 50% ethyl acetate in cyclohexane

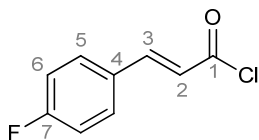
R_F = 0.28

Pink with Ninhydrin

Synthesis of dissymmetric diarylideneacetones *via* a coupling isomerization reaction

Synthesis of precursors

4-Fluorocinnamoyl chloride (**31**)



Gray needles

Chemical Formula: C₉H₆ClFO

Molecular Weight: 184.59 g.mol⁻¹

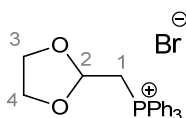
Yield: ≥ 95 %

4-fluorocinnamic acid (2 g, 12 mmol, 1.0 equiv.) was solubilized in thionyl chloride (10 mL). The reaction was refluxed for two hours under stirring and an atmosphere of argon. After being cooled at room temperature, thionyl chloride was co-evaporated with toluene three-times. The resulting gray residue was dried under high vacuum to afford desired product **31** as gray needles (2.2 g, 12 mmol, quantitative) which was used in the next steps without further purification.

¹H NMR (300 MHz, CDCl₃) δ (ppm): 7.82 (d, ³J_{trans} = 15.5 Hz, 1H, H3), 7.61 (dd, ³J = 8.5 Hz, ⁴J_{H-F} = 5.3 Hz, 2H, H5), 7.16 (t, ³J = 8.5 Hz, ³J_{H-F} = 8.5 Hz, 1H, H6), 6.67 (d, ³J_{trans} = 15.9 Hz, 1H, H2)

¹³C NMR (75.5 MHz, CDCl₃) δ (ppm): 166.0 (C=O), 164.9 (d, ¹J_{C-F} = 253 Hz, C7), 149.2 (C2), 131.2 (d, ³J_{C-F} = 8.9 Hz, C5), 129.3 (d, ⁴J_{C-F} = 3.5 Hz, C4), 122.1 (d, ⁵J_{C-F} = 2.4 Hz, C3), 116.6 (d, ²J_{C-F} = 22.1 Hz, C6)

(1,3-Dioxolan-2-ylmethyl)triphenylphosphonium bromide (**33**)



White powder

Chemical Formula: C₂₂H₂₂BrO₂P

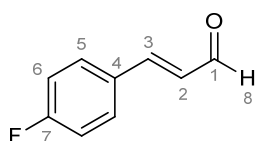
Molecular Weight: 429.29 g.mol⁻¹

Yield: 50 %

Triphenylphosphine (5.25 g, 20 mmol, 1.0 equiv.) was solubilized in 2-(bromoethyl)-1,3-dioxolane (8.6 mL, 80 mmol, 4.0 equiv.). The reaction was refluxed overnight. After being allowed to cool at room temperature, cold acetone (20 mL) was added in the crude and the resulting precipitate in filtered and thoroughly washed with cold acetone to give desired product **33** as a white fine powder (4.32 g, 10 mmol, 50 %).

¹H NMR (300 MHz, CDCl₃) δ (ppm): 7.9 (m, 15H, Ph₃), 5.44 (dt, ³J_{H-P} = 13.2 Hz, ³J = 3.9 Hz, 1H, H2), 4.42 (dd, ²J_{H-P} = 12.6 Hz, ³J = 3.9 Hz, 2H, H1), 3.57 (m, 4H, H3-H4)

¹³C NMR (75.5 MHz, CDCl₃) δ (ppm): 135.0 (d, ⁴J_{C-P} = 2 Hz, Ar in *para* to P), 134.2 (d, ³J_{C-P} = 8 Hz, Ar in *meta* to P), 130.5 (d, ²J_{C-P} = 12 Hz, Ar in *ortho* to P), 119.7 (d, ¹J_{C-P} = 88 Hz, C_qP), 99.2 (d, ²J_{C-P} = 8 Hz, C2), 65.5 (C3-C4), 30.1 (d, ¹J_{C-P} = 52 Hz, C1)

4-Fluorocinnamaldehyde (32)

Yellow oil

Chemical Formula: C₉H₇FOMolecular Weight: 150.15 g.mol⁻¹**Procedure I: Reduction of 31**

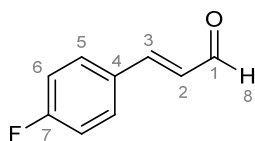
Previously prepared 4-fluorocinnamoyl chloride **31** (1 g, 5.4 mmol, 1.0 equiv.) was dissolved in anhydrous THF (15 mL). The solution was cooled to -78 °C and lithium tri-*tert*-butoxyaluminumhydride 1 M in THF (5.4 mL, 5.4 mmol, 1.0 equiv.) was added dropwise. The reaction was carried on for one hour, at -78 °C, under stirring and an atmosphere of argon. After being allowed to warm at room temperature the crude mixture was quenched by saturated ammonium chloride (10 mL) and 3N hydrochloric acid (15 mL). The product was extracted with DCM (2 x 40 mL). The combined organic layers were dried over MgSO₄ and evaporated under reduced pressure. The residue was purified by flash chromatography (SiO₂, CyHex/EtOAc) to afford desired product **32** as a yellow oil (444 mg, 3.0 mmol, 55 %).

Procedure II: Wittig reaction

Previously prepared phosphonium salt **33** (3.4 g, 8.0 mmol, 2.0 equiv.) was suspended in anhydrous THF (35 mL) and cooled to 0 °C. To this was added potassium *tert*-butoxide (900 mg, ~7.7 mmol, 1.9 equiv.) portionwise, under stirring at 0 °C and an atmosphere of argon. The orange suspension was kept at -0 °C for half an hour. 4-Fluorobenzaldehyde (500 mg, 4.03 mmol, 1.0 equiv.) in THF (5 mL) was then added dropwise over ten minutes at 0 °C. The reaction was then allowed to warm at room temperature and carried on for one night heated at 55 °C under argon. The crude mixture was quenched by 2 M hydrochloric acid (30 mL) and stirred for another two hours. The product was extracted with diethyl ether (2 x 50 mL) and the combined organic layers were washed with saturated potassium carbonate (2 x 40 mL), dried over MgSO₄ and evaporated to dryness under reduced pressure. The resulting orange solid was triturated and washed three times with a 1:3 cold solution of diethyl ether in *n*-pentane and the resulting liquid layers were filtered over a pad of Celite and evaporated to afford desired product **32** (580 mg, 3.9 mmol, 96 %).

Procedure III: Grignard reaction

In a dry three-necked round-bottomed flask under argon was introduced magnesium (470 mg, 19.3 mmol, 1.2 equiv) and anhydrous THF (1 mL). Few drops of 2-bromomethyl-1,3-dioxolane (3.23 g, 19.3 mmol, 1.2 equiv.) in anhydrous THF (20 mL) were added on the stirred suspension of magnesium. After addition of a crystal of iodine, the mixture started to boil. The addition of bromide was carried on, keeping a gentle reflux. At the end of the addition, external heating was required to keep the mixture refluxing for one hour, under argon. 4-Fluorobenzaldehyde (2 g, 16.1 mmol, 1.0 equiv.) in anhydrous THF (10 mL) was then added dropwise and the deep red solution was refluxed for another two hours under argon. After being cooled to room temperature, the crude was quenched by 3 M hydrochloric acid (25 mL) and the yellowish solution was stirred for two hours. The pH was then adjusted to 12 by addition of concentrated sodium hydroxide and the crude mixture was transferred in a separating funnel. Product was extracted with diethyl ether (3 x 75 mL), the combined organic layers were dried over MgSO₄ and evaporated under reduced pressure. The resulting yellowish oil was distilled under reduced pressure (60 °C, ~1mBar) to afford desired product **32** as a yellow oil (1.08 g, 7.2 mmol, 45 %).

4-Fluorocinnamaldehyde (32) (continued)

Yellow oil

Chemical Formula: C₉H₇FOMolecular Weight: 150.15 g.mol⁻¹

¹H NMR (300 MHz, CDCl₃) δ (ppm): 9.71 (d, ³J = 7.6 Hz, 1H, H8), 7.59 (dd, ³J = 8.5 Hz, ⁴J_{H-F} = 5.3 Hz, 2H, H5), 7.46 (d, ³J_{trans} = 15.9 Hz, 1H, H3), 7.15 (t, ³J = 8.5 Hz, ³J_{H-F} = 8.5 Hz, 1H, H6), 6.67 (dd, ³J_{trans} = 15.9 Hz, ³J = 7.6 Hz, 1H, H2)

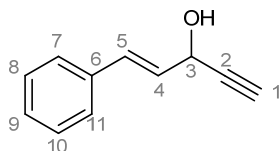
¹³C NMR (75.5 MHz, CDCl₃) δ (ppm): 193.4 (C=O), 164.5 (d, ¹J_{C-F} = 253 Hz, C7), 151.3 (C2), 130.5 (d, ³J_{C-F} = 8.3 Hz, C5), 130.3 (d, ⁴J_{C-F} = 3.3 Hz, C4), 128.4 (d, ⁵J_{C-F} = 2.2 Hz, C3), 116.4 (d, ¹J_{C-F} = 22.1 Hz, C6)

LC/MS (ESI): [M+H]⁺ m/z 151.2

TLC (SiO₂): 20% ethyl acetate in cyclohexane

R_F = 0.36

Bright orange with 2,4-DNPH

(E)-1-phenylpent-1-en-4-yn-3-ol (36)

Creamy-white powder

Chemical Formula: C₁₁H₁₀OMolecular Weight: 158.20 g.mol⁻¹

Yield: 81 %

In a dry three necked round bottomed flask equipped with a P₂O₅ guard, a septa and a nitrogen inlet, were introduced anhydrous THF (20 mL), and ethynylmagnesium bromide 0.5M in THF (50 mL, 25 mmol, 1.25 equiv.). This solution was cooled to -10 °C (salted ice) and once the temperature was raised, cinnamaldehyde (2.52 mL, 20 mmol, 1.0 equiv) in anhydrous THF (5 mL) was introduced dropwise over five minutes. The reaction mixture was kept at -10 °C for fifteen minutes under stirring and nitrogen. The mixture was subsequently allowed to warm at room temperature and the reaction was carried on for two hours, still under stirring and nitrogen. The reaction was quenched with a saturated solution of ammonium chloride and the product was extracted with diethylether (3 x 50 mL). The combined organic layers were washed with saturated ammonium chloride (2 x 20 mL), dried over Na₂SO₄ and solvent were removed under reduced pressure. Resulting residue was recrystallized in a mixture of 30 % EtOAc in *n*-hexane to afford desired product **36** as a creamy white powder (2.54 g, 16 mmol, 81 %).

¹H NMR (300 MHz, CDCl₃) δ (ppm): 7.32 (m, 5H, Ph), 6.80 (d, ³J_{trans} = 15.9 Hz, 1H, H5), 6.29 (dd, ³J_{trans} = 15.9 Hz, ³J = 5.8 Hz, 1H, H4), 5.05 (td, ³J = 5.9 Hz, ⁴J = 2.2 Hz, 1H, H3), 2.63 (d, ⁴J = 2.2 Hz, 1H, H1), 2.01 (bd, *J* ≈ 6.0 Hz, 1H, OH)

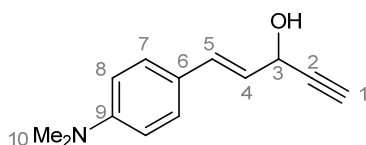
¹³C NMR (75.5 MHz, CDCl₃) δ (ppm): 135.6 (C6), 131.8 (Ph), 128.8 (CH), 128.4 (Ph), 127.4 (CH), 126.7 (Ph), 82.8 (C2), 74.6 (C1), 62.2 (C3)

LC/MS (ESI): [M+H]⁺ m/z 159.3

TLC (SiO₂): DCM

R_F = 0.32

Brown with *p*-anisaldehyde

(E)-1-(4-aminophenyl)pent-1-en-4-yn-3-ol (37)

Brownish powder

Chemical Formula: C₁₁H₁₁NOMolecular Weight: 201.26 g.mol⁻¹

Yield: 79 %

In a dry three-necked round bottomed flask were introduced anhydrous THF (5 mL) and ethynylmagnesium bromide 0.5M in THF (18 mL, 9 mmol, 1.25 equiv.). The solution was cooled at -78°C and commercially available (*E*)-3-(4-(dimethylamino)phenyl)acrylaldehyde (1.23 g, 7 mmol, 1.0 equiv.) in anhydrous THF (7 mL) was added dropwise over 10 min at -78°C under stirring and argon. Reaction mixture was next allowed to warm at room temperature and reaction was carried out for two hours under stirring and argon. Reaction was subsequently quenched by saturated ammonium chloride (20 mL). Product was extracted with diethyl ether (3 x 30 mL) after the aqueous was adjusted to pH~10 with sodium hydrogen carbonate. Combined organic layers were dried over MgSO₄ and evaporated to dryness. The orange crude powder was recrystallized in a mixture of 40% *n*-hexane in toluene to give desired product **37** as a brownish powder (1.10 g, 5.5 mmol, 79 %).

¹H NMR (300 MHz, CDCl₃) δ (ppm): 7.30 (d, ³J = 8.7 Hz, 2H, H7), 6.71 (d, ³J = 8.7 Hz, 2H, H8), 6.63 (d, ³J_{trans} = 15.8 Hz, 1H, H5), 6.10 (dd, ³J_{trans} = 15.8 Hz, ³J = 6.3 Hz, 1H, H4), 4.97 (ddd, ³J = 6.3 Hz, 5.9 Hz, ⁴J = 2.0 Hz, 1H, H3), 4.53 (d, ³J = 5.9 Hz, 1H, OH), 2.98 (d, ⁴J = 2.0 Hz, 1H, H1), 2.95 (s, 6H, NMe₂)

¹³C NMR (50.3 MHz, Acetone-*d*₆) δ (ppm): 151.5 (C6), 131.8 (CH), 128.5 (CH), 125.6 (CH), 125.4 (C9), 113.2 (CH), 85.5 (C2), 74.4 (C1), 63.1 (C9), 40.5 (NMe₂)

Elemental analysis: Calcd. C 77.58 H 7.51

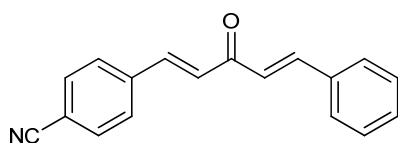
Found C 77.37 H 7.52

m.p. = 124 °C (Toluene/*n*-hexane)

TLC (SiO₂): DCM R_F = 0.18 Brown with PMA
2.5 % (NH₃ 1M in MeOH) in DCM R_F = 0.63

Synthesis of dissymmetric diarylideneacetones**General procedure E for the synthesis of dissymmetric diarylideneacetones via the the coupling isomerization reaction**

Aryl halide starting material (1 mmol, 1.0 equiv.), unsaturated propargyl alcohol previously synthesized (1.2 mmol, 1.2 equiv.), commercial bis-(triphenylphosphine)palladium(II) dichloride (21 mg, 0.03 mmol, 0.03 equiv.), copper iodide (4 mg, 0.02 mmol, 0.02 equiv.) and triphenylphosphine (52 mg, 0.2 mmol, 0.2 equiv.) were introduced in a 10 mL microwave vial flushed with argon. This was solubilized with a solution of anhydrous triethylamine (700 μL, 5 mmol, 5.0 equiv.) in anhydrous degassed 1,4-dioxane (1.3 mL). The solution was heated under microwave irradiation at 120 °C for 45 min. The reaction mixture was poured into a mix of 1M aqueous solution of hydrochloric acid (10 mL, except when pyridyl or aniline derivatives were used) and saturated aqueous ammonium chloride solution (10 mL), and this was extracted with ethyl acetate (3 x 15 mL). The combined organic layers were dried over MgSO₄, filtered, and evaporated to dryness to give crude product which was purified by flash chromatography as mentioned in the following examples.

4-((1E,4E)-3-oxo-5-phenylpenta-1,4-dien-1-yl)benzotrile (39)

Light yellow powder

Chemical Formula: C₁₈H₁₃NOMolecular Weight: 259.30 g.mol⁻¹

Yield: 65 % (Scale-up: 68 %)

Commercially available 4-bromobenzotrile (182 mg, 1 mmol) and previously prepared unsaturated propargyl alcohol **36** (190 mg, 1.2 mmol) were used as the starting material and treated according to general procedure E. Product was purified by flash chromatography (SiO₂, EtOAc/*n*-hexane) to give desired product **39** as a light yellow powder (169 mg, 0.65 mmol, 65%).

Scale-up

4-bromobenzotrile (1.82 g, 10 mmol, 1.0 equiv.), phenylpent-1-en-4-yn-3-ol **36** (1.90 g, 12.5 mmol, 1.25 equiv), bis(triphenylphosphine)palladium(II) dichloride (210 mg, 0.3 mmol, 0.03 equiv.), copper iodide (40 mg, 0.2 mmol, 0.02 equiv.) and triphenylphosphine (520 mg, 2 mmol, 0.2 equiv.) were introduced in a 25 mL microwave vial flushed with argon. This was diluted with anhydrous triethylamine (7 mL, 50 mmol, 5.0 equiv.) in anhydrous degassed 1,4-dioxane (13 mL). The solution was heated under microwave irradiation at 120 °C for 45 min. The reaction mixture was poured into a mix of 3M hydrochloric acid (40 mL) and saturated aqueous ammonium chloride solution (60 mL), and this was extracted with ethyl acetate (3 x 50 mL). The combined organic layers were dried over MgSO₄, filtered, and evaporated to dryness to give crude product. Product was purified by flash chromatography (SiO₂, EtOAc/*n*-hexane) to give desired product **39** as a light yellow powder (1.75 g, 6.8 mmol, 68 %).

¹H NMR (500 MHz, CD₂Cl₂) δ (ppm): 7.75 (d, ³J_{trans} = 16.4 Hz, 1H, H_{vin}), 7.72 (m, 4H, ArH), 7.69 (d, ³J_{trans} = 15.5 Hz, 1H, H_{vin}), 7.64-7.66 (m, 2H, ArH), 7.44 (m, 3H, ArH), 7.18 (d, ³J_{trans} = 15.5 Hz, 1H, H_{vin}), 7.09 (d, ³J_{trans} = 16.4 Hz, 1H, H_{vin})

¹³C NMR (125 MHz, CD₂Cl₂) δ (ppm): 188.3 (C=O), 144.1 (CH), 140.7 (CH), 139.6 (C_q), 135.0 (C_q), 133.0 (CH), 131.1 (CH), 129.4 (CH), 129.0 (CH), 128.8 (CH), 128.5 (CH), 125.7 (CH), 118.8 (CH), 113.7 (C_q)

IR (neat) ν (cm⁻¹): 1674, 1601, 1337, 1188, 982, 826, 763, 695

HRMS (ESI+): [M+Na]⁺ Calcd. m/z 282.089

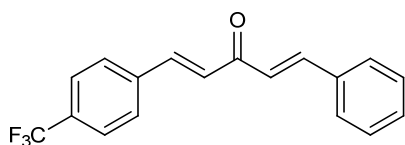
Found m/z 282.089

m.p. = 146 °C

TLC (SiO₂): DCM

R_F = 0.69

Yellow with Mostaine

(1E,4E)-1-phenyl-5-(4-(trifluoromethyl)phenyl)penta-1,4-dien-3-one (40)

Light yellow powder

Chemical Formula: C₁₈H₁₃F₃OMolecular Weight: 302.29 g.mol⁻¹

Yield: 55 %

Commercially available 4-iodobenzotrifluoride (272 mg, 1 mmol) and previously prepared unsaturated propargyl alcohol **36** (190 mg, 1.2 mmol) were used as the starting material and treated according to general procedure E. Product was purified by flash chromatography (SiO₂, DCM/*n*-hexane) to give desired product **40** as a light yellow powder (166 mg, 0.55 mmol, 55%).

¹H NMR (300 MHz, CDCl₃) δ (ppm): 7.79 (d, ³J_{trans} = 16.0 Hz, 1H, H_{vin}), 7.76 (d, ³J_{trans} = 16.0 Hz, 1H, H_{vin}), 7.77-7.67 (m, 4H, Ar), 7.67-7.60 (m, 2H, Ph), 7.45 (m, 3H, Ph), 7.17 (d, ³J_{trans} = 16.0 Hz, 1H, H_{vin}), 7.10 (d, ³J_{trans} = 16.0 Hz, 1H, H_{vin})

¹³C NMR (75.5 MHz, CDCl₃) δ (ppm): 188.7 (C_q), 144.2 (CH), 144.4 (CH), 138.4 (m, C_q), 134.8 (C_q), 132.1 (q, ²J_{C-F} = 32 Hz, C_q), 131.0 (CH), 129.2 (CH), 128.7 (CH), 128.6 (CH), 127.6 (CH), 125.9 (q, ³J_{C-F} = 3.6 Hz, CH), 125.5 (CH), 123.8 (q, ¹J_{C-F} = 271 Hz, CF₃)

IR (neat) ν (cm⁻¹): 1653, 1593, 1322, 1107, 1066, 981, 826, 760, 695

HRMS (ESI+): [M+Na]⁺ Calcd. m/z 325.081

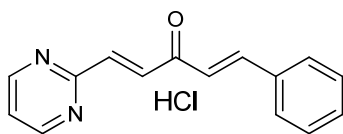
Found m/z 325.081

m.p. = 142-143°C

TLC (SiO₂): 50 % DCM in *n*-hexane

R_F = 0.33

Yellow with PMA

(1E,4E)-1-phenyl-5-(pyrimidin-2-yl)penta-1,4-dien-3-one hydrochloride (41)

Fine yellow powder

Chemical Formula: C₁₅H₁₃ClN₂OMolecular Weight: 272.24 g.mol⁻¹

Yield: 65 %

Commercially available bromopyrimidine (159 mg, 1 mmol) and previously prepared unsaturated propargyl alcohol **36** (190 mg, 1.2 mmol) were used as the starting material and treated according to general procedure E. Product was purified by flash chromatography (SiO₂, EtOAc/*n*-hexane) to give the desired free base (FB). This was dissolved in diethyl ether (5 mL) and commercial hydrogen chloride 1.25 M in ethanol (2 mL) was added. The suspension was filtered to recover the hydrochloric salt of desired product **41** as a fine yellow powder (178 mg, 0.65 mmol, 65 %).

¹H NMR (300 MHz, DMSO-*d*₆) δ (ppm): 8.92 (d, ³*J* = 4.7 Hz, 2H, H in *ortho* to the nitrogens), 7.83 (m, 2H, Ph), 7.78 (d, ³*J*_{trans} = 16.0 Hz, 1H, H_{vin}), 7.77 (d, ³*J*_{trans} = 15.8 Hz, 1H, H_{vin}), 7.64 (d, ³*J*_{trans} = 15.8 Hz, 1H, H_{vin}), 7.52 (d, ³*J* = 4.7 Hz, 1H, H in *meta* to the nitrogens), 7.47 (d, ³*J*_{trans} = 16.0 Hz, 1H, H_{vin}), 7.46 (m, 3H, Ph)

¹³C NMR (75.5 MHz, DMSO-*d*₆) δ (ppm): 188.7 (C=O), 162.3 (C_q pyrimidine), 157.7 (Ar), 143.9 (CH), 140.6 (CH), 134.4 (C_q), 133.3 (CH), 130.8 (CH), 128.9-128.8 (CH), 125.2 (CH), 121.0 (Ar)

IR (neat) ν (cm⁻¹): 1662, 1604, 1595, 1504, 1386, 1238, 1200, 1061, 994, 986, 813, 780, 692

HRMS (ESI+): [M+Na]⁺ Calcd. m/z 259.084

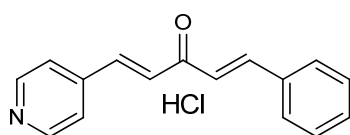
Found m/z 259.084

m.p. = 164°C dec.

TLC (SiO₂): 50 % EtOAc in *n*-hexane

R_F = 0.38 (FB)

Orange with PMA

(1E,4E)-1-phenyl-5-(pyridin-4-yl)penta-1,4-dien-3-one hydrochloride (42)

Fine yellow powder

Chemical Formula: C₁₆H₁₄ClNOMolecular Weight: 271.74 g.mol⁻¹

Yield: 42 %

Commercially available 4-bromopyridinium hydrochloride (194 mg, 1 mmol) (neutralized prior use by aqueous potassium carbonate washing/extraction) and previously prepared unsaturated propargyl alcohol **36** (190 mg, 1.2 mmol) were used as the starting material and treated according to general procedure E. Product was purified by flash chromatography (SiO₂, EtOAc/*n*-hexane) to give the desired free base (FB). This was dissolved in 1,4-dioxane (15 mL) and commercial hydrogen chloride 1.25M in ethanol (2 mL) was added. The suspension was filtered to recover the hydrochloric salt of desired product **42** as a fine yellow powder (115 mg, 0.42 mmol, 42 %).

¹H NMR (300 MHz, DMSO-*d*₆) δ (ppm): 8.97 (d, ³*J* = 6.4 Hz, 2H, H in *ortho* to the nitrogen), 8.38 (d, ³*J* = 6.4 Hz, 2H, H in *meta* to the nitrogen), 8.05-7.85 (m, 3H, H_{vin}), 7.82 (m, 2H, Ph), 7.49 (m, 3H, Ph), 7.33 (d, ³*J*_{trans} = 16.8 Hz, 1H, H_{vin})

¹³C NMR (75.5 MHz, DMSO-*d*₆) δ (ppm): 188.4 (C=O), 150.2 (C_q pyridine), 144.8 (CH), 143.0 (CH), 137.0 (CH), 134.4 (C_q), 133.4 (CH), 131.0 (CH), 129.1 (CH), 128.7 (CH), 125.7 (CH), 125.1 (CH)

IR (neat) ν (cm⁻¹): 1655, 1634, 1602, 1505, 1335, 1189, 979, 812, 767, 729, 691

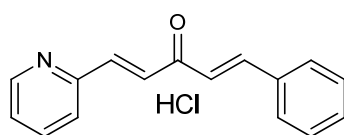
HRMS (ESI+): [M+H]⁺ Calcd. m/z 236.107
Found m/z 236.106

m.p. = 190 °C dec.

TLC (SiO₂): 70 % EtOAc in *n*-hexane

R_F = 0.33 (FB)

Orange with PMA

(1E,4E)-1-phenyl-5-(pyridin-2-yl)penta-1,4-dien-3-one hydrochloride (43)

Duck-yellow powder

Chemical Formula: C₁₆H₁₄ClNOMolecular Weight: 271.74 g.mol⁻¹

Yield: 50 %

Commercially available 2-iodopyridine (205 mg, 1 mmol) and previously prepared unsaturated propargyl alcohol **36** (190 mg, 1.2 mmol) were used as the starting material and treated according to general procedure E. Product was purified by flash chromatography (SiO₂, EtOAc/*n*-hexane) to give the desired free base (FB). This was dissolved in diethyl ether (5 mL) and commercial hydrogen chloride 1.25M in ethanol (2 mL) was added. The suspension was filtered to recover the hydrochloric salt of desired product **43** as a fine duck-yellow powder (136 mg, 0.5 mmol, 50 %).

¹H NMR (300 MHz, DMSO-*d*₆) δ (ppm): 8.83 (d, ³J = 5.6 Hz, 1H, H in *ortho* to the nitrogen), 8.38-8.26 (m, 2H, H pyridine), 8.09 (d, ³J_{trans} = 16.4 Hz, 1H, H_{vin}), 7.99 (d, ³J_{trans} = 15.9 Hz, 1H, H_{vin}), 7.84 (d, ³J_{trans} = 16.4 Hz, 1H, H_{vin}), 7.84-7.81 (m, 1H, H pyridine), 7.81 (m, 2H, Ph), 7.47 (m, 3H, Ph), 7.29 (d, ³J_{trans} = 15.9 Hz, 1H, H_{vin})

¹³C NMR (75.5 MHz, DMSO-*d*₆) δ (ppm): 188.2 (C=O), 149.5 (C_q pyridine), 145.5 (CH), 144.7 (CH), 142.6 (CH), 135.7 (C_qPh), 134.4 (CH), 131.5 (CH), 130.9 (CH), 129.1 (Ar), 128.8 (Ar), 126.3 (CH), 126.0 (CH), 125.9 (CH)

IR (neat) ν (cm⁻¹): 1661, 1614, 1462, 1304, 1197, 1109, 979, 771, 692

HRMS (ESI+): [FB+Na]⁺ Calcd. m/z 258.089

Found m/z 258.088

Elemental analysis: Calcd. C 70.72 H 5.15

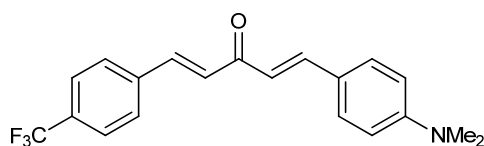
Found C 70.45 H 5.03

m.p. = 155 °C dec.

TLC (SiO₂): 30 % EtOAc in *n*-hexane

R_F = 0.33 (FB)

Orange with PMA

(1E,4E)-1-(4-(dimethylamino)phenyl)-5-(4-(trifluoromethyl)phenyl)penta-1,4-dien-3-one (44)

Bright yellow powder

Chemical Formula: C₂₀H₁₈F₃NOMolecular Weight: 345.36 g.mol⁻¹

Yield: 58 %

Commercially available 4-iodobenzotrifluoride (272 mg, 1 mmol) and previously prepared unsaturated propargyl alcohol **37** (242 mg, 1.2 mmol) were used as the starting material and treated according to general procedure E. Product was purified by flash chromatography (SiO₂, 30% EtOAc/DCM). The resulting yellow solid was triturated in diethyl ether to give desired product **44** as a bright yellow powder (200 mg, 0.58 mmol, 58 %).

¹H NMR (500 MHz, CDCl₃) δ (ppm): 7.76 (d, ³J_{trans} = 15.6 Hz, 1H, H_{vin}), 7.72 (d, ³J_{trans} = 16 Hz, 1H, H_{vin}), 7.70 (m, 4H, ArH), 7.55 (d, ³J = 9 Hz, 2H, ArH aniline), 7.17 (d, ³J_{trans} = 16 Hz, 1H, H_{vin}), 6.89 (d, ³J_{trans} = 15.6 Hz, 1H, H_{vin}), 6.72 (d, ³J = 8.5 Hz, 2H, ArH aniline), 3.07 (s, 6H, NMe₂)

¹³C NMR (75.5 MHz, CDCl₃) δ (ppm): 188.5 (C=O), 152.4 (C_q), 145.2 (CH), 140.1 (CH), 138.9 (C_q), 131.4 (q, ²J_{C-F} = 32.5 Hz, C_q), 130.7 (CH), 128.5 (CH), 128.1 (CH), 126.0 (q, ³J_{C-F} = 3.8 Hz, Ar), 123.9 (q, ¹J = 269 Hz, CF₃), 122.5 (C_q), 120.8 (CH), 112.1 (CH), 40.3 (NMe₂)

IR (neat) ν (cm⁻¹): 1648, 1600, 1587, 1524, 1321, 1162, 1118, 1108, 1065, 981, 826, 810

HRMS (ESI+): [M+H]⁺ Calcd. m/z 346.141

Found m/z 346.140

Elemental analysis: Calcd. C 69.56 H 5.25

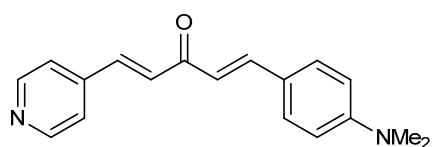
Found C 69.57 H 5.54

m.p. = 179-180 °C

TLC (SiO₂): 20 % DCM in *n*-hexane

R_F = 0.31

Visible orange spot

(1E,4E)-1-(4-(dimethylamino)phenyl)-5-(pyridin-4-yl)penta-1,4-dien-3-one (45)

Dark purple crystals

Chemical Formula: C₁₈H₁₈N₂OMolecular Weight: 278.35 g.mol⁻¹

Yield: 54 %

Commercially available 4-bromopyridinium hydrochloride (194 mg, 1 mmol) (neutralized prior use) and previously prepared unsaturated propargyl alcohol **37** (242 mg, 1.2 mmol) were used as the starting material and treated according to general procedure E. Product was purified by flash chromatography (SiO₂, MeOH/DCM) to give desired product **45** as dark purple crystals (190 mg, 0.54 mmol, 54 %).

¹H NMR (300 MHz, CDCl₃) δ (ppm): 8.68 (d, ³J = 6.0 Hz, 2H, H in *ortho* to the nitrogen), 7.76 (d, ³J_{trans} = 15.6 Hz, 1H, H_{vin}), 7.61 (d, ³J_{trans} = 15.9 Hz, 1H, H_{vin}), 7.54 (d, ³J = 8.5 Hz, 2H, ArH aniline), 7.46 (d, ³J = 6.0 Hz, 2H, H in *meta* to the nitrogen), 7.25 (d, ³J_{trans} = 15.9 Hz, 1H, H_{vin}), 6.87 (d, ³J_{trans} = 15.6 Hz, 1H, H_{vin}), 6.71 (d, ³J = 8.5 Hz, 2H, ArH aniline), 3.07 (s, 6H, NMe₂)

¹³C NMR (75.5 MHz, CDCl₃) δ (ppm): 186.0 (C=O), 152.3 (C_q), 150.5 (CH), 145.4 (CH), 142.5 (C_q), 138.7 (CH), 130.6 (CH), 129.6 (CH), 122.1 (C_q), 122.0 (CH), 120.4 (CH), 111.9 (CH), 40.1 (NMe₂)

IR (neat) ν (cm⁻¹): 1662, 1634, 1609, 1509, 1197, 1131, 1114, 992, 836, 819

HRMS (ESI+): [M+H]⁺ Calcd. m/z 346.141

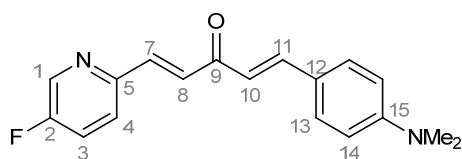
Found m/z 346.140

m.p. = 192 °C dec.

TLC (SiO₂): 5 % MeOH in DCM

R_F = 0.40

Visible orange spot

(1E,4E)-1-(4-(dimethylamino)phenyl)-5-(5-fluoropyridin-2-yl)penta-1,4-dien-3-one (46)

Orange powder

Chemical Formula: C₁₈H₁₇FN₂OMolecular Weight: 296.34 g.mol⁻¹

Yield: 52 %

Commercially available 2-bromo-5-fluoropyridine (176 mg, 1 mmol) and previously prepared unsaturated propargyl alcohol **37** (242 mg, 1.2 mmol) were used as the starting material and treated according to general procedure E. Product was purified by flash chromatography (SiO₂, 5 % (NH₃ 1M in MeOH) in DCM) to give desired product **46** as an orange powder (154 mg, 0.52 mmol, 52 %).

¹H NMR (300 MHz, CDCl₃) δ (ppm): 8.54 (d, ³J_{H-F} = 2.7 Hz, 1H, H1), 7.77 (d, ³J_{trans} = 15.9 Hz, 1H, H11), 7.68 (d, ³J_{trans} = 15.6 Hz, 1H, H7), 7.57 (d, ³J_{trans} = 15.6 Hz, 1H, H8), 7.54 (d, ³J = 8.6 Hz, 2H, H13), 7.5-7.4 (m, 2H, H3-H4), 6.89 (d, ³J_{trans} = 15.9 Hz, 1H, H10), 6.72 (d, ³J = 8.6 Hz, 2H, H14), 3.07 (s, 6H, NMe₂)

¹³C NMR (75.5 MHz, CDCl₃) δ (ppm): 188.8 (C=O), 159.4 (d, ¹J_{C-F} = 260 Hz, C2), 152.1 (C15), 150.1 (d, ⁴J_{C-F} = 4 Hz, C5), 145.0 (C11), 138.8 (C7), 138.7 (d, ²J_{C-F} = 24 Hz, C1), 130.5 (C13), 128.8 (C8), 125.8 (d, ³J_{C-F} = 5 Hz, C4), 123.3 (d, ²J_{C-F} = 19 Hz, C3), 122.5 (C12), 121.4 (C10), 112.0 (C14), 40.2 (NMe₂)

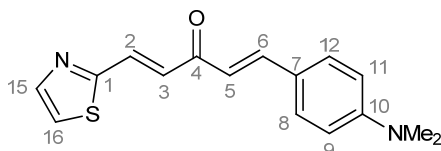
IR (neat) ν (cm⁻¹): 1605, 1559, 1523, 1475, 1434, 1371, 1345, 1226, 1186, 1098, 982, 855, 803

HRMS (ESI+): [M+H]⁺ Calcd. m/z 297.140

Found m/z 297.139

m.p. = 164 °C dec.

TLC (SiO₂): 50 % [10 % (NH₃ 1M in MeOH) in DCM] in CyHex R_F = 0.45 Dark green with PMA

(1E,4E)-1-(4-(dimethylamino)phenyl)-5-(thiazol-2-yl)penta-1,4-dien-3-one (47)

Dark purple powder

Chemical Formula: C₁₆H₁₆N₂OSMolecular Weight: 284.38 g.mol⁻¹

Yield: 62 %

Commercially available 2-bromothiazole (164 mg, 1 mmol) and previously prepared unsaturated propargyl alcohol **37** (242 mg, 1.2 mmol) were used as the starting material and treated according to general procedure E. Product was purified by flash chromatography (SiO₂, EtOAc/CyHex) to give desired product **47** as a dark purple powder (176 mg, 0.62 mmol, 62 %).

¹H NMR (300 MHz, CDCl₃) δ (ppm): 7.96 (d, ³J = 3.2 Hz, 1H, H15), 7.80 (d, ³J_{trans} = 15.8 Hz, 1H, H2), 7.76 (d, ³J_{trans} = 15.8 Hz, 1H, H6), 7.53 (d, ³J = 8.7 Hz, 2H, H8-H12), 7.46 (d, ³J = 3.2 Hz, 1H, H16), 7.43 (d, ³J_{trans} = 15.8 Hz, 1H, H3), 6.88 (d, ³J_{trans} = 15.8 Hz, 1H, H5), 6.73 (d, ³J = 8.7 Hz, 2H, H9-H11), 3.07 (s, 6H, NMe₂)

¹³C NMR (75.5 MHz, CDCl₃) δ (ppm): 187.9 (C=O), 164.6 (C1), 152.1 (C10), 145.3 (C6), 144.7 (C15), 132.5 (C2), 130.6 (C8-C12), 129.5 (C3), 122.5 (C7), 121.2 (C16), 120.7 (C5), 112.0 (C9-C11), 40.2 (NMe₂)

IR (neat) ν (cm⁻¹): 1594, 1558, 1524, 1346, 1186, 1099, 1074, 1000, 811, 771

HRMS (ESI+): [M+H]⁺ Calcd. m/z 285.106

Found m/z 285.105

m.p. = 176 °C

TLC (SiO₂): 50% ethyl acetate in cyclohexane R_F = 0.38 Orange with Dragendorff

Diastereoselective synthesis of 2,6-diaryl-4*H*-tetrahydrothiopyran-4-ones

Foreword

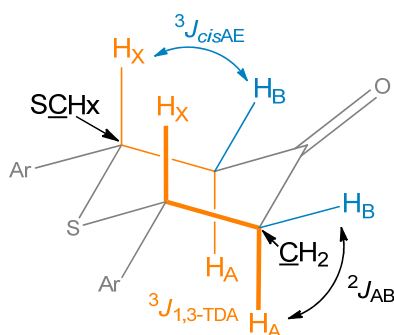
About the nomenclature of 2,6-diaryl-4*H*-tetrahydrothiopyran-4-ones

Very various nomenclatures have been used in the past to name this scaffold. IUPAC seems to recommend the use of "2,6-diarylthian-4-one", ChemBioDraw Ultra is generating "2,6-diaryldihydro-2*H*-thiopyran-4(3*H*)-one", and in the literature it is possible to read "2,6-diarylthiopyran-4-one", "2,6-diaryl-2,3,5,6-tetra-hydrothiopyran-4-one", "2,6-diaryltetrahydro-1-thio-4-pyrone", "2,6-diaryl-4-thianone", "2,6-diaryltetrahydropyran-4-one", "2,6-diarylthia-cyclohexanone", "2,3,5,6-Tetrahydro-2,6-diarylthiopyran-4-one" etc. (non-exhaustive list). Facing this difficulty, we chose the nomenclature "2,6-diaryl-4*H*-tetrahydrothiopyran-4-one" as mentioned in the most complete and reliable article on the subject (Ingall, A. H. Thiopyrans and Fused Thiopyrans. In *Comprehensive Heterocyclic Chemistry*; Elsevier, **1984**; pp. 885–942.). However, this choice was arbitrary.

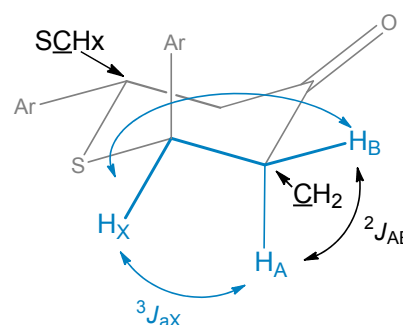
About the attribution of signals on the NMR spectra

The following conventions will be applied:

A) *cis* isomer



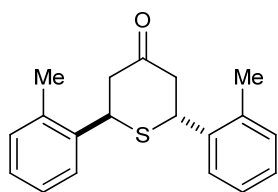
B) *trans* isomer



Synthesis of (\pm)-*trans* isomers

General procedure F for the diastereoselective synthesis of (\pm)-*trans*-2,6-diaryl-4*H*-tetrahydrothiopyran-4-ones

Diarylideneacetone starting material (15 mmol, 1.0 equiv.) was dissolved in THF (100 mL) and an 1.2 M aqueous solution of potassium phosphate dibasic (50 mL, 60 mmol, 4.0 equiv.). The mixture was cooled to 4 °C under vigorous stirring and an atmosphere of argon. To this was added sodium hydrosulfide 75 wt% (3.36 g, 45 mmol, 3.0 equiv.). The reaction was carried on for 26 h at 4 °C, under vigorous stirring and argon. 1 M Hydrochloric acid (15 mL, except when pyridyl- or aniline-substituted compounds were synthesized) and saturated ammonium chloride (15 mL) were subsequently added to quench the reaction. The product was extracted with DCM (3 x 50 mL). The combined organic layers were dried over MgSO₄ and evaporated to dryness. Unless otherwise mentioned, desired product was purified by flash chromatography (SiO₂, EtOAc/CyHex).

(±)-trans-2,6-di-(*o*-tolyl)-4*H*-tetrahydrothiopyran-4-one (48)

White powder

Chemical Formula: C₁₉H₂₀OSMolecular Weight: 296.43 g.mol⁻¹

Yield: 96 %

d.r.(*cis/trans*) 1:32 d.e. 94 %

Previously prepared diarylideneacetone **2** (3.94 g, 15 mmol) was used as the starting material and treated according to general procedure F to afford desired product **48** as a white powder (4.27 g, 14.4 mmol, 96 %).

¹H NMR (300 MHz, CDCl₃) δ (ppm): 7.19 (m, 8H, ArH), 4.43 (ABX, $J_{AX} = 4.4$ Hz, $J_{BX} = 7.7$ Hz, 2H, H_X), 3.13 (ABX, $J_{AB} = 15.6$ Hz, $J_{AX} = 4.4$ Hz, $J_{BX} = 7.7$ Hz, $\Delta\nu = 44$ Hz, 4H, H_AH_B), 2.15 (s, 6H, Me)

¹³C NMR (75.5 MHz, CDCl₃) δ (ppm): 209.9 (C=O), 138.2 (C_q), 136.1 (C_q), 131.0 (Ar), 127.6 (Ar), 126.1 (Ar), 125.9 (Ar), 48.2 (CH₂), 39.9 (SCH_x), 18.9 (Me)

HRMS (ESI+): [M+Na]⁺ Calcd. m/z 319.113

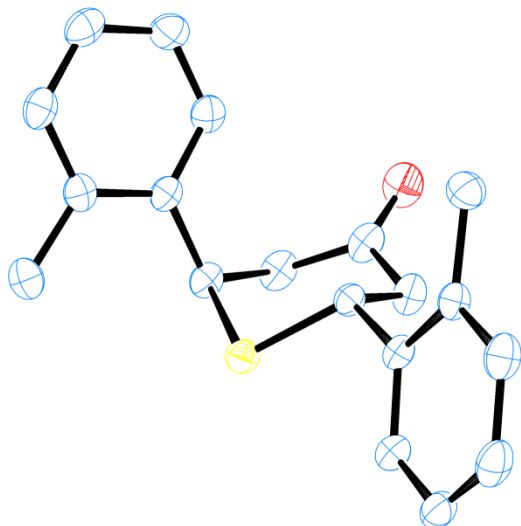
Found m/z 319.114

m.p. = 102 °C

TLC (SiO₂): 70% dichloromethane in cyclohexane

R_F = 0.46

Dark green with PMA

X-ray crystallography:

Space group (Hall): -P 2ybc

Space group (HM): P 1 21/c 1

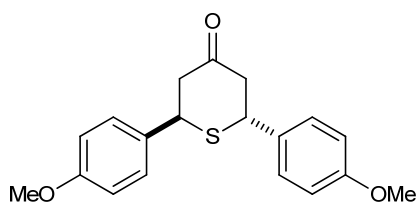
Crystal class: Monoclinic

International table #: 14

Space group multiplicity: 4

Parameters:

a = 10.4721	b = 9.0606	c = 17.1612
α = 90.00	β = 108.76	γ = 90.00

(±)-trans-2,6-di-(p-anisyl)-4H-tetrahydrothiopyran-4-one (50)

White powder
 Chemical Formula: C₁₉H₂₀O₃S
 Molecular Weight: 328.43 g.mol⁻¹
 Yield: 76 %
 d.r.(cis/trans) 1:40 d.e. 95 %

Previously prepared diarylideneacetone **1** (4.41 g, 15 mmol) was used as the starting material and treated according to general procedure F to afford desired product **50** as a white powder (3.74 g, 11.4 mmol, 76 %).

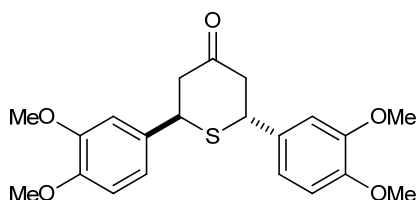
¹H NMR (300 MHz, CDCl₃) δ (ppm): 7.28 (d, ³J = 8.8 Hz, 4H, ArH), 6.87 (d, ³J = 8.8 Hz, 4H, ArH), 4.31 (ABX, ³J_{AX} = 8.1 Hz, ³J_{BX} = 4.5 Hz, 2H, H_X), 3.81 (s, 6H, OMe), 3.07 (ABX, ²J_{AB} = 14.9 Hz, ³J_{AX} = 4.5 Hz, ³J_{BX} = 8.2 Hz, 4H, H_AH_B)

¹³C NMR (75.5 MHz, CDCl₃) δ (ppm): 208.9 (C=O), 158.9 (C_q), 132.4 (C_q), 128.6 (Ar), 114.0 (Ar), 55.3 (OMe), 48.8 (CH₂), 43.3 (SCH_x)

Elemental analysis: Calcd. C 69.48 H 6.14
 Found C 69.27 H 5.97

m.p. = 144-147 °C

TLC (SiO₂): 20% ethyl acetate in cyclohexane R_F = 0.30 Red with Mostaïne

(±)-trans-2,6-di-(3,4-dimethoxyphenyl)-4H-tetrahydrothiopyran-4-one (51)

White powder
 Chemical Formula: C₂₁H₂₄O₅S
 Molecular Weight: 388.48 g.mol⁻¹
 Yield: 63 %
 d.r.(cis/trans) 1:9 d.e. 80 %

Previously prepared diarylideneacetone **6** (5.31 g, 15 mmol) was used as the starting material and treated according to general procedure F to afford desired product **51** as a white powder (3.67 g, 9.45 mmol, 63 %).

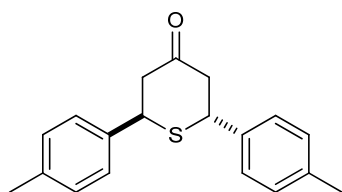
¹H NMR (300 MHz, CDCl₃) δ (ppm): 6.88 (m, 6H, ArH), 4.29 (ABX, ³J_{AX} = 7.9 Hz, ³J_{BX} = 4.4 Hz, 2H, H_X), 3.88 (s, 12H, OMe), 3.08 (ABX, ²J_{AB} = 15.0 Hz, ³J_{AX} = 7.9 Hz, ³J_{BX} = 4.4 Hz, Δv = 37 Hz, 4H, H_AH_B)

¹³C NMR (75.5 MHz, CDCl₃) δ (ppm): 208.8 (C=O), 149.0 (C_q), 148.5 (C_q), 132.9 (C_q), 119.4 (Ar), 110.9 (Ar), 110.8 (Ar), 55.9 (OMe), 48.9 (CH₂), 43.8 (SCH_x)

HRMS (ESI+): [M+Na]⁺ Calcd. m/z 411.124
 Found m/z 411.123

m.p. = 133 °C

TLC (SiO₂): 50% ethyl acetate in cyclohexane R_F = 0.36 Purple with Mostaïne

(±)-trans-2,6-di-p-tolyl-4H-tetrahydrothiopyran-4-one (52)

White powder

Chemical Formula: C₁₉H₂₀OSMolecular Weight: 296.43 g.mol⁻¹

Yield: 70 %

d.r.(cis/trans) 1:15 d.e. 88 %

Previously prepared diarylideneacetone **5** (3.94 g, 15 mmol) was used as the starting material and treated according to general procedure F to afford desired product **52** as a white powder (3.11 g, 10.5 mmol, 70 %).

¹H NMR (300 MHz, CDCl₃) δ (ppm): 7.24 (d, ³J = 8.0 Hz, 4H, ArH), 7.15 (d, ³J = 8.0 Hz, 4H, ArH), 4.33 (ABX, ³J_{AX} = 9.2 Hz, ³J_{BX} = 4.3 Hz, 2H, H_X), 4.33 (ABX, ²J_{AB} = 15.0 Hz, ³J_{AX} = 9.2 Hz, 2H, H_A), 3.08 (ABX, ²J_{AB} = 15.0 Hz, ³J_{BX} = 4.3 Hz, 2H, H_B), 2.36 (s, 6H, Me)

¹³C NMR (75.5 MHz, CDCl₃) δ (ppm): 208.8 (C=O), 137.4 (C_q), 137.3 (C_q), 129.3 (Ar), 129.4 (Ar), 48.6 (CH₂), 43.5 (SCH_x), 21.0 (Me)

HRMS (ESI+): [M+Na]⁺ Calcd. m/z 319.113

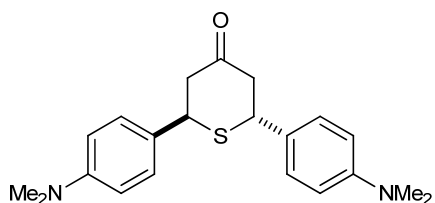
Found m/z 319.114

m.p. = 99 °C

TLC (SiO₂): 30% ethyl acetate in cyclohexane

R_F = 0.72

Brown with Mostaïne

(±)-trans-2,6-di-4-(dimethylamino)phenyl-4H-tetrahydrothiopyran-4-one (53)

Light orange powder

Chemical Formula: C₂₁H₂₆N₂OSMolecular Weight: 354.51 g.mol⁻¹

Yield: 10 %

d.r.(cis/trans) 1:19 d.e. 90 %

Previously prepared diarylideneacetone **3** (3.93 g, 15 mmol) was used as the starting material and treated according to general procedure F to afford desired product **53** as a light orange powder (532 mg, 1.5 mmol, 10 %).

¹H NMR (300 MHz, CDCl₃) δ (ppm): 7.23 (d, ³J = 8.7 Hz, 4H, ArH), 6.69 (d, ³J = 8.7 Hz, 4H, ArH), 4.31 (ABX, ³J_{AX} = 8.1 Hz, ³J_{BX} = 4.5 Hz, 2H, H_X), 3.09 (ABX, ²J_{AB} = 15.3 Hz, ³J_{AX} = 8.1 Hz, ³J_{BX} = 4.5 Hz, Δv = 43 Hz, 4H, H_AH_B), 2.95 (s, 12H, NMe₂)

¹³C NMR (75.5 MHz, CDCl₃) δ (ppm): 209.7 (C=O), 149.7 (C_q), 128.3 (Ar), 128.1 (C_q), 112.5 (Ar), 48.9 (CH₂), 43.4 (SCH_x), 40.5 (NMe₂)

HRMS (ESI+): [M+Na]⁺ Calcd. m/z 377.166

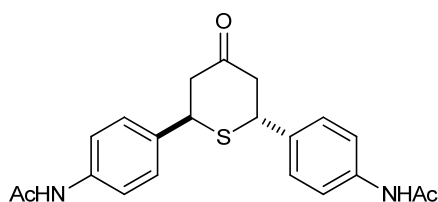
Found m/z 377.167

m.p. = 149 °C

TLC (SiO₂): ethyl acetate

R_F = 0.68

Blue with Mostaïne

(±)-trans-2,6-di-4-(N-penylacetamide)-4H-tetrahydrothiopyran-4-one (54)

White powder
 Chemical Formula: C₂₁H₂₂N₂O₃S
 Molecular Weight: 322.88 g.mol⁻¹
 Yield: 74 %
 d.r.(cis/trans) 1:19 d.e. 90 %

Previously prepared diarylideneacetone **4** (5.23 g, 15 mmol) was used as the starting material and treated according to general procedure F to afford desired product **54** as a white powder (3.58 g, 11.1 mmol, 74 %).

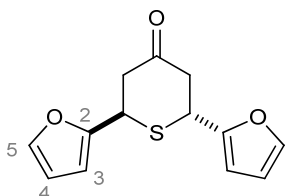
¹H NMR (400 MHz, DMSO-*d*₆) δ (ppm): 9.96 (bs, 2H, NH), 7.53 (d, ³J = 8.6 Hz, 4H, ArH), 7.28 (d, ³J = 8.6 Hz, 4H, ArH), 4.47 (ABX, ³J_{AX} = 9.0 Hz, ³J_{BX} = 4.4 Hz, 2H, H_X), 3.09 (ABX, ²J_{AB} = 15.2 Hz, ³J_{AX} = 9.0 Hz, ³J_{BX} = 4.4 Hz, Δν = 75 Hz, 4H, H_AH_B), 2.03 (s, 6H, Me)

¹³C NMR (75.5 MHz, DMSO-*d*₆) δ (ppm): 208.3 (C=O), 207.31 (C=O), 168.21 (C=O), 138.7 (C_q), 138.3 (C_q), 135.2 (C_q), 134.2 (C_q), 127.6 (Ar), 119.1 (Ar), 49.4 (CH₂), 47.7 (CH₂), 46.1 (SCH_x), 42.5 (SCH_x), 23.8 (Me)

HRMS (ESI+): [M+Na]⁺ Calcd. m/z 405.124
 Found m/z 405.125

m.p. > 250 °C (dec.)

TLC (SiO₂): 25 % ethyl acetate in cyclohexane R_F = 0.22 Blue with Mostaïne

(±)-trans-2,6-di-(furan-2-yl)-4H-tetrahydrothiopyran-4-one (55)

Yellowish sticky oil
 Chemical Formula: C₁₃H₁₂O₃S
 Molecular Weight: 248.30 g.mol⁻¹
 Yield: 69 %
 d.r.(cis/trans) 1:14 d.e. 87 %

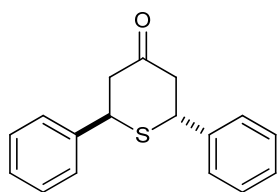
Previously prepared diarylideneacetone **24** (3.21 g, 15 mmol) was used as the starting material and treated according to general procedure F to afford desired product **55** as a yellowish oil (2.57 g, 10.35 mmol, 69 %).

¹H NMR (300 MHz, CDCl₃) δ (ppm): 7.39 (d, ³J = 2.0 Hz, 2H, H5), 6.33 (dd, ³J = 3.3 Hz, 2.0 Hz, 2H, H4), 6.21 (d, ³J = 3.3 Hz, 2H, H3), 4.46 (ABX, ³J_{AX} = 6.7 Hz, ³J_{BX} = 5.6 Hz, 2H, H_X), 3.09 (ABX, m, 4H, H_AH_B)

¹³C NMR (75.5 MHz, CDCl₃) δ (ppm): 206.2 (C=O), 152.3 (C2), 142.4 (C5), 110.4 (C4 or C3), 107.4 (C3 or C4), 46.9 (CH₂), 38.3 (SCH_x).

HRMS (ESI+): [M+Na]⁺ Calcd. m/z 271.040
 Found m/z 271.042

TLC (SiO₂): 20 % ethyl acetate in cyclohexane R_F = 0.43 Blue with Mostaïne

(±)-trans-2,6-diphenyl-4H-tetrahydrothiopyran-4-one (56)

Creamy-white solid
 Chemical Formula: C₁₇H₁₆O
 Molecular Weight: 268.37 g.mol⁻¹
 Yield: 67 %
 d.r.(cis/trans) 1:14 d.e. 87 %

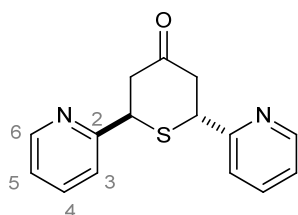
Commercial dibenzylideneacetone (3.51 g, 15 mmol) was used as the starting material and treated according to general procedure F to afford desired product **56** as a creamy-white solid after being stored in the fridge (2.7 g, 10.05 mmol, 67 %).

¹H NMR (300 MHz, CDCl₃) δ (ppm): 7.36 (m, 10H, Ph), 4.37 (ABX, ³J_{AX} = 8.0 Hz, ³J_{BX} = 4.5 Hz, 2H, H_X), 3.11 (ABX, ²J_{AB} = 15 Hz, ³J_{AX} = 8.0 Hz, ³J_{BX} = 4.5 Hz, Δv = 40 Hz, 4H, H_AH_B)

¹³C NMR (75.5 MHz, CDCl₃) δ (ppm): 208.6 (C=O), 140.3 (C_q), 128.7 (Ar), 127.6 (Ar), 127.4 (Ar), 48.5 (C_H), 43.8 (S_CH_x)

HRMS (ESI+): [M+Na]⁺ Calcd. m/z 291.081
 Found m/z 291.080

TLC (SiO₂): 15 % ethyl acetate in cyclohexane R_F = 0.3 KMnO₄

(±)-trans-2,6-di-(pyridin-2-yl)-4H-tetrahydrothiopyran-4-one (57)

White powder
 Chemical Formula: C₁₅H₁₄N₂O
 Molecular Weight: 270.35 g.mol⁻¹
 Yield: 64 %
 d.r.(cis/trans) 1:3.5 d.e. 55 %

Previously prepared diarylideneacetone **28** (3.54 g, 15 mmol) was used as the starting material and treated according to general procedure F to afford desired product **57** as a white powder (2.6 g, 9.6 mmol, 64 %). This was purified by slow elution on a flash chromatography to separate both isomers which were isolated, fully characterized and used in the next reactions as pure diastereoisomers. Description of the *cis* diastereoisomer **63** is given (*vide infra*).

¹H NMR (300 MHz, CDCl₃) δ (ppm): 8.54 (dd, ³J = 4.2 Hz, ⁴J = 1.8 Hz, 2H, H₆), 7.64 (td, ³J = 7.7 Hz, ⁴J = 1.8 Hz, 2H, H₄), 7.26 (bd, ³J = 7.7 Hz, 2H, H₃), 7.19 (ddd, ³J = 4.2 Hz, 7.7 Hz, ⁴J = 1.8 Hz, 2H, H₅), 4.61 (ABX, t, ³J = 7.0 Hz, 4.8 Hz, 2H, H_X), 3.11 (ABX, ²J_{AB} = 15.3 Hz, ³J_{AX} = 7.0 Hz, ³J_{BX} = 4.8 Hz, Δv = 26.6 Hz, 4H, H_AH_B)

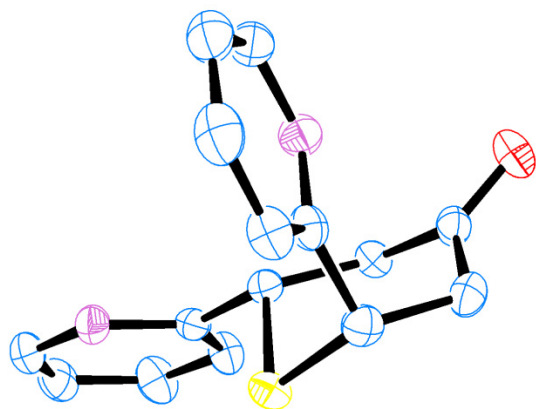
¹³C NMR (75.5 MHz, CDCl₃) δ (ppm): 206.9 (C=O), 159.8 (C₂), 149.1 (C₆), 136.9 (C₄), 122.4 (C₃ or C₅), 122.2 (C₃ or C₅), 47.0 (C_H), 45.6 (S_CH_x)

IR (neat) ν (cm⁻¹): 1702 (C=O), 1589 (C=C pyr.), 1467, 1432, 804, 749 (C-H pyr.)

Elemental analysis: Calcd. C 66.64 H 5.22 N 10.36
 Found C 66.39 H 5.16 N 10.36

m.p. = 97 °C

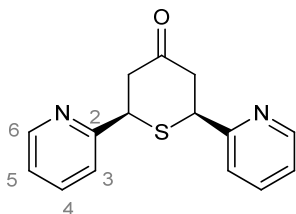
TLC (SiO₂): 70 % ethyl acetate in cyclohexane R_F = 0.39 Dark spot with PMA

(±)-trans-2,6-di-(pyridin-2-yl)-4H-tetrahydrothiopyran-4-one (57) (continued)**X-ray crystallography:**

Space group (Hall): -P 2ybc
 Space group (HM): P 1 21/c 1
 Crystal class: Monoclinic
 International table #: 14
 Space group multiplicity: 4

Parameters:

a = 11.5646 b = 9.9729 c = 23.1227
 α = 90.00 β = 98.57 γ = 90.00

cis-2,6-di-(pyridin-2-yl)-4H-tetrahydrothiopyran-4-one (63)

White powder
 Chemical Formula: C₁₅H₁₄N₂OS
 Molecular Weight: 270.35 g.mol⁻¹
 Yield: 64 %
 d.r.(cis/trans) 1:3.5 d.e. 55 %

Isolated after slow chromatography of the cude of **57**.

¹H NMR (300 MHz, CDCl₃) δ (ppm): 8.61 (d, ³J = 4.9 Hz, ⁴J = 1.9 Hz, 2H, H₆), 7.64 (td, ³J = 7.7 Hz, ⁴J = 1.9 Hz, 2H, H₄), 7.38 (bd, ³J = 7.7 Hz, 2H, H₃), 7.23 (ddd, ³J = 4.9 Hz, 7.7 Hz, ⁴J = 1.9 Hz, 2H, H₅), 4.61 (dd, ³J_{1,3-TDA} = 12.2 Hz, ³J_{cisAE} = 3.0 Hz, 2H, H_X), 3.31 (dd, ²J_{AB} = 14.0 Hz, ³J_{1,3-TDA} = 12.2 Hz, 2H, H_A), 3.04 (dd, ²J_{AB} = 14.0 Hz, ³J_{cisAE} = 3.0 Hz, 2H, H_B)

¹³C NMR (75.5 MHz, CDCl₃) δ (ppm): 208.3 (C=O), 157.9 (C₂), 149.7 (C₆), 137.0 (C₄), 123.0 (C₃ or C₅), 122.3 (C₃ or C₅), 49.7 (S-CH_X), 48.6 (CH₂)

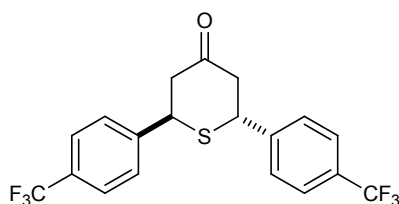
IR (neat) ν (cm⁻¹): 1696 (C=O), 1587 (C=C pyr.), 1469, 1436, 745 (C-H pyr.)

Elemental analysis:

Calcd.	C 66.64	H 5.22	N 10.36
Found	C 66.43	H 5.16	N 10.35

m.p. = 165°C dec.

TLC (SiO₂): 70 % ethyl acetate in cyclohexane R_F = 0.27 Light spot with PMA

(±)-trans-2,6-di-(4-(trifluoromethyl)phenyl)-4H-tetrahydrothiopyran-4-one (58)

White powder

Chemical Formula: C₁₉H₁₄F₆OSMolecular Weight: 404.37 g.mol⁻¹

Yield: 80 %

d.r.(cis/trans) 1:2 d.e. 33 %

Previously prepared diarylideneacetone **NW267** (5.38 g, 15 mmol) was used as the starting material and treated according to general procedure F to afford desired product **58** as a white powder (4.85 g, 12 mmol, 80 %). This was purified by slow elution on a flash chromatography to separate both isomers which were isolated, fully characterized and the (±)-trans was sent for biological evaluation as pure diastereoisomer. Description of the *cis* diastereoisomer is given (*vide infra*).

Characterization of the (±)-trans 58

¹H NMR (400 MHz, CDCl₃) δ (ppm): 7.63 (bd, ³J = 8.2 Hz, 4H, ArH), 7.49 (bd, ³J = 8.2 Hz, 4H, ArH), 4.39 (ABX, ³J_{AX} = 8.0 Hz, ³J_{BX} = 4.7 Hz, 2H, H_X), 3.13 (ABX, ²J_{AB} = 14.9 Hz, ³J_{AX} = 8.0 Hz, ³J_{BX} = 4.7 Hz, Δv = 48 Hz, 4H, H_AH_B)

¹³C NMR (100 MHz, CDCl₃) δ (ppm): 207.2 (C=O), 143.9 (C_q), 130.2 (q, ²J_{C-F} = 32.5 Hz, C_q), 127.9 (Ar), 125.8 (q, ³J_{C-F} = 3.7 Hz, Ar), 123.9 (q, ¹J_{C-F} = 272 Hz, CF₃), 48.1 (C_{H2}), 43.7 (S_CH_X)

HRMS (ESI): [M-H]⁻ Calcd. m/z 403.059

Found m/z 403.056

m.p. = 99 °C

TLC (SiO₂): 50 % ethyl acetate in cyclohexane

R_F = 0.69

Green with Mostaïne

Spectroscopic characterization of the cis isomer

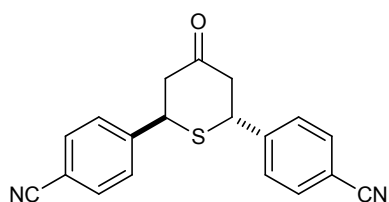
¹H NMR (400 MHz, CDCl₃) δ (ppm): 7.66 (bd, ³J = 8.3 Hz, 4H, ArH), 7.53 (d, ³J = 8.3 Hz, 4H, ArH), 4.41 (ABX, ³J_{1,3-TDA} = 11.5 Hz, ³J_{cisAE} = 4.1 Hz, 2H, H_X), 3.03 (ABX, ²J_{AB} = 13.7 Hz, ³J_{1,3-TDA} = 11.5 Hz, ³J_{cisAE} = 4.1 Hz, Δv = 44 Hz, 2H, H_AH_B)

¹³C NMR (100 MHz, CDCl₃) δ (ppm): 206.4 (C=O), 142.9 (C_q), 130.6 (q, ²J_{C-F} = 32.7 Hz, C_q), 127.7 (Ar), 126.1 (q, ³J_{C-F} = 3.6 Hz, Ar), 123.8 (q, ¹J_{C-F} = 272 Hz, CF₃), 50.1 (C_{H2}), 48.1 (S_CH_X)

TLC (SiO₂): 50 % ethyl acetate in cyclohexane

R_F = 0.54

Green with Mostaïne

(±)-trans-2,6-di-(p-benzonitrile)-4H-tetrahydrothiopyran-4-one (59)

White powder
 Chemical Formula: C₁₉H₁₄N₂OS
 Molecular Weight: 318.39 g.mol⁻¹
 Yield: 50 %
 d.r.(cis/trans) n.d. d.e. ≥ 95 %

Previously prepared diarylideneacetone **16** (4.26 g, 15 mmol) was used as the starting material and treated according to general procedure F to afford desired product **59** as a white powder (2.39 g, 7.5 mmol, 50 %).

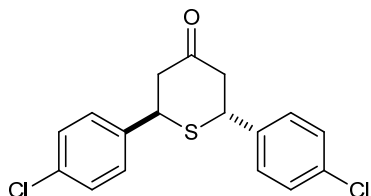
¹H NMR (300 MHz, CDCl₃) δ (ppm): 7.70 (d, ³J = 8.3 Hz, 4H, ArH), 7.52 (d, ³J = 8.3 Hz, 4H, ArH), 4.39 (ABX, ³J_{AX} = 10.5 Hz, ³J_{BX} = 5.0 Hz, 2H, H_X), 3.01 (ABX, m, 4H, H_AH_B)

¹³C NMR (75.5 MHz, CDCl₃) δ (ppm): 206.1 (C=O), 144.9 (C_q), 132.8 (Ar), 128.4 (Ar), 118.4 (C_q), 110.6 (C_q), 48.3 (CH₂), 40.2 (SCH_x)

HRMS (ESI+): [M+Na]⁺ Calcd. m/z 341.072
 Found m/z 341.073

m.p. = 202 °C

TLC (SiO₂): 10 % ethyl acetate in toluene R_F = 0.26 Green with Mostaine

(±)-trans-2,6-di-(4-chlorophenyl)-4H-tetrahydrothiopyran-4-one (60)

White powder
 Chemical Formula: C₁₇H₁₄Cl₂OS
 Molecular Weight: 337.26 g.mol⁻¹
 Yield: 77 %
 d.r.(cis/trans) 1:11 d.e. 83 %

Previously prepared diarylideneacetone **10** (4.55 g, 15 mmol) was used as the starting material and treated according to general procedure F to afford desired product **60** as a white powder (4.20 g, 12.45 mmol, 83 %).

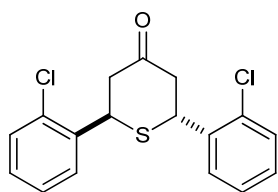
¹H NMR (300 MHz, CDCl₃) δ (ppm): 7.30 (m, 8H, ArH), 4.3 (ABX, ³J_{AX} = 8.0 Hz, ³J_{BX} = 4.7 Hz, 2H, H_X), 3.07 (ABX, ²J_{AB} = 15.0 Hz, ³J_{AX} = 8.0 Hz, ³J_{BX} = 4.7 Hz, 4H, H_AH_B)

¹³C NMR (75.5 MHz, CDCl₃) δ (ppm): 207.7 (C=O), 138.6 (C_q), 133.6 (C_q), 128.9 (Ar), 128.8 (Ar), 48.3 (CH₂), 43.4 (SCH_x)

LC/MS (ESI): [M+H]⁺ m/z 338

m.p. = 83 °C

TLC (SiO₂): 20 % ethyl acetate in cyclohexane R_F = 0.40 Yellow with Mostaine

(±)-trans-2,6-di-(2-chlorophenyl)-4H-tetrahydrothiopyran-4-one (61)

White powder

Chemical Formula: C₁₇H₁₄Cl₂OSMolecular Weight: 337.26 g.mol⁻¹

Yield: 63 %

d.r.(cis/trans) 1:7 d.e. 75 %

Previously prepared diarylideneacetone **11** (4.55 g, 15 mmol) was used as the starting material and treated according to general procedure F to afford desired product **61** as a white powder (3.19 g, 9.45 mmol, 63 %).

¹H NMR (300 MHz, CDCl₃) δ (ppm): 7.38 (m, 4H, ArH), 7.26 (m, 4H, ArH), 4.82 (ABX, t, ³J = 6.4 Hz, 2H, H_X), 3.09 (ABX, overlapping, ³J = 6.4 Hz, 4H, H_AH_B)

¹³C NMR (75.5 MHz, CDCl₃) δ (ppm): 208.48 (C=O), 137.7 (C_q), 133.5 (C_q), 130.2 (Ar), 128.9 (Ar), 127.8 (Ar), 127.1 (Ar), 47.8 (CH₂), 40.1 (SCH_x)

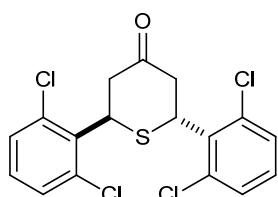
LC/MS (ESI): [M+H]⁺ m/z 338

m.p. = 119 °C

TLC (SiO₂): 20 % ethyl acetate in cyclohexane

R_F = 0.40

Yellow with Mostaine

(±)-trans-2,6-di-(2,6-dichlorophenyl)-4H-tetrahydrothiopyran-4-one (62)

White powder

Chemical Formula: C₁₇H₁₂Cl₄OSMolecular Weight: 406.15 g.mol⁻¹

Yield: 67 %

d.r.(cis/trans) n.d. d.e. ≥ 95 %

Previously prepared diarylideneacetone **12** (5.58 g, 15 mmol) was used as the starting material and treated according to general procedure F to afford desired product **62** as a white powder (4.08 g, 10.05 mmol, 67 %).

¹H NMR (300 MHz, CDCl₃) δ (ppm): 7.35 (d, ³J = 8.0 Hz, 4H, ArH in *ortho* to ArCl), 7.16 (t, ³J = 8.0 Hz, 2H, ArH in *meta* to ArCl), 5.82 (ABX, ³J_{AX} = 12.0 Hz, ³J_{BX} = 4.4 Hz, 2H, H_X), 3.91 (ABX, ²J_{AB} = 17.3 Hz, ³J_{AX} = 12.0 Hz, 2H, H_A), 2.84 (ABX, ²J_{AB} = 17.3 Hz, ³J_{BX} = 4.4 Hz, 2H, H_B)

¹³C NMR (75.5 MHz, CDCl₃) δ (ppm): 207.4 (C=O), 135.8 (C_q), 134.0 (C_q), 129.3 (Ar), 128.8 (Ar), 42.9 (CH₂), 39.0 (SCH_x)

HRMS (ESI+): [M+Na]⁺ Calcd. m/z 426.926

Found m/z 426.925

m.p. = 177 °C

TLC (SiO₂): 20 % ethyl acetate in cyclohexane

R_F = 0.41

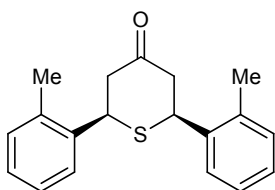
Green with Mostaine

Synthesis of *cis* isomers

General procedure G for the diastereoselective synthesis of *cis*-2,6-diaryl-4H-tetrahydrothiopyran-4-ones in purely organic medium

Diarylideneacetone starting material (15 mmol, 1.0 equiv.) and sodium hydrosulfide 75 wt% (2.22 g, 30 mmol, 2.0 equiv.) were suspended in methanol (70 mL). The mixture was refluxed under vigorous stirring and an atmosphere of argon for two hours. After being cooled to room temperature, the mixture is quenched by addition of cold 1 M hydrochloric acid (30 mL) and product was allowed to precipitate a low temperature (4 °C or -20 °C). The resulting suspension was filtered; solid was thoroughly washed with a 1:3 cold mixture of water and ethanol, and dried under high vacuum. Unless otherwise mentioned, desired product was purified by recrystallization

cis-2,6-di(*o*-tolyl)-4H-tetrahydrothiopyran-4-one (**49**)



White powder

Chemical Formula: C₁₉H₂₀OS

Molecular Weight: 296.43 g.mol⁻¹

Yield: 83 %

d.r.(*cis/trans*) n.d. d.e. ≥ 95 %

Previously prepared diarylideneacetone **2** (3.94 g, 15 mmol) was used as the starting material and treated according to general procedure G. Recrystallization in a mixture of ethyl acetate and *n*-hexane gave desired product **49** as a white powder (3.7 g, 12.45 mmol, 83 %).

¹H NMR (300 MHz, CDCl₃) δ (ppm): 7.44 (d, ³J = 7.4 Hz, 2H, ArH), 7.22 (m, 6H, ArH), 4.50 (ABX, ³J_{1,3-TDA} = 12.6 Hz, ³J_{cisAE} = 2.6 Hz, 2H, H_X), 3.03 (ABX, ²J_{AB} = 13 Hz, ³J_{1,3-TDA} = 12.6 Hz, ³J_{cisAE} = 2.6 Hz, Δν = 64 Hz, 4H, H_AH_B), 2.47 (s, 6H, Me)

¹³C NMR (75.5 MHz, CDCl₃) δ (ppm): 208.7 (C=O), 137.3 (C_q), 135.7 (C_q), 130.8 (Ar), 127.9 (Ar), 126.7 (Ar), 126.1 (Ar), 50.0 (C_{H2}), 44.6 (S_CH_X), 19.2 (Me)

HRMS (ESI+): [M+Na]⁺ Calcd. m/z 319.113

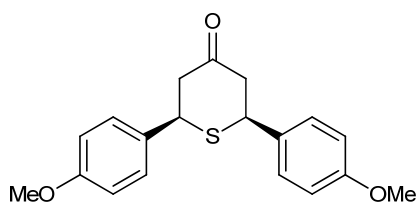
Found m/z 319.114

m.p. = 102 °C (EtOAc/*n*-hexane)

TLC (SiO₂): 20 % ethyl acetate in cyclohexane

R_F = 0.46

Green with Mostaine

***cis*-2,6-di-(*p*-anisyl)-4*H*-tetrahydrothiopyran-4-one (64)**

White powder
 Chemical Formula: C₁₉H₂₀O₃S
 Molecular Weight: 328.43 g.mol⁻¹
 Yield: 73 %
 d.r.(*cis/trans*) 32:1 d.e. 94 %

Previously prepared diarylideneacetone **1** (4.41 g, 15 mmol) was used as the starting material and treated according to general procedure G. Recrystallization in acetonitrile gave desired product **64** as a white powder (3.6 g, 11 mmol, 73 %).

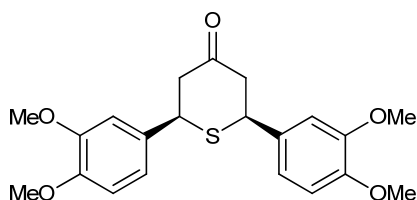
¹H NMR (300 MHz, CDCl₃) δ (ppm): 7.32 (d, ³J = 8.6 Hz, 4H, ArH), 6.9 (d, ³J = 8.6 Hz, 4H, ArH), 4.28 (ABX, ³J_{1,3-TDA} = 12.0 Hz, ³J_{cisAE} = 2.6 Hz, 2H, H_X), 3.81 (s, 6H, OMe), 2.95 (ABX, ²J_{AB} = 13.3 Hz, ³J_{AX} = 12.0 Hz, ³J_{cisAE} = 2.6 Hz, 4H, H_AH_B)

¹³C NMR (75.5 MHz, CDCl₃) δ (ppm): 208.3 (C=O), 159.1 (C_q), 131.5 (C_q), 128.3 (Ar), 114.2 (Ar), 55.2 (OMe), 50.74 (CH₂), 47.88 (SCH_X)

Elemental analysis: Calcd. C 69.48 H 6.14
 Found C 69.35 H 6.04

m.p. = 166-169 °C (Acetonitrile)

TLC (SiO₂): 10 % ethyl acetate in toluene R_F = 0.43 Red with Mostaïne

***cis*-2,6-di-(3,4-dimethoxyphenyl)-4*H*-tetrahydrothiopyran-4-one (65)**

White powder
 Chemical Formula: C₂₁H₂₄O₅S
 Molecular Weight: 388.48 g.mol⁻¹
 Yield: 67 %
 d.r.(*cis/trans*) 2,3:1 d.e. 40 %

Previously prepared diarylideneacetone **6** (5.32 g, 15 mmol) was used as the starting material and treated according to general procedure G. Recrystallization in a mixture of ethyl acetate and cyclohexane gave desired product **65** as a white powder (3.9 g, 10.1 mmol, 67 %). Subsequent column of chromatography slowly eluted (SiO₂, EtOAc/CyHex) afforded pure *cis* diastereoisomer for biological tests (spectroscopic data of this pur isomer are detailed below).

¹H NMR (300 MHz, CDCl₃) δ (ppm): 6.9 (m, 6H, ArH), 4.28 (ABX, ³J_{1,3-TDA} = 11.6 Hz, ³J_{cisAE} = 3.9 Hz, 2H, H_X), 3.91 (s, 6H, OMe), 3.89 (s, 6H, OMe), 3.05 (ABX, m, 4H, H_AH_B)

¹³C NMR (75.5 MHz, CDCl₃) δ (ppm): 208.0 (C=O), 149.2 (C_q), 148.8 (C_q), 131.9 (C_q), 119.2 (Ar), 111.3 (Ar), 110.4 (Ar), 56.0 (OMe), 50.8 (CH₂), 48.3 (SCH_X)

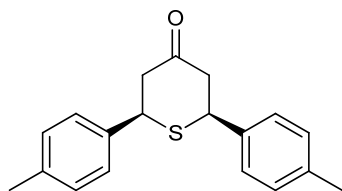
HRMS (ESI+): [M+Na]⁺ Calcd. m/z 411.124
 Found m/z 411.123

m.p. = 160 °C

TLC (SiO₂): 50 % ethyl acetate in cyclohexane R_F = 0.34 KMnO₄

General procedure H for the diastereoselective synthesis of cis-2,6-diaryl-4H-tetrahydrothiopyran-4-ones under phase-transfer catalysis

Diarylideneacetone starting material (2 mmol, 1.0 equiv.) and Aliquot® 336 (92 µL, 0.2 mmol, 0.1 equiv.) were introduced in a mixture of MTBE (20 mL) and 1.2 M aqueous solution of potassium phosphate dibasic (7 mL, 8 mmol, 4.0 equiv.) in a round-bottomed flask under argon. To this vigorously stirred diphasic solution was added sodium hydrosulfide 75 wt% (300 mg, 4 mmol, 2.0 equiv.). The reaction was heated at 55 °C for nine hours under argon and the maximal stirring. After being cooled to room temperature, the mixture was quenched by addition of cold 1 M hydrochloric acid (10 mL, except when aniline-substituted derivatives were synthesized) and saturated ammonium chloride (10 mL). Product was extracted with DCM (3 x 20 mL). The combined organic layers were dried over MgSO₄, evaporated to dryness under reduced pressure. The residue was purified by flash chromatography (SiO₂, EtOAc/CyHex unless otherwise notice).

cis-2,6-di-(p-tolyl)-4H-tetrahydrothiopyran-4-one (68)

White powder

Chemical Formula: C₁₉H₂₀OSMolecular Weight: 296.43 g.mol⁻¹

Yield: 90 %

d.r.(cis/trans) 5.7:1 d.e. 70 %

Previously prepared diarylideneacetone **5** (520 mg, 2 mmol) was used as the starting material and treated according to general procedure H. Purification by flash chromatography gave desired product **68** as a white powder (533 mg, 1.8 mmol, 90 %).

¹H NMR (300 MHz, CDCl₃) δ (ppm): 7.29 (d, ³J = 7.9 Hz, 4H, ArH), 7.18 (d, ³J = 7.9 Hz, 4H, ArH), 4.30 (ABX, ³J_{1,3-TDA} = 12.1 Hz, ³J_{cisAE} = 3.3 Hz, 2H, H_X), 2.97 (ABX, ²J_{AB} = 13.3 Hz, ³J_{1,3-TDA} = 12.1 Hz, ³J_{cisAE} = 3.3 Hz, Δv = 21 Hz, 4H, H_AH_B), 2.36 (s, 6H, Me)

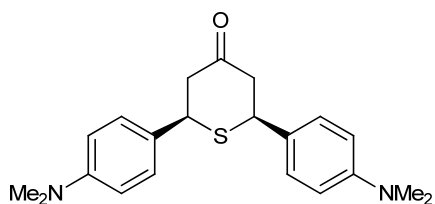
¹³C NMR (75.5 MHz, CDCl₃) δ (ppm): 208.3 (C=O), 137.9 (C_q), 136.5 (C_q), 129.6 (Ar), 127.1 (Ar), 50.6 (CH₂), 48.3 (SCH_x), 21.1 (Me)

LC/MS (ESI): [M+H]⁺ m/z 297

TLC (SiO₂): 30% ethyl acetate in cyclohexane

R_F = 0.70

Brown with Mostaine

cis-2,6-di-(4-(dimethylamino)phenyl)-4H-tetrahydrothiopyran-4-one (69)

Light orange powder
 Chemical Formula: C₂₁H₂₆N₂OS
 Molecular Weight: 354.51 g.mol⁻¹
 Yield: 82 %
 d.r.(cis/trans) 2.3:1 d.e. 40 %

Previously prepared diarylideneacetone **3** (640 mg, 2 mmol) was used as the starting material and treated according to general procedure H. Purification by flash chromatography gave desired product **69** as a light orange powder (581 mg, 1.64 mmol, 82 %).

¹H NMR (300 MHz, CDCl₃) δ (ppm): 7.13 (d, ³J = 8.9 Hz, 4H, ArH), 6.63 (d, ³J = 8.9 Hz, 4H, ArH), 4.15 (ABX, ³J_{1,3-TDA} = 12.3 Hz, ³J_{cisAE} = 3.1 Hz, 2H, H_X), 2.81 (ABX, ²J_{AB} = 13.5 Hz, ³J_{1,3-TDA} = 12.3 Hz, ³J_{cisAE} = 3.1 Hz, Δv = 14 Hz, 2H, H_AH_B), 2.87 (s, 12H, NMe₂)

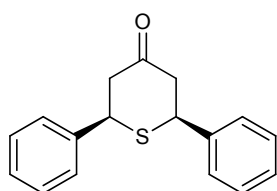
¹³C NMR (75.5 MHz, CDCl₃) δ (ppm): 209.0 (C=O), 150.1 (C_q), 127.9 (Ar), 127.3 (C_q), 112.6 (Ar), 50.9 (CH₂), 47.9 (SCH_X), 40.5 (NMe₂)

LC/MS (ESI): [M+H]⁺ m/z 355-356

TLC (SiO₂): ethyl acetate

R_F = 0.72

Orange whitth Dragendroff

cis-2,6-diphenyl-4H-tetrahydrothiopyran-4-one (70)

White powder
 Chemical Formula: C₁₇H₁₆OS
 Molecular Weight: 268.37 g.mol⁻¹
 Yield: 88 %
 d.r.(cis/trans) 4:1 d.e. 54 %

Commercial dibenzylideneacetone (470 mg, 2 mmol) was used as the starting material and treated according to general procedure H. Purification by flash chromatography gave desired product **70** as a white powder (472 mg, 1.8 mmol, 88 %).

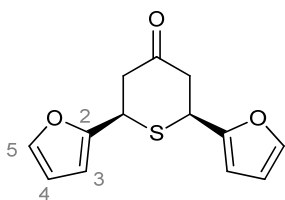
¹H NMR (300 MHz, CDCl₃) δ (ppm): 7.35 (m, 10H, ArH), 4.34 (ABX, ³J_{1,3-TDA} = 12.1 Hz, ³J_{cisAE} = 3.5 Hz, 2H, H_X), 3.00 (ABX, ²J_{AB} = 12.8 Hz, ³J_{1,3-TDA} = 12.1 Hz, ³J_{cisAE} = 3.5 Hz, 4H, H_AH_B)

¹³C NMR (75.5 MHz, CDCl₃) δ (ppm): 207.9 (C=O), 139.4 (C_q), 128.9 (Ar), 128.2 (C_q), 127.2 (Ar), 50.6 (CH₂), 48.5 (SCH_X)

TLC (SiO₂): 15 % ethyl acetate in cyclohexane

R_F = 0.3

KMnO₄

cis-2,6-di-(furan-2-yl)-4H-tetrahydrothiopyran-4-one (67)

Light orange powder

Chemical Formula: C₁₃H₁₂O₃SMolecular Weight: 248.30 g.mol⁻¹

Yield: 75 %

d.r.(cis/trans) 3:1 d.e. 50 %

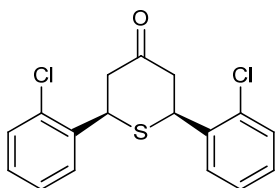
Previously prepared diarylideneacetone **24** (mg, 2 mmol) was used as the starting material and treated according to general procedure H. Purification by flash chromatography gave desired product **67** as a light orange powder (372 mg, 1.5 mmol, 75 %).

¹H NMR (300 MHz, CDCl₃) δ (ppm): 7.39 (d, ³J = 2.0 Hz, 2H, H₅), 6.34 (m, 2H, H₄), 6.24 (d, ³J = 3.4 Hz, 2H, H₃), 4.46 (ABX, ³J_{1,3-TDA} = 12.0 Hz, ³J_{cisAE} = 6.2 Hz, 2H, H_X), 3.05 (ABX, m, 4H, H_AH_B)

¹³C NMR (75.5 MHz, CDCl₃) δ (ppm): 207.0 (C=O), 152.3 (C₂), 142.5 (C₅), 110.4 (C₄ or C₃), 107.0 (C₃ or C₄), 47.5 (CH₂), 40.3 (SCH_X).

TLC (SiO₂): 20 % ethyl acetate in cyclohexaneR_F = 0.45

Blue with Mostaine

cis-2,6-di-(2-chlorophenyl)-4H-tetrahydrothiopyran-4-one (66)

White powder

Chemical Formula: C₁₇H₁₄Cl₂OSMolecular Weight: 337.26 g.mol⁻¹

Yield: 85 %

d.r.(cis/trans) 2.3:1 d.e. 40 %

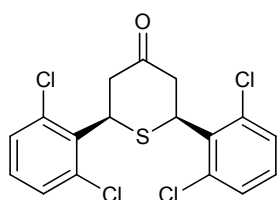
Previously prepared diarylideneacetone **11** (610 mg, 2 mmol) was used as the starting material and treated according to general procedure H. Purification by flash chromatography gave desired product **66** as a white powder (573 mg, 1.7 mmol, 85 %).

¹H NMR (300 MHz, CDCl₃) δ (ppm): 7.55 (d, ³J = 7.6, ⁴J = 1.6 Hz, 2H, ArH), 7.42 (d, ³J = 7.4, ⁴J = 1.6 Hz, 2H, ArH), 7.28 (m, 4H, ArH), 4.89 (ABX, ³J_{1,3-TDA} = 11.3 Hz, ³J_{cisAE} = 4.1 Hz, 2H, H_X), 3.01 (ABX, m, 4H, H_AH_B)

¹³C NMR (75.5 MHz, CDCl₃) δ (ppm): 208.48 (C=O), 137.6 (C_q), 132.4 (C_q), 130.2 (Ar), 128.9 (Ar), 127.8 (Ar), 127.0 (Ar), 47.2 (CH₂), 44.8 (SCH_X)

TLC (SiO₂): 20 % ethyl acetate in cyclohexaneR_F = 0.43

Yellow with Mostaine

cis-2,6-di-(2,6-dichlorophenyl)-4H-tetrahydrothiopyran-4-one (71)

White powder

Chemical Formula: C₁₇H₁₂Cl₄OSMolecular Weight: 406.15 g.mol⁻¹

Yield: 93 %

d.r.(cis/trans) 4.2:1 d.e. 62 %

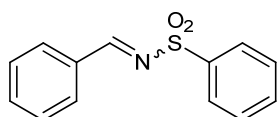
Previously prepared diarylideneacetone **12** (740 mg, 2 mmol) was used as the starting material and treated according to general procedure H. Purification by flash chromatography gave desired product **71** as a white powder (755 mg, 1.86 mmol, 93 %).

¹H NMR (300 MHz, CDCl₃) δ (ppm): 7.34 (m, 4H, ArH), 7.16 (t, ³J = 8.1 Hz, 2H, ArH in meta to ArCl), 5.25 (ABX, ³J_{1,3-TDA} = 12.8 Hz, ³J_{cisAE} = 3.0 Hz, 2H, H_x), 3.93 (ABX, bt, J ≈ 13.0 Hz, 2H, H_A), 2.84 (ABX, ²J_{AB} = 14.7 Hz, ³J_{cisAE} = 3.1 Hz, 2H, H_B)

¹³C NMR (75.5 MHz, CDCl₃) δ (ppm): 206.5 (C=O), 135.7 (C_q), 133.4 (C_q), 130.7 (Ar), 129.5 (Ar), 45.9 (CH₂), 44.6 (SCH_x)

TLC (SiO₂): 20 % ethyl acetate in cyclohexaneR_F = 0.47

Green with Mostaïne

Synthesis of the S-oxides**Synthesis of sulfoxide derivatives****N-benzylidenebenzenesulfonamide (75)**

White crystals

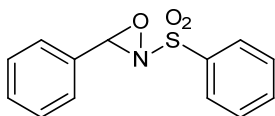
Chemical Formula: C₁₃H₁₁NO₂SMolecular Weight: 245.30 g.mol⁻¹

Yield: 80 %

Powdered 4Å molecular sieves (7 g), Amberlyst® 15 (120 mg), benzenesulfonamide (6.28 g, 40 mmol, 1.0 equiv.) and benzaldehyde (4.50 mL, 44 mmol, 1.1 equiv.) were introduced in a round-bottomed flask equipped with a Dean-Stark apparatus, in anhydrous toluene (66 mL). The suspension was then heated at 150 °C, under stirring and argon for 17 h. The reaction was then allowed to cool at room temperature and was filtered. Solid was washed with toluene (3 x 10 mL) and the liquid phase was evaporated under reduced pressure. The resulting light yellow oil was crystallized with cold *n*-pentane (if necessary the flask was stored in the fridge for two hours). Subsequent recrystallization of the white solid in ethyl acetate and pentane afforded the pure desired product **75** as white crystals (7.81 g, 31.8 mmol, 80 %)

¹H NMR (300 MHz, CDCl₃) δ (ppm): 9.07 (s, 1H, imine), 8.00 (m, 4H), 7.6 (m, 6H)

Fine for product according to the litterature.

3-Phenyl-2-(phenylsulfonyl)-1,2-oxaziridine, "Davis's oxaziridine" (74)

White crystals

Chemical Formula: C₁₃H₁₁NO₃SMolecular Weight: 261.30 g.mol⁻¹

Yield: 90 %

Previously synthesized *N*-benzylidenebenzenesulfonamide **75** (3 g, 12 mmol, 1.0 equiv.) and potassium carbonate (13.8 g, 100 mmol, 8.4 equiv.) were suspended in toluene (60 mL) and water (42 mL) in a two-necked round-bottomed flask cooled at 0 °C. Oxone[®] (8.9 g, 14.4 mmol, 1.2 equiv.) in water (42 mL) was introduced in a dropping funnel and added dropwise in the flask over 15 min, under stirring, at 0 °C. At the end of the addition, the reaction was allowed to warm at room temperature and was carried on for 45 min. The aqueous phase was separated and extracted with toluene and the combined organic layers were dried over MgSO₄ and evaporated under reduced pressure. *Warning*: evaporation must not reach dryness and rotary bath must be kept under 40 °C. Product was crystallized in the fridge and the resulting white solid was gently recrystallized in ethyl acetate and *n*-pentane to afford desired product **74** (2.82 g, 10.8 mmol, 90 %). Stored at -20 °C under argon.

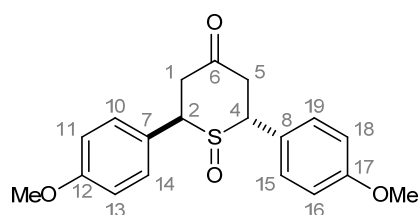
¹H NMR (300 MHz, CDCl₃) δ (ppm): 8.05 (bd d, 2H, Ar), 7.76 (m, 1H, Ar), 7.65 (m, 2H, Ar), 7.44 (m, 5H, Ar), 5.5 (s, 1H, H oxaziridine)

¹³C NMR (75.5 MHz, CDCl₃) δ (ppm): 135.0 (Ar), 134.7 (C_q), 131.5 (Ar), 130.5 (C_q), 129.4 (Ar), 129.3 (Ar), 128.8 (Ar), 128.3 (Ar), 76.3 (CH oxaziridine)

Fine for product according to the literature.

General procedure I for the synthesis of sulfoxide derivatives

Sulfide starting material (1.0 equiv.) was dissolved in anhydrous dichloromethane and the solution was cooled at -20 °C under argon. To this was added Davis's oxaziridine **74** (1.1 equiv.) in anhydrous dichloromethane (final concentration 0.05 mol.L⁻¹). The reaction was carried on for 1h30 at -20 °C under argon and then allowed to warm at room temperature for another half hour. The crude was transferred in a separating funnel with DCM, and the organic layer was washed twice with sodium thiosulfate (0.25 M). The organic layer was dried over MgSO₄ and evaporated to dryness. The resulting residue was purified by column of chromatography as mentioned in the following examples.

(±)-trans-2,6-di-(p-anisyl)-4H-tetrahydrothiopyran-4-one 1-oxide (76)

White powder

Chemical Formula: C₁₉H₂₀O₄SMolecular Weight: 344.42 g.mol⁻¹

Yield: 82 %

Previously synthesized sulfide **50** (328 mg, 1 mmol) was used as the starting material and treated according to general procedure I. Purification by flash chromatography (SiO₂, EtOAc/CyHex) gave desired product **76** as a white powder (283 mg, 0.82 mmol, 82 %).

¹H NMR (400 MHz, CDCl₃) δ (ppm): 7.28 (d, ³J = 8.7 Hz, 2H, H10-H14), 7.07 (d, ³J = 8.8 Hz, 2H, H15-H19), 6.97 (d, ³J = 8.8 Hz, 2H, H11-H13), 6.86 (d, ³J = 8.8 Hz, 2H, H16-H18), 4.78 (dd, ³J = 6.1 Hz, 2.5 Hz, 1H, H2), 3.85 (s, 3H, OMe), 3.80 (s, 3H, OMe), 3.74 (m, 1H, H_X), 3.70 (m, 1H, H5_{ax}), 3.62 (dd, ²J = 15.5 Hz, ³J = 6.1 Hz, 1H, H1_{ax}), 3.02 (ddd, ²J = 15.5 Hz, ³J = 2.5 Hz, ⁴J = 1.7 Hz, 1H, H1_{eq}), 2.59 (bdd, ²J = 12 Hz, ⁴J = 1.7 Hz, 1H, H5_{eq})

¹³C NMR (100 MHz, CDCl₃) δ (ppm): 207.2 (C6), 159.9 (C12 or C17), 159.6 (C12 or C17), 129.3 (C15-19), 129.2 (C10-14), 126.8 (C7 or C8), 125.1 (C7 or C8), 115.0 (C11-C13), 114.4 (C16-C18), 61.8 (C2), 55.5 (OMe), 55.4 (OMe), 54.9 (C4), 38.3 (C5), 35.6 (C1)

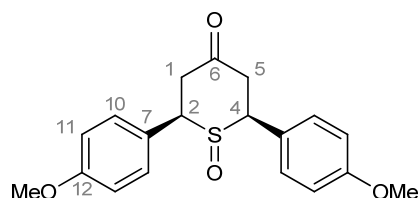
IR (neat) ν (cm⁻¹): 1713 (C=O), 1610, 1512, 1255, 1185-1176, 1038 (C-OMe), 959 (S=O), 838-829 (Ar-H)

m.p. = 173 °C dec.

TLC (SiO₂): 70 % ethyl acetate in chloroform

R_F = 0.27

Dark blue with Mostaine

cis-2,6-di-(p-anisyl)-4H-tetrahydrothiopyran-4-one 1-oxides (77 and 78)

White powder

Chemical Formula: C₁₉H₂₀O₄SMolecular Weight: 344.42 g.mol⁻¹

Yield: 86 %

d.e. 46 %

Previously synthesized sulfide **64** (328 mg, 1 mmol) was used as the starting material and treated according to general procedure I. Purification by flash chromatography (SiO₂, EtOAc/chloroforme) gave the two desired diastereoisomers, products **77** (218 mg, 0.63 mmol, 63 %) and **78** (78 mg, 0.23 mmol, 23 %) as two white powders.

Major diastereoisomer 77

¹H NMR (300 MHz, CDCl₃) δ (ppm): 7.31 (d, ³J = 8.7 Hz, 4H, H10), 6.94 (d, ³J = 8.7 Hz, 4H, H11), 4.07 (ABX, ³J_{1,3-TDA} = 13.8 Hz, ³J_{cisAE} = 2.8 Hz, 2H, H_X), 3.83 (s, 6H, OMe), 3.73 (ABX, ²J_{AB} = 14.4 Hz, ³J_{1,3-TDA} = 13.8 Hz, 2H, H_A), 2.67 (ABX, dd, ²J_{AB} = 14.4 Hz, ³J_{cisAE} = 2.8 Hz, 2H, H_B)

¹³C NMR (75.5 MHz, DMSO-d₆) δ (ppm): 205.4 (C=O), 159.7 (C12), 129.7 (C10), 128.9 (C_q), 114.7 (C11), 59.9 (S-CH_X), 55.6 (OMe), 37.9 (CH₂)

IR (neat) ν (cm⁻¹): 1709 (C=O), 1609, 1513, 1243, 1180, 1028 (C-OMe), 958 (S=O), 837 (Ar-H)

Elemental analysis: Calcd. C 66.26 H 5.85

Found C 65.96 H 5.66

m.p. = 190 °C dec.

TLC (SiO₂): 30 % ethyl acetate in chloroform

R_F = 0.38

Purple with Mostaine

cis-2,6-di-(p-anisyl)-4H-tetrahydrothiopyran-4-one 1-oxides (77 and 78) (continued)**Minor diastereoisomer 78**

¹H NMR (300 MHz, CDCl₃) δ (ppm): 7.29 (d, ³J = 9.0 Hz, 4H, H₁₀), 6.93 (d, ³J = 8.8 Hz, 4H, H₁₁), 4.11 (ABX, ³J_{1,3-TDA} = 13.6 Hz, ³J_{cisAE} = 3.0 Hz, 2H, H_X), 3.82 (s, 6H, OMe), 3.24 (ABX, ²J_{AB} = 15.0 Hz, ³J_{1,3-TDA} = 13.6 Hz, 2H, H_A), 3.01 (dd, ²J_{AB} = 15.0 Hz, ³J_{cisAE} = 3.0 Hz, 2H, H_B)

¹³C NMR (75.5 MHz, CDCl₃) δ (ppm): 203.2 (C=O), 160.1 (C₁₂), 129.4 (C₁₀), 126.3 (C₇), 114.6 (C₁₁), 66.0 (S-CH₂), 55.3 (OMe), 44.1 (CH₂)

IR (neat) ν (cm⁻¹): 1715 (C=O), 1609, 1512, 1253, 1177, 1059 (S=O), 1028 (C-OMe), 839 (Ar-H)

Elemental analysis: Calcd. C 66.26 H 5.85

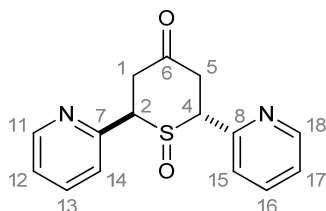
Found C 66.08 H 5.76

m.p. = 166 °C dec.

TLC (SiO₂): 30 % ethyl acetate in chloroform

R_F = 0.20

Purple with Mostaine

(±)-trans-2,6-di-(pyridin-2-yl)-4H-tetrahydrothiopyran-4-one 1-oxide (79)

White powder

Chemical Formula: C₁₅H₁₄N₂O₂S

Molecular Weight: 286.35 g.mol⁻¹

Yield: 73 %

Previously synthesized sulfide **57** (650 mg, 2.4 mmol) was used as the starting material and treated according to general procedure I. Purification by flash chromatography (SiO₂, MeOH/DCM) gave desired product **79** as a white powder (500 mg, 1.75 mmol, 73 %).

¹H NMR (300 MHz, CDCl₃) δ (ppm): 8.65 (dd, ³J = 4.8 Hz, ⁴J = 1.5 Hz, 2H, H₁₁ or 18), 8.60 (dd, ³J = 4.8 Hz, ⁴J = 1.5 Hz, 2H, H₁₁ or 18), 7.71 (td, ³J = 7.7 Hz, ⁴J = 1.8 Hz, 2H, H₁₃ or 16), 7.72 (td, ³J = 7.7 Hz, ⁴J = 1.8 Hz, 2H, H₁₃ or 16), 7.33 (bd, ³J = 7.9 Hz, 2H, H₁₄₋₁₅), 7.28 (m, 2H, H₁₂₋₁₇), 4.73 (t, ³J = 5.1 Hz, 1H, H_{2eq}), 4.56 (dd, ³J_{1,3-TDA} = 11.1 Hz, ³J_{cisAE} = 3.9 Hz, 1H, H_{4ax}), 3.55 (dd, ²J = 15.8 Hz, ³J_{1,3-TDA} = 11.1 Hz, 1H, H_{5ax}), 3.41 (dd, ²J = 15.8 Hz, ³J = 5.1 Hz, 1H, H_{1ax}), 3.06 (ddd, ²J = 15.8 Hz, ³J = 5.1 Hz, ⁴J = 1.3 Hz, 1H, H_{1eq}), 2.93 (ddd, ²J = 15.8 Hz, ³J = 3.9 Hz, ⁴J = 1.3 Hz, 1H, H_{5eq})

¹³C NMR (75.5 MHz, CDCl₃) δ (ppm): 203.5 (C=O), 154.0 (C₇ or C₈), 153.2 (C₇ or C₈), 150.4 (C₁₁ or C₁₈), 149.7 (C₁₁ or C₁₈), 137.2 (C₁₃ or C₁₆), 137.0 (C₁₃ or C₁₆), 124.8 (C₁₄ or C₁₅), 124.9 (C₁₄ or C₁₅), 123.7 (C₁₂ or C₁₇), 123.4 (C₁₂ or C₁₇), 64.3 (C₂), 59.7 (C₄), 38.0 (C₅), 37.0 (C₁)

IR (neat) ν (cm⁻¹): 1710 (C=O), 1587 (C=C pyr.), 1471, 1435, 1126, 1037 (S=O), 798-790 (Ar-H)

Elemental analysis: Calcd. C 62.92 H 4.93 N 9.78

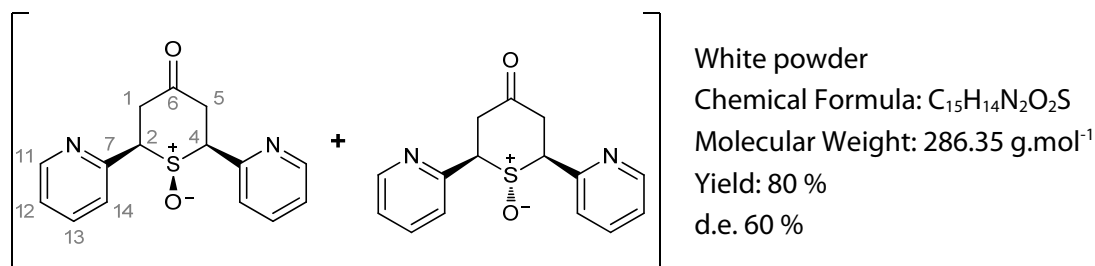
Found C 62.76 H 4.83 N 9.66

m.p. = 149 °C dec.

TLC (SiO₂): 5 % methanol in dichloromethane

R_F = 0.27

Dark blue with Mostaine

cis-2,6-di-(pyridin-2-yl)-4H-tetrahydrothiopyran-4-one 1-oxide, diastereoisomeric mixture (80)

Previously synthesized sulfide **63** (500 mg, 1.76 mmol) was used as the starting material and treated according to general procedure I. Purification by flash chromatography (SiO₂, MeOH/DCM) gave desired product **80** as a white powder (403 mg, 1.41 mmol, 80 %) as a mixture of both diastereoisomers.

Analysis performed on the mixture*Major diastereoisomer (80 mol%)*

¹H NMR (300 MHz, CDCl₃) δ (ppm): 8.66 (d, ³J = 5 Hz, 2H, H₁₁), 7.72 (td, ³J = 7.7 Hz, ⁴J = 1.9 Hz, 2H, H₁₃), 7.40 (d, ³J = 7.7 Hz, 2H, H₁₄), 7.30 (m, 2H, H₁₂), 4.30 (ABX, ³J_{1,3-TDA} = 13 Hz, ³J_{cisAE} = 3.1 Hz, 2H, H_X), 3.64 (ABX, ²J_{AB} = 16 Hz, ³J_{1,3-TDA} = 13.1 Hz, 2H, H_A), 3.02 (ABX, ²J_{AB} = 16 Hz, ³J_{cisAE} = 3.1 Hz, 2H, H_B)

¹³C NMR (75.5 MHz, CDCl₃) δ (ppm): 204.6 (C=O), 153.6 (C₇), 150.3 (C₁₁), 136.9 (C₃), 125.1 (C₁₄), 123.7 (C₁₂), 68.1 (S-CH_x), 42.1 (CH₂)

Minor diastereoisomer (20 mol%)

¹H NMR (300 MHz, CDCl₃) δ (ppm): 8.66 (d, ³J = 5 Hz, 2H, H₁₁), 7.75 (td, ³J = 7.7 Hz, ⁴J = 1.6 Hz, 2H, H₁₃), 7.40 (d, ³J = 7.7 Hz, 2H, H₁₄), 7.30 (m, 2H, H₁₂), 4.48 (ABX, ³J_{1,3-TDA} = 14.1 Hz, ³J_{cisAE} = 3 Hz, 2H, H_X), 3.83 (dd, ²J = 14.7 Hz, ³J_{1,3-TDA} = 14.1 Hz, 2H, H_A), 2.85 (dd, ²J = 14.7 Hz, ³J_{cisAE} = 3 Hz, 2H, H_B)

¹³C NMR (75.5 MHz, CDCl₃) δ (ppm): 204.8 (C=O), 154.5 (C₇), 149.9 (C₁₁), 137.3 (C₃), 125.1 (C₁₄), 122.7 (C₁₂), 64.5 (S-CH_x), 36.41 (CH₂)

IR (neat) ν (cm⁻¹): 1717 (C=O), 1587 (C=C pyr.), 1466, 1294, 1037/994 (S=O), 835-782 (Ar-H)

Elemental analysis: Calcd. C 62.92 H 4.93 N 9.78
Found C 62.75 H 5.04 N 9.51

TLC (SiO₂): 10 % methanol in dichloromethane R_F = 0.40

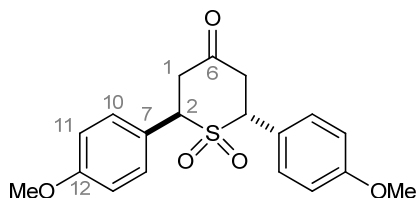
Dark blue with Mostaine

Synthesis of sulfone derivatives

General procedure J for the synthesis of sulfone derivatives

Sulfoxide starting material (1.0 equiv.) was solubilized in dichloromethane (final concentration: 0.07 mol.L⁻¹). The solution was cooled to 0 °C. When pyridyl-substituted starting materials were used, trifluoroacetic acid (2.0 equiv.) was added in the cold mixture. To this was added portionwise *m*-chloroperbenzoic acid (1.25 equiv). The reaction was carried on overnight, under argon, between 0 °C and 4 °C. The crude was transferred in a separating funnel with DCM, and the organic layer was washed twice with sodium thiosulfate (0.25 M). The organic layer was dried over MgSO₄ and evaporated to dryness. The resulting residue was purified as mentioned in the following examples.

(±)-*trans*-2,6-di-(*p*-anisyl)-4*H*-tetrahydrothiopyran-4-one 1,1-dioxide (**81**)



White powder

Chemical Formula: C₁₉H₂₀O₅S

Molecular Weight: 360.42 g.mol⁻¹

Yield: 77 %

Previously synthesized sulfoxide **76** (325 mg, 0.94 mmol) was used as the starting material and treated according to general procedure J. Purification by flash chromatography (SiO₂, EtOAc/CyHex) gave desired product **81** as a white powder (262 mg, 0.72 mmol, 77 %).

¹H NMR (300 MHz, CDCl₃) δ (ppm): 7.32 (d, ³J = 8.8 Hz, 4H, H₁₀), 6.94 (d, ³J = 8.8 Hz, 4H, H₁₁), 4.37 (ABX, ³J_{AX} = 8.2 Hz, ³J_{BX} = 5.0 Hz, 2H, H_X), 3.83 (s, 6H, OMe), 3.42 (ABX, ²J_{AB} = 16 Hz, ³J_{AX} = 8.2 Hz, ³J_{BX} = 5.0 Hz, Δν = 42 Hz, 4H, H_AH_B)

¹³C NMR (75.5 MHz, CDCl₃) δ (ppm): 203.9 (C=O), 160.5 (C₁₂), 130.7 (C₁₀), 122.0 (C₇), 114.5 (C₁₁), 60.5 (S-CH_x), 55.3 (OMe), 44.9 (CH₂)

IR (neat) ν (cm⁻¹): 1715 (C=O), 1608, 1299, 1252, 1120 (-SO₂), 1029-1021 (C-OMe), 837 (Ar-H)

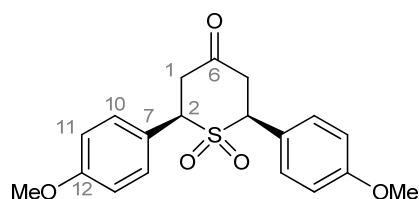
Elemental analysis: Calcd. C 63.32 H 5.59

Found C 63.19 H 5.61

m.p. = 160 °C

TLC (SiO₂): 70 % ethyl acetate in cyclohexane R_F = 0.54

Dark blue with Mostaine

(±)-cis-2,6-di-(p-anisyl)-4H-tetrahydrothiopyran-4-one 1,1-dioxide (73)

White powder

Chemical Formula: C₁₉H₂₀O₅SMolecular Weight: 360.42 g.mol⁻¹

Yield: 80 %

Previously synthesized sulfoxide (mixture of **77** and **78** without separation) (344 mg, 1 mmol) was used as the starting material and treated according to general procedure J. Purification by flash chromatography (SiO₂, EtOAc/CyHex) gave desired product **73** as a white powder (288 mg, 0.8 mmol, 80 %).

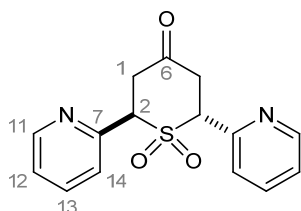
¹H NMR (300 MHz, CDCl₃) δ (ppm): 7.35 (d, ³J = 9.1 Hz, 4H, H₁₀-H₁₄), 6.93 (d, ³J = 9.1 Hz, 4H, H₁₁-H₁₃), 4.47 (ABX, ³J_{1,3-TDA} = 14.2 Hz, ³J_{cisAE} = 2.4 Hz, 2H, H_x), 3.83 (s, 6H, OMe), 3.42 (ABX, bt, J ≈ 15 Hz, H_A), 2.93 (ABX, bd, J ≈ 15 Hz, H_B)

¹³C NMR (75.5 MHz, CDCl₃) δ (ppm): 202.5 (C=O), 160.9 (C₁₂), 130.9 (C₁₀), 122.5 (C₇), 114.7 (C₁₁), 64.0 (SCH_x), 55.5 (OMe), 46.2 (CH₂)

m.p. = 190-192 °C

TLC (SiO₂): 50 % ethyl acetate in cyclohexaneR_F = 0.22

Purple with Mostaïne

(±)-trans-2,6-di-(pyridin-2-yl)-4H-tetrahydrothiopyran-4-one 1,1-dioxide (82)

White powder

Chemical Formula: C₁₅H₁₄N₂O₃SMolecular Weight: 302.35 g.mol⁻¹

Yield: 36 %

Previously synthesized sulfoxide **82** (315 mg, 1.1 mmol) was used as the starting material and treated according to general procedure J. Purification by recrystallization in a boiling mixture of methanol and chloroform (1:1) gave desired product **82** as a white powder (120 mg, 0.4 mmol, 36 %).

¹H NMR (300 MHz, DMSO-*d*₆) δ (ppm): 8.61 (dd, ³J = 4.9 Hz, ⁴J = 1.8 Hz, 2H, H₁₁), 7.87 (td, ³J = 7.7 Hz, ⁴J = 1.8 Hz, 2H, H₁₃), 7.50 (bd, ³J = 7.7 Hz, 2H, H₁₄), 7.47 (ddd, ³J = 7.7 Hz, 4.9 Hz, ⁴J = 1.0 Hz, 2H, H₁₂), 5.23 (ABX, ³J = 7.8 Hz, 5.1 Hz, 2H, H_x), 3.4-3.3 (ABX, m, 2H, H_A), 3.22 (ABX, dd, ²J_{AB} = 16.1 Hz, ³J_{BX} = 5.1 Hz, 2H, H_B)

¹³C NMR (75.5 MHz, DMSO-*d*₆) δ (ppm): 201.5 (C=O), 150.9 (C₇), 149.4 (C₁₁), 137.2 (C₁₃), 125.9 (C₁₄), 124.1 (C₁₂), 63.3 (SCH_x), 43.2 (CH₂)

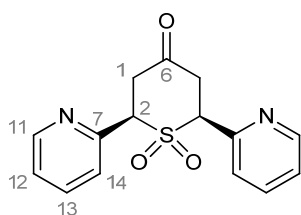
IR (neat) ν (cm⁻¹): 1716 (C=O), 1589 (C=C pyr.), 1471, 1119 (-SO₂), 838-750 (Ar-H)HRMS (ESI⁺): [M+Na]⁺ Calcd. m/z 325.062

Found m/z 325.062

m.p. = 207 °C dec. (MeOH/Chloroform)

TLC (SiO₂): 5 % methanol in dichloromethaneR_F = 0.55

Orange with Dragendorff

cis-2,6-di-(pyridin-2-yl)-4H-tetrahydrothiopyran-4-one 1,1-dioxide (83)

White powder

Chemical Formula: C₁₅H₁₄N₂O₃SMolecular Weight: 302.35 g.mol⁻¹

Yield: 92 %

Previously synthesized diastereoisomeric mixture of sulfoxide **80** (236 mg, 0.82 mmol) was used as the starting material and treated according to general procedure J. Purification by recrystallization in boiling chloroform gave desired product **83** as a white powder (230 mg, 0.75 mmol, 92 %).

¹H NMR (300 MHz, DMSO-*d*₆) δ (ppm): 8.68 (dd, ³*J* = 4.8 Hz, ⁴*J* = 1.8 Hz, 2H, H₁₁), 7.76 (td, ³*J* = 7.8 Hz, ⁴*J* = 1.8 Hz, 2H, H₁₃), 7.50 (bd, ³*J* = 7.8 Hz, 2H, H₁₄), 7.47 (ddd, ³*J* = 7.8 Hz, 4.8 Hz, ⁴*J* = 1.0 Hz, 2H, H₁₂), 4.93 (ABX, ³*J*_{1,3-TDA} = 13.0 Hz, ³*J*_{cisAE} = 3.8 Hz, 2H, H_X), 4.05 (ABX, ²*J*_{AB} = 15.5 Hz, ³*J*_{1,3-TDA} = 13.0 Hz, 2H, H_A), 3.09 (ABX, ²*J*_{AB} = 15.5 Hz, ³*J*_{cisAE} = 3.8 Hz, 2H, H_B)

¹³C NMR (75.5 MHz, DMSO-*d*₆) δ (ppm): 201.5 (C=O), 150.1 (C₁₁), 148.2 (C₇), 136.9 (C₁₃), 125.5 (C₁₄), 124.3 (C₁₂), 66.2 (SCH_X), 43.8 (CH₂)

HRMS (ESI+): [M+Na]⁺ Calcd. m/z 325.062

Found m/z 325.061

m.p. = 210 °C dec. (Chloroform)

TLC (SiO₂): 10 % methanol in dichloromethane

R_F = 0.74

Orange with Dragendorff

Biological assays

University of Paris-Sud 11 (Prof. Loiseau, BioCIS, UMR 8076 CNRS)

***L. donovani* (MHOM/ET/67/HU3) – Promastigote stage**

L. donovani Promastigote forms from logarithmic phase culture were suspended to yield 106 cells/mL. Miltefosine was used as antileishmanial reference compound. Compounds to be evaluated and Miltefosine were distributed in the plates by making a serial dilution. The final concentrations used were between 100 mM and 50 nM. Triplicates were used for each concentration. After a 3-day incubation period at 27 °C in the dark and under a 5% CO₂ atmosphere, the viability of the promastigotes was assessed using the tetrazolium-dye (MTT) colourimetric method, which measures the reduction of a tetrazolium component (MTT) into an insoluble formazan product by the mitochondria of viable cells. After incubation of the cells with the MTT reagent, a detergent solution (Triton X100, HCl) was added to lyse the cells and dissolve the coloured crystals. The absorbance at 570 nm, directly proportional to the number of viable cells, was measured using an ELISA plate reader. The results are expressed as the concentrations inhibiting parasite growth by 50% (IC₅₀)±SD after a 3-day incubation period.

***L. donovani* (MHOM/ET/67/HU3) – Amastigote stage**

L. donovani Amastigote forms were suspended to yield 107 cells/mL. The final compound concentrations used were 100 mM, 10 mM, 1 mM, 500 nM and 50 nM. Duplicates were used for each concentration. Cultures were incubated at 37 °C for 72 h in the dark and under a 5% CO₂ atmosphere, then the viability of the amastigotes was assessed using the SYBR[®] green I (Invitrogen, France) incorporation method. Parasite growth is determined by using SYBR[®] Green I, a dye with marked fluorescence enhancement upon contact with parasite DNA. Parasites were lysed following Direct PCReCell Genotyping without DNA isolation protocol (Euromedex, France). 10 ml of SYBR Green I was added to each well, and the contents were mixed. Fluorescence was measured with Mastercycler[®] ep realplex (Eppendorf, France). Fluorescence obtained was compared to those from the range obtained with different parasite densities.

University of Antwerp (Prof. Maes)

Trypanosoma brucei brucei

A suramin-sensitive strain (Squib 427) is incubated in 96-wells plates with five different concentrations of the product (64, 16, 4, 1 and 0.25 μM). After three days, parasite growth is assessed fluorimetrically following addition of resazurin. After 24 hours at 37 °C, fluorescence is measured ($\lambda_{\text{ex}} = 550 \text{ nm}$, $\lambda_{\text{em}} = 590 \text{ nm}$). The results are expressed as percentage reduction in parasite growth/viability compared to control wells, and a 50 % inhibitory concentration (IC_{50}) is calculated. Suramin is included as the reference drug ($\text{IC}_{50} = 0.12 \pm 0.07 \mu\text{M}$).

Trypanosoma cruzi

A nifurtimox-sensitive strain (Tulahuen CL2 β -galactosidase) in human lung fibroblast hMRC-5_{SV2} cells is incubated seven days in 96-wells plates with five different concentrations of the product (64, 16, 4, 1 and 0.25 μM). The parasitic burden is evaluated through the activity of the enzyme β -galactosidase on a specific substrate, the chlorophenol red β -D-galactopyranoside (CPRG). Alive parasites convert the yellow-orange CPRG substrate into the red chromophore chlorophenol red, yielding a dark red solution which can be quantitatively measured at 540 nm after 4 hours incubation at 37 °C. The results are expressed as percentage reduction in parasite growth/viability compared to control wells, and an IC_{50} is calculated. Nifurtimox is included as a reference drug ($\text{IC}_{50} = 0.845 \pm 0.2 \mu\text{M}$).

Leishmania spp.

L. infantum (MHOM/MA(BE)/67 strain) amastigote are incubated five days in 96-wells plates with five different concentrations of the product (64, 16, 4, 1 and 0.25 μM). Primary peritoneal mouse macrophages are used as host cells. Parasite burdens (i.e. number of amastigotes per macrophage) are microscopically assessed. The results are expressed as percentage reduction in parasite burden compared to untreated control wells and an IC_{50} is calculated. Pentostam[®] ($\text{IC}_{50} = 6.8 \pm 0.9 \mu\text{M}$) and miltefosin ($\text{IC}_{50} = 5.2 \pm 0.8 \mu\text{M}$) are included as the reference drug.

Toxicity

Cytotoxicity of compounds is evaluated toward human diploid embryonic lung fibroblast hMRC-5_{SV2} cells; this cell strain derived from fetal lung tissues and was firstly described in 1970. hMRC-5_{SV2} cells are cultured in 96-well plates with five different concentrations of the product (64, 16, 4, 1 and 0.25 μM). After 3 days incubation, the cell viability is assessed fluorimetrically after addition of resazurin and fluorescence is measured ($\lambda_{\text{ex}} = 550 \text{ nm}$, $\lambda_{\text{em}} = 590 \text{ nm}$). The results are expressed as percentage reduction in cells growth/viability compared to control wells, and a 50 % cytotoxic concentration is calculated. Reference cytotoxic drugs are usually not included in the test because of health hazards for laboratory personnel.

Additionally, toxicity toward mouse macrophages is qualitatively observed. Three concentrations are tested toward these cells (64, 16 and 4 μM) and the range of toxicity is indicated as follows, from the less toxic compound to the most toxic one: T1 (toxic at 64 μM), T2 (toxic at 64 and 16 μM) and T3 (toxic at 64, 16 and 4 μM).

References

- (1) Guddat, L. Editorial [Hot Topic: Drug Targets for the Treatment of Protozoan Parasitic Diseases (Guest Editor: Luke Guddat)]. *Current Topics in Medicinal Chemistry* **2011**, *11*, 2010–2011.
- (2) Singer, P. A.; Berndtson, K.; Tracy, C. S.; Cohen, E. R. M.; Masum, H.; Lavery, J. V.; Daar, A. S. A tough transition. *Nature* **2007**, *449*, 160–163.
- (3) O’Connell, D. Neglected Diseases. *Nature* **2007**, *449*, 157–157.
- (4) Feasey, N.; Wansbrough-Jones, M.; Mabey, D. C. W.; Solomon, A. W. Neglected tropical diseases. *British Medical Bulletin* **2009**, *93*, 179–200.
- (5) Butler, D. Lost in translation. *Nature* **2007**, *449*, 158–159.
- (6) Pink, R.; Hudson, A.; Mouriès, M.-A.; Bendig, M. Opportunities and Challenges in Antiparasitic Drug Discovery. *Nature Reviews Drug Discovery* **2005**, *4*, 727–740.
- (7) Cavalli, A.; Bolognesi, M. L. Neglected Tropical Diseases: Multi-Target-Directed Ligands in the Search for Novel Lead Candidates against Trypanosoma and Leishmania. *Journal of Medicinal Chemistry* **2009**, *52*, 7339–7359.
- (8) Hopkins, A. L.; Witty, M. J.; Nwaka, S. Mission possible. *Nature* **2007**, *449*, 166–169.
- (9) Hotez, P. J.; Molyneux, D. H.; Fenwick, A.; Kumaresan, J.; Sachs, S. E.; Sachs, J. D.; Savioli, L. Control of Neglected Tropical Diseases. *N Engl J Med* **2007**, *357*, 1018–1027.
- (10) Beverley, S. M. Protozoomics: trypanosomatid parasite genetics comes of age. *Nature Reviews Genetics* **2003**, *4*, 11–19.
- (11) Simpson, A. G. B.; Stevens, J. R.; Lukeš, J. The evolution and diversity of kinetoplastid flagellates. *Trends in Parasitology* **2006**, *22*, 168–174.
- (12) Stevens, J. R.; Noyes, H. A.; Dover, G. A.; Gibson, W. C. The ancient and divergent origins of the human pathogenic trypanosomes, *Trypanosoma brucei* and *T. cruzi*. *Parasitology* **1999**, *118*, 107–116.
- (13) Nwaka, S.; Ridley, R. G. Virtual drug discovery and development for neglected diseases through public–private partnerships. *Nature Rev. Drug Discov.* **2003**, *2*, 919–928.
- (14) Wenzel, I. N. Synthesis and Mechanism of Antiparasitic Mannich Base Derivatives Affecting the Redox Equilibrium of Trypanosomes and Malaria Parasites, Ruprecht-Karls-Universität Heidelberg: Heidelberg, 2009.
- (15) Brun, R.; Blum, J.; Chappuis, F.; Burri, C. Human African trypanosomiasis. *The Lancet* **2010**, *375*, 148–159.
- (16) Welburn, S.; Picozzi, K.; Fèvre, E.; Coleman, P.; Odiit, M.; Carrington, M.; Maudlin, I. Identification of human-infective trypanosomes in animal reservoir of sleeping sickness in Uganda by means of serum-resistance-associated (SRA) gene. *The Lancet* **2001**, *358*, 2017–2019.
- (17) Simarro, P. P.; Diarra, A.; Ruiz Postigo, J. A.; Franco, J. R.; Jannin, J. G. The Human African Trypanosomiasis Control and Surveillance Programme of the World Health Organization 2000–2009: The Way Forward. *PLoS Neglected Tropical Diseases* **2011**, *5*, e1007.
- (18) WHO Human African trypanosomiasis (sleeping sickness): epidemiological update. *Wkly Epidemiol Rec* **2006**, *81*, 71–80.
- (19) Barrett, M. P. The rise and fall of sleeping sickness. *The Lancet* **2006**, *367*, 1377–1378.
- (20) Checchi, F.; Filipe, J. A.; Haydon, D. T.; Chandramohan, D.; Chappuis, F. Estimates of the duration of the early and late stage of gambiense sleeping sickness. *BMC Infect Dis* **2008**, *8*, 16.
- (21) Odiit, M.; Kansime, F.; Enyaru, J. C. Duration of symptoms and case fatality of sleeping sickness caused by *Trypanosoma brucei rhodesiense* in Tororo, Uganda. *East Afr Med J* **1997**, *74*, 792–795.
- (22) Barrett, M. P.; Boykin, D. W.; Brun, R.; Tidwell, R. R. Human African trypanosomiasis: pharmacological re-engagement with a neglected disease. *British Journal of Pharmacology* **2007**, *152*, 1155–1171.
- (23) Masocha, W.; Rottenberg, M. E.; Kristensson, K. Migration of African trypanosomes across the blood–brain barrier. *Physiology & Behavior* **2007**, *92*, 110–114.
- (24) Grab, D. J.; Kennedy, P. G. Traversal of human and animal trypanosomes across the blood-brain barrier. *Journal of Neurovirology* **2008**, *14*, 344–351.

- (25) Vanhamme, L.; Pays, E. The trypanosome lytic factor of human serum and the molecular basis of sleeping sickness. *International Journal for Parasitology* **2004**, *34*, 887–898.
- (26) De Koning, H. P. Uptake of Pentamidine in *Trypanosoma brucei brucei* Mediated by Three Distinct Transporters: Implications for Cross-Resistance with Arsenicals. *Molecular Pharmacology* **2001**, *59*, 586–592.
- (27) Keiser, J. Investigations of the metabolites of the trypanocidal drug melarsoprol. *Clinical Pharmacology & Therapeutics* **2000**, *67*, 478–488.
- (28) Carter, N. S.; Fairlamb, A. H. Arsenical-resistant trypanosomes lack an unusual adenosine transporter. *Nature* **1993**, *361*, 173–176.
- (29) Jennings, F. W.; Atouguia, J. M.; Murray, M. The importance of 2,3-dimercaptopropinol (British anti-lewisite, BAL) in the trypanocidal activity of topical melarsoprol. *Acta Tropica* **1996**, *62*, 83–89.
- (30) Loiseau, P. M.; Lubert, P.; Wolf, J.-G. Contribution of Dithiol Ligands to *In Vitro* and *In Vivo* Trypanocidal Activities of Dithiaarsanes and Investigation of Ligand Exchange in an Aqueous Solution. *Antimicrobial Agents and Chemotherapy* **2000**, *44*, 2954–2961.
- (31) Fairlamb, A. H.; Henderson, G. B.; Cerami, A. Trypanothione is the primary target for arsenical drugs against African trypanosomes. *PNAS* **1989**, *86*, 2607–2611.
- (32) Iten, M.; Mett, H.; Evans, A.; Enyaru, J. C.; Brun, R.; Kaminsky, R. Alterations in ornithine decarboxylase characteristics account for tolerance of *Trypanosoma brucei rhodesiense* to D,L-alpha-difluoromethylornithine. *Antimicrobial Agents and Chemotherapy* **1997**, *41*, 1922–1925.
- (33) Bouteille, B.; Oukem, O.; Bisser, S.; Dumas, M. Treatment perspectives for human African trypanosomiasis. *Fundamental and Clinical Pharmacology* **2003**, *17*, 171–181.
- (34) Simarro, P. P.; Franco, J.; Diarra, A.; Postigo, J. A. R.; Jannin, J. Update on field use of the available drugs for the chemotherapy of human African trypanosomiasis. *Parasitology* **2012**, *139*, 842–846.
- (35) Vansterkenburg, E. L. M.; Coppens, I.; Wilting, J.; Bos, O. J. M.; Fischer, M. J. E.; Janssen, L. H. M.; Opperdoes, F. R. The uptake of the trypanocidal drug suramin in combination with low-density lipoproteins by *Trypanosoma brucei* and its possible mode of action. *Acta Tropica* **1993**, *54*, 237–250.
- (36) International Drug Price Indicator Guide **2009**.
- (37) Rassi, A.; Rassi, A.; Marin-Neto, J. A. Chagas disease. *The Lancet* **2010**, *375*, 1388–1402.
- (38) Rabinovich, J. E.; Wisnivesky-Colli, C.; Solarz, N. D.; Gurtler, R. E. Probability of transmission of Chagas disease by *triatoma infestans* (Hemiptera: *Reduviidae*) in an endemic area of Santiago del Estero, Argentina. *Bull. WHO* **1990**, *68*, 737–746.
- (39) Schmunis, G. A. Prevention of Transfusional *Trypanosoma cruzi* Infection in Latin America. *Mem Inst Oswaldo Cruz* **1999**, *94* (suppl 1), 93–101.
- (40) Bern, C.; Montgomery, S. P.; Katz, L.; Caglioti, S.; Stramer, S. L. Chagas disease and the US blood supply. *Curr Opin Infect Dis* **2008**, *21*, 476–482.
- (41) Castro, E. Chagas' disease: lessons from routine donation testing. *Transfus. Med.* **2009**, *19*, 16–23.
- (42) Signori Pereira, K.; Luis Schmidt, F.; M. A. Guaraldo, A.; M. B. Franco, R.; L. Dias, V.; A. C. Passos, L. Chagas' Disease as a Foodborne Illness. *J. Food Prot.* **2009**, *72*, 441–446.
- (43) World Health Organization Control of Chagas Disease. *WHO technical report series* **2002**.
- (44) Gascon, J.; Bern, C.; Pinazo, M.-J. Chagas disease in Spain, the United States and other non-endemic countries. *Acta Tropica* **2010**, *115*, 22–27.
- (45) Sanchez-Sancho, F.; Campillo, N. E.; Paez, J. A. Chagas Disease: Progress and New Perspectives. *Current Medicinal Chemistry* **2010**, *17*, 423–452.
- (46) Rassi, A. J.; Rassi, S. G.; Rassi, A. Sudden Death in Chagas' Disease. *Arq Bras Cardiol* **2001**, *76*, 86–96.

- (47) Maya, J. D.; Cassels, B. K.; Iturriaga-Vásquez, P.; Ferreira, J.; Faúndez, M.; Galanti, N.; Ferreira, A.; Morello, A. Mode of action of natural and synthetic drugs against *Trypanosoma cruzi* and their interaction with the mammalian host. *Comparative Biochemistry and Physiology - Part A: Molecular & Integrative Physiology* **2007**, *146*, 601–620.
- (48) Richard, J. V.; Werbovetz, K. A. New antileishmanial candidates and lead compounds. *Current Opinion in Chemical Biology* **2010**, *14*, 447–455.
- (49) Faucher, B.; Piarroux, R. Actualités sur les leishmanioses viscérales. *La Revue de Médecine Interne* **2011**, *32*, 544–551.
- (50) Pagliano, P. Visceral leishmaniasis in pregnancy: a case series and a systematic review of the literature. *Journal of Antimicrobial Chemotherapy* **2005**, *55*, 229–233.
- (51) Antinori, S.; Cascio, A.; Parravicini, C.; Bianchi, R.; Corbellino, M. Leishmaniasis among organ transplant recipients. *The Lancet Infectious Diseases* **2008**, *8*, 191–199.
- (52) Kubar, J.; Quaranta, J.-F.; Marty, P.; Lelièvre, A.; Fichoux, Y. L.; Aueuvre, J.-P. Transmission of *L. infantum* by blood donors. *Nature Medicine* **1997**, *3*, 368–368.
- (53) Cruz, I.; Morales, M.; Noguera, I.; Rodriguez, A.; Alvar, J. *Leishmania* in discarded syringes from intravenous drug users. *The Lancet* **2002**, *359*, 1124–1125.
- (54) Chawla, B.; Madhubala, R. Drug targets in *Leishmania*. *Journal of Parasitic Diseases* **2010**, *34*, 1–13.
- (55) World Health Organization. WHO Expert Committee on control of Leishmaniasis (Geneva); Meeting of the WHO Expert Committee on the Control of Leishmaniasis *Control of the leishmaniasis : report of a meeting of the WHO Expert Committee on the Control of Leishmaniasis, Geneva, 22-26 March 2010.*; World Health Organization: Geneva, 2010.
- (56) Seaman, J.; Mercer, A. J.; Sondorp, E. The Epidemic of Visceral Leishmaniasis in Western Upper Nile, Southern Sudan: Course and Impact from 1984 to 1994. *International Journal of Epidemiology* **1996**, *25*, 862–871.
- (57) Alvar, J.; Aparicio, P.; Aseffa, A.; Den Boer, M.; Canavate, C.; Dedet, J.-P.; Gradoni, L.; Ter Horst, R.; Lopez-Velez, R.; Moreno, J. The Relationship between Leishmaniasis and AIDS: the Second 10 Years. *Clinical Microbiology Reviews* **2008**, *21*, 334–359.
- (58) Mary, C.; Faraut, F.; Drogoul, M.-P.; Xeridat, B.; Schleinitz, N.; Cuisenier, B.; Dumon, H. Reference values for *leishmania infantum* parasitemia in different clinical presentations: quantitative polymerase chain reaction for therapeutic monitoring and patient follow-up. *Am. J. Trop. Med. Hyg.* **2006**, *75*, 858–863.
- (59) Haldar, A. K.; Sen, P.; Roy, S. Use of Antimony in the Treatment of Leishmaniasis: Current Status and Future Directions. *Molecular Biology International* **2011**, *2011*, 1–23.
- (60) Goodwin, L. G. Pentostam® (sodium stibogluconate); a 50-year personal reminiscence. *Transactions of the Royal Society of Tropical Medicine and Hygiene* **1995**, *89*, 339–341.
- (61) Verma, N. K.; Dey, C. S. Possible Mechanism of Miltefosine-Mediated Death of *Leishmania donovani*. *Antimicrob. Agents Chemother.* **2004**, *48*, 3010–3015.
- (62) Marinho, F. de A.; Gonçalves, K. C. da S.; Oliveira, S. S. de; Oliveira, A.-C. de S. C. de; Bellio, M.; d'Avila-Levy, C. M.; Santos, A. L. S. dos; Branquinha, M. H. Miltefosine induces programmed cell death in *Leishmania amazonensis* promastigotes. *Memórias do Instituto Oswaldo Cruz* **2011**, *106*, 507–509.
- (63) Berman, J. D. Editorial Response: U.S. Food and Drug Administration Approval of AmBisome (Liposomal Amphotericin B) for Treatment of Visceral Leishmaniasis. *Clinical Infectious Diseases* **1999**, *28*, 49–51.
- (64) Fernandez, M. M.; Malchiodi, E. L.; Algranati, I. D. Differential Effects of Paromomycin on Ribosomes of *Leishmania mexicana* and Mammalian Cells. *Antimicrob. Agents Chemother.* **2010**, *55*, 86–93.
- (65) Chawla, B.; Jhingran, A.; Panigrahi, A.; Stuart, K. D.; Madhubala, R. Paromomycin Affects Translation and Vesicle-Mediated Trafficking as Revealed by Proteomics of Paromomycin – Susceptible – Resistant *Leishmania donovani*. *PLoS ONE* **2011**, *6*, e26660.

- (66) Tebbey, P. W.; Rink, C. Target Product Profile: A renaissance for its definition and use. *J. Med. Market.* **2009**, *9*, 301–307.
- (67) G. Wyatt, P.; H. Gilbert, I.; D. Read, K.; H. Fairlamb, A. Target Validation: Linking Target and Chemical Properties to Desired Product Profile. *Current Topics in Medicinal Chemistry* **2011**, *11*, 1275–1283.
- (68) Nwaka, S.; Hudson, A. Innovative lead discovery strategies for tropical diseases. *Nature Reviews Drug Discovery* **2006**, *5*, 941–955.
- (69) Bern, C.; Adler-Moore, J.; Berenguer, J.; Boelaert, M.; Boer, M. den; Davidson, R. N.; Figueras, C.; Gradoni, L.; Kafetzis, D. A.; Ritmeijer, K.; Rosenthal, E.; Royce, C.; Russo, R.; Sundar, S.; Alvar, J. Reviews Of Anti-infective Agents: Liposomal Amphotericin B for the Treatment of Visceral Leishmaniasis. *Clinical Infectious Diseases* **2006**, *43*, 917–924.
- (70) Ashburn, T. T.; Thor, K. B. Drug repositioning: identifying and developing new uses for existing drugs. *Nature Reviews Drug Discovery* **2004**, *3*, 673–683.
- (71) Reichert, J. M. A guide to drug discovery: Trends in development and approval times for new therapeutics in the United States. *Nature Reviews Drug Discovery* **2003**, *2*, 695–702.
- (72) H. Gilbert, I.; Leroy, D.; A. Frearson, J. Finding New Hits in Neglected Disease Projects: Target or Phenotypic Based Screening? *Current Topics in Medicinal Chemistry* **2011**, *11*, 1284–1291.
- (73) Swinney, D. C.; Anthony, J. How were new medicines discovered? *Nature Reviews Drug Discovery* **2011**, *10*, 507–519.
- (74) Berriman, M. *et al.* The Genome of the African Trypanosome *Trypanosoma brucei*. *Science* **2005**, *309*, 416–422.
- (75) El-Sayed, N. M. *et al.* The Genome Sequence of *Trypanosoma cruzi*, Etiologic Agent of Chagas Disease. *Science* **2005**, *309*, 409–415.
- (76) Ivens, A. C. *et al.* The Genome of the Kinetoplastid Parasite, *Leishmania major*. *Science* **2005**, *309*, 436–442.
- (77) El-Sayed, N. M. *et al.* Comparative Genomics of Trypanosomatid Parasitic Protozoa. *Science* **2005**, *309*, 404–409.
- (78) Opperdoes, F. R. Compartmentation of Carbohydrate Metabolism in Trypanosomes. *Annu. Rev. Microbiol.* **1987**, *41*, 127–151.
- (79) Aronov, A. M. Structure-based design of submicromolar, biologically active inhibitors of trypanosomatid glyceraldehyde-3-phosphate dehydrogenase. *Proc. Natl. Acad. Sci. USA* **1999**, *96*, 4273–4278.
- (80) Ruda, G. F.; Wong, P. E.; Alibu, V. P.; Norval, S.; Read, K. D.; Barrett, M. P.; Gilbert, I. H. Aryl Phosphoramidates of 5-Phospho Erythronhydroxamic Acid, A New Class of Potent Trypanocidal Compounds. *Journal of Medicinal Chemistry* **2010**, *53*, 6071–6078.
- (81) Apt, W.; Arribada, A.; Zulantay, I.; Solari, A.; Sánchez, G.; Mundaca, K.; Coronado, X.; Rodríguez, J.; Gil, L. C.; Osuna, A. Itraconazole or allopurinol in the treatment of chronic American trypanosomiasis: the results of clinical and parasitological examinations 11 years post-treatment. *Annals of Tropical Medicine and Parasitology* **2005**, *99*, 733–741.
- (82) Molina, J.; Martins-Filho, O.; Brener, Z.; Romanha, A. J.; Loebenberg, D.; Urbina, J. A. Activities of the Triazole Derivative SCH 56592 (Posaconazole) against Drug-Resistant Strains of the Protozoan Parasite *Trypanosoma (Schizotrypanum) cruzi* in Immunocompetent and Immunosuppressed Murine Hosts. *Antimicrobial Agents and Chemotherapy* **2000**, *44*, 150–155.
- (83) Urbina, J. A.; Payares, G.; Sanoja, C.; Lira, R.; Romanha, A. J. *In vitro* and *in vivo* activities of ravuconazole on *Trypanosoma cruzi*, the causative agent of Chagas disease. *International Journal of Antimicrobial Agents* **2003**, *21*, 27–38.
- (84) Fernandes Rodrigues, J. C.; Concepcion, J. L.; Rodrigues, C.; Caldera, A.; Urbina, J. A.; de Souza, W. *In Vitro* Activities of ER-119884 and E5700, Two Potent Squalene Synthase Inhibitors, against *Leishmania amazonensis*: Antiproliferative, Biochemical, and Ultrastructural Effects. *Antimicrob. Agents Chemother.* **2008**, *52*, 4098–4114.

- (85) Wang, M. Z.; Zhu, X.; Srivastava, A.; Liu, Q.; Sweat, J. M.; Pandharkar, T.; Stephens, C. E.; Riccio, E.; Parman, T.; Munde, M.; Mandal, S.; Madhubala, R.; Tidwell, R. R.; Wilson, W. D.; Boykin, D. W.; Hall, J. E.; Kyle, D. E.; Werbovetz, K. A. Novel Arylimidamides for Treatment of Visceral Leishmaniasis. *Antimicrob. Agents Chemother.* **2010**, *54*, 2507–2516.
- (86) Bridges, D. J.; Gould, M. K.; Nerima, B.; Maser, P.; Burchmore, R. J. S.; de Koning, H. P. Loss of the High-Affinity Pentamidine Transporter Is Responsible for High Levels of Cross-Resistance between Arsenical and Diamidine Drugs in African Trypanosomes. *Molecular Pharmacology* **2007**, *71*, 1098–1108.
- (87) Willert, E.; Phillips, M. A. Regulation and function of polyamines in African trypanosomes. *Trends in Parasitology* **2012**, *28*, 66–72.
- (88) Casero, R. A.; Marton, L. J. Targeting polyamine metabolism and function in cancer and other hyperproliferative diseases. *Nature Reviews Drug Discovery* **2007**, *6*, 373–390.
- (89) Krauth-Siegel, R. L.; Bauer, H.; Schirmer, R. H. Dithiol Proteins as Guardians of the Intracellular Redox Milieu in Parasites: Old and New Drug Targets in Trypanosomes and Malaria-Causing Plasmodia. *Angewandte Chemie International Edition* **2005**, *44*, 690–715.
- (90) Williams, C. H. J. Lipoamide dehydrogenase, glutathione reductase, thioredoxin reductase, and mercuric ion reductase – A family of flavoenzyme transhydrogenases. In *Chemistry and biochemistry of flavoenzymes*; CRC Press: Boca Raton, 1991; Vol. III, pp. 121–211.
- (91) Argyrou, A.; Blanchard, J. Flavoprotein Disulfide Reductases: Advances in Chemistry and Function. In *Progress in Nucleic Acid Research and Molecular Biology*; Elsevier, 2004; Vol. 78, pp. 89–142.
- (92) Fairlamb, A. H.; Cerami, A. Metabolism and Functions of Trypanothione in the Kinetoplastida. *Annual Review of Microbiology* **1992**, *46*, 695–729.
- (93) Fairlamb, A. H.; Cerami, A. Identification of a novel, thiol-containing co-factor essential for glutathione reductase enzyme activity in trypanosomatids. *Molecular and Biochemical Parasitology* **1985**, *14*, 187–198.
- (94) Shames, S. L.; Fairlamb, A. H.; Cerami, A.; Walsh, C. T. Purification and characterization of trypanothione reductase from *Crithidia fasciculata*, a new member of the family of disulfide-containing flavoprotein reductases. *Biochemistry* **1986**, *25*, 3519–3526.
- (95) Montrichard, F.; Le Guen, F.; Laval-Martin, D. L.; Davioud-Charvet, E. Evidence for the co-existence of glutathione reductase and trypanothione reductase in the non-trypanosomatid Euglenozoa: *Euglena gracilis* Z. *FEBS Letters* **1999**, *442*, 29–33.
- (96) Fairlamb, A.; Henderson, G.; Cerami, A. The biosynthesis of trypanothione and N1-glutathionylspermidine in *Crithidia fasciculata*. *Molecular and Biochemical Parasitology* **1986**, *21*, 247–257.
- (97) Shames, S. L.; Kimmel, B. E.; Peoples, O. E.; Agabian, N.; Walsh, C. T. Trypanothione reductase of *Trypanosoma congolense*: gene isolation, primary sequence determination, and comparison to glutathione reductase. *Biochemistry* **1988**, *27*, 5014–5019.
- (98) Faerman, C. H.; Savvides, S. N.; Strickland, C.; Breidenbach, M. A.; Ponasik, J. A.; Ganem, B.; Ripoll, D.; Luise Krauth-Siegel, R.; Andrew Karplus, P. Charge is the major discriminating factor for glutathione reductase versus trypanothione reductase inhibitors. *Bioorganic & Medicinal Chemistry* **1996**, *4*, 1247–1253.
- (99) Zhang, Y.; Bond, C. S.; Bailey, S.; Cunningham, M. L.; Fairlamb, A. H.; Hunter, W. N. The crystal structure of trypanothione reductase from the human pathogen *Trypanosoma cruzi* at 2.3 Å resolution. *Protein Science* **2008**, *5*, 52–61.
- (100) Scrutton, N. S.; Raine, A. R. Cation-pi bonding and amino-aromatic interactions in the biomolecular recognition of substituted ammonium ligands. *Biochem. J.* **1996**, *319*, 1–8.
- (101) Moutiez, M.; Meziane-Cherif, D.; Aumercier, M.; Sergheraert, C.; Tartar, A. Compared Reactivities of Trypanothione and Glutathione in Conjugation Reactions. *Chemical and Pharmaceutical Bulletin* **1994**, *42*, 2641–2644.
- (102) Maya, J. D.; Bollo, S.; Nuñez-Vergara, L. J.; Squella, J. A.; Repetto, Y.; Morello, A.; Périé, J.; Chauvière, G. *Trypanosoma cruzi*: effect and mode of action of nitroimidazole and nitrofurans derivatives. *Biochemical Pharmacology* **2003**, *65*, 999–1006.

- (103) Boiani, M.; Piacenza, L.; Hernández, P.; Boiani, L.; Cerecetto, H.; González, M.; Denicola, A. Mode of action of Nifurtimox and N-oxide-containing heterocycles against *Trypanosoma cruzi*: Is oxidative stress involved? *Biochemical Pharmacology* **2010**, *79*, 1736–1745.
- (104) Dumas, C.; Ouellette, M.; Tovar, J.; Cunningham, M. L.; Fairlamb, A. H.; Tamar, S.; Olivier, M.; Papadopoulou, B. Disruption of the trypanothione reductase gene of *Leishmania* decreases its ability to survive oxidative stress in macrophages. *The EMBO Journal* **1997**, *16*, 2590–2598.
- (105) Krieger, S.; Schwarz, W.; Ariyanayagam, M. R.; Fairlamb, A. H.; Krauth-Siegel, R. L.; Clayton, C. Trypanosomes lacking trypanothione reductase are avirulent and show increased sensitivity to oxidative stress. *Molecular Microbiology* **2000**, *35*, 542–552.
- (106) Cunningham, M. L.; Zvelebil, M. J. J. M.; Fairlamb, A. H. Mechanism of inhibition of trypanothione reductase and glutathione reductase by trivalent organic arsenicals. *Eur. J. Biochem.* **1994**, *221*, 285–295.
- (107) Werbovets, K. A. Target-based drug discovery for malaria, leishmaniasis, and trypanosomiasis. *Curr. Med. Chem.* **2000**, *7*, 835–860.
- (108) Li, Z.; Fennie, M. W.; Ganem, B.; Hancock, M. T.; Kobašljija, M.; Rattendi, D.; Bacchi, C. J.; O'Sullivan, M. C. Polyamines with N-(3-phenylpropyl) substituents are effective competitive inhibitors of trypanothione reductase and trypanocidal agents. *Bioorganic & Medicinal Chemistry Letters* **2001**, *11*, 251–254.
- (109) Khan, M. O. F.; Austin, S. E.; Chan, C.; Yin, H.; Marks, D.; Vaghjiani, S. N.; Kendrick, H.; Yardley, V.; Croft, S. L.; Douglas, K. T. Use of an Additional Hydrophobic Binding Site, the Z Site, in the Rational Drug Design of a New Class of Stronger Trypanothione Reductase Inhibitor, Quaternary Alkylammonium Phenothiazines. *Journal of Medicinal Chemistry* **2000**, *43*, 3148–3156.
- (110) Fernandez-Gomez, R.; Moutiez, M.; Aumercier, M.; Bethegnies, G.; Luyckx, M.; Ouaiissi, A.; Tartar, A.; Sergheraert, C. 2-Amino diphenylsulfides as new inhibitors of trypanothione reductase. *International Journal of Antimicrobial Agents* **1995**, *6*, 111–118.
- (111) Girault, S.; Davioud-Charvet, E.; Salmon, L.; Berecibar, A.; Debreu, M.-A.; Sergheraert, C. Structure-activity relationships in 2-aminodiphenylsulfides against trypanothione reductase from *Trypanosoma cruzi*. *Bioorganic & Medicinal Chemistry Letters* **1998**, *8*, 1175–1180.
- (112) Girault, S.; Davioud-Charvet, E.; Maes, L.; Dubremetz, J.-F.; Debreu, M.-A.; Landry, V.; Sergheraert, C. Potent and specific inhibitors of trypanothione reductase from *Trypanosoma cruzi*. *Bioorganic & Medicinal Chemistry* **2001**, *9*, 837–846.
- (113) Stump, B.; Eberle, C.; Kaiser, M.; Brun, R.; Krauth-Siegel, R. L.; Diederich, F. Diaryl sulfide-based inhibitors of trypanothione reductase: inhibition potency, revised binding mode and antiprotozoal activities. *Organic & Biomolecular Chemistry* **2008**, *6*, 3935.
- (114) Henderson, G. B.; Ulrich, P.; Fairlamb, A. H.; Rosenberg, I.; Pereira, M.; Sela, M.; Cerami, A. "Subversive" substrates for the enzyme trypanothione disulfide reductase: alternative approach to chemotherapy of Chagas disease. *Proceedings of the National Academy of Sciences* **1988**, *85*, 5374–5378.
- (115) Blumenstiel, K.; Schöneck, R.; Yardley, V.; Croft, S. L.; Krauth-Siegel, R. L. Nitrofurans as common subversive substrates of *Trypanosoma cruzi* lipoamide dehydrogenase and trypanothione reductase. *Biochemical Pharmacology* **1999**, *58*, 1791–1799.
- (116) Julião, M. S. da S.; Ferreira, E. I.; Ferreira, N. G.; Serrano, S. H. P. Voltammetric detection of the interactions between RNO₂⁻ and electron acceptors in aqueous medium at highly boron doped diamond electrode (HBDDE). *Electrochimica Acta* **2006**, *51*, 5080–5086.
- (117) Hall, B. S.; Bot, C.; Wilkinson, S. R. Nifurtimox Activation by Trypanosomal Type I Nitroreductases Generates Cytotoxic Nitrile Metabolites. *Journal of Biological Chemistry* **2011**, *286*, 13088–13095.
- (118) Stewart, M. L.; Bueno, G. J.; Baliani, A.; Klenke, B.; Brun, R.; Brock, J. M.; Gilbert, I. H.; Barrett, M. P. Trypanocidal Activity of Melamine-Based Nitroheterocycles. *Antimicrobial Agents and Chemotherapy* **2004**, *48*, 1733–1738.
- (119) Baliani, A.; Peal, V.; Gros, L.; Brun, R.; Kaiser, M.; Barrett, M. P.; Gilbert, I. H. Novel functionalized melamine-based nitroheterocycles: synthesis and activity against trypanosomatid parasites. *Organic & Biomolecular Chemistry* **2009**, *7*, 1154.

- (120) Davies, C.; Cardozo, R. M.; Negrette, O. S.; Mora, M. C.; Chung, M. C.; Basombrio, M. A. Hydroxymethylnitrofurazone Is Active in a Murine Model of Chagas' Disease. *Antimicrobial Agents and Chemotherapy* **2010**, *54*, 3584–3589.
- (121) Davioud-Charvet, E.; McLeish, M. J.; Veine, D.; Giegel, D.; Andricopulo, A. D.; Becker, K.; Müller, S. Mechanism-based inactivation of thioredoxin reductase from *Plasmodium falciparum* by Mannich bases. Implications for drug design. In *Flavins and flavoproteins 2002*; Chapman, S.; Perham, R.; Scrutton, N., Eds.; Weber, Agency for Scientific Publ.: Berlin, 2002; pp. 845–851.
- (122) Davioud-Charvet, E.; McLeish, M. J.; Veine, D. M.; Giegel, D.; Arscott, L. D.; Andricopulo, A. D.; Becker, K.; Müller, S.; Schirmer, R. H.; Williams, C. H.; Kenyon, G. L. Mechanism-Based Inactivation of Thioredoxin Reductase from *Plasmodium falciparum* by Mannich Bases. Implication for Cytotoxicity. *Biochemistry* **2003**, *42*, 13319–13330.
- (123) Lee, B.; Bauer, H.; Melchers, J.; Ruppert, T.; Rattray, L.; Yardley, V.; Davioud-Charvet, E.; Krauth-Siegel, R. L. Irreversible Inactivation of Trypanothione Reductase by Unsaturated Mannich Bases: A Divinyl Ketone as Key Intermediate. *Journal of Medicinal Chemistry* **2005**, *48*, 7400–7410.
- (124) Krauth-Siegel, R. L.; Davioud-Charvet, E. Trypanothione reductase and other flavoenzymes as targets of antiparasitic drugs. In *Flavins and Flavoproteins 2005*; Nishino, T.; Miura, R.; Tanokura, M.; Fukui, K., Eds.; Tokyo, Japan, 2005; pp. 867–876.
- (125) Wenzel, I. N.; Wong, P. E.; Maes, L.; Müller, T. J. J.; Krauth-Siegel, R. L.; Barrett, M. P.; Davioud-Charvet, E. Unsaturated Mannich Bases Active Against Multidrug-Resistant *Trypanosoma brucei* Strains. *ChemMedChem* **2009**, *4*, 339–351.
- (126) Esatbeyoglu, T.; Huebbe, P.; Ernst, I. M. A.; Chin, D.; Wagner, A. E.; Rimbach, G. Curcumin-From Molecule to Biological Function. *Angewandte Chemie International Edition* **2012**, *51*, 5308–5332.
- (127) Masuda, T.; Jitoe, A.; Isobe, J.; Nakatani, N.; Yonemori, S. Anti-oxidative and anti-inflammatory curcumin-related phenolics from rhizomes of *Curcuma domestica*. *Phytochemistry* **1993**, *32*, 1557–1560.
- (128) Kanai, M.; Yoshimura, K.; Asada, M.; Imaizumi, A.; Suzuki, C.; Matsumoto, S.; Nishimura, T.; Mori, Y.; Masui, T.; Kawaguchi, Y.; Yanagihara, K.; Yazumi, S.; Chiba, T.; Guha, S.; Aggarwal, B. B. A phase I/II study of gemcitabine-based chemotherapy plus curcumin for patients with gemcitabine-resistant pancreatic cancer. *Cancer Chemotherapy and Pharmacology* **2010**, *68*, 157–164.
- (129) Carroll, R. E.; Benya, R. V.; Turgeon, D. K.; Vareed, S.; Neuman, M.; Rodriguez, L.; Kakarala, M.; Carpenter, P. M.; McLaren, C.; Meyskens, F. L.; Brenner, D. E. Phase IIa Clinical Trial of Curcumin for the Prevention of Colorectal Neoplasia. *Cancer Prevention Research* **2011**, *4*, 354–364.
- (130) Weber, W. M.; Hunsaker, L. A.; Abcouwer, S. F.; Deck, L. M.; Vander Jagt, D. L. Anti-oxidant activities of curcumin and related enones. *Bioorganic & Medicinal Chemistry* **2005**, *13*, 3811–3820.
- (131) Smerbeck, R. V.; Pittz, E. P. Dibenzalacetone and benzylcinnamate as non-steroidal anti-inflammatory compounds and compositions thereof **1986**. US Patent 4587260
- (132) Wang, Y.; Xiao, J.; Zhou, H.; Yang, S.; Wu, X.; Jiang, C.; Zhao, Y.; Liang, D.; Li, X.; Liang, G. A Novel Monocarbonyl Analogue of Curcumin, (1E, 4E)-1,5-Bis(2,3-dimethoxyphenyl)penta-1,4-dien-3-one, Induced Cancer Cell H460 Apoptosis via Activation of Endoplasmic Reticulum Stress Signaling Pathway. *Journal of Medicinal Chemistry* **2011**, *54*, 3768–3778.
- (133) Otori, H.; Yamakoshi, H.; Tomizawa, M.; Shibuya, M.; Kakudo, Y.; Takahashi, A.; Takahashi, S.; Kato, S.; Suzuki, T.; Ishioka, C.; Iwabuchi, Y.; Shibata, H. Synthesis and biological analysis of new curcumin analogues bearing an enhanced potential for the medicinal treatment of cancer. *Molecular Cancer Therapeutics* **2006**, *5*, 2563–2571.
- (134) Pati, H. N.; Das, U.; Quail, J. W.; Kawase, M.; Sakagami, H.; Dimmock, J. R. Cytotoxic 3,5-bis(benzylidene)piperidin-4-ones and N-acyl analogs displaying selective toxicity for malignant cells. *European Journal of Medicinal Chemistry* **2008**, *43*, 1–7.
- (135) Liang, G.; Shao, L.; Wang, Y.; Zhao, C.; Chu, Y.; Xiao, J.; Zhao, Y.; Li, X.; Yang, S. Exploration and synthesis of curcumin analogues with improved structural stability both in vitro and in vivo as cytotoxic agents. *Bioorganic & Medicinal Chemistry* **2009**, *17*, 2623–2631.

- (136) Yuan, K.; Song, B.; Jin, L.; Xu, S.; Hu, D.; Xu, X.; Yang, S. Synthesis and biological evaluation of novel 1-aryl, 5-(phenoxy-substituted)aryl-1,4-pentadien-3-one derivatives. *MedChemComm* **2011**, *2*, 585.
- (137) Weber, W. M.; Hunsaker, L. A.; Roybal, C. N.; Bobrovnikova-Marjon, E. V.; Abcouwer, S. F.; Royer, R. E.; Deck, L. M.; Vander Jagt, D. L. Activation of NF κ B is inhibited by curcumin and related enones. *Bioorganic & Medicinal Chemistry* **2006**, *14*, 2450–2461.
- (138) Qiu, X.; Du, Y.; Lou, B.; Zuo, Y.; Shao, W.; Huo, Y.; Huang, J.; Yu, Y.; Zhou, B.; Du, J.; Fu, H.; Bu, X. Synthesis and Identification of New 4-Arylidene Curcumin Analogues as Potential Anticancer Agents Targeting Nuclear Factor- κ B Signaling Pathway. *Journal of Medicinal Chemistry* **2010**, *53*, 8260–8273.
- (139) Cui, M.; Ono, M.; Kimura, H.; Liu, B.; Saji, H. Synthesis and Structure–Affinity Relationships of Novel Dibenzylideneacetone Derivatives as Probes for β -Amyloid Plaques. *Journal of Medicinal Chemistry* **2011**, *54*, 2225–2240.
- (140) Changtam, C.; de Koning, H. P.; Ibrahim, H.; Sajid, M. S.; Gould, M. K.; Suksamrarn, A. Curcuminoid analogs with potent activity against Trypanosoma and Leishmania species. *European Journal of Medicinal Chemistry* **2010**, *45*, 941–956.
- (141) Suarez, J. A. Q.; Maria, D. A.; Rando, D. G.; Martins, C. A. S.; Pardi, P. C.; De, S. Methods to prepare penta-1,4-dien-3-ones and substituted cyclohexanones and derivatives with antitumoral and antiparasitic properties, the compounds and their uses. **2008**, 98 pp. WO2008003155A2
- (142) Angiolini, L.; Ghedini, N.; Tramontini, M. The Mannich Bases in Polymer Synthesis. 10. Synthesis of poly(b-ketothioethers) and their behaviour towards hydroperoxyde reagents. *Polymer Communications* **1985**, *26*, 218–221.
- (143) Fairlamb, I. J. S.; Kapdi, A. R.; Lee, A. F. η^2 -dba Complexes of Pd(0): The Substituent Effect in Suzuki–Miyaura Coupling. *Organic Letters* **2004**, *6*, 4435–4438.
- (144) Qadir, M.; Möchel, T.; Hii, K. K. (Mimi) Examination of Ligand Effects in the Heck Arylation Reaction. *Tetrahedron* **2000**, *56*, 7975–7979.
- (145) Kürti, L.; Czako, B. *Strategic applications of named reactions in organic synthesis : background and detailed mechanisms*; Elsevier: Amsterdam, 2005.
- (146) Howell, J. A. S.; O'Leary, P. J.; Yates, P. C.; Goldschmidt, Z.; Gottlieb, H. E.; Hezroni-Langerman, D. Acyclic O- and N-substituted pentadienyl cations: Structural characterisation, cyclisation and computational results. *Tetrahedron* **1995**, *51*, 7231–7246.
- (147) Nair, V.; Mathew, S. C.; Biju, A. T.; Suresh, E. A Novel Reaction of the "Huisgen Zwitterion" with Chalcones and Dienones: An Efficient Strategy for the Synthesis of Pyrazoline and Pyrazolopyridazine Derivatives. *Angewandte Chemie International Edition* **2007**, *46*, 2070–2073.
- (148) Conard, C. R.; Dolliver, M. A. Dibenzalacetone. *Organic Syntheses* **1932**, *12*, 22.
- (149) Furniss, B. S.; Vogel, A. I. *Vogel's textbook of practical organic chemistry*; Longman: New York [u.a.], 2000.
- (150) Rule, N. G.; Detty, M. R.; Kaeding, J. E.; Sinicropi, J. A. Syntheses of 4H-Thiopyran-4-one 1,1-Dioxides as Precursors to Sulfone-Containing Analogs of Tetracyanoquinodimethane. *The Journal of Organic Chemistry* **1995**, *60*, 1665–1673.
- (151) Marvel, C. S.; Stille, J. K. Preparation of the Pyridalacetones and the Inductive Effect of Nitrogen on the Dehydration of the Intermediate Aldols. *Journal of Organic Chemistry* **1957**, *22*, 1451–1457.
- (152) Sehna, P.; Taghzouti, H.; Fairlamb, I. J. S.; Jutand, A.; Lee, A. F.; Whitwood, A. C. Heteroaromatic Analogues of Dibenzylideneacetone (dba) and Pd₂(het-dba)₃ Complexes: Effect of a Thienyl Moiety on the Reactivity of Pd(η^2 -th[n]-dba)(PPh₃)₂/Pd(PPh₃)₂ (n=1 or 2) and Pd(η^2 -th₂-dba)(dppe)/Pd(dppe) in Oxidative Addition Reactions with Iodobenzene. *Organometallics* **2009**, *28*, 824–829.
- (153) Corbel, B.; Medinger, L.; Haelters, J. P.; Sturtz, G. An Efficient Synthesis of Dialkyl 2-Oxoalkanephosphonates and Diphenyl-2-oxoalkylphosphine Oxides from 1-Chloroalkyl Ketones. *Synthesis* **1985**, *1985*, 1048–1051.

- (154) Perkow, W. Umsetzungen mit Alkylphosphiten. I. Mitteil.: Umlagerungen bei der Reaktion mit Chloral und Bromal. *Chemische Berichte* **1954**, *87*, 755–758.
- (155) Cao, B.; Wang, Y.; Ding, K.; Neamati, N.; Long, Y.-Q. Synthesis of the pyridinyl analogues of dibenzylideneacetone (pyr-dba) via an improved Claisen–Schmidt condensation, displaying diverse biological activities as curcumin analogues. *Organic & Biomolecular Chemistry* **2012**, *10*, 1239.
- (156) Braun, R. U.; Ansorge, M.; Müller, T. J. J. Coupling–Isomerization Synthesis of Chalcones. *Chemistry - A European Journal* **2006**, *12*, 9081–9094.
- (157) Müller, T. Synthesis of Carbo- and Heterocycles via Coupling–Isomerization Reactions. *Synthesis* **2011**, *2012*, 159–174.
- (158) Schramm (née Dediu), O. G.; Müller, T. J. J. Microwave-Accelerated Coupling–Isomerization Reaction (MACIR) – A General Coupling–Isomerization Synthesis of 1,3-Diarylprop-2-en-1-ones. *Advanced Synthesis & Catalysis* **2006**, *348*, 2565–2570.
- (159) Brandsma, L.; Heus-Kloos, Y. A.; Heiden, R. van der; Verkruijse, H. D. *Preparative acetylenic chemistry*; Elsevier: Amsterdam; New York, 1988.
- (160) Kuijl, C.; Savage, N. D. L.; Marsman, M.; Tuin, A. W.; Janssen, L.; Egan, D. A.; Ketema, M.; van den Nieuwendijk, R.; van den Eeden, S. J. F.; Geluk, A.; Poot, A.; van der Marel, G.; Beijersbergen, R. L.; Overkleeft, H.; Ottenhoff, T. H. M.; Neefjes, J. Intracellular bacterial growth is controlled by a kinase network around PKB/AKT1. *Nature* **2007**, *450*, 725–730.
- (161) Kim, P.; Kang, S.; Boshoff, H. I.; Jiricek, J.; Collins, M.; Singh, R.; Manjunatha, U. H.; Niyomrattanakit, P.; Zhang, L.; Goodwin, M.; Dick, T.; Keller, T. H.; Dowd, C. S.; Barry, C. E. Structure–Activity Relationships of Antitubercular Nitroimidazoles. 2. Determinants of Aerobic Activity and Quantitative Structure–Activity Relationships. *Journal of Medicinal Chemistry* **2009**, *52*, 1329–1344.
- (162) Maruta, Y. Antimicrobial stress compounds from *Hypochoeris radicata*. *Phytochemistry* **1995**, *38*, 1169–1173.
- (163) White, J.; Grether, U.; Lee, C.-S. (R)-(+)-3,4-dimethylcyclohex-2-en-1-one. *Organic Syntheses* **2005**, *82*, 108–114.
- (164) Rosenmund, K. W. Über eine neue Methode zur Darstellung von Aldehyden. 1. Mitteilung. *Berichte der deutschen chemischen Gesellschaft* **1918**, *51*, 585–593.
- (165) Wu, Z.; Minhas, G. S.; Wen, D.; Jiang, H.; Chen, K.; Zimniak, P.; Zheng, J. Design, Synthesis, and Structure–Activity Relationships of Haloenol Lactones: Site-Directed and Isozyme-Selective Glutathione S-Transferase Inhibitors. *Journal of Medicinal Chemistry* **2004**, *47*, 3282–3294.
- (166) Kim, M. S.; Choi, Y. M.; An, D. K. Lithium diisobutyl-t-butoxyaluminum hydride, a new and efficient reducing agent for the conversion of esters to aldehydes. *Tetrahedron Letters* **2007**, *48*, 5061–5064.
- (167) Sydorenko, N.; Hsung, R. P.; Vera, E. L. Torquoselective 6π -Electron Electrocyclic Ring Closure of 1-Azatrienenes Containing Acyclic Chirality at the C-Terminus. *Organic Letters* **2006**, *8*, 2611–2614.
- (168) Eitel, M.; Pindur, U. Selective Wittig Reactions for the Synthesis of Variously Substituted 2-Vinylindoles. *Synthesis* **1989**, *1989*, 364–367.
- (169) de Figueiredo, R. M.; Berner, R.; Julis, J.; Liu, T.; Türp, D.; Christmann, M. Bidirectional, Organocatalytic Synthesis of Lepidopteran Sex Pheromones. *The Journal of Organic Chemistry* **2007**, *72*, 640–642.
- (170) Sís̃a, M.; Pla, D.; Altuna, M.; Francesch, A.; Cuevas, C.; Albericio, F.; Álvarez, M. Total Synthesis and Antiproliferative Activity Screening of (\pm)-Aplicyanins A, B and E and Related Analogues. *Journal of Medicinal Chemistry* **2009**, *52*, 6217–6223.
- (171) Cresp, T. M.; Sargent, M. V.; Vogel, P. A synthesis of $\alpha\beta$ -unsaturated aldehydes. *Journal of the Chemical Society, Perkin Transactions 1* **1974**, *37*.
- (172) Nielsen, T. E.; Quement, S. L.; Tanner, D. Palladium-Catalyzed Silastannation of Secondary Propargylic Alcohols and their Derivatives. *Synthesis* **2004**, *2004*, 1381–1390.
- (173) Darcel, C. Stereoselective synthesis of β -ketoesters from prop-2-yn-1-ols. *Tetrahedron* **1997**, *53*, 9241–9252.

- (174) Midland, M. M. Preparation of monolithium acetylide in tetrahydrofuran. Reaction with aldehydes and ketones. *The Journal of Organic Chemistry* **1975**, *40*, 2250–2252.
- (175) Leardi, R. Experimental design in chemistry: A tutorial. *Analytica Chimica Acta* **2009**, *652*, 161–172.
- (176) Kappe, C. O. Controlled Microwave Heating in Modern Organic Synthesis. *Angewandte Chemie International Edition* **2004**, *43*, 6250–6284.
- (177) Chinchilla, R.; Nájera, C. The Sonogashira Reaction: A Booming Methodology in Synthetic Organic Chemistry. *Chemical Reviews* **2007**, *107*, 874–922.
- (178) Box, G. E. P.; Behnken, D. W. Some New Three Level Designs for the Study of Quantitative Variables. *Technometrics* **1960**, *2*, 455–475.
- (179) Ferreira, S. L. C.; Bruns, R. E.; Ferreira, H. S.; Matos, G. D.; David, J. M.; Brandão, G. C.; da Silva, E. G. P.; Portugal, L. A.; dos Reis, P. S.; Souza, A. S.; dos Santos, W. N. L. Box-Behnken design: An alternative for the optimization of analytical methods. *Analytica Chimica Acta* **2007**, *597*, 179–186.
- (180) Derringer, G.; Suich, R. Simultaneous Optimization of Several Response Variables. *Journal of Quality Technology* **1980**, *12*, 214–219.
- (181) Jacobs, J. P.; Jones, C. M.; Baille, J. P. Characteristics of a Human Diploid Cell Designated MRC-5. *Nature* **1970**, *227*, 168–170.
- (182) Tetko, I. V.; Gasteiger, J.; Todeschini, R.; Mauri, A.; Livingstone, D.; Ertl, P.; Palyulin, V. A.; Radchenko, E. V.; Zefirov, N. S.; Makarenko, A. S.; Tanchuk, V. Y.; Prokopenko, V. V. Virtual Computational Chemistry Laboratory – Design and Description. *Journal of Computer-Aided Molecular Design* **2005**, *19*, 453–463.
- (183) On-line Lipophilicity/Aqueous Solubility Calculation Software <http://www.vcclab.org/lab/alogps/> (accessed Sep 10, 2012).
- (184) Kuhl, H. Comparative Pharmacology of Newer Progestogens. *Drugs* **1996**, *51*.
- (185) Kuhn, W.; Fritze, K. H.; Hegele-Hartung, C.; Krattenmacher, R. Comparative progestational activity of norgestimate, levonorgestrel-oxime and levonorgestrel in the rat and binding of these compounds to the progesterone receptor. *Contraception* **1995**, *51*, 131–139.
- (186) Jousserandot, A.; Boucher, J.-L.; Henry, Y.; Niklaus, B.; Clement, B.; Mansuy, D. Microsomal Cytochrome P450 Dependent Oxidation of N-Hydroxyguanidines, Amidoximes, and Ketoximes: Mechanism of the Oxidative Cleavage of Their CN(OH) Bond with Formation of Nitrogen Oxides. *Biochemistry* **1998**, *37*, 17179–17191.
- (187) Kumpulainen, H.; Mähönen, N.; Laitinen, M.-L.; Jaurakkajärvi, M.; Raunio, H.; Juvonen, R. O.; Vepsäläinen, J.; Järvinen, T.; Rautio, J. Evaluation of Hydroxyimine as Cytochrome P450-Selective Prodrug Structure. *Journal of Medicinal Chemistry* **2006**, *49*, 1207–1211.
- (188) Chung, M. C.; Ferreira, E. I.; Santos, J. L.; Giarolla, J.; Rando, D. G.; Almeida, A. E.; Bosquesi, P. L.; Menegon, R. F.; Blau, L. Prodrugs for the Treatment of Neglected Diseases. *Molecules* **2007**, *13*, 616–677.
- (189) Patrick, G. L.; Spencer, J. *An introduction to medicinal chemistry*; Oxford University Press: New York, 2009.
- (190) Rollema, H.; Skolnik, M.; D’Engelbronner, J.; Igarashi, K.; Usuki, E.; Castagnoli, N. MPP(+)-like neurotoxicity of a pyridinium metabolite derived from haloperidol: in vivo microdialysis and in vitro mitochondrial studies. *Journal of Pharmacology and Experimental Therapeutics* **1994**, *268*, 380–387.
- (191) Gregory, J. D.; Robbins, P. W. Metabolism of Sulfur Compounds (Sulfate Metabolism). *Annual Review of Biochemistry* **1960**, *29*, 347–364.
- (192) Mathew, J.; Balasubramanian, A. S. Mammalian sulfoconjugate metabolism. *Journal of Biosciences* **1987**, *11*, 7–21.
- (193) Carroll, K. S.; Gao, H.; Chen, H.; Stout, C. D.; Leary, J. A.; Bertozzi, C. R. A Conserved Mechanism for Sulfonucleotide Reduction. *PLoS Biology* **2005**, *3*, e250.

- (194) Bauchart-Thevret, C.; Stoll, B.; Burrin, D. G. Intestinal metabolism of sulfur amino acids. *Nutrition Research Reviews* **2009**, *22*, 175.
- (195) Block, E. The Organosulfur Chemistry of the Genus *Allium* - Implications for the Organic Chemistry of Sulfur. *Angewandte Chemie International Edition in English* **1992**, *31*, 1135–1178.
- (196) Oae, S. *Organic Sulfur Chemistry: Structure and mechanism.*; CRC Press: Boca Raton [u.a.], 1991.
- (197) Rayner, C. M. *Advances in sulfur chemistry*; JAI Press: Stamford, Conn., 2000.
- (198) Cubbage, J. W.; Vos, B. W.; Jenks, W. S. Ei Elimination: An Unprecedented Facet of Sulfone Chemistry. *Journal of the American Chemical Society* **2000**, *122*, 4968–4971.
- (199) Cubbage, J. W.; Guo, Y.; McCulla, R. D.; Jenks, W. S. Thermolysis of Alkyl Sulfoxides and Derivatives: A Comparison of Experiment and Theory. *The Journal of Organic Chemistry* **2001**, *66*, 8722–8736.
- (200) Lanfranchi, D. A.; Bour, C.; Hanquet, G. Enantioselective Access to Key Intermediates for Salvinorin A and Analogues. *European Journal of Organic Chemistry* **2011**, *2011*, 2818–2826.
- (201) Bordwell, F. G.; Happer, D. A. R.; Cooper, G. D. Concerning driving forces for β -elimination reactions. *Tetrahedron Letters* **1972**, *13*, 2759–2762.
- (202) Marshall, D. R.; Thomas, P. J.; Stirling, C. J. M. Elimination and addition reactions. Part 30. Leaving group abilities in alkene-forming eliminations activated by sulphonyl groups. *Journal of the Chemical Society, Perkin Transactions 2* **1977**, 1898.
- (203) Redman, R. P.; Thomas, P. J.; Stirling, C. J. M. Elimination and addition reactions. Part 35. Substituent effects on alkene-forming eliminations from carbanions. *Journal of the Chemical Society, Perkin Transactions 2* **1978**, 1135.
- (204) Baciocchi, E.; Del Giacco, T.; Lanzalunga, O.; Mencarelli, P.; Procacci, B. Photosensitized Oxidation of Alkyl Phenyl Sulfoxides. C–S Bond Cleavage in Alkyl Phenyl Sulfoxide Radical Cations. *The Journal of Organic Chemistry* **2008**, *73*, 5675–5682.
- (205) Ramalingam, K.; Berlin, K. D.; Loghry, R. A.; Van der Helm, D.; Satyamurthy, N. Preparation and stereochemistry of some substituted 4-thianones and 4-thianols. Single-crystal analysis of (R)-2,trans-6-diphenyl-cis-3-methyl-4-thianone and (R)-2,trans-6-diphenyl-cis-3-ethyl-4-thianone. *The Journal of Organic Chemistry* **1979**, *44*, 477–486.
- (206) Powers, T. A.; Evans, S. A.; Pandiarajan, K.; Benny, J. C. N. Oxygen-17 nuclear magnetic resonance spectroscopy of organosulfur compounds. 2. ^{17}O NMR lanthanide-induced shifts (LIS) of diastereotopic sulfonyl oxygens in substituted six-membered-ring sulfones. *The Journal of Organic Chemistry* **1991**, *56*, 5589–5594.
- (207) Narasimhamurthy, T.; Krishnakumar, R. V.; Benny, J. C. N.; Pandiarajan, K.; Viswamitra, M. A. 2,6-Diphenylthiopyran-4-one. *Acta Crystallographica Section C Crystal Structure Communications* **2000**, *56*, 870–871.
- (208) Narasimhamurthy, T.; Benny, J. C. N.; Pandiarajan, K.; Rathore, R. S. Herring-bone π - π interactions in trans-2,6-diphenyl-2,3,5,6-tetrahydrothiopyran-4-one. *Acta Crystallographica Section C Crystal Structure Communications* **2003**, *59*, o620–o621.
- (209) Ingall, A. H. Thiopyrans and Fused Thiopyrans. In *Comprehensive Heterocyclic Chemistry*; Elsevier, 1984; pp. 885–942.
- (210) Sankarapapavinasam, S.; Pushpanaden, F.; Ahmed, M. . Piperidine, piperidones and tetrahydrothiopyrones as inhibitors for the corrosion of copper in H_2SO_4 . *Corrosion Science* **1991**, *32*, 193–203.
- (211) Chen, C. H.; Reynolds, G. A.; Luss, H. R.; Perlstein, J. H. Chemistry of 1,1-dioxothiopyrans. 1. Syntheses and reactions of 2,6-diphenyl-4H-thiopyran-4-one 1,1-dioxide and 4H-thioflaven-4-one 1,1-dioxide. *The Journal of Organic Chemistry* **1986**, *51*, 3282–3289.
- (212) Detty, M. R.; Sinicropi, J. A.; Cowdery-Corvan, R. J.; Young, R. H. Electrophotographic elements and soluble cyclic sulfone electron transport agents **1996**, *23*. EP0691579A1
- (213) El-Ghanam, A. M. Fused Heterocyclic Systems Derived from 2,6-Diaryl-3,5-dibenzylidenetetrahydro-4H-thiopyran-4-ones. *Phosphorus, Sulfur, and Silicon and the Related Elements* **2006**, *181*, 1419–1425.

- (214) Amutha, P.; Nagarajan, S. Synthesis of Novel Spiropyrimidinones. *Helvetica Chimica Acta* **2010**, *93*, 430–434.
- (215) Chaykovsky, M.; Lin, M.; Rosowsky, A.; Modest, E. J. 2,4-Diaminothiemo[2,3-d]pyrimidines as antifolates and antimalarials. 2. Synthesis of 2,4-diaminopyrido[4',3':4,5]thieno[2,3-d]pyrimidines and 2,4-diamino-8H-thiopyrano[4',3':4,5]thieno[2,3-d]pyrimidines. *Journal of Medicinal Chemistry* **1973**, *16*, 188–191.
- (216) Jayabharathi, J.; Thanikachalam, V.; Thangamani, A.; Padmavathy, M. Synthesis, AM1 calculation, and biological studies of thiopyran-4-one and their azine derivatives. *Medicinal Chemistry Research* **2007**, *16*, 266–279.
- (217) Gopalakrishnan, M.; Thanusu, J.; Kanagarajan, V. A facile solid-state synthesis and in vitro antimicrobial activities of some 2,6-diarylpiperidin/tetrahydrothiopyran and tetrahydropyran-4-one oximes. *Journal of Enzyme Inhibition and Medicinal Chemistry* **2009**, *24*, 669–675.
- (218) Parthiban, P.; Aridoss, G.; Rathika, P.; Ramkumar, V.; Kabilan, S. Synthesis, spectral, crystal and antimicrobial studies of biologically potent oxime ethers of nitrogen, oxygen and sulfur heterocycles. *Bioorganic & Medicinal Chemistry Letters* **2009**, *19*, 2981–2985.
- (219) Arndt, F.; Nachtwey, P.; Pusch, J. Über 1-Thiopyrone und 1-Thiopyranone; Beiträge zum Pyron-Problem. *Berichte der deutschen chemischen Gesellschaft (A and B Series)* **1925**, *58*, 1633–1644.
- (220) Baxter, C. A. R.; Whiting, D. A. Stereochemistry and structure in the tetrahydro-1-thio-4-pyrone and tetrahydro-4-pyrone series. *Journal of the Chemical Society C: Organic* **1968**, 1174.
- (221) Chen, C. H.; Reynolds, G. A.; Van Allan, J. A. Synthesis of 4H-thiopyran-4-ones. *The Journal of Organic Chemistry* **1977**, *42*, 2777–2778.
- (222) Ivanchikova, I. D.; Lebedeva, N. I.; Shvartsberg, M. S. A Simple Synthesis of Angular Anthrathiophenediones via Acetylenic Derivatives of Anthraquinone. *Synthesis* **2004**, *2004*, 2131–2134.
- (223) Willy, B.; Müller, T. J. J. A Novel Consecutive Three-Component Coupling-Addition-SNAr (CASNAR) Synthesis of 4H-Thiochromen-4-ones. *Synlett* **2009**, *2009*, 1255–1260.
- (224) Abramovitch, R. A.; Struble, D. L. Stereochemistry of the Michael addition. An interesting solvent effect. *Tetrahedron Letters* **1966**, *7*, 289–294.
- (225) Kalinowski, H.-O.; Berger, S.; Braun, S. *Carbon-13 NMR spectroscopy*; Wiley: Chichester; New York, 1988.
- (226) Lanfranchi, D. A.; Bour, C.; Boff, B.; Hanquet, G. Ring-Closing of 1,7- and 1,8-Enynes of Propargylic O,O-Acetals by Ruthenium-Catalysed Intramolecular Metathesis. *European Journal of Organic Chemistry* **2010**, *2010*, 5232–5247.
- (227) Lanfranchi, D. A. Vers la synthèse totale de la Salvinorine A et d'analogues structuraux, Université Louis Pasteur: Strasbourg, 2006.
- (228) Glennon, R. A.; Liebowitz, S. M.; Anderson, G. M. Serotonin receptor affinities of psychoactive phenalkylamine analogs. *Journal of Medicinal Chemistry* **1980**, *23*, 294–299.
- (229) Klein, J.; Stollar, H. The stereochemistry of thiane oxidation. *Tetrahedron* **1974**, *30*, 2541–2548.
- (230) Thiruvalluvar, A.; Balamurugan, S.; Butcher, R. J.; Pandiarajan, K.; Devanathan, D. 2-(4-Fluorophenyl)-6-phenyltetrahydro-2H-thiopyran-4-one 1-oxide. *Acta Crystallographica Section E Structure Reports Online* **2007**, *63*, o4486–o4486.
- (231) Thiruvalluvar, A.; Balamurugan, S.; Butcher, R. J.; Pandiarajan, K.; Devanathan, D. 2-r -(4-Chlorophenyl)-6-c-phenyl-3,4,5,6-tetrahydro-2H -thiopyran-4-one 1-oxide. *Acta Crystallographica Section E Structure Reports Online* **2008**, *64*, o2367–o2367.
- (232) Wojaczyńska, E.; Wojaczyński, J. Enantioselective Synthesis of Sulfoxides: 2000–2009. *Chemical Reviews* **2010**, *110*, 4303–4356.
- (233) Brunel, J. M.; Kagan, H. B. Catalytic Asymmetric Oxidation of Sulfides With High Enantioselectivities. *Synlett* **1996**, *1996*, 404–406.
- (234) Page, P. C. B. *Organosulfur Chemistry: Synthetic and stereochemical aspects*; Academic Press: San Diego, CA; London, 1998; Vol. 2.

- (235) Potvin, P. G.; Fieldhouse, B. G. On the structure of the Kagan–Modena catalysts for asymmetric oxidation of sulfides. *Tetrahedron: Asymmetry* **1999**, *10*, 1661–1672.
- (236) Hogan, P. J.; Hopes, P. A.; Moss, W. O.; Robinson, G. E.; Patel, I. Asymmetric Sulfoxidation of an Aryl Ethyl Sulfide: Modification of Kagan Procedure to Provide a Viable Manufacturing Process. *Organic Process Research & Development* **2002**, *6*, 225–229.
- (237) Song, Z. J. Asymmetric Catalysis Special Feature Part II: An efficient asymmetric synthesis of an estrogen receptor modulator by sulfoxide-directed borane reduction. *Proceedings of the National Academy of Sciences* **2004**, *101*, 5776–5781.
- (238) Andrae, S.; Schmitz, E. Electrophilic Aminations with Oxaziridines. *Synthesis* **1991**, *1991*, 327–341.
- (239) Davis, F. A.; Sheppard, A. C. Applications of oxaziridines in organic synthesis. *Tetrahedron* **1989**, *45*, 5703–5742.
- (240) Davis, F. A.; Jenkins, R.; Yocklovich, S. G. 2-Arenesulfonyl-3-aryloxaziridines: A new class of aprotic oxidizing agents (oxidation of organic sulfur compounds). *Tetrahedron Letters* **1978**, *19*, 5171–5174.
- (241) Davis, F. A.; Stringer, O. D.; Billmers, J. M. Oxidation of selenides to selenoxides using 2-sulfonyloxaziridines. *Tetrahedron Letters* **1983**, *24*, 1213–1216.
- (242) Davis, F. A.; Rizvi, S. Q. A.; Ardecky, R.; Gosciniak, D. J.; Friedman, A. J.; Yocklovich, S. G. Chemistry of sulfenic acids. 1. Synthesis of trimethylsilyl arenesulfenates (arenesulfenic acids). *The Journal of Organic Chemistry* **1980**, *45*, 1650–1653.
- (243) Davis, F. A.; Jenkins, R. H. Chemistry of sulfenic acids. 2. Formation of hydrogen peroxide from sulfenic acids. *Journal of the American Chemical Society* **1980**, *102*, 7967–7969.
- (244) Davis, F. A.; Billmers, R. L. Chemistry of sulfenic acids. 4. The first direct evidence for the involvement of sulfenic acids in the oxidation of thiols. *Journal of the American Chemical Society* **1981**, *103*, 7016–7018.
- (245) Davis, F. A.; Mancinelli, P. A.; Balasubramanian, K.; Nadir, U. K. Coupling and hydroxylation of lithium and Grignard reagents by oxaziridines. *Journal of the American Chemical Society* **1979**, *101*, 1044–1045.
- (246) Davis, F. A.; Vishwakarma, L. C.; Billmers, J. G.; Finn, J. Synthesis of alpha-hydroxycarbonyl compounds (acyloins): direct oxidation of enolates using 2-sulfonyloxaziridines. *The Journal of Organic Chemistry* **1984**, *49*, 3241–3243.
- (247) Davis, F. A.; Abdul-Malik, N. F.; Awad, S. B.; Harakal, M. E. Epoxidation of olefins by oxaziridines. *Tetrahedron Letters* **1981**, *22*, 917–920.
- (248) Davis, F. A.; Abdul-Malik, N. F.; Jenkins, L. A. Chemistry of oxaziridines. 6. Hydroxylation of anisole by 2-sulfonyloxaziridines. *The Journal of Organic Chemistry* **1983**, *48*, 5128–5130.
- (249) Davis, F. A.; Vishwakarma, L. C. Asymmetric synthesis of α -hydroxy carboxylic acids: direct oxidation of chiral amide enolates using 2-sulfonyloxaziridines. *Tetrahedron Letters* **1985**, *26*, 3539–3542.
- (250) Evans, D. A.; Morrissey, M. M.; Dorow, R. L. Asymmetric oxygenation of chiral imide enolates. A general approach to the synthesis of enantiomerically pure α -hydroxy carboxylic acid synthons. *Journal of the American Chemical Society* **1985**, *107*, 4346–4348.
- (251) Davis, F. A.; Chattopadhyay, S.; Towson, J. C.; Lal, S.; Reddy, T. Chemistry of oxaziridines. 9. Synthesis of 2-sulfonyl- and 2-sulfamoyloxaziridines using potassium peroxymonosulfate (oxone). *The Journal of Organic Chemistry* **1988**, *53*, 2087–2089.
- (252) Vishwakarma, L. C.; Stringer, O. D.; Davis, F. A. (\pm)-trans-2-(phenylsulfonyl)-3-phenyloxaziridine. *Organic Syntheses* **1988**, *66*, 203.
- (253) Foster, A. B.; Inch, T. D.; Qadir, M. H.; Webber, J. M. Assignment of sulphoxide configuration by the nuclear magnetic resonance method. *Chemical Communications (London)* **1968**, 1086.
- (254) Devanathan, D.; Pandiarajan, K. ¹H and ¹³C NMR Spectral Study of Some 2r-Aryl-6c-phenylthian-4-ones, Their 1-Oxides and 1,1-Dioxides. *Spectroscopy Letters* **2009**, *42*, 147–155.

- (255) Williams, D. R.; Fu, L. General Methodology for the Preparation of 2,5-Disubstituted-1,3-oxazoles. *Organic Letters* **2010**, *12*, 808–811.
- (256) Bos, P. H.; Maciá, B.; Fernández-Ibáñez, M. Á.; Minnaard, A. J.; Feringa, B. L. Catalytic asymmetric conjugate addition of dialkylzinc reagents to α,β -unsaturated sulfones. *Organic & Biomolecular Chemistry* **2010**, *8*, 47.

Synthesis and evaluation of the antiparasitic activity of diarylideneacetones and their related thiopyranone and S-oxide prodrugs

Résumé

La trypanosomiase humaine africaine, la maladie de Chagas et les leishmanioses sont des maladies parasitaires qui représentent un problème majeur de santé publique dans de nombreux pays et notamment ceux en voie de développement. Afin de trouver de nouveaux candidats-médicaments contre ces parasites, deux séries chimiques ont été étudiées : les diarylidèneacétones et les 2,6-diaryl-4*H*-tétrahydrothiopyranones.

Précédemment initiée au laboratoire, l'étude approfondie de la série diarylidèneacétone a nécessité la mise au point et l'optimisation de protocoles. Une nouvelle méthodologie de synthèse des (hétéro)diarylidèneacétones dissymétriques par palladocatalyse a ainsi été développée en collaboration avec le Pr. T. J. Müller (Université de Düsseldorf). En dépit d'excellentes activités antiparasitaires, la plupart des diarylidèneacétones synthétisées se sont révélées trop toxiques sur les cellules humaines.

Les 2,6-diaryl-4*H*-tétrahydrothiopyranones et leurs S-oxydes ont été conçues pour résoudre ce problème de toxicité. Agissant comme prodrogues, ces molécules sont susceptibles de régénérer les diarylidèneacétones parentes par β -élimination du groupement soufré intracyclique. Peu décrite dans la littérature, la synthèse diastéréosélective de ces structures a été intégralement mise au point et généralisée à de nombreuses substitutions. Les résultats obtenus prouvent que la toxicité des produits a été grandement diminuée tout en maintenant une activité antiparasitaire importante, ce qui valide l'approche de la stratégie prodrogue.

Mot-clefs: antiparasitaire, synthèse diastéréosélective, hétérocycle, addition de Michael, Palladium, S-oxydes

Résumé en anglais

Human African trypanosomiasis, Chagas disease and leishmaniasis are parasitic diseases that significantly affect the populations and thus the economy of many developing countries. With the aim of developing new therapeutic agents to cure these diseases, we focused our research on two series: the diarylideneacetone and the 2,6-diaryl-4*H*-tetrahydrothiopyranone series.

To complete and extend preliminary results that had been previously obtained in our laboratory, a generalization and an optimization of the protocols was intended. Thus, a novel Palladium-catalyzed synthesis of (hetero)dissymmetric diarylideneacetones was developed and optimized in collaboration with Prof. T. J. Müller (University of Düsseldorf). In spite of excellent antiparasitic activities, most of the diarylideneacetones were toxic toward human cells.

2,6-Diaryl-4*H*-tetrahydrothiopyranones and their related S-oxides were designed to cope with major toxicity issues. Acting as prodrugs, these molecules are prone to undergo β -elimination of the sulfurated intracyclic group, regenerating the parent diarylideneacetone. The diastereoselective synthesis of this scaffold is not extensively described in the literature. Consequently, novel diastereoselective methodologies have been developed and generalized to a wide panel of substitution patterns. Results of the biological assays demonstrated that sulfide and S-oxide prodrugs displayed a lowered toxicity while the potency was maintained, thus confirming the validity of the prodrug strategy.

Keywords: antiparasitic, diastereoselective synthesis, heterocycle, Michael addition, Palladium, S-oxides